


UNIVERSITY OF
ILLINOIS LIBRARY
AT URBANA-CHAMPAIGN
BOOK



Digitized by the Internet Archive
in 2012 with funding from
University of Illinois Urbana-Champaign


<http://archive.org/details/organicsemi199700univ>

ORGANIC SEMINAR ABSTRACTS 1997-98, SEMESTER I

University of Illinois

Department of Chemistry
Box 68 Roger Adams Laboratory
600 South Matthews Avenue
Urbana, Illinois 61801

January, 1998

UNIVERSITY OF
ILLINOIS LIBRARY
AT URBANA-CHAMPAIGN


Q. 547
Il6s
1997-98:1

SEMINAR TOPICS

Semester I, 1997-98

	Page
Dynamic Kinetic Resolution	1
Recent Developments in t	9
Synthetic Approaches to	17
Recent Advances in Stille C Copper(I) Salts.....	25
Autocatalysis and the O	33

NOTICE: Return or renew all Library Materials! The Minimum Fee for each Lost Book is \$50.00.

The person charging this material is responsible for its return to the library from which it was withdrawn on or before the **Latest Date** stamped below.

Theft, mutilation, and underlining of books are reasons for disciplinary action and may result in dismissal from the University.
To renew call Telephone Center, 333-8400


UNIVERSITY OF ILLINOIS LIBRARY AT URBANA-CHAMPAIGN

CHEMISTRY LIBRARY

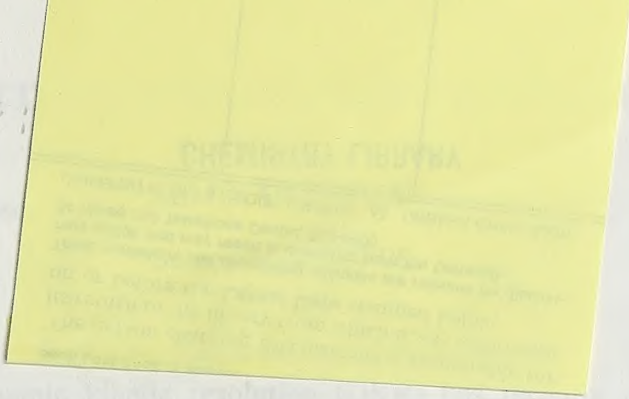
L161—O-1096

REQUIREMENTS FOR DYNAMIC KINETIC RESOLUTIONS

An important factor to be considered in a DKR process is the rate of racemization or epimerization relative to that of resolution. This rate must at least equal or exceed the rate of the resolution step ($k_{res} > k_{rac}$) to prevent a gross increase in the concentration of the slower-reacting species.

UNIVERSITY OF
ILLINOIS LIBRARY
AT URBANA-CHAMPAIGN


Q. 547
IL65
1997-98



Page

Dynamic Kinetic Resolutions in Asymmetric Synthesis.....	1
Julie L. Thompson	
Recent Developments in the Catalytic Pauson-Khand Reaction.....	9
Matthew T. Epperson	
Synthetic Approaches to Epothilones.....	17
A. Dawn Bounds	
Recent Advances in Stille Coupling Methodology: Effects of Ligands and Copper(I) Salts.....	25
Marvin J. Meyers	
Autocatalysis and the Origin of Homochirality.....	33
Son M. Pham	

UNIVERSITY OF
ILLINOIS LIBRARY
AT URBANA-CHAMPAIGN
CHEMISTRY

DYNAMIC KINETIC RESOLUTIONS IN ASYMMETRIC SYNTHESIS

Reported by Julie L. Thompson

September 18, 1997

INTRODUCTION

The concept of dynamic kinetic resolution (DKR) has recently gained attention because it surpasses the inherent limit of traditional kinetic resolution, in which there is a maximum 50% yield of a single stereoisomer.¹ This higher yield is the result of the coupling of two processes, a rapid *in situ* racemization or epimerization of starting material and an efficient kinetic resolution step, as depicted in Figure 1b.

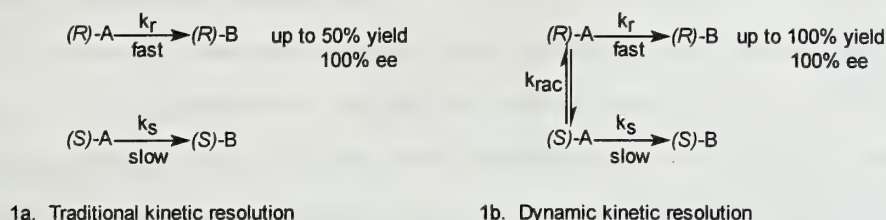


Figure 1. Comparison of traditional and dynamic kinetic resolution of racemates.

In traditional kinetic resolution (Figure 1a), the isolated product may be either the unreacted enantiomer of the starting material (i.e., (S)-A) or the product resulting from reaction of the other enantiomer (i.e., (R)-B). The yield and the ee are affected greatly by the extent of conversion. DKR differs greatly from traditional kinetic resolution methods in that there is no possibility of isolating an unreacted substrate with high ee. Thus, it is not a method to be used for the purification of final products. In DKR, racemization followed by resolution depletes all starting material and has the potential of creating (R)-B in 100% yield and 100% ee (Figure 1b). There are many ways to racemize configurationally labile substrates, and this topic has been reviewed very recently.² This abstract briefly addresses the requirements for DKR processes and provides examples to illustrate the concept as it has been applied to the resolution of diastereomers and enantiomers.

REQUIREMENTS FOR DYNAMIC KINETIC RESOLUTIONS

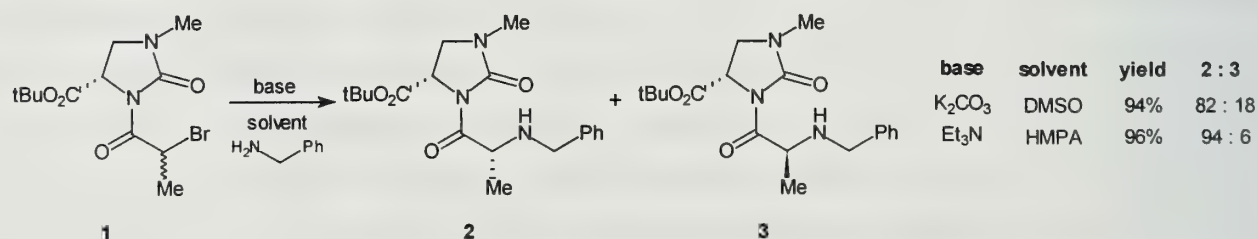
An important factor to be considered in a DKR process is the rate of racemization or epimerization relative to that of resolution. This rate must at least equal or exceed the rate of the resolution step ($k_{\text{rac}} > k_{\text{res}}$) to prevent a great increase in the concentration of the slower-reacting species

relative to the remaining faster-reacting species. As in normal kinetic resolutions, the more favorable the ratio of k_r/k_s , the higher the ee. Finally, the resolution reaction must be irreversible and the product must be configurationally stable under the reaction conditions in order to prevent product distributions that are thermodynamically derived. Noyori has developed a mathematical treatment of these kinetic parameters to show the relationships between k_{rac}/k_{res} , k_r/k_s , ee, and conversion.³

“DYNAMIC KINETIC RESOLUTION” OF DIASTEREOMERS

By definition, kinetic resolution is a separation of enantiomers and dynamic kinetic resolution involves equilibration of racemates with an inherent equilibrium constant equal to one. In the literature, however, the term is expanded to include the analogous process using mixtures of two diastereomers, which usually arise from placement of chiral, non-racemic auxiliaries onto racemates. Due to energy differences, the diastereomers may not be present in equal amounts in solution. Regardless, the process is typically used to resolve enantiomers, using the chiral auxiliary to direct the asymmetric transformation reaction with an achiral reagent. For example (Scheme 1), the diastereomers **1** arose from the reaction of (*S*)-2-oxoimidazolidine-4-carboxylate with a racemic substrate.⁴ Epimerization of the 2-bromopropanoyl group is base catalyzed in polar solvents; reaction with benzylamine gives a high yield and dr of **2**.

Scheme 1



This diastereomeric substrate has been used with other nucleophiles (malonic ester enolate⁵ and potassium phthalimide⁶) under different conditions and consistently provides high yields and de's. Oppolzer's camphorsultam⁷ is another chiral auxiliary used in DKR for the preparation of α -bromo amides leading to α -amino, α -hydroxy and α -thiocarboxylic acid derivatives. Pantolactone⁸ and various chiral pyrrolidinones⁹ and pyrrolidines¹⁰ have also been used extensively as covalent chiral auxiliaries in DKR. A major disadvantage of using covalently bound chiral auxiliaries for chiral information transfer is that they must be removed. Often, this removal is not described, which leaves unanswered the question of whether high de's will extend to high ee's, i.e., whether the intermediates are configurationally stable to the conditions of auxiliary removal. There are some recent examples of DKR using non-covalently bound auxiliaries on an epimerizing substrate.¹¹

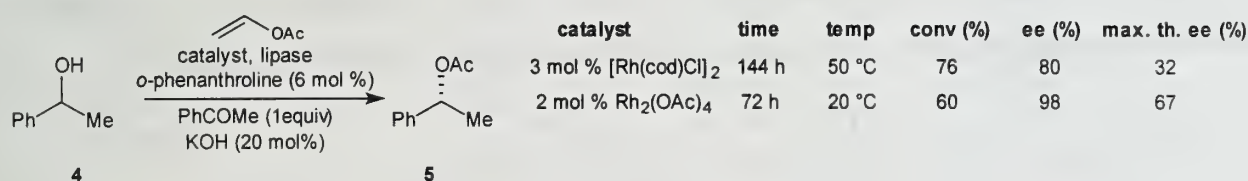
DYNAMIC KINETIC RESOLUTION OF ENANTIOMERS

There are three basic ways to resolve racemates by kinetic resolution. The use of enzymatic and whole cell methods is the most widely explored, and a thorough review has been published on biocatalytic DKR techniques.¹² A few recent novel examples are discussed here to illustrate the concept of DKR. Chemical resolution methods used in DKRs are not as well developed, but several successful examples are known. The use of synthetic chiral catalysts for the resolution step is discussed, including those reactions that create a new stereocenter, preferentially generating one of four possible diastereomers. The last chemical method is the reaction of racemates with chiral reagents.

DKR of enantiomers using enzymatic resolution

Recently, an enzymatic DKR was performed on a configurationally labile alcohol that included a catalytic racemization by Oppenauer oxidation/Meerwein-Ponndorf-Verley reduction.¹³ The racemization was performed using rhodium catalysts with phenanthroline as a coligand, acetophenone as a hydride acceptor, and KOH as base (KOH was not used with the $\text{Rh}_2(\text{OAc})_4$ system). The enzyme used was a lipase from *P. fluorescens*. This is the first example of a transition metal-catalyzed racemization coupled with an enzymatic resolution (Scheme 2). In the table, the maximum theoretical ee of a traditional kinetic resolution at the particular level of conversion is given as proof of the concept that higher ee's and yields can be obtained by DKR. A similar method employing a palladium-catalyzed racemization/lipase resolution was shown to dynamically resolve phenylethylamine in 64% yield and 99% ee.¹⁴

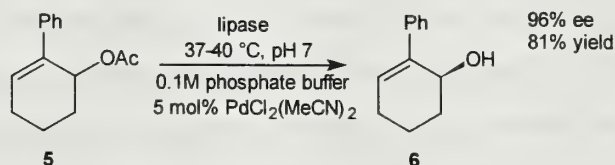
Scheme 2



An example of DKR of racemic phenyl-substituted cyclohexenyl acetate **5** is depicted in Scheme 3. Racemization was effected by a Pd-catalyzed [1,3]-sigmatropic acetate shift. Enantioselective hydrolysis with lipase from *P. fluorescens* gave the (*S*)-alcohol **6** in 81% yield and 96% ee after 19 days. The authors note that 50% conversion had been reached within two days and that, therefore, racemization must be the rate-limiting step for the completion of the DKR.¹⁵ Although this may appear to be contrary to the basic principle of DKR that requires racemization to be faster than resolution, it

must be noted that there are *two* rates to consider in the resolution step. For DKR to be effective, the rate of racemization must exceed the *slower* of these two rates (i.e., $k_{\text{rac}} > k_s$ from Figure 1b).

Scheme 3



There are many instances of lipases catalyzing esterifications in DKR, and many examples of racemization of various substrates, such as racemization of hemiacetals of pyranones¹⁶ and hemithioacetals have been reported.¹⁷ D-hydantoinases have been used to resolve various racemizing phenyl derivatives of hydantoins to ultimately yield synthetically important D-phenylglycine derivatives.¹⁸ Efforts to access the L-derivatives using L-hydantoinases were unsuccessful, however. DKR using microbes has also been demonstrated. Most notable are the number of reported dynamic kinetic resolutions of β -ketoesters containing one and two epimerizing stereocenters effected by Baker's yeast.¹⁹ In many instances enzymatic reactions have been shown to be useful for DKR, but they often suffer from long reaction times. Also, finding the appropriate enzyme to accomplish a given transformation is of major concern. When whole cell reactions (rather than pure enzymes) are used, competing enzymes can affect product ratios and various enzyme inhibitors must be used to control activity.

DKR of enantiomers using chiral catalysts

The asymmetric hydrogenations of β -keto esters with chiral Ru-BINAP complexes yield β -hydroxy esters with high enantioselectivity.²⁰ With an α -carbon substituent, there is potential for dynamic kinetic resolution with racemization arising from keto-enol tautomerism (Figure 2).

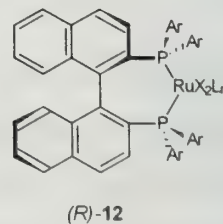
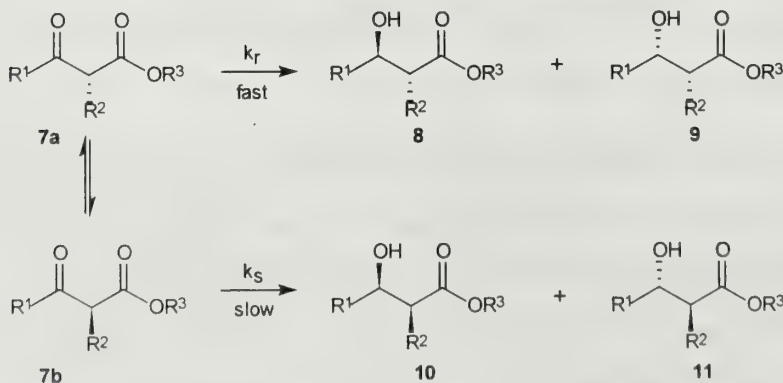
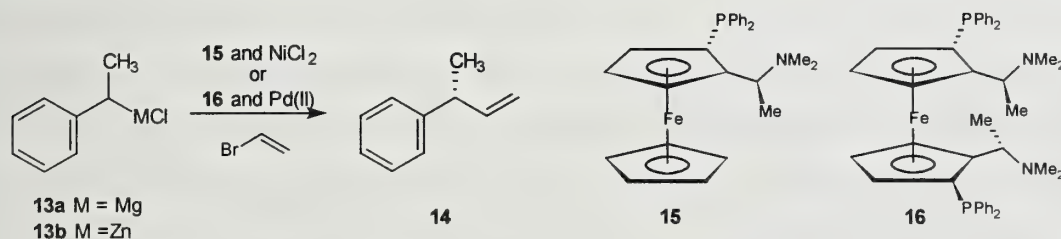


Figure 2. Possible products from DKR of enantiomers using asymmetric hydrogenation

Noyori has extensively studied chiral Ru-BINAP catalyzed reduction of these substituted esters and has demonstrated the ability to control product formation under DKR conditions to favor one out of the four possible diastereomers. The configuration of the β -hydroxy moiety is determined solely by the chirality of the catalyst, which for the (*R*)- catalyst would give the (*R*)-hydroxy products **8** or **10**. The configuration at the α -carbon is substrate, and sometimes solvent, dependent. The *syn* product **10** predominates if the substituent R^2 can hydrogen bond with the ester; however, for some alkyl substituents the *anti* product **8** is formed. As an example demonstrating the concept, when $R^1=R^3=Me$ and $R^2=NHAc$, the yield of the DKR in CH_2Cl_2 is 100%, with *syn:anti* (**10:8**) of 99:1 and 94% ee.²¹ This type of DKR has been extended to several other substrates, including cyclic β -ketoesters, β -ketophosphonates, and diastereomeric β -keto esters.²¹ All demonstrate successfully the concept of dynamic kinetic resolution, in which yields greater than 50% of the product with high ee can be achieved. Major benefits of using this method of DKR include the mild conditions required for racemization and the fact that the method has been thoroughly investigated (including computational analysis of product distributions) and applied.

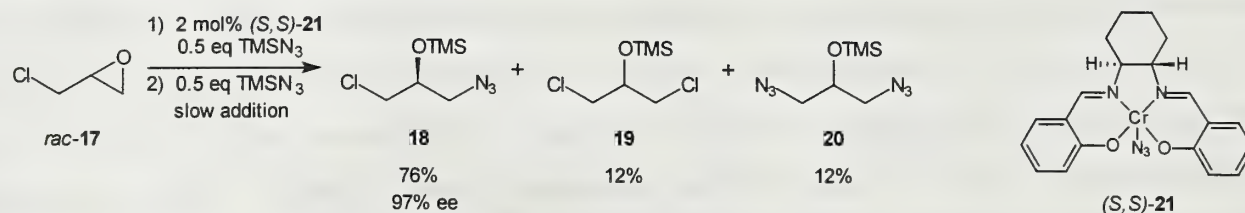
Kumada has exploited the chiral lability of secondary Grignard reagents in an asymmetric Grignard cross-coupling reaction catalyzed by chiral transition metal complexes (Scheme 4). The chiral ferrocenyl ligand **15** was used with $NiCl_2$ to catalyze the coupling of **13a** with vinyl bromide to yield **14** in 95% yield and 66% ee.²² When the organozinc reagent **13b** was used with Pd catalysis and the chiral phenyl butene ligand **16**, the coupling reaction resulted in quantitative yield and 93% ee.²²

Scheme 4



Jacobsen has recently demonstrated a DKR of racemic epichlorohydrin **17** by enantioselective ring opening with $TMSN_3$ catalyzed by the (salen)Cr(III) N_3 complex **21**. This DKR of an enantiomer with a chiral catalyst, shown in Scheme 5, is an example of resolution without creation of an additional stereocenter.²³

Scheme 5

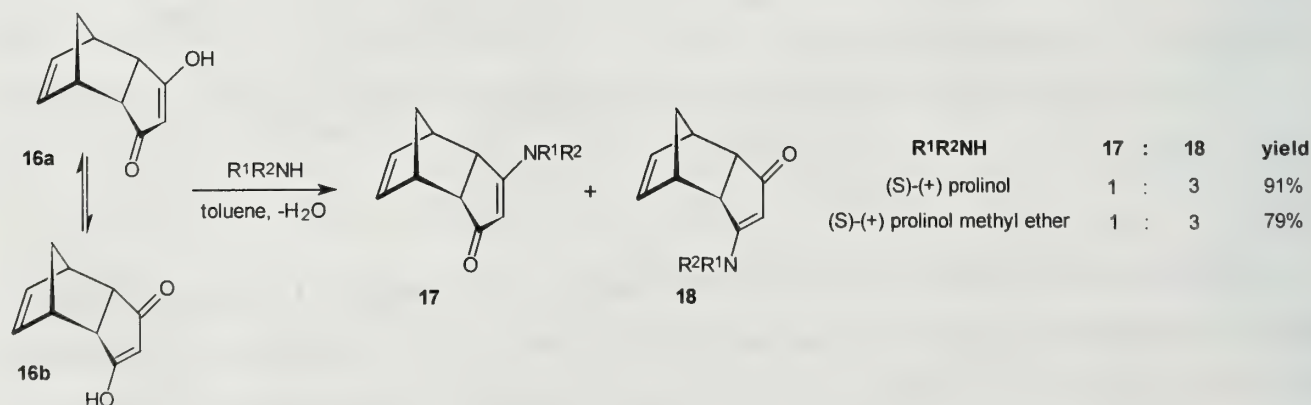


Careful addition of TMSN_3 was necessary to ensure that the rate of racemization exceeded that of ring opening. The side products **19** and **20** provided some evidence for the mechanism of the *in situ* racemization, which was postulated to require chlorine ion transfer from the chromium to the slower reacting enantiomer, opening the epoxide, which then recloses non-selectively. This reaction is appealing because it resolved a commodity chemical (**17**) into an azide intermediate **18** which can be converted into synthetically valuable building blocks.

DKR of enantiomers with chiral reagents

The selective addition of a chiral reagent to racemic, equilibrating starting materials under DKR conditions can provide a diastereomeric excess of products, as shown in Scheme 6. In the case shown, the racemization occurs via tautomerization of **16a** and **16b**. When L-prolinol was used as the chiral amine reagent, a de of 50% was obtained with 91% yield.²⁴ The diastereomers **17** and **18** had to be converted into the corresponding acetates to be separated by column chromatography. This DKR process provided a novel route to the *endo*-tricyclodecadienone from readily accessible **16**.

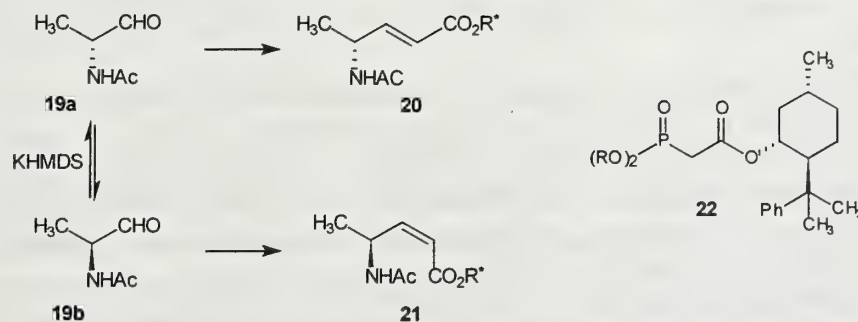
Scheme 6



Recently, the first DKR of α -amino aldehydes was reported; this involved their conversion to alkenes using chiral phosphonates.²⁵ Racemization was catalyzed by an excess of base, and kinetic

resolution was effected by an asymmetric Horner-Wadsworth-Emmons reaction using chiral phosphonate **22** as shown in Scheme 7.

Scheme 7



The authors were able to affect product ratios by selection of the R groups on the phosphonate reagent. For example, the *Z* alkene was favored when the R groups on the phosphonates were CF_3CH_2- , and the *E* alkene was favored when the R groups were Me, Et, or *i*Pr. To demonstrate that this process was DKR, it was shown that without excess base, the interconversion of **19a** and **19b** was too slow for a DKR, which resulted in decreased *E/Z* selectivity and diastereoselectivity. Also, products **20** and **21** were shown to be stable to epimerization in the presence of excess base required for racemization. Thus, two of the important criteria of DKR were demonstrated in these experiments. A few other examples of chiral discrimination in DKR by the use of chiral reagents are known.^{1,26}

CONCLUSIONS

The examples presented in this abstract illustrate the concept and utility of dynamic kinetic resolution of enantiomers and diastereomers. The practical use of this concept, particularly the use of chemical resolution methods, is quite recent. Few extensive studies have been undertaken to expand individual systems (asymmetric hydrogenations of β -keto esters are an exception). It may be difficult to optimize reaction conditions to meet the criteria of DKR. There are many factors to take into account, particularly the rate issues. Innovative ways to racemize substrates² combined with logical design of a resolution method should lead to more opportunities for exploiting DKR in asymmetric synthesis. Certainly, many more papers using this technique will be forthcoming.

REFERENCES

- (1) (a) Kagan, H.B.; Fiaud, J.C. *Topics in Stereochem.*, **1988**, 18, 249. (b) Ward, R.S. *Tetrahedron: Asymmetry* **1995**, 6, 1475. (c) Noyori, R.; Tokunaga, M.; Kitamura, M. *Bull. Chem. Soc. Jpn.* **1995**, 68, 36. (d) Caddick, S.; Jenkins, K. *Chem. Soc. Rev.* **1996**, 447.
- (2) Ebbers, E.J.; Ariaans, G.J.A.; Houbiers, J.P.M.; Bruggink, A.; Zwanenburg, B. *Tetrahedron* **1997**, 53, 9417.
- (3) Kitamura, M.; Tokunaga, M.; Noyori, R. *Tetrahedron* **1993**, 49, 1853.
- (4) Nunami, K.; Kubota, H.; Kubo, A. *Tetrahedron Lett.* **1994**, 35, 8639.
- (5) (a) Kubo, A.; Takahashi, M.; Kubota, H.; Nunami, K. *Tetrahedron Lett.* **1995**, 36, 6251. (b) Kubo, A.; Takahashi, M.; Kubota, H.; Nunami, K. *J. Org. Chem.* **1997**, 62, 5830.
- (6) Kubo, A.; Kubota, H.; Takahashi, M.; Nunami, K. *Tetrahedron Lett.* **1996**, 37, 4957.
- (7) (a) Ward, R.S.; Pelter, A.; Goubet, D.; Pritchard, M.C. *Tetrahedron: Asymmetry* **1995**, 6, 469. (b) Ward, R.S.; Pelter, A.; Goubet, D.; Pritchard, M.C. *Tetrahedron: Asymmetry* **1995**, 6, 93.
- (8) (a) Koh, K.; Ben, R.N.; Durst, T. *Tetrahedron Lett.* **1993**, 34, 4473. (b) Koh, K.; Ben, R.N.; Durst, T. *Tetrahedron Lett.* **1994**, 35, 375. (c) Koh, K.; Durst, T. *J. Org. Chem.* **1994**, 59, 4683.
- (9) Camps, P.; Pérez, F.; Soldevilla, N. *Tetrahedron: Asymmetry* **1997**, 8, 1877.
- (10) Devine, P.N.; Dolling, U.; Heid, R.M.; Tschaen, D.M. *Tetrahedron Lett.* **1996**, 37, 2683.
- (11) (a) Thayumanavan, S.; Basu, A.; Beak, P. *J. Am. Chem. Soc.* **1997**, 119, 8209. (b) Seebach, D.; Jaeschke, G.; Gottwald, K.; Matsuda, K.; Formisano, R.; Chaplin, D.A. *Tetrahedron* **1997**, 53, 7539.
- (12) Stecher, H.; Faber, K. *Synthesis-Stuttgart* **1997**, 1, 1.
- (13) Dinh, P.M.; Howarth, J.A.; Hudnott, A.R.; Williams, J.M.J. *Tetrahedron Lett.* **1996**, 37, 7623.
- (14) Reetz, M.T.; Schimossek, K. *Chimia* **1996**, 50, 668.
- (15) Allen, J.V.; Williams, J.M.J. *Tetrahedron Lett.* **1996**, 37, 1859.
- (16) van den Heuvel, M.; Cuiper, A.D.; van der Deen, H.; Kellogg, R.M.; Feringa, B.L. *Tetrahedron Lett.* **1997**, 38, 1655.
- (17) Brand, S.; Jones, M.F.; Rayner, C.M. *Tetrahedron Lett.* **1995**, 36, 8493.
- (18) Garcia, M.J.; Azerad, R. *Tetrahedron: Asymmetry* **1997**, 8, 85.
- (19) (a) Kawai, Y.; Hida, K.; Nakamura, K.; Ohno, A. *Tetrahedron Lett.* **1995**, 36, 591. (b) Nakamura, K.; Kawai, Y.; Miyai, T.; Honda, S.; Nakajima, N.; Ohno, A. *Bull. Chem. Soc. Jpn.* **1991**, 64, 1467. (c) Sato, T.; Tsurumaki, M.; Fujisawa, T. *Chemistry Letters*, **1986**, 1367.
- (20) Noyori, R. *Acta Chem. Scand.* **1996**, 50, 380
- (21) Noyori, R.; Ikeda, T.; Ohkuma, T.; Widhalm, M.; Kitamura, M.; Takaya, H.; Akutagawa, S.; Sayo, N.; Saito, T.; Taketomi, T.; Kumobayashi, H. *J. Am. Chem. Soc.* **1989**, 111, 9134.
- (22) (a) Hayashi, T.; Konishi, M.; Fukushima, M.; Kanehira, K.; Hioki, T.; Kumada, M. *J. Org. Chem.* **1983**, 48, 2195. (b) Hayashi, T.; Yamamoto, A.; Hojo, M.; Ito, Y. *J. Chem. Soc., Chem. Commun.* **1989**, 495
- (23) Schaus, S.E.; Jacobsen, E.N. *Tetrahedron Lett.* **1996**, 37, 7937.
- (24) Bakkeren, F.J.A.D.; Ramesh, N.G.; de Groot, D.; Klunder, A.J.H.; Zwanenburg, B. *Tetrahedron Lett.* **1996**, 37, 8003.
- (25) Rein, T.; Kreuder, R.; von Zezschwitz, P.; Wulff, C.; Reiser, O. *Angew. Chem. Int. Ed. Engl.* **1995**, 34, 1023.
- (26) (a) Yamada, S.; Mori, Y.; Morimatsu, K.; Ishizu, Y.; Ozaki, Y.; Yoshioka, R.; Nakatani, T.; Seko, H. *J. Org. Chem.* **1996**, 61, 8586. (d) Sugi, K.D.; Nagata, T.; Yamada, T.; Mukaiyama, T. *Chem. Lett.* **1996**, 1081.

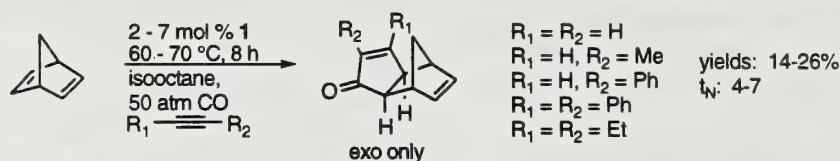
Initial studies¹ eliminated alkene complexes of (**1**) as intermediates and established the intermediacy of alkynehexacarbonyldicobalt complexes (**2**) along the cycloaddition reaction pathway. However, no intermediates have been observed following alkyne complexation, suggesting that the rate-determining step occurs early in the ensuing sequence.⁵ According to Schore,⁴ reversible alkene complexation follows the formation of **2**. Subsequent irreversible insertion of the complexed face of the alkene π bond into the less hindered cobalt-carbon bond results in carbon-carbon bond formation at the alkyne carbon possessing the smaller substituent. This is consistent with the observation that the larger alkyne substituent invariably appears α to the carbonyl in the cyclopentenone product. Thus, alkene insertion is believed to be the regio- and rate-determining step. Sequential CO insertion, reductive elimination of one cobalt, and decomplexation of the other give the final product. Recently, Rautenstrauch and coworkers⁶ proposed a catalytic cycle based on the Magnus-Schore mechanism with **1** as the active catalyst (refer to Scheme 1).

COBALT-BASED CATALYTIC METHODS

Conventional $\text{Co}_2(\text{CO})_8$ Catalyzed Procedures

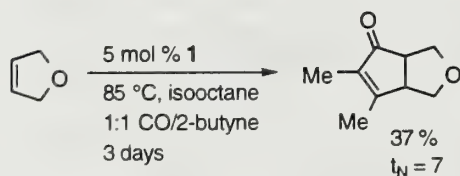
Attempts to promote the PKR catalytically began with the pioneering efforts of Pauson and Khand.¹ Their approach was based on the observation that cyclopentenones were formed when carbon monoxide, acetylene, and strained cyclic alkenes were heated in the presence of a catalytic quantity of **1**. However, heating a mixture of **1** and norbornadiene with a variety of alkynes in isooctane under an atmosphere of CO resulted in poor turnover, low yields, and substantial byproduct formation (Scheme 2).

Scheme 2



Billington,^{8,9} noting the thermal instability of alkynehexacarbonyldicobalt complexes, attempted to recycle the degraded complex in the reaction of 2-butyne and 2,5-dihydrofuran by performing the reaction under an atmosphere of 1:1 2-butyne/CO with a generous excess of the alkene (Scheme 3).

Scheme 3



Unfortunately, this method required extended reaction times and also produced modest amounts of the desired adducts. Subsequently, Rautenstrauch and coworkers⁶ were able to achieve more efficient turnover than Pauson and Khand by heating a toluene

solution of ethylene, 1-heptyne, and **1** (0.22 mol %) in an autoclave under a CO atmosphere. However, this procedure necessitated the use of ethylene as the olefin, resulted in irreproducible yields, and afforded byproducts resulting from alkyne cyclotrimerization and alkyne-alkene cocyclotrimerization.

Several inherent problems arise when **1** is used as the active catalyst. These include (1) the dimerization of $[\text{Co}_2(\text{CO})_6]$ to the inert $\text{Co}_4(\text{CO})_{12}$ which is competitive with CO capture¹⁰, (2) the recycling of $[\text{Co}_2(\text{CO})_6]$ to **1** which requires high CO pressures that prevent alkene complexation,⁶ (3) the thermal decomposition of the alkynehexacarbonyldicobalt complexes which occurs at the temperatures required for dissociative carbon monoxide/alkene exchange,⁸ and (4) the possibility of several side reactions between the alkynehexacarbonyldicobalt complex and remaining alkyne molecules when there is an excess of alkyne relative to **1**.⁶

Photochemical Promotion

It has been demonstrated that **1** undergoes photolytic conversion to $[\text{Co}_2(\text{CO})_7]$,¹¹ the suspected intermediate in the reaction of **1** with alkynes. Presumably, irradiation of **1** with high intensity light weakens the metal-carbonyl bond via a $\pi \rightarrow \sigma^*$ transition¹² and avoids the difficulties encountered with high temperatures and CO pressures. Further irradiation should also favor CO loss from the alkynehexacarbonyldicobalt complex, facilitating alkene complexation and rate-determining insertion. Livinghouse and Pagenkopf¹³ were able to effect the photochemical conversion of various 1,6-enynes to bicyclooctenones in 12 h with 5 mol % **1** at 55 °C under CO (1 atm) in good to excellent yields (Table 1).

Table 1. Photochemical catalytic Pauson-Khand cycloadditions

Substrate	Product	% Yield	Substrate	Product	% Yield
		95			67
		75			74
		91			67
		80			

Phosphite Coligand Approach

Several attempts to promote the catalytic Pauson-Khand reaction with modified cobalt reagents have been recently explored. In 1994 Jeong and coworkers¹⁴ reported that 10-20 mol % triphenylphosphite combined with 3-5 mol % **1** in DME under CO (3 atm) successfully promoted the conversion of enynes to bicyclic cyclopentenones (Table 2). This approach was based on the earlier hypothesis by Magnus¹⁰ that the formation of inert cobalt clusters such as $\text{Co}_4(\text{CO})_{12}$ prevent catalytic turnover. Although the specific role of the triphenylphosphite was not determined, it was assumed to prevent the dimerization of $[\text{Co}_2(\text{CO})_6]$ by occupying the empty coordination sites on the cobalt atoms.

Table 2. Catalytic Pauson-Khand reaction with triphenylphosphite coligand.

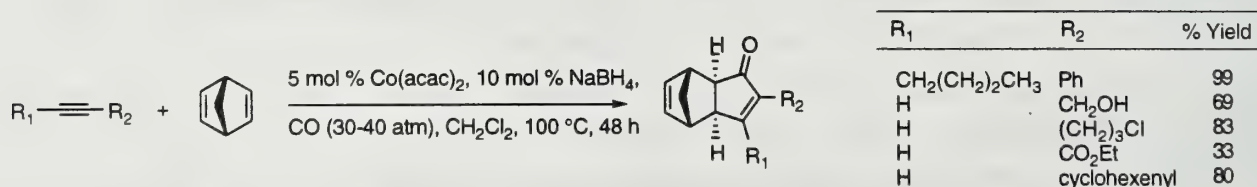
Substrate	Product	% Yield	Substrate	Product	% Yield
		82			58
		94			19
		90			

Low turnover numbers (4-5) were observed when the reaction was carried out under 1 atm of CO in refluxing dimethoxyethane. However, under a higher pressure of CO (3 atm), the reactions proceeded in good yields. Substrates containing internal and terminal alkynes, monosubstituted and disubstituted alkenes, and heteroatom containing tethers reacted successfully. In contrast to the photochemical reaction, allylic acetates in the enyne afforded products derived from the elimination of acetic acid in significant amounts. When the intermolecular cycloaddition between phenylacetylene and norbornadiene was attempted, a 1:1 mixture of triphenylbenzene and a cyclopentenone was obtained in 20% yield.

In Situ Generation of Cobalt Carbonyls With Co(acac)₂/NaBH₄

Chung and Lee¹⁵ have reported a method for promoting the catalytic PKR using Co(acac)₂/NaBH₄ (Scheme 4). This approach was based on the premise that low valent cobalt carbonyl complexes, generated *in situ* under a CO atmosphere, would not undergo dimerization and could continue to react with alkynes. The presence of NaBH₄ was believed to inhibit the formation of cobalt clusters, allowing the catalytic cycle to continue. Small amounts of cobalt carbonyl complexes were observed in every reaction. In fact, when 1-hexyne was employed as the alkyne, (1-hexyne)Co₂(CO)₆ was isolated

Scheme 4



This system is compatible with alkyl halides and accepts acetylene and ethyl propionate as the alkyne. However, it is unable to catalyze the reaction with less reactive and unstrained alkenes. Intramolecular cycloadditions have been accomplished but proceed less efficiently than the intermolecular cycloadditions (Table 3).

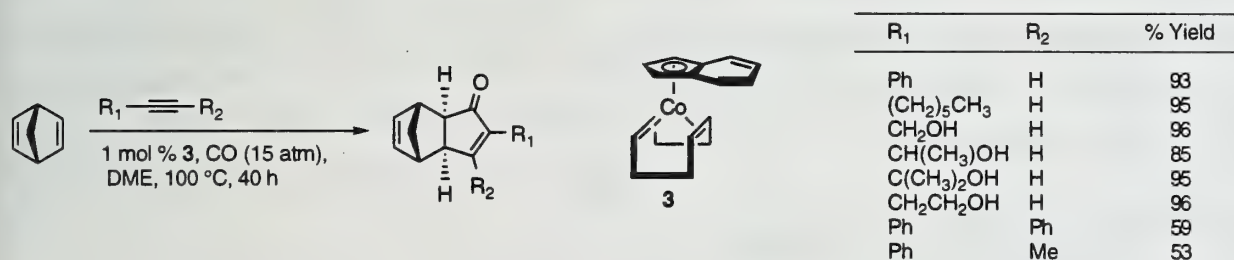
Table 3. Intramolecular Cycloadditions Catalyzed by $\text{Co}(\text{acac})_2/\text{NaBH}_4$

Substrate	$\text{Co}(\text{acac})_2$, mol %	NaBH_4 , mol %	Product	% Yield
	5	10		66
	4.6	9.2		85
	10	20		59
	10	20		82 (3.7 : 1)

Cobalt(I) Catalysis

More recently, Jeong's group developed another catalytic PKR.¹⁶ This method was the first successful catalytic PKR not based on **1**. When strained cyclic alkenes such as norbornadiene were exposed to a variety of alkynes in the presence of 1,5-cyclooctadiene(indenyl)cobalt(I) (**3**) under an atmosphere of CO (Scheme 5), high turnover was achieved. Both terminal and internal alkynes produced the desired adducts in high yields with low catalyst loading. Reactions with propargyl alcohol, a notoriously poor substrate in the stoichiometric PKR, and 1,7-octadiynes (which often give [2+2+2] adducts) were successful.

Scheme 5



This catalyst was comparable to the $\text{Co}(\text{acac})_2/\text{NaBH}_4$ system in its inability to catalyze the reaction with less reactive and unstrained olefins such as ethylene, cyclopentene, allyl alcohol, and methyl acrylate; however, the process was completely diastereoselective and useful in both intermolecular and intramolecular cases. During the course of this study, it was realized that the indenyl ligand is required for the cycloaddition since $\text{Cp}(\text{Co})\text{COD}$ and $\text{CpCo}(\text{CO})_2$ failed to catalyze the reaction. However, no explanation was provided for this observation.

RUTHENIUM-BASED CATALYTIC METHODS

In addition to cobalt, other transition metals are known to promote the stoichiometric PKR including zirconium,¹⁷ molybdenum,¹⁸ tungsten,¹⁹ iron,²⁰ and nickel.²¹ Furthermore, it has been reported that ruthenium complexes catalyze [2+2] cycloadditions between alkynes and norbornenes via the formation of ruthenacyclopentenes.²² Earlier this year, the groups of Mitsudo²³ and Murai²⁴ expanded the scope of the catalytic PKR beyond the use of Co-based systems with their independent reports of $\text{Ru}_3(\text{CO})_{12}$ catalysis. Their approaches were based on the prospect of inserting CO into the ruthenacyclopentene intermediate.²³ Mitsudo reported that 1,6-enynes equipped with internal alkynes (attempts with terminal alkynes were unsuccessful) and monosubstituted, 1,1-disubstituted, or 1,2-disubstituted alkenes undergo cyclization to bicyclooctenones in moderate yields (Table 4). The reactions

Table 4. $\text{Ru}_3(\text{CO})_{12}$ -catalyzed Pauson-Khand reactions

Substrate	Product	% Yield
		89
		90
		41 (5.6 : 1)

were conducted in the presence of 2 mol % $\text{Ru}_3(\text{CO})_{12}$ under CO (15 atm) in amide solvents at elevated temperatures. Murai's group reported almost identical conditions with similar substrates. Neither group reported intermolecular cycloadditions with this catalyst. Other ruthenium complexes were tried with little success. For example, $[\text{RuCl}(\text{CO})_3]_2$ provided byproducts derived from β -hydride elimination, whereas $(\text{Cp}^*)\text{Ru}(\text{COD})\text{Cl}$

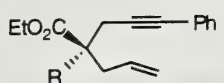
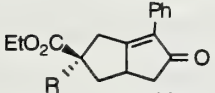
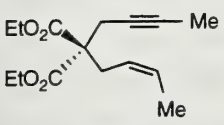
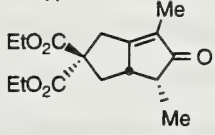
failed to catalyze the reaction (Cp^* = pentamethylcyclopentadienyl). Both groups tentatively proposed a mechanism in which the key intermediate is a ruthenacyclopentene, with Murai citing Pearson's iron carbonyl promoted reaction mechanism.²⁰

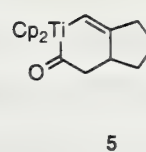
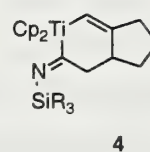
TITANIUM-BASED CATALYTIC SYSTEMS

$\text{Cp}_2\text{Ti}(\text{CO})_2$ Catalysis

Buchwald and Hicks²⁵ recently developed the first successful catalytic PKR based on titanium. Cyclopentenones were formed in good yields under relatively low CO pressures (~1 atm) in the presence of catalytic amounts of $\text{Cp}_2\text{Ti}(\text{CO})_2$. This method also extended the scope of the catalytic PKR to cyclic enynes and added ketones and nitriles to the list of compatible functional groups (Table 5). However, the reactions employing acyclic 1,2-disubstituted olefins were highly dependent on CO pressure, and significant isomerization occurred during the cyclization of highly enriched Z-isomers. The pressure dependence was attributed to the competition between CO and the olefin for titanium, since lowering the CO pressure allowed the reactions to proceed to completion.²⁵

Table 5. Catalytic Pauson-Khand reaction with $\text{Cp}_2\text{Ti}(\text{CO})_2$.

Substrate	Product	$\text{Cp}_2\text{Ti}(\text{CO})_2$ mol %	% Yield
		R = CO_2Et , 5 R = CN , 7.5 R = COMe , 7.5	95 75 (1:1) 93 (1:1)
		20	58



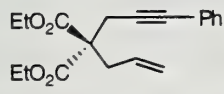
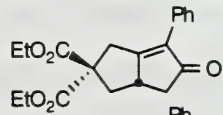

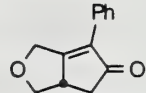
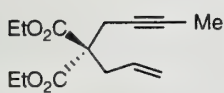
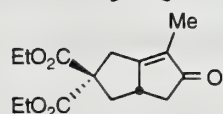
The mechanistic details of this process have not been resolved. Previously, it was shown that the conversion of enynes to iminocyclopentenones with catalytic $\text{Cp}_2\text{Ti}(\text{PMe}_3)_2$ proceeded through metallacycle **4**.²⁶ Thus, it was initially assumed that the reaction with $\text{Cp}_2\text{Ti}(\text{CO})_2$ proceeded through the analogous metallacycle **5**. However, **5** has been eliminated as an intermediate, since striking differences in stereochemical behavior between the two systems has been observed with chiral enynes.²⁶

(S,S)-(EBTHI)Ti(CO)₂ Catalysis

Buchwald and Hicks²⁷ have reported the first catalytic asymmetric PKR utilizing (S,S)-(EBTHI)Ti(CO)₂ (**6**), generated *in situ* from (S,S)-(EBTHI)TiMe₂, where EBTHI = ethylenebis(tetrahydroindene). This catalyst demonstrated functional group compatibility comparable to the $\text{Cp}_2\text{Ti}(\text{CO})_2$ system and effected the cyclization of a variety of 1,6-enynes with good to excellent enantioselectivity. Enynes with geminally disubstituted backbones required less catalyst, a manifestation of the Thorpe-Ingold effect⁴ (Table 6). Catalyst efficiency was dependent on CO pressure, and no intermolecular cycloadditions were reported.

The observed enantioselectivity was attributed to steric interactions between enyne backbone and the EBTHI ligand.²⁷

Table 6. (S,S)-(EBTHI)Ti(CO)₂-catalyzed PKR.

Substrate	Product	(S,S) Cat mol %	ee(%)	% Yield
		7.5	94	92
		20	96	85
		5	87	90

CONCLUSIONS

Significant improvements in efficiency, substrate variability, and stereochemical control have been made in the catalytic Pauson-Khand reaction. Conventional cobalt-based methods have been largely superseded by modified cobalt catalysts. Ruthenium and titanium are useful alternatives to cobalt, demonstrating increased functional group compatibility and potential for asymmetric catalysis; however, these methods have not effected the corresponding intermolecular cycloadditions. Future studies should focus on (1) elucidating the mechanistic details of these processes, (2) effecting asymmetric cycloadditions with chiral cobalt complexes derived from (indenyl)Co(COD), (3) accomplishing ruthenium- and titanium-catalyzed intermolecular cycloadditions, and (4) exploring ligand design in the ruthenium and titanium systems.

REFERENCES

1. Khand, I. U.; Knox, G. R.; Pauson, P. L.; Watts, W. E.; Foreman, M. I. *J. Chem. Soc. Perkin Trans. 1* **1973**, 977.
2. Schore, N. E. *Chem. Rev.* **1988**, 88, 1081.
3. Schore, N. E. *Org. React.* **1991**, 40, 1.
4. Schore, N. E. In *Comprehensive Organometallic Chemistry II*; Abel, E. W.; Stone, F. G. A.; Wilkinson, G., Eds.; Pergamon: Kidlington, 1995; Vol. 12, p 703.
5. Ojima, I.; Tzamarioudaki, M.; Li, Z.; Donovan, R. J. *Chem. Rev.* **1996**, 96, 635.
6. Rautenstrauch, V.; Mégard, P.; Conesa, J.; Küster, W. *Angew. Chem., Int. Ed. Engl.* **1990**, 29, 1413.
7. (a) Magnus, P.; Principe, L. M. *Tetrahedron Lett.* **1985**, 26, 4851. (b) La Belle, B. E.; Knudsen, M. J.; Olmstead, M. M.; Hope, H.; Yanuck, M. D.; Schore, N. E. *J. Org. Chem.* **1985**, 50, 5215. (c) Magnus, P.; Exon, C.; Albaugh-Robertson, P. *Tetrahedron* **1985**, 41, 5861.
8. Billington, D. C. *Tetrahedron Lett.* **1983**, 24, 2905.
9. Billington, D. C.; Kerr, W. J.; Pauson, P. L.; Farnocchi, C. F. *J. Organomet. Chem.* **1988**, 356, 213.
10. Magnus, P.; Principe, L. M.; Slater, M. J. *J. Org. Chem.* **1987**, 52, 1483.
11. Sweany, R. L.; Brown, T. L. *Inorg. Chem.* **1977**, 16, 421.
12. Cotton, F. A.; Wilkinson, G. *Advanced Inorganic Chemistry*; Wiley-Interscience: New York, 1988; p 1047.
13. Pagenkopf, B. L.; Livinghouse, T. *J. Am. Chem. Soc.* **1996**, 118, 2285.
14. Jeong, N.; Hwang, S. H.; Lee, Y.; Chung, Y. K. *J. Am. Chem. Soc.* **1994**, 116, 3159.
15. Lee, N. Y.; Chung, Y. K. *Tetrahedron Lett.* **1996**, 37, 3145.
16. Lee, B. Y.; Chung, Y. K.; Jeong, N.; Lee, Y.; Hwang, S. H. *J. Am. Chem. Soc.* **1994**, 116, 8793.
17. Negishi, E.; Holmes, S. J.; Tour, J. M.; Miller, J. A.; Cederbaum, R. E.; Swanson, D. R.; Takahashi, T. *J. Am. Chem. Soc.* **1989**, 111, 3336.
18. Kent, J. L.; Wan, H.; Brummond, K. M. *Tetrahedron Lett.* **1995**, 36, 2407.
19. Hoyer, T. R.; Suriano, J. A. *J. Am. Chem. Soc.* **1993**, 115, 1154.
20. Pearson, A. J.; Cubbert, R. A. *Organometallics* **1994**, 13, 1656.
21. Pages, L.; Llebaria, A.; Camps, F.; Molins, E.; Miravittles, C.; Moretó, J. M. *J. Am. Chem. Soc.* **1992**, 114, 10449.
22. Mitsudo, T.; Naruse, H.; Kondo, T.; Ozaki, T.; Watanabe, Y. *Angew. Chem., Int. Ed. Engl.* **1994**, 33, 580.
23. Kondo, T.; Suzuki, N.; Okada, T.; Mitsudo, T. *J. Am. Chem. Soc.* **1997**, 119, 6187.
24. Morimoto, T.; Chatani, N.; Fukumoto, Y.; Murai, S. *J. Org. Chem.* **1997**, 62, 3762.
25. Hicks, F. A.; Kablaoui, N. M.; Buchwald, S. L. *J. Am. Chem. Soc.* **1996**, 118, 9450.
26. Berk, S. C.; Grossman, R. B.; Buchwald, S. L. *J. Am. Chem. Soc.* **1993**, 115, 4912.
27. Hicks, F. A.; Buchwald, S. L. *J. Am. Chem. Soc.* **1996**, 118, 11688.

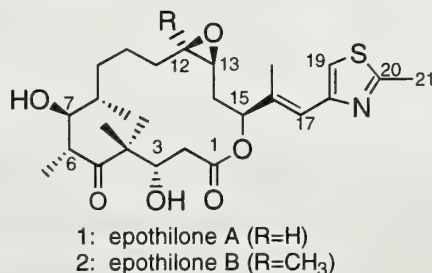
SYNTHETIC APPROACHES TO EPOTHILONES

Reported by A. Dawn Bounds

October 6, 1997

INTRODUCTION

Epothilones A and B were isolated from myxobacteria *Sorangium cellulosum*, and their structure and preferred conformation were elucidated by X-ray crystallographic and spectroscopic analysis in 1996. Both compounds show antifungal activity and are active against breast and colon cancer cell lines. Epothilone, like paclitaxel (Taxol), effects cytotoxicity by binding and stabilizing microtubules.



Beyond its interesting chemotherapeutic activity, epothilone's structure presents intriguing synthetic challenges. The 16-membered macrolactone contains seven stereogenic centers and two elements of geometric isomerism.¹ Of particular interest are the *gem* dimethyl moiety at C4, the epoxide arising from a *Z* olefin, and the stereo and regioselective requirements for formation of this epoxide.²

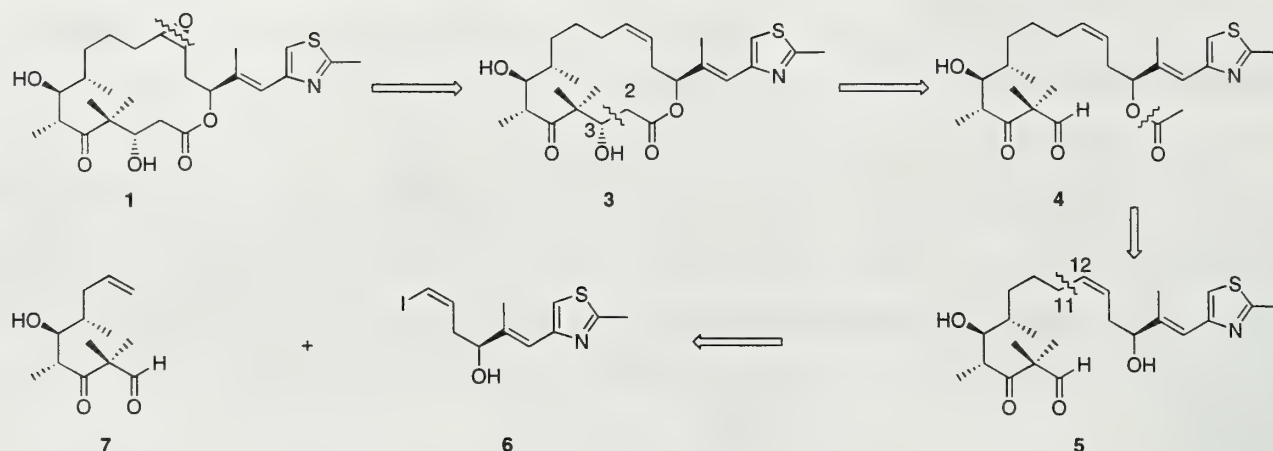
Because of its therapeutic potential and complex structure, it is not surprising that the total synthesis of epothilone has received much attention. Danishefsky and coworkers have recently completed the total syntheses of both epothilones A and B by macroaldolization,³ while Nicolaou et al. have synthesized epothilones A and B by macrolactonization.⁴ Schinzer, Nicolaou, and Danishefsky have each synthesized epothilone A using an olefin metathesis route.^{1,5,6} In addition, several groups are currently working on various fragments of the molecule.⁷⁻⁹

RETROSYNTHETIC ANALYSIS

The first of Danishefsky's two syntheses (Scheme 1) entailed three key disconnections. The first simplification involves removal of the epoxide. Fragment 4 arises from subsequent scission of the C2/C3 bond of macrocycle 3, which might be formed via a macroaldol. The final disconnection of 5, between C11 and C12, is projected to occur via a retro-Suzuki coupling reaction, leads back to fragments 6 and 7.¹⁰

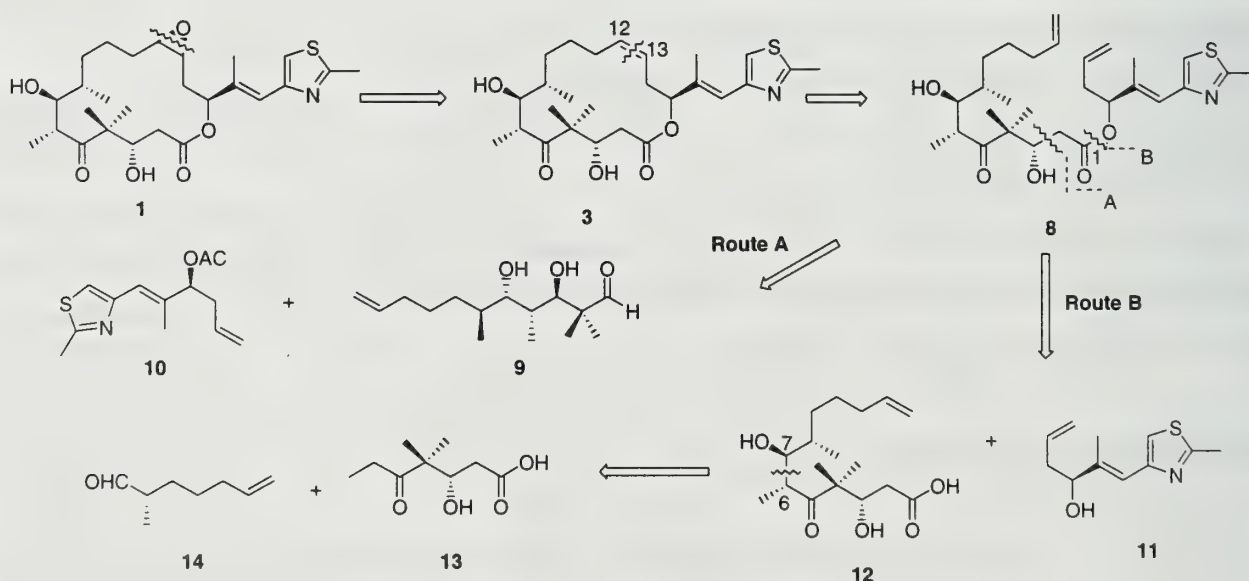
Copyright © 1997 by A. Dawn Bounds

Scheme 1



Another retrosynthetic approach devised by Danishefsky et al. is depicted in Scheme 2 (Route A). Following removal of the epoxide, a scission of the C12/C13 double bond of **3** leads back to acyclic fragment **8**. Cyclization of this precursor should be possible via an olefin metathesis reaction. Fragments **9** and **10** arise from subsequent disconnection of the C2/C3 bond via a retro-aldol (Route A).³

Scheme 2

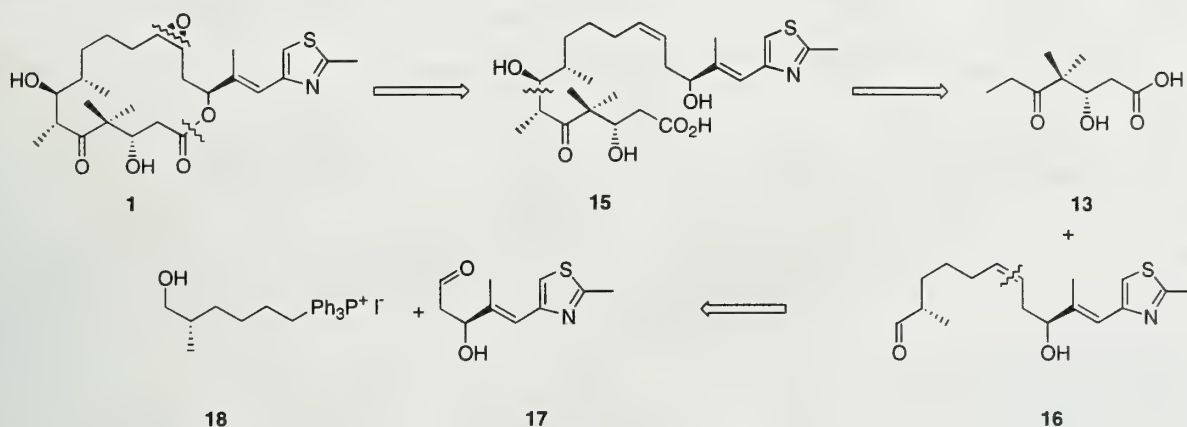


In a similar manner, Nicolaou et al. developed a retrosynthetic strategy toward epothilone utilizing olefin metathesis (Scheme 2). Removal of the epoxide and disconnection of the indicated carbon-carbon bond in **3** by retro-metathesis lead back to precursor **8**. Disassembly of **8** (Route B) at the

C-O ester bond generates fragments **11** and **12**.¹ Scission of the indicated C6-C7 bond via a retro-aldol of **12** leads back to a ketone component **13** and an aldehyde component **14**.

In an alternate approach (Scheme 3), Nicolaou et al. propose the initial disconnection at the indicated C-O bond via a retro-macrolactonization to generate the acyclic precursor **15**, the further simplification of which would potentially give **13** and **16**. Finally, scission of **16** at the double bond by a retro-Wittig reaction was conceived to give fragments **17** and **18**.⁴

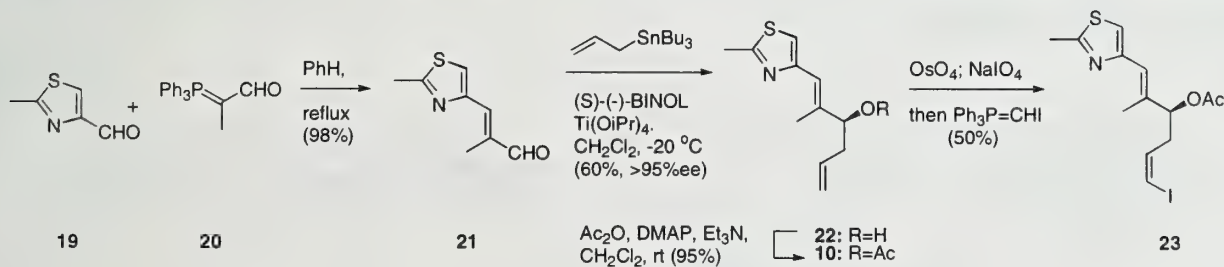
Scheme 3



SYNTHETIC APPROACHES

The total synthesis of epothilone A proposed by Danishefsky (Scheme 1) necessitated the design and synthesis of two key components, vinyl iodide **23** and acetal **33**. In pursuit of the thiazole fragment (**23**), which would form the C12-C21 unit of epothilone (Scheme 4), heterocyclic aldehyde **19** was homologated by Wittig methodology to give thiazole enal **21**.² Catalytic asymmetric allylation of **21** gave diene **22**, and the ensuing acylation provided ester **10**. Oxidative cleavage of the primary alkene in **10** was followed by a Wittig to give vinyl iodide **23**.⁶

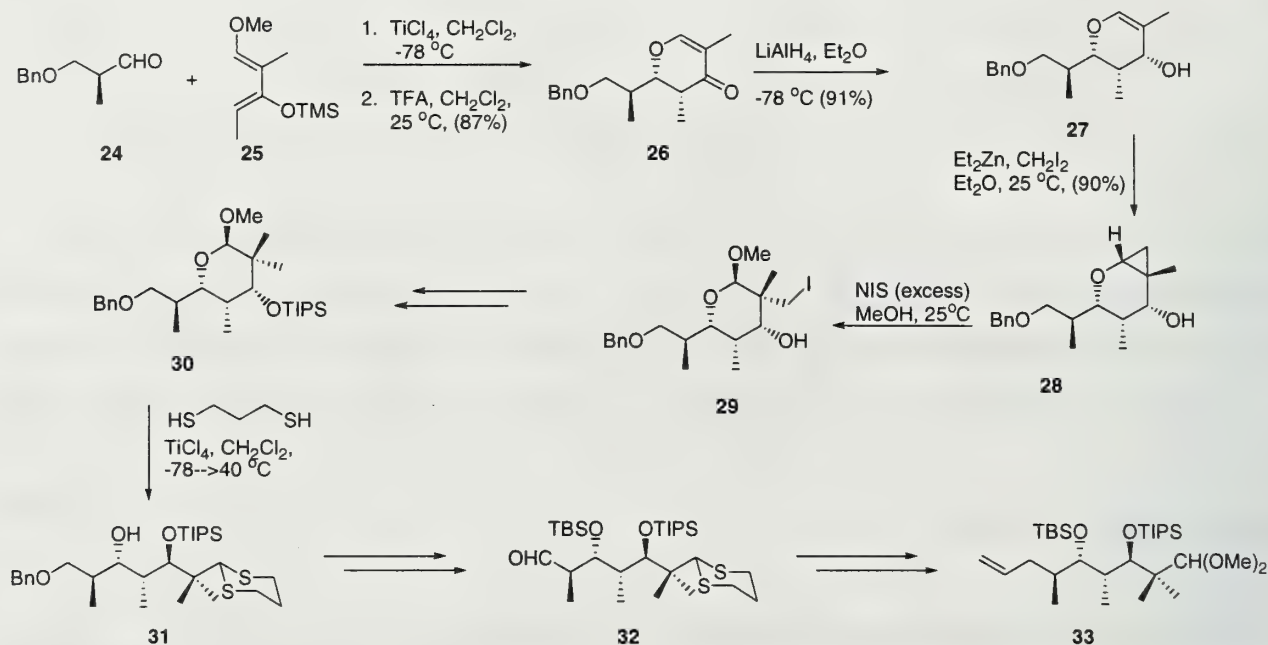
Scheme 4



Key fragment **33**, the source of the C2-C11 portion of **1** (Scheme 5), was synthesized beginning with a chelation-controlled cyclocondensation of **24** and **25** to give dihydropyrone **26**. After reduction to

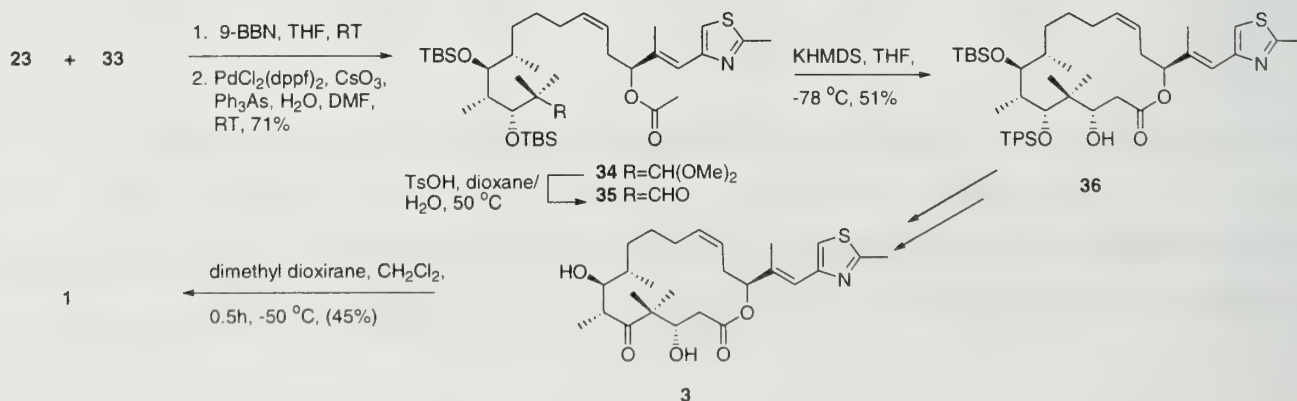
glycal **27**, Simmons-Smith cyclopropanation gave cyclopropane **28**. Oxidative ring-opening with *N*-iodosuccinimide produced the iodomethyl glycoside **29**, and various functional group manipulations provided glycoside **30** bearing the necessary *gem*-dimethyl moiety.¹¹ Protection of the aldehyde as the dithiane, followed by cleavage of the glycosidic bond lead to intermediate **31**. Further manipulations yielded aldehyde **32**, which, after removal of the dithiane moiety, was transformed to acetal **33**.¹⁰

Scheme 5



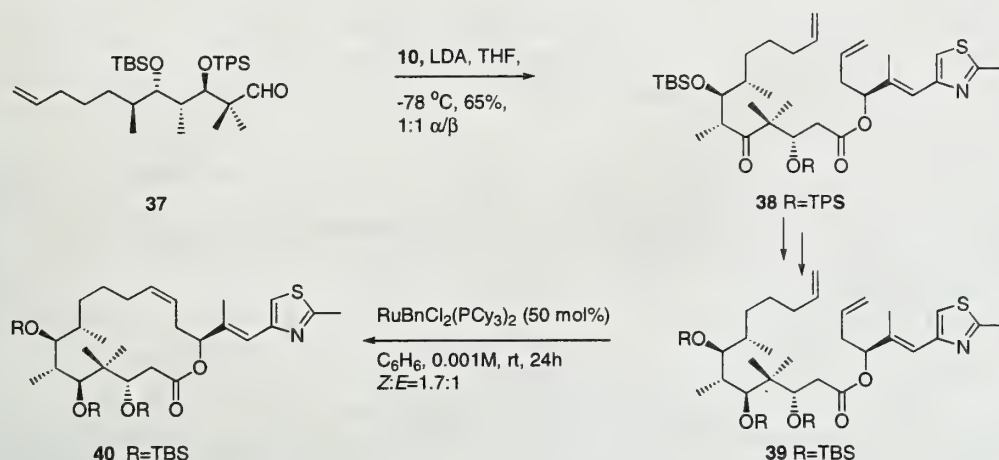
With the key components in hand, the assembly of the complete skeleton began via hydroboration of fragment **33** with 9-BBN and subsequent coupling with iodoalkene **23**, forming aldehyde **35** after acetal cleavage. The final strategic connection was accomplished by a stereoselective macroaldol reaction, which gave predominantly the desired (*S*) alcohol **36**. Cyclic precursor **36** was selectively deprotected and oxidized at C5 to the ketone. Complete deprotection and epoxidation gave epothilone A.¹⁰ The synthesis required twenty-five steps overall. The longest linear sequence was twenty steps from aldehyde **19** with a yield of 2.2%

Scheme 6



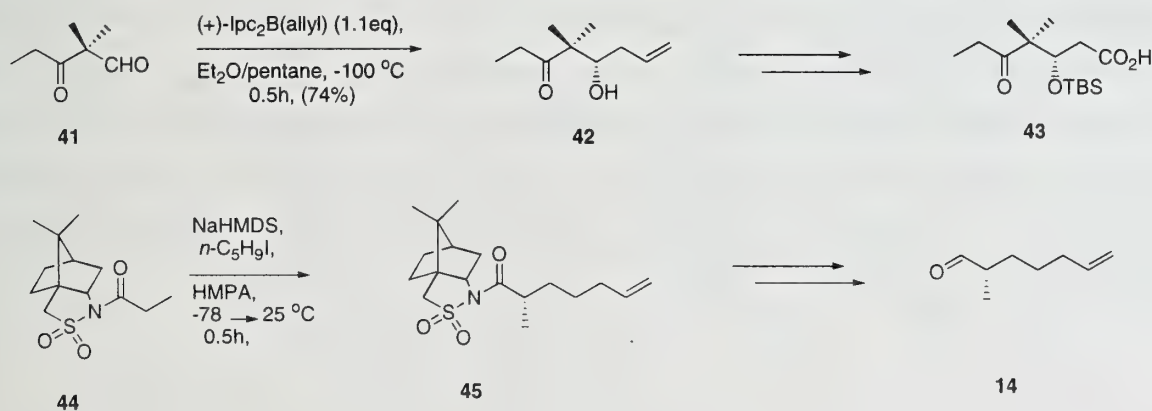
An alternative approach explored by Danishefsky et al. utilized closely related precursors, but reversed the order of the coupling and ring-forming steps. The aldehyde **37** first underwent aldol addition with ester **10** to give a 1:1 mixture of C3 epimers. Subsequent ring closure was accomplished by olefin metathesis using catalytic $\text{RuBnCl}_2(\text{Pcy}_3)_2$, which produced the macrolide as a 1.7:1 mixture of Z:E isomers. Precursor **40** was deprotected and epoxidized in the same manner demonstrated in Scheme 6.³ The synthesis required twenty-five steps overall. The longest linear sequence was twenty steps and provided **1** in 4.1% yield from **22**.

Scheme 7



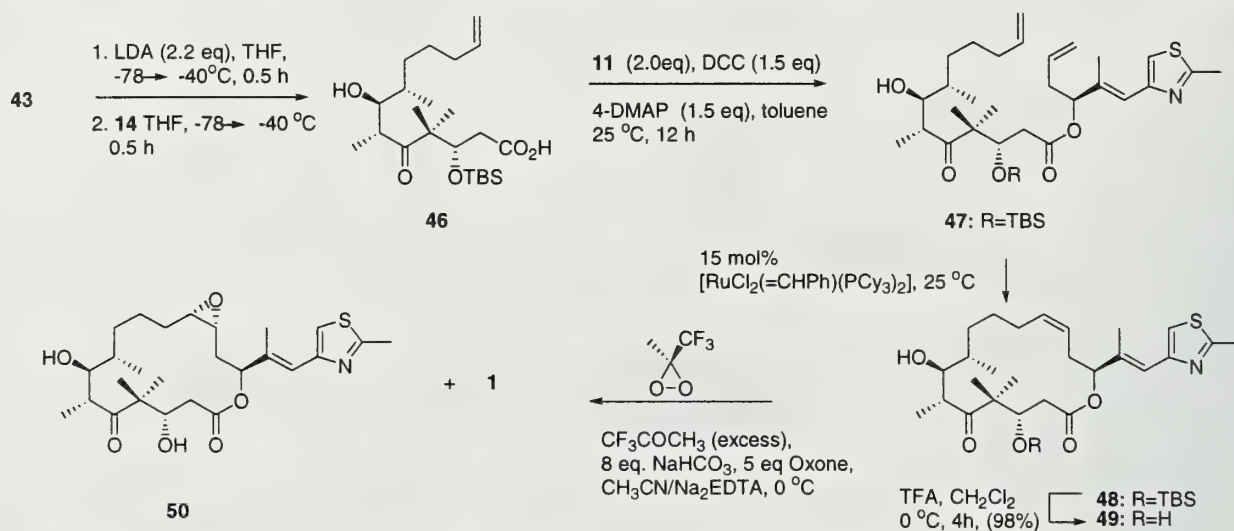
Nicolaou and coworkers also developed a three-component convergent synthesis based on olefin metathesis (Scheme 8). Ketoaldehyde **41**, synthesized in several steps from propionyl chloride, was allylated with (+)- $\text{Ipc}_2\text{B}(\text{allyl})$ to give **42**. Further manipulation provided the first component, protected keto acid **43**. The second key component, the unsaturated alcohol **11** (Scheme 2), was also obtained by asymmetric allylation from the same aldehyde used in Danishefsky's synthesis (Scheme 4) (**31**). Oppolzer's acylated sultam was alkylated and carried through a number of manipulations to give the third key fragment, aldehyde **14**.¹

Scheme 8



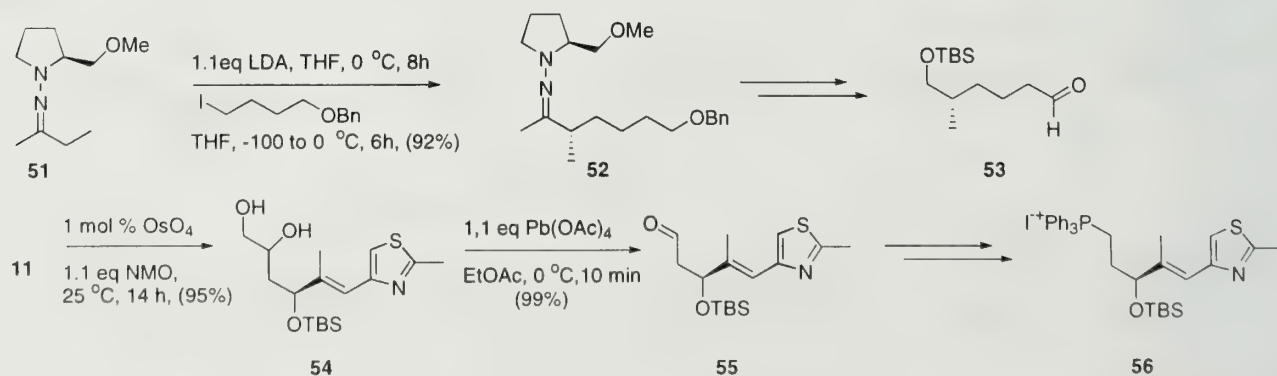
To complete the synthesis, aldehyde **14** and ketoacid **43** were joined via aldolization to provide a 2:1 mixture of **46** and the 6*S*,7*R* diastereomer. Esterification with alcohol **11** gave acyclic precursor **47**, which was subsequently cyclized with $[\text{RuCl}_2(=\text{CHPh})(\text{Pcy}_3)_2]$ to give **48** as a 1.4:1 *Z:E* mixture of olefins. Deprotection followed by epoxidation with methyl(trifluoromethyl)dioxirane gave a 62% yield of **1**, with a small percentage of the epoxide epimer **50**.¹ The synthesis of **1** required nine linear steps (fifteen total) and gave a 4.6% yield from aldehyde **19**.

Scheme 9



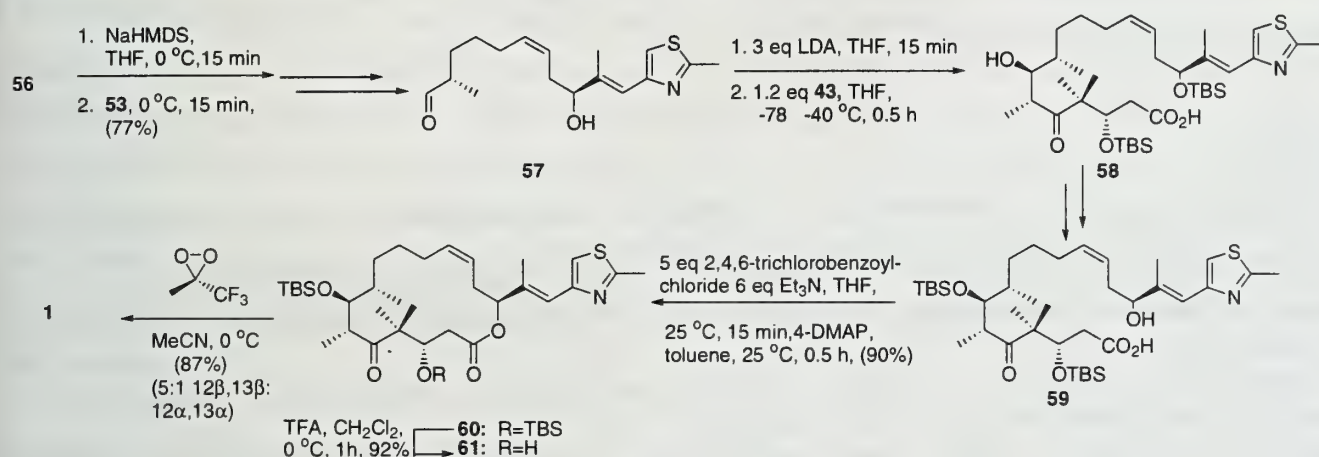
Nicolaou devised another approach that required the union of three key pieces in the same locations as the olefin metathesis approach. The components, however, were modified to accommodate the different methodology. Propionaldehyde was asymmetrically alkylated via its SAMP derivative **51** to give **52** in >98% de. Several manipulations provided **53**, the analog of **14**. Thiazole fragment **56** was synthesized beginning with **11**, which was dihydroxylated nonstereoselectively to give **54**. Subsequent cleavage of the diol epimers with $\text{Pb}(\text{OAc})_4$ gave aldehyde **55**, which was transformed into phosphonium salt **56**.⁴

Scheme 10



Key fragments **53** and **56** were combined (Scheme 11) via a Wittig reaction in the presence of NaHMDS, followed by several steps involving protecting group interchanges to give aldehyde **57** with *Z:E* = 9:1. An aldol condensation with fragment **43** followed, giving **58** as a 1:1 mixture of diastereomers (**58:6*S*,7*R*-diastereomer). Several protecting group manipulations, followed by ring closure of hydroxyacid **59** under Yamaguchi conditions, gave macrolactone **60**. Deprotection of the remaining hydroxyl groups followed by regio and stereoselective epoxidation with methyl(trifluoromethyl)dioxirane afforded **1**.⁴ The synthesis of **1** was completed by Nicolaou and coworkers with a yield of 5.05%. The macrolactone route required thirty-one total steps; the longest linear sequence contained seventeen steps from **43**.**

Scheme 11



CONCLUSION

Danishefsky presents two approaches to epothilone A which are the more linear of the routes presented above. Each of these syntheses employs an aldol reaction to create the C2/C3 bond and give the required (*S*) stereochemistry at C3. The macroaldol version shows moderate selectivity and yield, whereas the standard aldol used in the olefin metathesis approach shows no selectivity and proceeds in a low yield.^{6,10} Despite the noted selectivity problems, however, Danishefsky has developed an innovative approach. The dihydropyrone system, while not a new concept,¹¹ is certainly an elegant methodology for creation of the C6-C8 stereocenters. In addition, ring closure via a macroaldol has been a virtually unexplored application of the aldol reaction. Its use in this synthesis contributes to the overall uniqueness of Danishefsky's synthesis.

Nicolaou, on the other hand, has developed two highly convergent approaches, olefin metathesis and macrolactonization, each of which provide epothilone A in good yields.^{1,4} While Nicolaou's macrolactonization approach requires a high number of total steps, the olefin metathesis approach is efficient, requiring only fifteen total steps. While this synthesis suffers from difficulties in the stereoselective formation of the C6/C7 bond,¹ it is still the most efficient of the methodologies reported thus far. Nicolaou has also adapted this approach to solid phase synthesis.¹² Despite the large excesses of reagents needed, this methodology shows promise as a viable approach to the synthesis of epothilone and analogs of possible medicinal interest.

None of the total syntheses reported to date are as efficient as fermentation for the production of epothilone.⁸ However, they have employed interesting, if not always practical, methodologies to overcome the synthetic challenges inherent in epothilone. In addition, these methodologies do provide avenues for the synthesis of a variety of analogs, including epothilone B, which is an advantage that fermentation does not readily offer.

References

- 1) Nicolaou, K.C.; He, Y.; Vourloumis, D.; Vallberg, H.; Roschangar, F.; Sarabia, F.; Ninkovic, S.; Yang, Z.; Trujillo, J.I. *J. Am. Chem. Soc.* 1997, *119*, 7960-7973.
- 2) Meng, D.; Sorenson, E.; Bertinato, P.; Danishefsky, S. *J. Org. Chem.* 1996, *61*, 7998-7999.
- 3) Meng, D.; Bertinato, P.; Balog, A.; Su, D.; Kamenecka, T.; Sorensen, E.; Danishefsky, S. *Submitted for Publication*,
- 4) Nicolaou, K.C.; Ninkovic, S.; Sarabia, F.; Vourloumis, D.; He, Y.; Vallberg, H.; Finlay, M.R.V.; Yang, Z. *J. Am. Chem. Soc.* 1997, *119*, 7974-7991.
- 5) Schinzer, D.; Limberg, A.; Bohm, O.M.; Cordes, M. *Angew. Chem. Int. Ed. Engl.* 1997, *36*, 523-524.
- 6) Meng, D.; Su, D.; Balog, A.; Bertinato, P.; Sorenson, E.; Danishefsky, S.; Zheng, Y.; Chou, T.; He, L.; Horwitz, S. *J. Am. Chem. Soc.* 1997, *119*, 2733-2734.
- 7) Taylor, R.; Haley, J. 2061-2064 1997,
- 8) Wessjohann, L. *Angew. Chem. Int. Ed. Engl.* 1997, *36*, 715-718.
- 9) Gabriel, T.; Wessjohann, L. *Tetrahedron Lett.* 1997, *38*, 1363-1366.
- 10) Balog, A.; Meng, D.; Kamenecka, T.; Bertinato, D.; Sorenson, E.; Danishefsky, S. *Angew. Chem. Int. Ed. Engl.* 1996, *35*, 2801-2803.
- 11) Bertinato, P.; Sorenson, E.; Meng, D.; Danishefsky, S. *J. Org. Chem.* 1996, *61*, 8000-8001.
- 12) Nicolaou, K.C.; Winssinger, N.; Pastor, J.; Ninkovic, S.; Sarabia, F.; He, Y.; Vourloumis, D.; Yang, Z.; Li, T.; Glannakakou, P.; Hamel, E. *Nature* 1997, *387*, 268-272.

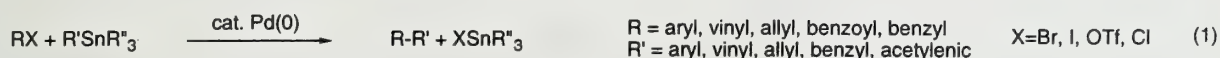
RECENT ADVANCES IN STILLE COUPLING METHODOLOGY: EFFECTS OF LIGANDS AND COPPER(I) SALTS

Reported by Marvin J. Meyers

October 23, 1997

INTRODUCTION

Transition metal couplings to form carbon-carbon bonds are invaluable tools for the construction of complex molecules. In particular, the Stille coupling has demonstrated usefulness because of its compatibility with a wide variety of functional groups. By definition, a Stille coupling is the palladium(0) catalyzed cross-coupling of an organostannane and an unsaturated halide or triflate (eq 1).¹ The scope and usefulness of the Stille coupling has been reviewed.^{1,2}



The organotin precursors containing various functional groups can be prepared by a variety of means and are surprisingly stable to moisture and air.¹ However, increased stability compromises the reactivity of some of these species. While many Stille couplings can be performed under mild conditions, others require long reaction times at temperatures of 100 °C. This may lead to significantly reduced yields due to the instability of substrates, products, or catalysts.³ These problems have been circumvented by two important developments over the past decade: (1) the optimization of the ligands on palladium and (2) the addition of copper(I) salts. This abstract reviews these two improvements and their mechanistic implications.

EFFECT OF LIGAND CHOICE

Typical reaction conditions for this coupling, as originally described by Stille,¹ usually involve $\text{Pd}(\text{PPh}_3)_4$ or $(\text{Ph}_3\text{P})_2\text{PdCl}_2$ (which is reduced in situ) as catalysts, where triphenylphosphine is the ligand for palladium. Farina investigated a wide variety of ligands and showed that tri-2-furylphosphine (TFP) and triphenylarsine were far superior to PPh_3 , exhibiting rate accelerations of up to 1100-fold over PPh_3 , in the coupling of aryl and vinyl stannanes with aryl, vinyl, allyl, and benzoyl halides and triflates.^{3,4} No correlation for ligand steric bulk was seen in the reaction rates; rather, good σ -donors (i.e., PPh_3) were poor at promoting coupling, whereas weak donor ligands (i.e., AsPh_3) were considerably better. The general trend of reaction rates was $\text{AsPh}_3 > \text{TFP} > \text{PPh}_3$. In fact, of all ligands tested, PPh_3 -promoted couplings were consistently the slowest. The mechanistic implications of this trend will be discussed in a later section.

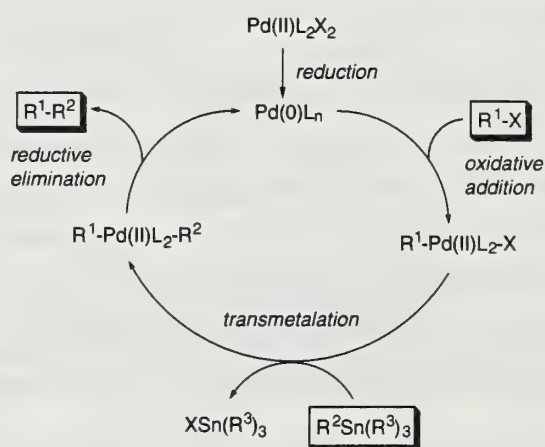
In general, optimal catalysts were generated in situ from tris(dibenzylideneacetone)dipalladium (Pd_2dba_3) utilizing a Pd:L ratio of 1:2 for TFP and 1:4 for AsPh_3 . Vinyl and aryl halides were coupled best in *N*-methyl-2-pyrrolidinone (NMP) with either catalyst, whereas allylic halides were best coupled in

THF with AsPh_3 .³ Triphenylarsine was also found to be the best catalyst for the coupling of aryltriflates with tetramethyltin and vinyltriflates with arylstannanes, a reaction which is very poor under typical Stille conditions.⁴

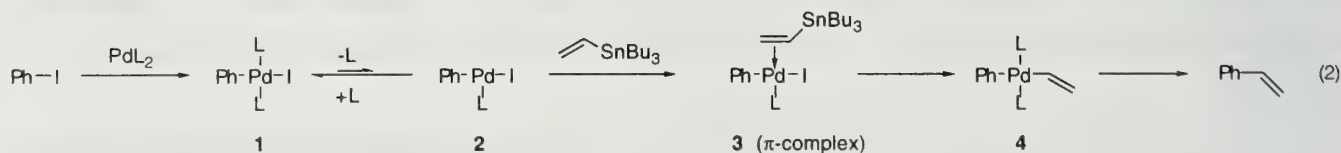
Mechanism

The generally accepted catalytic cycle for the Stille coupling is depicted in Scheme 1. Oxidative addition requires an electron rich $\text{Pd}(0)$, whereas transmetalation requires an electron deficient $\text{Pd}(\text{II})$ to permit nucleophilic attack by the stannane. Both processes require prior ligand dissociation. However, strong σ -donor ligands stabilize the catalytic $\text{Pd}(0)$ species, whereas weak donor ligands allow decomposition of the catalyst. Therefore, intermediate σ -donors should be the best ligands in this cycle.³ This explains the dramatic rate differences between PPh_3 , TFP, and AsPh_3 .

Scheme 1



^{31}P NMR studies were conducted to examine the mechanistic implications of the ligand effect.³ When Pd_2dba_3 (0.5 eq.) and PPh_3 (4 eq.) were added to iodobenzene, two signals corresponding to complex **1** ($\text{L}=\text{PPh}_3$) and the free PPh_3 were observed. The equivalent complex was observed for TFP, although the formation of the complex was considerably slower due to the intermediate donor character of this phosphine. Addition of PPh_3 to **1** ($\text{L}=\text{TFP}$) showed an immediate consumption of the Pd complex to form complex **1** ($\text{L}=\text{PPh}_3$) plus free TFP, demonstrating the stronger affinity of PPh_3 for Pd. It was found that the presence of excess ligand inhibited reaction rates. This effect was greatest for the ligands with the slowest reaction rates (i.e. PPh_3), supporting ligand dissociation as important for the transmetalation (eq 2).



It was proposed that a π -complex (**3**) forms between **2** and the organostannane after the required ligand dissociation.³ This is supported by the observation of very little ligand effect (<1 order of magnitude) in the coupling of aryl triflates with tetramethyltin, which cannot form the suggested π -

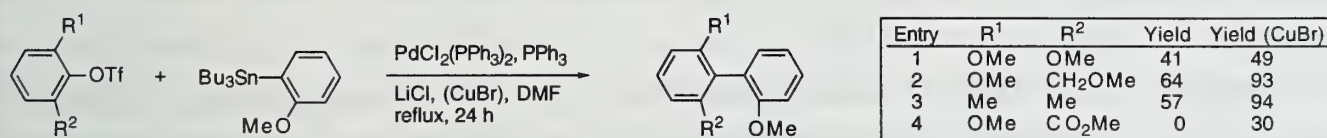
complex. Weak donors, such as AsPh_3 and TFP, will allow facile dissociation leading to formation of the π -complex, whereas good donors will strengthen the $\text{Pd}-\pi$ bond by favoring the back donation of the metal into the olefin π^* orbital.⁵ Thus, the rate enhancing ability of ligand is dependent on the strength, or σ -donor ability, of the $\text{Pd}-\text{L}$ bond.

THE "COPPER EFFECT"

Another important improvement in the Stille coupling was the introduction of co-catalytic Cu(I) salts by Liebeskind.⁶ Conventional Stille conditions required high temperatures for the arylation of stannylcyclobutenediones to achieve only 70% yields. However, modified conditions utilizing CuI in DMF allowed 99% conversion at room temperature. The addition of a second metal salt in cross-coupling reactions to improve rates and selectivity is not new.⁷ In fact, it is well known that alkynylation of aryl and vinyl halides is co-catalyzed by Pd and CuI through a copper acetylide species.⁸ However, this was the first example for a Stille cross-coupling and presents some interesting mechanistic implications. This system has been expanded to allow the use of inexpensive Pd/C (0.5%) in conjunction with CuI and 20% AsPh_3 as an efficient catalytic system.⁹ Stang has expanded the scope of Stille electrophiles to include alkenyl(phenyl)iodonium triflates via co-catalytic CuI .¹⁰ In general, the "copper effect" has allowed increased reaction rates and yields, milder reaction conditions, and increased chemo- and stereoselectivity. This will be briefly illustrated in the examples to follow.

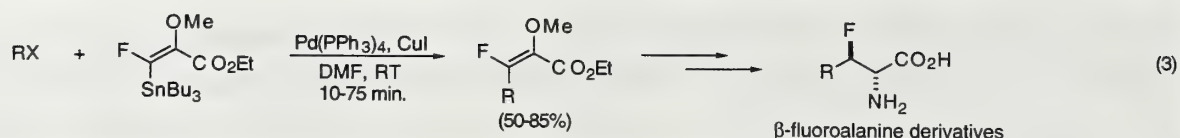
Ortho-substituted biaryl compounds derived from the Stille coupling of highly hindered, electron-rich aryl triflates are obtained in very poor yields in the absence of copper (Scheme 2). However, in the presence of catalytic CuBr or CuI , reaction efficiencies were improved considerably.¹¹ Stannylindoles and heteroarylstannanes have also been shown to couple to aryl iodides in the presence of catalytic CuI in good yields.^{12,13}

Scheme 2



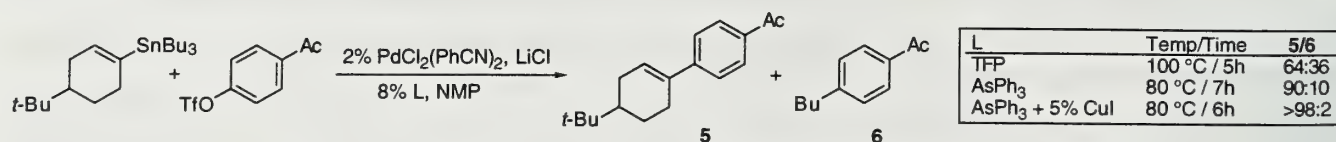
The coupling of aryl triflates and stannylallenes to generate arylallenes using DMF, TFP and 10% CuI doubled yields (20-70%) over Pd -only systems.¹⁴ A route from α,β -unsaturated ketones via the easily generated α -iodoenones, allowed the efficient synthesis of aryl and vinyl α -substituted enones in 53-95% yields using CuI , AsPh_3 , and NMP.¹⁵ Standard Stille coupling techniques with readily available α -bromo enones generally yielded less than 20% conversion. Coupling of α -stannyl enones was also enhanced with Cu(I) salts.¹⁶

A route to β -fluoro- α -keto acid derivatives was devised in which CuI allowed lower reaction temperatures and minimized homocoupled byproducts that were prevalent in the Pd -only version (eq 3).¹⁷

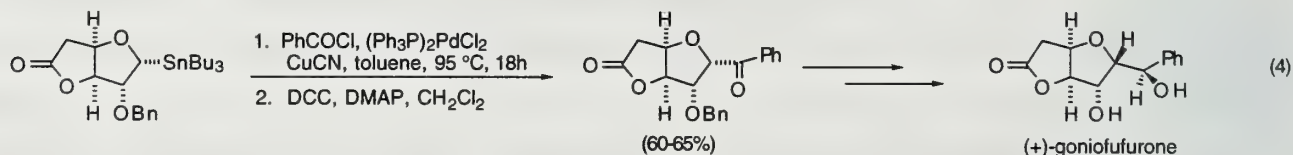


In some cases, Pd-only Stille conditions allow the transfer of an alkyl group from the stannane to compete with desired transfer (Scheme 3). While a ligand change from TFP to AsPh₃ gave substantial improvements, the addition of 5% CuI made the selectivity virtually complete.¹⁸

Scheme 3



Conventional Stille couplings of α -alkoxy- and α -aminostannanes with acyl chlorides is quite sluggish.¹⁹ The addition of CuCN promoted the coupling of these substrates in toluene at 75 °C with 98% retention of stereochemistry, in contrast to Pd-only conditions, where complete inversion of stereochemistry is observed.²⁰ This methodology was utilized in the stereoselective synthesis of (+)-goniofufurone (eq 4).²¹ Pd and Cu were both required to obtain satisfactory yields. Pd(0)/Cu(I) co-catalyzed processes have facilitated the synthesis of a number of other natural products and their derivatives.²²⁻²⁵

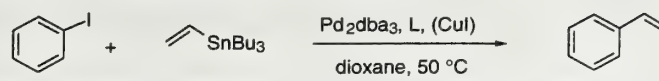


Mechanism

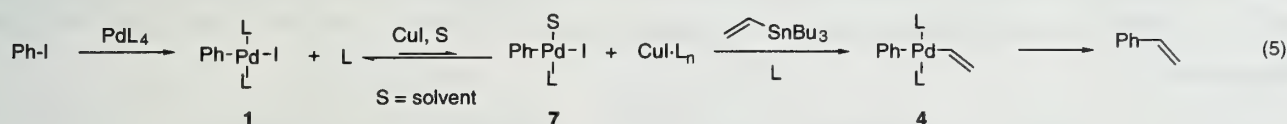
Farina and Liebeskind have conducted detailed investigations of the mechanism of the copper effect and have proposed two different mechanisms based on the solvent and ligands used.²⁶ For Pd/Cu co-catalyzed reactions carried out in ethereal solvents such as dioxane, a predissociation mechanism is proposed. In contrast, in the presence of aprotic polar solvents such as NMP and weak donor ligands, a double transmetalation mechanism is proposed.

Predissociation. The cross-coupling of iodobenzene with tributylvinylstannane in dioxane was examined (Table 1).²⁶ The kinetic studies show a strong dependence on the ratio of ligand to CuI rather than the ratio of Pd to CuI (entries 1-4). The observed reaction rate constant (k_{obs}) was inversely proportional to ligand concentration. Increasing CuI concentration led to an increase in k_{obs} and thus in the overall reaction rate. However, excess CuI resulted in lower yields (entry 3), presumably due to the copper removing ligands from the active Pd catalyst, causing catalyst decomposition. The rate dependence was determined to be first order with respect to the stannane regardless of whether CuI was present.

Table 1. Kinetic Studies of the Copper Effect in Dioxane²⁶

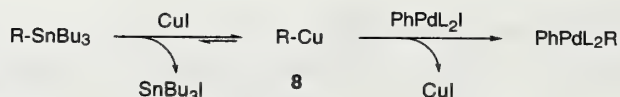
				
entry	ligand	Pd:L:CuI	10 ⁵ k _{obs} (min ⁻¹)	Yield
1	PPh ₃	1:4:0	2.66	85
2	PPh ₃	1:4:2	303	>95
3	PPh ₃	1:4:4	523	45
4	PPh ₃	1:2:2	547	56
5	AsPh ₃	1:4:0	7210	>95
6	AsPh ₃	1:4:2	9640	>95

These results suggest that Cu(I) acts as a phosphine scavenger for free ligand from solution (eq 5). Cu(I) complexes with phosphines are known.²⁷ Based on the earlier investigation of the ligand effect, ligand dissociation is considered to play a key role in the rate determining transmetalation step.²⁶ Since the dissociation of **1** is thermodynamically unfavorable for strong donor ligands such as PPh₃, the complexation of CuI with any free ligand will drive the equilibrium to the more reactive **7**, facilitating transmetalation. Copper had little effect in the presence of weak donors such as AsPh₃ (entries 5-6), since predissociation is readily accomplished without any additives. Further evidence for this mechanism was provided by ³¹P NMR studies.²⁶ When CuI was added to **1** (L=PPh₃), the resonance due to free ligand was broadened substantially, presumably due to complexation with copper.



Double Transmetalation. Studies of the Stille coupling in highly polar solvents with catalytic quantities of CuI presented another possible mechanism. Kinetic studies on the coupling of *p*-iodoanisole with phenyltributylstannane were carried out in NMP.²⁶ In the absence of CuI, first order kinetics were observed; however, non-first order kinetics were observed in the presence of CuI, suggesting the reaction rate was dependent on the concentration of a second species in addition to the stannane. It was observed that increased CuI concentration tended to give increased initial reaction rates and slightly higher yields. When strong donor ligands such as PPh₃ were used, CuI induced a 20-fold increase in the initial reaction rate. More interestingly, in contrast to the dioxane experiments, CuI induced a 5-fold rate increase when AsPh₃ was used. Thus, a different mechanism must be operating to some extent.

¹¹⁹Sn NMR experiments were conducted to test the hypothesis that copper may be transmetalating with the tin reagent (eq 6).²⁶ Phenyl- and vinyltributyltin reagents were added to one equivalent of CuI in the absence of Pd. In THF and dioxane, no reaction was observed. However, in the highly polar solvents NMP and DMF, a majority of the signal from the organostannane was consumed to give a broad peak corresponding to SnBu₃I. These observations strongly suggest that an organocopper species (**8**) is formed in equilibrium with the organostannane; the copper species is favored, assuming that it is stable. The reaction was not affected by the addition of one equivalent of AsPh₃, but was strongly suppressed by PPh₃. The presence of PPh₃ presumably binds the CuI, preventing it from reacting with the tin species.



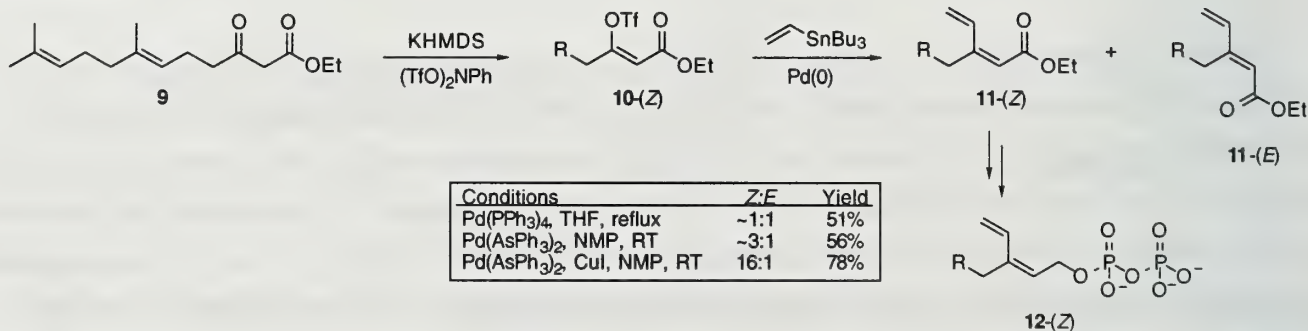
(6)

Thus, the data strongly support the involvement of double transmetalation mechanism for highly polar solvents when weak donor ligands are used. The group transfer selectivity mentioned earlier also supports this interpretation, since the organocopper species would react more quickly than the stannane, minimizing the transfer of the alkyl group.¹⁸ In the presence of PPh_3 , a predissociation mechanism, as described earlier, is more likely, as demonstrated by the NMR experiments.

The generality of these observations was affirmed by the coupling of a variety of stannanes (vinyl, allyl, butyl, furyl, pyridyl, and alkynyl) to iodobenzene. Typical yields were improved by 10-20% and small rate enhancements were consistently observed in the presence of 8 mol% CuI in both NMP and DMF.²⁶

Stereoselectivity. Gibbs has observed substantially enhanced stereoselectivity in olefin substitution via a Pd(0)/CuI -catalyzed route to synthesize 3-substituted farnesyl analogs (Scheme 4).²⁸ Attempts to couple triflate **10-(Z)** with a vinylstannane using conventional Stille techniques led to a 1:1 mixture of *Z* and *E* isomers. Employing AsPh_3 and NMP improved the selectivity of *Z*:*E* to 3:1. The addition of 10 mol% CuI dramatically improved the selectivity (16:1) as well as the overall yield. Couplings were also achieved with tetraalkyl-, acetyltributyl-, and phenyltributylstannanes in 33-77% yields and in very good *Z*:*E* selectivities (all >20:1).²⁹ Coupling of the (*E*)-vinyl triflate with PhSnBu_3 and CuI generated only the (*E*)-phenyl- α,β -unsaturated ester.

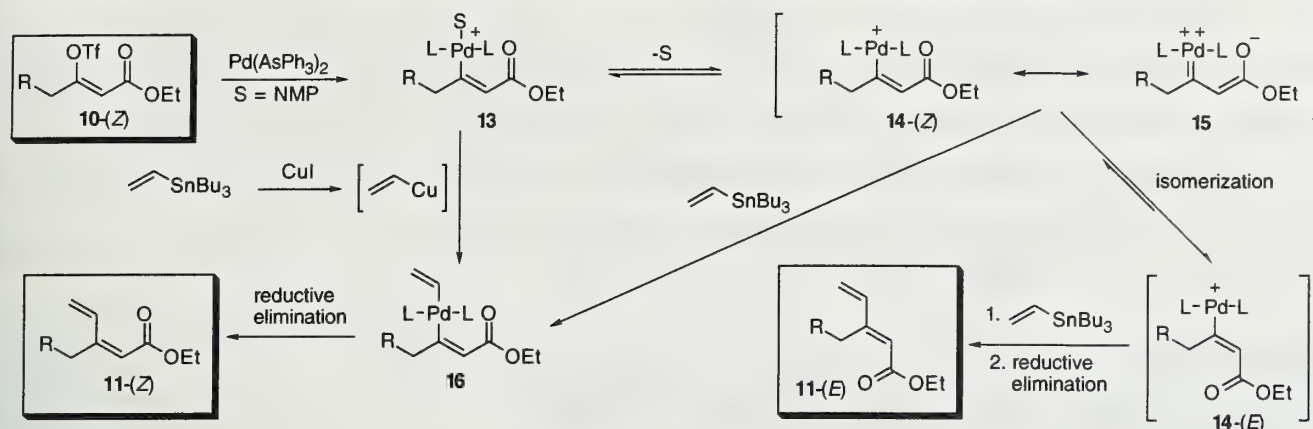
Scheme 4



These results were rationalized by the following mechanism (Scheme 5).²⁸ The oxidative addition of triflate **10-(Z)** to Pd(0) generates vinylpalladium species **13** which may be attacked quickly by the vinyl copper species via a pentacoordinate transition state to give divinylpalladium species **16**. Rapid reductive elimination generates the desired *Z* product. However, in the absence of CuI , the slower reacting vinylstannane may require the dissociation of the coordinating solvent species before it can transmetalate. Vinylpalladium species **14-(Z)** may be in resonance with palladium carbene species **15**. Similar Pd-carbenes have been proposed³⁰ and some evidence has been provided for their existence.³¹ This resonance character would weaken the α,β -bond and allow isomerization to the (*E*)-vinylpalladium species **14-(E)**. Transmetalation and reductive elimination would generate the *E* product. This proposal is

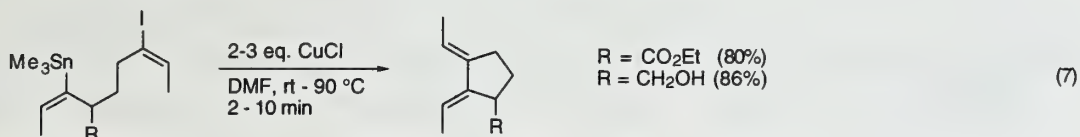
supported by the observation that the (*Z*)-vinyltriflate from acetoacetate coupled with an arylstannane yielded the thermodynamically more stable (*E*)-vinylarene (19:1) in the absence of CuI.⁴

Scheme 5



COPPER-MEDIATED STILLE-TYPE COUPLINGS WITHOUT PALLADIUM

Several reports of Stille-type couplings mediated by copper(I) salts without Pd catalyst have been reported recently. Piers has reported a rapid intramolecular coupling of vinyl iodides and stannanes using 2-3 equiv. of CuCl in good to excellent yields (eq 7).³² This methodology was highly stereospecific and demonstrated significant functional group tolerance.



Intermolecular couplings were accomplished by Liebeskind using 1.5 equiv copper(I) thiophene-2-carboxylate (CuTC).³³ CuTC was found to be the best Cu(I) reagent and efficiently caused the rapid coupling (5-30 min) of aryl, heteroaryl, and vinyl stannanes with vinyl iodides in NMP at 0 °C to room temperature.³³ In contrast to Stille couplings, most aryl iodides and bromides did not react under these conditions, making this a valuable complement as well as an alternative for Stille couplings. Paterson applied this new method in a double Stille cross-coupling cyclodimerization model reaction for the synthesis of macrolide elaiophyllin with good success.³⁴

Takeda was able to employ substoichiometric amounts of CuI to promote the allylation of vinylstannanes which exhibited poor yields even in Pd/Cu co-catalyzed systems.³⁵ While catalytic amounts of CuI generated the desired products in moderate yields, the use of 0.5-1.0 equivalents gave considerably better yields. Falck was able to couple alkyl- α -heterostannanes with a variety of electrophiles using 8 mol% of CuCN in fair yields.³⁶ Yields were substantially improved with the inclusion of a proximal sulfur atom in the substrates. The sulfur was proposed to stabilize the copper intermediate. Kang has also reported catalytic couplings with CuI and one equivalent of NaCl to keep the SnBu_3I from participating in the reversible transmetalation.³⁷ Caution must be exercised when reviewing

claims of Cu(I)-only catalyzed couplings, as it has been reported that traces of Pd metal embedded in stirbars are sufficient to catalyze Stille couplings in the presence of catalytic copper(I).⁹

CONCLUSIONS

The two important advances in the Stille coupling, the use of TFP and AsPh₃ ligands and co-catalytic Cu(I) salts, have been demonstrated to be of particular importance. These improvements have allowed faster reactions, higher yields, chemo- and stereoselectivity, and milder reaction conditions. Further investigation into the copper/tin transmetalation is necessary. Initial reports of the cost-efficient copper-only couplings are promising, and more work is needed to determine the generality of this methodology as well as the mechanism.

REFERENCES

1. Stille, J.K. *Angew. Chem., Int. Ed. Engl.* **1986**, *25*, 508-524.
2. Mitchell, T.N. *Synthesis* **1992**, 803-815.
3. Farina, V.; Krishnan, B. *J. Am. Chem. Soc.* **1991**, *113*, 9585-9595.
4. Farina, V.; Krishnan, B.; Marshall, D.R.; Roth, G.P. *J. Org. Chem.* **1993**, *58*, 5434-5444.
5. Tolman, C.A.; Seidel, W.C.; Gerlach, D.H. *J. Am. Chem. Soc.* **1972**, *94*, 2669-2676.
6. Liebeskind, L.S.; Fengl, R.W. *J. Org. Chem.* **1990**, *55*, 5359-5364.
7. Negishi, E.-I. *Acc. Chem. Res.* **1982**, *15*, 340-348.
8. Hobbs, F.W., Jr. *J. Org. Chem.* **1989**, *54*, 3420.
9. Roth, G.P.; Farina, V.; Liebeskind, L.S.; Peña-Cabrera, E. *Tetrahedron Lett.* **1995**, *36*, 2191-2194.
10. Hinkle, R.J.; Poulter, G.T.; Stang, P.J. *J. Am. Chem. Soc.* **1993**, *115*, 11626-11627.
11. Saá, J.M.; Martorell, G. *J. Org. Chem.* **1993**, *58*, 1963-1966.
12. Achab, S.; Guyot, M.; Potier, P. *Tetrahedron Lett.* **1993**, *34*, 2127-2130.
13. Ciattini, P.G.; Morera, E.; Ortar, G. *Tetrahedron Lett.* **1994**, *35*, 2405-2408.
14. Badone, D.; Cardamone, R.; Guzzi, U. *Tetrahedron Lett.* **1994**, *35*, 5477-5480.
15. Johnson, C.R.; Adams, J.P.; Braun, M.P.; Senanayake, C.B.W. *Tetrahedron Lett.* **1992**, *33*, 919-922.
16. Levin, J.I. *Tetrahedron Lett.* **1993**, *34*, 6211-6214.
17. Shi, G.-Q.; Cao, Z.-Y.; Zhang, X.-B. *J. Org. Chem.* **1995**, *60*, 6608-6611.
18. Farina, V. *Pure & Appl. Chem.* **1996**, *68*, 73-78.
19. Ye, J.; Bhatt, R.K.; Falck, J.R. *J. Am. Chem. Soc.* **1994**, *116*, 1-5.
20. Labadie, J.W.; Stille, J.K. *J. Am. Chem. Soc.* **1983**, *105*, 6129-6137.
21. Ye, J.; Bhatt, R.K.; Falck, J.R. *Tetrahedron Lett.* **1993**, *34*, 8007-8010.
22. de Frutos, O.; Echavarren, A.M. *Tetrahedron Lett.* **1996**, *37*, 8953-8956.
23. Ciattini, P.G.; Morera, E.; Ortar, G. *Synth. Commun.* **1995**, *25*, 2883-2894.
24. Gómez-Bengoa, E.; Echavarren, A.M. *J. Org. Chem.* **1991**, *56*, 3497-3501.
25. Palmisano, G.; Santagostino, M. *Tetrahedron Lett.* **1993**, *49*, 2533-2542.
26. Farina, V.; Kapadia, S.; Krishnan, B.; Wang, C.; Liebeskind, L.S. *J. Org. Chem.* **1994**, *59*, 5905-5911.
27. Reichle, W.T. *Inorg. Chim. Acta* **1971**, *5*, 325-332.
28. Gibbs, R.A.; Krishnan, U.; Dolence, J.M.; Poulter, C.D. *J. Org. Chem.* **1995**, *60*, 7821-7829.
29. Gibbs, R.A.; Krishnan, U. *Tetrahedron Lett.* **1994**, *35*, 2509-2512.
30. Murakami, M.; Yoshida, T.; Kawanami, S.; Ito, Y. *J. Am. Chem. Soc.* **1995**, *117*, 6408-6409.
31. Farina, V.; Hossain, M.A. *Tetrahedron Lett.* **1996**, *37*, 6997-7000.
32. Peirs, E.; Wong, T. *J. Org. Chem.* **1993**, *58*, 3609-3610.
33. Allred, G.D.; Liebeskind, L.S. *J. Am. Chem. Soc.* **1996**, *118*, 2748-2749.
34. Paterson, I.; Man, J. *Tetrahedron Lett.* **1997**, *38*, 695-698.
35. Takeda, T.; Matsunaga, K.; Kabasawa, Y.; Fujiwara, T. *Chem. Lett.* **1995**, 771-772.
36. Falck, J.R.; Bhatt, R.K.; Ye, J. *J. Am. Chem. Soc.* **1995**, *117*, 5973-5982.
37. Kang, S.-K.; Kim, J.-S.; Choi, S.-C. *J. Org. Chem.* **1997**, *62*, 4208-4209.

INTRODUCTION

The search for the origin of chirality is an interesting challenge. Numerous biotic and abiotic hypotheses have been proposed, in particular those that suppose a gradual selection of one enantiomer from a racemic mixture (Figure 1). However, many scientists are convinced that these theories are somewhat speculative and will be at best very difficult to verify experimentally.

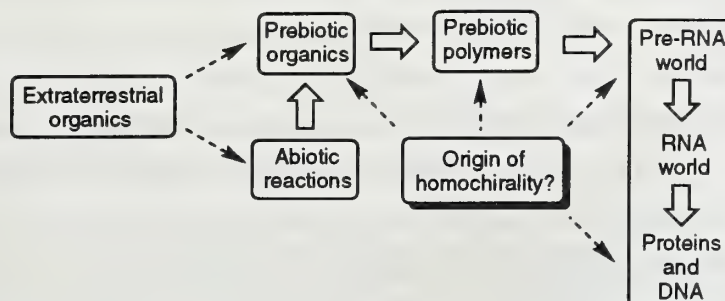


Figure 1. Where did homochirality begin?

It is generally accepted that life, as we know it, could not exist on a racemic basis.¹ It is therefore not surprising that interest in the origin of molecular chirality remains considerable. Early hypotheses concerning the origin of homochirality were developed in the 1950s with proposals by Frank² and Havinga.³ Although mechanistically different, both concluded that symmetry breaking was a spontaneous yet random event. Frank proposed a homogeneous chemical kinetic mechanism for an open flow reactor system, which he called *spontaneous asymmetric synthesis*.² The mechanism contained no internal bias, and the dominance of one enantiomeric form seemed to be entirely a matter of chance. Alternatively, Havinga proposed the possibility of forming optically active crystals from an initially racemic mixture.³ Regardless of the mechanism, both concepts require the notion of autocatalysis.^{4,5}

Typically, for a catalytic process to be effective the catalyst must remain unaffected by the newly formed product in order to maintain its catalytic nature. Wynberg realized the great potential of having the product itself be a catalyst and, moreover, a catalyst for its own asymmetric synthesis.^{1,6} At the outset, it is necessary to distinguish between various forms of autocatalysis. Self-replication is an autocatalytic process in which molecular recognition is a key factor. The nature of molecular recognition in self-replicating systems is based on either physical structure or template effects. These effects generally involve weak forces working within dynamic systems. Molecular multiplication is another example of autocatalysis, in which the product catalyzes its own formation without the recognition events characteristic of self-replicating systems. The design of systems which display high stereoselectivity in addition to kinetic enhancement have been developed to attempt to demonstrate the concept of asymmetric autocatalysis. Although still in its infancy, the development of asymmetric autocatalytic systems may constitute the next generation of asymmetric synthesis.

AUTOCATALYSIS

Self-replicating Systems

Self-replication is a form of autocatalysis in which molecular recognition plays a key role. The two different types of systems displaying these characteristics are those based on the replication of physical structures, which has been extensively examined by Luisi, on the autogeneration of micelles and reverse micelles,⁷ and those based on template effects, which have been examined by von Kiedrowski^{8,9} and Rebek.¹⁰

Luisi's work on self-replicating systems has focused on the self-reproduction of structures with clear chemically defined boundaries.⁷ The boundaries define an operationally distinct inside and outside, and a network of interactions take place within the bounded structure. The production of boundary components by way of the reaction network and spontaneous assembly led to self-generation. Luisi and coworkers were able to generate micelles which can host 1-octanol, using sodium octanoate as a surfactant in water. The addition of permanganate provided the final component to the autocatalytic system; the oxidant is believed to be either localized in the water pool or to act as a cosurfactant at the micellar surface. Nonetheless, slow oxidation of the alcohol to the cognate acid is thought to take place at the structural boundary (Figure 2). The result was growth and replication of the micelle by production of the surfactant of which it is composed. Control experiments without initial surfactant showed very slow consumption of permanganate as well as slow formation of micelles. Luisi described the observed rate enhancement as an example of "micellar catalysis." The experiments were repeated in isooctane to generate reverse micelles using octylamine as a cosurfactant. In this example, the oxidant is sequestered inside the reverse micelle. Again, oxidation of the alcohol was enhanced through interactions with the micellar interface.

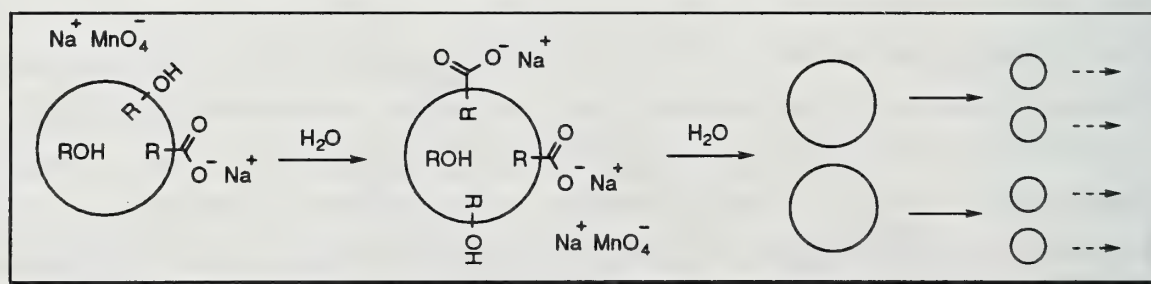


Figure 2. 1-Octanol oxidation in aqueous micelles

An example of template-based autocatalysis was brought forth in 1986 when von Kiedrowski showed that a short self-complementary segment of DNA could act as a template for its own formation without the need for enzymes.⁸ It was found that complementary trideoxynucleotides CCG and GGC could be coupled in the presence of a water soluble condensing agent to form a self-complementary hexadeoxynucleotide by an autocatalytic process. Subsequent improvements were made to give parabolic growth in the hexamer concentration to reflect the exponential nature of an autocatalytic process.⁹

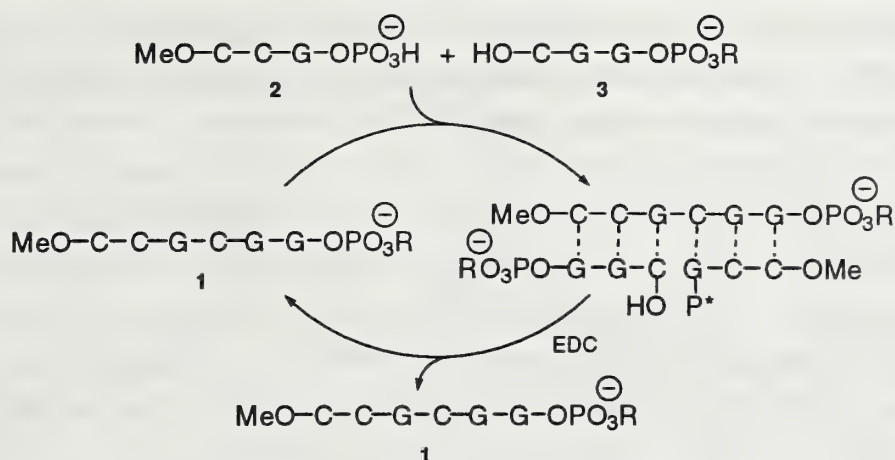
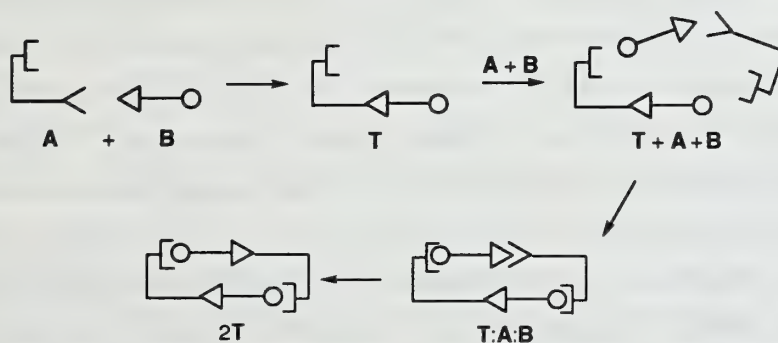


Figure 3. Reaction pathway for the template production of complementary hexadeoxynucleotides

With these results, Rebek investigated self-replicating systems using the weak intermolecular forces which give rise to molecular recognition, such as hydrogen-bonding, aryl stacking and hydrophobic effects. These forces provide a dynamic system with short-lived complexes where small modifications within the molecules can yield self-replicating structures. Schematically, two complementary components **A** and **B** react in an intermolecular fashion to form a template **T** (Scheme 1). Due to the self-complementary nature of the template, two additional units of **A** and **B** can form a termolecular complex with the template (**T:A:B**). An intramolecular reaction process can then produce the dimer **2T**, which dissociates and repeats the process.

Scheme 1



Rebek's first attempts at a self-replicating system was based on the hydrogen-bonding recognition of adenine and an imide of Kemp's triacid (Figure 4).¹¹ The naphthoyl ester **4** reacts with 5'-amino-5'-deoxy-2',3'-isopropylideneadenosine (**5**) to form a self-complementary autocatalytic template. In addition, seeding the reaction with its product resulted in a 50% rate enhancement, further suggesting the reaction was autocatalytic in nature. However, because the product contains several functional groups, it was unclear whether the enhanced rate was a result of chemical catalysis or template effects. To probe for template effects, Rebek designed a series of overlapping control experiments to exclude

each individual function of the product molecule as a source of simple chemical catalysis.¹² His results supported the notion of template effected autocatalysis. However, there has been recent controversy regarding the nature of catalysis in these systems.¹³⁻¹⁵

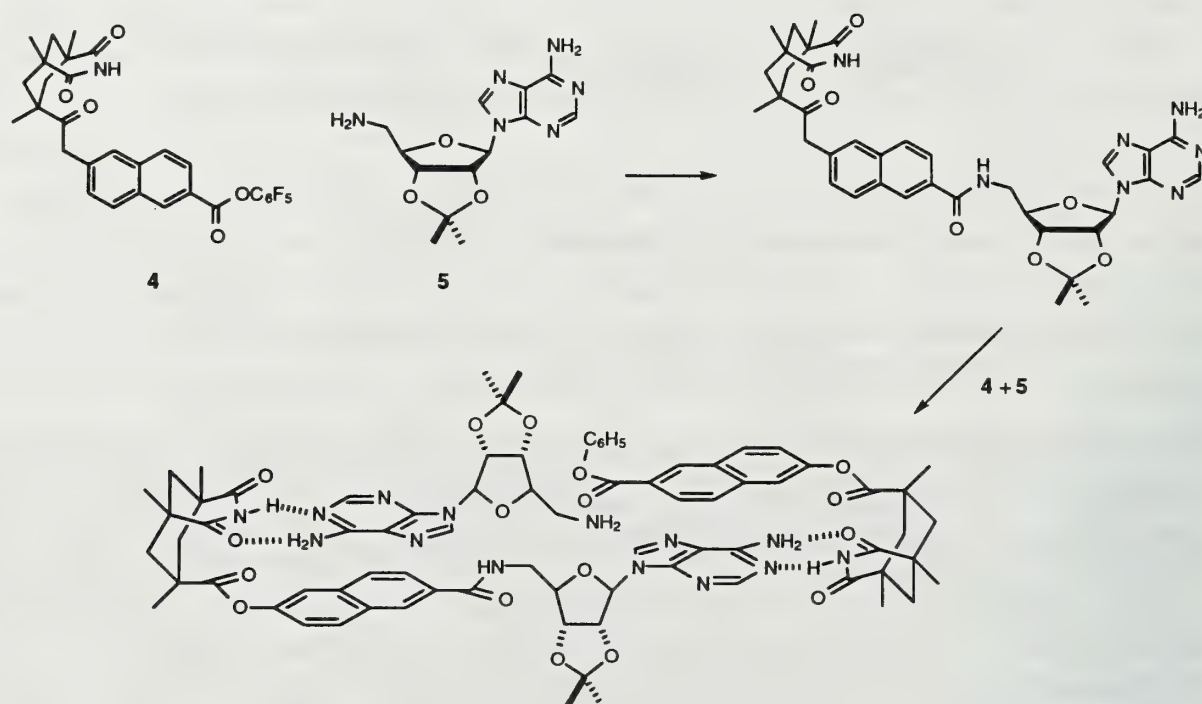
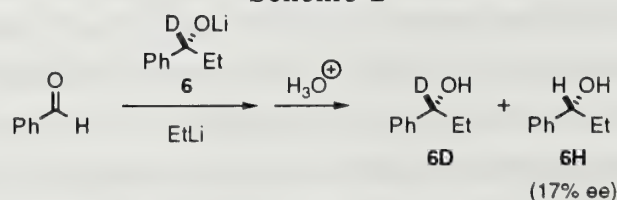


Figure 4. Template based self-replication

Asymmetric Autocatalysis

It was discovered by Seebach and coworkers that in stereoselective reactions with organometallic reagents, differing diastereo- and enantioselectivities could arise due to the formation of various mixed complexes during the course of product development.^{16,17} This led Alberts and Wynberg to investigate the asymmetric addition of ethyllithium to benzaldehyde (Scheme 2).^{18,19} By adding **6** to the initial reaction mixture, they showed the stereochemical course of the reaction could be influenced using both stoichiometric and sub-stoichiometric (50 mol %) amounts of metal-containing product molecules, in this case lithium alkoxides. Yields were slightly lower than 50% with the enantiomeric excess being roughly 17% with high reproducibility. Although **6** does not catalyze the addition of ethyllithium, it nonetheless governs the stereochemical outcome of the product. Alberts and Wynberg coined the term “enantioselective induction” to describe this effect.

Scheme 2



Danda made a remarkable discovery when studying the cyclic dipeptide catalyzed hydrocyanation of arylbenzaldehydes (Scheme 3).²⁰ In the hydrocyanation of 3-phenoxybenzaldehyde (7), dipeptide **9** alone showed poor stereoselectivity at early reaction times, yet with increasing time the enantiomeric excess of **8** increased (Table 1). Using only 0.5 mol % (*R,R*)-**9**, the optical purity of (*S*)-**8** was 33% after 30 minutes, but steadily increased to 92% after four hours. However, when 8 mol % of (*S*)-**8** (92% ee) is initially added, the product is consistently formed with high enantioselectivity. As in the previous example, **8** is not a catalyst, but the interaction between the correct product enantiomer with the cyclic dipeptide leads to increased stereoselection. Additionally, the absolute configuration of the product is determined not by the configuration of the catalyst but by the added cyanohydrin (Table 2).

Scheme 3

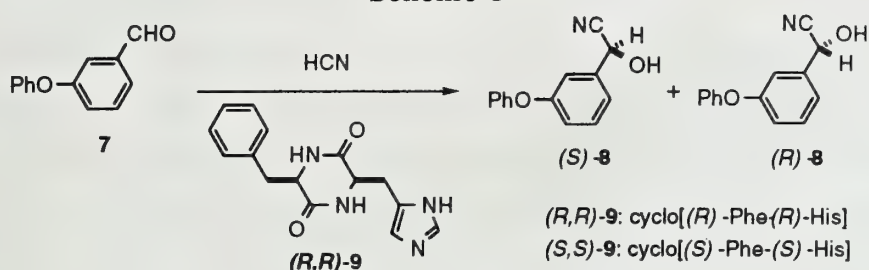


Table 1. Effect of the initial presence of (*S*)-**8**

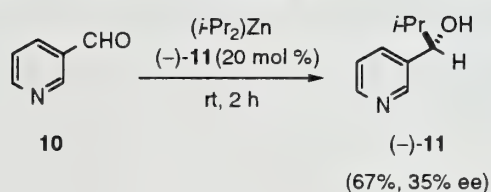
(<i>S</i>)- 8	time (h)	conversion (%)	optical purity of (<i>S</i>)- 8 (% ee)
0 mol %	0.5	21	34.4
	1	39	66.2
	2	92	91.6
	4	94	92.0
8 mol %	0.5	55	95.8
	1	79	96.4
	2	92	96.8
	4	95	96.6

Table 2. Effect of the optical purity (*R,R*)-**9** on the enantioselective autoinduction

(<i>R,R</i>)- 9	optical purity of (<i>R,R</i>)- 9 (% ee)	8	conversion (%)	optical purity of 8 (% ee)
0.5 mol %	2.0	8 mol % (<i>S</i>)- 8	43	81.6 (<i>S</i>)
0 mol %	2.0	no reaction		
0.5 mol %	2.0	8 mol % (<i>R</i>)- 8	39	74.0 (<i>R</i>)
0 mol %	2.0	no reaction		

The first successful reactions with a chiral “autocatalyst” were reported by Soai and coworkers in 1990.²¹ They discovered that the pyridinyl alcohol (–)-**11** catalyzed its own formation from pyridine-3-carboxaldehyde (**10**) and diisopropylzinc via the isopropylzinc alcoholate. When using 20 mol % of (–)-**11** (86% ee), they were able to isolate (–)-**11** in 67% yield with 35% enantiomeric excess after correcting for the initial amount added (Scheme 4).

Scheme 4



Until 1995, asymmetric autocatalytic organozinc additions consistently gave products with lower enantiomeric excess than that of the catalyst used. At this time, Soai showed pyrimidyl alcohol (*S*)-**8** (94.8% ee) could catalyze its own formation in 48% yield and 95.7% enantiomeric excess (Scheme 5).²² Additionally, Soai showed the catalyst behaved in a positive non-linear fashion²³ as defined by Kagan.²⁴ With an ee of only 2%, the autocatalytic reaction gave the newly produced alcohol in 16% ee (Table 3). Subsequent studies showed the enantiomeric excess increased from 10% to 88% after four cycles, resulting in a 940-fold increase in the amount of product

Scheme 5

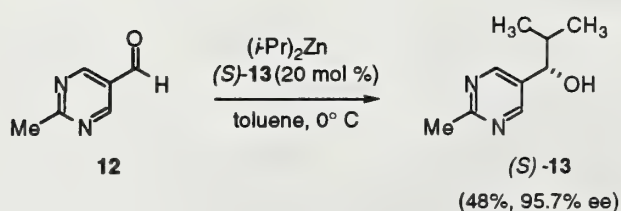


Table 3. Asymmetric autocatalysis of chiral pyrimidyl alcohol **13**

Run	Catalyst(<i>S</i>)- 13 (% ee)	Yield of newly formed(<i>S</i>)- 13	% ee of newly formed(<i>S</i>)- 13
1	2	26%	16
2	10	55%	74
3	57	60%	89
4	81	55%	90
5	88	59%	88

ORIGINS OF HOMOCHIRALITY

When Frank wrote his mathematical treatise on the possibility of asymmetric autocatalysis, he clearly predicted that “a laboratory demonstration is not necessarily impossible.”² Although autocatalysis displaying sigmoidal kinetics has yet to be achieved asymmetrically, work by Soai and others is making great progress. The basis for Frank’s calculations were that a substance A and B react to form C, where A and B are both achiral whereas C is chiral. The assumptions Frank made were that substance C catalyzes its own formation, specifically one enantiomer of C; for example (*R*)-C, catalyzes the formation of (*R*)-C and inhibits the formation of (*S*)-C, while (*S*)-C catalyzes its own formation and inhibits the formation of (*R*)-C (Figure 5). Should these conditions ever be met and at any time slightly more of one enantiomer is formed, the process leads to rapid formation of that single enantiomer, ultimately resulting in autocatalytic symmetry breaking without interference from external sources. Using pyrimidyl alcohol (*S*)-**8** as a chiral autocatalyst, Soai achieved a milestone in the development of true autocatalytic systems. Although a sigmoidal rate profile was never attained, these results should continue to drive further research.

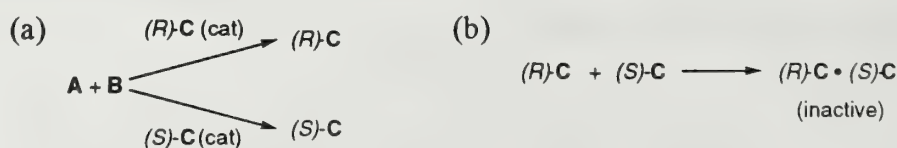


Figure 5. Boundary conditions for Frank’s model of “spontaneous asymmetric synthesis”

Like Frank's model, Havinga's model for the spontaneous crystallization of optically active crystals from a racemic source,³ is based merely on chance. Symmetry breaking crystallization into separate (+) or (-)-crystals requires no external intervention. Havinga argued that the free surface energy of chiral crystal could potentially be lower than that of the racemic mixture resulting in random, yet spontaneous crystallization of chiral entities. Recently, Kondepudi has shown that sodium perchlorate could spontaneously crystallize into optically active units.²⁵

A more recent hypothesis has been developed by Eschenmoser, based on oligomerization and base-pairing studies of pyranosyl-RNA.²⁶ The studies predict a mixture of the racemic pairs of enantiomers of the complete set of eight diastereomers of tetrameric pyranosyl-oligonucleotides should auto-oligomerize to a mixture of oligomers containing predominantly, if not exclusively, homochiral (D) and (L) sequences. Using this prediction as the basis for a gedanken experiment, Eschenmoser proposed that stochastic, chirospecific oligomerization of a mixture of all 4⁶ possible oligonucleotide tetamers, would lead to two libraries of equal amounts of homochiral (D) and (L) oligomers. However, the two libraries taken together would no longer constitute a racemic mixture. Symmetry breaking would be an inevitable consequence, because the number of possible sequences with growing oligomer length would rise beyond the number of sequences actually formed. Thus, the composition of the D- and L-libraries would not be identical and could not constitute a racemic mixture.

CONCLUSIONS

In addition to the models proposed by Frank, Havinga and Eschenmoser, other theoreticians have invoked esoteric concepts such as parity-violating energy differences (PVED),²⁷ weak neutral currents²⁸ and nuclear β -decay²⁹ as possible mechanisms for the origin of molecular dissymmetry. Thus, these theoreticians view homochirality as an inevitable consequence of universal, fundamental, physical processes. If correct, these explanations would predict that wherever life exists, the molecular handedness would be the same as on Earth. In comparison, the models of Frank and Havinga envision that life throughout the universe would be equally divided with respect to left and right molecular handedness. This debate has fueled the development of autocatalytic systems.

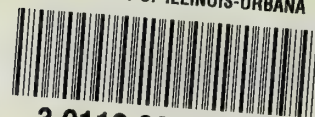
Although work in asymmetric autocatalysis is still in its infancy, recent results have demonstrated its potential to be a viable tool in asymmetric synthesis. The practicality of a chiral molecule asymmetrically catalyzing its own formation is unquestionable. An ever increasing concern for environmentally sound and chemically efficient synthetic methods constantly challenge chemists' abilities to invent innovative methodologies. By removing the requirement for an external catalyst and subsequently bypassing the need to remove and recycle precious chiral catalysts, methods such as asymmetric autocatalysis appear poised to meet future chemical challenges.

REFERENCES

- (1) Wynberg, H. *Chimia* **1989**, *43*, 150.
- (2) Frank, F. C. *Biochim. Biophys. Acta* **1953**, *11*, 459.
- (3) Havinga, E. *Biochim. Biophys. Acta* **1954**, *13*, 171.
- (4) Bolm, C.; Bienewald, F.; Seger, A. *Angew. Chem., Int. Ed. Engl.* **1996**, *35*, 1657.
- (5) Mason, S. *Nature* **1985**, *314*, 400.
- (6) Wynberg, H. *J. Macromol. Sci.-Chem.* **1989**, *A26*, 1033.
- (7) Bachmann, P. A.; Walde, P.; Luisi, P. L.; Lang, J. *J. Am. Chem. Soc.* **1991**, *113*, 8204.
- (8) von Kiedrowski, G. *Angew. Chem., Int. Ed. Engl.* **1986**, *25*, 932.
- (9) von Kiedrowski, G.; Wlotzka, B.; Helbing, J.; Matzen, M.; Jordan, S. *Angew. Chem., Int. Ed. Engl.* **1991**, *30*, 423.
- (10) Wintner, E. A.; Conn, M. M.; Rebek, J., Jr. *Acc. Chem. Res.* **1994**, *27*, 198.
- (11) Tjivikua, T.; Ballester, P.; Rebek, J., Jr. *J. Am. Chem. Soc.* **1990**, *112*, 1249.
- (12) Conn, M. M.; Wintner, E. A.; Rebek, J., Jr. *J. Am. Chem. Soc.* **1994**, *116*, 8823.
- (13) Menger, F. M.; Eliseev, A. V.; Khanjin, N. A. *J. Am. Chem. Soc.* **1994**, *116*, 3613.
- (14) Menger, F. M.; Eliseev, A. V.; Khanjin, N. A.; Sherrod, M. J. *J. Org. Chem.* **1995**, *60*, 2870.
- (15) Wintner, E. A.; Tsao, B.; Rebek, J., Jr. *J. Org. Chem.* **1995**, *60*, 7997.
- (16) Seebach, D.; Amstutz, R.; Dunitz, J. D. *Helv. Chim. Acta* **1981**, *64*, 2622.
- (17) Seebach, D. *Angew. Chem., Int. Ed. Engl.* **1988**, *27*, 1624.
- (18) Alberts, A. H.; Wynberg, H. *J. Am. Chem. Soc.* **1989**, *111*, 7265.
- (19) Alberts, A. H.; Wynberg, H. *J. Chem. Soc., Chem. Commun.* **1990**, 453.
- (20) Danda, H.; Nishikawa, H.; Otaka, K. *J. Org. Chem.* **1991**, *56*, 6740.
- (21) Soai, K.; Niwa, S.; Hori, H. *J. Chem. Soc., Chem. Commun.* **1990**, 982.
- (22) Shibata, T.; Morioka, H.; Hayase, T.; Choji, K.; Soai, K. *J. Am. Chem. Soc.* **1996**, *118*, 471.
- (23) Soai, K.; Shibata, T.; Morioka, H.; Choji, K. *Nature* **1995**, *378*, 767.
- (24) Guillaneaux, D.; Zhao, S.-H.; Samuel, O.; Rainford, D.; Kagan, H. B. *J. Am. Chem. Soc.* **1994**, *116*, 9430.
- (25) Kondepudi, D. K.; Kaufman, R. J.; Singh, N. *Science* **1990**, *250*, 1249.
- (26) Bolli, M.; Micura, R.; Eschenmoser, A. *Chem Biol* **1997**, *4*, 309.
- (27) Tranter, G. E. *Nature* **1985**, *318*, 172.
- (28) Kondepudi, D. K.; Nelson, G. W. *Nature* **1985**, *314*, 438.
- (29) Meiring, W. J. *Nature* **1987**, *329*, 712.



UNIVERSITY OF ILLINOIS-URBANA



3 0112 033109304

Q.547

I l 6s

1997/98:2

ORGANIC SEMINAR ABSTRACTS
1997-98, SEMESTER II

University of Illinois

Department of Chemistry
Box 68 Roger Adams Laboratory
600 South Matthews Avenue
Urbana, Illinois 61801

June, 1998

NOTICE: Return or renew all Library Materials! The *Minimum Fee* for each Lost Book is \$50.00.

The person charging this material is responsible for its return to the library from which it was withdrawn on or before the **Latest Date** stamped below.

Theft, mutilation, and underlining of books are reasons for disciplinary action and may result in dismissal from the University.
To renew call Telephone Center, 333-8400

UNIVERSITY OF ILLINOIS LIBRARY AT URBANA-CHAMPAIGN

CHEMISTRY LIBRARY

JAN 20 2003

LIBRARY U. OF
CHAMPAIGN

L161—O-1096

8.547
265
7/1/98:2

SEMINAR TOPICS

Semester II, 1997-98

	Page
Recent Advances in Palladium-Catalyzed Metallo-ene Cyclization Reactions.....1 Ewa Fredette	
Lewis Acid Promoted Asymmetric Radical Reactions in Acyclic Systems.....9 Jason Laumer	
Boron Dienophiles as Diels Alder Synthetic Equivalents.....17 Bryce Assink	
Techniques for the Structural Identification of Active Molecules Within Combinatorial Libraries.....25 Jennifer Poole	
Recent Developments in the Secondary Structure of β -peptides.....33 Shreyasi Lahiri	
Chirality in Molecular Encapsulation.....41 Chad Baker	
Functionalization of Olefins Using Chiral Selenium Reagents.....49 Sergio Duron	
Computational Solvation Models for Organic Chemists.....57 Jane Owens	

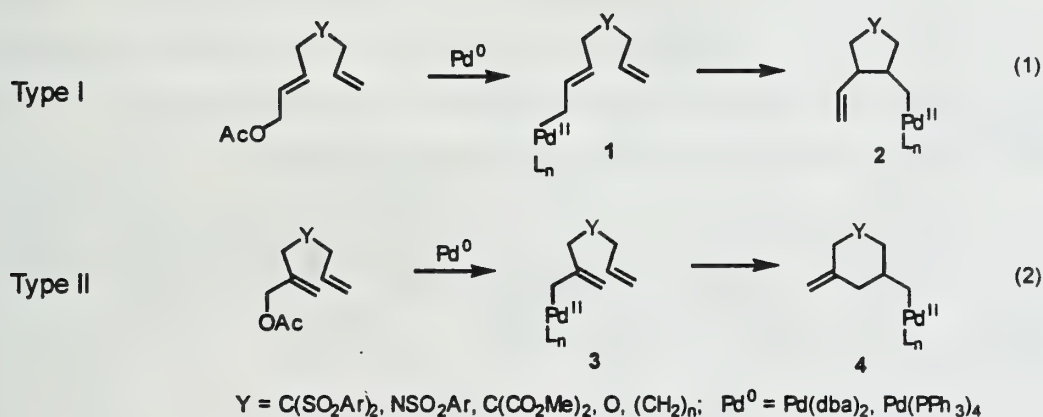
RECENT ADVANCES IN PALLADIUM-CATALYZED METALLO-ENE CYCLIZATION REACTIONS

Reported by Ewa Fredette

February 19, 1998

INTRODUCTION

Palladium-catalyzed metallo-ene cyclization reactions represent a useful synthetic tool for carbon-carbon bond formation at sp^2 centers, efficiently leading to formation of carbo- and heterocyclic compounds.¹ The cyclization process involves reaction between the 'enophile' unit (alkene or alkyne) and the 'ene' (allyl) unit, which is connected by a suitable bridge to either the proximal (Type I) or distal carbon atom (Type II) of the enophile component (eqs 1, 2). Typical reaction involves heating palladium adducts **1** or **3** in acetic acid or methanol to obtain the cyclization products **2** or **4**. This report describes the most recent developments in Type-I palladium-catalyzed metallo-ene reactions, including their mechanistic aspects and synthetic utility.

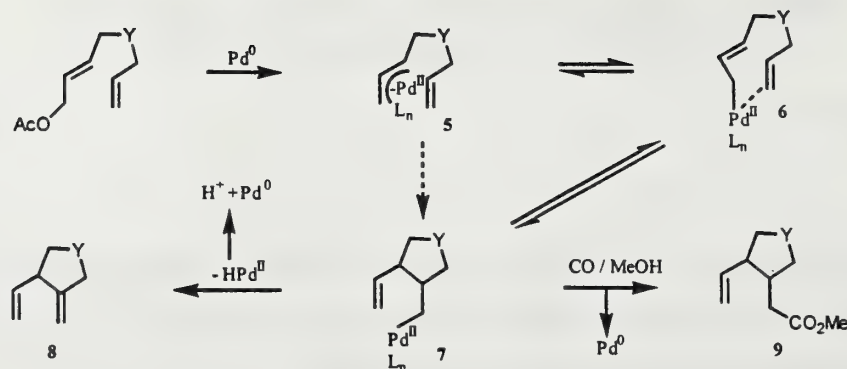


MECHANISTIC ASPECTS

General Mechanism and Catalytic Cycle

The cyclization step in Type-I palladium-catalyzed metallo-ene reaction involves insertion of the enophile component of **1** into the π -allylpalladium(II) (**5**)- or σ -allylpalladium(II) (**6**) complex of the ene unit to regioselectively form a carbon-carbon bond between the proximal centers of the two components (Scheme 1).² Reductive β -elimination of the initial cyclization product **7** (**7**→**8**) or C-C bond insertion/elimination (**7**→**9**) steps furnish the final products and regenerate Pd^0 that may then reenter the catalytic cycle by oxidative addition to the ene unit. Analogous transformations for Type-II substrates, having the enophile unit tethered to the distal sp^2 carbon of the ene, have also been described.³

Scheme 1



Topicity

An extensive study of the topicity of the carbon-palladium bond cleavage and carbon-carbon bond formation by Oppolzer and co-workers⁴ suggests that both events proceed in a suprafacial manner, syn with respect to the metal. Palladium-catalyzed metallo-ene reactions of *trans*- and *cis*-acetoxydienes **10** and **12** led to formation of *cis*- and *trans*-fused products **11** and **13**, respectively, with very high specificity (Scheme 2, Table 1). This efficient chirality transfer from the carbon-palladium bond to the newly formed stereogenic center allows for the selective and predictable preparation of both *cis*- and *trans*-fused ring systems of various size from readily available substrates.⁵

Scheme 2

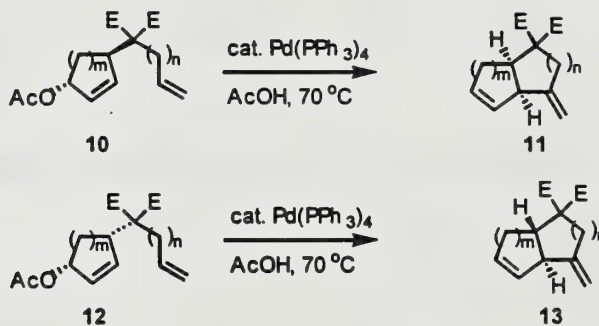
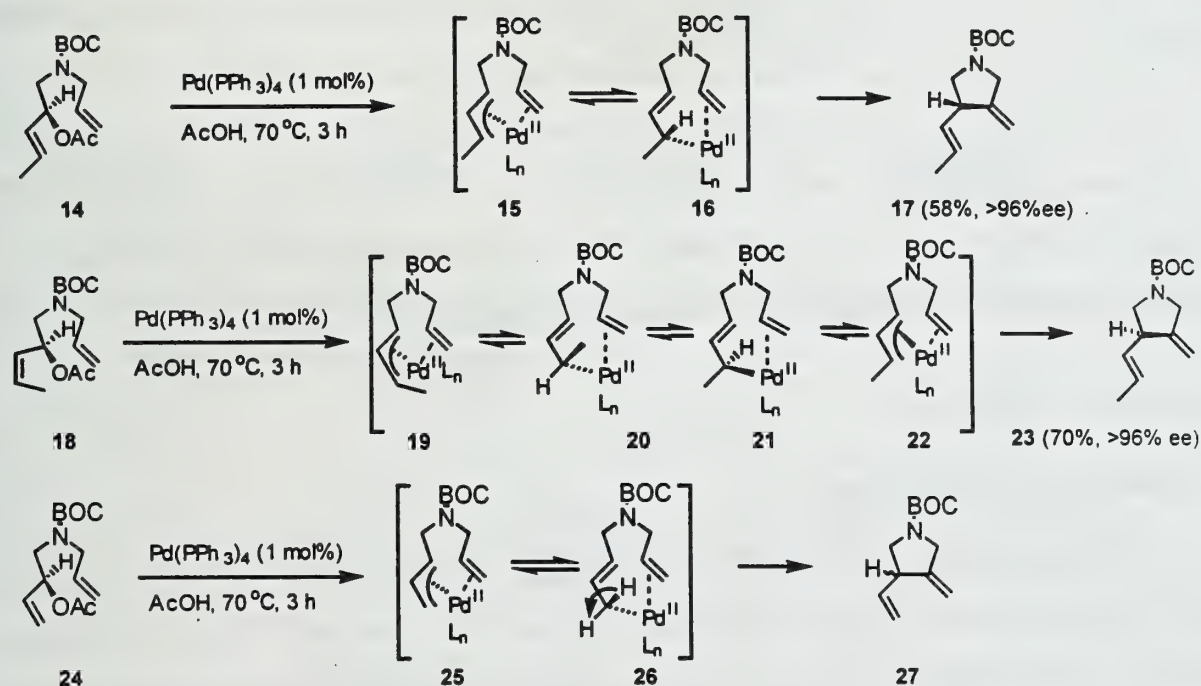


Table 1. Stereocontrolled Ring Closures of Acetoxydienes **10** and **12** by Pd Catalysis in AcOH.

Entry	Diene	m	n	Pd(PPh ₃) ₄		Yield (11 + 13) %	Ratio 11 / 13
				(equiv)	Time (h)		
1	10	2	1	0.07	1.1	84	98 : 2
2	10	2	2	0.07	3.0	60	99 : 1
3	12	2	2	0.07	3.0	69	5 : 95
4	10	3	1	0.10	4.0	73	99 : 1
5	12	3	1	0.05	1.8	80-92	2 : 98

Further evidence for of the *syn*-type olefin insertion into the allyl unit derives from the cyclizations of open-chain acetoxydienes (Scheme 3).⁶ Thus, palladium-catalyzed metallo-ene reactions of enantiomerically pure acetoxydienes **14** and **18**, followed by β -elimination, led to highly stereospecific formation of exocyclic alkenes **17** and **23**, respectively. The net retention at C(3), observed in the cyclization of **18**, is presumably due to the isomerization of the initially formed *anti* / *syn*- π -allyl complex **19** to the more stable *syn* / *syn*- π -allyl isomer **22**, which allows one to conclude that the olefin inserts into the more stable E-ene component and that the *anti*→*syn* isomerization is faster than the subsequent cyclization step. Consequently, analogous transformations of enantiomerically pure terminally unsubstituted acetoxydiene **24** resulted in a complete loss of stereochemical integrity at C(3) in the product (**27**), due to a facile rotation about C(1)-C(2) bond in a σ -allylpalladium complex **26**.

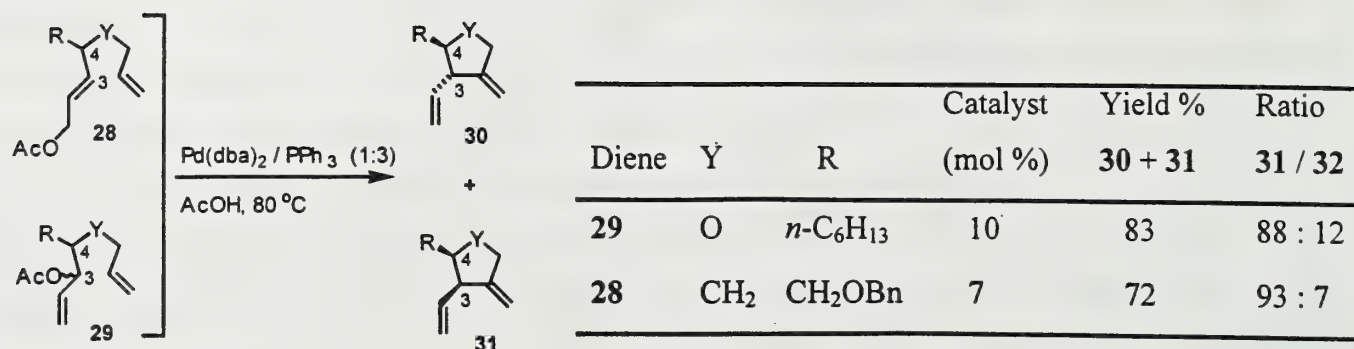
Scheme 3



Stereodirecting Control

Several studies concerning the influence of pre-existing stereogenic centers within the bridge connecting ene and enophile on the developing stereogenic centers in the cyclization step revealed that C(5)⁷- and C(6)⁸-substituted acetoxydienes show no preference for either cis- or trans-disubstituted products. However, palladium-catalyzed cyclization of 4-substituted acetoxydienes allowed selective formation of trans-1,2-disubstituted cyclopentanes and tetrahydrofurans in good yield.¹⁰

Scheme 4



The observed 1,2-*trans* stereodirecting effect is presumably a result of a high *endo* / *exo* preference in the transition state: examination of four plausible transition structures, consistent with the suprafacial olefin insertion into the ene unit through (E)- σ -allyl- or *syn*- π -allylpalladium species, reveals less steric crowding in the *endo*, *trans*-predisposed transition structure (34 or 35, Figure 2) than in the corresponding *exo* transition structure (32 or 33).¹⁰

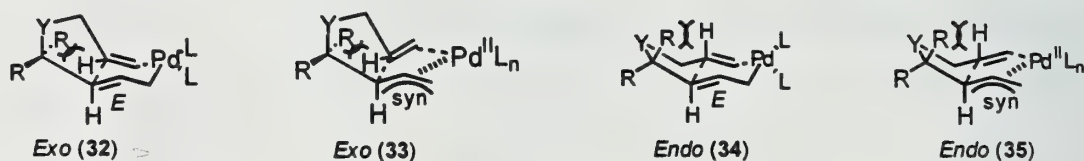


Figure 2. Transition structures for cyclizations of 28 and 29.

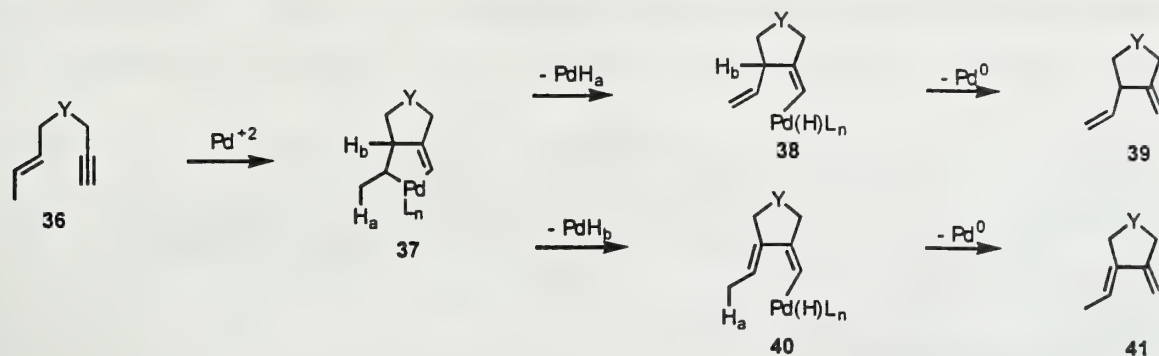
SYNTHETIC UTILITY

Cycloisomerization of Enynes

Metallo-ene reaction of 1,6-enynes is a particularly attractive pathway for the synthesis of 1,3-dienes, which can then serve as substrates in the Diels-Alder reaction.⁹ In this event, the ability to divert the metallo-ene pathway away from the Alder-ene product 39 (Scheme 5) and toward 1,3-diene 41 depends on regioselectivity of the β -hydrogen elimination step.¹⁰ Geometrical constraints associated with *syn* β -elimination of PdH from the ene component in 37, coupled with thermodynamic stability of 38 relative to 40, are the driving forces in preferential formation of 1,4-dienes in the ene reaction.^{1,13} Study of the allylic substituent effect on regioselectivity of the β -elimination step revealed that the metallo-ene pathway can be successfully diverted toward 1,3-diene product. This involves formation of the pseudocyclic intermediate 43 (Scheme 6), afforded by binding of the remote olefin to palladium and thus geometrically precluding elimination of the exocyclic hydrogen H_a.¹³ In this event, the geometrical

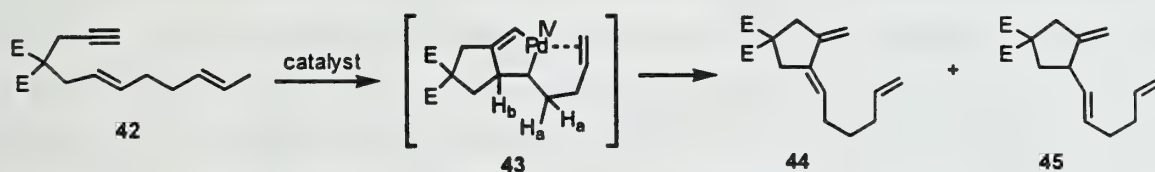
constraints of H_a and H_b eliminations being equal, the lower bond strength of allylic hydrogen relative to the methylene hydrogen favors formation of 1,3-diene **44**.¹³

Scheme 5



The effect of catalyst type on the differences in regioselectivity provides evidence of remote binding: the regioselectivity diminishes in the presence of phosphine ligands (entries 2-4), presumably a result of competitive olefin binding, and it parallels the trend in ligation strength of phosphines. Thus, careful choice of catalyst allows selective formation of either of the diene products and, with the recent development of a more efficient 'ligandless' palladium catalyst,¹¹ this metallo-ene pathway offers a useful tool for synthesis of Diels-Alder substrates. A very elegant application of this catalyst-dependent control of regioselectivity in the β -elimination step was recently demonstrated in the enantioselective synthesis of (+)-cassiol, an antiulcerogenic agent.¹²

Scheme 6



Entry	1	2	3	4
Catalyst	Pd(OAc) ₂	[(<i>o</i> -tol) ₃ P] ₂ Pd(OAc) ₂	(Ph ₃ P) ₂ Pd(OAc) ₂	3PPh ₃ , 2Pd(OAc) ₂
Ratio 44 / 45 (%yield)	21:1 (76%)	20:1 (ND)	2.7:1 (ND)	1:2.3 (24%)

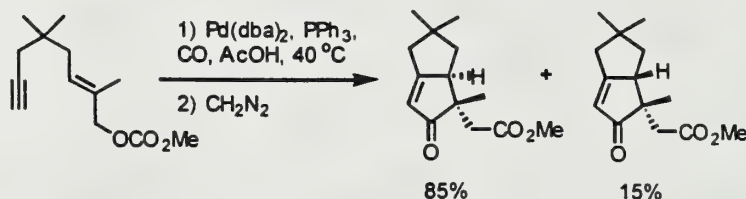
E = CO₂Me, ND = not determined

Cyclization / Carbonylation Sequences

Functionalization of the carbon-palladium bond in the initial cyclization product by carbonylation leads to formation of a bicyclic structure with two stereogenic centers.¹³ This methodology was

particularly well demonstrated in the total synthesis of (\pm)-hirsutene, where the key cyclization / carbonylation step, forming a quaternary carbon center, proceeded with high diastereoselectivity (Scheme 7).¹⁴ Analogous tandem cyclization / carbonylation allowed stereoselective formation of the heterocyclic skeleton in the total synthesis of (+)-isorauniticine.¹⁵

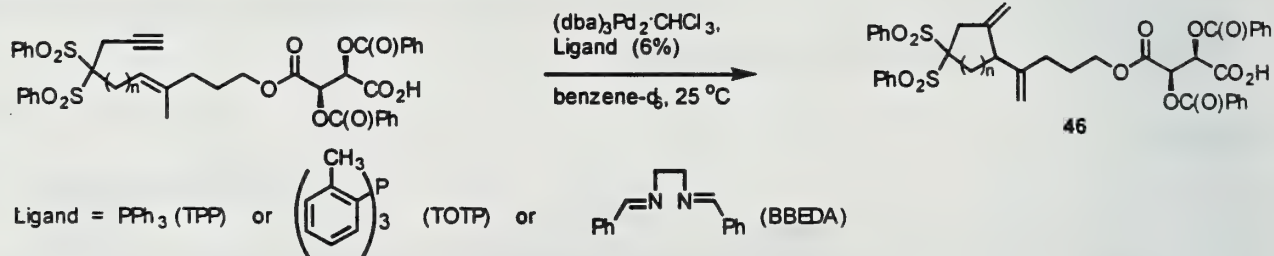
Scheme 7



ASYMMETRIC INDUCTION

Although many stereoselective syntheses of natural products have employed the metallo-ene reaction as a convenient means to form carbo- and heterocycles,¹⁶ the more recent attempts to control the absolute stereochemistry of the cyclization step may enhance the overall synthetic utility of this atom-efficient reaction. The first attempt at achieving asymmetric induction involved the use of tartaric acid derivatives as a chiral auxiliary.¹²

Scheme 8



n	1	1	1	2
Ligand	BBEDA	TPP	TOTP	TOTP
% de (46)	21	27	50	71

Depending on the catalyst system used, a moderate to good diastereomeric excess was observed in cyclizations of 1,6- and 1,7-enynes (Scheme 8). In this event, the free acid in the auxiliary serves as a coordinating site for palladium, which presumably accounts for its ability to induce chirality despite the relatively remote location from the reaction center.¹² Attempts to improve the asymmetric induction by employing several chiral ligands failed to improve diastereoselectivities relative to achiral ligands under similar reaction conditions.¹²

A more recent study toward the asymmetric palladium-catalyzed metallo-ene reaction focused on enantioselective cyclization of cyclopentadiene derivative **47** (Scheme 9).¹⁷ Best results were obtained with Trost's ligands¹⁸ TI and TIII, while no asymmetric induction was observed when monodentate phosphine ligand MOP¹⁹ was employed (Table 2).¹⁷ Further studies, involving different substrates as well as new developments in this area, will no doubt lead to further improvements in enantioselectivity.

Scheme 9

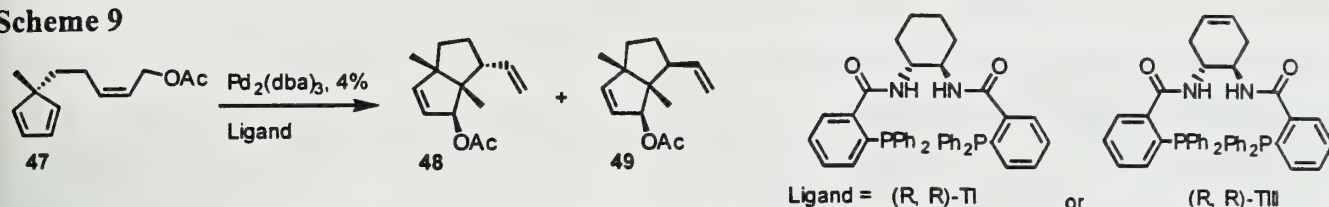


Table 2. Asymmetric induction in palladium-catalyzed cyclization of **47**.

Entry	Ligand	Conditions	Conversion (%)	Ratio 48 / 49	ee 48	ee 49
1	10% (S,S)-TI	MeOH, 70 °C, 8h	100	88 / 12	34	19
2	18% (R,R)-TI	MeOH, 40 °C, 36h	100	93 / 7	45	10
3	12% (R,R)-TIII	MeOH, 72 °C, 24h	100	88 / 12	40	ND
4	15% (R,R)TIII	MeOH, 45 °C, 36h	97	87 / 13	47	15

CONCLUSIONS

Recent developments in palladium-catalyzed metallo-ene cyclization reactions broadened the scope of their synthetic utility and opened new ways toward stereoselective synthesis of carbo- and heterocyclic systems. Full elucidation of the reaction mechanism and further studies in the area of asymmetric catalysis should be the focus of the future research.

REFERENCES

- ¹ Oppolzer, W. *Angew. Chem. Int. Ed. Engl.* **1989**, 28, 38.
- ² Oppolzer, W., Gaudin, J.-M. *Helv. Chim. Acta* **1987**, 70, 1477.
- ³ Oppolzer, W., Gaudin, J.-M. *Tetrahedron Lett.* **1988**, 29, 5529.
- ⁴ Oppolzer, W., Gaudin, J.-M., Birkinshaw, T.N. *Tetrahedron Lett.* **1988**, 29, 4705.
- ⁵ Backvall, J.-E., Nystrom, J. E., Nordberg, R. E. *J. Am. Chem. Soc.* **1985**, 107, 3676.
- ⁶ Oppolzer, W., Birkinshaw, T. N., Bernadinelli, G. *Tetrahedron Lett.* **1990**, 31, 6995.
- ⁷ Oppolzer, W., Keller, T. H., Kuo, D. L., Puchinger, W. *Tetrahedron Lett.* **1990**, 31, 1265.

- ⁸ Oppolzer, W., Gaudin J.-M., Bedoya-Zurita, M., Hueso-Rodriguez, J., Raynham, T. M., Robyr, C. *Tetrahedron Lett.* **1988**, 29, 4709.
- ⁹ Trost, B. M., Czekis, B. A. *Tetrahedron Lett.* **1994**, 35, 211.
- ¹⁰ Trost, B. M., Tanoury, G. J., Lautens, M., Chan, C., MacPherson, D. T. *J. Am. Chem. Soc.* **1994**, 116, 4255.
- ¹¹ Trost, B. M., Lee, D. C., Rise, F. *Tetrahedron Lett.* **1989**, 30, 651.
- ¹² Trost, B. M., Li, Y. *J. Am. Chem. Soc.* **1996**, 118, 6625.
- ¹³ Oppolzer, W., Keller, T. H., Bedoya-Zurita, M., Stone, C. *Tetrahedron Lett.* **1989**, 30, 5883.
- ¹⁴ Oppolzer, W., Robyr, C. *Tetrahedron*, **1994**, 50, 415.
- ¹⁵ Oppolzer, W., Bienayme, H., Genevois-Borella, A. *J. Am. Chem. Soc.* **1991**, 113, 9660.
- ¹⁶ Oppolzer, W. *Pure & Appl. Chem.* **1981**, 53, 1181.
- ¹⁷ Oppolzer, W., Kuo, D. L., Hutzinger, M. W., Leger, R., Durand, J.-O., Leslie, C. *Tetrahedron Lett.* **1997**, 38, 6213.
- ¹⁸ Trost, B. M., Van Vranken, D. L. *Chem. Rev.* **1996**, 96, 395.
- ¹⁹ Uozumi, Y., Tanahashi, A., Lee, S. Y., Hayashi, T. *J. Org. Chem.* **1993**, 58, 1945.

LEWIS ACID PROMOTED ASYMMETRIC RADICAL REACTIONS IN ACYCLIC SYSTEMS

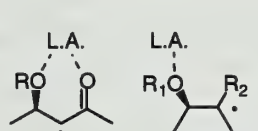
Reported by Jason M. Laumer

February 23, 1998

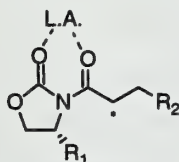
INTRODUCTION

Over the past several decades, free radical chemistry has become common in organic synthesis; however, until the mid-Eighties, stereochemical control was rarely realized in radical based methods.^{1,2} Early advances in stereoselective radical reactions came in the area of intramolecular cyclizations³ and reactions with cyclic substrates,^{3,4} while stereochemical control with acyclic substrates remained elusive.

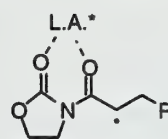
Recently, with stereoselective radical reactions of cyclic substrates generally understood, significant progress has been made toward understanding reactions of acyclic substrates.³⁻⁶ Three general methods of asymmetric induction in which Lewis acids play an important role have been developed for acyclic systems. In two of these methods, 1,2-asymmetric induction and use of chiral auxiliaries, Lewis acids provide control of the reactive conformation of the substrate through chelation. The third method involves the use of chiral Lewis acids. This abstract discusses these three methods and their application to substrates similar to those represented below.



1,2-asymmetric induction



chiral auxiliary



chiral Lewis acid

LEWIS ACIDS IN 1,2-ASYMMETRIC INDUCTION

The driving force for 1,2-asymmetric induction in radical reactions is considered to arise from either minimization of allylic 1,3-strain ($A^{1,3}$ strain) or minimization of electronic interactions. Allylic 1,3-strain is the main factor in substrates bearing one oxygen substituent. Monodentate Lewis acids have been successful in inducing stereoselectivity in substrates affected by $A^{1,3}$ strain. Electronic interactions are dominant in substrates with 1,2-dioxy substitution or β -oxy carbonyls. Bidentate Lewis acids have been utilized to enhance the diastereoselectivity in reactions of these types of substrates.

Monodentate Lewis Acids: Reactions Controlled by $A^{1,3}$ Strain

Renaud's work illustrates the stereochemical effect Lewis acids have on the deuteration of

2-sulfinylated benzylic radicals with tributyltindeuteride (Table 1).⁷ In the absence of Lewis acid, the reaction provided **3** and **4** in 59-87% combined yield, with diastereomeric ratios ranging from 50:50 to 93:7 favoring **3**. In the presence of Lewis acids, **4** is obtained as the major diastereomer in most cases.

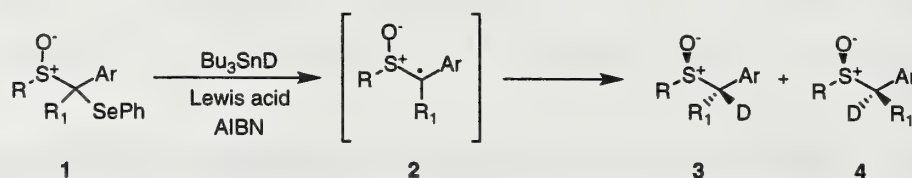


Table 1. Effect of Lewis Acid on Deuteration of 1a-c

Entry	Compound	R	R ₁	Ar	Lewis Acid	Yield	3:4
1	1a	Ph	H	Ph	---	87%	66:34
2	1a	Ph	H	Ph	LiClO ₄	51%	58:42
3	1a	Ph	H	Ph	[Eu(dpm) ₃] ^a	95%	54:46
4	1a	Ph	H	Ph	MAD ^b	85%	3:97
5	1a	Ph	H	Ph	MABR ^c	84%	<3:97
6	1b	Me	H	Ph	---	59%	50:50
7	1b	Me	H	Ph	MAD ^b	77%	4:96
8	1c	Ph	Me	Ph	---	59%	93:7
9	1c	Ph	Me	Ph	MAD ^b	73%	14:86

a) dpm = 2,2,6,6-tetramethylheptane-3,5-dionato b) MAD = methylaluminum bis[2,6-di(*tert*-butyl)-4-methylphenoxide]

c) MABR = methylaluminum bis[4-bromo-2,6-di(*tert*-butyl)phenoxide]

Several trends can be noted in these results. The size of the R group on sulfur plays a small but discernible role in the stereochemical outcome of the reaction (entries 1 and 6). Abstraction of deuterium by a tertiary radical is much more selective than abstraction by a secondary radical (entries 1, 6 and 8). The major product formed in all reactions in the absence of Lewis acid is **3**. Upon the addition of lithium perchlorate and [Eu(dpm)₃] the selectivity of the reaction was decreased with the major product still being **3** (entries 2 and 3). A very interesting result was found with the addition of the bulky aluminum-based Lewis acids MAD and MABR (entries 4, 5, 7 and 9). Not only was the diastereoselectivity very good in all cases, but the major product was found to be **4**.

The inversion resulting from the addition of MAD and MABR can be explained by a change of the minimum energy conformations of radical **2**, from **5** and **6** to **7** and **8** (Figure 1). With no chelated Lewis acid, the R group is assigned as the large substituent on sulfur, and conformers **5** and **6** may be considered. One can imagine attack from either face of the radical in both conformations. This explains the importance of the size of the R group. A large R group will achieve two things, a preference for conformation **5** and attack of the radical anti to the large group. Attack anti to R in conformation **5** leads to product **3**. Chelation of a bulky Lewis acid causes the lowest energy conformations to become **7** and **8**. One can now imagine exclusive attack of the radical anti to the bulky Lewis acid. The size of the R group can again be seen as playing an important role. When R is not H there is a preference for **7** to relieve A^{1,3} strain. Attack anti to the Lewis acid in **7** leads to **4**.

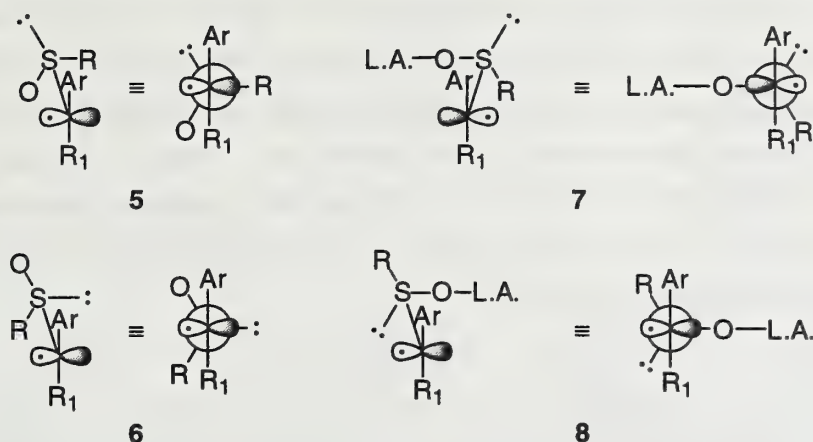


Figure 1. Minimum energy conformations of nonchelated and chelated substrates.

In **5-8** the importance of R_1 in controlling the conformation can also be seen. When R_1 is not H, **5** is preferred over **6** to relieve $A^{1,3}$ strain. This conformational preference rationalizes the increased selectivity of **1c** versus **1a** (entries 8 and 1, Table 1). In conformations **7** and **8**, when R_1 is not H there is a decrease in the preference for **7** versus **8**. This rationalizes the decreased selectivity of **1c** versus **1a** with Lewis acid (entries 9 and 4, Table 1).

Bidentate Lewis Acids: Reactions Controlled by Electronic Effects

Asymmetric deuteration and allylation of β -oxy esters has been achieved in radical reactions with the use of several different bidentate Lewis acids.⁸⁻¹³ Table 2 shows the results of the allylation of **9** using allyltributylstannane. The reaction has been carried out under various conditions by different research groups. When the β -substituent is an alkoxy group, **9a** and **9b**, the major products in the absence of a Lewis acid are the syn products, **11a** and **11b**, respectively (entries 1 and 3). When the β -substituent is a hydroxy group, **9c**, the major product in the absence of a Lewis acid is the anti product, **11c** (entry 5).

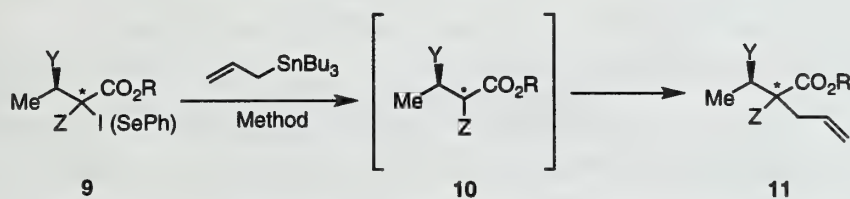


Table 2. Effect of Lewis Acid on Allylation of 9a-c

Entry	Compound	Method ^a	Y	Z	R	Lewis Acid	Yield	syn:anti 11
1	9a	A	OMe	H	Me	---	79%	75:25
2	9a	B	OMe	H	Me	MgBr ₂ ·OEt ₂	73%	2:98
3	9b	A	OMe	Me	Et	---	65%	82:18
4	9b	B	OMe	Me	Et	MgBr ₂ ·OEt ₂	44%	<1:99
5	9c	C	OH ^b	H	Et	---	98%	37:63
6	9c	C	OH ^b	H	Et	Me ₃ Al	>70%	3:97

a) A: 2.0 equiv of allylBu₃Sn, 0.2 equiv of AIBN, hexanes, reflux. B: 2.0 equiv of allylBu₃Sn, 3.0 equiv of MgBr₂·OEt₂, 0.2 equiv of Et₃B, CH₂Cl₂, -78 °C. C: allylBu₃Sn, AIBN, *hν*, 3.0 equiv of Me₃Al, 10 °C. b) opposite config. to that shown

Addition of a Lewis acid to the allylation reaction in Table 2 has a dramatic effect on the stereochemical outcome of the reaction. In the reactions of **9a** and **9b**, the addition of $\text{MgBr}_2 \cdot \text{OEt}_2$ results in a very high preference for the formation of the anti products, **11a** and **11b**, respectively (entries 2 and 4). Addition of Me_3Al to the reaction of **9c** results in an increased selectivity for the anti product **11c** (entry 6). The inversion caused by the Lewis acid is believed to be due to chelation to the β -oxygen and the carbonyl of the ester, as depicted in Figure 2. Attack opposite the methyl in both conformations leads to products of the opposite configuration.

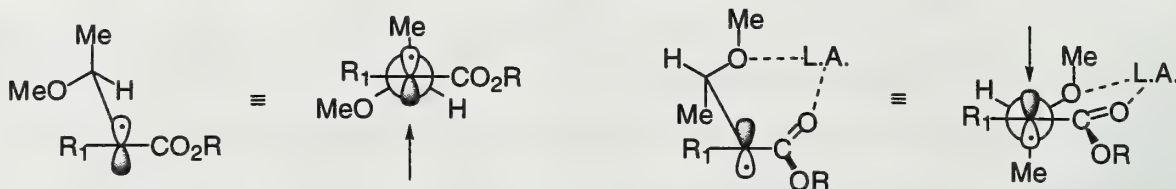


Figure 2. Unchelated and chelated conformations of β -methoxy esters.

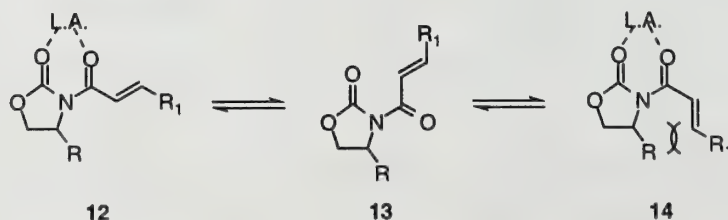
It has also been noted that the syn and anti diastereomers of starting materials **9a-9c** do not react with the same degree of stereoselectivity. The results given in Table 2 are with anti compounds **9a-9c**. If the syn starting material is used the product ratio in the presence of Lewis acid is decreased dramatically or even reversed. Both diastereomers of the starting materials react identically in the absence of Lewis acid. One possible explanation for this observation is that the syn Lewis acid-chelated reactant is less reactive than the non-chelated reactant.

LEWIS ACIDS WITH CHIRAL AUXILIARIES

An alternate approach to controlling the stereoselectivity of acyclic radical reactions involves the use of chiral auxiliaries. Oxazolidinones have been used with Lewis acids because they provide an additional site for chelation; they are also easily hydrolyzed and recovered. The key to this methodology lies in controlling the conformation of the substrate and blocking one face of the prostereogenic center. Lewis acids can be employed to rigidify the substrate in a single conformation.

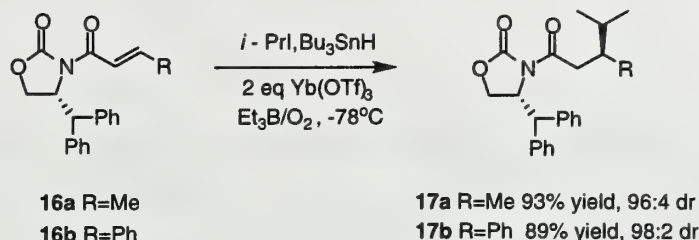
Conjugate additions to α,β -unsaturated systems with an oxazolidinone chiral auxiliary have been investigated by Sibi.¹⁴⁻¹⁶ For this type of substrate several conformations are conceivable (Scheme 1). The combination of chelation to a Lewis acid and steric effects would lead to **12** as the preferred conformer. With the proper choice of R group on the oxazolidinone, one face of the olefin can be blocked.

Scheme 1



Sibi has carried out extensive studies and found that the best results are obtained when the R substituent of the oxazolidinone is the large diphenylmethyl group. This chiral auxiliary was employed in several different conjugate radical additions. The addition of 2-iodopropane to the crotonate and cinnamate derivatives, **16a** and **16b**, in the presence of ytterbium triflate provided the addition products in high yields with excellent selectivity (Scheme 2).

Scheme 2



In the absence of Lewis acid, the reaction of **16a** provided **17a** in 60% yield and with a 56:44 dr. The major diastereomer in all of these reactions is the same. It has been proposed that the Bu_3SnI , which is a byproduct of the reaction, may serve as a weak Lewis acid. Although initial reactions were run in the presence of excess Lewis acid, the process has been shown to be catalytic in Lewis acid. The reaction of **16a** in the presence of 0.3 equivalents $\text{Yb}(\text{OTf})_3$ (relative to substrate) provided **17a** in 90% yield and with a 95:5 dr.

Sibi also investigated the conjugate radical addition to **18**. Orientation reactions involving ethyl radical addition and trapping of the intermediate radical with allyltributylstannane indicated $\text{MgBr}_2 \cdot \text{Et}_2\text{O}$ and $\text{Yb}(\text{OTf})_3$ to be the Lewis acids of choice. The effect of various R groups on the outcome of the reaction was also studied (Table 3).

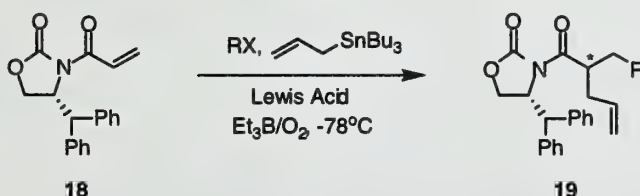


Table 3. Effect of the RX Group in Conjugate Radical Additions

Entry	RX	Lewis Acid	Product	Yield	Ratio ^a
1	EtI	---	19a	90%	50:50
2	EtI	$\text{MgBr}_2 \cdot \text{Et}_2\text{O}$	19a	93%	>99:1
3	MeI	$\text{MgBr}_2 \cdot \text{Et}_2\text{O}$	19b	82%	>99:1
4	<i>i</i> -PrI	$\text{MgBr}_2 \cdot \text{Et}_2\text{O}$	19c	85%	>99:1
5	<i>t</i> -BuI	$\text{MgBr}_2 \cdot \text{Et}_2\text{O}$	19d	94%	>99:1
6	$\text{C}_6\text{H}_{11}\text{I}$	$\text{MgBr}_2 \cdot \text{Et}_2\text{O}$	19e	93%	>99:1
7	MeOCH_2Br	$\text{Yb}(\text{OTf})_3$	19f	70%	98:2
8	MeCOBr	$\text{MgBr}_2 \cdot \text{Et}_2\text{O}$	19h	55%	98:2
9	PhCOBr	$\text{MgBr}_2 \cdot \text{Et}_2\text{O}$	19i	90%	98:2

a) absolute configuration of the newly formed stereogenic center in **19a** was determined to be S by hydrolysis and comparison to authentic compound, all other products were assumed to have the same absolute configuration as **19a**.

Addition of ethyl iodide in the absence of a Lewis acid provided racemic **19a** (entry 1). Addition of various alkyl iodides in the presence of $\text{MgBr}_2 \cdot \text{Et}_2\text{O}$ provided essentially one diastereomer (entries 2-6). Other functionalized radicals, including acyl radicals, could also be added and subsequently trapped by allyltributylstannane with excellent diastereoselectivity (entries 7-8).

The mode of stereo-induction for substrates **16** and **18** can be explained using the model shown in Figure 3. One of the large phenyl groups blocks the bottom face of the olefin (**16**) or the newly formed radical (**18**).

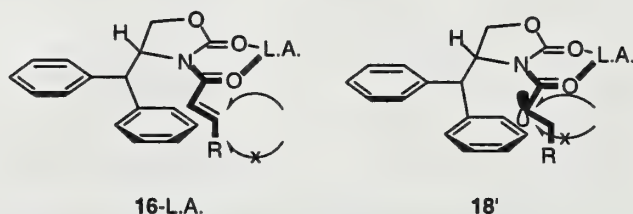
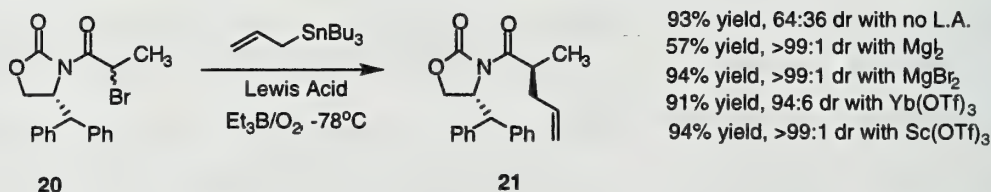


Figure 3. Model for the mode of stereo-induction in reactions involving chiral auxiliaries.

Another type of reaction employing the 4-(diphenylmethyl)-2-oxazolidinone auxiliary is that of a radical group transfer. As shown in Scheme 3, treating α -bromide **20** with allyltributylstannane in the presence of a Lewis acid provides the allyl product **21**. The extremely high stereoselectivity induced in **21** can be explained using the same models as proposed in Figure 3.

Scheme 3

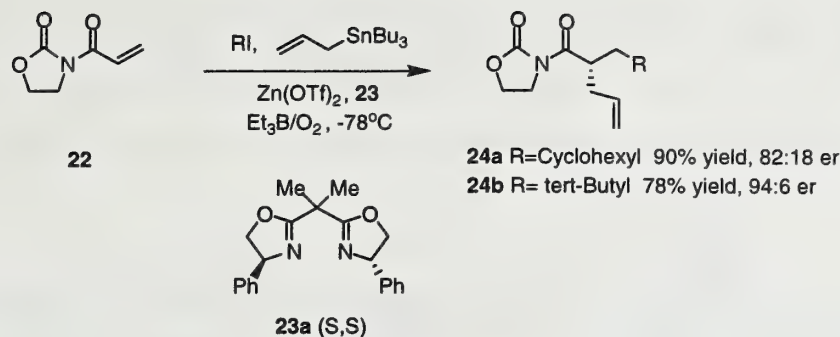


CHIRAL LEWIS ACIDS

The most recent advance in asymmetric radical reactions involves the utilization of Lewis acids in conjunction with chiral ligands. The resulting "chiral Lewis acids" require two sites for coordination to hold the substrate in a single conformation. An achiral auxiliary, commonly an oxazolidinone, has been used in most cases as the second site of coordination.

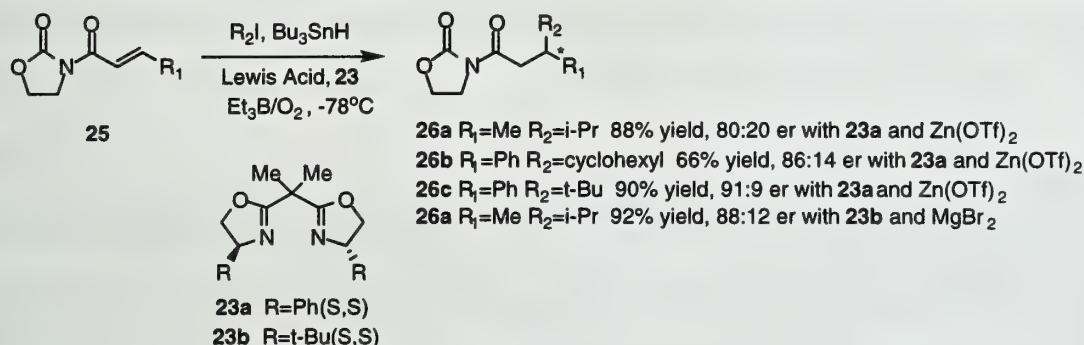
Porter developed the first successful chiral Lewis acid mediated radical reaction.¹⁷ A conjugate radical addition sequence similar to that shown in Table 3 was employed with the oxazolidinone auxiliary unsubstituted in the four position. Zinc triflate was chosen as the Lewis acid and a variety of chiral bisoxazolines were explored as ligands. Cyclohexyl and *tert*-butyl radicals were added to **22** in the presence of **23a** to provide the addition products (Scheme 4).

Scheme 4

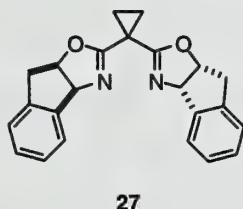


Sibi has extended the work with chiral Lewis acids,¹⁸ using **23a** and **23b** in radical conjugate additions of the type shown in Scheme 5. Cinnamate and crotonate were used as the starting substrates, with the addition of *i*-Pr, *tert*-Bu, and cyclohexyl radicals providing the addition products **26**. Some general trends were found in these experiments: the chiral ligand **23a** gave the best results when used with zinc triflate while **23b** performed better when used with a magnesium Lewis acid.

Scheme 5



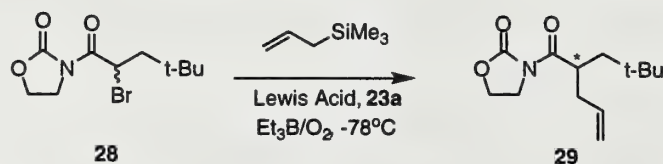
More recently it has been shown that utilization of more rigid chiral bisoxazolines results in greater selectivity.¹⁹ The bisoxazoline **27** was found to give the highest selectivity. With MgI₂ and **27** the addition of *i*-Pr radical to the cinnamate derivative of **25** (R₁ = Ph) provided **26** (R₁ = Ph R₂ = *i*-Pr) in 88% yield with a 96:4 er. It was also demonstrated that **27** was effective catalytically in the same reaction, providing the product in 92% yield (95:5 er) with only 5 mole % of Lewis acid and ligand.



Porter²⁰ and Renaud²¹ have both recently reported that chiral Lewis acids are also fairly successful in enantioselective group transfer reactions. Porter has used the chiral ligands **23a** and **23b** in allyl transfer reactions with good enantioselectivity. Scheme 6 shows the reaction of **28** with

allyltrimethylsilane. When zinc triflate was used as the Lewis acid, (R)-**29** was formed in 88% yield with a 95:5 er. Interestingly, when magnesium iodide was used as the Lewis acid (S)-**29** was formed in 86% yield with a 84:16 er. Therefore, the same chiral ligand can provide either configuration of **29** depending on the partner Lewis acid. This reversal of selectivity is not entirely understood at this time.

Scheme 6



CONCLUSIONS

Significant advances have been made in asymmetric radical reactions on acyclic systems. Much of the progress in this area is due to the employment of Lewis acids which can stabilize a single conformer of a reactive intermediate. Lewis Acids have been effective in enhancing the diastereoselectivity in 1,2-induction and chiral auxiliary reactions. They have also allowed for enantioselective reactions using chiral Lewis acids.

REFERENCES

- (1) Motherwell, W. B. and Crich, D. *Free Radical Chain Reaction in Organic Synthesis*; Academic Press: San Diego, 1993.
- (2) Giese, B. *Angew. Chem. Int. Ed. Engl.* **1983**, *22*, 753.
- (3) Curran, P. C.; Porter, N. A.; Giese, B. *Stereochemistry of Radical Reactions*; VCH: Weinheim, 1996.
- (4) Giese, B. *Angew. Chem. Int. Ed. Engl.* **1989**, *28*, 969.
- (5) Porter, N. A.; Giese, B.; Curran, D. P. *Acc. Chem. Res.* **1991**, *24*, 296.
- (6) Smadja, W. *Synlett* **1994**, 1.
- (7) Renaud, P.; Bourquard, T.; Gerster, M.; Moufid, N. *Angew. Chem. Int. Ed. Engl.* **1994**, *33*, 1601.
- (8) Guindon, Y.; Lavallee, J.; Brunet, M.; Horner, G.; Rancourt, J. *J. Am. Chem. Soc.* **1991**, *113*, 9701.
- (9) Nagano, H.; Kuno, Y. *J. Chem. Soc., Chem. Commun.* **1994**, 987.
- (10) Guindon, Y.; Guerin, B.; Chabot, C.; Mackintosh, N.; Ogilvie, W. *Synth. Lett.* **1995**, 449.
- (11) Gerster, M.; Audergon, L.; Moufid, N.; Renaud, P. *Tetrahedron Lett.* **1996**, *37*, 6335.
- (12) Renaud, P. *Chimia* **1996**, *50*, 135.
- (13) Guindon, Y.; Guerin, B.; Chabot, C.; Ogilvie, W. *J. Am. Chem. Soc.* **1996**, *118*, 12528.
- (14) Sibi, M.; Jasperse, C.; Ji, J. *J. Am. Chem. Soc.* **1995**, *117*, 10779.
- (15) Sibi, M.; Ji, J. *J. Org. Chem.* **1996**, *61*, 6090.
- (16) Sibi, M.; Ji, J. *Angew. Chem. Int. Ed. Engl.* **1997**, *36*, 274.
- (17) Wu, J.; Radinov, R.; Porter, N. *J. Am. Chem. Soc.* **1995**, *117*, 11029.
- (18) Sibi, M.; Ji, J. *J. Am. Chem. Soc.* **1996**, *118*, 9200.
- (19) Sibi, M.; Ji, J. *J. Org. Chem.* **1997**, *62*, 3800.
- (20) Porter, N.; Wu, J.; Zhang, G.; Reed, A. *J. Org. Chem.* **1997**, *62*, 6702.
- (21) Fhal, A.; Renaud, P. *Tetrahedron Lett.* **1997**, *38*, 2661.

VINYL BORANES AS SYNTHONS TO UNREACTIVE AND UNSTABLE DIENOPHILES FOR USE IN DIELS ALDER REACTIONS

Reported by Bryce Assink

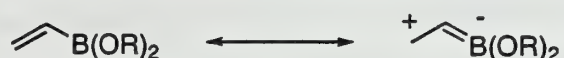
March 2, 1998

INTRODUCTION

The use of synthetic equivalents in Diels Alder reactions has allowed access to desired products unattainable from certain dienophiles due to their low reactivity (e.g.: ethylene, acetylene, vinyl alcohol), self-destructive nature (e.g.: ketene), or lack of regioselectivity (e.g.: unactivated olefins). Vinyl boranes can be used as synthetic equivalents of these ineffective dienophiles. In most cases the regioselectivity, and in some cases the stereoselectivity can be controlled through simple modifications of the olefin and boron substituents.¹⁻³ Compatibility with electron-rich, electron-poor, and neutral dienes lends general synthetic utility to these dienophiles.⁴ This report will discuss the mechanism of Diels Alder reactions with boron dienophiles, explore the reactivity of the dienophiles, and discuss the various olefins and boron substituents to date.

MECHANISM

Vinyl boronic esters were first predicted to be dienophiles by Matteson⁵ in 1960. Based on electron densities derived from molecular orbital calculations, Matteson proposed the existence of resonance between the vinyl group and the empty 'p' orbital on the boron. The possibility of resonance



inspired the prediction that 1 would be a good dienophile and could also be subjected to electrophilic and nucleophilic attack at C_α and C_β, respectively. Subsequent research^{1,6-8} proved his prediction of dienophilicity to be correct, but not entirely for the right reason.^{4,9} In 1992, ¹³C NMR experiments on vinyl borane showed that the double bond character between C and B is very limited.⁴ This apparent lack of appreciable resonance casts doubt upon the hypothesis that vinyl boranes and boronic esters are electron-poor dienophiles. Furthermore, detailed *ab initio* calculations of the exo/endo transition states gave surprising results (Figure 1).⁹ The exo transition state was [4 + 2] in character. The endo transition structure, however, was [4 + 3] in character, showing C₁ to be closer to the boron atom than to C_α. In support of this transition state, calculated LUMO coefficients were consistently small for C_α and large for boron and C_β. The *ab initio* calculations also showed a preference for the endo transition structure

over the *exo* by 2.3 kcal·mol⁻¹. Thus, for the preferred *endo* pathway, boron is not an activating group, but instead an active participant in the Diels Alder reaction.

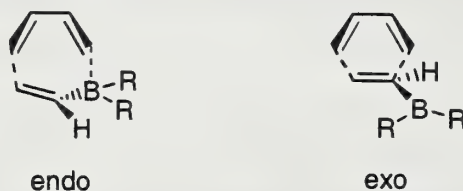
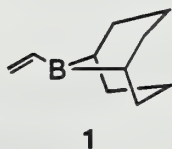


Figure 1. *Ab initio* calculated transition structures for *endo* and *exo* dienophile orientation. *Endo* structure has boron positioned under the diene. *Exo* structure has hydrogen positioned under the diene.

REPRESENTATIVE BORON DIENOPHILE: VINYL-9-BBN

Selectivity

Early work in this area dealt with vinyl boronic esters and vinyl dihaloboranes as dienophiles. These papers report high temperatures, long reaction times, low reactivity, and low selectivity for reactions of these dienophiles with various dienes.^{6,7,10} Against this backdrop Singleton and coworkers decided to test the dienophilicity of vinyl dialkylboranes, specifically vinyl-9-BBN (**1**). They discovered that **2** is highly regio- and *endo*-stereoselective (Table 1) and that **1** is significantly more



reactive than many other neutral activated dienophiles.^{1,4} The only examined dienophiles faster were Lewis Acid complexed dienophiles and α,β -unsaturated Fischer carbene complexes.¹ The observed regioselectivities are influenced by the steric bulk of the borabicyclononane group. For the most part, the regioisomer favored is the one that minimizes the interactions of the borabicyclononane with substituents on the diene: “*para*” is preferred to “*meta*” and “*meta*” is preferred to “*ortho*.” The observed stereoselectivities are notable because they are greater than those reported for Lewis Acid catalyzed Diels Alder reactions, with the exception of cyclopentadiene. The *endo* stereoselectivity is a result of the transition structure preference discussed earlier. The reduced *endo:exo* ratio with the cyclopentadiene adducts is a result of steric interactions with the methylene group of cyclopentadiene.

Omniphilicity

One intriguing aspect of vinylboranes is its classification of dienophile. Because the boron plays an active role in the preferred [4 + 3] transition state, the diene has very little influence upon the reaction rate. 9-Vinyl-BBN is known to react with electron-rich, electron-poor, and unactivated dienes with minimal rate change (Table 2). A σ - ρ study using 2-arylbutadienes gave a ρ value of -0.01 ± 0.10 . These results compelled Singleton, and co-workers to describe vinylboranes as omniphilic dienophiles.⁴

Table 1. Products and Yields for Diels-Alder Reactions with Vinyl-9-BBN


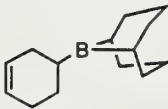
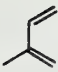
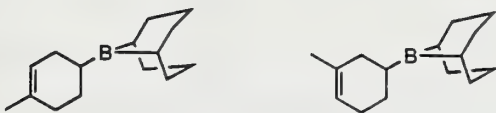

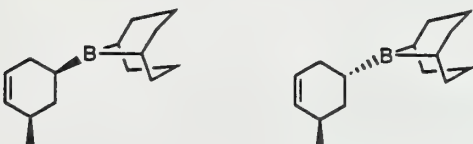
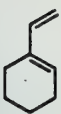
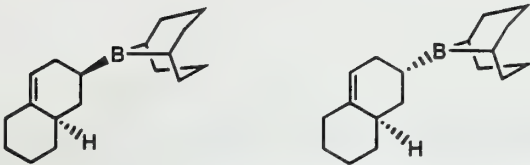

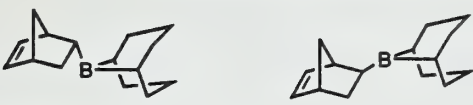
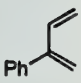
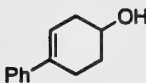
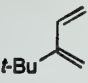
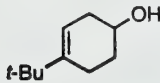
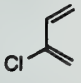
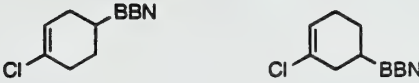
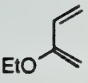
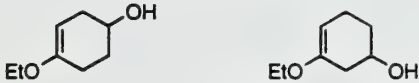
Diene	Reaction Conditions	Yield	Ratio	Product(s)
	25 °C, 30 h MeCl ₂	82%	NA	
	25 °C, 30 h MeCl ₂	79%	93:7	
	25 °C, 30 h MeCl ₂	71%	92:8	
	55 °C, 48 h MeCl ₂	72%	96:4	
	25 °C, 3.5 h MeCl ₂	86%	2:1	
	1. 25 °C, MeCl ₂ , 23 h 2. NaBO ₃ ·4H ₂ O	97%	NA	
	1. 25 °C, MeCl ₂ , 24 h 2. H ₂ O ₂ , NaOH	93%	NA	
	55 °C, 12 h MeCl ₂	75%	91:10	
	1. 55 °C, MeCl ₂ , 4 days 2. H ₂ O ₂ , NaOH	58%	69:31	

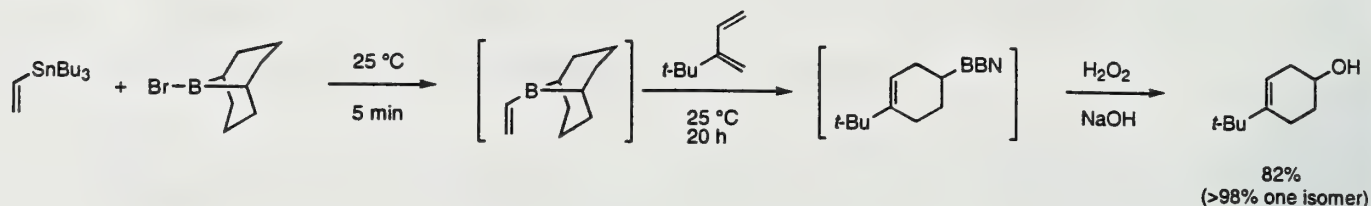
Table 2. Diene Structure vs. Reactivity for Vinyl-9-BBN and Maleic Anhydride

Diene	k_{rel} (25 °C) Vinyl-9-BBN	k_{rel} (25 °C) Maleic anhydride
2,3-Dichlorobutadiene	0.34	0.0047
2-Chlorobutadiene	1.3	0.1
Butadiene	1	1
	($k=3.2 \times 10^{-6}$)	($k=5.3 \times 10^{-5}$)
Isoprene	0.94	3
2-(M)ethoxybutadiene ^a	0.17	10
2-Phenylbutadiene	72	8.8
2-tert-Butylbutadiene	13	28
Cyclopentadiene	22	1160

^a2-Ethoxybutadiene for vinyl-9-BBN, 2-methoxybutadiene for maleic anhydride

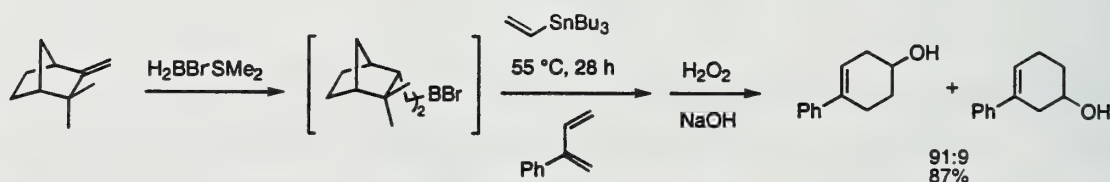
Preparation and Catalytic Cycle

The high reactivity and selectivities of vinyl boranes make them attractive dienophiles, but instability and a highly pyrophoric nature are practical drawbacks that prevent widespread use. The recent developments of *in situ* preparations of vinylboranes overcome these limitations (Scheme 1).^{11,12} The tin-boron exchange is fast, efficient, and proceeds at room temperature. Reaction with diene and oxidation of the carbon-boron bond is clean and takes place in the same reaction vessel. An extension of

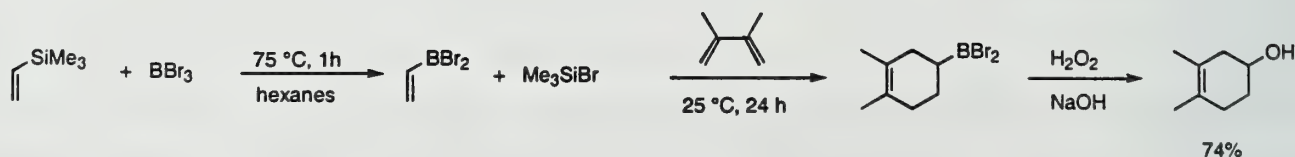


this scheme provides one with the option of choosing the boron substituent (Scheme 2).¹¹ Silicon-boron exchange was recently suggested as a way to avoid using tin reagents. This exchange is slower and requires heat, yet the yields are similar to those for tin-boron exchange for the dienes reacted (Scheme 3).¹²

Scheme 2



Scheme 3



Based on the boron-tin exchange, acetylene synthetic equivalents have been proposed utilizing a catalytic amount of either BCl_3 or 9-halo-BBN (Scheme 4).¹³ BCl_3 works faster and at a lower temperature than 9-halo-BBN, yet both give similar yields (Table 3). Similarly, 9-BBN has been used to catalytically activate 1-octyne for Diels Alder reaction (Scheme 5). 9-BBN adds across the triple bond to give a trans dienophile which eliminates 9-BBN after cyclizing with a diene. The reaction conditions shown are not ideal, but this does show considerable generality for the idea of temporary covalent activation.¹³

Scheme 4

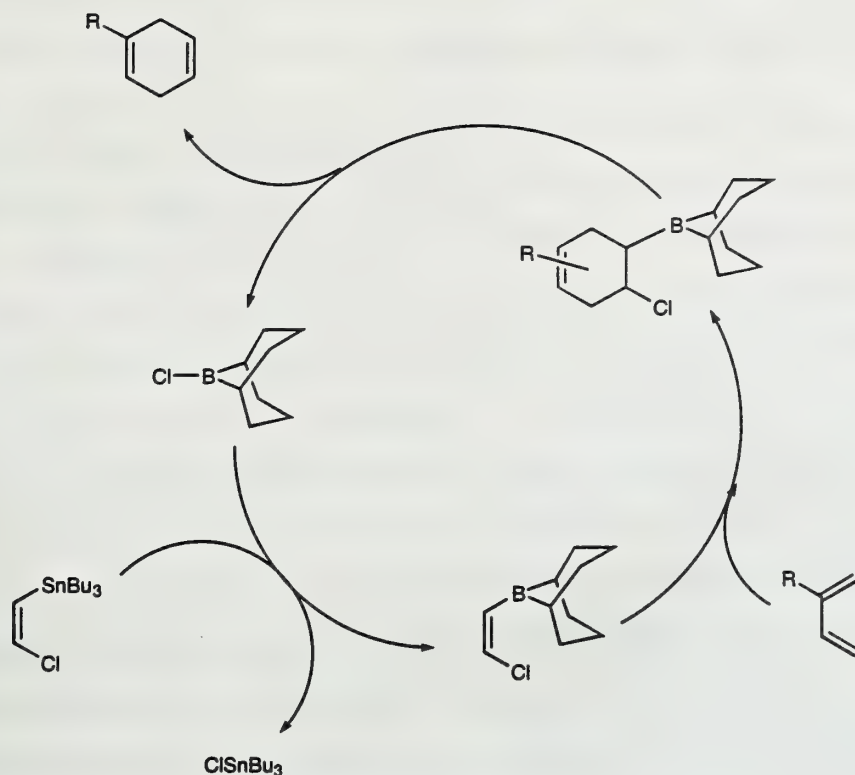
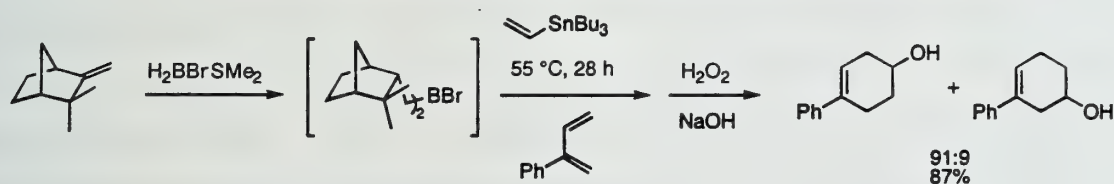


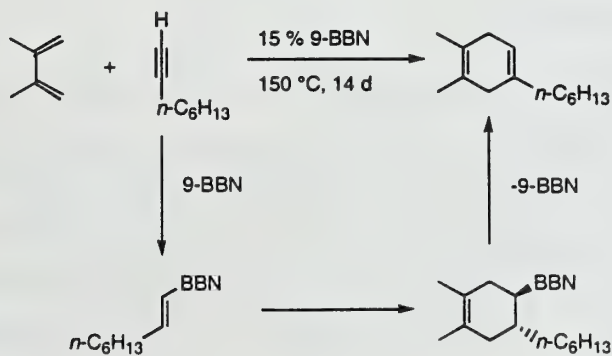
Table 3. Conditions and Yields for Catalytic Vinylborane Reactions



R = Ph		
Reaction Conditions	Yield	
140 °C, 24 h	3%	
15 mol % BCl ₃ 25 °C, 48 h	71 %	
15 mol % Br-BBN 60 °C, 144 h	78 %	

R = <i>t</i> -Bu		
Reaction Conditions	Yield	
80 °C, 120 h	5%	
15 mol % BCl ₃ 25 °C, 96 h	74 %	
20 mol % Cl-BBN 80 °C, 240 h	73 %	

Scheme 5



VARIATIONS OF THE BORON SUBSTITUENTS

Different substituents on boron will alter the reactivity and the selectivity of the dienophile. Most early work in this area concentrated on boronic esters and acids. Unfortunately, vinylboronates are among the less reactive and selective dienophiles, so most research was for comparison purposes. For example, Matteson reported yields ranging from 65% to as little as 1% for the reaction of cyclopentadiene with various vinylboronates. Endo:exo ratios varied from 3:2 to 1:4 for boronic acid and the more bulky ester groups, respectively.⁶ Experiments with 1,3-cyclohexadiene showed slight improvement with 71% yield, 4:1 endo:exo isomer.¹⁰ In a paper on ketene equivalents, Evans compared the Diels Alder reactions of 2-acetoxyacrylonitrile, 2-chloroacrylonitrile and di-*tert*-butyl vinylboronate with some dienes. Besides requiring higher temperatures and longer reaction times, the stereoselectivity of the boronate was the lowest.⁷ Overall product yield for boronate, however, was the highest of the three. For this reason, Evans employed di-*n*-butyl vinylboronate as a ketene equivalent in the total synthesis of (\pm)-dihydrocannivonine.⁸ Fresneda reported the first synthesis and Diels Alder reaction of pinacol vinylboronates β -substituted with an electron withdrawing group on the olefin.¹⁴ These would be expected to have better reactivity than an unsubstituted vinyl boronate. The reaction conditions for the vinylboronate synthesis were mild and the yields were quite good. Subsequent reaction with cyclopentadiene gave reasonable endo stereoselectivity with high yields. Vaultier recently recognized that the electron-withdrawing groups could also act as synthetic equivalents.¹⁵ This recognition opened up a pathway for several subsequent transformations with reasonable yields.¹⁵

After the success of vinyl-9-BBN, the synthesis of other vinylalkylboranes was inevitable. Reports describing the synthesis, handling, reactivity, regioselectivity and stereoselectivity of vinylalkylboranes followed.^{3,16} Although all displayed consistent reactivity and endo selectivity, the regioselectivity could be controlled to a very high degree. The synthesis and handling of each vinylalkylborane was made trivial by the *in situ* procedure described earlier.¹¹

VARIATIONS OF THE DIENOPHILE

Vinylboranes have proved to be good ethylene and vinyl alcohol equivalents. By adding substituents or changing the structure of the dienophile, various other synthetic equivalents are possible. Dibutyl acetyleneboronate is a moderate acetylene equivalent and a poor ketene equivalent,¹⁷ but 2-TMS-ethynyl-9-BBN proved to be an effective acetylene equivalent with an unusual preference for the 1,3-disubstituted ("meta") product.¹⁸ *Ab initio* calculations provided a transition state in which the

boron was closer to the diene than C $_{\alpha}$ (similar to that shown in Figure 1). In this case, however, there was advanced bonding between boron and C $_1$ compared to C $_4$ and C $_{\beta}$ (Figure 2). This resulted in a relatively positive charge on C $_2$ compared to C $_3$. The presence of a donating group on C $_2$ would stabilize this charge, leading to the observed adduct. Alternatively, Diels Alder cycloaddition of 2-TMS-vinylborane followed by oxidation and elimination gave the 1,4-disubstituted ("para") product.²⁰

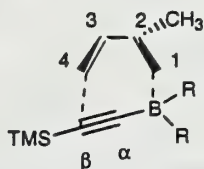
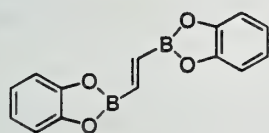
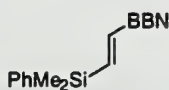


Figure 2. Transition structure for 2-TMS-ethynyl-9-BBN reacting with piperylene. C $_1$ is closer to the boron atom than C $_4$ is to C $_{\beta}$.

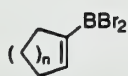
Other interesting olefin substituent variations include *trans*-1,2-bis(catecholboryl)ethylene (**3**) and 2-phenyldimethylsilylvinyl-9-BBN (**4**).¹⁹ Both work well as *trans*-1,2-vinyl alcohol equivalents: **3** having greater reactivity and higher yield, **4** having differentiable latent alcohols. Cycloalkenyldibromoboranes (**5**) have been shown to be highly reactive and, in most cases, completely regio- and stereoselective. The product bridgehead bicyclic alcohols can exhibit diverse functionality in good yield with conveniently chosen dienes.²⁰ There are also reports about intramolecular Diels Alder reactions to produce bicyclic adducts.^{21,22} Both involve hydroboration or transmetalation across a terminal alkyne which, thus activated, reacts stereoselectively with a nearby diene to give the bicycle with three new, contiguous stereocenters (**6**).



3

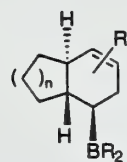


4



n=1,2

5



n=1,2

6

CONCLUSIONS

Highly reactive dienophiles with controllable regioselectivity and endo stereoselectivity are readily available with a wide variety of inherent synthetic equivalency. The options for catalytic use, *in situ* reagent preparation, and polycyclic products make these attractive dienophiles. Future work should explore the possibilities of asymmetric induction and photochemical cycloaddition.

REFERENCES

1. Singleton, D. A.; Martinez, J. P. *J. Am. Chem. Soc.* **1990**, *112*, 7423.
2. Singleton, D. A.; Martinez, J. P. *Tetrahedron Lett.* **1991**, *32*, 7365.
3. Singleton, D. A.; Martinez, J. P.; Watson, J. V.; Ndip, G. M. *Tetrahedron* **1992**, *48*, 5831.
4. Singleton, D. A.; Martinez, J. P.; Watson, J. V. *Tetrahedron Lett.* **1992**, *33*, 1017.
5. Matteson, D. S. *J. Am. Chem. Soc.* **1960**, *82*, 4228.
6. Matteson, D. S.; Waldbillig, J. O. *J. Org. Chem.* **1962**, *28*, 366.
7. Evans, D. A.; Scott, W. L.; Truesdale, L. K. *Tetrahedron Lett.* **1972**, 121.
8. Evans, D. A.; Golob, A. M.; Mandel, N. S.; Mandel, G. S. *J. Am. Chem. Soc.* **1978**, *100*, 8170.
9. Singleton, D. A. *J. Am. Chem. Soc.* **1992**, *114*, 6563.
10. Matteson, D. S.; Talbot, M. L. *J. Am. Chem. Soc.* **1967**, *89*, 1123.
11. Singleton, D. A.; Martinez, J. P.; Ndip, G. M. *J. Org. Chem.* **1992**, *57*, 5768.
12. Singleton, D. A.; Leung, S. W. *J. Organomet. Chem.* in press.
13. Singleton, D. A.; Leung, S. W.; Martinez, J. P.; Lee, Y. K. *Tetrahedron Lett.* **1997**, *38*, 3163.
14. Martinez-Fresneda, P.; Vaultier, M. *Tetrahedron Lett.* **1989**, *30*, 2929.
15. Rasset, C.; Vaultier, M. *Tetrahedron* **1994**, *50*, 3397.
16. Singleton, D. A.; Kim, K.; Martinez, J. P. *Tetrahedron Lett.* **1993**, *34*, 3071.
17. Matteson, D. S.; Peacock, K. *J. Am. Chem. Soc.* **1960**, *82*, 5759.
18. Singleton, D. A.; Leung, S. W. *J. Org. Chem.* **1992**, *57*, 4796.
19. Singleton, D. A.; Redman, A. M. *Tetrahedron Lett.* **1994**, *35*, 509.
20. Lee, Y. K.; Singleton, D. A. *J. Org. Chem.* **1997**, *62*, 2255.
21. Singleton, D. A.; Lee, Y. K. *Tetrahedron Lett.* **1995**, *36*, 3473.
22. Batey, R. A.; Lin, D.; Wong, A.; Hayhoe, C. L. S. *Tetrahedron Lett.* **1997**, *38*, 3699.

TECHNIQUES FOR THE STRUCTURAL IDENTIFICATION OF ACTIVE MOLECULES WITHIN COMBINATORIAL LIBRARIES

Reported by Jennifer L. Poole

March 12, 1998

INTRODUCTION

Combinatorial chemistry has become one of the most promising approaches for generating molecular diversity. New methodologies are continually emerging for the rapid synthesis of large libraries of peptides and oligonucleotides,¹ as well as for small organic molecules.^{2,3} Screening of these libraries has led to the discovery of compounds with novel biological activity. Historically, combinatorial chemistry has focused on the construction of peptide and oligonucleotide libraries for drug discovery because their synthesis is well established.¹ However, these compounds have limited utility as therapeutic agents due to their poor bioavailability and rapid *in vivo* clearance.² Small organic molecules, on the other hand, have favorable pharmacokinetic properties and emphasis has been focused on the combinatorial synthesis of libraries of these compounds.

Although library design, synthesis and activity screening are important issues in the development and application of combinatorial libraries, structural elucidation of the active member(s) in an assay provides a major challenge for the combinatorial process.⁴ Peptide and oligonucleotide libraries are easily "deconvoluted" because their structures are readily revealed using standard sequencing methodologies.^{5,6} Small molecule (< 600 – 700 molecular weight) libraries, on the other hand, are difficult to characterize because there is a high probability that many different compounds will have similar molecular weights, complicating structural identification.² This report describes several novel techniques that have been reported to circumvent the structural elucidation problem of small molecule combinatorial libraries.

SYNTHESIS STRATEGIES FOR SMALL MOLECULE LIBRARIES

Combinatorial chemistry encompasses the rapid synthesis of large, organized collections of compounds called libraries. The rise of this technology has been primarily facilitated by the application of solid-phase synthesis (SPS).³ A solid support allows for the production of products as separate entities such that reagents and by-products not bound to the resin can be washed away. Numerous examples of the application of solid-phase synthesis to the construction of small molecule libraries have been reported.²

In general, libraries of compounds are produced either as discrete units (i.e. individual compounds in the wells of a 96-well plate) or as large mixtures of many different compounds.

Identification of compounds synthesized in a discrete format (parallel synthesis) is easily accomplished because the identity of a library member is confirmed by its location in the array. Due to advances in automation, the parallel synthesis of small ($10^1 - 10^3$) libraries of organic compounds has been readily achieved.⁷ In addition, Fodor has introduced the use of photolabile protecting groups to direct the synthesis of larger ($> 10^4$) libraries of spatially separate compounds.^{8,9}

Very high volume ($10^4 - 10^6$) library synthesis, however, is best accomplished using the "split and mix" strategy pioneered by Furka for the generation of peptide libraries.¹⁰ Solid supports upon which reactions occur are repooled for each step in a combinatorial synthesis such that $a + b + c$ reactions result in the production of $a \times b \times c$ reaction products. Although great diversity in structure can be achieved, the major challenge to the generation of combinatorial libraries in this manner is the structural elucidation of biologically active compounds in the mixture. A number of different strategies have been developed for the evaluation of libraries that are prepared by split synthesis. These techniques follow two basic strategies: (1) the production and deconvolution of untagged libraries and (2) the production and decoding of tagged libraries.

DECONVOLUTION STRATEGIES

Iterative Deconvolution

Geysen¹¹ was the first to report the use of a technique for the deconvolution of a soluble compound library after cleavage from the solid support. In this approach, pools of compounds are generated with one or more defined positions and the remaining sites built from all combinations of building blocks (Figure 1). Screening of these pools for biological activity identifies the optimal building block at the defined position. Iterative synthesis and screening of compound pools with this defined site(s) ultimately identifies the most active compound in the library. The number of library elements in each sublibrary decreases until only a single compound is present in each pool, thus identifying the active compound. This process has been employed in the deconvolution of a 100-member dihydropyridine library.¹²

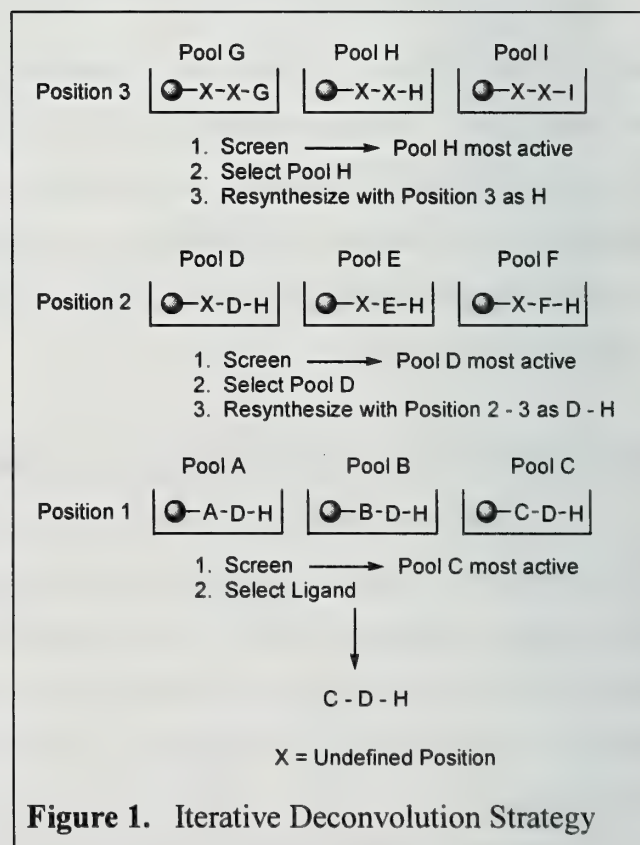


Figure 1. Iterative Deconvolution Strategy

A simpler procedure, termed “recursive deconvolution” was reported by Janda *et al.*¹³ By saving a portion of the library pool after each combinatorial step in a “split and mix” synthesis, a series of partial sublibraries are available for resynthesis and deconvolution. Screening and identification of the active compound is then achieved by screening of the final library pools and proceeding backward through the partial libraries saved.

A virtue of these iterative methods is that the multiplicity of components decreases with each step so that there is an enrichment process.¹⁴ However, several issues must be addressed when considering this technique. First, as the number of compounds in a library increases, the concentration of individual compounds decreases. Thus, even compounds with modest activity may not be detected. In addition, the pool with the most potent compound may not show the greatest biological activity, because activity depends greatly upon the abundance of the active compound in the pool.

Positional Scanning

Positional scanning is a modification to the traditional iterative deconvolution strategy where all sublibraries of a combinatorial library, each having one defined position, are individually synthesized. Determination of the most active position in each subset of libraries elucidates the structure of an active compound. This technique attempts to address the limitations to iterative deconvolution by obviating the need for time-consuming resynthesis and rescreening of sublibraries. Although pioneered by Houghten for the synthesis of peptide libraries,¹⁵ an identical strategy has emerged for the preparation of small organic molecule libraries. Pirrung has developed a positional scanning technique that involves the solution pool synthesis of an indexed combinatorial library.¹⁶ In a representative

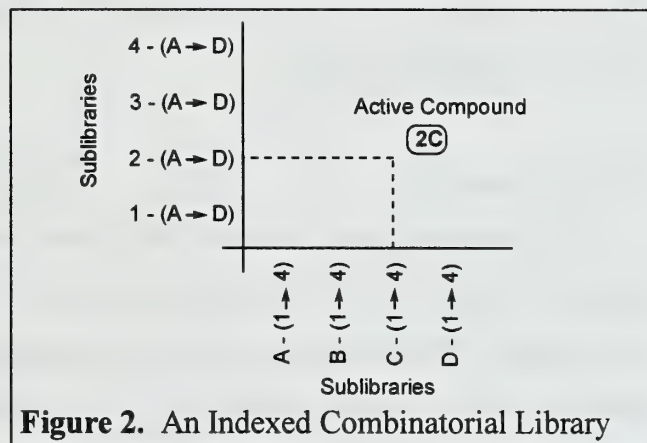


Figure 2. An Indexed Combinatorial Library

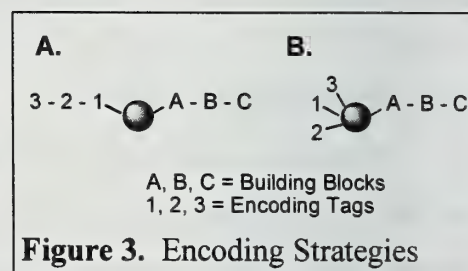
combinatorial synthesis, each member of a building block set ($A \rightarrow D$, Figure 2) was individually coupled with a mixture of the building blocks in the second set ($1 \rightarrow 4$, Figure 2) to make 4 sublibraries of 4 compounds with one position defined in each sublibrary. The same procedure was used to couple individual building blocks $1 \rightarrow 4$ with a mixture of $A \rightarrow D$, to form 4 more sublibraries. These sublibraries are considered to form a 2-D matrix in which the first position of a ‘dimer’ varies along one axis and the second position varies along the other axis. Organization of these pools along a matrix allows two pools on different axes to have only one single compound in common. Thus, identification

of the two most active pools identifies a potent compound in the library. This strategy has been used to identify a novel acetylcholinesterase inhibitor from a 54-member carbamate library and a 72-member tetrahydroacridine library.¹⁷

ENCODING STRATEGIES

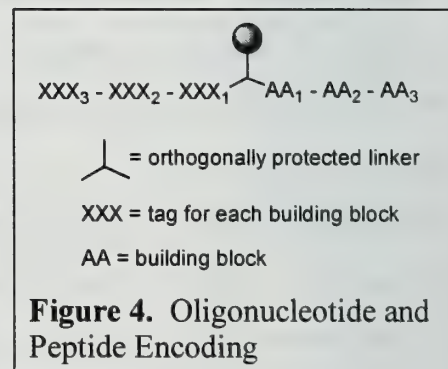
Alternatives to deconvolution strategies involve the encoding of a resin bound library member with a tag or code that 'carries' information concerning the compound within it. In this approach, readable tags that record a reaction sequence are attached to the resin bead concurrently with the synthesis of the compound. Decoding of the tag identifies the structure of the library compound attached to the resin bead. Thus, no resynthesis of compound libraries is needed.

Two methods for encoded combinatorial chemistry have been explored. The first involves the co-synthesis of an encoding sequence, made of individual tag molecules on a resin bead (Figure 3A). The structure of each tag identifies a unique building block in the library synthesis and the location of each tag in the sequence indicates the synthesis step in which the building block was added. In an alternative method, each tag can be added directly to the resin bead such that it individually identifies the building block as well as the library synthesis step in which it was added (Figure 3B). The use of both chemical and non-chemical tags has been reported.



Chemical Encoding

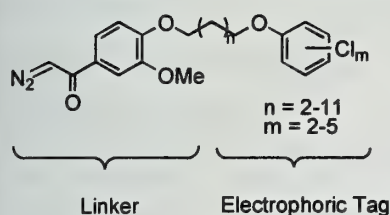
Brenner and Lerner were the first to propose a novel strategy that allows for the co-synthesis of a sequenceable tag with that of the library element.¹⁸ The tag and the corresponding library element are associated via an orthogonally protected linker group attached to a resin bead (Figure 4). Alternating combinatorial syntheses are performed to chemically link the tag (coding strand) with the library element (binding strand). Following identification and isolation of an active library member, detachment of the linker group from the resin bead and subsequent sequencing of the coding strand leads to structure determination of the library element. The ordering of each individual tag in the full tag sequence encodes the sequence of individual steps of the library synthesis. Both oligonucleotides¹⁸⁻²⁰ and peptides²¹⁻²³ have been reported for this technique because sequencing of their structures is a facile process.^{5,6} These tagging strands, however, may have the



potential to be mutually incompatible with the library synthesis strategy. In addition, extensive protecting group manipulations, due to the orthogonally protected linker group, require selective synthetic strategies that may not be amenable to certain compound classes. Moreover, the oligonucleotide or peptide tags may themselves interact with biological receptors, negating the effect of the library member or falsely identifying an inactive molecule.

Ohlmeyer and Still have devised an alternative tagging method that circumvents the limitations associated with oligonucleotide or peptide tagging.²⁴ They have reported the use of GC-separable, chemically inert haloaromatic alkanol tags to encode a set of chemical reactions (or reagents) in a combinatorial synthesis (Figure 5). At each step of the synthesis, the tag(s) are attached directly to the polymer resin bead through a linker group. Hence, no co-synthesis or orthogonal protecting groups are needed and the code is not directly connected to the library element. Tag addition to the resin is controlled so that only a small percentage of the growing library element is capped or modified by the tag. After synthesis and screening, tag mixtures are cleaved from the resin and analyzed by electron capture gas chromatography. The presence or absence of the individual tagging molecule forms a binary record of the synthetic steps performed on that bead.

I. Diazaketone Linker



II. Nitrobenzoic Acid Linker

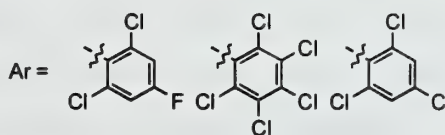
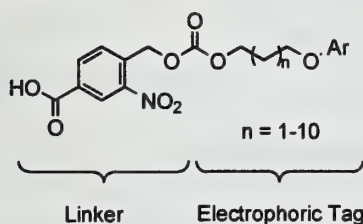


Figure 5. Haloaromatic Alkanol Tags

Two different tag attachment and detachment mechanisms have been reported for the generation of small molecule combinatorial libraries. Tags containing a diazaketone functionality can be attached directly to any unfunctionalized resin bead (I, Figure 5).²⁵ Alternatively, a nitrobenzoic acid linker can be used to attach the tag to any amine functionalized resin (II, Figure 5).^{24, 26}

Ni *et al.* reported a variation to this methodology using chemically robust secondary amines as tagging molecules (Figure 6).²⁷ The tags were attached to each other through an amide bond. An orthogonal

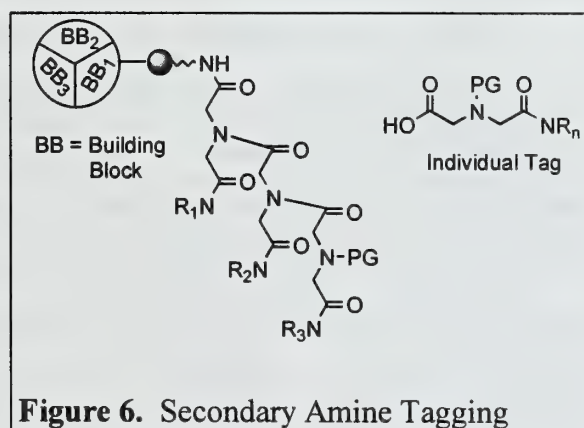


Figure 6. Secondary Amine Tagging

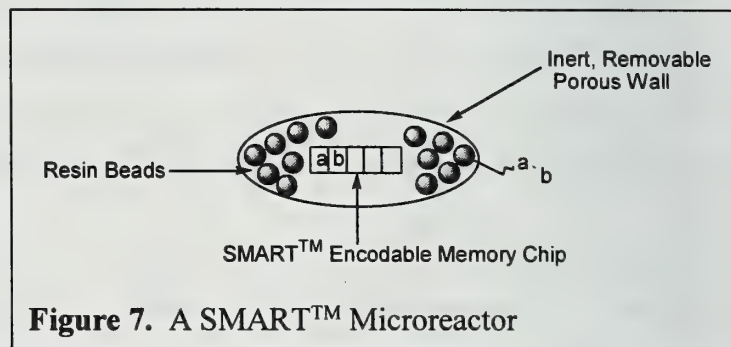
amine protecting group was used to differentiate tag addition from library synthesis. Thus, ligand corruption is avoided. Tag detachment was achieved by acidic hydrolysis, and the secondary amines were analyzed as their dansyl derivatives by reverse-phase HPLC. This approach has been used in the generation of a large (~50,000 member) encoded library of various heterocyclic compounds and a small library of functionalized pyrrolidines.²⁸

Through the introduction of chemically inert tags such as halocarbons and secondary amines, the stability problems associated with oligonucleotide and peptide tagging are avoided. In addition, the possible interference of the tag during biological assays is eliminated to a degree. However, the use of a molecular tagging system requires tedious tag synthesis, attachment, analysis and subsequent decoding that may not be compatible with the combinatorial chemical synthesis being explored.

Radiofrequency Tagging

Nicolaou, in conjunction with IRORI Quantum Microchemistry, has introduced a new concept for encoding combinatorial libraries based on radiofrequency (RF) signals and semiconductor memory devices.²⁹

“Radiofrequency Encoded Combinatorial Chemistry (REC)” uses a Single or Multiple Addressable Radiofrequency Tag (SMARTTM), rather than a chemical label, to record relevant information along the synthetic pathway of a combinatorial synthesis. A SMARTTM



microreactor (Figure 7) was assembled from three components: (1) a chemically inert, porous support enclosure, (2) functionalized solid-phase resin beads and (3) a glass-encased SMARTTM semiconductor unit (8 x 1 x 1 mm) capable of receiving, storing and emitting RF signals from a distance of 75-150 mm.

During a representative ‘split-mix’ combinatorial synthesis, solid-phase reactions take place on the resin beads inside the porous enclosure and the relevant encoding information is recorded on the RF tag. Identification of the active library members is then achieved by retrieval of the information via a specially designed radiofrequency memory-retrieving device that provides a history of the memory chips’ manipulation throughout any experiment. The RF tag is stable to most organic solvents and reagents, can be reused, and has been submitted to reaction temperatures ranging from -78 to 100 °C. Additionally, the most current REC memory chips have a large encoding capacity capable of storing large amounts of various types of information.

The inert nature of the RF tag permits the broader application of encoded combinatorial libraries to a vast array of chemistries. This methodology allows for the reliable, straightforward, nonchemical and noninvasive encoding and decoding of combinatorial libraries. Validation of this approach was achieved through the generation of a 400-member taxoid library³⁰ and a 400-member tyrostatin library³¹ by a modified "split and mix" synthesis. A variation of this methodology utilizing a read-only radiofrequency microchip was introduced by Armstrong *et al.* for the generation of a 64-member library employing the Ugi reaction.³² This example is the first use of multi-component chemistry in encoded combinatorial libraries.

Laser Optical Encoding

IRORI recently reported an extension to REC methodology using laser optical encoding to achieve chemically inert, noninvasive encoding of a combinatorial library.³³ Laser Optical Synthesis Chips (LOSC's) were assembled from the combination of a two-dimensional 16-digit bar code and a polymeric support that is grafted with low cross-linking polystyrene (Figure 8). LOSC's, like the RF tag, can be manipulated through a "split and mix" combinatorial synthesis and 'reading' of the bar code identifies the synthetic transformations of the substrate bound to the chip. These chips are inert to most organic solvents and synthesis conditions and can provide a low cost, non-invasive, highly reliable form of molecular encoding. The utility of this strategy was demonstrated via the chemical synthesis of a library of 27 trimeric oligonucleotides.

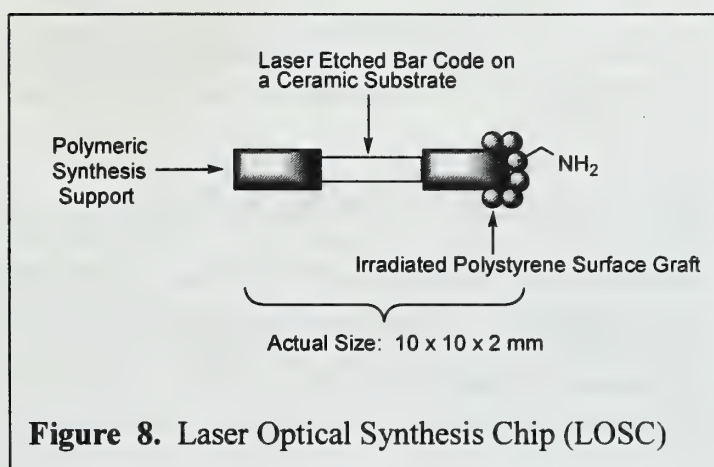


Figure 8. Laser Optical Synthesis Chip (LOSC)

CONCLUSIONS

Advancement in the field of combinatorial synthesis and screening has lead to the development of a wide range of methodologies for the identification of active lead compounds in a large, complex combinatorial library. The ease of structural identification will, in turn, allow for the synthesis of larger, more diverse libraries of compounds. Whether a library is defined spatially or in a pool, tagged or untagged, ultimately depends on the chemistry used to design the array. With the increasing sophistication of methods for the generation and screening of these libraries, additional and more general techniques for structural elucidation will continue to emerge.

REFERENCES

- 1) Gallop, M. A.; Barrett, R. W.; Dower, W. J.; Fodor, S. P. A.; Gordon, E. M. *J. Med. Chem.* **1994**, *37*, 1233.
- 2) Thompson, L. A.; Ellman, J. A. *Chem. Rev.* **1996**, *96*, 555.
- 3) Terrett, N. K.; Gardner, M.; Gordon, D. W.; Kobylecki, R. J.; Steele, J. *Tetrahedron* **1995**, *51*, 8135.
- 4) Xiao, X.-Y.; Nova, M. P. *Radiofrequency Encoding and Additional Techniques for the Structure Elucidation of Synthetic Combinatorial Libraries*; Wilson, S. R. and Czarnik, A. W. ; John Wiley & Sons, Inc.: New York, 1997, pp 135.
- 5) Stevanovic, S.; Jung, G. *Anal. Biochem.* **1993**, *212*, 212.
- 6) Ellington, A. D.; Szostak, J. W. *Nature* **1990**, *346*, 818.
- 7) DeWitt, S. H.; Czarnik, A. W. *Acc. Chem. Res.* **1996**, *29*, 114.
- 8) Fodor, S. P. A.; Read, J. L.; Pirrung, M. C.; Stryer, L.; Lu, A. T.; Solas, D. *Science* **1991**, *251*, 767.
- 9) Cho, C. Y.; Moran, E. J.; Cherry, S. R.; Stephans, J. C.; Fodor, S. P. A.; Adams, C. L.; Sundaram, A.; Jacobs, J. W.; Schultz, P. G. *Science* **1993**, *261*, 1303.
- 10) Furka, A.; Sebestyen, F.; Asgedom, M.; Dibo, G. *Int. J. Peptide Prot. Res.* **1991**, *37*, 487.
- 11) Geysen, H. M.; Rodda, S. J.; Mason, T. J.; Tribbick, G.; Schooks, P. G. *J. Immunol. Methods* **1987**, *102*, 259.
- 12) Gordeev, M. F.; Patel, D. V.; Gordon, E. M. *J. Org. Chem.* **1996**, *61*, 924.
- 13) Erb, E.; Janda, K. D.; Brenner, S. *Proc. Natl. Acad. Sci. U.S.A.* **1994**, *91*, 11422.
- 14) Janda, K. D. *Proc. Natl. Acad. Sci. U.S.A.* **1994**, *91*, 10779.
- 15) Dooley, C. T.; Houghten, R. A. *Life. Sci.* **1993**, *52*, 1509.
- 16) Pirrung, M. C.; Chen, J. *J. Am. Chem. Soc.* **1995**, *117*, 1240.
- 17) Pirrung, M. C.; Chau, J. H.-L.; Chen, J. *Chem. Biol.* **1995**, *2*, 621.
- 18) Brenner, S.; Lerner, R. A. *Proc. Natl. Acad. Sci. U.S.A.* **1992**, *89*, 5381.
- 19) Nielsen, J.; Brenner, S.; Janda, K. D. *J. Am. Chem. Soc.* **1993**, *115*, 9812.
- 20) Needels, M. C.; Jones, D. G.; Tate, E. H.; Heinkel, G. L.; Kochersperger, L. M.; Dower, W. J.; Barrett, R. W.; Gallop, M. A. *Proc. Natl. Acad. Sci. U.S.A.* **1993**, *90*, 10700.
- 21) Kerr, J. M.; Banville, S. C.; Zuckermann, R. N. *J. Am. Chem. Soc.* **1993**, *115*, 2529.
- 22) Kerr, J. M.; Banville, S. C.; Zuckermann, R. N. *Bioorg. Med. Chem. Lett.* **1993**, *3*, 463.
- 23) Younquist, R. S.; Fuentes, G. R.; Lacey, M. P.; Keough, T. *J. Am. Chem. Soc.* **1995**, *117*, 3900.
- 24) Ohlmeyer, M. H. J.; Swanson, R. N.; Dillard, L. W.; Reader, J. C.; Asouline, G.; Kobayashi, R.; Wigler, M.; Still, W. C. *Proc. Natl. Acad. Sci. U.S.A.* **1993**, *90*, 10922.
- 25) Baldwin, J. J.; Burbaum, J. J.; Henderson, I.; Ohlmeyer, M. H. J. *J. Am. Chem. Soc.* **1995**, *117*, 5588.
- 26) Borchardt, A.; Still, C. W. *J. Am. Chem. Soc.* **1994**, *116*, 373.
- 27) Ni, Z.-J.; Maclean, D.; Holmes, C. P.; Murphy, M. M.; Ruhland, B.; Jacobs, J. W.; Gordon, E. M.; Gallop, M. A. *J. Med. Chem.* **1996**, *39*, 1601.
- 28) Maclean, D.; Schullek, J. R.; Murphy, M. M.; Ni, Z.-J.; Gordon, E. M.; Gallop, M. A. *Proc. Natl. Acad. Sci. U.S.A.* **1997**, *94*, 2805.
- 29) Nicolaou, K. C.; Xiao, X.-Y.; Parandoosh, Z.; Senyei, A.; Nova, M. P. *Angew. Chem., Int. Ed. Engl.* **1996**, *34*, 2289.
- 30) Xiao, X.-Y.; Parandoosh, Z.; Nova, M. P. *J. Org. Chem.* **1997**, *62*, 6029.
- 31) Czarnik, T.; Nova, M. *Chem. Br.* **1997**, *33*, 39.
- 32) Armstrong, R. W.; Tempest, P. A.; Cargill, J. F. *Chimia* **1996**, *50*, 258.
- 33) Xiao, X.-Y.; Zhao, C.; Potash, H.; Nova, M. P. *Angew. Chem., Int. Ed. Engl.* **1997**, *36*, 780.

RECENT DEVELOPMENTS IN THE SECONDARY STRUCTURE OF β -PEPTIDES

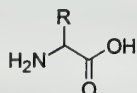
Reported by Shreyasi Lahiri

March 16, 1998

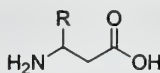
INTRODUCTION

In recent years there has been a growing interest in synthetic compounds with structural motifs similar to those found in nature. However, before synthetic molecules that are as complex as proteins can be realized and produced, structured oligomers that elucidate the interactions involved in the organization of these molecules must be found and studied. There have been numerous reports discussing the secondary structure of non-natural oligomers.¹⁻⁵ A goal of this work is to develop a system which is architecturally close to that of natural α -amino acid oligomers. The similar structure might allow these peptides to exhibit biological activity without being susceptible to cleavage by enzymes specific to α -amino acids. This report will focus on recent research on secondary structure formation in β -peptides.

Beta-peptides, oligomers of β -amino acids, are gaining attention as first generation synthetic analogs to regular peptides. The interest in β -amino acids originated from their presence in biological compounds such as the anticancer agent paclitaxel,⁶ macrocyclic peptides from marine organisms,⁷ and β -lactam antibiotics.⁸



α -amino acid

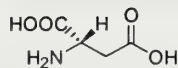


β -amino acid

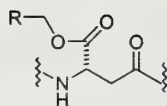
Early investigations on peptides of β -amino acids focused on their biological properties when incorporated into α -peptides.⁹ Secondary structure formation in β -amino acid polymers was not extensively studied. Recently, however, with an increased interest in supramolecular chemistry and peptidomimetics, interest in the secondary structure of β -peptides has re-emerged.

BACKGROUND: β -PEPTIDES OF NATURAL α -AMINO ACIDS

There have been extensive studies of derivatives of aspartic acid (1), which is a natural α -amino acid with β -carboxylic acid site.¹⁰⁻¹²



1



- | | |
|---|--|
| 2 | R: -H |
| 3 | R: -CH ₃ |
| 4 | R: -CH ₂ -O-CH ₃ |
| 5 | R: -CH(CH ₃) ₂ |
| 6 | R: -(CH ₂) _{n-2} -CH ₃ |

Studies of poly(β -L-aspartate)s show that these polymers exhibit different helical conformations depending on the nature of their alkyl side group.¹¹ Three types of helices with two types of hydrogen bonding patterns were formed. The helices were of the form, 3.25₁ (3.25 residues per 1 turn of helix), 4₁, and 4.25₁ and exhibited hydrogen bonding either between the first and third residue, or the first and fourth residue. Furthermore, some of the polymers adopted more than one helical form.

It was also found that in the crystalline state 4 underwent a conformational change from a 3.25₁ helix with hexagonal packing to a 4₁ helix with tetragonal packing upon heating. The change was attributed to the displacement of the helices across the basal plane of the crystal as well as a rearrangement of the molecular conformation. The mechanism of this was not elucidated. This conformational change was also observed when a solvent such as ethanol was added to a solution of 4 in chloroform.

The different conformations of these poly(β -L-aspartate)s might allow some insight into which of the two factors, the constitution of the side chain or the interactions involved in the packing, are dominant in the determination of conformation. These studies on the secondary structure formation of aspartic acid derivatives prompted speculation about whether oligomers made of unnatural β -amino acids would exhibit a similar structure, and thus motivated further studies investigating secondary structure formation.

SECONDARY STRUCTURE OF β -PEPTIDES

β -Peptides of Val-Ala-Leu

Seebach and co-workers constructed β -analogs of the natural peptide, Val-Ala-Leu (Figure 1), which have been the subject of numerous structural investigations.^{13,14} The synthesis of the β -analog

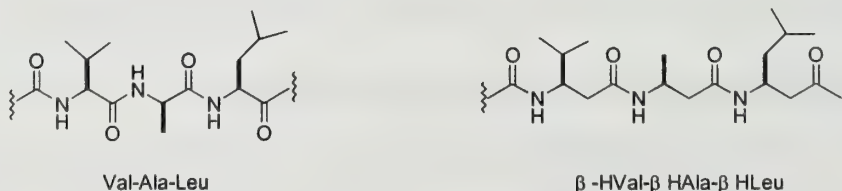
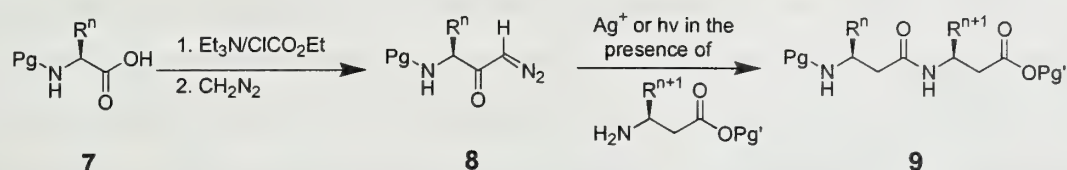


Figure 1. The structures of Val-Ala-Leu and its β -amino acid counterpart

was accomplished by methodology developed by Seebach where β -amino acid synthesis could be

coupled concomitantly with peptide formation.¹⁵ The Arndt-Eistert homologation of N-protected α -amino acids, followed by trapping of the intermediate with an amine functionality (Scheme 1), led directly to chain elongation.

Scheme 1



Initially, a hexamer was synthesized and characterized to determine its secondary structure.¹⁶⁻¹⁸ One of the characterization methods used was circular dichroism (CD). Circular dichroism has been used extensively for the detection and determination of the secondary structure of α -peptides. A right handed 3.6₁ helix with a pitch of 5.6 Å containing 13-membered hydrogen bonded rings gives rise to a CD maximum of 208 nm and minimum of 222 nm (208/222). In order for an α -helix to be observed in a protic solvent such as methanol or water, the chain needs to be at least 15 amino acid residues long. When a CD spectrum was taken of the β -substituted hexamer, an intense CD absorbance at 200 nm and 215 nm was observed. This was independent of the presence or absence of terminal protecting groups and of the concentration, indicating formation of secondary structure. The concentration independence suggested that the secondary structure was formed due to intramolecular interactions and not intermolecular interactions. This prompted the synthesis of a series of oligomers with different substitutions on the backbone. The nomenclature used for Seebach's β -peptides is outlined in Figure 2. The compounds are numbered from 1 to 3 starting with the carbonyl carbon as position 1 and the carbon adjacent to the amino group as 3. If the substituent is on the 3-position, then it is termed a β^3 -peptide. Similarly, if the substituent is on the 2-position, then it is known as a β^2 -peptide.

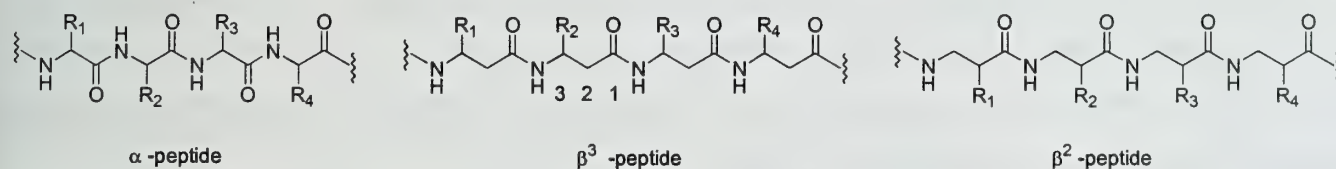
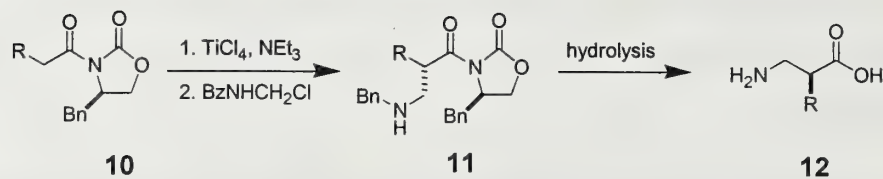


Figure 2. Nomenclature of the different peptides

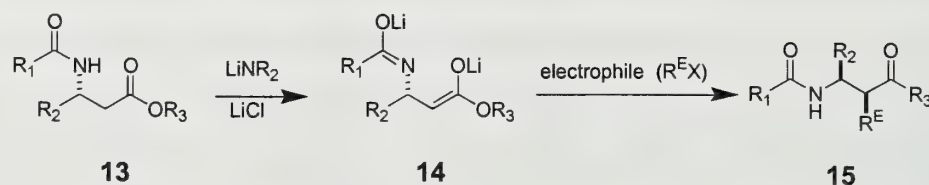
The β^3 -peptides were synthesized by the Arndt-Eistert homologation shown in Scheme 1. The synthesis of the β^2 -peptides was accomplished with the utilization of Evans' chiral auxiliary methodology (Scheme 2).¹⁸

Scheme 2



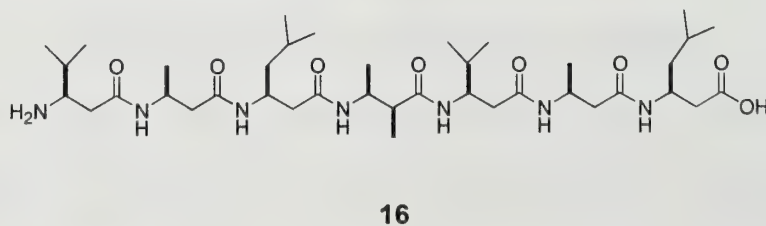
α,β -Disubstituted derivatives were also synthesized utilizing enolate chemistry in converting the β^3 -amino acid (Scheme 3).¹⁹

Scheme 3



Of the oligomers synthesized,^{16,20} the most intense CD absorptions were observed with the $\beta^{2,3}$ -hexapeptide consisting of β -amino acids with methyl groups in the 2-position and Val, Ala, and Leu side chains in the 3-position. This $\beta^{2,3}$ hexamer, along with a β^3 hexamer and a β^2 hexamer exhibited a maximum at 200 nm and a minimum at 215 nm in its CD spectrum. The β^3 -hexamer was a left handed helix and the β^2 -helix was a right handed helix. Mixed oligomers of the form $(\beta^2\beta^3)_3$ and $\beta^2\beta^2\beta^2\beta^3\beta^3\beta^3$ were also synthesized and characterized. The CD absorptions of these mixed oligomers depended on the sequence and upon the presence or absence of terminal protecting groups. Only the deprotected $\beta^2\beta^2\beta^2\beta^3\beta^3\beta^3$ peptide showed the expected 200 and 215 nm absorptions. All the other mixed peptides exhibited a single maxima at 205 nm. The secondary structures of these mixed compounds were unusual in that they consisted of a wide (12-membered turn), a narrow (10-membered turn), and another wide turn (12-membered turn).

Molecular dynamics calculations were performed on a β -heptapeptide (16) in methanol. These calculations showed that after a sudden temperature increase from 298 K to 350 K, the 3_1 helix unwound itself. However, when the temperature was kept constant at 350 K, the helix spontaneously reformed within 400 ps, and was still stable after 2000 ps.



The helix-forming peptides bearing natural amino acid side chains have not been crystallized yet,

however, a pleated sheet arrangement of a β -peptide fragment was found in the crystal structure of Boc- β^3 -HVal- β^3 HAla- β^3 -HLeu-OMe, with intermolecular hydrogen bonding in 14-membered rings.

Comparison with α -peptides

Seebach compared his work on the β -derivatives with the work of Karle.^{13,14} The comparative structural analysis of an α -peptide 3_6 helix with the 3_1 and 2.5_1 helices of β -peptides brought out the following points: (i) the helices have different polarities with respect to their C and N termini, and (ii) their shapes and sizes differ greatly in that the α -peptide has a pitch of 5.4 Å, the 3_1 helix a pitch of 5.0 Å, and the 2.5_1 helix a pitch of 5.6 Å. These structural differences suggest that β -peptides might show stability to peptidases that would normally cleave an α -peptide.

Seebach synthesized eight β -amino acids derived from proline, alanine, threonine, glutamic acid, leucine, phenylalanine, tryptophan, and lysine. Studies of their mutagenic properties using the Ames test, indicated that none of these amino acids were mutagenic under standard conditions.²¹ In other words, if the β -peptides were to undergo enzymatic cleavage, the resulting compounds would not be toxic. Other tests were conducted to determine whether these β -peptides were indeed stable to enzymes. The β -peptides were tested with enzymes, some of which were pepsin, chymotrypsin, trypsin, elastase, and carboxypeptidase A. There was no evidence of cleavage in any of these β -peptides over a period of up to two days. So, potentially, these β -peptides could be used as antigens in the future.

Constrained Oligomers of β -Alanine Derivatives

Previous work on the conformational properties of β -alanine oligomers by Narita and coworkers indicated that these oligomers formed sheet-like packing patterns in the solid state but they were disordered in solution.²² The lack of a discrete solution structure was attributed to the large amount of conformational freedom arising from the extra methylene group in the backbone. To induce solution structure formation, Gellman and coworkers introduced small rings into the backbone to minimize the conformational freedom by constraining rotation about the C_α - C_β bond.²³⁻²⁵

Molecular mechanics calculations using an AMBER force field were conducted on a β -alanine decamer to evaluate intramolecular hydrogen bonding interactions and determine which monomer would be the optimum one to study.²³ There are six possible helices that the β -alanine decamer could form (Figure 3).²⁴ The curved lines on Figure 1 represent the hydrogen bonding interactions between the amide NH and the carbonyl groups that would define one turn of a helix. For example, for the 18-helix, there would be 18 atoms constituting one turn of the helix (including the hydrogen atom of the

amide and the oxygen of the carbonyl). The calculations indicated that all six of the possible helices constituted a local minima on the conformational energy surface. Further modeling experiments were carried out to determine if any particular helix/small ring combination would lead to enhanced conformational stability.

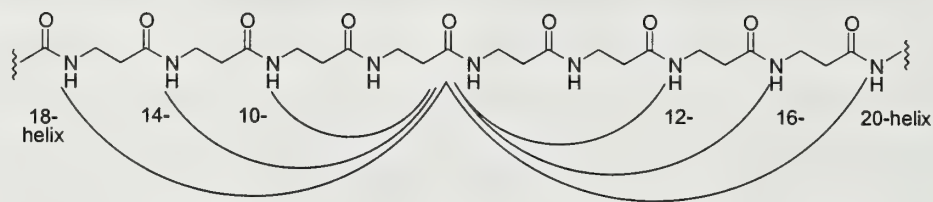
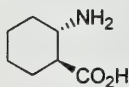
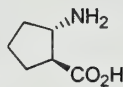


Figure 3. Hydrogen bonds defining the six possible helices for poly- β -alanine

The modeling studies predicted that the 14-helix of the decamer of trans-2-aminocyclohexane carboxylic acid (trans-ACHC) (17) would be the most stable, followed by the 12-helical form formed from the trans-2-aminocyclopentane carboxylic acid (trans-ACPC) (18). To test these predictions, Gellman synthesized the hexamers of both trans-ACHC and trans-ACPC by standard methods.^{26,27} The hexamers were characterized by amide proton exchange, proton NMR, X-ray crystallography and CD.



17



18

The crystal structure of the trans-ACHC hexamer showed a 14-membered helix in the solid state. Proton exchange behavior of the hexamer suggested that it adopted a very stable intramolecularly hydrogen bonded secondary structure in methanol. Three of the six protons of the hexamer showed very slow exchange rates, with one proton exchanging within 20 hours, and the other two requiring more than 48 hours for complete exchange. Proton exchange studies on the dimer were conducted as a control experiment and showed the amide proton of the dimer to be completely exchanged within 6 minutes. This experiment illustrated a more than 100-fold protection for two of the amide protons of the hexamer in CD_3OD , suggesting that the hexamer was very stable conformationally.

CD data for the trans-ACPC hexamer (204/221 nm) suggested that there was a distinctive secondary structure formed. The hexamer exhibited the predicted 12-helical form in the solid state and two-dimensional ^1H NMR also suggested this in solution. The combined CD and proton exchange

experiments indicated that the helical formation of these β -peptides could be controlled by manipulation of the $C_\alpha - C_\beta$ bond torsional angle of individual residues.

β -Peptide Sheet Structures

Gellman and coworkers also studied sheet structure formation of β -peptides.²⁸ There are two types of antiparallel sheet structures, anti and gauche (Figure 4), of which the anti-conformation is of

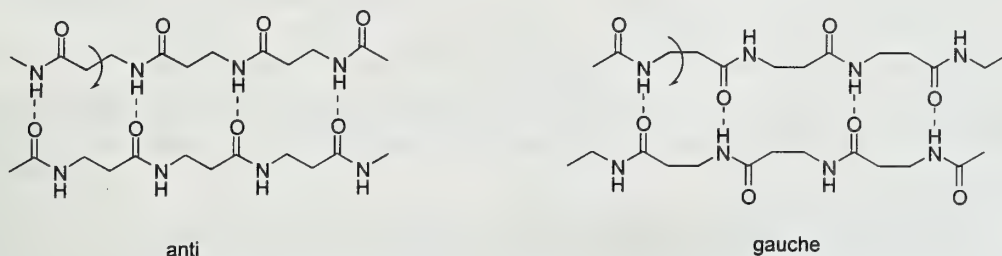


Figure 4. Different conformations of the sheet structures

particular interest because of its inherent net dipole. They reasoned that placing sterically bulky groups anti to one another at the α and β positions would promote anti β -sheet formation (Figure 5). A proline linker was used to promote sheet formation of the two strands and avoid intermolecular aggregation.

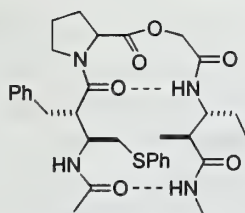


Figure 5

X-ray crystallography confirmed the structure of this anti sheet structure. Further studies investigating sheet formation were conducted by synthesizing a sheet that did not have the bulky side groups. This structure was found to prefer the gauche conformation. These results indicated that the conformation of sheet structures can be manipulated by changing the constitution of the substituents; bulky side groups anti to one another should prefer the anti-conformation, while less sterically hindered side groups should promote the gauche conformation.

CONCLUSIONS

The research on the secondary structure of β -peptides has grown over the years. The studies could lend some insight into the interactions involved in protein folding and the formation of

supramolecular structures. The potential of future applications in biological systems is immense and it will be interesting to see what roles β -amino acids and their peptides will play in the future.

REFERENCES

- 1) Hamilton, A.D.; Hamuro, Y.; Geib, S. J. *J. Am. Chem. Soc.* **1997**, *119*, 10587-10593.
- 2) Iverson, B. L.; Lokey, R. S. *Nature* **1995**, *375*, 303-305.
- 3) Iverson, B. L.; Lokey, R.; Kwok, Y.; Guelev, V.; Pursel, C.; Hurley, L. *J. Am. Chem. Soc.* **1997**, *119*, 7202-7210.
- 4) Lehn, J.-M.; Zarges, W.; Hall, J.; Bolm, C. *Helv. Chim. Acta* **1991**, *74*, 1843.
- 5) Stoddart, J. F.; Philp, D. *Angew. Chem. Int. Ed. Engl.* **1996**, *35*, 1154-1196.
- 6) Georg, G. I.; Chen, T. T.; Ojima, I.; Vyas, D. M. *Taxane Anticancer Agents: Basic Science and Current Status*; Georg, G. I.; Chen, T. T.; Ojima, I.; Vyas, D. M., Ed.; American Chemical Society: Washington, D.C., 1995.
- 7) Cardillo, G.; Tomasini, C. *Chem. Soc. Rev.* **1996**, 117.
- 8) Georg, G. I., Ed. *Bioorg. Med. Chem. Lett* **1993**, *3*, 2135-2486.
- 9) Drey, C. N. C.; Drey, C. N. C., Ed.; Chapman and Hall, London, 1985, pp 25.
- 10) Munoz-Guerra, S.; Lopez-Carrasquero, F.; Aleman, C. *Biopolymers* **1995**, *36*, 263-271.
- 11) Munoz-Guerra, S.; Aleman, C.; Navas, J. J. *Biopolymers* **1997**, *41*, 721.
- 12) Subirana, J. A.; Fernandez-Santin, J. M.; Munoz-Guerra, S.; Rodriguez-Galan, A.; Aymami, J.; Lloveras, J. *Macromolecules* **1987**, *20*, 62-68.
- 13) Karle, I. L.; Balaram, P. *Biochemistry* **1990**, *29*, 6747.
- 14) Karle, I. L.; Flippen-Anderson, J. L.; Sukumar, M.; Uma, K.; Balaram, P. *J. Am. Chem. Soc.* **1991**, *113*, 3952-3956.
- 15) Seebach, D.; Podlech, J. *Angew. Chem. Int. Ed. Engl.* **1995**, *34*, 471.
- 16) Seebach, D.; Matthews, J. L. *Chem. Commun.* **1997**, 2015.
- 17) Seebach, D.; Overhand, M.; Kuhnle, F. N. M.; Martinoni, B. *Helv. Chim. Acta* **1996**, *79*, 913.
- 18) Seebach, D.; Hintermann, T. *Synlett* **1997**, 437.
- 19) Seebach, D.; Podlech, J. *Liebigs Ann.* **1995**, 1217-1228.
- 20) Seebach, D.; Gademann, K.; Schreiber, J. V.; Matthews, J. L.; Hintermann, T.; Jaun, B. *Helv. Chim. Acta* **1997**, *80*, 2033.
- 21) Seebach, D.; Hintermann, T. *Chimia* **1997**, *51*, 244.
- 22) Narita, M.; Doi, M.; Kudo, K.; Terauchi, Y. *Bull. Chem. Soc. Jpn.* **1986**, *59*, 3553-3557.
- 23) Gellman, S. H.; Dado, G. P. *J. Am. Chem. Soc.* **1994**, *116*, 1054-1062.
- 24) Gellman, S. H.; Appella, D. H.; Christianson, L. A.; Karle, I. L.; Powell, D. R. *J. Am. Chem. Soc.* **1996**, *118*, 13071-13072.
- 25) Gellman, S. H.; Appella, D. H.; Christianson, L. A.; Klein, D. A.; Powell, D. R.; Huang, X.; Barch, J. J. *Nature* **1997**, *387*, 381.
- 26) Nohira, H.; Ehara, K.; Miyashita, A. *Bull. Chem. Soc. Jpn.* **1970**, *43*, 2230-2233.
- 27) Seebach, D.; Herradon, B. *Helv. Chim. Acta* **1989**, *72*, 690.
- 28) Gellman, S. H.; Krauthauser, S.; Christianson, L. A.; Powell, D. R. *J. Am. Chem. Soc.* **1997**, *119*, 11719-11720.

CHIRALITY IN MOLECULAR ENCAPSULATION

Reported by W. Chad Baker

April 6, 1998

INTRODUCTION

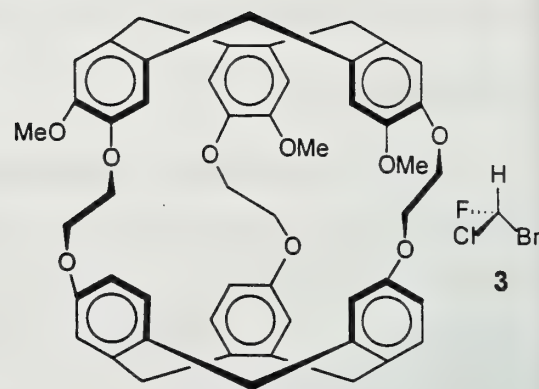
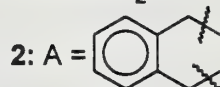
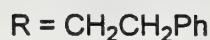
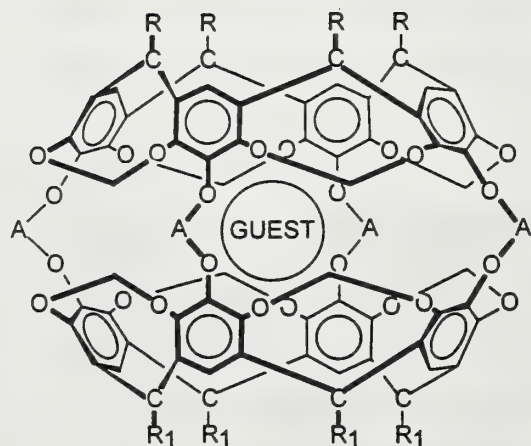
Since the pioneering work by Cram¹ and Collet², molecular container compounds have gained interest due to their potential as artificial receptors, molecular switches, and miniature reaction chambers.^{3,4} These molecule-within-molecule complexes, which differ from zeolites in that they reside in solution, consist of spherical hosts that bind molecules within their hollow interiors. The non-covalent interactions involved in their formation provide insight into molecular recognition and self-assembly processes.

Early work in the design of molecular capsules focused on covalently-assembled hosts which trapped guests within their interiors during synthesis.⁵ The field has since expanded to include reversible formation of self-assembled capsules held together through non-covalent interactions.⁴ Despite considerable activity in this area, limited attention has been paid to aspects of chirality in these systems. This report provides a brief background on the history and uses of molecular encapsulation and discusses recent work involving chirality in both covalently- and self-assembled systems.

BACKGROUND

Cram and coworkers proposed⁶ and synthesized¹ the first example of a carcerand, a molecule which incarcerates another molecule. This host is a closed-surface, spherical molecule with a hollow interior large enough to complex small neutral molecules. The irreversible complexation of a carcerand with a guest during closure of the two hemispheres results in formation of a carceplex (1).

The ability to control the liberation of the guest drove the synthesis of the first hemicarcerand⁷, a host with portals large enough to allow the entrance and egress of molecules. Encapsulation of guests to form a hemicarceplex (2) occurred through expansion/contraction of the portal at high/low temperatures. Hemicarplexes are kinetically stable and retain their guests for hours or longer, making them potentially useful as molecular reactors.^{5,8-10} Recently, studies have shown the ability of a hemicarceplex to stabilize reactive intermediates such as cyclobutadiene and *o*-benzyne in the host interior.⁸ Other studies in molecular encapsulation have demonstrated the acceleration of a Diels-Alder reaction inside the capsule.⁹ Due to altered physical properties of incarcerated guests, Cram and Sherman suggested that the inner spaces of molecular capsules can be considered new phases of matter.¹⁰



4

CHIRALITY IN COVALENTLY-ASSEMBLED CAPSULES

Chiral Cryptophanes

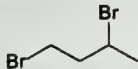
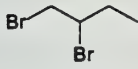
In 1985, Collet showed that chiral cryptophanes could be used to resolve enantiomers of bromochlorofluoromethane (**3**).² Cryptophane-C (**4**), a chiral host designed to fit substrates of small size, contains two cyclotribenzylenes which act as “rims.” The C_3 symmetry of the capping cyclotribenzylenes resulted in a pair of enantiomers of **4**. Molecules of the type CH_2XY were found to enter the host easily, making them suitable guests for **4**. At 53 °C, addition of 300-fold excess of racemic **3** to (+)-**4** resulted in the appearance of a pair of upfield-shifted doublets (due to shielding effects of the aromatic rings) in the ^1H NMR spectrum of **3**. This shift was interpreted as the imprisonment of the enantiomers of **3** to form two diastereomeric complexes. Integration of the signals revealed a 2:1 ratio of $[(-)\text{-}\mathbf{3}\cdot(+)\text{-}\mathbf{4}]$ to $[(+)\text{-}\mathbf{3}\cdot(+)\text{-}\mathbf{4}]$, a difference in thermodynamic stability of $\Delta\Delta G^\circ = 0.26 \text{ kcal mol}^{-1}$. Molecular dynamics simulations¹¹ in chloroform showed a preferential orientation for **3** in the capsule with the C-H bond parallel to the length of the capsule and showed the $[(R)\text{-}\mathbf{3}\cdot(-)\text{-}\mathbf{4}]$ complex to be 0-0.62 kcal mol^{-1} more stable than its diastereomer. The assignment of the (*R*)-configuration to $(-)\text{-}\mathbf{3}$ was consistent with experimental observations. Despite these simulations, no information about the structural origin of the enantioselective binding was deduced.

Collet and coworkers have also synthesized other inherently chiral cryptophanes.¹² These systems possess D_3 symmetry and consist of enantiomers having right- and left-handed helical twists. To date, no complexation properties have been reported with these cryptophanes.

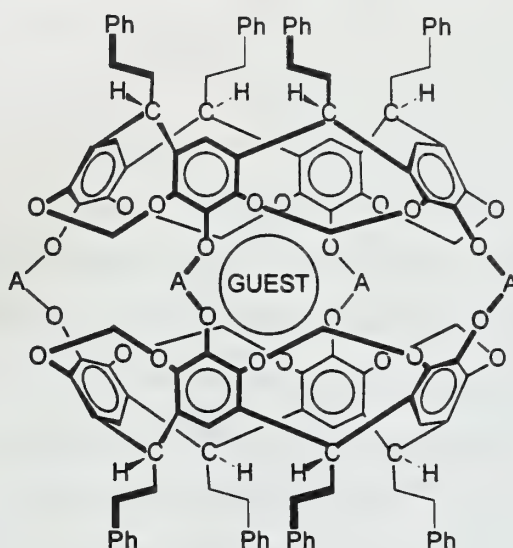
Chiral Recognition in Hemicarceplexes

The first chiral hemicarceplexes (**5** and **6**) were reported by Cram in 1991.¹³ These hemicarceplexes contained four equivalent chiral portals generated by the use of either (*R*)- or (*S*)-binaphthyl bridging units. Racemic mixtures of guests were trapped within the interior of **6** by heating solutions of the host and guest at 100 °C until diastereomeric equilibration was observed, followed by cooling to room temperature (Table 1). The differences in free energy of association for the enantiomers in both cases were ~300 cal mol⁻¹. Differences in chiral selectivity in decomplexation were theorized to be due to differential steric repulsions between the host and guest.

Table 1. Selectivity during host-guest decomplexation.

host	racemic guest	dr	$k_{\text{fast}}/k_{\text{slow}}^a$
6		2:1	5
6		2:1	9

^a Ratio of dissociation rate constants for diastereomeric complexes at 23 °C

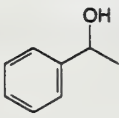
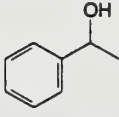
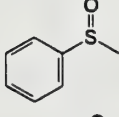
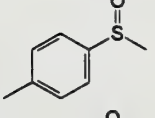
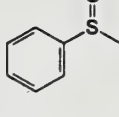
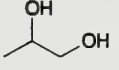


6: A = (*S*)-binap

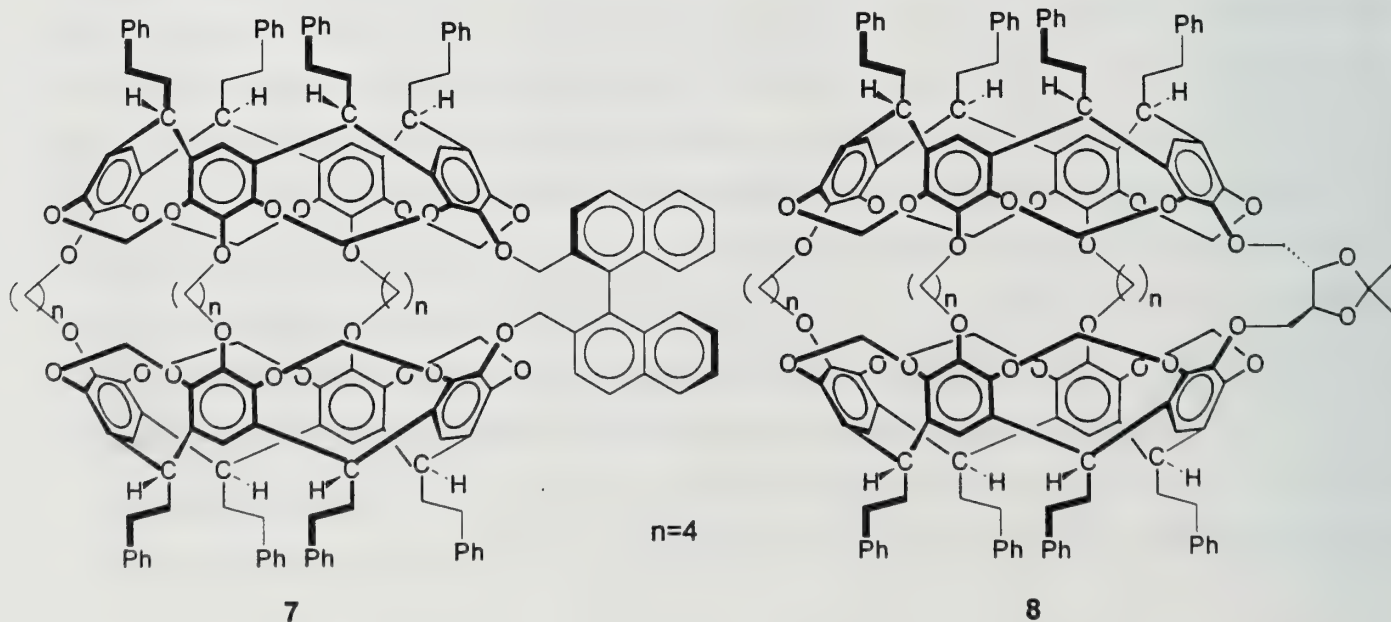
Additional studies identified the roles of chiral portals in host-guest complexation (Table 2).¹⁴ Host **7** contained one (*S*)-binaphthyl ligand as a bridging unit, creating two identical flexible chiral portals which were larger (28 vs. 26 membered rings) and more likely to be used than the two achiral portals. In contrast, **8** possessed one (*S,S*)-acetonide ligand, creating two rigid chiral portals equal in size but less likely to be used than the achiral portals. Several important trends were noted in the complexation studies. Host **7** showed enhanced enantioselection over **8** for racemic PhS(O)CH₃ as a result of discrimination via the chiral portals. In addition, enhanced diastereomeric ratios were observed for thermodynamically incarcerated guests over guests kinetically sealed in during closure of the two hemispheres of the hemicarcerand. The most dramatic enantioselection was observed for *p*-tol-S(O)CH₃, in contrast to poor differentiation of PhS(O)CH₃. Comparison of CPK models of (±)-PhS(O)CH₃ and (±)-*p*-tol-S(O)CH₃ showed that all four guests entered the portals relatively easily. Both enantiomers of PhS(O)CH₃ easily rotated within the cavity of **7**, while (*R*)-*p*-tol-S(O)CH₃ “locked into place” by rotating 90°, aligning the long axes of host and guest. This rotation created an activation

barrier to the egress of (*R*)-*p*-tol-S(O)CH₃. In contrast, (*S*)-*p*-CH₃PhS(O)CH₃ resisted rotation and was free to exchange in and out of the host.

Table 2. Selectivity during guest complexation.

host	racemic guest	method	% yield	dr
7		sealed in	35%	1.5:1
7		guest, 160 °C	97%	2.5:1
7		guest, 125 °C	96%	1.6:1
7		guest, 125 °C	30%	>20:1
8		sealed in	33%	1:1
8		guest, reflux	93%	1:1

In addition to these complexation studies, host-guest configurational relationships were studied via chromatography. The two diastereomeric complexes of **7** with racemic PhS(O)CH₃ showed different *R_f* values by TLC. In contrast, the corresponding complexes of **8** showed no difference in *R_f* values.



The binaphthyl bridge of **7** can adjust its naphthyl-to-naphthyl dihedral angle, allowing the capsule to adapt its shape to the configuration of the host, while the rigid acetonide bridge of **8** precludes such flexibility. Thus, adaptability of the host allows communication between the guest and the capsule environment despite multi-Angstrom separation of the guest from the exterior of the complex.

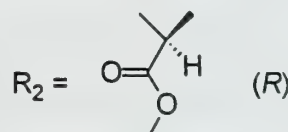
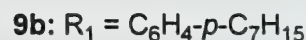
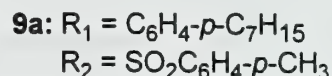
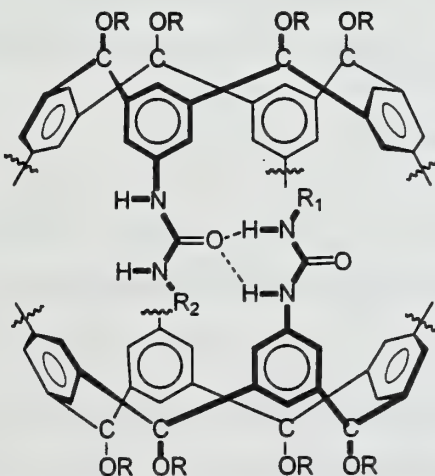
Novel Types of Stereoisomerism in Calixarene-Based Carceplexes

During the synthesis of a carceplex from a calix[4]arene and a resorcin[4]arene unit, Reinhoudt and coworkers observed differing orientations of achiral guests within the internal cavity.¹⁵ Trapping of DMF, DMA, and NMP during closure of the two hemispheres and cooling of the samples to <0 °C led to doubling of resonances in the ¹H NMR spectrum. NOE correlations between methyl groups of the amide guests and protons on the upper and lower rims of the carceplex suggested two differing orientations of the guests within the capsule. This form of isomerism between molecules that are not covalently attached has been termed “carceroisomerism.” In studies of templation effects of guests during formation of an asymmetric carceplex, Sherman observed a preferred orientation for pyrazine at room temperature.¹⁶ Other guests which adopt preferred orientations in carceplexes at room temperature have also been reported, leading to the potential use of these complexes as molecular switches.¹⁷

CHIRALITY IN SELF-ASSEMBLED SYSTEMS

Calixarene-Based Dimers

Encapsulation of optically active guests by self-assembled calix[4]arene-based heterodimers (**9a**) bearing sulfonyl urea functionalities at the upper rim and aryl ureas on the lower rim led to the observation of diastereomeric complexes in the corresponding ¹H NMR spectra.¹⁸ Molecular modeling of these complexes showed that guests such as (1*R*)-(+)-camphor have a pair of preferred orientations in the capsules, resulting in the observation of two different encapsulated species. Other calixarene-based capsules with different upper and lower rim components have been synthesized, although no recognition studies of these systems have been reported.^{19,20}

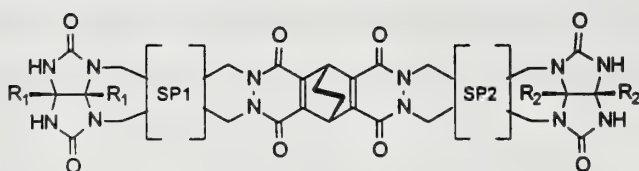


A heterodimeric capsule with an optically-active lining (**9b**) was constructed by substitution of the upper-rim urea with (*R*)-CH(CH₃)Ph.²² Encapsulation of racemic nopinone (**11**) led to the formation of equal amounts of diastereomeric products. This transition from racemic capsules to capsules with optically active linings did not result in transfer of steric information to the guest, thus failing to achieve enantioselective complexation.

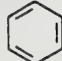
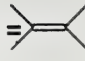
Glycouril-Based Self-Assembling Capsules

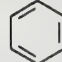
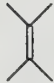
Rebek and coworkers have recently assembled a molecular capsule through approach of two C-shaped fused-ring structures with terminal glycouril units (**10**).²¹ This assembly is driven through the interaction of hydrogen bond acceptors (N-H bonds on the terminal glycourils) with hydrogen bond donors (the four carbonyl oxygens). Due to the hydrogen bonding "seams" of the capsule and the shape of the final self-assembled system, these dimers have been referred to as "softballs." These hosts contain interior volumes of ~300 Å³ and are able to complex guests the size of ferrocene or adamantane. The presence of encapsulated guest is usually observed through upfield shifts of the guest ¹H NMR signals.

Initial work on capsule formation centered on the use of symmetric units to build an achiral spherical capsule. Recently softballs with asymmetric surfaces have been synthesized.²² Substitution of the outward-facing R groups on one of the terminal glycourils reduces the symmetry of the resulting assembly, leading to the formation of enantiomeric capsules in the presence of achiral guests. Encapsulation of chiral guests, such as (1*R*)-(+)-camphor, resulted in the formation of equally-populated



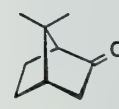
10a: R₁ = CO₂isopentyl R₂ = *p*-PhOC₆H₁₃

10b: R₁ = R₂ = 4-*n*-heptylphenyl SP1 =  SP2 = 

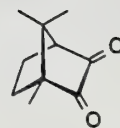
10c: R₁ = R₂ = 4-*n*-heptylphenyl SP1 =  SP2 = 



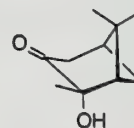
11



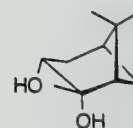
12



13



14



15

diastereomeric capsules. This result suggests that the asymmetric surface does not transmit steric information to the chiral guests within the interior cavity.

In an attempt to synthesize capsules with chiral spaces, Rebek employed two different ethylene spacers within the same monomer unit (**10b** and **10c**).^{23,24} Although these monomers still have a mirror plane, their dimerization results in decreased symmetry, yielding racemic mixtures of enantiomeric capsules in the presence of an achiral guest. In contrast to the softballs with asymmetric surfaces, these

Table 3. Selectivity of self-assembled chiral capsules.

Host	Guest	de (%)	$\Delta\Delta G^\circ$ (kcal mol ⁻¹)	Host	Guest	de (%)	$\Delta\Delta G^\circ$ (kcal mol ⁻¹)
10b	11	0	0	10c	11	0	0
10b	12	12	0.1	10c	12	17	0.2
10b	13	6	0.1	10c	13	12	0.2
10b	14	19	0.2	10c	14	29	0.4
10b	15	32	0.4	10c	15	35	0.4

capsules contain deformed chiral spaces and are able to form diastereomers with some preference (Table 3). Selectivities increased with increasing size of guest and were larger for the smaller **10c**, a result that can be rationalized by the presence of increased surface contacts between the host and guest. Although the diastereomeric excesses in this system are low, enantioselection is nonetheless possible.

Large Chiral Capsules

Atwood has recently reported the synthesis of a chiral capsule held together by 60 hydrogen bonds.²⁵ This complex, composed of six C-methylcalix[4]resorcinarene units and several water molecules, exists as a pair of enantiomers and contains an internal cavity volume of ~1,400 Å³. Formation of this complex in the solid state has been verified by x-ray crystallography; however, only limited proof exists regarding persistence of this complex in solution.

CONCLUSION

Covalently- and self-assembled chiral capsules are capable of discriminating between enantiomers of captured guests. Communication between the guest and the environment of the complex is possible despite multi-Angstrom separation of the guest from the capsule exterior. Movement of asymmetric elements from the periphery of these capsules (chiral portals, surfaces, and linings) toward the interiors of these systems (chiral spaces) may allow the construction of miniature reactors capable of

asymmetric catalysis. Though a number of chiral capsules have been synthesized, more studies are necessary to probe the nature of the stereochemical interactions in their interiors.

REFERENCES

- (1) Cram, D. J.; Karbach, S.; Kim, Y. H.; Baczynskyj, L.; Kallemeyn, G. W. *J. Am. Chem. Soc.* **1985**, *107*, 2575.
- (2) Canceill, J.; Lacombe, L.; Collet, A. *J. Am. Chem. Soc.* **1985**, *107*, 6993.
- (3) Sherman, J. C. *Tetrahedron*. **1995**, *51*, 3395.
- (4) Conn, M. M.; Rebek, Jr. J. *Chem. Rev.* **1997**, *97*, 1647.
- (5) Cram, D. J.; Cram, J. M. *Container Molecules and Their Guests*. Stoddart, J. F., Ed.; Monographs in Supramolecular Chemistry 4; Royal Society of Chemistry. Cambridge **1994**.
- (6) Cram, D. J. *Science* **1983**, *219*, 1177.
- (7) Tanner, M. E.; Knobler, C. B.; Cram, D. J. *J. Am. Chem. Soc.* **1990**, *112*, 1659.
- (8) Cram, D. J.; Tanner, M. E.; Thomas, R. *Angew. Chem., Int. Ed. Engl.* **1991**, *30*, 1024.
- (9) Kang, J.; Rebek, Jr. J. *Nature (London)* **1997**, *385*, 50.
- (10) Sherman, J. C.; Cram, D. J. *J. Am. Chem. Soc.* **1989**, *111*, 4527.
- (11) Costante-Crassous, J.; Marrone, T. J.; Briggs, J. M.; McCammon, J. A.; Collet, A. *J. Am. Chem. Soc.* **1997**, *119*, 3818.
- (12) Garcia, C.; Aubry, A. Collet, A. *Bull. Soc. Chim. Fr.* **1996**, *133*, 853.
- (13) Judice, J. K.; Cram, D. J.; *J. Am. Chem. Soc.* **1991**, *113*, 2790.
- (14) Yoon, J.; Cram, D. J. *J. Am. Chem. Soc.* **1997**, *119*, 11796.
- (15) Timmerman, P.; Verboom, W.; van Veggel, F. C. J. M.; van Duynhoven, J. P. M.; Reinhoudt, D. N. *Angew. Chem., Int. Ed. Engl.* **1994**, *33*, 2345.
- (16) Fraser, J. R.; Borecka, B.; Trotter, J.; Sherman, J. C. *J. Org. Chem.* **1995**, *60*, 1207.
- (17) van Wageningen, A. M. A.; van Duynhoven, J. P. M.; Verboom, W.; Reinhoudt, D. N. *J. Chem. Soc., Chem. Commun.* **1995**, 1941.
- (18) Castellano, R. K.; Kim, B. H.; Rebek, Jr. J. *J. Am. Chem. Soc.* **1997**, *119*, 12671.
- (19) Mogck, O.; Böhmer, V.; Vogt, W. *Tetrahedron* **1996**, *52*, 8489.
- (20) Koh, K.; Araki, K.; Shinkai, S. *Tetrahedron Lett.* **1994**, *44*, 8255.
- (21) Meissner, R. S.; Rebek, Jr. J.; de Mendoza, J. *Science* **1995**, *270*, 1485.
- (22) Tokunaga, Y.; Rebek, Jr. J. *J. Am. Chem. Soc.* **1998**, *120*, 66.
- (23) Rivera, J. M.; Martín, T.; Rebek, Jr. J. *J. Am. Chem. Soc.* **1998**, *120*, 819.
- (24) Rivera, J. M.; Martín, T.; Rebek, Jr. J. *Science* **1998**, *279*, 1021.
- (25) MacGillivray, L. R.; Atwood, J. L. *Nature* **1997**, *389*, 469.

FUNCTIONALIZATION OF OLEFINS USING CHIRAL SELENIUM REAGENTS

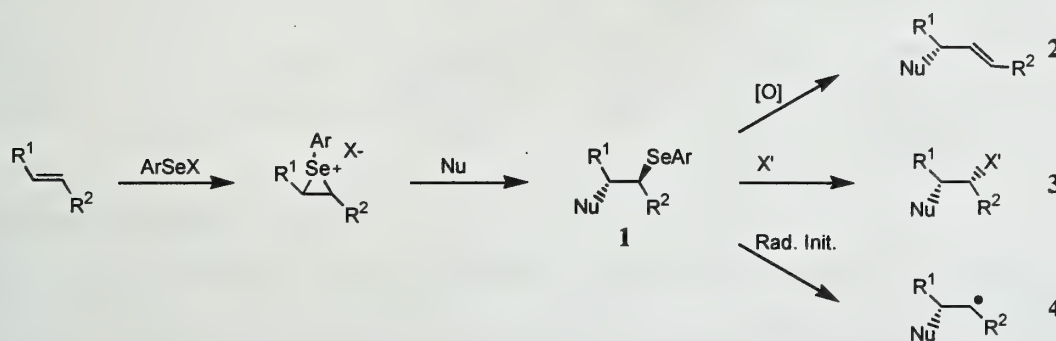
Reported by Sergio G. Duron

April 13, 1998

INTRODUCTION

The utility of organoselenium reagents in organic synthesis is well established.^{1,2} Electrophilic selenium reagents have been used to functionalize olefins under relatively mild conditions providing organoselenium intermediates of the type **1** (Scheme 1). Intermediate **1** is an extremely versatile agent, which can be (1) converted to an olefin **2** by selenoxide eliminations, (2) undergo substitution through nucleophilic displacement **3**, or (3) undergo functionalization by radical pathways through homolytic cleavage of the carbon-selenium bond **4**.

Scheme 1

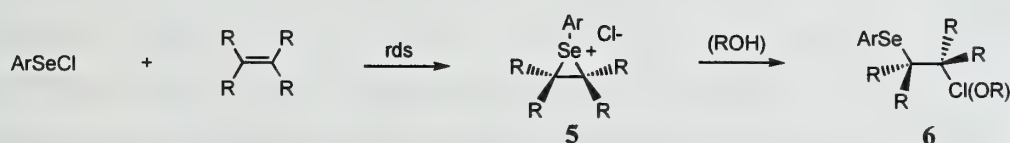


The addition of electrophilic organoselenium reagents across carbon-carbon double bonds is accompanied by the generation of two new chiral centers; therefore, the use of chiral selenium reagents provides a potential avenue for asymmetric induction. This report describes recent advances in the use of chiral electrophilic selenium reagents for the asymmetric functionalization of olefins.

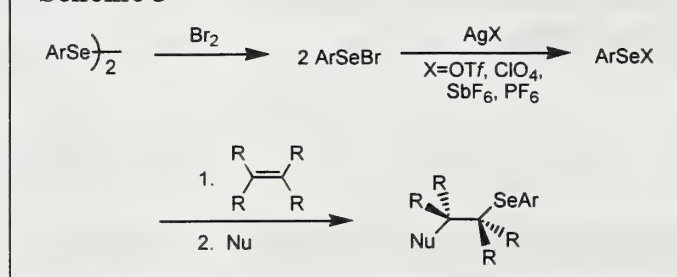
ADDITION OF ELECTROPHILIC SELENIUM TO OLEFINS

A two step mechanism has been proposed for the addition of electrophilic selenium reagents to olefins.³⁻⁵ The reaction proceeds via a three-membered seleniranium cation and typically provides Markovnikov products derived from the *anti* addition of a nucleophile to the seleniranium cation **5**.

Scheme 2



(Scheme 2). The formation of **5** is the rate-determining step (rds) and involves nucleophilic displacement at bivalent selenium by an olefin. The product-determining step then involves the addition

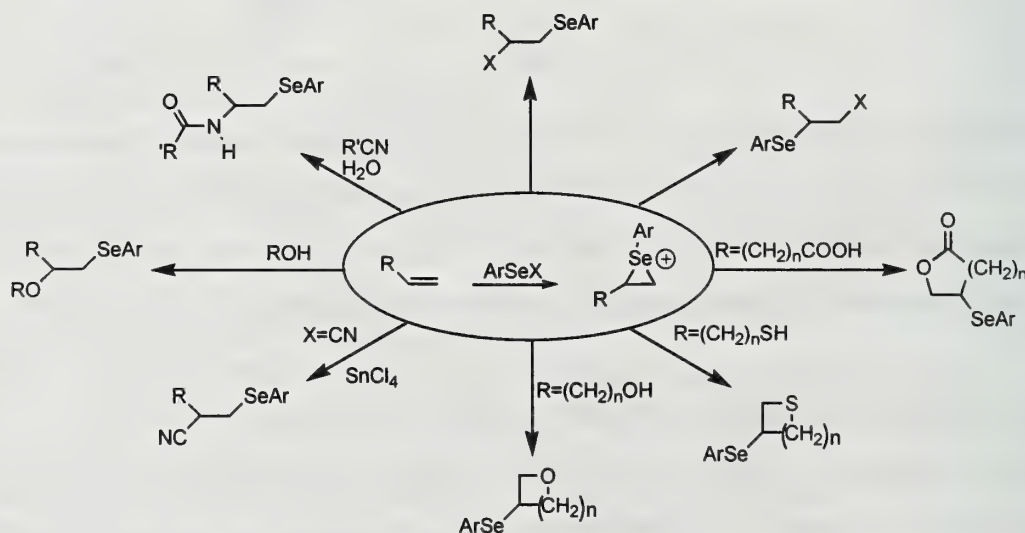
Scheme 3

of a nucleophile to the seleniranium by an $\text{S}_{\text{N}}2$ mechanism, to produce 1,2 *anti*-adducts, **6**. The free halide ion produced from the selenenyl halide can serve as a nucleophile. However, if nucleophiles other than halides are desired, exchange of the halide with less nucleophilic

counter ions can be accomplished using silver salts. Less nucleophilic counter ions also increase the electrophilicity of the selenium reagent providing a more reactive seleniranium intermediate.

Diselenides are typically employed as a source of electrophilic selenium due to their stability and accessibility and can easily be converted to their corresponding electrophilic intermediates for use in addition reactions to olefins (Scheme 3).

Achiral electrophilic selenium reagents have been used to provide a variety of intermolecular and intramolecular 1,2-adducts. Several examples are shown in Scheme 4. In most cases the organoselenium intermediates provide products with high regioselectivity and stereospecificity affording only *anti* products.

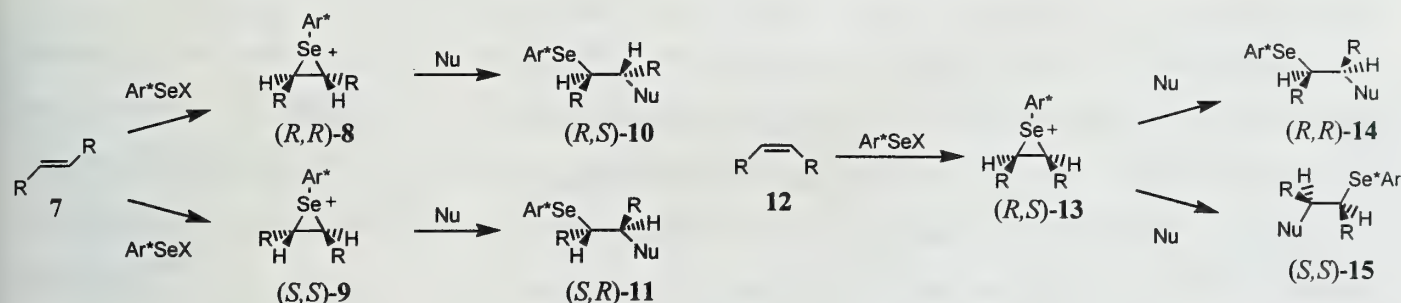
Scheme 4

ASYMMETRIC ELECTROPHILIC SELENENYLATIONS

The addition of electrophilic organoselenium reagents across carbon-carbon double bonds generates new chiral centers; therefore, the possibility exists that diastereoselective reactions can be performed by employing chiral selenyl reagents.⁶ Several chiral variants of diselenenides have been shown to provide high diastereoselectivities. It is important to note that the diastereo-determining step is different for *trans* and symmetrical *cis* olefins, as shown in Scheme 5. The addition of electrophilic

selenium to *trans* alkenes, **7**, is the diastereo-determining step. This affords two intermediates, **8** and **9**, resulting from enantiofacial addition, which provide products **10** and **11** after addition of a nucleophile. The addition of bivalent selenium to *cis* alkenes such as **12**, provides only one intermediate, **13**; therefore, the diastereo-determining step in this case is the addition of the nucleophile to the seleniranium intermediate **13**, yielding two possible products, **14** and **15**. Therefore, use of chiral organoselenium reagents with *cis* olefins is not as effective as with *trans* olefins because the approach of the nucleophile occurs far removed from the chiral influence of the selenium moiety.

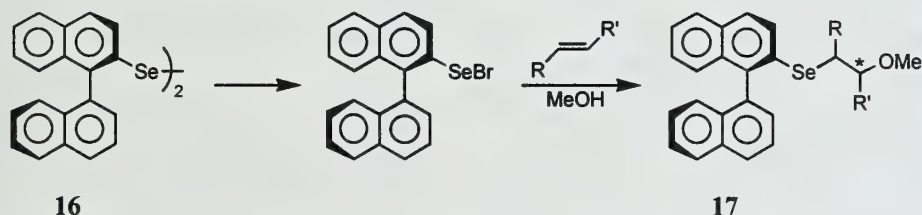
Scheme 5



Chiral Binaphthyl Selenides

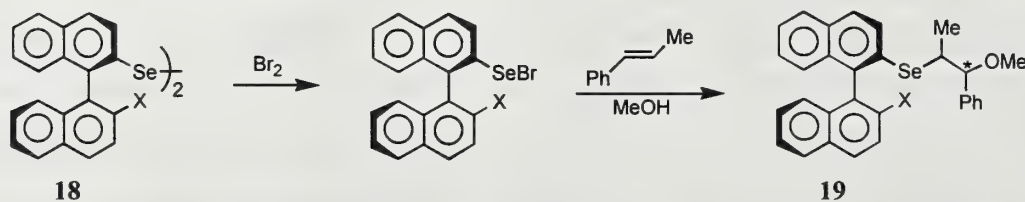
One of the first attempts to promote asymmetric induction using chiral selenium reagents utilized binaphthyl diselenide **16** to induce facial discrimination of simple olefins (Scheme 6).⁷ With methanol as the nucleophile, the methoxyselenenated products **17** were provided in yields of 48%-95% and *de*'s up to 49%. Although the diastereoselectivities achieved with these reagents were modest, they demonstrated that chiral selenium reagents could be used for asymmetric *trans*-addition to olefins.

Scheme 6

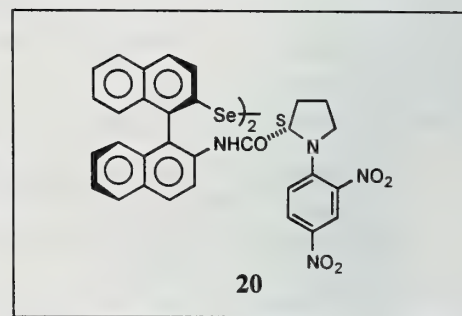


The asymmetric methoxyselenenylation was further investigated, using analogs of enantiomerically pure di(2'-N-substituted amido-2-binaphthyl) diselenides (Scheme 7, **18**) which contain a heteroatom at the 2'-position.^{8,9} The heteroatom provides a coordinating group that interacts with selenium in the chiral reagent. Heteroatoms such as oxygen and nitrogen have been observed spectroscopically to have intramolecular interactions with divalent selenium.¹⁰⁻¹² This coordination is thought to create a more rigid transition state, thus enhancing the stereoselectivities.

The use of binaphthyl derivative **18** ($X = \text{NHCOMe}$) with β -methyl styrene and methanol provided the methoxyselenide **19** in 63% yield as the only product with a de of 54%. This is a **Scheme 7**

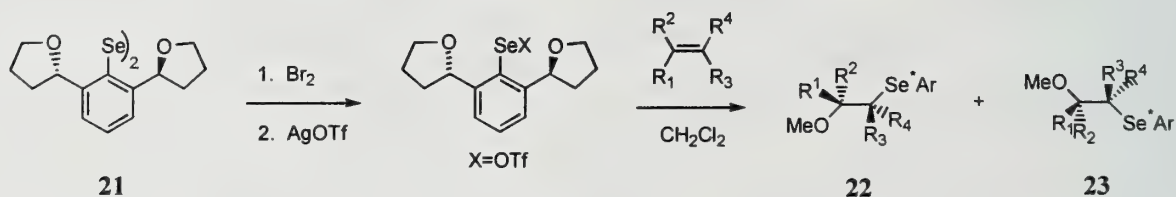


substantial enhancement compared to the unsubstituted case (**18**, $X = \text{H}$), which provided the methoxyselenide **19** with a de of 24%. Therefore the coordination of selenium with the amide group was a contributing factor in obtaining high selectivities. Using diselenide **20** provided **19** with a de of 79%. This was the highest de obtained to this point in the asymmetric *trans*-addition to alkenes and was the first to provide a practical level of asymmetric induction. This again demonstrated the importance of a selenium-nitrogen interaction and its ability to enhance the selectivities of the addition of electrophilic selenium to olefins.



C₂ Symmetrical Electrophilic Organoselenium Reagents

Numerous reports have shown that reagents possessing C_2 symmetry are efficient chiral reagents for the transfer of chiral information.¹³⁻¹⁵ Chiral C_2 symmetric organoselenium reagents, such as **21** (Scheme 8), demonstrated high facial selectivities with alkenes substituted with a phenyl



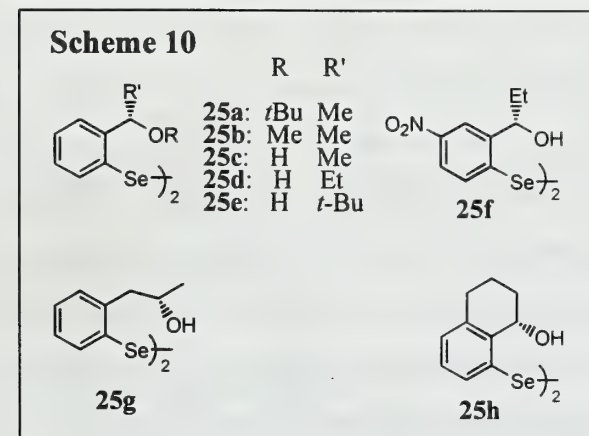
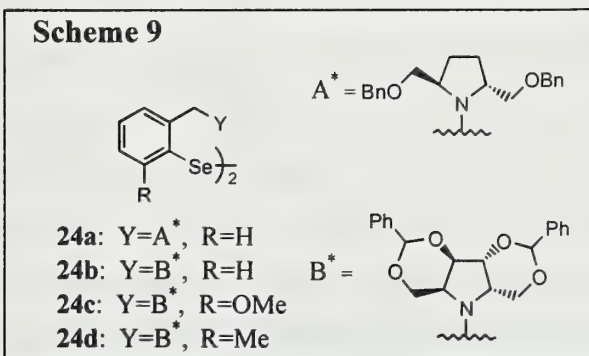
group or a bulky substituent, such as a *tert*-butyl or a cyclohexyl group. The products **22** and **23**, were obtained in good yield and with de's up to 98 % for 1,2-disubstituted (*E*)-olefins.

Diaryl diselenides with chiral pyrrolidine rings possessing C_2 symmetry at the ortho position were also shown to be efficient chiral inducers (Scheme 9).¹⁶⁻¹⁸ The utility of C_2 symmetrical diselenides **24**, bearing the stereogenic center at the coordinating amine, were demonstrated as chiral inducers in reactions with β -methyl styrene. Conversion of the selenenyl bromide to the

selenoperchlorate, which possesses a less nucleophilic counter ion, led to significant enhancement in the selectivities (de = 97 %).

Diaryl Diselenides

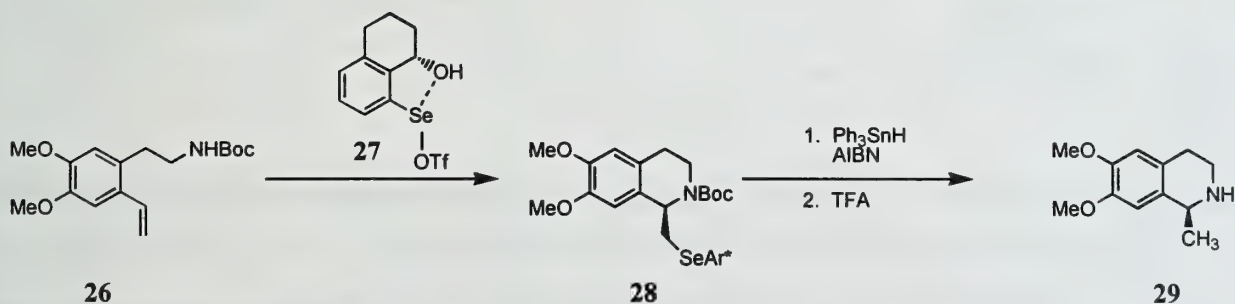
Simple chiral diaryl diselenides **25a-25h** have been developed that provide good facial selectivities and can be synthesized in relatively few steps from readily available starting materials (Scheme 10).¹⁹ Exchanging the halide with less nucleophilic counter ions, such as triflates, provide better selectivities presumably by allowing the reactions to be carried out at lower temperatures due to the increased reactivity of the electrophiles.



INTRAMOLECULAR CYCLIZATIONS

Alkenes incorporating a nucleophilic functionality within their scaffold can cyclize by reaction with chiral selenides to provide the corresponding heterocycles with high diastereoselectivities. The use of C₂ symmetrical optically active diaryl diselenides **24b** was extended to include asymmetric intramolecular selenoetherifications and selenolactonizations.^{20,21} The diastereofacial selectivities of mono, di, and trisubstituted alkenes were shown to provide the ether and lactone products in good yields (62%-100%, de = 13%-98%). Wirth and coworkers investigated intramolecular aminoselenenylations for applications in alkaloid synthesis (Scheme 11).²² In the synthesis of salsolidine, it was found that the

Scheme 11



counter ion of the electrophilic selenium reagent, as well as the substituents on the phenyl ring, play an important role in determining the yield and selectivity. Using selenenyl triflate **27** provided the product (-)-(*S*)-salsolidine **29** in 66% overall yield (de = 79 %) from **26**.

MECHANISTIC BASIS FOR ASYMMETRIC INDUCTION

The coordination of the heteroatom with selenium has been demonstrated to be a significant source of asymmetric induction by creating a more rigid and confined transition state. The nonbonding selenium-heteroatom interaction has been proposed to predominately be an $n \rightarrow \sigma^*$ -type orbital interaction between the heteroatom and the

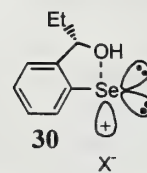
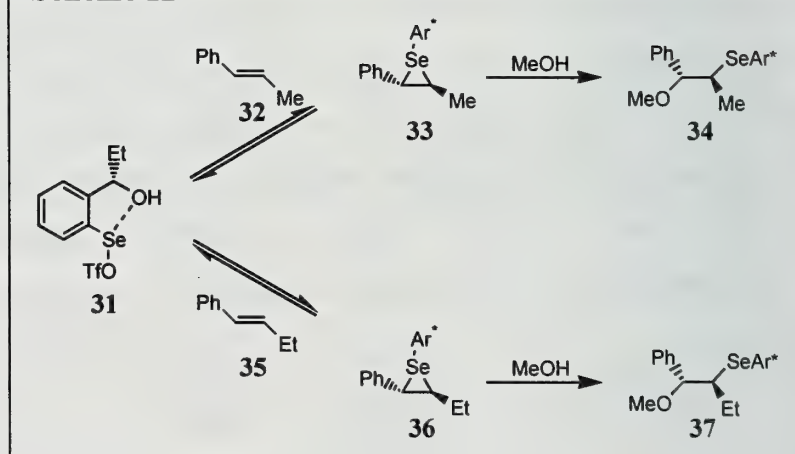


Figure 1. $n \rightarrow \sigma^*$ interaction

selenium moiety as shown in **30** (Figure 1). Wirth and coworkers investigated the mechanistic course of asymmetric induction using the chiral selenium electrophile **31** (Scheme 12).²³ The methoxyselenide **34** was provided by reaction of **32** with **31** followed by addition of methanol. Formation of **34** corresponds to approach on the *re* face of styrene. Therefore, it was proposed that the reaction proceeded through preferential formation of only one of the two possible seleniranium intermediates. In addition, the formation of the seleniranium ion **33** was found to be reversible under the reaction conditions by means of a decomplexation-complexation mechanism. The establishment of an equilibrium between the seleniranium ion **33** and **31** was demonstrated by formation of seleniranium ion **33** followed by addition of a second alkene **35** to the reaction mixture. Addition of methanol provided both methoxyselenides **34** and **37** in high diastereomeric excesses.

The equilibrium between **33** and **36** did not effect the stereoselectivity of the reaction; therefore, it was concluded that the formation of the diastereomeric seleniranium ions **33** and **36** are preferentially formed by approach to the *re* face of styrene due to an enhanced stability in comparison to the seleniranium ion formed from approach of the *si* face.

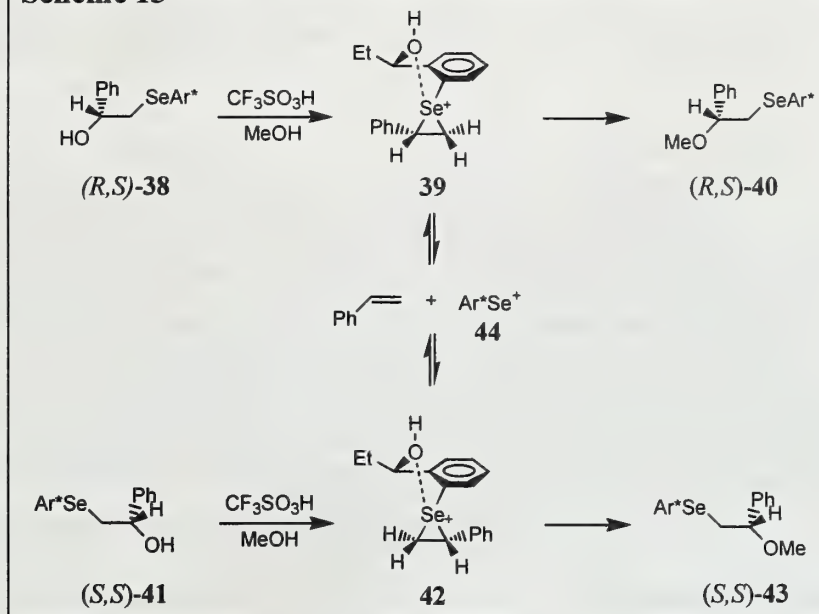
Scheme 12



To demonstrate that preferential formation of only one intermediate is a result of the different stabilities of the seleniranium intermediates, both intermediates **39** and **42** corresponding to approach of the *re* and *si* face were synthesized independently by treatment of both enantiomers of β-hydroxy selenides **38** and **41** with trifluoromethanesulfonic acid (Scheme 13).²³ Formation of the seleniranium ion intermediate **39** corresponds to the product of addition to the *re* face of styrene by **44**, which is presumably the more stable intermediate. Addition of methanol provided exclusively the β-methoxy

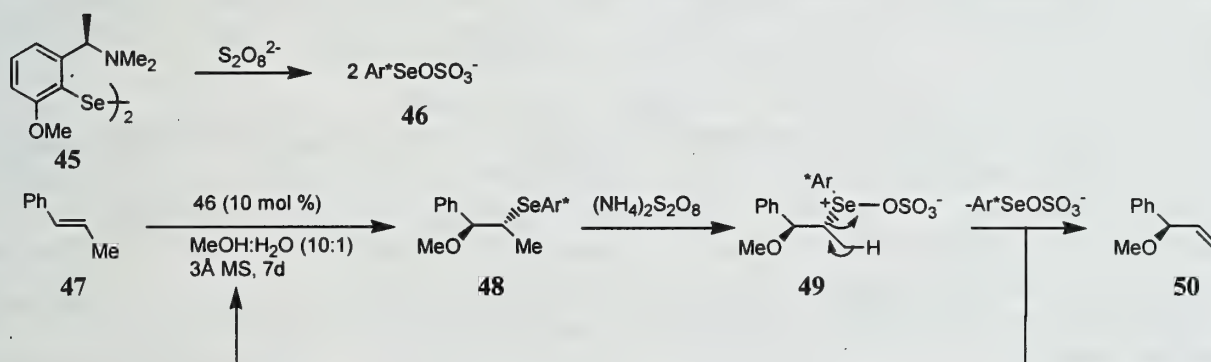
selenide (*R,S*)-**40**. The same conditions were applied to the seleniranium ion intermediate **42** corresponding to the product of addition to the *si* face of styrene by **44**, which is presumably the less stable intermediate. Addition of methanol provided a 3:1 mixture of (*S,S*)-**43** to (*R,S*)-**40** demonstrating that the less stable intermediate **42** converts to **39** by equilibrating to the more stable intermediate.

Scheme 13



CATALYTIC ASYMMETRIC OXYSELENYLATION-ELIMINATION

Until recently only stoichiometric amounts of chiral diselenides have been used successfully in the stereoselective functionalization of olefins. Wirth and coworkers investigated counter ions such as peroxodisulfates for the generation of the chiral selenium electrophiles to provide conditions favorable for catalytic turnovers (Scheme 14).²⁴ Formation of the electrophilic chiral selenenyl sulfate **46** by **Scheme 14**



reaction of the chiral diselenide **45** and the peroxodisulfate in the presence of 10 mol% of the metal salt $\text{Ni}(\text{NO}_3)_2 \cdot 6\text{H}_2\text{O}$, followed by addition of alkene **47** produces **48**. The methoxyselenenylated intermediate **48** is oxidized by the peroxodisulfate to provide **49** which then undergoes a selenoxide elimination to provide the chiral allylic ether **50**, releasing the electrophilic chiral selenenyl sulfate **46** which can undergo another addition reaction. The highest ee obtained for this catalytic conversion was 75% using

10 mol % of diselenide **45**. Although the catalytic turnovers are not very high this is the best enantioselectivity reported for the catalytic asymmetric methoxylation using chiral selenium reagents.

CONCLUSION

Significant advancements have been made in the asymmetric selenenylation of olefins. Many of the advancements are due to the synthesis of easily accessible chiral diselenides and the incorporation of coordinating heteroatoms. The methods have been successfully applied in the asymmetric synthesis of heterocycles and in the total synthesis^{25,26} of several natural occurring furofurans. Catalytic amounts of chiral diselenides have also been shown to provide products with good enantiomeric excesses in asymmetric methoxyselenenylation of olefins.

REFERENCES

1. *Organoselenium Chemistry*; Liotta, D., Ed.; Wiley: New York, 1987.
2. Paulmier, C. *Selenium Reagents and Intermediates in Organic Synthesis*; Pergamon; Oxford, 1986.
3. Schmid, G. H.; Garratt, D. G. *Tetrahedron Lett.* **1975**, 46, 3991-3994.
4. Garratt, D. G.; Kabo, A. *Can. J. Chem.* **1980**, 1030-1041.
5. Schmid, G. H.; Garratt, D. G. *J. Org. Chem.* **1983**, 4169-4172.
6. Review: Wirth, T. *Liebigs Ann./Recl.* **1997**, 2189-2196.
7. Tomoda, S.; Iwaoka, M. *Chem. Let.* **1988**, 1895-1898.
8. Tomoda, S.; Fujita, K.; Iwaoka, M. *J. Chem. Soc., Chem. Commun.* **1990**, 129-131.
9. Tomoda, S.; Fujita, K.; Iwaoka, M. *Phosphorus Sulfur* **1992**, 67, 247-252.
10. Tomoda, S.; Iwaoka, M. *Phosphorous Sulfur* **1992**, 67, 125-130.
11. Barton, D. H. R.; Hall, M. B.; Lin, Z.; Parekh, S. I.; Reibenspies, J. *J. Am. Chem. Soc.* **1993**, 115, 5056-5059.
12. Tomoda, S.; Iwaoka, M. *J. Am. Chem. Soc.* **1996**, 118, 8077-8084.
13. Déziel, R.; Goulet, S.; Grenier, L.; Bordeleau, J.; Bernier, J. *J. Org. Chem.* **1993**, 58, 3619-3621.
14. Déziel, R.; Malfenfant, E.; Bélanger, G. *J. Org. Chem.* **1996**, 61, 1875-1876.
15. Déziel, R.; Malfenfant, E.; Thibault, C.; Fréchette, S.; Gravel, M. *Tetrahedron Lett.* **1997**, 38, 4753-4756.
16. Tomoda, S.; Fujita, K.; Iwaoka, M. *Chem. Let.* **1994**, 923-926.
17. Tomoda, S.; Fujita, K.; Iwaoka, M.; Murata, K. *Tetrahedron Lett.* **1995**, 36, 5219-5222.
18. Tomoda, S.; Fujita, K.; Iwaoka, M.; Murata, K. *Tetrahedron* **1997**, 53, 2029-2048.
19. Wirth, T. *Angew. Chem., Int. Ed. Engl.* **1995**, 34, 1726-1728.
20. Tomoda, S.; Fujita, K.; Iwaoka, M.; Murata, K. *J. Chem. Soc., Chem. Commun.* **1995**, 1641-1642.
21. Déziel, R.; Malfenfant, E. *J. Org. Chem.* **1995**, 60, 4660-4662.
22. Wirth, T.; Fragle, G. *Synthesis* **1998**, 162-166.
23. Wirth, T.; Fragle, G.; Spichty, M. *J. Am. Chem. Soc.* **1998**, 120, 3376-3381.
24. Wirth, T.; Häuptli, S.; Leuenberger, M. *Tetrahedron: Asymmetry* **1998**, 547-550.
25. Wirth, T.; Kulicke, K. J.; Fragle, G.; *J. Org. Chem.* **1996**, 61, 2686-2689.
26. Wirth, T. *Liebigs Ann./Recl.* **1997**, 1155-1158.

INTRODUCTION

The use of computer simulations to elucidate reaction mechanisms and the structures of organic and biological molecules has increased greatly in the last two decades. However, for these simulations to be of more general use to organic chemists, they must account for solvation effects. Such methods have truly become accessible in recent years. To take full advantage of these models, an understanding of their theoretical basis is necessary. Three of the most widely used methods of accounting for solvation effects in computer simulations are the inclusion of explicit solvent molecules, the GB/SA model, and the SMx models. This review describes the theory, development, and application of these models.

EXPLICIT INCLUSION OF SOLVENT MOLECULES

Conceptually, the simplest way of accounting for the effects of solvation in computer simulations is to include explicit solvent molecules in the description of the system. Typically, 200 to 400 solvent molecules are needed to effectively simulate a small to medium sized organic solute molecule¹ and this number generally increases with the size of the solute molecule. Due to the large number of atoms in such a system, the calculations usually employ a classical mechanics forcefield in either Monte Carlo or molecular dynamics simulations.

The general form of the potential energy function of such a forcefield model is given by Equation 1. The first and second terms are summations over all bonds and all bond angles, respectively,

$$V = \sum_{\text{bonds}} \frac{1}{2} K_b (b - b_0)^2 + \sum_{\text{angles}} \frac{1}{2} K_\theta (\theta - \theta_0)^2 + \sum_{\text{dihed.}} K_\phi [1 + \cos(n\phi - \delta)] + \sum_{\substack{\text{pairs} \\ i \neq j}} \left(\frac{A_{ij}}{r_{ij}^{12}} - \frac{C_{ij}}{r_{ij}^6} + \frac{q_i q_j}{r_{ij}} \right) \quad (1)$$

where each bond and angle is treated as a harmonic oscillator. The third term accounts for changes in dihedral angle where n determines the number of minima and δ their position. The last summation corresponds to all long-range, non-bonded interactions including the interaction between the solute and the solvent molecules. These interactions are modeled by the combination of a Lennard-Jones potential for all atoms and a Coulomb potential between charged atoms. A common variation of this last term is the addition of interaction sites for lone pairs or at a virtual, non-atom-centered site. In another variation,

the united atom approach, each CH_n group is treated as one interaction site centered on the carbon atom. All constants in Equation 1 are parameters that must be fitted to either experimental data or results of ab initio calculations.

The accuracy of the non-bonded parameters is the main determinant of the effectiveness of including explicit solvent molecules as a solvation model. As an example of how these parameters are determined, the generation of Jorgensen's OPLS (optimized potentials for liquid simulations) model is considered.² As in most classical mechanics forcefields, the atoms in this model are separated into types determined by their functionality and connectivity. To lessen computational costs, all CH_n units are treated by the united atom approach and, with the exception of water, no non-atom-centered interaction sites are used. It should also be noted that $A_{ij} = (A_{ii}A_{jj})^{1/2}$, $C_{ij} = (C_{ii}C_{jj})^{1/2}$, $A_{ii} = 4\sigma_i\epsilon_i^{12}$, and $C_{ii} = 4\sigma_i\epsilon_i^6$. Thus, determining σ_i and ϵ_i for each interaction site determines all A_{ij} and C_{ij} .

Most OPLS parameters were optimized utilizing liquid simulations of small organic molecules.² Monte Carlo simulations of 100-200 molecules per unit cell were used to fit the simulated values of liquid densities and heats of vaporization to the experimental values. These parameters were first determined for liquid hydrocarbons,³ and the procedure followed serves as an illustrative example of the general methods used. The bond lengths and angles were fixed at standard geometries and, only in this specific case of hydrocarbons, all charges were set to zero. Cyclopentane was used to optimize the $\text{CH}_2(\text{sp}^3)$ parameters, which were subsequently applied in simulations of *n*-butane to optimize the CH_3 parameters. However, while attempting to optimize the CH parameters with simulations of isobutane, no reasonable values could be obtained without changing ϵ for CH_3 . This result indicated that more than one type of CH_3 was required to adequately fit the data. In fact, four types were required, defined by the branching of the adjacent carbon and labeled $\text{CH}_3(\text{C}_n)$, where *n* is the number of non-hydrogen substituents on the adjacent carbon. Simulations of isobutane were then used to simultaneously optimize the parameters for $\text{CH}(\text{sp}^3)$ and $\text{CH}_3(\text{C}_3)$, requiring that ϵ decrease and σ increase relative to the previously determined values for $\text{CH}_3(\text{C}_2)$. Parameters for the all other types of CH_n groups in hydrocarbons were determined in a similar manner. Liquid simulations of molecules with other functionalities were used to optimize σ and ϵ for several other atom types, the number of different types being kept to a minimum whenever feasible. For example, all amide carbonyls were considered the same type as were all alcoholic oxygens.

When parameters for an atom type cannot be fitted to experimental data of a liquid molecule because the experimental data is not reliable or because the functionality is charged, these parameters are instead fitted to ab initio calculations. For example, ammonium and carboxylate group parameters were optimized to reproduce the geometries and interaction energies determined by ab initio calculations with

the 6-31G(d) basis set for complexes of water with ammonium, methylammonium, and formate ions. These parameters were also required to accurately predict the experimental heats of hydration for tetrabutyl ammonium, acetate, and the three previously mentioned ions.⁴

Following the methodology illustrated above, parameters for a multitude of functionalities have been developed. The OPLS parameters can be combined with the bond length and angle parameters of a forcefield such as AMBER to fully characterize a system. Hydrocarbons, amides, esters, amines, azoles, thiols, and proteins are just a few of the solutes that can be effectively modeled with the OPLS/AMBER parameters. This model can also be readily extended to other molecules as was done for carbohydrates by simply adding parameters for the acetal carbon. These parameters were fitted to both ab initio calculations of dimethoxymethane and experimental data for liquid dimethoxymethane and 1,3-dioxolane.⁵ An additional advantage of this method is that any molecule that can be modeled as a solute can also be used as a solvent, although smaller, simpler molecules give faster results.

The OPLS/AMBER parameters are available as part of the BOSS program. Other programs, including AMBER,⁶ CHARMM,⁷ and GROMOS,⁸ can also be used to model solvation by including explicit solvent in the system description.

THE GENERALIZED BORN/SURFACE AREA (GB/SA) SOLVATION MODEL

Simulations using explicit solvent molecules have been widely used and are generally quite accurate; however, they can be very time consuming, especially when converged energies are required. One alternative is to treat the solvent as a statistical continuum. Continuum models have long been employed in the numerical calculation of free energies of solvation and were applied to computer simulations by Still and co-workers in 1990 when they developed the GB/SA model for use with a classical mechanics forcefield.⁹

In the GB/SA model, the free energy of solvation (G_{sol}) is considered to be the sum of two separate terms: one the result of electrostatic interactions between the solute and solvent (G_{pol}) and the other due to cavitation, dispersion, and solvent restructuring effects (G_{CDS}). The first assumption made in this model is to set $G_{CDS} = \sum_k \sigma_k SA_k$, where σ_k is a parameter that can be optimized for each atom type and SA_k is the solvent accessible surface area of each atom. This assumption can be partially justified by the linear dependence of G_{sol} for saturated hydrocarbons on the solvent accessible surface area because G_{pol} for such compounds should be negligible. Conceptually, SA_k is the area of the surface mapped out by the center of a sphere of radius R_s , representing the solvent, when it is rolled over the van der Waals

surface of radius R_k of the molecule. Thus, SA_k is the surface area of the parts of the sphere centered on the atom k of radius (R_s+R_k) which are not contained in any similarly defined sphere centered on another atom (Figure 1). Each SA_k varies with the structure and is analytically approximated in this model although it can also be numerically estimated.

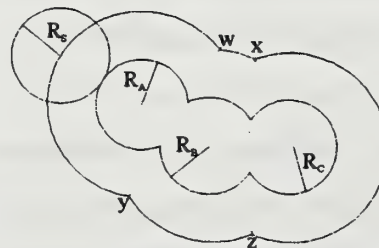


Figure 1. Schematic view of SASA

The electrostatic term is calculated using the generalized Born equation for a system of N interacting particles with charges q and Born radii α in a medium of dielectric constant ϵ (Equation 2). Still and co-workers combined the two terms to yield the right side of Equation 2 with f_{GB} defined to approximate classical behavior as in Equation 3. The Born radius is larger than the Coulomb radius p

$$G_{pol} = -332 \left(1 - \frac{1}{\epsilon} \right) \sum_{i=1}^{N-1} \sum_{j=i+1}^N \frac{q_i q_j}{r_{ij}} - 166 \left(1 - \frac{1}{\epsilon} \right) \sum_{i=1}^N \frac{q_i^2}{\alpha_i} = -166 \left(1 - \frac{1}{\epsilon} \right) \sum_{i=1}^N \sum_{j=1}^N \frac{q_i q_j}{f_{GB}} \quad (2)$$

$$f_{GB} = \left(r_{ij}^2 + \alpha_i \alpha_j \exp \left\{ r_{ij}^2 / 4 \alpha_i \alpha_j \right\} \right)^{1/2} \quad (3)$$

and is determined by assuming that the other atoms serve to screen the charge from the dielectric medium. Thus, each α_i depends on its own Coulomb radius as well as the location and Coulomb radius of every other atom. In the GB/SA model, p is set equal to the atomic radius from the OPLS forcefield minus an offset, δ , determined by the solvent.

The GB/SA model is applicable to most solutes and solvents and generally gives reliable results. It is very simple to integrate into preexisting forcefields and is available as part of MacroModel. The model can be applied to all solutes that are well simulated by a classical mechanics forcefield, and only two parameters, σ and δ , need to be determined to adequately model a solvent. The hydration energies calculated by the GB/SA model generally correlate well with the experimental values and only require two to four times more computer time than the corresponding gas-phase calculations.⁹ This is a vast improvement over the free energy perturbation calculations needed to achieve converged energies using explicit solvent molecules.

THE SM_x SOLVATION MODELS

Although the GB/SA model is better suited for some purposes than explicitly including solvent molecules, there are still aspects of solvation that are not adequately addressed by either model. Indeed, two of these, the inability to account for the effects of solvent induced charge reorganization and to

analyze reactive species or transition states, cannot be easily treated by any classical mechanics forcefield. Both of these issues are addressed by the extension of Still's generalized Born/solvent accessible surface area model to semiempirical molecular orbital theory as accomplished by Cramer and Truhlar.¹⁰⁻¹⁶

This extension was developed in a series of models where each successive model is more accurate, and usually more detailed, than the preceding one. Because of this escalation in complexity, these models are reviewed sequentially to aid in the understanding of the latest model. The concepts behind the extension of Still's model are relatively simple; however, the mathematics involved are convoluted. For this reason, this review only discusses the mathematics in a qualitative way that should be sufficient for understanding what types of interactions are taken into account and what assumptions are made.

The AM1-SM1 Model

AM1-SM1 is a model for aqueous solvation only and is a very straightforward adaptation of Still's method to the semiempirical Austin Model 1 (AM1).^{10,17} The non-electrostatic free energy is still calculated as $G_{\text{CDS}} = \sum_k \sigma_k SA_k$; however, the surface area is calculated numerically rather than analytically.

In this model, σ_k depends only on the atomic number of the atom and was optimized for $k = \text{C, N, O, F, S, Cl, Br, and I}$. Hydrogen's value for σ_k was set to zero because optimization for different classes of solute yielded widely varying values. The free energy due to electrostatic interactions is calculated according to Equation 2 with only a few changes in its implementation. The most important of these changes is that the charges are determined by Mulliken population analysis instead of being set at a constant defined by atom type as in the GB/SA model. In this way, the charges are altered by the solvation-induced changes in the density matrix. In addition, damping factors were added to f_{GB} to correct for systematic error in the treatment of O-O and N-H pairs. The method of calculation of the Born radius was also slightly modified in that the Coulomb radius ρ depends only on atomic number and charge and is determined by a smooth sigmoidal function with empirically optimized parameters. The effects of solvation are incorporated into the Fock matrix that is defined as the partial derivative of G with respect to the density matrix. Thus, as the Fock matrix affects the orbitals, the charges also change. These altered orbitals effect a change in the matrix, and the cycle continues until the energies have converged. All parameters in this model were optimized to reproduce the experimental free energies of solvation for a set of 141 neutral molecules including a wide variety of mono- and polyfunctional compounds. The root mean square (rms) error for this set is 1.52 kcal/mol.

Models SM2 and SM3

SM2 and SM3 are also only parameterized for aqueous solvation, are conceptually very similar to SM1, and, in form, are identical to each other.¹¹ The sole difference between SM2 and SM3 is that SM2 is optimized for the AM1 semiempirical Hamiltonian, while SM3 is based on the semiempirical Hamiltonian of Parameterized Model 3 (PM3).¹⁸ In contrast to SM1, SM2 and SM3 contain parameters for phosphorus, but these parameters may not be optimal since little data was available for their fitting. Presumably for this reason, no other SM models contain parameters for phosphorus. Additionally, the treatment of hydrogen was modified so that these models would better account for the hydrophobic effect. This modification is not implemented in the newest model and therefore it is not detailed here. SM2.1 and 3.1 differ from SM2 and 3 only in the improved algorithms used to calculate certain values.¹²

The SM4 model

SM4 was parameterized for use with all alkane solvents and all solutes containing H, C, N, O, F, S, Cl, Br, and I.^{13,14} In addition to the changes required to parameterize for many solvents, two important revisions were made in the development of SM4. The first modification is the use of CM1A or CM1P charges instead of charges taken directly from Mulliken population analysis. CM1 charges are calculated from the charges determined by Mulliken population analysis by an empirically determined mapping function.¹⁹ The SMx models are very dependent on the partial charges used and the CM1 models calculate these values more accurately. A change needed to correctly fit experimental data is the separation of the G_{CDS} terms into the sum of G_{CS} and G_{CD} terms as $G_{CDS} = \sum_k \sigma_k^{CD} SA_k^{CD} + \sigma^{CS} \sum_k SA_k^{CS}$.

This can be motivated by the fact that, while dispersion terms can be generally limited to the parts of the solvent in direct contact with the solute, solvent restructuring effects must extend further. R_s , used in the calculation of the solvent accessible surface area, is 2.0 Å for the CD terms and 4.9 Å for the CS term. Although σ^{CS} is assumed to be independent of the solute atom and linearly dependent on the macroscopic surface tension, σ_k^{CD} is assumed to differ with atom type but to be the same for all alkane solvents. The other important change is that σ_H^{CD} is no longer set to zero, but is instead dependent on hydrogen's bond order to other elements. This replaces the changes made in SM2 and SM3. Also, σ_C^{CD} contains a term dependent on carbon's bond order to other carbons, correcting a consistent source of error. These changes remove the need for the damping parameter in f_{GB} for N-H pairs but not for O-O pairs. The rms error in G_{sol} for this model across 506 solute-solvent pairings for either Hamiltonian is only 0.45 kcal/mol.

The SM5.4-aqueous Model

Differences between SM5.4 and previous models are small but they result in significant improvement.¹⁵ CM1P or CM1A charges are used, the Coulomb radius is constant for all atoms but hydrogen, and all bond order dependencies are geometry-based instead. The first change results in a more accurate model and the last results in a more stable parameterization. The radius of hydrogen atoms is dependent on the location of other atoms, which eliminates the need for the charge-dependent radii used previously. The G_{CDs} terms are not separated in the aqueous model; however, the form of σ_k is similar to that used in SM4. Thus, σ_{H} depends on the hydrogen's location relative to nearby C, O, N, and S atoms; σ_{C} on the relation to other C atoms; σ_{O} on other C, N, and O atoms; σ_{S} on other S atoms; and σ_{N} on the relative location of nearby C atoms. When the surface tensions are defined in this way, both damping terms in f_{GB} can be removed. This model is parameterized for solutes containing H, C, N, O, F, S, Cl, Br, and I. The rms error in G_{sol} across 215 solutes is 0.72 kcal/mol with AM1 and 0.62 kcal/mol with PM3.

The SM5.4/A-organic Model

This model is designed for almost all organic solvents and is very similar to SM5.4-aqueous, except that G_{CDs} is split into G_{CD} and G_{CS} as in SM4.¹⁶ The solvent parameters that are used in determining the σ_k^{CD} and σ^{CS} for each solvent are the index of refraction (n), the macroscopic surface tension (γ), and Abraham's acidity parameter (α) and basicity parameter (β).²⁰ Each σ^{CS} is the sum of two terms: one proportional to n and the other to γ . Each σ_k^{CD} is the sum of four terms: one proportional to n , one to α , one to β , and one dependent on the atom's location relative to other atoms as described for SM5.4-aqueous. This last term, however, consists of a geometry factor multiplied by the sum of three terms proportional to n , α , and β , respectively. In total, not including the parameters equal to zero, 41 surface tension parameters are optimized in this model. The mean unsigned error in G_{sol} for this model across 90 solvents, 27 solute classes, and 1784 total measurements is 0.5 kcal/mol.

Summary Of SMx Models

The SMx models give good agreement with experiment over a wide range of solutes and solvents. Since no typing of atoms is needed, these models are applicable to a large range of solutes including transition states, reactive intermediates, and non-traditional compounds. With the development of SM5.4-organic, a wide variety of solvents can be used since Abraham's α and β parameters are known or

can be well-estimated for almost any solvent. These models are available as part of the AMSOL program.

CONCLUSION

Not only are all three of these models discussed here widely used and readily available, but each also has certain advantages over the other two. The inclusion of explicit solvent molecules can better model systems where solvent molecules are active participants or where the structure of the first solvation shell is important. For many other systems, the GB/SA model gives comparably accurate results at a fraction of the computational cost. The SMx models are more computationally expensive than GB/SA, but they are still less expensive than modeling explicit solvent and can be used to model systems not easily or well described by classical forcefields. Thus, the question is not which model is best, but which model is better suited to a particular purpose.

REFERENCES

- (1) Jorgensen, W. L. *Acc. Chem. Res.* 1989, 22, 184.
- (2) Jorgensen, W. L.; Tirado-Reves, J. J. *Am. Chem. Soc.* 1988, 110, 1657.
- (3) Jorgensen, W. L.; Madura, J. D.; Swenson, C. J. *J. Am. Chem. Soc.* 1984, 106, 6638.
- (4) Jorgensen, W. L.; Gao, J. J. *Phys. Chem.* 1986, 90, 2174.
- (5) Jorgensen, W. L.; Morales de Tirado, P. I.; Severance, D. L. *J. Am. Chem. Soc.* 1994, 116, 2199.
- (6) Weiner, S. J.; Kollman, P. A.; Nguyen, D. T.; Case, D. A. *J. Comput. Chem.* 1986, 7, 230.
- (7) Brooks, B. R.; Bruccoleri, R. E.; Olafson, B. D.; States, D. J.; Swaminathan, S.; Karplus, M. J. *Comput. Chem.* 1983, 4, 187.
- (8) Hermans, J.; Berendsen, H. J. C.; van Gunsteren, W. F.; Postma, J. P. M. *Biopolymers* 1984, 23, 1513.
- (9) Still, W. C.; Tempczyk, A.; Hawley, R. C.; Hendrickson, T. *J. Am. Chem. Soc.* 1990, 112, 6127.
- (10) Cramer, C. J.; Truhlar, D. G. *J. Am. Chem. Soc.* 1991, 113, 8305.
- (11) Cramer, C. J.; Truhlar, D. G. *J. Comput.-Aided Mol. Des.* 1992, 6, 629.
- (12) Liotard, D. A.; Hawkins, G. D.; Lynch, G. C.; Cramer, C. J.; Truhlar, D. G. *J. Comput. Chem.* 1995, 16, 422.
- (13) Giesen, D. J.; Storer, J. W.; Cramer, C. J.; Truhlar, D. G. *J. Am. Chem. Soc.* 1995, 117, 1057.
- (14) Giesen, D. J.; Cramer, C. J.; Truhlar, D. G. *J. Phys. Chem.* 1995, 99, 7137.
- (15) Chambers, C. C.; Hawkins, G. D.; Cramer, C. J.; Truhlar, D. G. *J. Phys. Chem.* 1996, 100, 16385.
- (16) Giesen, D. J.; Gu, M. Z.; Cramer, C. J.; Truhlar, D. G. *J. Org. Chem.* 1996, 61, 8720.
- (17) Dewar, M. J. S.; Zoebisch, E. G.; Healy, E. F.; Stewart, J. J. P. *J. Am. Chem. Soc.* 1985, 107, 3902.
- (18) Stewart, J. J. P. *J. Comput.-Aided Mol. Des.* 1990, 4, 1.
- (19) Storer, J. W.; Giesen, D. J.; Cramer, C. J.; Truhlar, D. G. *J. Comput.-Aided Mol. Des.* 1995, 9, 87.
- (20) a) Abraham, M. H. *Chem. Soc. Rev.* 1993, 73. b) Abraham, M. H. *J. Phys. Org. Chem.* 1993, 6, 660.



UNIVERSITY OF ILLINOIS-URBANA



3 0112 002395504

Q.547
I16s
1998-99:1

ORGANIC SEMINAR ABSTRACTS

SEMESTER I

FALL 1998

University of Illinois

**Department of Chemistry
600 South Mathews Avenue
271 Roger Adams Laboratory
Urbana, IL 61801**

January 1999

NOTICE: Return or renew all Library Materials! The *Minimum Fee* for each Lost Book is \$50.00.

The person charging this material is responsible for its return to the library from which it was withdrawn on or before the **Latest Date** stamped below.

Theft, mutilation, and underlining of books are reasons for disciplinary action and may result in dismissal from the University.
To renew call Telephone Center, 333-8400

UNIVERSITY OF ILLINOIS LIBRARY AT URBANA-CHAMPAIGN

CHAMPAIGN LIBRARY

MAY 19 2002

FEB 13 2003

JAN 17 2003

SEMINAR TOPICS

SEMESTER I

FALL 1998

	<u>PAGE</u>
CHIRAL SULFONIUM YLIDE MEDIATED ASYMMETRIC CYCLIZATION REACTIONS MARN C. WHISLER	3
DEVELOPMENT OF $\alpha_v\beta_3$ INTEGRIN INHIBITORS FOR SUPPRESSION OF ANGIOGENESIS ALICE L. RODRIGUEZ	11
RING OPENING CYCLOADDITIONS OF METHYLENECYCLOPROPANES AND VINYL CYCLOPROPANES NICOLE M. OKELEY	19
CARBOMETALATIONS OF CARBON-CARBON MULTIPLE BONDS BY ORGANOZINC COMPOUNDS..... ERIC MERTZ	27
VANCOMYCIN: AN APPLICATION OF BIARYL ETHER SYNTHESIS..... JEROMY COTTELL	35

DESIGNING MOLECULAR-SCALE ORGANIC DEVICES	43
DAVID J. HILL	
CHIRAL LITHIUM AMIDES FOR THE ENANTIOSELECTIVE DEPROTONATION OF KETONES AND EPOXIDES	51
CORY STIFF	
THE APPLICATION OF POLYMERIC CATALYSTS TO ASYMMETRIC SYNTHESIS	59
JOSHUA A. ORLICKI	
FUSED TETRAHYDROPYRAN AND OXEPANE SYNTHESIS TOWARDS HEMIBREVETOXIN B	67
STEPHEN THORN	
CATALYTIC ASYMMETRIC NUCLEOPHILIC RING OPENING OF MESO EPOXIDES AND KINETIC RESOLUTION OF TERMINAL EPOXIDES	75
SUNG H. LIM	
ORGANIC SYNTHESIS BY ELECTROCHEMICAL METHODS	83
JIPING FU	
THE STRUCTURAL AND MECHANISTIC RELATIONSHIP OF ISOPENICILLIN N SYNTHASE AND 2-KETOGLUTARATE-DEPENDENT ENZYMES	91
ELLEN D. EBERHARD HILL	
CHEMISTRY OF ARTEMISININ AND OTHER RELATED ANTIMALARIAL COMPOUNDS	99
JUSTIN SHEY	

CHIRAL SULFONIUM YLIDE MEDIATED ASYMMETRIC CYCLIZATION REACTIONS

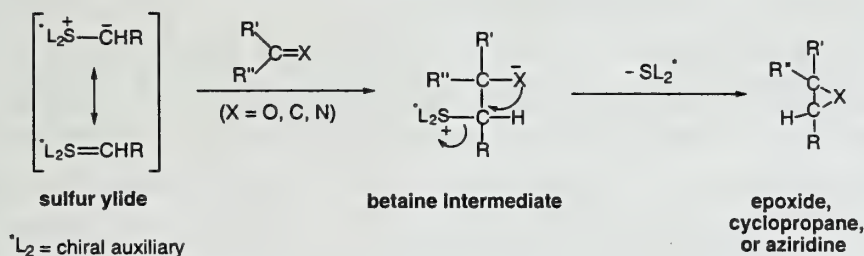
Reported by Marna C. Whisler

October 1, 1998

INTRODUCTION

Sulfur ylide chemistry has recently emerged as a powerful method for the stereoselective formation of carbon-carbon bonds.^{1,2} Sulfonium ylide addition to carbonyls, enones, and imines provides a synthetically versatile and mechanistically interesting route to epoxides, cyclopropanes, and aziridines. The nucleophilic attack of an ylide on an electrophilic C=X (X = O, C, N) carbon is believed to give rise to a betaine intermediate. Subsequent displacement of the sulfide leaving group (SL₂^{*}) by X⁻ generates the three-membered ring. With an asymmetric ligand on sulfur, attack of the ylide on the electrophilic carbon can occur stereoselectively, giving rise to an enantioenriched epoxide, cyclopropane, or aziridine.

Asymmetric sulfonium ylide mediated reactions were first investigated by Trost and coworkers in 1973.³ However, the low levels of asymmetric induction dissuaded further research until Furukawa's breakthrough work of 1989.⁴ The research prior to 1995 has been summarized in a recent report.^{1, 5-9} This review focuses on asymmetric epoxidation of carbonyl compounds with sulfonium ylides and also highlights recent advances in sulfonium ylide mediated cyclopropanation and aziridination since 1995.

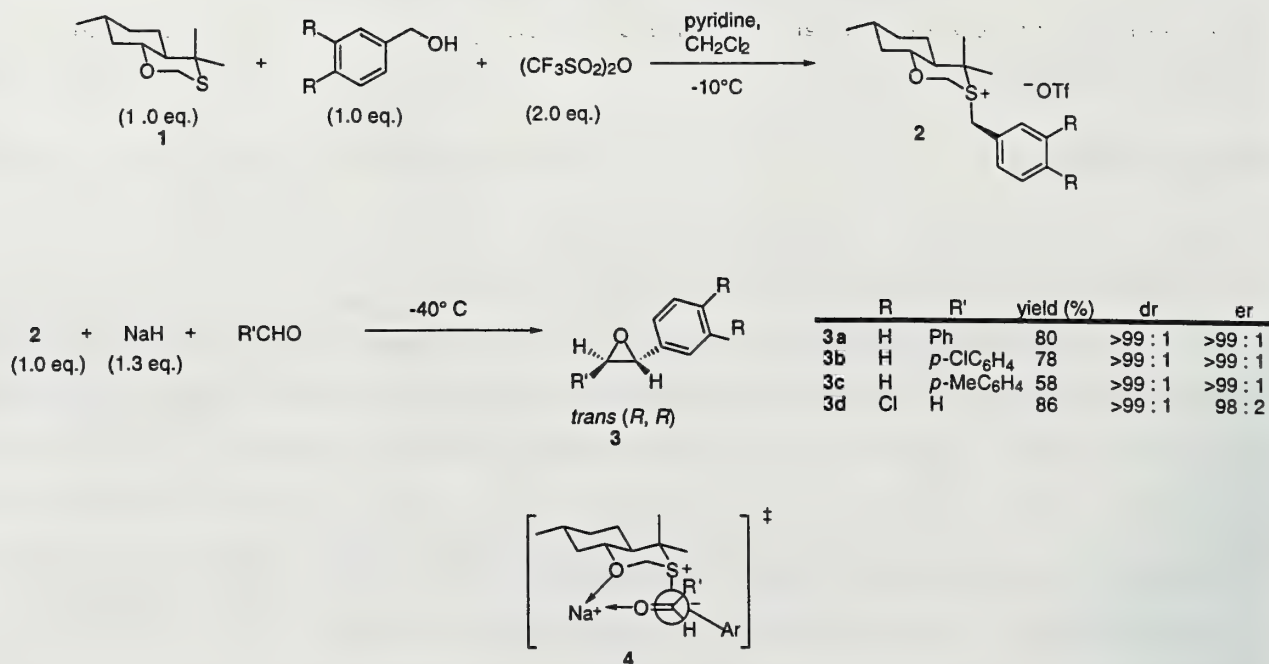


EPOXIDATION

Stoichiometric Epoxidation of Carbonyl Compounds with Chiral Sulfonium Ylides

Solladié-Cavallo and coworkers have developed the chiral oxathiane auxiliary **1** for epoxidations with non-enolizable aldehydes (Scheme 1).^{10, 11} After S-alkylation of the oxathiane, the ylide is formed by deprotonation of **2** with NaH, and then treated with an aromatic aldehyde¹⁰ or paraformaldehyde¹¹ to provide epoxide products **3** with high enantiomeric ratios. This stereoselectivity is attributed to a plausible transition structure **4** in which chelation of the Na⁺ cation to the oxygen atoms of the oxathiane and the incoming aldehyde governs the facial selectivity of the ylide. The facial selectivity of the aldehyde is attributed to steric effects between the two aromatic rings in the betaine intermediate. Although recoverable and reusable, this sulfonium auxiliary must be used in stoichiometric amounts.

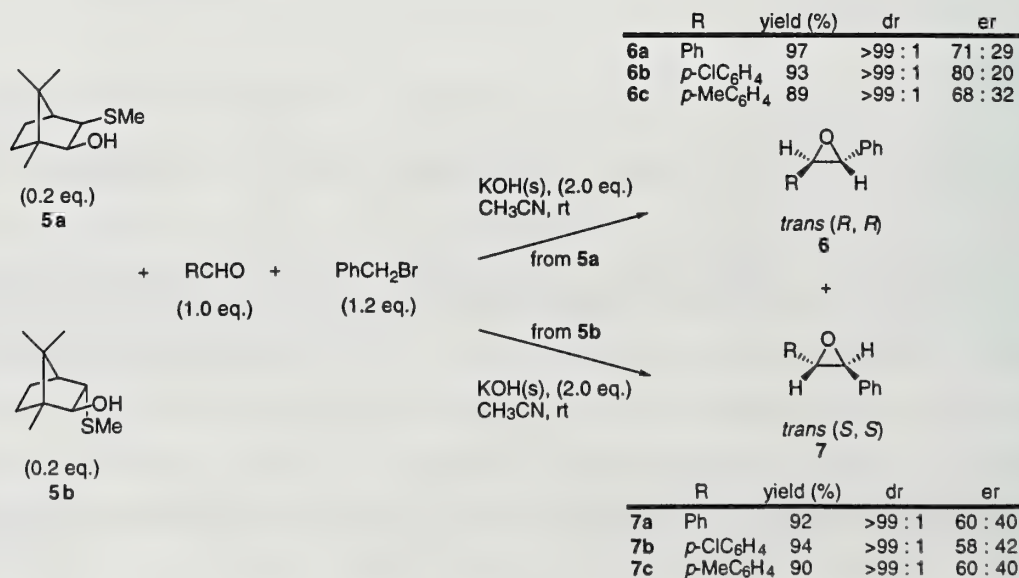
Scheme 1



Catalytic Epoxidation of Carbonyls with Chiral Sulfonium Ylides

Chiral sulfonium ylides may also be used in catalytic amounts to induce asymmetric epoxide ring formation.¹²⁻¹⁹ Asymmetric epoxidations mediated by various D-(+)-camphor-derived sulfides **5** have been demonstrated to provide products in excellent yields and with good stereoselectivities (Scheme 2).¹² When used as a benzylidene transfer reagent, methylated sulfides need only be present in catalytic amounts (0.2 equivalents).

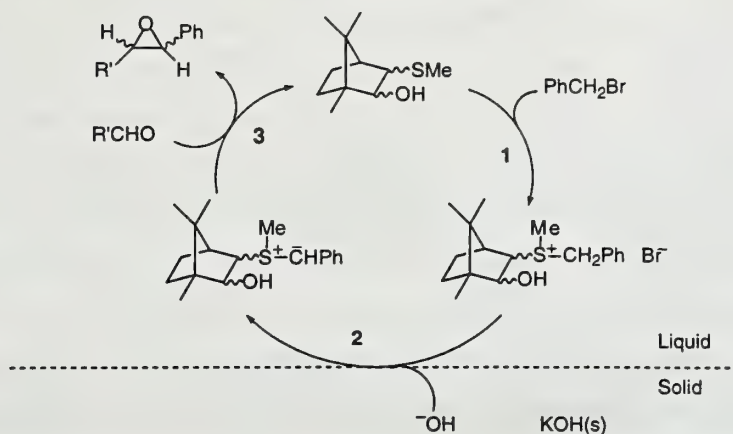
Scheme 2



The proposed catalytic cycle (Scheme 3) includes (1) sulfonium salt preparation by addition of benzyl bromide to the sulfonium auxiliary, (2) deprotonation by base under phase transfer conditions to

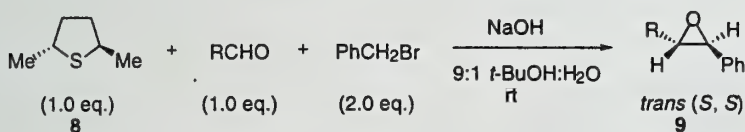
afford the corresponding ylide, and (3) attack of the ylide on the aldehyde giving the newly-formed epoxide and regeneration of the original sulfonium compound. This methodology provides convenient

Scheme 3



access to both (+)- and (-)- *trans*-diaryloxiranes, depending on whether *exo*-**5a** or *endo*-**5b** alkylthio groups are employed. Although this catalytic method is convenient, proceeds with complete diastereoselectivity, and allows direct access to the enantiomer of choice, the enantiomeric ratios (er) are poor.

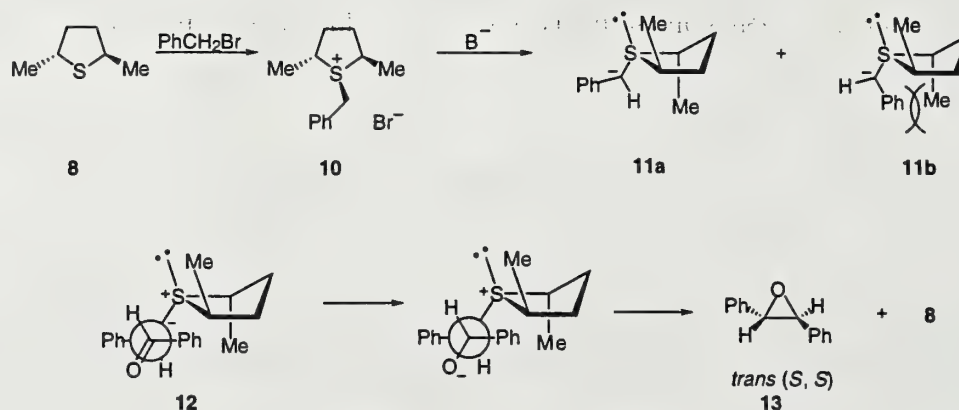
Julienne and Metzner have reported that the C_2 symmetric sulfide **8** transfers a benzylidene unit to aldehydes to produce epoxides **9** with high diastereomeric ratios (dr), enantiomeric ratios, and yields.¹³ The catalytic cycle is comparable to that for auxiliary **5** shown in Scheme 3 (*vide supra*). This sulfide can be prepared in two steps and its symmetry allows for the formation of only one diastereomeric sulfonium salt **10** upon reaction with benzyl bromide. The sulfide has been shown to be effective in catalytic amounts (0.1 equivalent) in a reaction with benzaldehyde (1 equivalent) and benzyl bromide (2 equivalents). Although the reaction took one month to complete, the yield (92%), dr (92:8), and er (95:5) are all high. The C_2 symmetric sulfide was tested in stoichiometric amounts with three other aldehydes.



	R	yield (%)	dr	er
9a	Ph	92	93 : 7	94 : 6
9b	<i>p</i> -ClC ₆ H ₄	89	92 : 8	93 : 7
9c	<i>p</i> -MeC ₆ H ₄	88	92 : 8	94 : 6
9d	Cy	87	65 : 35	97 : 3

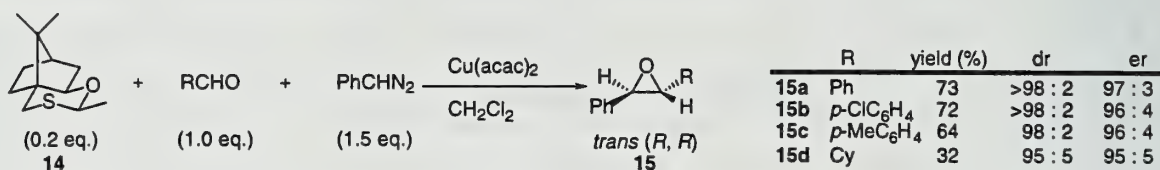
Deprotonation of the sulfonium salt by base affords the ylide **11**, which could in theory assume two different conformations, **11a** and **11b** (Scheme 4). The conformer **11a** is hypothesized to be the preferred conformer, as it minimizes repulsion between the phenyl group and the methyl group of the thiolane ring. The aldehyde approaches from the *si* face of the ylide since the *re* face is blocked by the methyl group of the five-membered ring. Furthermore, to avoid unfavorable steric interactions with the phenyl ring of the benzyl group, the incoming aldehyde approaches from its *re* face, as in conformation **12**, inducing diastereoselectivity in epoxide **13**.

Scheme 4



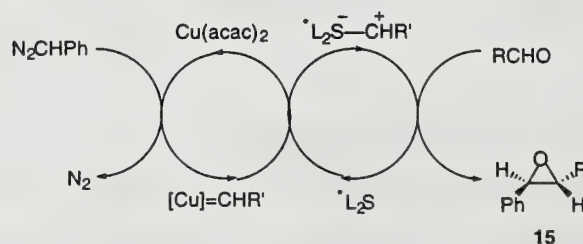
Although the aforementioned methods stereoselectively provide epoxides in good yield, the reactions require strongly basic conditions for deprotonation which limits the type of aldehydes suitable for reaction.

Generation of sulfur ylides via a metal carbenoid, an alternate method to the deprotonation of sulfonium salts, has been explored by Aggarwal and coworkers.¹⁴⁻¹⁹ Initially, a $\text{Cu}(\text{acac})_2$ complex reacts with a diazo compound to form a metal carbenoid.^{14,15} The chiral sulfur catalyst **14**, which need only be present in catalytic amounts, then reacts with the metallocarbene, forming the sulfur ylide *in situ*.



Nucleophilic attack of the ylide on the carbonyl carbon of the aldehyde followed by elimination of the chiral bicyclic sulfonium auxiliary generates the asymmetric epoxide **15** (Scheme 5). Because this method allows for catalytic sulfur ylide formation under neutral conditions, base-sensitive aldehydes may be employed.¹⁶

Scheme 5

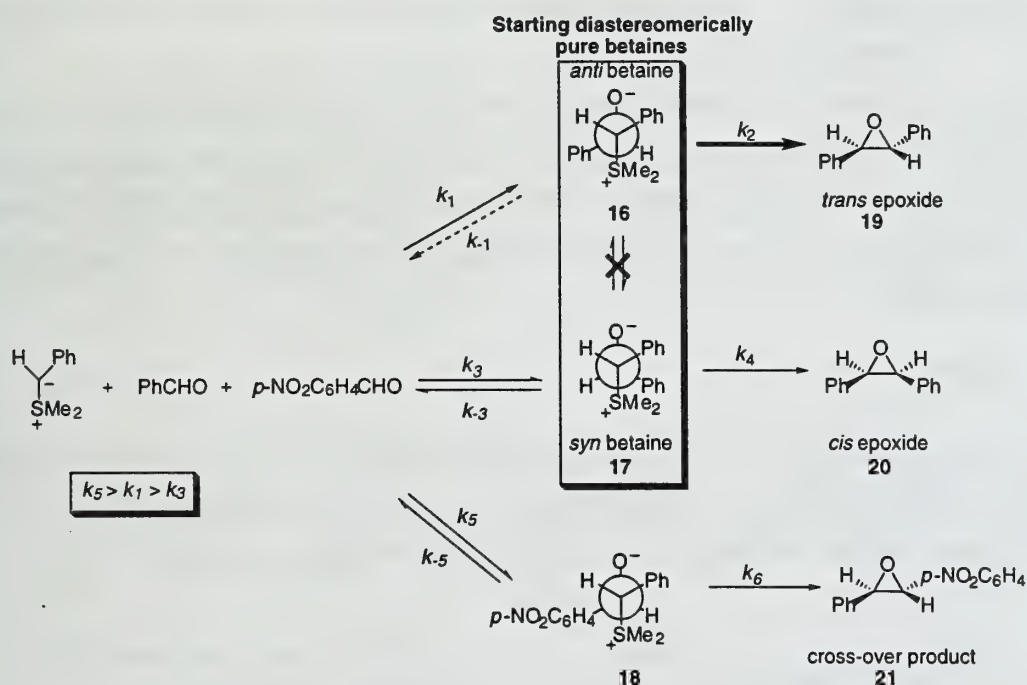


Origin of Diastereoselectivity

Reaction of a sulfonium ylide with a carbonyl compound has been assumed to proceed through a betaine intermediate. The betaine may adopt either a *syn* or *anti* conformation. $\text{S}_\text{N}2$ displacement of the

sulfur auxiliary from the *anti* diastereomer would provide a *trans* epoxide, while the *syn* diastereomer would provide the *cis* epoxide (Scheme 6). Aggarwal and coworkers in an elegant study¹⁷ have produced a complete reaction profile for the diastereomerically pure intermediate betaines **16** and **17** in the presence of a more reactive aldehyde (4-nitrobenzaldehyde). If formation of the betaine intermediate is reversible, reversion to starting materials would necessarily cause preferential reaction with the 4-nitrobenzaldehyde, affording a new betaine **18**. This newly-formed betaine may again revert to starting materials or collapse to give a cross-over epoxide product **21** into which 4-nitrobenzaldehyde is incorporated. Experimental data indicates that the *anti* sulfonium betaine intermediate gave the expected *trans* epoxides **19** only, while *syn* betaines derived from aromatic aldehydes afforded no *cis* epoxide **20**, but gave only *trans* cross-over product **21** ($k_{-3} > k_4$, $k_5 > k_1 > k_3$). This result demonstrates that formation of the *anti* betaine is irreversible ($k_2 \gg k_{-1}$), and leads necessarily to products. However, the *syn* betaine, once formed, will dissociate to starting materials ($k_{-3} > k_4$) and react with the more reactive aldehyde ($k_5 > k_1 > k_3$). Additionally, the *trans* and *anti* betaines do not interconvert, as the *syn* betaine **17** did not provide *trans* epoxide product **19**.

Scheme 6

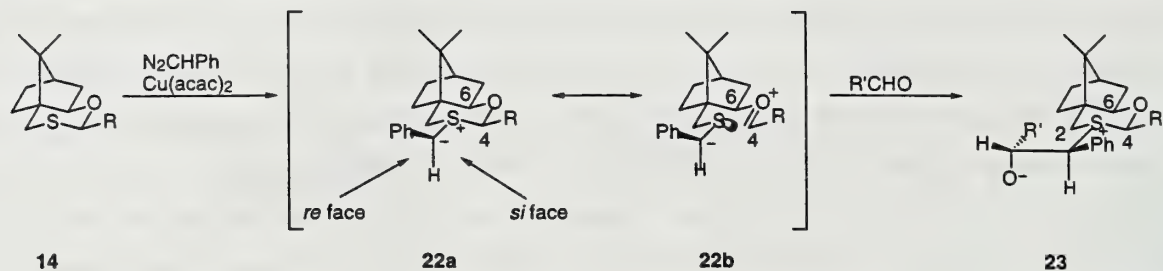


Origin of Enantioselectivity

The enantioselectivity of chiral sulfonium ylide asymmetric epoxidation depends on the conformation and facial selectivity of the ylide in the diastereomeric transition state of the addition to the carbonyl.¹⁶ This may be illustrated by considering the chiral sulfonium oxathiane developed by Aggarwal (Scheme 7).¹⁸ In this case, the $-\text{CHPh}$ group, transferred from the metal carbenoid, adds preferentially in the equatorial position. The axial lone pair of electrons on sulfur, which would react to form the opposite diastereomeric ylide, is sterically blocked by the bridge of the bicyclic oxathiane. The approach of the

aldehyde can occur on either the *re* or *si* face of the ylide **22** and apparently does not depend on the size of the R group of the oxathiane **14**. In fact, the highest stereoselectivities are reported when R=Me. The aldehyde preferentially approaches the *re* face of the ylide, to produce the betaine **23**.

Scheme 7

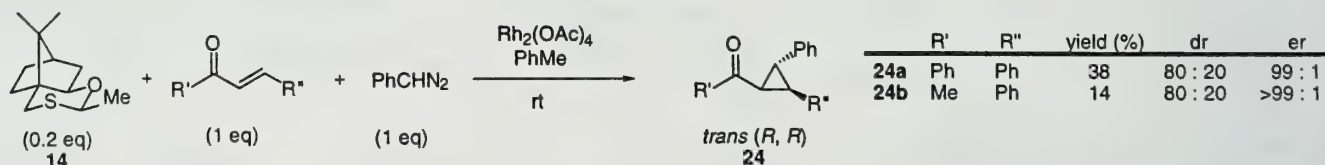


To explain the *re* facial selectivity of the aldehyde in this case, the Cieplak effect²⁰ is invoked. The Cieplak effect predicts that nucleophilic reaction will occur on the face of the ylide opposite the richer electron donor. The *re* face of **22** is opposite the richer electron donor, as shown by the resonance structure **22b**, an illustration of the anomeric effect. The electron rich $\text{C}_4\text{—S}$ σ bond donates electron density into the nucleophile's σ^* orbital of the forming σ bond. This donation lowers the energy of the σ^* and thus promotes formation of the σ bond.

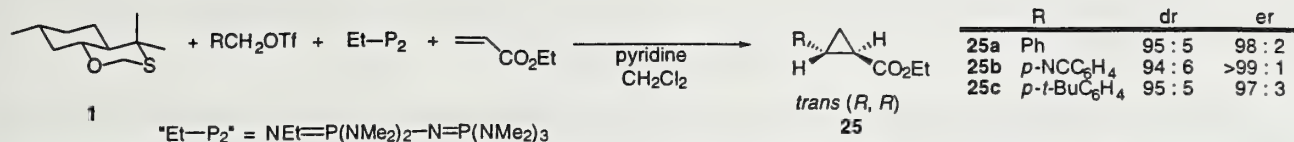
The electronic structure predicted by the resonance hybrid is experimentally corroborated by X-ray crystallography of a corresponding sulfoxide, which is electronically analogous to the reactive sulfonium ylide. In the solid state, the $\text{C}_4\text{—O}$ bond is shorter than the $\text{C}_6\text{—O}$ bond, while the $\text{C}_4\text{—S}$ bond is lengthened relative to the $\text{C}_2\text{—S}$ bond. In the absence of the oxygen atom at the C_5 position, the C—S bond lengths are similar.

CYCLOPROPANATION

Both of the chiral sulfonium auxiliaries **14** and **1** developed by Aggarwal and Solladié-Cavallo have been successfully applied to cyclopropanations of α,β -unsaturated ketones and esters. These asymmetric cyclopropanations can be rationalized by Aggarwal's catalytic cycle.²¹

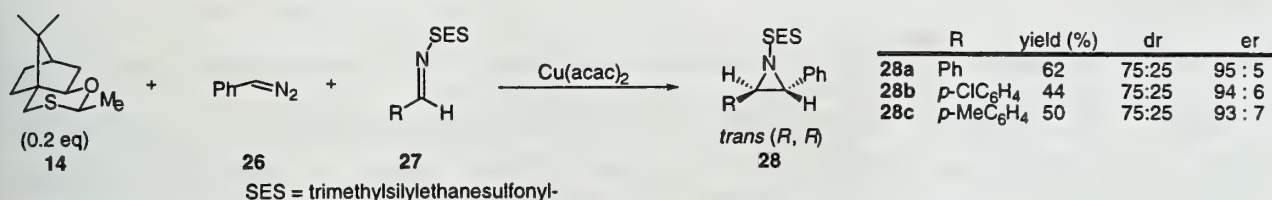


Similarly, oxathiane **1** can be used in the preparation of *trans*-2-arylcylopropane carboxylates **25**.²² High stereoselectivities are achieved when $\text{EtN}=\text{P}(\text{NMe}_2)_2\text{—N}=\text{P}(\text{NMe}_2)_3$ ("Et- P_2 "), a strong phosphazene base, is used. The chiral oxathiane is recoverable and reuseable, and the phosphazene base is recoverable. The chelation of the oxygen to the metal is believed to guide the Michael acceptor as it approaches the ylide from the side opposite of the *gem*-dimethyl group (*vide supra*).



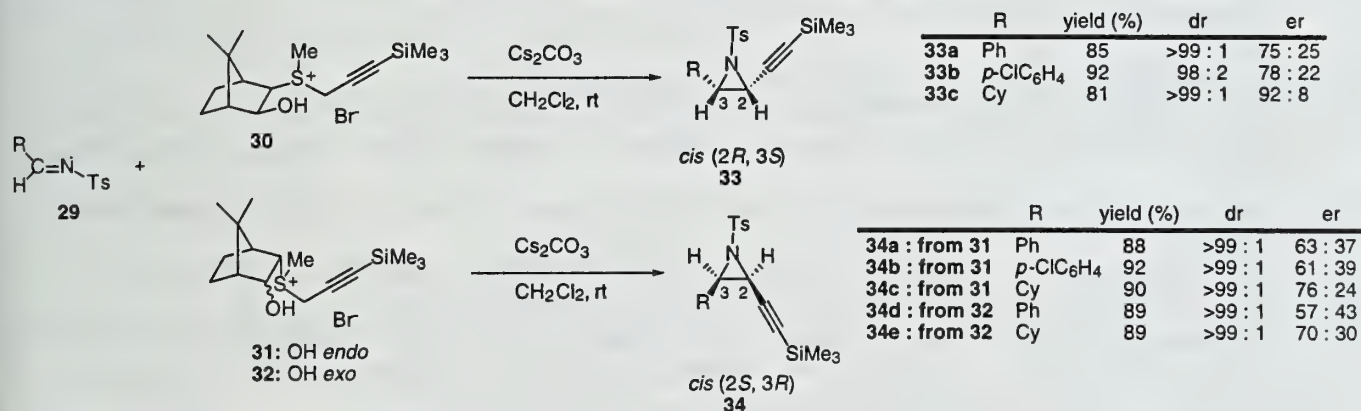
AZIRIDINATION

The 1,3-oxathiane auxiliary **14** has been applied to the preparation of aziridines **28** from activated imines **27**.²³ The necessary diazo starting materials have been prepared *in situ*, due to their high reactivity. An additional feature of this sequence is the fact that functionalized diazo compounds can be used for the preparation of functionalized aziridines.



Finally, the *N*-sulfonylimines **29** have been used in reactions with chiral propargylic ylides **30**, **31**, and **32** to afford enantiomerically enriched aziridines **33** and **34** (Scheme 8).²⁴ Aromatic imines, aliphatic imines, and ketimines can be successfully employed as substrates. The enantiocontrol provided by this method is synthetically useful, as the *endo*- and *exo*-sulfonium groups allow access to opposite enantiomers. The chiral sulfides are recoverable in >80% yields without loss of optical purity. Either 3-trimethylsilyl, 3-phenyl, or 3-alkyl-substituted sulfonyl propargylides can be used to effect the aziridination.

Scheme 8



CONCLUSIONS

The asymmetric preparation of three-membered rings has become a matter of considerable synthetic importance, as these compounds serve as versatile reactive intermediates.²⁵⁻²⁸ Catalytic and substrate-recoverable methods which are synthetically useful, efficient, and economical have been reported. The opportunity for development and improvement of this methodology exists, as the stereoselective addition of aliphatic aldehydes to chiral sulfonium ylides remains relatively unexplored. This methodology has only recently been applied to cyclopropanation and aziridination; thus, the current limited scope of these reactions provides ample opportunity for further investigation.

REFERENCES

- (1) Li, A.-H.; Dai, L.-X.; Aggarwal, V.K. *Chem. Rev.* **1997**, *97*, 2341.
- (2) Müller, P.; Fernandez, D.; Nury, P.; Rossier, J.-C. *J. Phys. Org. Chem.* **1998**, *11*, 321.
- (3) Trost, B.M.; Hammen, R.F. *J. Am. Chem. Soc.* **1973**, *95*, 962.
- (4) Furukawa, N.; Sugihara, Y.; Fujihara, H. *J. Org. Chem.* **1989**, *54*, 4222.
- (5) Breau, L.; Ogilvie, L.L.; Durst, T. *Tetrahedron Lett.* **1990**, *31*, 35.
- (6) Solladié-Cavallo, A.; Adib, A.; *Tetrahedron* **1992**, *48*, 2453.
- (7) Aggarwal, V.K.; Kalomiri, M.; Thomas, A.P. *Tetrahedron: Asymmetry* **1994**, *5*, 723.
- (8) Aggarwal, V.K.; Abdel-Rahman, H.; Jones, R.V.H.; Lee, H.Y.; Reid, B.D. *J. Am. Chem. Soc.* **1994**, *116*, 5973.
- (9) Breau, L.; Ogilvie, W.W.; Durst, T. *Tetrahedron Lett.* **1990**, *31*, 35.
- (10) Solladié-Cavallo, A.; Diep-Vohuule, A. *Tetrahedron: Asymmetry* **1996**, *7*, 1783.
- (11) Solladié-Cavallo, A.; Diep-Vohuule, A. *J. Org. Chem.* **1995**, *60*, 3494.
- (12) Li, A.-H.; Dai, L.-X.; Hou, X.-L.; Huang, Y.-Z.; Li, F.-W. *J. Org. Chem.* **1996**, *61*, 489.
- (13) Julienne, K.; Metzner, P.; Henryon, V.; Greiner, A. *J. Org. Chem.* **1998**, *63*, 4532.
- (14) Aggarwal, V.K. *Synth. Lett.* **1998**, 329.
- (15) Aggarwal, V.K.; Ford, J.G.; Fonquerna, S.; Adams, H.; Jones, R.V.H.; Fieldhouse, R. *J. Am. Chem. Soc.* **1998**, *120*, 8328.
- (16) Aggarwal, V.K.; Hesham, A.-R.; Jones, R.V.H.; Standen, M.C.H. *Tetrahedron Lett.* **1995**, *36*, 1731.
- (17) Aggarwal, V.K.; Calamai, S.; Ford, J.G. *J. Chem. Soc., Perkin Trans. 1* **1997**, 593.
- (18) Aggarwal, V.K.; Ali, A.; Coogan, M.P. *J. Org. Chem.* **1997**, *62*, 8628.
- (19) Aggarwal, V.K.; Bell, L.; Coogan, M.P.; Jubault, P. *J. Chem. Soc., Perkin Trans. 1* **1998**, 2037.
- (20) Cieplak, A.S. *J. Am. Chem. Soc.* **1981**, *103*, 4540.
- (21) Aggarwal, V.K.; Smith, H.W.; Jones, R.V.H.; Fieldhouse, R. *Chem. Commun.* **1997**, 1785.
- (22) Solladié-Cavallo, A.; Diep-Vohuule, A.; Isarno, T. *Angew. Chem. Int. Ed. Eng.* **1998**, *37*, 1689.
- (23) Aggarwal, V.K.; Thompson, A.; Jones, R.V.H.; Standen, M.C.H. *J. Org. Chem.* **1996**, *61*, 8368.
- (24) Li, A.-H.; Dai, L.-X.; Hou, X.-L.; Xia, L.-J.; Lin, L. *J. Org. Chem.* **1998**, *63*, 4338.
- (25) Kim, N.-S.; Choi, J.-R.; Cha, J.K. *J. Org. Chem.* **1993**, *58*, 7096.
- (26) Hudlicky, T.; Tian, X.; Königsberger, K.; Rouden, J. *J. Org. Chem.* **1994**, *59*, 4037.
- (27) Soulié, J.; Boyer, T.; Lallemand, J.Y. *Tetrahedron: Asymmetry* **1995**, *6*, 625.
- (28) Shao, H.; Zhu, Q.; Goodman, M. *J. Org. Chem.* **1995**, *60*, 790.

DEVELOPMENT OF $\alpha_v\beta_3$ INTEGRIN INHIBITORS FOR SUPPRESSION OF ANGIOGENESIS

Reported by Alice L. Rodriguez

October 5, 1998

INTRODUCTION

Angiogenesis is defined as the invasion, migration, and growth of smooth muscle and endothelial cells in the development of new blood vessels. These processes play critical roles in embryonic development, wound healing, and inflammation.¹⁻³ Uncontrolled angiogenesis can lead to a variety of pathological conditions such as diabetic retinopathy, rheumatoid arthritis, and tumor progression and metastasis. Tumor growth, for example, is dependent on the supply of nutrients by blood vessels formed by angiogenesis. Inhibition of angiogenesis has potential as a powerful therapeutic approach for the treatment of tumors and other vascular disorders. The development of potent, orally available antagonists of angiogenesis is an issue which involves considerable interdisciplinary effort. This report will address the mechanism of angiogenesis, the involvement of integrin proteins, the development of small molecule inhibitors, and their clinical potential.

THE MECHANISM OF ANGIOGENESIS

There are three major phases of angiogenesis (Figure 1).¹ The first is initiation, in which angiogenic signals such as growth factors and signaling molecules are released to bind a receptor on the endothelial or smooth muscle cells, causing the proteolytic degradation of the blood vessel basal lamina. The second phase is proliferation and migration of the targeted cells toward the stimulus. A class of transmembrane proteins called integrins are in part responsible for cell adhesion. Lastly, the third phase is maturation and differentiation of the endothelial cells. A capillary lumen and basal lamina forms in the new blood vessel enabling blood flow to the stimulus.

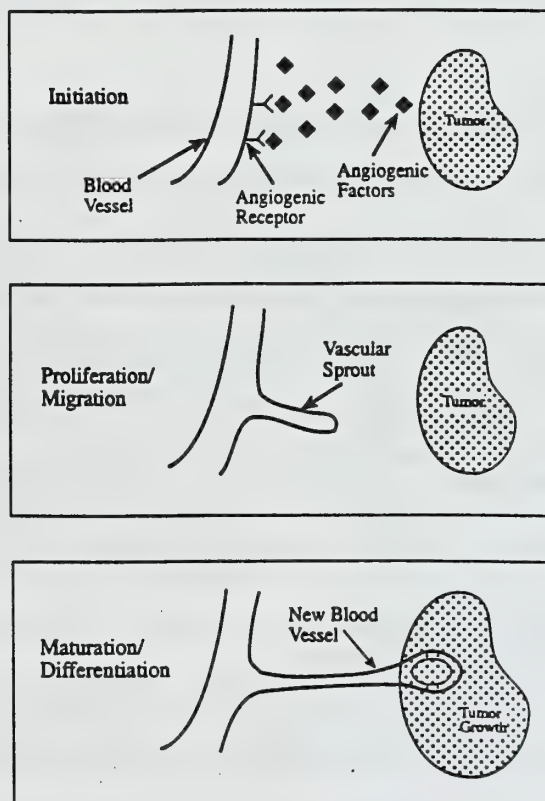


Figure 1. Mechanism of Angiogenesis

THE ROLE OF INTEGRIN PROTEINS

The family of integrin proteins plays a crucial part in angiogenesis via cell adhesion. Integrins are $\alpha\beta$ heterodimer transmembrane proteins expressed on the cell membranes of smooth muscle and endothelial cells. They are anchored to the cytoskeleton for support (Figure 2).

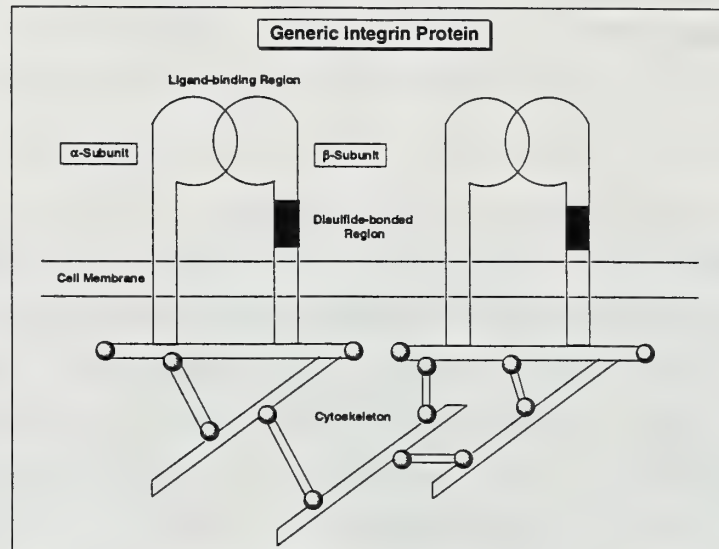


Figure 2. Schematic Diagram of a Generic Integrin Protein

Currently sixteen different α subunits and eight β subunits are known, with α and β referring to the heterogenous monomeric units in the dimer. Specifically, $\alpha_v\beta_3$ integrin, also known as the vitronectin receptor, allows endothelial cells to adhere to a variety of extracellular matrix (ECM) components such as fibronectin (Fn), vitronectin (Vn), and von Willebrand factor (vWF), as well as to the blood protein fibrinogen (Fg). Ligand binding leads to integrin clustering, which initiates a signal cascade resulting in migration of endothelial cells.⁴ The different classes of $\alpha_v\beta_3$ integrin antagonists include monoclonal antibodies, synthetic peptides, and naturally occurring venoms.¹ Several $\alpha_v\beta_3$ antagonists have been shown to inhibit angiogenesis induced by tumors⁵ and a number are scheduled to be tested in clinical trials.

The RGD Sequence

Rational design of potent and selective inhibitors can be based on understanding the structure and function of integrins. The first major breakthrough in understanding the relationship of integrins and cell adhesion was the elucidation of the binding sequence RGD (Arg-Gly-Asp).⁶ The ECM protein fibronectin was proteolysed and fragments tested for integrin binding activity. The only amino acid

sequence required for activity was found to be RGD. Mutation of any one of the three amino acids abolished all activity. The RGD sequence was found to be present in a variety of ECM proteins. The corresponding RGD-directed receptors were then isolated using affinity chromatography.¹

The Structure Of The α Subunit

Although integrins have been studied for some time, their structure is still not entirely understood. Until 1995, only information about the α subunit, which was known to contain a divalent cation binding region and a ligand binding site somewhere near the amino terminus, had been established. Recently, the first crystal structure of an integrin α subunit was determined in the presence of Mg^{2+} at 1.7 Å resolution.⁷ From the data, a model of the subunit was built from Asp132 to K315 (Figure 3).

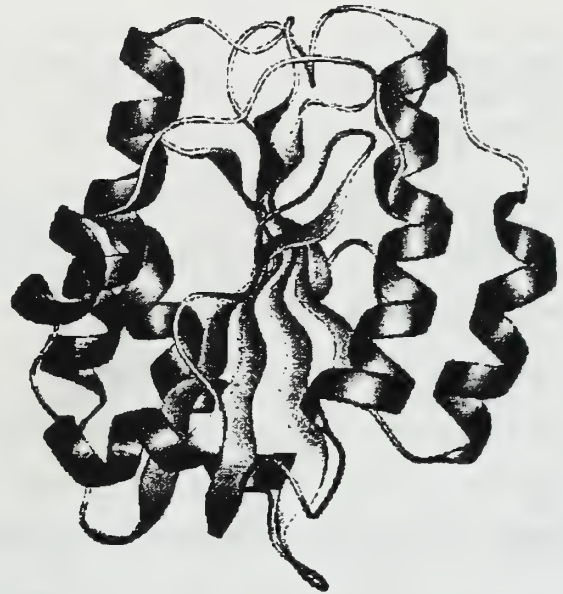


Figure 3. X-Ray Crystal Structure of α_M -Subunit

The domain has alternating amphipathic α -helices and hydrophobic β -strands. The structure forms a classic “Rossman fold” or α/β open sheet, with the β sheet in the center surrounded by the helices. This type of structure is often referred to as a Von Willebrand Factor A Domain and will be referred to as the A domain in following descriptions. The structure has a metal binding site at the top of the A domain. The divalent metal is bound by an aspartate and two serine residues in a (Asp-Xxx-Ser-Xxx-Ser-Xxx) motif and by two additional distal oxygenated residues, aspartate and threonine. In this crystal structure the sixth binding site is occupied by the A domain of another molecule. It is postulated that in monomeric form, the α subunit could bind ligand in the sixth coordination site on the metal. This hypothesis is referred to as the metal ion-dependent adhesion site or MIDAS motif. Two additional crystal structures of the A domain binding Mn^{2+} and Ca^{2+} have been elucidated.^{8,9} These structures show a similar A domain, but the sixth metal coordination site is occupied by a water molecule. Interestingly, the rest of the α subunit shows a dramatic shift in the conformation of the Mn^{2+} and Ca^{2+} bound structure relative to the Mg^{2+} bound model. Cations may interact indirectly, thereby causing a conformational change which alters the protein’s affinity for the ligand, although direct cation-

ligand binding as in the MIDAS motif has not been excluded. Other monoclonal antibody studies^{10,11} also support a two state binding model in which the integrin can be in an active state ready to bind ligand, or an inactive state, depending on stabilizing factors as shown in Figure 4.

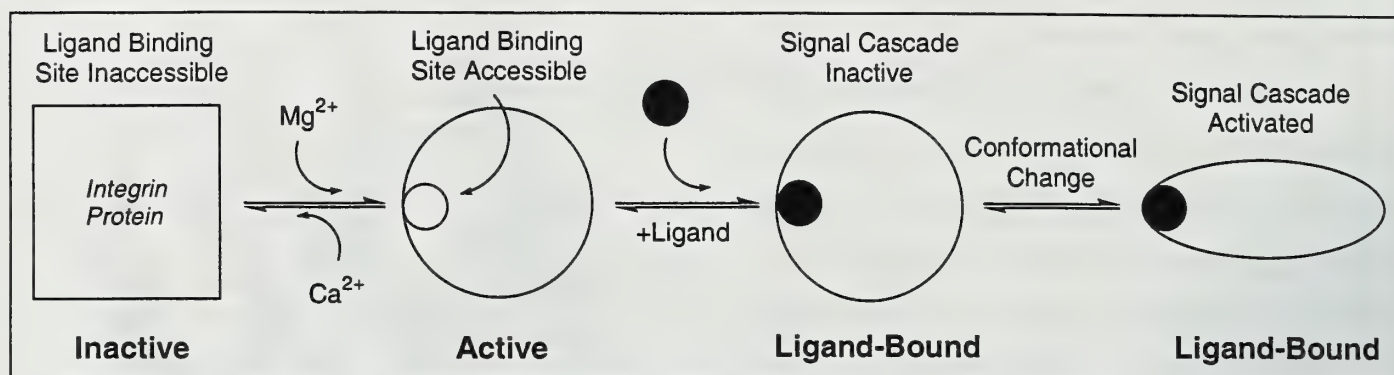


Figure 4. Two State Binding Model of the Integrin Family

The Predicted Structure Of The β -Subunit

The structure of the β subunit has not been elucidated. The traditional approaches for structure determination are cloning, expression, and crystallography. They have proven difficult for the β subunit because of the numerous disulfide bonds found in the protein. The β subunit is of particular importance in the $\alpha_v\beta_3$ integrins because the α subunit does not contain an A domain. Sequence homology, hydropathy plots, and molecular modeling on the β subunit suggest it has a similar three dimensional folding to the A domain.^{7,12} Mutagenesis studies were performed on the β_3 integrin subunit resulting in the identification of two critical residues, Asp-130 and Ser-132.¹³ They appear to be in a similar region as the oxygenated residues that bind the cation in the α crystal structure, further confirming the hypothesis that the β subunit also contains an A domain critical for ligand binding.

Binding Specificity

A recent study of the β_3 subunit has provided insight not only into ligand binding, but also binding specificity.¹⁴ A predicted loop in the β subunit containing a diverse disulfide linked region was investigated in a domain swap experiment. A specific sequence in a β_1 subunit was replaced by the corresponding sequence in a β_3 subunit. Both mutants were tested for activity with Fn, Fg, and vWF. The affinities of the mutants for these ligands were found to be reversed from the wild-type integrins. The study shows that the small disulfide region is a novel region of the β_1 and β_3 integrin subunits

critical for ligand specificity. This discovery should help in the ongoing development of specific integrin antagonists.

DEVELOPMENT OF $\alpha_v\beta_3$ INTEGRIN ANTAGONISTS

Introduction Of Cyclic Peptides

The lack of a thorough understanding of the structure-activity relationship of integrins has not prevented development of antagonists. Initial studies focused on anticoagulants for the $\alpha_{IIb}\beta_3$ integrin have afforded many orally available, nonpeptidic drugs which are currently in clinical trials. Recent studies have been geared towards developing inhibitors for $\alpha_v\beta_3$ integrins based on new insights into angiogenesis. The initial work was directed toward linear peptides containing the RGD sequence. These compounds bound well to $\alpha_{IIb}\beta_3$, but not to $\alpha_v\beta_3$. It was hypothesized that the introduction of conformational restrictions may lead to higher activity and selectivity for $\alpha_v\beta_3$, due to the possibility of the peptide forming a conformation closely related to that of the bioactive ligands. H. Kessler synthesized a series of cyclic peptides introducing a D-amino acid into various positions for conformational constraint.¹⁵ He saw an increase in inhibition 20-100 fold over the linear equivalent in the case of $\alpha_v\beta_3$, but no increase in $\alpha_{IIb}\beta_3$ inhibition, demonstrating that the $\alpha_v\beta_3$ integrin prefers ligands in a more restricted conformation. In 1994 Kessler's group synthesized a series of 18 pentapeptides to further study the conformation of the binding site.¹⁶ For most of the cyclic peptides, binding was lower compared to the linear peptide, thus defining them as mismatches to the receptor. Two of the cyclic peptides, cRGDfV and cRGDFv bound more strongly to the vitronectin receptor with an IC_{50} of 4.9 nM and 11.2 μ M, respectively, and were considered matches (Figure 5). The data supports the theory that the RGD peptide needs to be in its bioactive conformation in order to achieve maximal binding. The conformation of the analogue therefore must be very specific, leading to either a match or a mismatch.

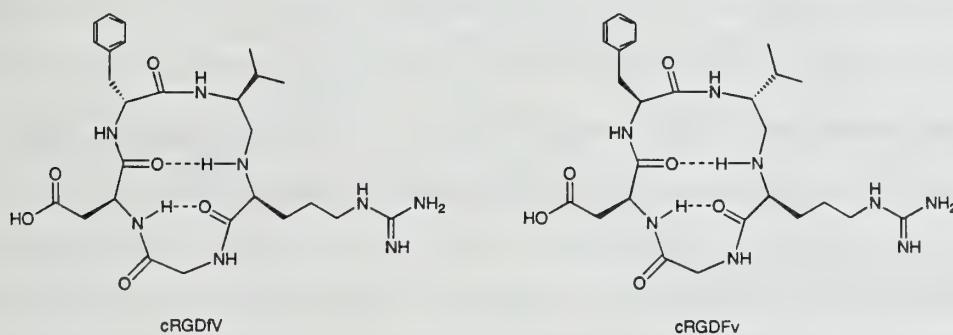


Figure 5. Cyclic (Arg-Gly-Asp-D-Phe-Val) and Cyclic (Arg-Gly-Asp-Phe-D-Val)

Studies were performed on the lead peptides to determine how the conformation of the peptide could be fixed by chirality and how this could affect inhibition.^{16,17} Two dimensional ¹HNMR and molecular dynamics simulations confirmed that the peptides were all trans and were arranged in a β II' turn and a γ -turn. The D-amino acid is in the *i*+1 position of the β II' turn. The distance between the R and D side chains is 6.6 Å in pentapeptides which bind better to $\alpha_v\beta_3$, while this distance is 7.8 Å in hexapeptides, demonstrating that a tighter ligand will have better specificity for the vitronectin receptor.

Structure-Activity Relationship

The two cyclic peptides, cRGDfV and cRGDFv, were used as lead structures in a study designed to elucidate the characteristics required by amino acids adjacent to RGD for binding.¹⁸ Selective substitutions were introduced into the lead structures, and the new peptides were divided into four categories based on the location and chirality of the substitution. Both hydrophobic and hydrophilic, natural and unnatural amino acids were used to probe the binding site limits. The structure of each peptide was determined and a structure-activity model was formulated (Figure 6). It appears that hydrophobic amino acids in position 4 increase activity as does serine in that position. Position 5 can tolerate both hydrophobic and hydrophilic residues. The amide proton between position 3 and 4 is essential for high activity and is hypothesized to be involved in hydrogen bonding contacts with the receptor. It also appears that peptides with a distance of 500 pm between the C $^\alpha$ R/C $^\alpha$ D fit the binding pocket most effectively.

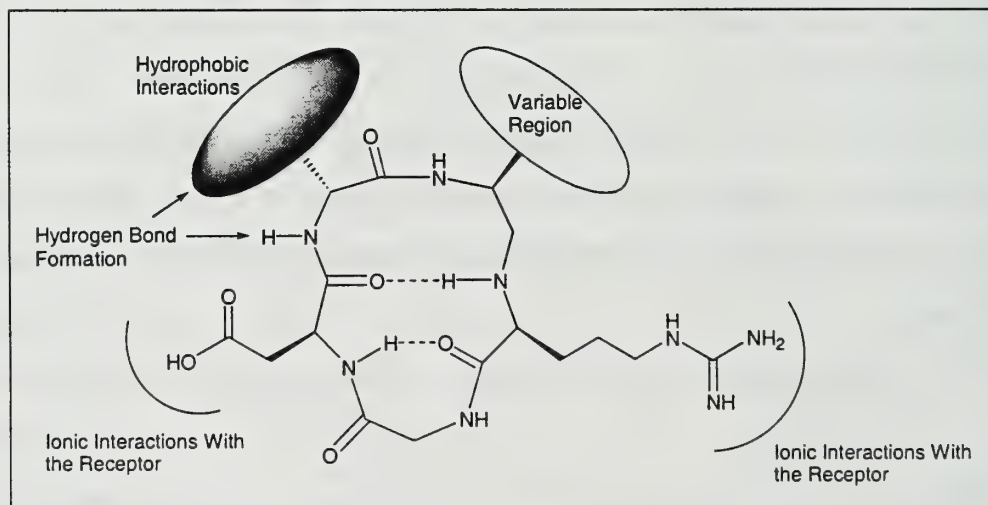


Figure 6. Structure-Activity Relationship

The role of the peptide backbone was seen as a structural platform until it was found that the amide proton between positions 3 and 4 was critical to binding. To study the backbone, a series of 18

retro-inverso cyclic peptides were synthesized.¹⁹ The hypothesis being tested was that total inversion of chirality combined with total inversion of sequence would achieve an orientation of the side chains identical to that of the parent compound (Figure 7). The only difference should be the location of the peptide bonds which are reversed. The compounds were tested for activity and conformational studies of select peptides were performed in detail. One of the retro-inverso compounds proved to be the most potent inhibitor in the series, even more so than the parent compound. Its conformation showed a change from the β II'/ γ turn motif to a β II/ γ_i conformation, which may explain the dramatic increase in activity. On the other hand, another retro-inverso compound showed an almost identical conformation as its parent compound, but had virtually no activity. This observation lead to the hypothesis that the peptide backbone may interact directly with the receptor.

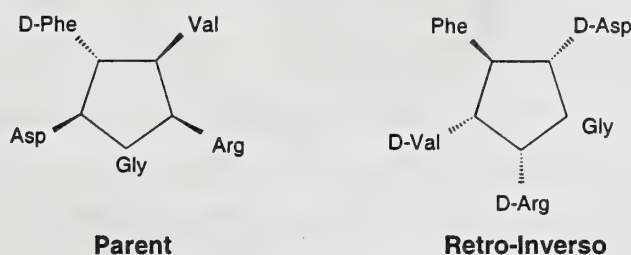


Figure 7. A schematic illustration of a parent compound and its retro-inverso isomer

Bioavailability Of Antagonists

Bioavailability is critical for an active drug. A useful compound needs to be stable through the appropriate route of administration and be able to localize to the target tissue before it is degraded or modified. Lipoderivatization, the addition of lipophilic building blocks, can improve cell permeability. In the case of the cyclic pentapeptides, position five is ideal for adding a lipophilic group, because of its tolerance for functional groups. A series of lipophilic cyclopentapeptides were synthesized using Fmoc-based Merrifield solid phase methodology and tested for biological activity against $\alpha_v\beta_3$ and $\alpha_{IIb}\beta_3$.²⁰ All the peptides but one proved to be selective for $\alpha_v\beta_3$, with two having an IC_{50} in the μ M range and one in the nM range. This reveals that lipoderivatization of active cyclic pentapeptides is possible and should be studied in greater detail. Another way to improve bioavailability of a drug is to avoid incorporating peptides. The conformation of the peptide backbone can be mimicked through the design of small organic molecules. One example is the use of a benzodiazepine backbone as a γ -turn mimic.²¹ Potent, selective vitronectin receptor antagonists have been synthesized using such a design and are currently being tested in clinical trials.

CONCLUSIONS

The future of integrin inhibitors has made leaps and bounds in the last three years. The elucidation of the first crystal structure of an integrin receptor protein greatly increased the understanding of integrin structure. The next important step is to crystalize the ligand-bound vitronectin receptor. With increased knowledge of the structure of the ligand binding pocket, rational design of potent inhibitors can become a more systematic process. Combining the knowledge of structural biochemists with that of creative synthetic chemists will prove a comprehensive and powerful approach to the field of receptor inhibitors.

REFERENCES

1. Stromblad, S. and Cheresch, D.A. *Chem. Biol.* **1996**, *3*, 881-885
2. Haubner, R.; Finsinger, D.; and Kessler, H. *Angew. Chem. Int. Ed.* **1997**, *36*, 1374-1389
3. Giannis, A. and Rubsam, F. *Angew. Chem. Int. Ed.* **1997**, *36*, 588-590
4. Humphries, M.J. *Curr. Opin. Cell Biol.* **1996**, *8*, 632-640
5. Brooks, P.C.; Clark, R.A.F.; Cheresch, D.A. *Science*, **1994**, *264*, 569-571
6. Pierschbacher, M.D. and Ruoslahti, E. *Nature* **1984**, *309*, 30-33
7. Lee, J.; Rieu, P.; Arnaout, M.A.; and Liddington, R. *Cell* **1995**, *80*, 631-638
8. Qu, A. and Leahy, D.J. *Proc. Natl. Acad. Sci.* **1995**, *92*, 10277-10281
9. Lee, J.; Bankston, L.A.; Arnaout, M.A.; and Liddington, R.C. *Structure*, **1995**, *3*, 1333-1340
10. Brooks, P.C. et al *Cell* **1994**, *79*, 1157-1164
11. Tozer, et al *J. Biol. Chem.* **1996**, *271*, 21978-21984
12. Tuckwell, D.S. and Humphries, M.J. *FEBS Lett.* **1997**, *400*, 297-303
13. Puzon-McLaughlin, W. and Takada, Y. *J. Biol. Chem.* **1996**, *271*, 20438-20443
14. Takagi, J. et al *J. Biol. Chem.* **1997**, *272*, 19794-19800
15. Aumailley, M. et al *FEBS Lett.* **1991**, *291*, 50-54
16. Pfaff, M. et al *J. Bio. Chem.* **1994**, *269*, 20233-20238
17. Muller, G.; Gurrath, M.; Kessler, H.; and Timpl, R. *Angew. Chem. Int. Ed.* **1992**, *31*, 326-328
18. Haubner, R. et al *J. Am. Chem. Soc.* **1996**, *118*, 7461-7472
19. Wermuth, J.; Goodman, S.L.; Jonczyk, A.; and Kessler, H. *J. Am. Chem. Soc.* **1997**, *119*, 1328-1335
20. Koppitz, M.; Huenges, M.; Gratias, R.; and Kessler, H. *Helv. Chim. Acta* **1997**, *80*, 1280-1300
21. Keenan, R.M. et al *J. Med. Chem.* **1997**, *40*, 2289-2292.

RING OPENING CYCLOADDITIONS OF METHYLENECYCLOPROPANES AND VINYLCYCLOPROPANES

Reported by Nicole M. Okeley

October 8, 1998

INTRODUCTION

Five- and seven-membered carbocyclic rings are important building blocks in organic synthesis. These rings are found in a large number of natural products and designed molecules which possess biological activities.¹⁻³ Efficient and stereoselective syntheses of these key ring structures can be envisioned through cycloaddition reactions in which simultaneous formation of two new C-C bonds occurs regio- and diastereoselectively. Although such stereoselective formation of substituted six-membered rings by the Diels-Alder reaction has been well developed, analogous cycloadditions for creating five- and seven-membered rings are less well known.

Two very promising cycloadditions that afford five- and seven-membered carbocyclic rings are the [3+2] cycloadditions involving methylenecyclopropanes⁴ and [5+2] cycloadditions using vinylcyclopropanes.⁵ This report will focus on the mechanism and synthetic utility of these reactions.

METHYLENECYCLOPROPANES

Methylenecyclopropanes are highly strained compounds that are stable at ambient temperatures. These compounds are also generally quite reactive, making them interesting from a structural as well as a synthetic point of view. In the past 20 years numerous methods have been developed to prepare substituted methylenecyclopropanes⁶ in good yields, so their use as a starting material in a subsequent synthesis is appropriate.

[3+2] Cycloadditions of Methylenecyclopropanes

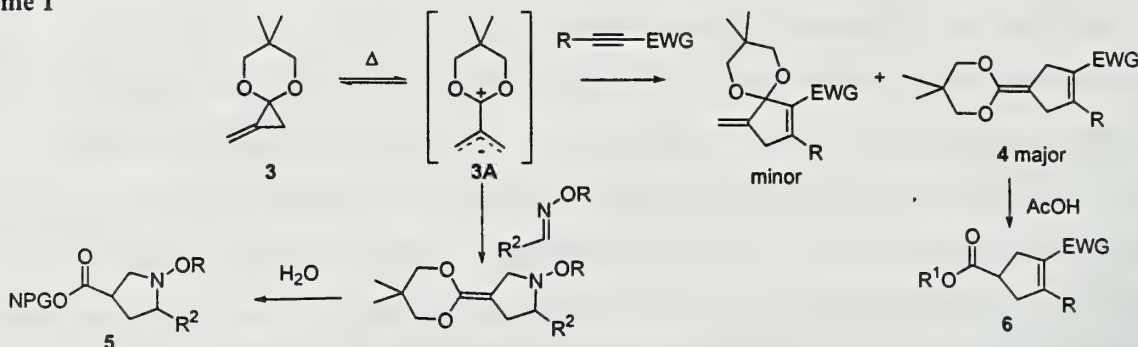
A generic [3+2] cycloaddition which involves the condensation of a three atom unit and a two atom unit to form a five membered ring is illustrated in Equation 1 for methylenecyclopropane (1) and ethylene. These reactions can occur between methylenecyclopropanes and olefins, carbonyl



compounds, or oximes at elevated temperatures.⁷⁻⁹

Thermal [3+2] cycloadditions of methylenecyclopropanes can lead to some synthetically useful products. For example, the reaction of methylenecyclopropane **3** with substituted alkynes provides ketene acetals, **4**, that can be converted to cyclopentene carboxylic acids, **6**, after hydrolysis (Scheme 1).⁸ Terminal unactivated acetylenes fail to undergo the addition.

Scheme 1

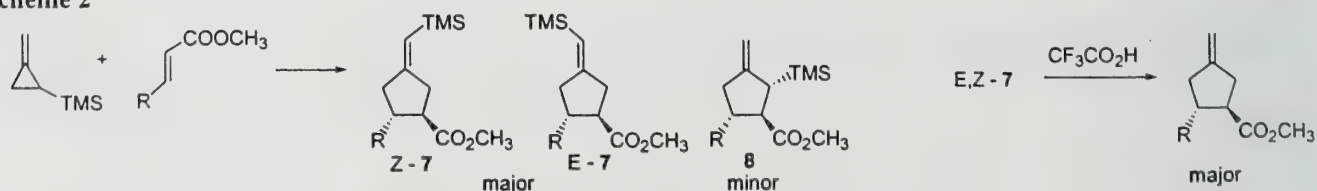


The methylenecyclopropane **3** and related compounds also react with *O*-alkyloximes to provide substituted alkoxy pyrrolidines, **5** (Scheme 1).⁹ The selectivity of these reactions increases from good to excellent with more substituted reactants. One limitation of these thermal [3+2] reactions is that they require the olefin or substrate to be electron deficient. This is most likely due to the dipolar nature of the trimethylenemethane intermediate **3A** involved in the addition.

[3+2] reactions can be promoted by transition metals and these are effective with either electron rich or electron poor olefins.¹⁰ The selectivity obtained in these reactions, however, is highly dependent on the transition metal catalyst employed, its ligands, and the substitution pattern of the methylenecyclopropane. Despite this case by case dependence, these reactions are quite synthetically useful. Some examples of the synthetic utility of these reactions are described in the following paragraphs.

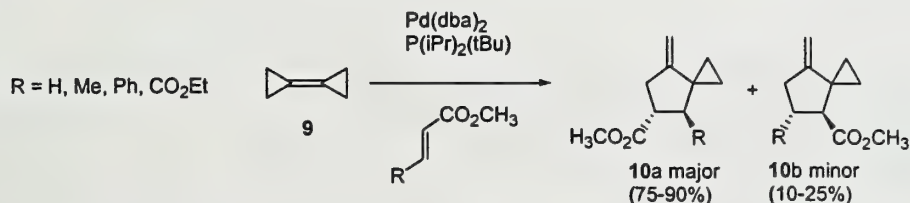
Methylenecyclopropane itself works well in many [3+2] cycloaddition reactions, but for some reactions it can be a poor substrate, yielding dimers and higher oligomers. The reaction of 1-methylene-2-(trimethylsilyl) cyclopropane can serve as a synthetic equivalent for methylenecyclopropane, as the TMS group can be removed after the reaction by protolysis with trifluoroacetic acid in yields as good as 95% (Scheme 2).¹¹ These reactions give better yields and selectivities than the corresponding reaction with unsubstituted methylenecyclopropane.

Scheme 2



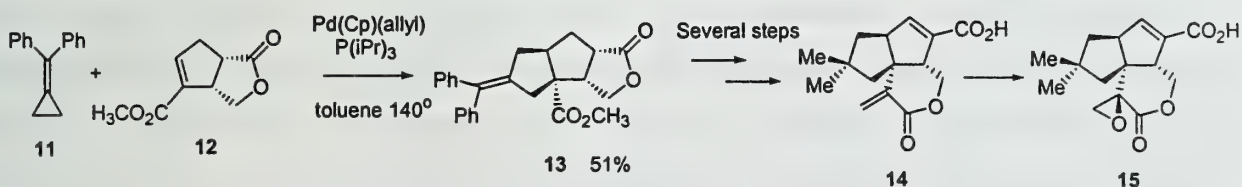
The reaction of bicyclopropyldiene (**9**) with olefins provides interesting 4-methylenespiro[2.4]heptane derivatives, **10**, that contain vinylcyclopropane functionalities (Scheme 3)¹² in acceptable to good yields with high regioselectivities. In addition, intramolecular [3+2] cycloadditions of methylenecyclopropanes provide a one-step route to bicyclic and heterobicyclic compounds with high regiocontrol.^{4,13}

Scheme 3



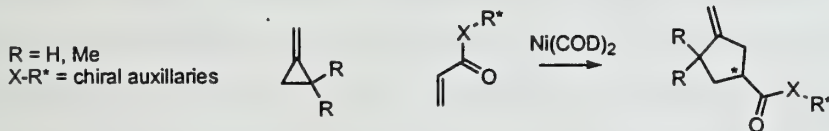
A recent example of an application of these reactions to natural product synthesis is the synthesis of the pentalenolactones **E** and **F**, **14** and **15** respectively.¹ The formation of the diquinane skeleton, **13**, was accomplished through the palladium catalyzed [3+2] cycloaddition of the bicyclic alkene **12** and diphenylmethylenecyclopropane (**11**).

Scheme 4



Diastereoselective cycloadditions have been accomplished with nickel (0) catalysts between chiral acrylic acid derivatives and methylenecyclopropanes (Scheme 5).¹⁴ The best dr of 99:1 was achieved when (-)-camphorsultam was the chiral auxiliary.

Scheme 5



Reaction Pathway

Two types of products are observed in the [3+2] cycloaddition reaction of methylenecyclopropanes. One product formally arises from distal cleavage of the cyclopropane ring, between C2 and C3 producing a trimethylenemethane (TMM) equivalent, **17**, which affords **16** (Figure 1). The other product formally arises from proximal cleavage, between C1 and C2, **18**, to provide **19** (Figure 1). As is evident in the structures of the proposed intermediate metal complexes

proximal cleavage; thus no scrambling would be expected in this reaction.¹⁰

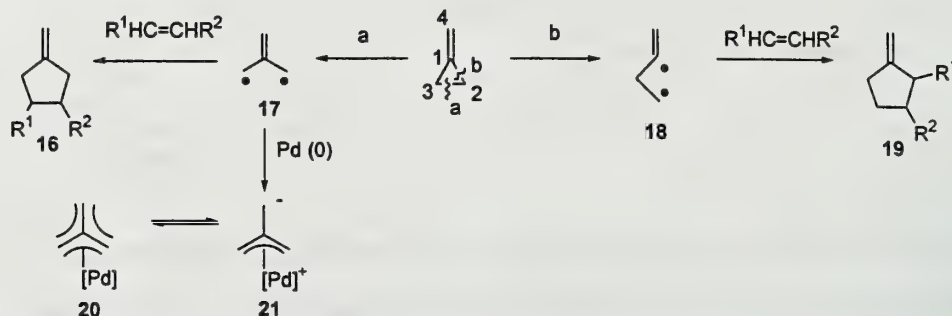
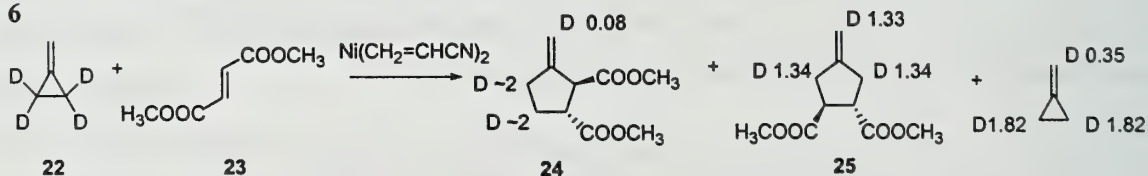


Figure 1. The two modes of cyclopropane ring opening and their products.

These pathways are supported by early deuterium labeling studies reported by Noyori on the nickel catalyzed [3+2] cycloaddition reaction of 2,2,3,3-tetradeuteriomethylenecyclopropane (**22**) and dimethyl fumarate (**23**, Scheme 6).¹⁵ Two products, **24** and **25**, were isolated along with unreacted starting material. Product **24** was formed by proximal cleavage, and little scrambling of the deuterium label was observed. Product **25** was formed via distal cleavage, and complete deuterium scrambling was detected. A small amount of deuterium was detected at the C4 position of the recovered starting material, indicating that distal cleavage must be, to some extent, reversible.

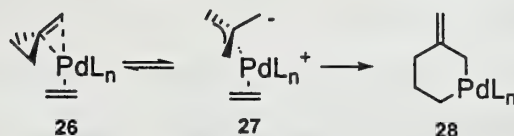


Mechanistic Investigations

Although products arising from the two mechanistic pathways are observed, the actual mode by which the metal catalyst coordinates with the starting materials and facilitates addition varies from case to case. Reactions with palladium (0) catalysts generally afford product **16** via the distal cleavage pathway, while proximal cleavage leads to the product, **19**, that has been observed in nickel catalyzed reactions. Fujimoto has performed *ab initio* calculations for the intermolecular palladium (0) catalyzed [3+2] cycloaddition of methylenecyclopropane and ethylene.¹⁶ The lowest energy intermediates suggest that the initial step is the pre-coordination of both methylenecyclopropane and

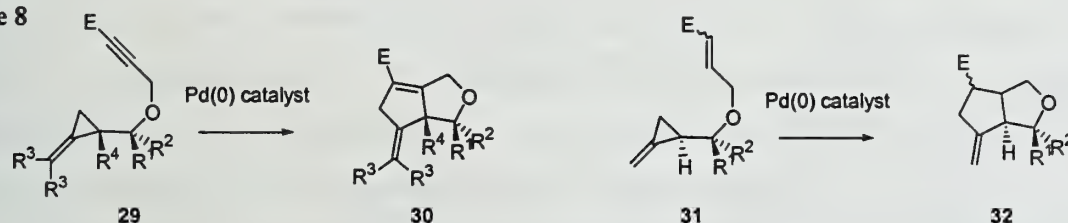
ethylene. Experimentally, this is supported by the fact that alkenes that are very strongly metal coordinating can prevent cycloaddition, presumably by forming a stable, unreactive complex.¹⁷ Calculations show the initial coordination to methylenecyclopropane to be an η^2 -complex, **26**, that evolves into the η^3 - π -allylic structure **27**. Once the η^3 -complex is generated, the first C-C bond can be formed between the olefin and the TMM, constructing a six-membered metallacycle, **28**.

Scheme 7



This mechanism is similar in some ways to one that has been suggested by Lautens for an intramolecular [3+2] cycloaddition reaction.¹⁸ His group has studied the formation of heterobicyclic compounds **30** and **32** via intramolecular [3+2] palladium (0) catalyzed cycloadditions of compounds **29** and **31** shown in Scheme 8.^{4, 18, 19}

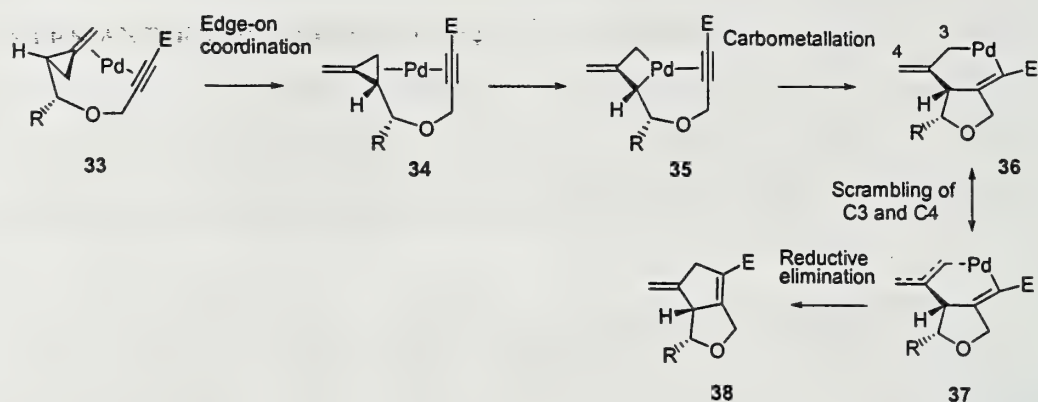
Scheme 8



A study of both alkenes and alkynes revealed that the stereochemistry at the substituted ring carbon on the cyclopropane is maintained throughout the reaction. Substitution at the exocyclic double bond could be tolerated and no scrambling of these substituents was observed. Different functional groups on the alkyne and alkene moieties were tolerated, although the nature of the group affected the reaction yields. Alkynes that had electron-withdrawing groups were more reactive than those bearing silicon. Based on the stereochemistry of the products observed, Lautens suggests a mechanism that does not involve a TMM-palladium intermediate (**20**). The difference between Fujimoto's calculation and Lautens' mechanism is in the metal intermediate. Lautens suggests coordination to the cyclopropane unit in an edge-on orientation, **34**, followed by insertion into the distal bond to form the metallacyclobutane **35** instead of an η^3 or TMM intermediate. Carbometallation followed by reductive elimination would complete the catalytic cycle (Scheme 9).

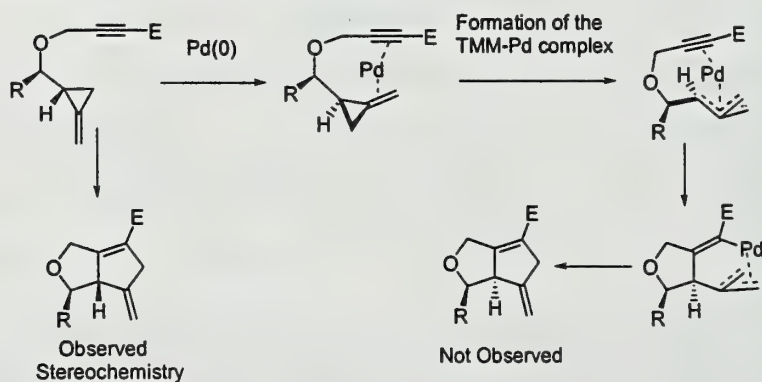
The formation of a metallacyclobutane is supported by two observations. First, the stereochemistry on the cyclopropyl ring would not be conserved if the second step were formation of a TMM-palladium or η^3 intermediate via disrotatory-out ring opening of the cyclopropane (Scheme

Scheme 9

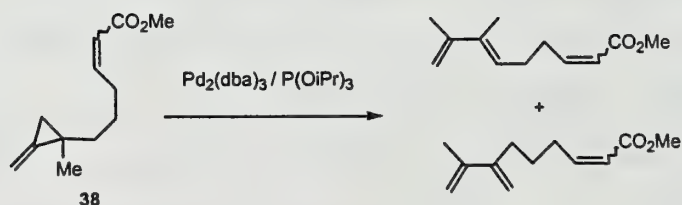


10)^{15,17}. In Lautens' mechanism, the stereochemical outcome can be explained by double-retention of configuration. Second, when **29**, R^4 = methyl, was used, a complex mixture of products was obtained. This mixture included dienes of unreported structure, presumably formed by β -elimination following metal insertion. This type of product was also observed when **38** was used in an intramolecular reaction studied by Motherwell (Scheme 11).¹³

Scheme 10



Scheme 11



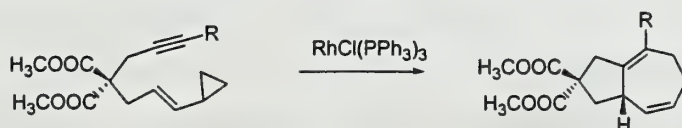
Perhaps the differences in the η^3 and metallacyclobutane mechanisms arise from the fact that the first is calculated for an intermolecular reaction while the second is proposed for an intramolecular reaction. However, other intramolecular reactions have been explained by an η^3 mechanism.^{13,20} Lautens' mechanism seems operative for his specific system. Nickel catalysis in these types of cycloadditions most likely occurs by a different mechanism due to their preference for proximal cleavage. Further studies are needed for the nickel catalyzed transformation.

VINYLCYCLOPROPANES

[5+2] Cycloadditions of vinylcyclopropanes

The formation of seven-membered rings via cycloaddition has been accomplished by several different methods including [6+1], [4+3], and [5+2] cycloadditions, but examples of such reactions are few.²¹ Wender recently reported a new method of intramolecular [5+2] cycloaddition of vinylcyclopropanes and alkynes which provide 5,7-fused ring systems with high yields and diastereoselectivities (Scheme 12).^{5, 21-23} Generally, vinylcyclopropanes do not react with dienophiles, but transition metal catalysts promote the [5+2] cycloaddition efficiently.

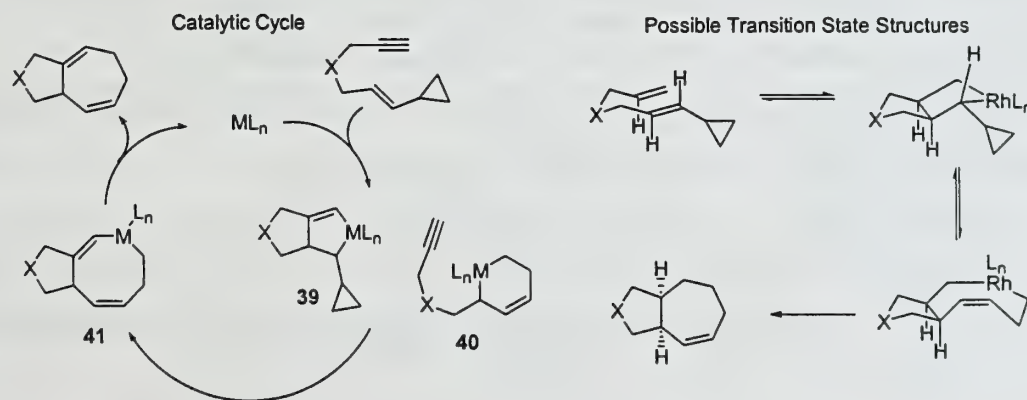
Scheme 12



Initial studies of the reaction showed that a wide range of alkynes could be incorporated and further studies revealed the viability of alkenes. In each system, it was determined that the geminal ester moiety is not crucial and that four carbon tethers can also be tolerated, creating 6,7-fused ring systems. The stereochemistry at the bridging carbon has proved to be independent of the vinylcyclopropane double bond geometry. Polar solvents and silver triflate increased the reaction efficiency, suggesting the participation of a cationic rhodium catalyst.

The mechanism of the reaction is not completely understood, although Wender has put forth a suggested catalytic cycle along with a transition state analysis that explains the observed stereochemistry (Scheme 13).²¹ The catalytic cycle begins with coordination of the metal to the yne-vinylcyclopropane and is followed by the formation of one of two metallacycles **39** or **40**. Subsequent rearrangement would lead to the eight-membered metallacycle **41**, which would be followed by reductive elimination to yield the products. The transition structures are based on structure **39** in this catalytic cycle, and provides a rationalization of the observed stereochemistry.

Scheme 13



In addition, Wender has performed preliminary studies²¹ with various chiral phosphorous ligands and the best er of 84:16 was achieved with CHIRAPHOS.

CONCLUSIONS

Recent developments in transition metal catalyzed cycloadditions have added the [3+2] and [5+2] reactions to the arsenal of synthetic methods to prepare five- and seven-membered rings. In the case of methylenecyclopropanes, mechanisms of the palladium (0) catalyzed reactions have been studied, although it is still not clear whether the same mechanism is operative for all cases. In addition, studies to help elucidate the mechanism of nickel catalyzed reactions need to be performed. The cycloaddition of vinylcyclopropanes, while still in its infancy may become a useful reaction for the synthesis of 5,7-fused ring systems and other seven-membered rings if the intramolecular reactions can be expanded and if intermolecular reactions can be developed.

REFERENCES

1. Rosenstock, B.; Gais, H.-J.; Herrmann, E.; Raabe, G.; Binger, P.; Freund, A.; Wedemann, P.; Krüger, C.; Lindner, H.J. *Eur. J. Org. Chem.* **1998**, 257.
2. Paquette, L.A. *Top. Curr. Chem.* **1984**, 119, 1.
3. Fraga, B. M. *Nat. Prod. Rep.* **1996**, 13, 307.
4. Lautens, M.; Ren, Y.; Delanghe, P.H.M. *J. Am. Chem. Soc.* **1994**, 116, 8821.
5. Wender, P.A.; Takahashi, H.; Witulski, B. *J. Am. Chem. Soc.* **1995**, 117, 4720.
6. Brandi, A.; Goti, A. *Chem. Rev.* **1998**, 98, 589.
7. Binger, P.; Büch, H.M. *Top. Curr. Chem.* **1987**, 135, 77.
8. Yamago, S.; Ejiri, S.; Nakamura, E. *Ang. Chem. Int. Ed. Engl.* **1995**, 34, 2154.
9. Yamago, S.; Nakamura, M.; Wang, X. Q.; Yanagawa, M.; Tokumitsu, S.; Nakamura, E. *J. Org. Chem.* **1998**, 63, 1694.
10. Binger, P.; Fox, D. In *Methods of Organic Chemistry* (Houben Weyl); Georg Thieme Verlag: Stuttgart, 1995; Vol. E 21C, p 2997.
11. Binger, P.; Sternberg, E.; Wittig, U. *Chem. Ber.* **1987**, 120, 1933.
12. Binger, P.; Wedemann, P.; Kozhushkov, S.I.; de Meijere, A. *Eur. J. Org. Chem.* **1998**, 113.
13. Motherwell, W.B.; Shipman, M. *Tetrahedron Lett.* **1991**, 32, 1103.
14. Binger, P.; Brinkmann, A.; Roefke, P.; Schäfer, B. *Liebigs Ann. Chem.* **1989**, 739.
15. Noyori, R.; Yamakawa, M.; Takaya, H. *Tetrahedron Lett.* **1978**, 48, 4823.
16. Oishi, Y.; Sakamoto, E.; Fujimoto, H. *Inorg. Chem.* **1996**, 35, 231.
17. Binger, P.; Schmidt, T. In *Methods of Organic Chemistry* (Houben Weyl); Georg Thieme Verlag: Stuttgart, 1997; Vol. E 17C, p 2217.
18. Lautens, M.; Ren, Y. *J. Am. Chem. Soc.* **1996**, 118, 9597.
19. Lautens, M.; Ren, Y. *J. Am. Chem. Soc.* **1996**, 118, 10668.
20. Corlay, H.; Motherwell, W.B.; Pennell, A.M.K.; Shipman, M.; Slawin, A.M.Z.; Williams, D.J. *Tetrahedron*, **1996**, 52, 4883.
21. Wender, P.A.; Husfeld, C.O.; Langkopf, E.; Love, J.A.; Pleuss, N. *Tetrahedron* **1998**, 54, 7203.
22. Wender, P. A.; Sperandio, D. *J. Org. Chem.* **1998**, 63, 4164.
23. Wender, P.A.; Husfeld, C.O.; Langkopf, E.; Love, J.A. *J. Am. Chem. Soc.* **1998**, 120, 1940.

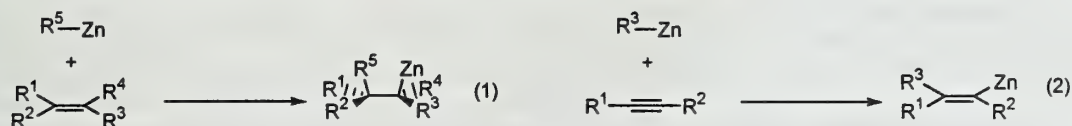
CARBOMETALATIONS OF CARBON-CARBON MULTIPLE BONDS BY ORGANOZINC COMPOUNDS

Reported by Eric Mertz

Oct. 15, 1998

INTRODUCTION

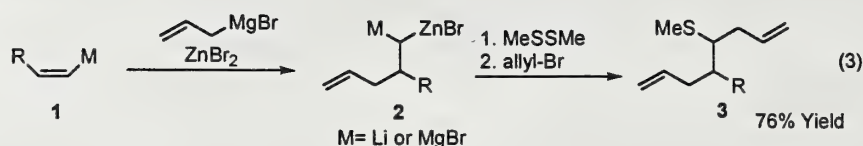
Carbometalation reactions have been developed as a practical method for the formation of new carbon-carbon bonds with particular emphasis on the construction of cyclic structures.¹ Due to the ability of zinc to complex with π bonds, additions of organozinc compounds to double and triple bonds (Eqs. 1-2) have emerged as a novel complement to more common organozinc reactions such as carbonyl additions, cross coupling reactions, and cyclopropanations.²



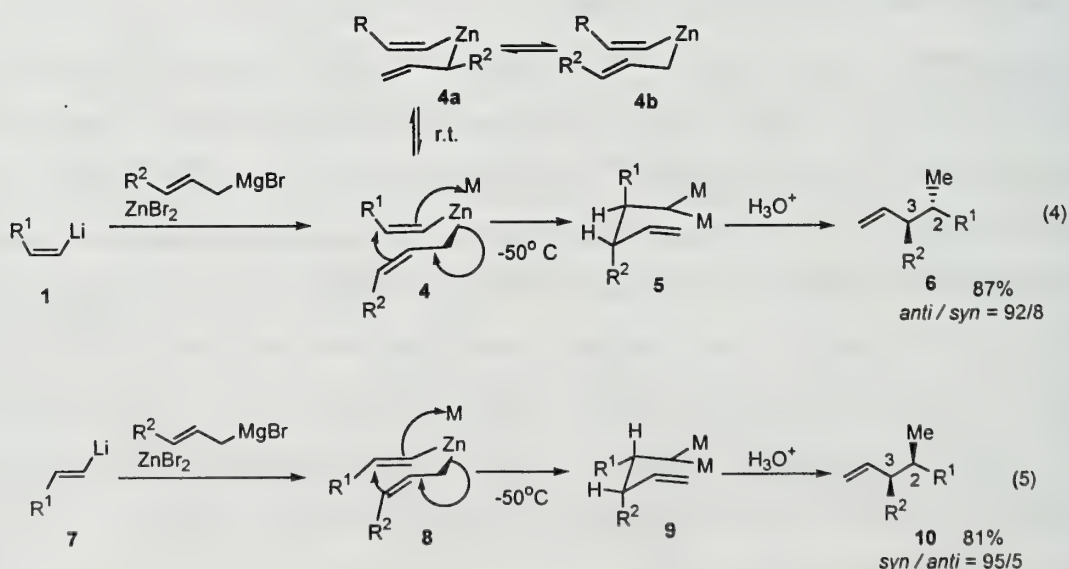
The first carbometalations with organozinc reagents to be reported involved simple alkyl and allyl zinc compounds adding to terminal alkenes and alkynes. Problems with stereoselectivity, side reactions, and the often harsh conditions initially limited the utility of these reactions. More recently, carbometalations using more complex allylic, propargyl, phenyl, vinyl and carbonyl containing organozinc reagents have been studied with particular attention paid to regioselectivity, mechanism, and stereoselectivity. This report describes advances in the understanding and application of carbometalations by unsaturated and carbonyl containing organozinc reagents.

UNSATURATED ORGANOZINC REAGENTS

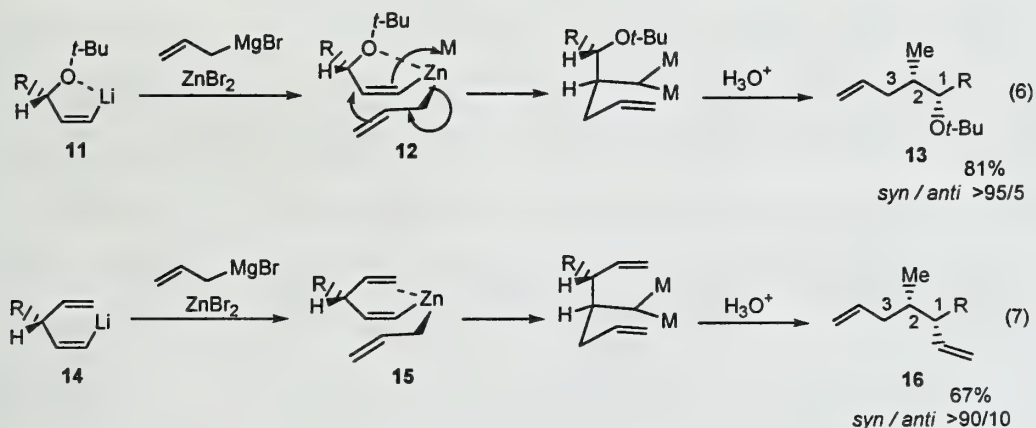
In an extension of carbometalation to organometallic olefins, Gaudemar and Knochel, followed by Normant and Marek, developed a mild addition of allylzinc compounds to vinyl metal reagents generalized by structure **1** to produce stable *gem*-bimetallic intermediates represented as **2** (Eq.3).³⁻⁴ The protocol for this reaction involves generation of an allylzinc reagent in situ through a transmetalation between an allyl Grignard reagent and ZnBr_2 . This method has synthetic appeal since it is applicable to a wide range of vinyl metal compounds, and **2** can react selectively with a variety of electrophiles. For example, treatment of **2** with methyl disulfide followed by allyl bromide yields the functionalized diene **3**. Allylzinc addition to vinyl metal compounds thus simultaneously forms a new carbon-carbon bond and affords a product which is activated for further substitution.



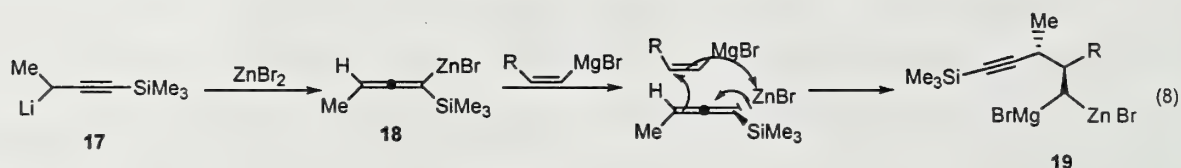
The geometry of the vinyl metal substrate plays an important role in determining the stereochemistry of the carbometallation products.^{4a} Substituted allyl metal reagents such as crotyl Grignard reagents add to (*Z*) vinyl lithium substrates generalized by structure **1** to form a *gem*-bismetallic species **5** (Eq. 4); hydrolysis of **5** affords the product **6** in which the C2 and C3 substituents are *anti* to each other. Similarly, an (*E*) vinyl metal substrate **7** reacts with crotylMgBr to form the *syn* analog **10** (Eq. 5). Normant and Marek rationalized the observed stereochemistry by suggesting the mixed zinc intermediates **4** and **8**. These intermediates undergo a Claisen or metallo-ene rearrangement through a chair transition state. The (*Z*) vinyl metal compounds must form an intermediate **4** in which R¹ and R² are on opposite faces while the (*E*) vinyl metal compounds must form an intermediate **8** in which R¹ and R² are on the same face. Significantly, diastereoselectivity depends strictly on the geometry of the vinyl group and not the initial geometry of the crotyl metal species. Equilibrium between (*E*) and (*Z*) configurations of the crotyl group in **4** is thought to create the possibility for two additional intermediates **4a** and **4b**. A similar equilibrium is proposed for the intermediate **8**. The (*Z*) configuration of the crotyl group in both **4** and **8** is thought to be kinetically favored due to an electrostatic attraction between hydrogens attached to R² and the carbanion adjacent to zinc. Therefore, stereocontrolled carbometallation between substituted allylzinc compounds and vinylmetal compounds must occur at low temperatures so that the (*Z*) configuration of the allyl moiety can be maintained.



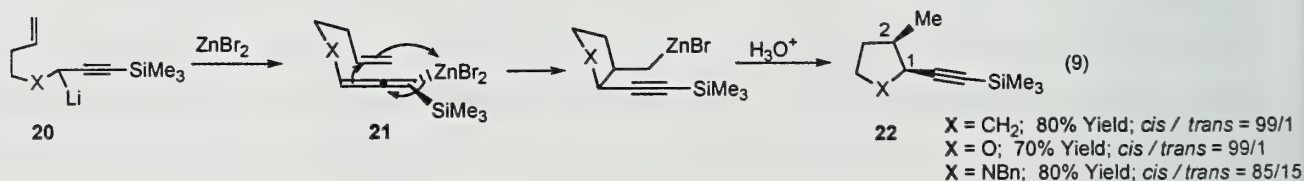
Diastereoselective allylzinc additions have also been observed with respect to C2 and C1 substituents using substituted vinyl metal compounds such as **11** which contain a γ chelating alkoxy group as well as a γ alkyl group R (Eq. 6).^{4b-c} Carbometalation of **11** followed by hydrolysis produces *syn* terminal alkenes of type **13**. Normant and Marek consider stereoselectivity to be controlled in the mixed zinc species **12** in which chelation between the γ oxygen and zinc causes the intermediate to be held rigidly in a chair-like conformation. Such a chair-like structure results in the *gem*-bismetallic group and the C1 alkoxy substituent having a *syn* relationship. Without chelation control, **12** could also access a boat-like conformation which leads to the *anti* diastereomer. The δ -alkenyl vinyl lithium reagent **14** (Eq. 7) affects the same type of stereocontrol without heteroatoms. The π bond of the terminal alkene coordinates to zinc such that **15** is also rigidly held in a chair-like conformation. Zinc coordination with either chelating heteroatoms or π bonds at the γ position thus provides another important element for controlling stereoselectivity of vinyl metal carbometalations.



Diastereoselective addition of propargylzinc reagents to vinyl metal compounds has also been observed using conditions similar to the allylzinc carbometalations. For example, the propargyl lithium compound **17** reacts with vinyl Grignard reagents to yield the alkyne **19** in the presence of ZnBr_2 (Eq. 8).^{4e} Normant and Marek argue that **17** transforms in situ into the zinc allene **18** immediately upon addition of zinc, but they do not propose a dialkyl zinc intermediate. Instead, reaction with the Grignard reagent is believed to occur through an $\text{S}_{\text{E}}2'$ mechanism. The *anti* diastereomer is formed due to the methyl substituent of the allene being orientated to avoid steric repulsion with the alkyl group R of the alkene. This same argument explains the stereochemistry of products resulting from (*E*) olefins which, in contrast to allylzinc additions, are also the *anti* diastereomer.



The power of propargylzinc additions for stereocontrolled carbocyclic synthesis has been realized by the intramolecular carbometalation of zinc enynes to afford substituted five membered rings (Eq. 9). Lithiated enynes generalized as structure **20** react with ZnBr_2 through a proposed zinc allene intermediate **21** similar to the intermolecular variant. Intermediate **21** is suggested to cyclize through a rarely observed metallo-ene-allene mechanism to form substituted cyclopentanes **22**. Unlike previous examples, this carbometalation does not occur on a metalated olefin. The C1 and C2 substituents in **22** selectively have a *cis* relationship due to the structural rigidity of the zinc allene in **21**. The zinc atom would be inaccessible to the alkene if the latter was on a different face than the allene. Heterocycles can also be produced by this cyclization method since replacement of X with oxygen or nitrogen affords a metallo-ene-allene pathway which yields substituted tetrahydrofurans and pyrrolidines (Eq. 9).⁶ Zinc mediated cyclization of enynes affords a versatile method for construction of various five membered rings and is a significant extension of Marek and Normant's carbometalation method to non-metalated alkenes.



Nakamura has reported carbometalation of the strained olefin in cyclopropanone ketal **23**.⁷ This reactive olefin, undergoes an $\text{S}_{\text{E}}2'$ type carbometalation with allylzinc bromide **24a** with moderate diastereoselectivity (Figure 1).⁷ When a bulky "dummy" ligand R^2 coordinates to zinc instead of bromine in **24b**, both yield and *syn* diastereoselectivity with respect to alkyl substituents at C3 and C4 in **25** improve. This result is explained by a twisted chair transition state model **26**. Both the ligand R^2 and the phenyl group at C3 are forced into pseudo equatorial positions in **26** by steric interactions with the alkoxy groups of the ketal. The effect of ligands on stereoselectivity initiated investigation of enantioselective carbometalations of **23** using allylzinc reagents such as **24c** which are coordinated to chiral bis(oxazoline) (BOX) ligands. An enantiomeric excess of 97% was obtained using **24c** which has a bulky R^1 group and a BOX ligand with bulky R^3 substituents. A twist chair transition state model can rationalize the observed enantioselectivity.

The orientation of the R^3 substituents of the BOX ligand directs **23** to approach **24c** with a single face. While Nakamura's studies of the carbometalation of **23** are specific to a single, reactive olefin, the concepts of ligand effects derived from these studies may assist in the further development of carbometalations of other cyclic and complex non-metalated olefins.

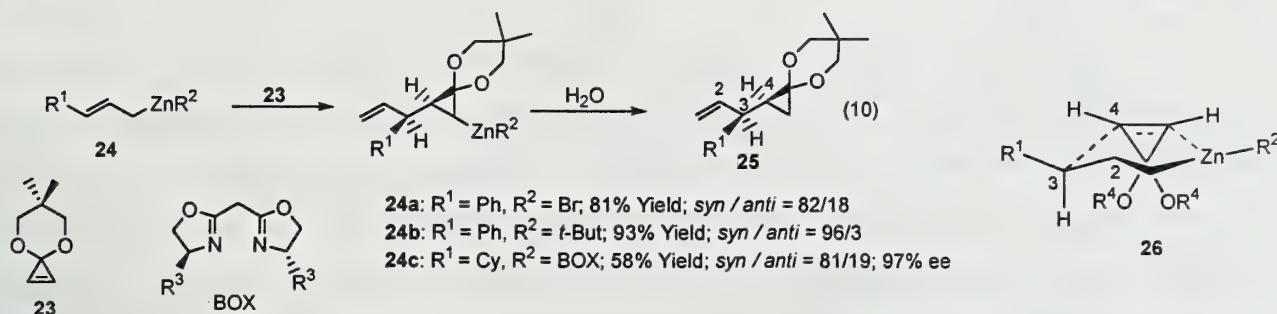
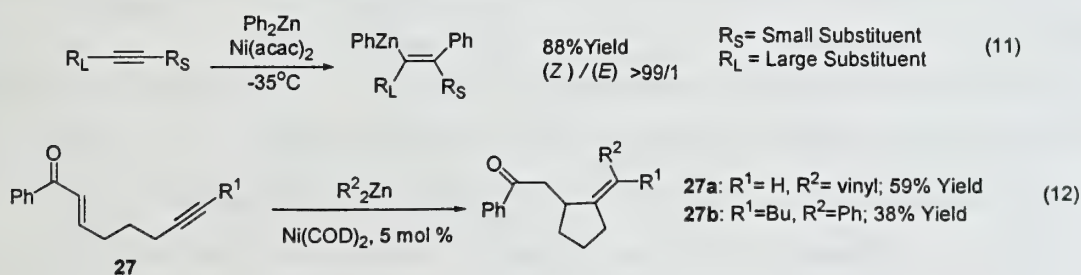


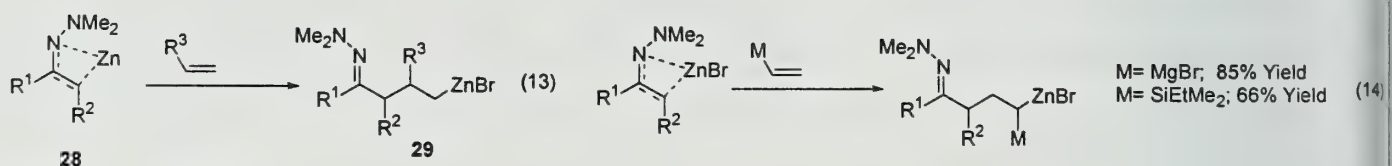
Figure 1. Allylzinc Addition to a Cyclopropenone Ketal

Organozinc addition to internal alkynes has had limited success due to poor regioselectivity until Knochel reported a nickel catalyzed *syn* addition of diphenylzinc to alkynes to produce alkenes with high stereo and regioselectivity (Eq. 11).⁹ Regioselectivity is thought to occur due to preferential addition of the phenyl group to the side of the alkyne attached to the smaller substituent. A mechanism which explains the role of nickel in this reaction involves a transmetalation of one phenyl group from zinc to nickel and then addition of the phenylnickel intermediate to the alkyne. Knochel has illustrated the utility of this method in an efficient synthesis of the anticancer drug (Z)-Tamoxifen. Montgomery has reported a similar Ni catalyzed carbometalation of alkynyl enones **27a-b** with phenyl and vinyl zinc reagents followed by intramolecular conjugate addition to form cyclic products (Eq. 12).¹⁰ While carbometalation is a plausible mechanism for this reaction, detailed studies also suggest an oxidative cyclization mechanism with the organozinc reagents playing only secondary roles.¹¹ Nevertheless, both Montgomery's and Knochel's nickel catalyzed variants of alkyne carbometalation increase the selectivity and scope of this reaction so that it has become more synthetically useful.



ZINC ENOLATES AND ENOLATE ANALOGS

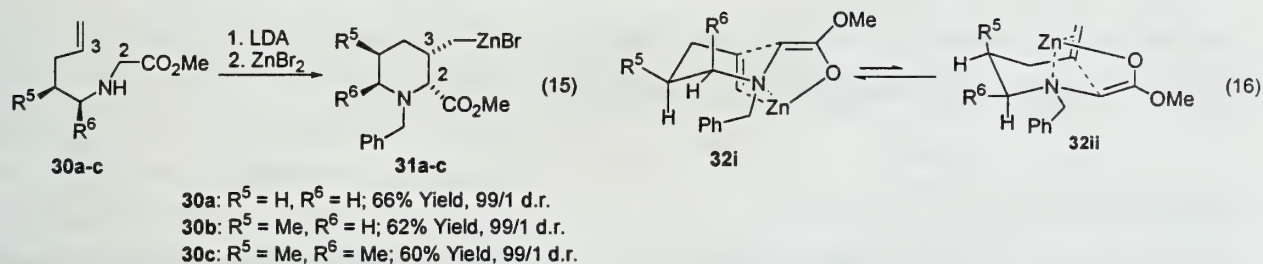
Although metallo-enolates are known to add to carbonyls, they have only rarely been observed to add to C-C π bonds. Zinc malonates have added across alkynes, but zinc enolate reactions with alkenes had been unknown until recently.^{1b} Nakamura has disclosed addition of zinc α -hydrazone anions generalized as structure **28** to **23** as well as to less reactive, isolated olefins to give γ -zinc hydrazone intermediates generalized by **29** (Eq. 13).¹²⁻¹³ These species can react with a variety of electrophiles in a manner similar to the *gem*-bismetallics produced by allylzinc additions. Nakamura's zinc hydrazone additions to substituted olefins are regioselective as the olefins used consistently react at the site of substitution to yield branched products instead of linear adducts. Zinc enolate and α -hydrazone carbometalations are a promising new extension of enolate chemistry. Because the hydrazones produced can readily be converted back to ketones, Nakamura describes this potentially useful alternative to carbometalation with ketone enolates as an "olefinic aldol reaction."



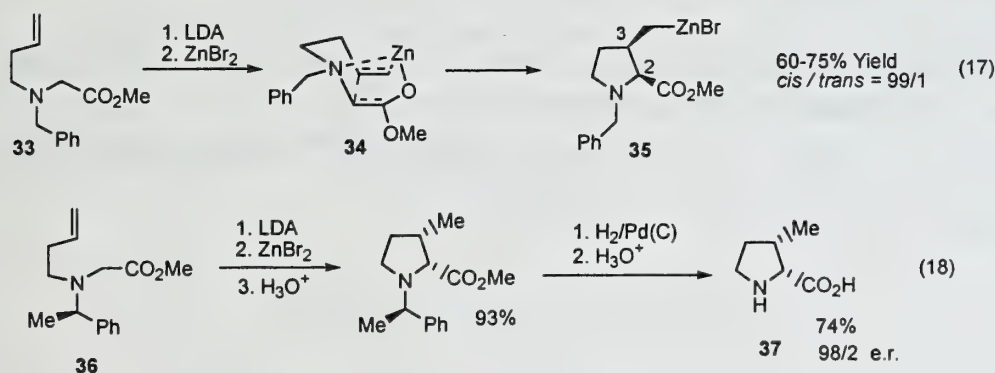
Zinc hydrazones have also been added to substituted vinyl silanes and vinyl Grignard reagents (Eq. 14).¹⁴ Both underwent carbometalation with regioselectivity opposite to that observed for non-metalated olefins. Nakamura argues that softer metal atoms are more capable of stabilizing an adjacent negative charge than alkyl or aryl groups. The less substituted carbon of the vinyl metal is somewhat electron deficient and thus the site for conjugate type addition of a zinc hydrazone. Vinyl Grignard species likely react through a dialkylzinc intermediate much like Normant proposed for the analogous allylzincation.¹⁴ Conversely, vinylsilanes are thought to react via a transition state more similar to those suggested for carbometalation of non-metallo olefins.^{14b} Additions to these silyl and magnesium vinyl derivatives further the synthetic potential of zinc azaenolate carbometalations since both branched and linear products can be accessed.

Normant and Marek have expanded on Nakamura's "olefinic aldol" chemistry by performing intramolecular diastereoselective carbometalations of unsaturated amino-zinc enolates.^{15a} Enolates of **30a-c** cyclize to form piperidines **31a-c** in which the C2 and C3 substituents selectively have a *cis* relationship (Eq. 15). This result is explained by zinc coordination to both the olefin and the partially negatively charged

oxygen of the enolate in a chair transition state **32** so that both groups are positioned on the same face. An unsubstituted starting material **30a** can access both transition state chair conformations **32i** and **32ii** (Eq. 16). However, a C5 substituted substrate, **30b**, is thought to react only through the transition state **32i** so that R⁵ is equatorial to avoid the 1,3 interactions with the olefin and the zinc atom which are evident in **32ii**. Hence, R⁵ is *trans* to C2 and C3 substituents in the product **31b**. Minimization of 1,3 interactions between a C5 substituent and the zinc-olefin complex appears to be the dominant element in determining the stereoselectivity of the cyclizations of disubstituted substrates. The major diastereomer in cyclizations of disubstituted enolates such as **30c** has R⁵ on the opposite face of the ring from the C1 and C2 substituents even if R⁶ is axial in the transition state **32i**.



Cyclizations to form pyrrolidines using the amino-zinc enolate method have also been reported (Eq. 17).^{15b} The enolate of **33** undergoes carbometalation through another chair like transition state **34** to form the pyrrolidine **35** which exhibits a *cis* relationship of the C2 and C3 substituents. Polysubstituted pyrrolidines in which all substituents are *cis* have also been formed, but the mechanism of this stereoselectivity is not clearly understood. An enantioselective amino-zinc enolate cyclization using the substrate **36** forms a benzyl protected precursor to **37**, the amino acid analog β-methylproline. This synthesis provides a practical application of the amino-zinc enolate carbometalation reaction (Eq. 18).¹⁶ Marek and Normant's cyclization methodology has the potential for further diastereoselective formations of a variety of pyrrolidine and piperidine derivatives.



CONCLUSION

Carbometalations of unsaturated organozinc reagents such as allylzinc and propargylzinc compounds have been developed into mild and general reactions. Stereoselectivity in the case of allylzinc additions is controlled by the geometry of the substrate, chelation effects of heteroatoms and π bonds, and the nature of the ligand bound to zinc. In additions of propargylzinc species to alkenes, stereoselectivity is governed both by steric effects and the rigidity of a proposed zinc allene intermediate, and the intramolecular propargylzinc carbometalation is a promising cyclization method. Nickel catalysts have improved the scope of carbometalations of alkynes so that more complex substrates can be used. The reaction conditions, mechanistic studies, and stereochemical models of propargyl and allyl zinc additions have led to the development of stereoselective zinc enolate and azaenolate additions to olefins. While the scope of the latter reactions is not yet well explored, these reactions hold promise as powerful new methods for carbon-carbon bond formations and stereoselective cyclizations.

REFERENCES

- (1) (a) Negishi, E. *Acc. Chem. Res.* **1987**, *20*, 65-72. (b) P. Knochel in *Comprehensive Organic Synthesis* (Eds. B. M. Trost, I. Fleming), Pergamon Press, **1991**, Vol. 4, p. 880.
- (2) Knochel, P.; Perea, J.; Jones, P. *Tetrahedron* **1998**, *54*, 8275-8319.
- (3) (a) Gaudemar, M.; Frangin, Y.; Bellassoued, M. *Synthesis*, **1977**, 205-207. (b) Knochel, P.; Normant, I.-F.; *Tetrahedron Lett.* **1986**, *27*, 1039-1042; 1043-1046; 4427-4430; 4431-4434; 5727-5730.
- (4) (a) Marek, I.; Lefrancois, J.; Normant, J. *J. Org. Chem.* **1994**, *59*, 4154-4161. (b) Marek, I.; Lefrancois, J.-M.; Normant, J.-F. *Bull. Soc. Chim. Fr.* **1994**, *131*, 910-918. (c) Brasseur, D.; Marek, I.; Normant, J.-F.; *Tetrahedron* **1996**, *52*, 7235-7250. (d) Marek, I.; Beruben, D.; Normant, J.-F.; *Tetrahedron Lett.* **1995**, *36*, 3695-3698.
- (5) Meyer, C.; Marek, I.; Coutemanch, G.; Normant, J. *J. Org. Chem.* **1995**, *60*, 863-871.
- (6) Marek, I.; Normant, J.; Lorthiois, E. *Tet. Lett.* **1997**, *38*, 89-92.
- (7) Nakamura, E.; Kubota, K.; Isaka, M.; Nakamura, M.; *J. Amer. Chem. Soc.* **1993**, *115*, 5867-5868.
- (8) Nakamura, M.; Nakamura, E.; Arai, M. *J. Amer. Chem. Soc.* **1995**, *117*, 1179-1180.
- (9) Knochel, P.; Studemann, T.; Ouali, M.I.; *Tetrahedron* **1998**, *54*, 1299-1316.
- (10) Montgomery, J.; Savchenko, A. *J. Amer. Chem. Soc.* **1996**, *118*, 2099-2100.
- (11) Montgomery, J.; Seo, J. *Tetrahedron* **1998**, *54*, 1131-1144.
- (12) Nakamura, E.; Kubota, K. *J. Org. Chem.* **1997**, *62*, 792-793.
- (13) Nakamura, E.; Kubota, K. *Angew. Chem. Int. Ed. Engl.* **1997**, *36*, 2591-2493.
- (14) (a) Nakamura, E.; Kubota, K.; Sakata, G. *J. Amer. Chem. Soc.* **1997**, *119*, 5457-5458. (b) Nakamura, E.; Kubota, K. *Tet. Lett.* **1997**, *38*, 7099-7102.
- (15) (a) Marek, I.; Normant, J.; Lorthiois, E. *J. Org. Chem.* **1998**, *63*, 566-574. (b) Marek, I.; Normant, J.; Lorthiois, E. *J. Org. Chem.* **1998**, *63*, 2442-2450.
- (16) Chassaing, G.; Karoyan, P. *Tet. Lett.* **1997**, *38*, 85-88.

VANCOMYCIN: AN APPLICATION OF BIARYL ETHER SYNTHESIS

Reported by Jeromy Cottell

October 19, 1998

INTRODUCTION

Vancomycin¹ (**1**) is a very powerful antibiotic that was isolated in 1956 from *Streptomyces orientalis*, a soil microorganism collected in Borneo.² Vancomycin has found clinical use in the treatment of Gram-positive bacteria which show resistance to penicillin,³ although side-effects, including auditory nerve and kidney damage, prevent wide-spread use of the drug. The structure of Vancomycin was proposed in 1983 after extensive NMR, X-ray, and chemical analysis by Williams and Harris.⁴ The full structure (Figure I) was confirmed by X-ray crystallography on **1** in 1997.⁵ Synthetically, **1** is a very complex glycopeptide. The aglycon is a heptapeptide with a tricyclic structure created through one biaryl linkage and two biaryl ether linkages. In addition to the stereogenic centers contained in the peptide backbone, each of the three macrocycles exist as a unique atropisomers. Though (5-7) tripeptide ring has been shown to isomerize at moderate temperatures, the (4-6) and (2-4) rings do not when fully functionalized. Therefore, atropiastereoselectivity must be achieved in the cyclization of the rings. This review will detail the development of biaryl ether syntheses as they are related to the construction of **1**.

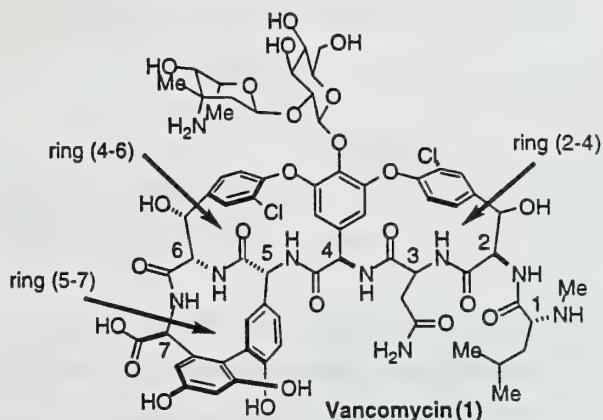
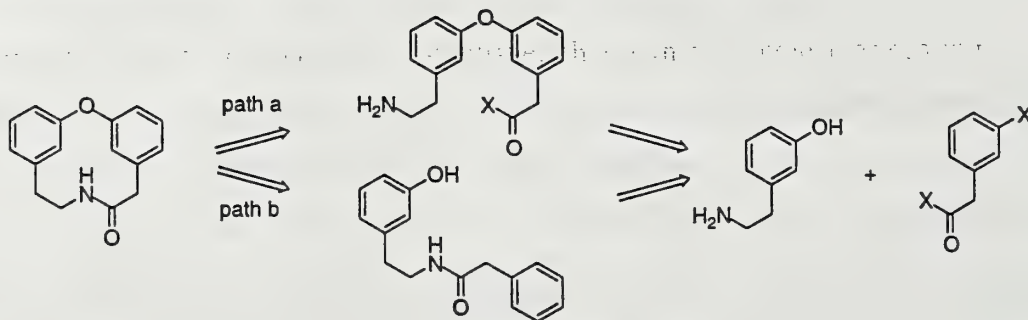


Figure I. Structure of Vancomycin.

SYNTHESIS

Work towards the formation of Vancomycin type macrocycles have followed two main approaches which differ in the timing of the biaryl ether formation (Scheme I). Earlier attempts began with the formation of a simple biaryl ether. This was subsequently functionalized to a precursor for macrolactamization (path a). Conversely, the formation of the peptide backbone can provide the coupling precursor for a macroetherification (path b). Investigations into the biosynthetic pathway of **1** indicate that the aryl rings are oxidatively coupled after peptide formation.¹

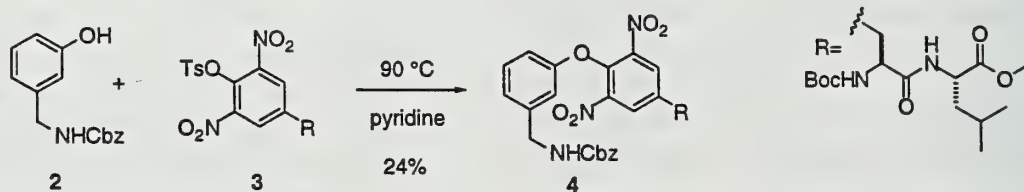
Scheme I.



Biaryl Ether Formation

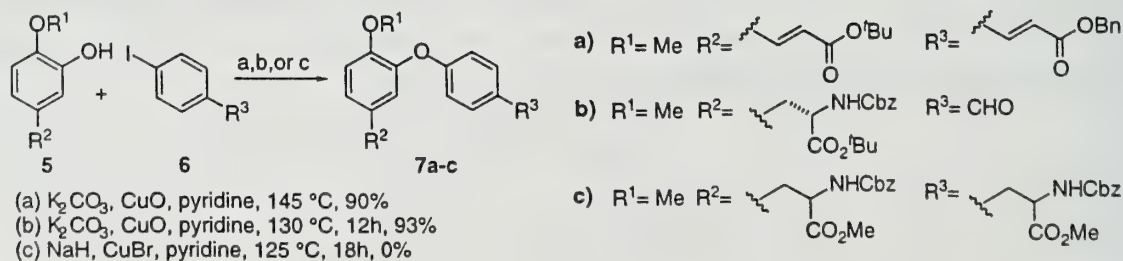
The formation of biaryl ethers is usually effected by the substitution of a leaving group on an aryl ring by a phenol.⁶ Typically performed under vigorous conditions which would not be compatible with labile groups, this process is facilitated by the presence of strongly electron withdrawing groups on the aryl acceptor. Thus the protected phenol **2** was coupled with tosylate **3** in pyridine at 90 °C to provide the aryl ether **4** without epimerization, but in low yield (Scheme II).⁷

Scheme II.



Another classical approach to the formation of the biaryl ethers is the copper facilitated Ullmann ether coupling^{8,9} of an aryl halide and a phenoxide. Standard reaction conditions include a weak base, a source of copper(I), and reaction at high temperatures in pyridine. Often these conditions preclude the coupling of partners with sensitive substituents. The application of the Ullmann reaction has been examined by several groups.¹⁰ Despite the vigorous reaction conditions, **7a** and **7b** were obtained in good yield, and in the case of **7b**, no epimerization was reported (Scheme III). However the reaction conditions prevented the direct coupling of two aryl amino acids (**7c**). Therefore one or both of the amino acids must be functionalized after the coupling.

Scheme III.



Other alternatives to the Ullmann coupling include the use of iodonium salts¹¹ and cationic ruthenium complexes¹² as the electrophilic aryl acceptor. Cationic iodine is a better leaving group which facilitates ether formation, but highly acidic conditions during their formation precludes the use of sensitive groups on the iodonium salt. In contrast, a cationic cyclopentadienyl ruthenium sufficiently activates the aryl acceptor by complexation. The conditions for the ruthenium assisted coupling have proven mild enough for the direct coupling of functionalized amino acids in good yields.

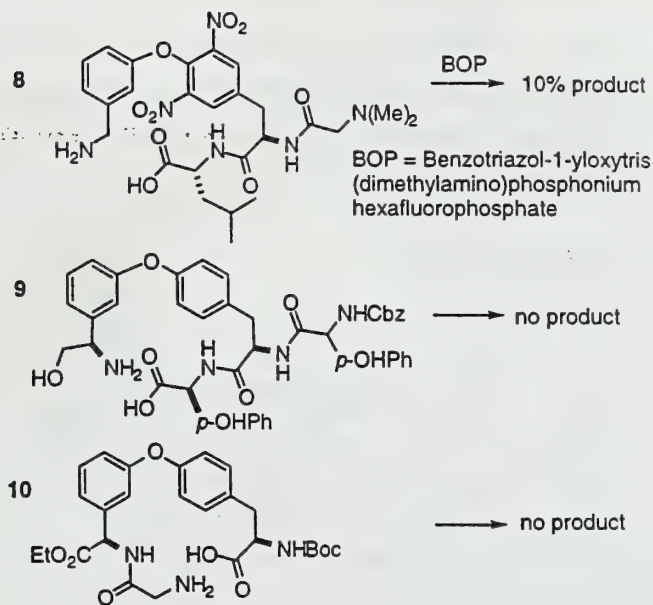
Moderate successes in the macrolactamization of several biaryl ether containing natural products, however attempts to cyclize model 16-membered rings present in **1** have not been successful (Scheme IV). Attempts by Brown and Hamilton yielded less than 10% of product, while lactamization of similar substrates by Williams and Pearson provided no product.^{6,10b,11a,13} A conformational restriction disfavoring the approach of the acyl group to the amine was believed to be responsible for the lack of reactivity. Although MM2 calculations done by Pearson suggest that the ground state conformer places the amine near the acyl coupling partner in the gas phase, they do not seem to apply to the preferred conformer in solution.

Despite the problems of cyclization, several biaryl ether methods have shown effective in the coupling of aryl amino acids. In the application to the synthesis of **1**, this initial work provided the basis for a biaryl ether macroetherification (Path b, Scheme I). Although the macroetherification adds complexity requiring an intramolecular ether formation, the flexibility in the peptide backbone may render this a more favorable process than macrolactamization.

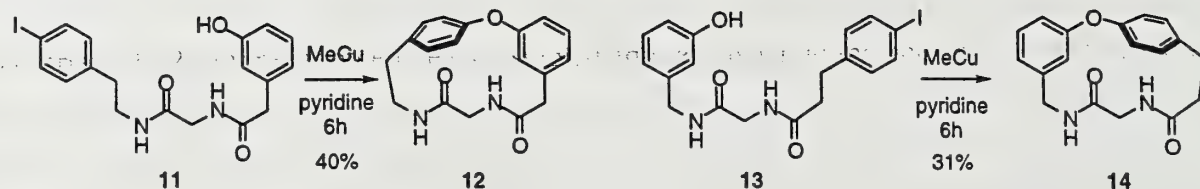
Macroetherification

Investigations into intramolecular Ullmann coupling were conducted mainly by Boger.¹⁴ Closure of nonfunctional 16-membered lactams **12** and **14** was effected in moderate yields (Scheme V). The use of MeCu was found to be necessary, eliminating the use of additional base during the reaction. Cyclization with an alanine linker provided the cyclic lactam in slightly higher yield, with 5% epimerization. This method has not been applied to a fully functionalized peptide chain, probably due to larger epimerization problems with the sensitive phenylglycine unit.

Scheme IV.

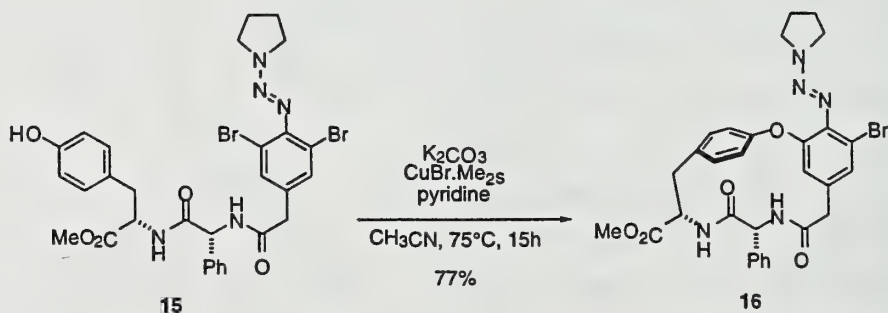


Scheme VI.



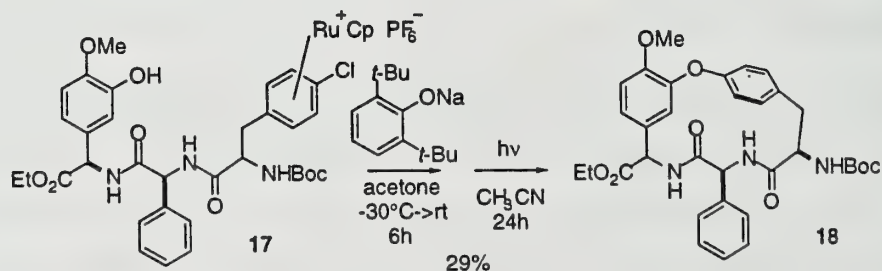
The problem of epimerization was addressed by Nicolaou which led to the use of a triazene group ortho to the leaving group (Scheme VII).^{15,16} The triazene group provides milder reaction conditions by the activation of the aryl ring as well as assistance to nucleophilic attack through complexation with the copper. An additional advantage of this approach is that the triazene unit can easily be transformed into a hydroxyl group.¹⁷ Thus, the cyclization product 16 can be obtained in 15h at 75 °C with good yield and minor epimerization.

Scheme VII.



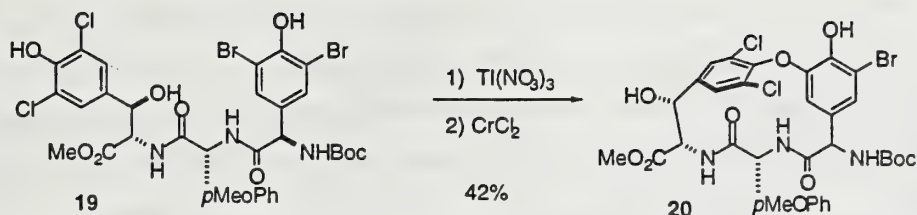
The cyclization of cationic aryl ruthenium complexes have been investigated by both Pearson and Rich.¹⁸ Application to several other biaryl ether natural products have yielded the desired lactams in moderate yields. However, cyclization of 17 (Scheme VIII) provided 18, a 16-membered ring, in only 29% yield.

Scheme VIII.



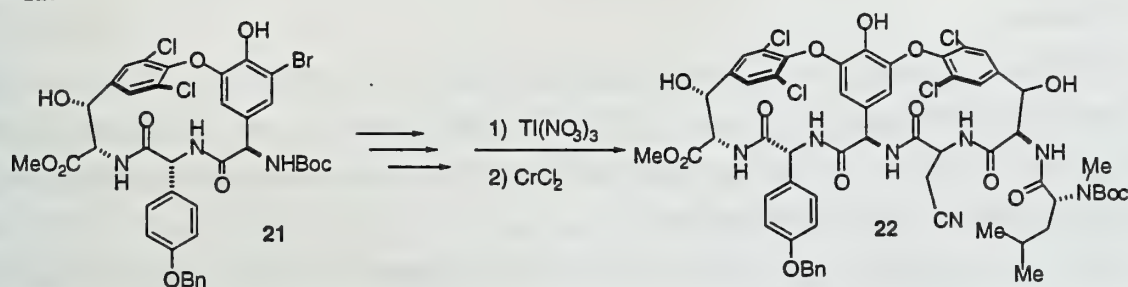
Studies by Yamamura found that thallium(III)nitrate could assist in the formation a quinone, which after reduction, gave a biaryl ether.¹⁹ Optimization and application of this two step procedure typically gave 15-20% yields.²⁰ A one-pot procedure eliminated the need for isolation of the quinone, and led to an increase in yield (Scheme IX).

Scheme IX.



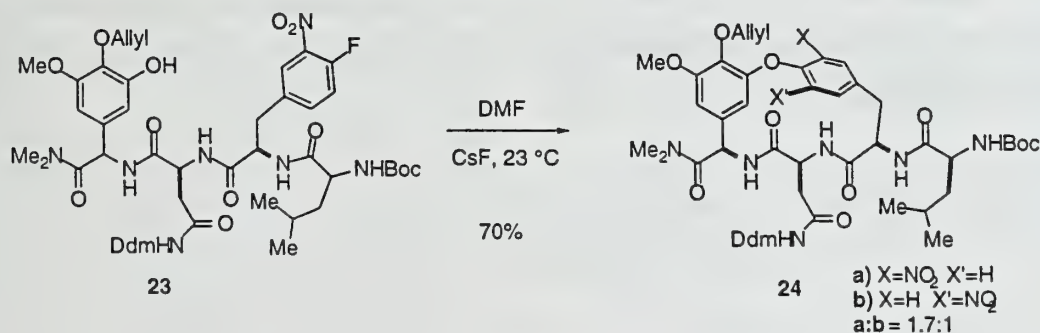
The thallium assisted coupling has led to the synthesis of the tetrahalogenated (2-4)/(4-6) bicyclic system **22** by both Evans and Yamamura (Scheme X).²¹ The dihalogenated starting material is needed for activation of the phenoxide, and therefore a selective dehalogenation would have to be used in the application to **1**. In addition, the cyclization of the (2-4) tripeptide ring in the presence the (5-7)/(4-6) bicyclic unit resulted in a compromised yield.²² A conformational bias was cited as the problem, however the effect of the unnatural (5-7) atropisomer was not investigated and the cyclization of the (4-6) tripeptide was shown to occur by other routes.

Scheme X.



Another method of biaryl ether cyclization is intramolecular nucleophilic aromatic substitution ($\text{S}_{\text{N}}\text{Ar}$), investigated by Zhu and Beugelmans.²³ In this case, an *o*-nitro aryl fluoride was chosen²⁴ as the aryl acceptor. During initial studies on the synthesis **14**, cyclization with K_2CO_3 in DMF (rt, 6h) provided the lactam in greater than 90% yield.²⁵ Subsequent work by Evans, Rao, Boger, and Zhu have shown that this methodology can be applied to fully functionalized lactams with yields between 50% and 70% using slightly varied procedures (Scheme XI).²⁶

Scheme XI



Several methods have been shown to be effective in the macroetherification of cyclic lactams. Importantly, this general route has proven more advantageous than the macrolactamization approach towards **1**. The nucleophilic aromatic substitution method developed by Zhu, and subsequently refined by others, is by far the most useful method, requiring very mild conditions and providing good yields with labile substrates.

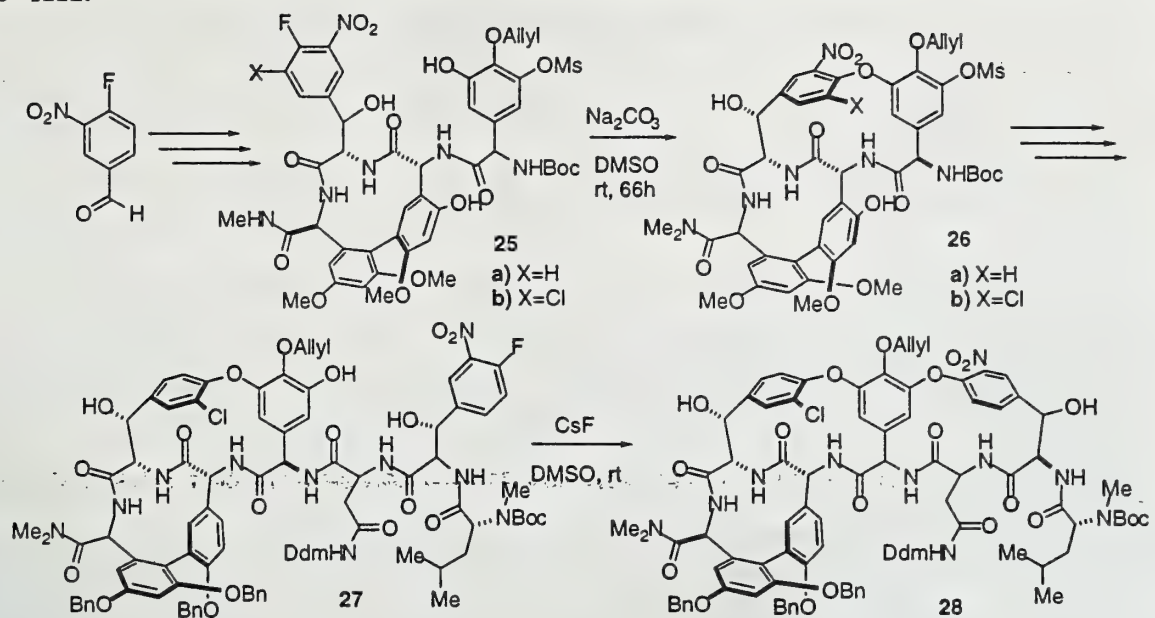
The issue of atropdiastereomers has only begun to be investigated, however none of the coupling methods show an inherent selectivity. In a study by Yamamura, the modification of the nucleophilic coupling partner to a *o*-bromo-*o*-chlorophenol allowed for the selective removal of the bromine, after cyclization, providing a mixture of atropisomers.²⁷ The use of an *o*-nitro aryl fluoride in the nucleophilic aromatic substitution method leads to the formation of atropisomers during the cyclization, although in most cases little or no selectivity is observed. During studies by Zhu, only once did the S_NAr cyclization provided a single diastereomer, however inspection of the lactam product did not provide any obvious reason for the selectivity observed.²⁸

Total Synthesis

After almost twenty years of synthetic work towards **1**, the total synthesis of the aglycon has recently been completed by Evans (Scheme XII).²⁹ The highlight of the synthesis was the construction of the biaryl ether rings following the S_NAr method, where the necessary atropdiastereoselectivity was obtained through substrate controlled cyclization.

Using asymmetric amino acid strategies and an oxidative biaryl cyclization method previously explored by Evans, the (5-7) ring was assembled with a >95:5 preference for the unnatural atropisomer. In earlier studies by Zhu it was observed that the macroetherification of the (2-4) tripeptide provided good selectivity when one atropisomer of the (4-6) subunit was used. This idea was extended to the cyclization of **25a**, where control of the unnatural (5-7) ring provided a 10:1 mixture of **26a**, favoring the unnatural atropisomer. Following the assumption that the selectivity could be preserved with additional aryl substitution, cyclization of the chlorinated analog **25b** yielded a 5:1 mixture favoring the same isomer in good yield. Reduction of the nitro group resulted in the desired atropisomer. The isomerization of the (5-7) tripeptide was then controlled by the (2-4) subunit resulting in a 95:5 preference for the natural atropisomer. Addition and cyclization of the (2-4) tripeptide occurred to give **28**, with 5:1 selectivity favoring the natural atropisomer. Subsequent deprotection provided the desired aglycon with 40 steps in the longest linear sequence.

Scheme XII.



CONCLUSION

The interest in the synthesis of Vancomycin has led to the development of several methods for the formation of biaryl ethers. Especially important is the ability to incorporate stereo labile functionality into the coupling partners. Macrolactamization of biaryl ether products, in efforts to produce 16-membered rings, gave unsatisfactory yields. Subsequent investigations into macroetherification have proven to be an effective alternative. In respect to the synthesis of Vancomycin, these cyclizations have not shown an ability to control atropdiastereoselectivity. Though additional work is necessary for complete selectivity, substrate control has been demonstrated to provide moderate selectivity in several examples. Exploitation of this fact has led to the first synthesis of the Vancomycin aglycon.

REFERENCES

- (1) Nagarajan, R. "Glycopeptide Antibiotics" Marcel Dekker, Inc.: New York, 1994.
- (2) McCormick, M. H.; Stark, W. M.; Pittenger, G. F.; Pittenger, R. C.; McGuiire, G. M. *Antibiot. Annu.* **1955-1956**, 606.
- (3) *Physicians' Desk Reference* vol. 96.
- (4) a) Williams, D. H. *Acc. Chem. Res.* **1984**, *17*, 364. b) Sheldrick, G. M.; Jones, P. G.; Kennard, O.; Williams, D. H.; Smith, G. A. *Nature*. **1978**, *271*, 223. c) Harris, C. M.; Kopecka, H.; Harris, T. M. *J. Am. Chem. Soc.* **1983**, *105*, 6915. d) Williams, D. H.; Kulman, J. R. *J. Am. Chem. Soc.* **1977**, *99*, 2768.
- (5) a) Schäfer, M.; Schneider, T. R.; Sheldrick, G. M. *Structure* **1996**, *4*, 1503. b) Loll, P. J.; Beviviro, A. E.; Korty, B. D.; Axelsen, D. H. *J. Am. Chem. Soc.* **1997**, *119*, 1516.
- (6) Pardisi, C. *Comprehensive Organic Synthesis* Pergamon Press: Oxford **1991**, *4*, 423.
- (7) Pant, N.; Hamilton, A. P. *J. Am. Chem. Soc.* **1988**, *110*, 2002.
- (8) Ullmann, F. *Chem. Ber.* **1904**, *37*, 853.
- (9) a) Moroz, A. A.; Shvartberg, M. S. *Russ. Chem. Rev.* **1974**, *43*, 679. b) Lindley, J. *Tetrahedron* **1984**, *40*, 1433.

- (10) a) Boger, D. L.; Yohannes, D. *Tetrahedron Lett.* **1989**, *30*, 2053. b) Boger, D. L.; Yohannes, D. *J. Org. Chem.* **1990**, *55*, 6000. c) Evans, D. A.; Ellman, J. A. *J. Am. Chem. Soc.* **1989**, *111*, 1063. d) Schmidt, U.; Weller, D.; Holder, A.; Lieberknecht, A. *Tetrahedron Lett.* **1988**, *29*, 3227
- (11) a) Chakraborty, T. K.; Reddy, G. V. *J. Org. Chem.* **1992**, *57*, 5462. b) Crimmin, M. J.; Brown, A. G. *Tetrahedron Lett.* **1990**, *31*, 2017.
- (12) a) Pearson, A. J.; Park, J. G. *J. Org. Chem.* **1992**, *57*, 1744. b) Pearson, A. J.; Park, J. G.; Zhu, P. Y. *J. Org. Chem.* **1992**, *57*, 3583. c) Pearson, A. J.; Lee, K. *J. Org. Chem.* **1994**, *59*, 2304.
- (13) Stone, M. J.; van Dyk, M. S.; Booth, P. M.; Williams, D. H. *J. Chem. Soc. Perkin Trans. I* **1991**, 1629.
- (14) a) Boger, D. L.; Yohannes, D. *J. Org. Chem.* **1991**, *56*, 1763. b) Boger, D. L.; Yohannes, D. *J. Am. Chem. Soc.* **1991**, *113*, 1427. c) Boger, D. L.; Nomoto, Y.; Teegarden, B. R. *J. Org. Chem.* **1993**, *58*, 1425. d) Boger, D. L.; Patane, M. A.; Zhou, J. *J. Am. Chem. Soc.* **1994**, *116*, 8544.
- (15) Nicolaou, K. C.; Boddy, N. C.; Natarajan, S.; Yue, T.-Y.; Li, H.; Brüse, S.; Ramanjulu, J. M. *J. Am. Chem. Soc.* **1997**, *119*, 3421.
- (16) For the synthesis for Vancomycin aglycon see published just prior to this review see: a) Nicolaou, K. C.; Natarajan, S.; Li, H.; Jain, N. F.; Hughes, R.; Solomon, M. E.; Ramanjulu, J. M.; Boddy, C. N. C.; Takayanagi, M. *Angew. Chem. Int. Ed.* **1998**, *37*, 2708. b) Nicolaou, K. C.; Jain, N. F.; Natarajan, S.; Hughes, R.; Solomon, M. E.; Li, H.; Ramanjulu, J. M.; Takayanagi, M.; Koumbis, A. E.; Bando, T. *Angew. Chem. Int. Ed.* **1998**, *37*, 2714. c) Nicolaou, K. C.; Takayangi, M.; Jain, N. F.; Natarajan, S.; Koumbis, A. E.; Bando, T.; Ramanjulu, J. M. *Angew. Chem. Int. Ed.* **1998**, *37*, 2717.
- (17) Sayamarthy, N.; Barrio, J. R.; Bida, G. T.; Phelps, M. E. *Tetrahedron Lett.* **1990**, *31*, 4409.
- (18) a) Janetka, J. W.; Rich, D. H. *J. Am. Chem. Soc.* **1995**, *117*, 10585. b) Janetka, J. W.; Rich, D. H. *J. Am. Chem. Soc.* **1997**, *119*, 6468. c) Pearson, A. J.; Bignan, G. *Tetrahedron Lett.* **1996**, *37*, 735.
- (19) Noda, H.; Niwa, M.; Yamamura, S. *Tetrahedron Lett.* **1981**, *22*, 3247
- (20) Nishiyama, S.; Suzuki, Y.; Yamamura, S. *Tetrahedron Lett.* **1989**, *30*, 379.
- (21) a) Evans, D. A.; Ellman, J. A.; DeVries, K. M. *J. Am. Chem. Soc.* **1989**, *111*, 8912. b) Suzuki, Y.; Nishiyama, S.; Yamamura, S. *Tetrahedron Lett.* **1990**, *31*, 4053
- (22) Evans, D. A.; Dinsmore, C. J.; Ratz, A. M. *Tetrahedron Lett.* **1997**, *38*, 3189.
- (23) Beugelmans, R.; Singh, G. P.; Zhu, J. *Tetrahedron Lett.* **1993**, *34*, 7741.
- (24) Vlasov, V. M. *J. Fluorine Chem.* **1992**, *61*, 193.
- (25) Beugelmans, R.; Singh, G. P.; Bois-Choussy, M.; Chastanet, J.; Zhu, J. *J. Org. Chem.* **1994**, *59*, 5535.
- (26) a) Boger, D. L.; Borzilleni, R. M.; Nukui, S. *Bioorg. Med. Chem. Lett.* **1995**, *5*, 3091. b) Zhu, J.; Bouillon, J.-P.; Singh, G. P.; Chastanet, J.; Beugelmans, R. *Tetrahedron Lett.* **1995**, *36*, 7081. c) Evans, D. A.; Barrow, J. C.; Ratz, A. M.; Dinsman, C. T.; Evard, D. A.; DeVries, K. M.; Ellman, J. A.; Rychnovsky, S. D.; Lacour, S. *J. Am. Chem. Soc.* **1997**, *119*, 3419.
- (27) Konishi, H.; Okano, T.; Nishiyama, S.; Yamamura, Y.; Koyasu, K.; Terada, Y. *Tetrahedron Lett.* **1996**, *37*, 8791.
- (28) Bois-Choussy, M.; Neuville, L.; Beugelmans, R.; Zhu, J. *J. Org. Chem.* **1996**, *61*, 9309.
- (29) a) Evans, D. A.; Wood, M. R.; Trotter, B. W.; Richardson, T. I.; Barrow, J. C.; Katz, J. L.; *Angew. Chem. Int. Ed.* **1998**, *37*, 2700. b) Evans, D. A.; Dinsmore, C. J.; Watson, P. S.; Wood, M. R.; Richardson, T. I.; Trotter, B. W.; Katz, J. C. *Angew. Chem. Int. Ed.* **1998**, *37*, 2704.

DESIGNING MOLECULAR-SCALE ORGANIC DEVICES

Reported by David J. Hill

October 29, 1998

INTRODUCTION

The twentieth century has seen the progress of technology from the age of machines into the age of computers. Nearing the century's close, there continues to be a tremendous effort to devise better machines by shrinking components and increasing efficiency. The traditional "top-down" engineering approach has inherent limitations including cost-effectiveness and construction feasibility. To overcome these problems, research into microelectromechanical systems (MEMS) has gained remarkable momentum in a variety of disciplines.

Within the MEMS community, molecular-scale organic devices (MSODs) have recently attracted considerable attention because of their potential as high-performance compact devices. From an engineering standpoint, the large number of reactions available to the organic chemist and the potential degree of resulting molecular control enables devices to be designed from the "bottom-up". Moreover, the MSOD would depend not on the bulk properties of the material for its function, but rather on the inherent properties of individual molecules. Bench-top "manufacturing" of an organic compound could produce 10^{23} devices, redefining the scale of mass production.

MSODs are molecular analogs of macroscopic devices, e.g., gears, switches, and wires. In order for MSODs to function, they must have a three-dimensional architecture with rotational, conformational, translational, or electronic properties that can respond to an external energy source. Control by heat, pH, light or electrochemistry can cause a the mechanical or electronic response. The focus of this report is to highlight recent advances in the design of MSODs and the strategies used for their synthesis and development.

MECHANICAL DEVICES

The ultimate goal in developing mechanical MSODs is to design and synthesize suitable components for building molecular machines, which are defined as any molecule or molecular assembly that can do work. Towards this end, a number of mechanical MSODs have been recently developed including a molecular turnstile¹ and molecular Tinkertoy[®] rods² but the largest effort has gone into developing molecular gears. Over the past twenty years, many investigations into the conformations of molecules have evolved into an ongoing search for molecular gearing devices. These molecules can be designed by taking advantage of the inherent rotation of juxtaposed organic groups.

Comprehensive studies by Yamamoto and Oki into rotational barriers in substituted triptycenes, which are triaryl [2.2.2] three-toothed gears, established their dynamic molecular gearing.³ Mislow and Iwamura simultaneously synthesized a variety of tethered bis-triptycene derivatives that act as bis-three-toothed bevel gears **1** and investigated their stereochemical relationships, correlated rotation, and barriers to gear slippage.⁴ The dynamic gearing of triptycenes has also been studied in crown ethers⁵ and as ligands in a cobalt complex.⁶ Throughout these studies, triptycenes have demonstrated their potential as organic gears. In order to develop functional molecular gears however, rotational restriction as well as directional control is required.

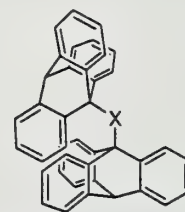
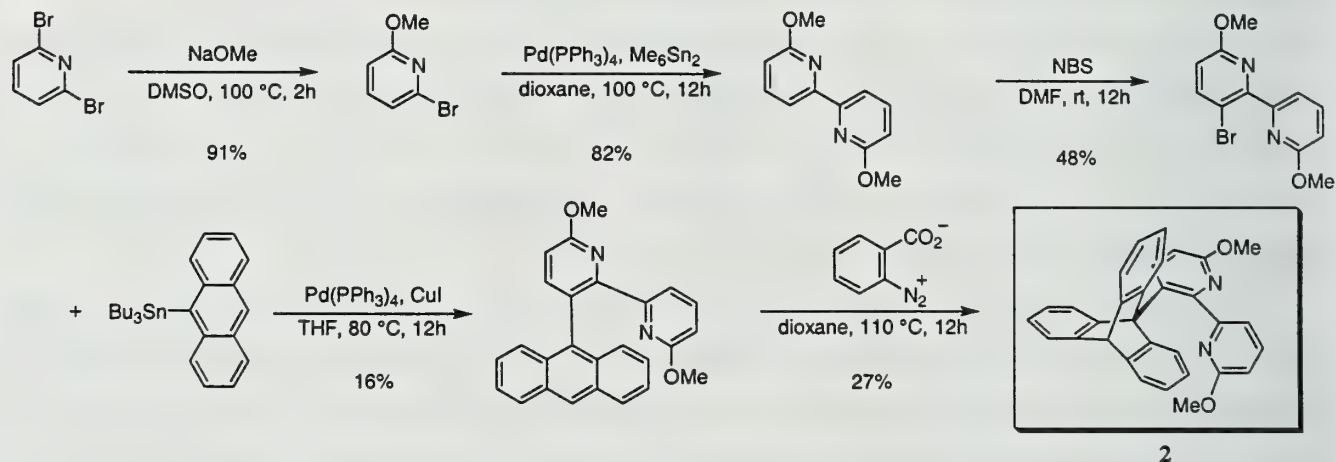


Figure 1. Triptycene Bevel Gear
(X = CH₂, CHOH, CO, O)

With the goal of hindering rotation in a triptycene gear, Kelly and coworkers recently pursued the development of a molecular brake.⁷ Their design for the device was a triptycene substituted with an

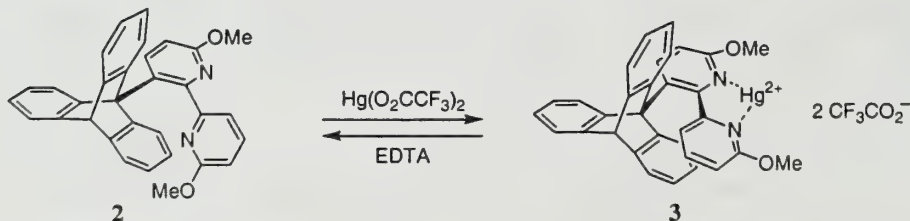
Scheme I



organic group that would become rigid when triggered embedding itself between two of the teeth and ceasing rotation. By taking advantage of two Pd couplings of aryl groups, they were able to synthesize the molecular brake **2** with a bis-pyridinal ligand designed to bind metal ions (Scheme I). In the triptycene **2** there is free rotation as seen by the broadening of the aryl peaks in the ¹H-NMR spectrum as

the temperature is lowered to -80 °C. The interpretation is that the bis-pyridinyl group is flexible and cannot impede rotation. Upon the addition of mercury(II), the bis-pyridinyl

Scheme II

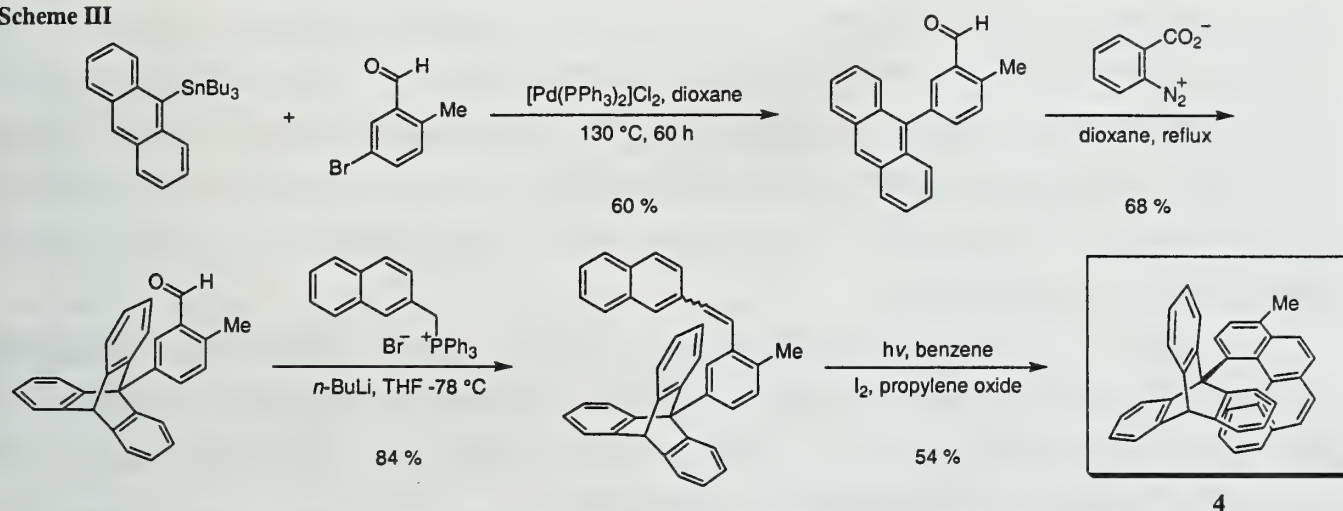


group binds the metal and is locked into a planar conformation **3**, wedging between two of the teeth (Scheme II). In the ¹H-NMR, the triptycene aryl peaks were broad from 30 °C to 0 °C, but sharpened at -30 °C, indicating that the triptycene was no longer rotating. The molecular braking process can be

reversed upon addition of a stronger mercury(II) chelating ligand such as EDTA. Further developments into non-chemical triggers as well as braking at room temperature are desired.

In a further effort to control molecular rotation, Kelly devised a molecular analogy to a macroscopic ratchet in which the direction of the gear's rotation could be biased by a sterically constrained pawl (Scheme III). The design of the molecular ratchet **4** involves a triptycene substituted with a helicene known to have spring-like properties.^{8,9} The concept is that the helicene would act as the pawl or catch that the triptycene gear must "push aside" in order to rotate. Since rotation "against the grain" of the helicene intuitively appears to be disfavored, the triptycene should prefer to rotate "with the grain" of the helicene. The mechanical device was prepared through the use of a Stille coupling, a

Scheme III



Wittig reaction and a photocyclization to produce **4** as a racemate. The presence of the methyl group prohibits formation of the diastereomeric cyclization product. After synthesizing a number of pawls and studying the rotational motion by spin polarization transfer ¹H-NMR,¹⁰ the authors concluded that there was no rotational bias in the system.

A similar theoretical molecular ratchet was proposed by Feynman to demonstrate that such a system could not rotate preferentially in one direction without violating the second law of thermodynamics.¹¹ Presumably, heat would provide the energy source for this system to do work, a result which would confirm the second law of thermodynamics that heat cannot be converted to work in an isothermal system. The system **4** fails since heat causes rotational and vibrational motion. When the helicene has significant vibration energy to lift away from the tooth, the triptycene can rotate freely in either direction, destroying any conformational bias induced by the helicene. This experiment demonstrates that traditional macroscopic mechanical engineering does not always scale down to the molecular level.

It is clear that the structural design of a mechanical MSOD is crucial to its function. Furthermore, the ability to control rotation in molecules will be a key design element in future systems

especially in sterically constrained molecules. Another approach to biasing rotation is required since it is implausible that thermodynamics can be circumvented. Overall, the potential for developing new mechanical MSODs has been improved by powerful synthetic and spectroscopic techniques.

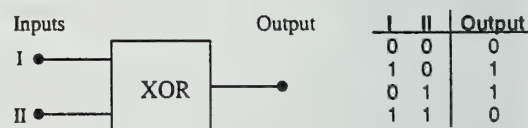
MOLECULAR SWITCHES

Switches, mechanical devices that control electronic signals, are common in macroscopic machines. Molecular switches are the most fully developed MSODs because they have the fewest structural requirements. A simple molecular switch must have two conformational or energetic states that are reversible with a high-energy barrier between them. An initiator must trigger the complete conversion of one state to the other and these "off" and "on" states must be physically distinct. Simple molecular switches which have been developed include slide switches^{12,13} where controlled translation of a molecule between two stations acts as a switch. The pursuit of more complex molecular switches and switch assemblies is stimulated by the possibility that they can act as logic gates and information storage devices for the binary code. The development of such sophisticated switches would be essential components of a molecular computer.

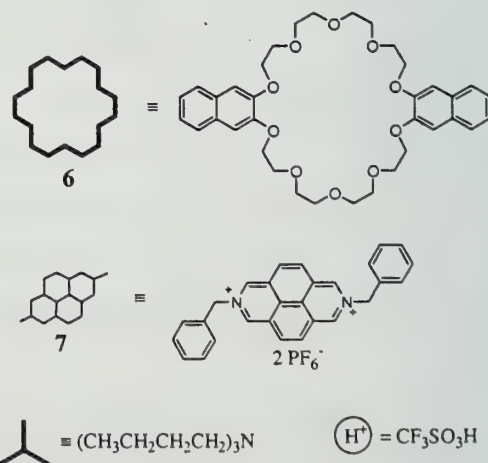
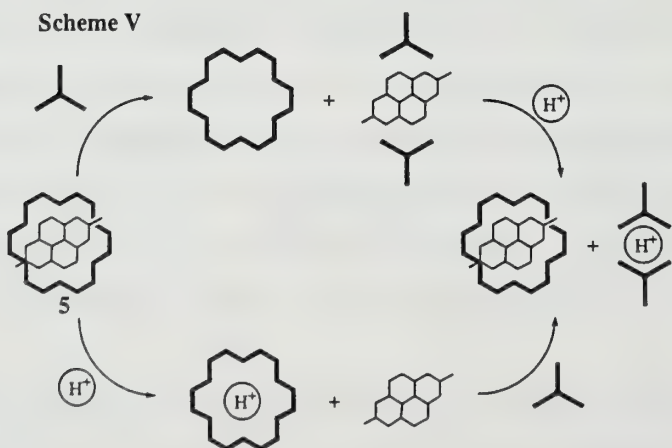
An assembly of molecular switches can act as a logic device, which can be the primary component of a digital processor. An important device in binary addition, an exclusive-or (XOR) logic gate contains two inputs and one output. When the states of the inputs are the same, whether 0 or 1, the output is 0. When either one of the inputs is 1, the output is 1.

A pseudorotaxane can act as a molecular logic gate where the inputs are reagents that disrupt the association and the fluorescent output comes from the free pseudorotaxane components. Stoddart and coworkers have developed a pseudorotaxane XOR logic gate (Scheme IV).¹⁴

Scheme IV



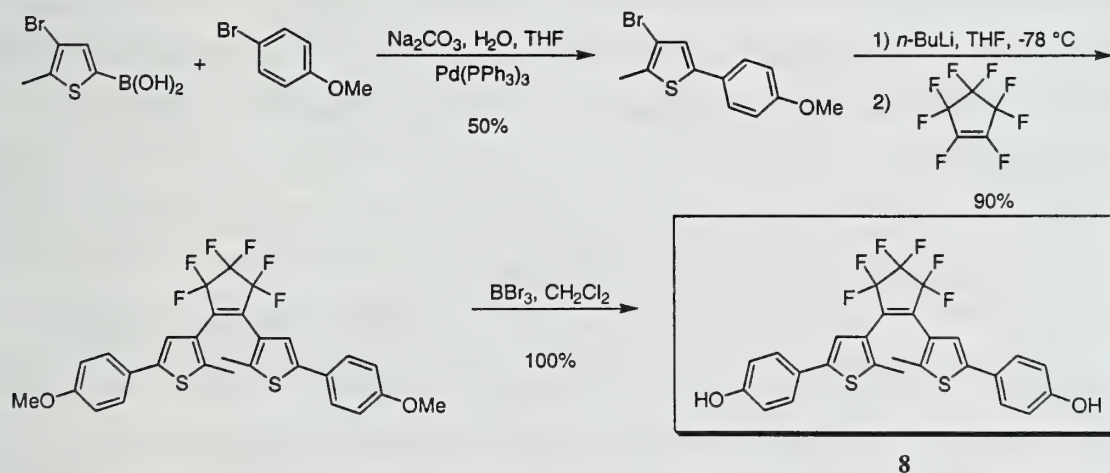
Scheme V



threading of bis-naphthyl-crown ether **6** with diazapyrenium dication **7** (Scheme V). When initially mixed in a 1.5:1 ratio, 60% of **6** and 85% of **7** are threaded as evaluated from fluorescence. Upon addition of an acid or an amine, 90-95% of **5** dethreads with the fluorescent signal of **6** increasing and that of **5** decreasing. Upon subsequent addition of either the amine or the acid, respectively, 90% of **6** and **7** rethread and the full fluorescent band of **5** returns. In this system, fluorescence is the output and the inputs are the acid and the amine. When one input is added to the pseudorotaxane and dethreading occurs, the fluorescence output produces a 1. When the other input is added, then the fluorescence output returns to 0. Although this system is effective in producing XOR logic, it suffers from the need to introduce more compounds into the system in order to function. For future designs, a photochemical or electrochemical initiator would be more efficient.

An erasable molecular memory device has been developed by Lehn and coworkers.^{15,16} In order to store information in any molecular device, the molecule's binary state must be able to be locked to protect the data and to be unlocked so that it can be modified. Furthermore, the locked state must be stable over time. This can be accomplished by a dual-mode switching process using photochemistry and electrochemistry in a conjugated system. The synthesis of the device is outlined in Scheme VI. Through the use of a Suzuki coupling, the arylthiophene precursor was obtained and further condensed with perfluorocyclopentene to yield the bisphenolic dithienylethene **8**. In its initial 0 state, the thiophene rings are out of plane to the alkene to minimize steric interactions between the interior methyl groups (Scheme VII). In the "write" cycle, photocyclization of the colorless **8** at 312 nm produces the blue **9** in >98% conversion. This system is "locked" by oxidation with ferricyanide(III) to generate the red-violet bisquinone **10** which can be "read" photochemically at >600 nm without destroying the state. The molecule can be "unlocked" by coulometric reduction to **9** and then "erased" to the 0 state by

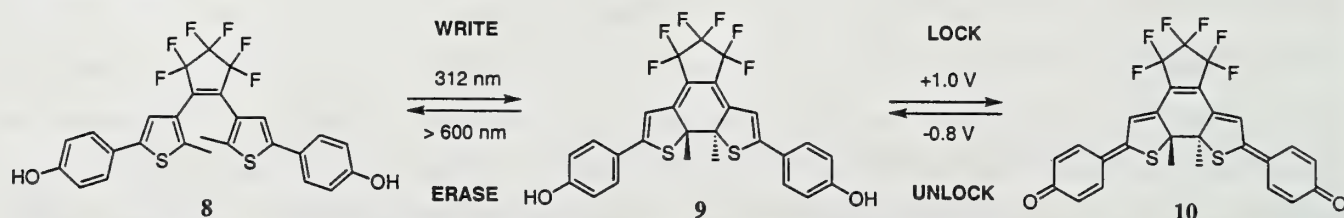
Scheme VI



photochemical ring opening at >600 nm to **8**. The strength of this system is that two different switching initiators are used and the states are stable. The "locked" **10** molecules are "write protected" when

exposed to “erasing” of **9** by light. Likewise, **8** cannot be oxidized directly to **10** ensuring that only **9** can be “locked” to **10**. This dual-mode switching is crucial to controlling the states of molecules necessary

Scheme VII



in the development of molecular memory suitable for temporary and permanent data storage. In the future, addressable molecular memory must be fabricated if large amounts of data are to be stored.

The design and development of switchable MSODs has benefited greatly from these recent investigations into more sophisticated devices. Ideally, the switching processes of logic gates should be initiated by an energy source to make these devices more uniform with other electronic MSODs. The possibility of information storage has been demonstrated although “reading” the data of one device in an array is a formidable task. These MSODs lay a strong foundation for future work in multi-component assemblies for the development of molecular microprocessors, but fabrication methodologies and techniques remain the major challenge in this area.

MOLECULAR WIRES

A network of copper wires connecting components forms the circuitry of modern electronic devices. These connections are required for both power and communication. For developing molecular computers, the wires that connect the devices are as important as the devices themselves. Progress towards molecular wires has focused on conjugated oligomers since the transmission of a signal could be accomplished either photochemically via excited states or electrochemically.¹⁷ Furthermore, the energy of π - π^* transitions in the conjugated oligomer can be controlled by length. It has also been suggested that merely perturbing a system's electron density with a charged species on one face can change the electrostatic potential on the other face, thereby transmitting a signal.¹⁸ Due to the advantages of molecular scale and speed, an estimated potential eleven-fold increase in computing performance has been predicted if functional molecular wires can be developed.

A number of potential molecular wires have been recently developed including phenyleneethynylene,¹⁹ thiophene, and thienylenevinylene²⁰ oligomers. The issue of whether single oligomeric molecules can be conductive has recently been addressed, although not conclusively. There is also the problem of how these components will be “soldered” together. Recent work in transition metal complexation of pyridinyl terminated oligomers may provide the solution.²¹ Another approach involves the use of thiol terminated oligomers that can bond to a gold connector similar to alligator clips.

In developing circuit layouts, the wires must be able to intersect without cross-communication, a strategy which can be accomplished by a molecular orthogonal junction.²² A spirobithiophene core **11** allows the two thiophene oligomers to “intersect” orthogonally while avoiding cross-conjugation between their π -systems. Altogether, the development of molecular wires should optimize signal transmission, allow for devices to communicate, and be versatile in length and geometry for the design of complex circuits.

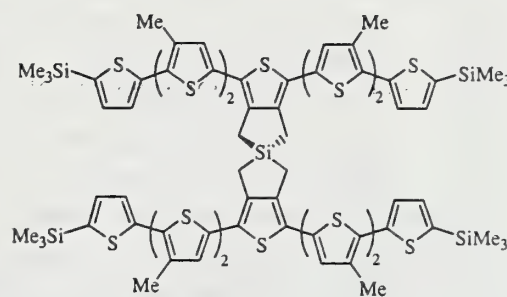


Figure 2. Spirobridged oligothiophene **11**

CONCLUSION

Based on the research to date, it is clear that there are a number of structural elements that are common in the development of molecular-scale organic devices. Triptycenes structurally resemble macroscopic gears and can be used for the task of rotational motion. Motifs with rigid structural units have controllable conformations and, therefore, are suitable for building the frameworks of machines. Incorporation of metal binding ligands into the device can allow for conformational changes upon addition of appropriate metals. Through π -stacking, electron-rich and electron-deficient aromatic units can self-assemble reversibly and are a useful construction method for supramolecular assemblies such as pseudorotaxanes.²³ Finally, π -conjugated systems are potentially useful for the transmission of information. Future MSODs will undoubtedly incorporate more than one of these functionalities in their design.

Development of molecular machines will involve bringing together MSODs in a highly organized manner whether in solution or on a surface. Furthermore, the molecular machine will require power. The energy required to drive molecular machines is still uncertain although photochemical or electrochemical sources have been suggested. Regardless, the ability to channel power and communicate between devices must be controlled by molecular wires. It will also be necessary to ensure that the components of a device are compatible with the conditions and the triggering stimulus used in neighboring components. These compatibility issues will need to be worked out in order to develop working molecular-scale machines. The design of MSODs may involve an entirely different approach than the strategy used in developing their macroscopic analogs. In the end, the development of MSODs for molecular machines is a fascinating pursuit and offers unimaginable technological gains.

REFERENCES

- [1] Bedard, T. C.; Moore, J. S. *J. Am. Chem. Soc.* **1995**, *117*, 10662.
- [2] Mazal, C.; Paraskos, A. J.; Michl, J. *J. Org. Chem.* **1998**, *63*, 2116.

- [3] Yamamoto, G.; Oki, M. *Bull. Chem. Soc. Jpn.* **1986**, *59*, 3597.
- [4] Iwamura, H.; Mislow, K. *Acc. Chem. Res.* **1988**, *21*, 175.
- [5] Gakh, A. A.; Sachleben, R. A.; Bryan, J. C. *Chemtech* **1997**, 26.
- [6] Stevens, A. M. *Tetrahedron Lett.* **1997**, *38*, 7805.
- [7] Kelly, T. R.; Bowyer, M. C.; Bhaskar, K. V.; Bebbington, D.; Garcia, A.; Lang, F.; Kim, M.; Jette, M. P. *J. Am. Chem. Soc.* **1994**, *116*, 3657.
- [8] Kelly, T. R.; Tellitu, I.; Sestelo, J. P. *Angew. Chem., Int. Ed. Engl.* **1997**, *36*, 1866.
- [9] Kelly, T. R.; Sestelo, J. P.; Tellitu, I. *J. Org. Chem.* **1998**, *63*, 3655.
- [10] Dahlquist, F. W.; Longmuir, K. J.; du Vernet, R. B. *J. Magn. Reson.* **1975**, *17*, 406.
- [11] Feynman, R. P.; Leighton, R. B.; Sands, M. ; *The Feynman Lectures on Physics, Vol. 1*; Addison-Wesley: Reading, MA, 1963; Chapter 46.
- [12] Amabilino, D. B.; Ashton, P. R.; Gómez-López, M.; Hayes, W.; Stoddart, J. F. *J. Org. Chem.* **1997**, *62*, 3062.
- [13] Anelli, P.-L.; Asakawa, M.; Ashton, P. R.; Bissell, R. A.; Clavier, G.; Górski, R.; Kaifer, A. E.; Langford, S. J.; Mattersteig, G.; Menzer, S.; Philp, D.; Slawin, A. M. Z.; Spencer, N.; Stoddart, J. F.; Tolley, M. S.; Williams, D. J. *Chem. Eur. J.* **1997**, *3*, 1113.
- [14] Credi, A.; Balzani, V.; Langford, S. J.; Stoddart, J. F. *J. Am. Chem. Soc.* **1997**, *119*, 2679.
- [15] Gilat, S. L.; Kawai, S. H.; Lehn, J. *Chem. Eur. J.* **1995**, *1*, 275.
- [16] Kawai, S. H.; Gilat, S. L.; Ponsinet, R.; Lehn, J. *Chem. Eur. J.* **1995**, *1*, 285.
- [17] Broo, A.; Hagen, S. *Chem. Phys. Lett.* **1992**, *196*, 239.
- [18] Tour, J. M.; Kozaki, M.; Seminario, J. M. *J. Am. Chem. Soc.* **1998**, *120*, 8486.
- [19] Schumm, J. S.; Pearson, D. L.; Tour, J. M. *Angew. Chem.* **1994**, *106*, 1445.
- [20] Jestin, I.; Frere, P.; Mercier, N.; Levillain, E.; Stievenard, D.; Roncali, J. *J. Am. Chem. Soc.* **1998**, *120*, 8150.
- [21] Harriman, A.; Ziessel, R. *Coord. Chem. Rev.* **1998**, *171*, 331.
- [22] Wu, R.; Schumm, J. S.; Pearson, D. L.; Tour, J. M. *J. Org. Chem.* **1996**, *61*, 6906.
- [23] Claessens, C. G.; Stoddart, J. F. *J. Phys. Org. Chem.* **1997**, *10*, 254.

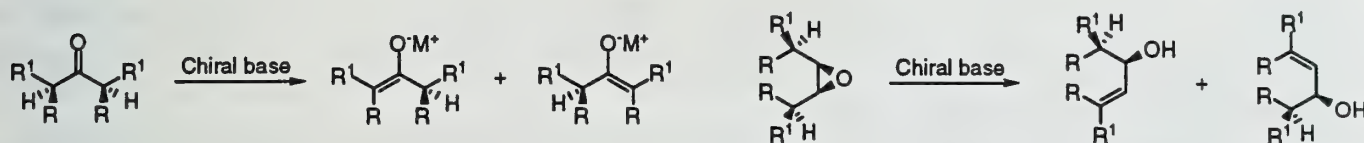
CHIRAL LITHIUM AMIDES FOR THE ENANTIOSELECTIVE DEPROTONATION OF KETONES AND EPOXIDES

Reported by Cory Stiff

Nov. 5, 1998

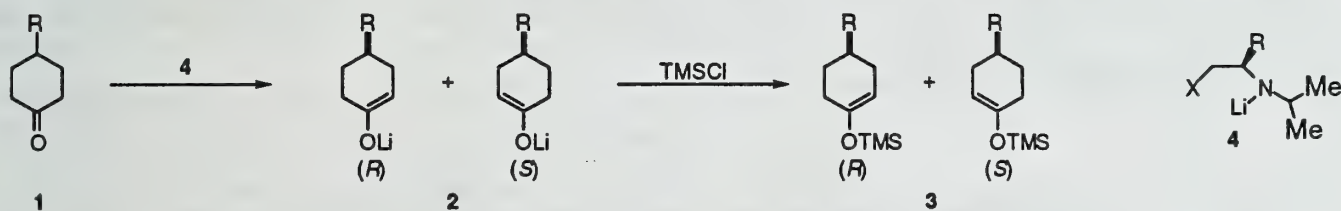
INTRODUCTION

There has been considerable interest in the desymmetrization of racemic compounds by differentiation of diastereo- or enantiotopic groups by a chiral reagent. A prototypical reaction of this type is the use of chiral lithium amides to preferentially abstract an enantiotopic hydrogen from an achiral molecule. The following will focus on the use of chiral lithium amides in enantioselective deprotonation of symmetrical ketones and the enantioselective rearrangement of *meso*-epoxides. In addition to empirical studies, recent computational, crystallographic and NMR studies which give insight into the solution structure of chiral lithium amides and possibly the reactive species will be presented.



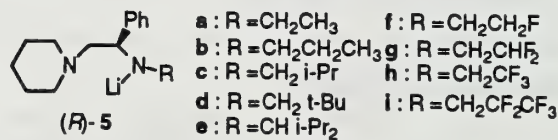
ENANTIOSELECTIVE ENOLIZATION OF KETONES

In 1986, Koga^{1a} and Simpkins^{2a} independently demonstrated that a chiral lithium base can differentiate between enantiotopic hydrogens of cyclic ketones. Koga's initial work involved the



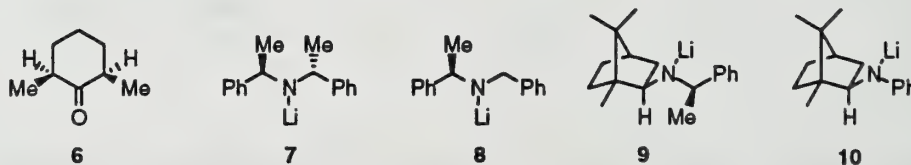
deprotonation of ketone 1 (R = *t*-butyl, *i*-Pr, Me) by lithium amides of the general structure 4, in tetrahydrofuran (THF) utilizing an internal quench with chlorotrimethyl silane (TMSCl) to isolate the chiral trimethylsilyl enol ether 3. This early study revealed that the selectivity of the reaction was highly dependent on lithium amide structure, with enantiomeric ratios (e.r.s) of up to 98:2 in favor of the (*R*) enantiomer being obtained. This study also indicated that the state of aggregation of the amide also plays a role in the selectivity of the reaction, as the addition of hexamethyl phosphoramide (HMPA) had a positive effect on the reaction.

Koga subsequently reported^{1b} a detailed study of lithium amide structures and reaction conditions. From his initial work Koga had determined that amides which offer a second site for chelation gave the highest enantioselectivity. Building on this information lithium amides **5a-i** were designed and used for the deprotonation of **1**. Koga considered that **5** could react *via* a five membered chelate where R is *trans* to the phenyl ring on the adjacent stereogenic carbon.



A general trend was seen for reactions in THF. The selectivity of the reaction increased with the size of the alkyl group at the β -position on the amide nitrogen, (Me < Et < i-Pr < t-Bu, CH₂F < CHF₂ < CF₃ < CF₂CF₃). This led Koga to investigate the amides **5d** and **5g-i** in more detail. By lowering the temperature of the reaction to -100 °C, he was able to obtain (*R*)-**3** in good yield and excellent enantiomeric ratios. A noticeable solvent effect was also seen in the reaction of **5h** with **1**. Poorly coordinating solvents such as toluene and diethyl ether showed a marked reduction of both chemical yield and selectivity. The addition of HMPA, however, reversed this effect. Koga believed that this was evidence for an active species of low aggregation state, as the lithium amide would aggregate to a higher degree in non-coordinating solvents. The addition of HMPA to the reaction disrupted the aggregates and produced the active species.

Simpkins' investigation^{2b} of the enantioselective deprotonation of **1** and **6** using monodentate lithium amides produced mixed results. In reactions with **1**, the chiral amides **7-10** yielded **3** in moderate enantioselectivity, with **7** giving the highest selectivity (85:15 e.r.). Reactions with **6** showed low selectivity with lithium amides **7-10**. In the course of Simpkins' studies it was noticed that the nature of the quench had a remarkable effect on the selectivity of the reaction.^{2c} If TMSCl was present with the lithium amide prior to addition of the ketone, i.e. an internal quench, the reaction yielded (*R*)-**3** in 85:15 er, if the addition of TMSCl followed mixing of the amide and ketone, i.e. an external quench, the product was formed in only a 62:38 e.r.

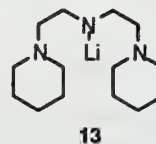


These results led Simpkins to investigate the effect of lithium chloride (LiCl), which is produced *in situ* by the internal quench method, but is absent in the external quench method. Work by Collum³ had shown that LiCl and other salts can effect the E/Z selectivity of ketone enolizations. Simpkins found that if 50 mol % of LiCl was added to the reaction of chiral amide **7** and ketone **1** the resulting enol ether from subsequent quench with TMSCl could be isolated in good yield and with improved enantioselectivity (91:9 er). A similar effect was seen when ZnCl₂ was used, but other salts such as LiBr, NaCl, and MgBr₂ did not lead to improved selectivity. This led to the rationalization that the

salts, LiCl or ZnCl₂, must modify the solution structure of the lithium amide to produce a more selective base. Simpkins did not speculate on the structure of this more selective species.

Catalytic deprotonation of cyclic ketones

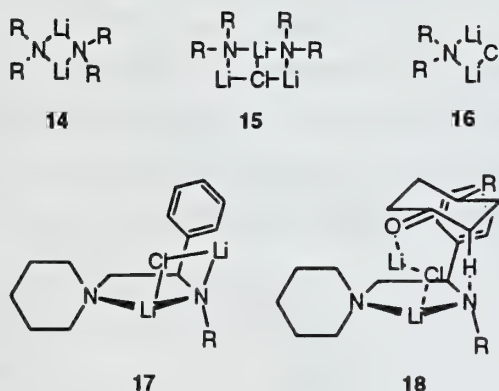
In his extensive survey of amide structures for the enantioselective enolization of cyclic ketones Koga discovered that a tridentate chiral amide gave lower chemical yields and optical purity.²⁶ He attributed this to the decreased Lewis acidity of lithium, which was coordinated to three nitrogens. This led him to propose that an achiral tridentate amide such as **13** may function efficiently as a lithium shuttle in a catalytic cycle. This developed to be the case. Using **13** as a stoichiometric lithium source, 30 mol % of **5h**, 2.4 equivalents of HMPA, and 1.5 equivalents of DABCO, Koga obtained enol ethers of 83% yield and 89:11 er, results virtually identical to the stoichiometric reaction.



Solution state structure

In his efforts to understand the structure of chiral lithium amides **5**, Koga has performed extensive crystallographic and NMR studies.⁵ The amide **5d** was found to be dimeric in the solid state, when crystallized from toluene. Crystallization of lithium amide **5h** from THF produced a monomeric structure in which two THF molecules coordinate to lithium. Subsequent ⁶Li and ¹⁵N NMR experiments on **5d** and **5h** showed that dimeric structures prevail in non-coordinating solvents but are replaced by a monomer in coordinating solvents or when HMPA is added to non-coordinating solvents. The coupling patterns observed were consistent with the five member chelating structure initially proposed by Koga for amides **5**.

Crystallographic⁶ and NMR^{5c} experiments with amide **7** have led to a better understanding of its structure as well. Similar to lithium diisopropyl amide (LDA) **7** crystallizes from THF as a dimer with each lithium coordinating two nitrogens and one molecule of solvent. ⁶Li and ¹⁵N NMR studies of **7** in THF have shown that the dimeric structure **14** dominates over monomeric **7** in solution. However, as LiCl is added to a solution of **7** two new species are formed. Using less than 50 mol % of LiCl it is found that **14**, **15**, **16**, are all present in solution. As the relative concentration of LiCl is increased the relative concentration of **16** increases. Lithium amide **5d** was also shown to form mixed dimers in the presence of LiCl.



The selectivity observed in the deprotonation of **1** with lithium amides **5** could not be rationalized *via* a

traditional six-member transition state. Coupling this information with crystallographic and spectroscopic data Koga has proposed that the deprotonation proceeds through an eight member transition structure **18** in which the selective species is the LiCl-lithium amide dimer **17**.⁷ The selectivity of the reaction is dictated by steric interactions between the chelated ketone and both the amide nitrogen substituent R and the group on the stereogenic carbon. However, Koga could not explain all of the results through steric interactions alone. Chiral amide **5h** produces higher enantioselectivity than **5c** and nearly the same as **5d**. Koga believes there may be an electrostatic interaction between lithium and fluorine which accounts for the improved selectivity with amide **5h**.

Synthetic applications

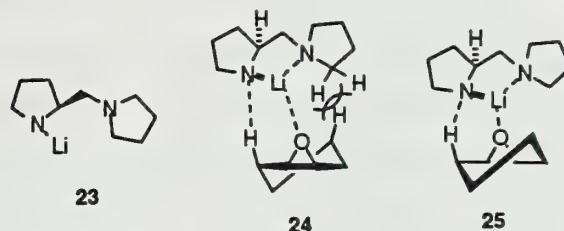
Optimization of lithium amide structures for the enantioselective enolization of 4-substituted cyclohexanones by Koga and Simpkins has led to their increased use in synthetic applications. Koga has applied chiral amides of type **5**, toward the synthesis of an intermediate important in the synthesis of carbacyclin, a platelet aggregation inhibitor.^{8b} Simpkins has used lithium amide **7** for the deprotonation of 8-oxabicyclo[3.2.1]octan-3-ones, which upon further elaboration affords access to *cis* tetrahydrofurans.^{9a} In a similar azabicyclic system Simpkins used **7** to prepare a intermediate in the synthesis of (-)-anatoxin.^{9b} Other groups have also used the chiral amides developed by Koga and Simpkins to pursue their own synthetic targets. Majewski and coworkers have reported that in the presence of LiCl, the naphthyl analog of **7** enolizes protected 4-hydroxycyclohexanones in 90% yield and 95:5 er.^{10a} Deprotonation of tropanone with **7** allows access to several tropane alkaloids.^{10b} Honda and co-workers have studied the reaction of cyclobutanones with chiral amides developed by both Koga and Simpkins for the synthesis of non-racemic γ -butyrolactones.¹¹ Chiral lithium amides have also been applied to several other syntheses employing an enantioselective enolization including savinin,^{12a} penitrem D,^{12b} chlorotetaine^{12c} and reischwigin A.^{12d}

ENANTIOSELECTIVE REARRANGEMENT OF EPOXIDES TO ALLYLIC ALCOHOLS

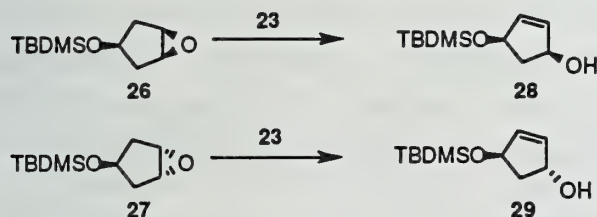
The ability of lithium amides to effect the rearrangement of epoxides to allylic alcohols has been known for some time.¹³ In cyclohexene oxide **21**, the researchers demonstrated that deprotonation is biased toward the *syn* proton occupying a pseudoaxial position. A chiral base must therefore differentiate between the enantiomeric conformations **A** and **B**. In 1980 Whitsell¹⁴ reported the formation of allylic alcohol (*R*)-**22** in 65:35 er using lithium amide **7**.



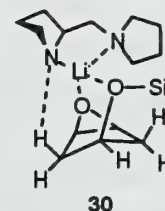
In another early report Asami¹⁵ showed that the bidentate lithium amide **23** could effect the same transformation in up to 96:4 er in favor of (*S*)-**22**. A major shortcoming of Asami's amide was its lack of generality. High selectivities were only seen in the reaction of cyclohexene oxide, whereas other cyclic and acyclic epoxides gave ers up to 85:15. This was, however, the first report of an acyclic epoxide reacting with some selectivity. Asami proposed that the reaction proceed through a six membered transition state similar to that suggested by Rickborn.¹³ The key to selectivity in Asami's reaction is the rigid structure produced by the internal chelation of lithium,



much like Koga's five member chelation. Unfavorable interactions in **24** leads to preferential reaction through **25**. Asami later investigated the reaction of **23** with the *meso*-epoxides **26** and **27**.^{15c} Previously reactions with cyclopentene oxide gave low selectivity, but the addition of the silyl ether afforded the protected diol in improved er. Asami proposed that the silyl ether provided the opportunity to form a tight complex around lithium, **30**. Support for this hypothesis was given in two forms. First the use of non-coordinating solvents led to further enhancement of selectivity. Secondly, lower selectivity was seen in the reaction of *trans* epoxide **27**, which should not be able to form the tight complex.

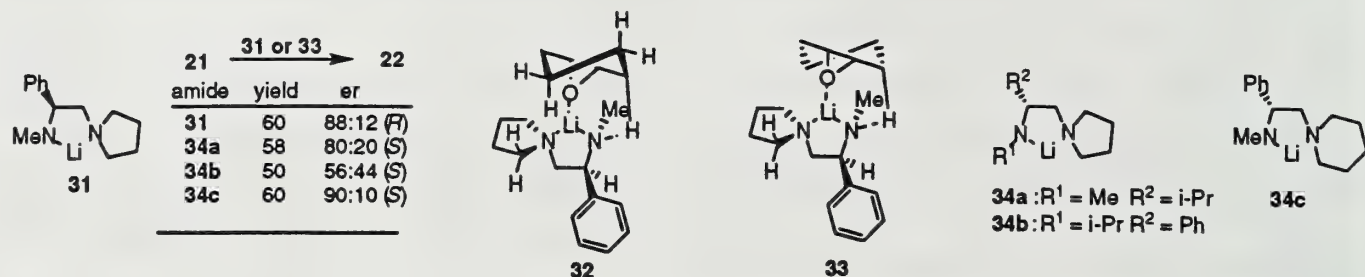


epoxide	solvent	yield	er
26	THF	76	83:17
26	benzene	92	95:5
27	THF	78	79:21

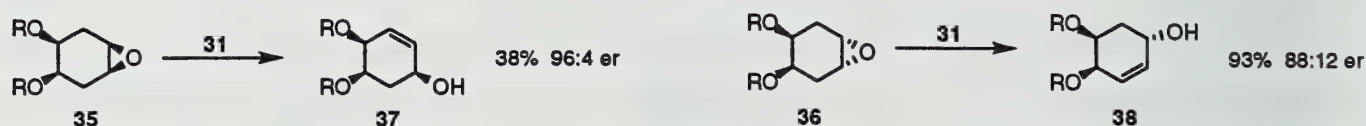


One drawback of Asami's approach to the problem is that the amine precursor to **23** is synthesized from proline, which is readily available in (*S*) form but expensive and impractical in the enantiomeric (*R*) form. Efforts to produce a more readily available chiral amide were recently reported by Singh and co-workers.¹⁶ Their initial studies found that chiral amide **31**, produced (*R*)-**22** in good er (88:12). Singh proposed a transition structure similar to that of Asami. In the disfavored transition structure **32** two non-bonding interactions are present. This should favor **33**, where there is only one such interaction. In order to test this hypothesis and attempt to improve selectivity, the lithium amides **34a-c** were synthesized and used in the rearrangement of cyclohexene oxide.^{16b} The results lend support for Singh's proposal. Change to a smaller substituent at the stereogenic carbon lowered the selectivity of the reaction, while substitution of a piperidine for pyrrolidine ring produced a slight increase. Additionally change the nitrogen alkyl group to isopropyl leads to a substantial decrease of selectivity. In the reaction with *cis* epoxide **26** Singh saw the same solvent effect

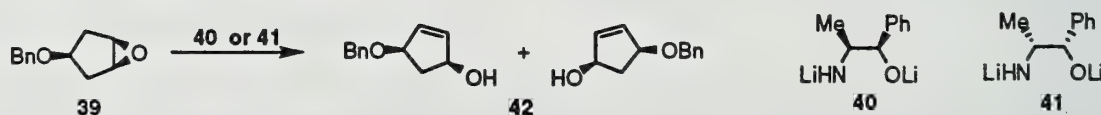
as Asami, that non-coordinating solvents gave higher selectivity.^{16b} Indeed, Singh was able to produce the highest selectivity seen in such reactions (98:2 er) by the use of amide **34c**.



O'Brien¹⁷ used **31** to effect the enantioselective rearrangement of *cis* and *trans* epoxides **35** and **36**. The allylic alcohols were recovered in good er's, although a poor chemical yield was obtained in the case of the *cis* epoxide. These workers believe the lower reactivity of *cis* epoxides is due to unfavorable steric interactions between the axial substituent and the chelating chiral amide.

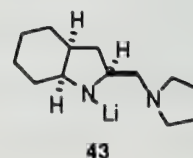


In 1993, Murphy and Milne reported that dilithiated aminoalcohols gave good results in the reaction with epoxide **39**.¹⁸ Their investigations were stimulated by a report that potassium alkoxides increased the rate of lithium dialkylamide deprotonation of epoxides.¹⁹ They found that (1*R*, 2*S*) and (1*S*, 2*R*) norephedrine **40** and **41** provided **42** in excellent yield (92-98%) and good er (90:10).



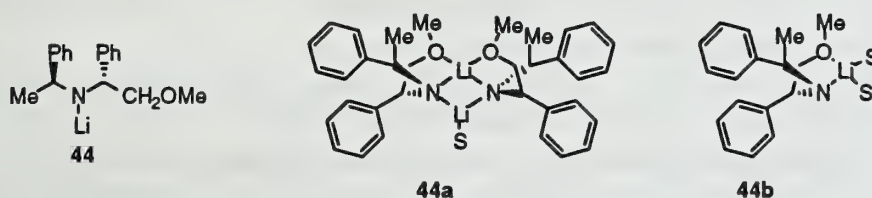
Catalytic deprotonation of epoxides

Asami^{27, 28} has developed a catalytic method for the enantioselective rearrangement of epoxides to allylic alcohols. He found that lithium dialkyl amides were not as reactive towards epoxides as the bidentate amide, **23**. Asami's initial studies showed that although a catalytic process was possible, slight erosion of selectivity may be inevitable due to the reactivity of LDA, the stoichiometric lithium source used in these reactions. However, Asami was able to improve the selectivity of the reaction by using chiral amine **43**, which in stoichiometric amounts produced **15** in good yield and er's. These improvements were also observed catalytically, using 20 mol % of **43** provided **22** in 89% yield and 97:3 er. Furthermore **43** showed unprecedented selectivity in the reaction with (*Z*)-4-octene oxide, giving er's up to 93:7.



Solution state structure

In an effort to better understand the reactive species in the deprotonation of cyclohexene oxide with the chiral amide **44**, Davidsson has performed extensive computational, spectroscopic and crystallographic investigations.²¹ Like many of the amides studied by Koga, **44** is a dimer in the solid state as well as in non-coordinating solvents. Likewise, in coordinating solvents such as THF **44** exists as a disolvated monomer as shown by ^6Li and ^{15}N NMR experiments. Because the reaction of cyclohexene oxide with **44** does not take place below 0 °C the authors were able to obtain spectra of the chiral amide in the presence of the epoxide. Upon addition of cyclohexene oxide to the solution of **44** in diethyl ether, the characteristic ^6Li NMR signals disappear and three new signals appear. Multiple correlation and variable temperature experiments allowed the authors to identify two new species, **44a** and **44b**. The dimer **44a** is associated with a single molecule of cyclohexene oxide while the monomer **44b** coordinates two molecules of the epoxide. The authors believe that the selective species in the reaction is the dimeric form of **44**. They do note however, that the studies only give information about initial ground states, which may not be consistent with transition states, nor does it eliminate the possibility of a monomeric transition state.



Synthetic applications

In addition to **28** and **42**, which are potential intermediates in the synthesis of prostaglandins, several synthetic targets have been approached *via* the enantioselective rearrangement of epoxides. Both Asami^{22a} and Hodgson^{22b} have reported a synthesis of carbovir, a potent anti-HIV carbocyclic nucleoside. Other synthetic efforts involving the enantioselective rearrangement of cyclic epoxides include untenone A,^{23a} furanal,^{23b} iridomyrmecin^{23c} and leukotriene.^{23d}

CONCLUSION

Extensive studies on the optimal reaction conditions and substrates have led to the development of chiral lithium amides as useful reagents in organic synthesis. The enolization of symmetrical ketones and the rearrangement of epoxides to allylic alcohols can be effected in good yields and high enantiomeric ratios, both stoichiometrically and catalytically. Further investigation of the solution structure and kinetics of the reactions should lead to a better understanding of the reactive and selective species. Such insight may allow for the development of a more general chiral lithium amide. Expanding the scope of the reactions will grant greater access to a wide variety of synthetic targets.

REFERENCES

- (1) a) Shirai, R.; Tanaka, M.; Koga, K. *J. Am. Chem. Soc.* **1986**, *108*, 543. b) Aoki, K.; Tomioka, K.; Noguchi, H.; Koga, K. *Tetrahedron* **1997**, *53*, 13641.
- (2) a) Simpkins, N. *J. Chem. Soc., Chem. Comm.* **1986**, 88. b) Cain, C.; Cousins, R.; Coumbarides, G.; Simpkins, N. *Tetrahedron* **1990**, *46*, 523. c) Bunn, B.; Simpkins, N.; Spavold, Z.; Crimmin, M. *J. Chem. Soc., Perkin Trans. 1* **1993**, 3113.
- (3) Hall, L.; Gilchrist, H.; Collum, D. *J. Am. Chem. Soc.* **1991**, *113*, 9571.
- (4) Yamashita, T.; Sato, D.; Kiyoto, T.; Kumar, A.; Koga, K. *Tetrahedron* **1997**, *53*, 16987.
- (5) a) Sato, D.; Kawasaki, H.; Shimada, I.; Arata, Y.; Okamura, K.; Date, T.; Koga, K. *J. Am. Chem. Soc.* **1992**, *114*, 761. b) Sato, D.; Kawasaki, H.; Shimada, I.; Arata, Y.; Okamura, K.; Date, T.; Koga, K. *Tetrahedron* **1997**, *53*, 7191. c) Sugasawa, K.; Shindo, M.; Noguchi, H.; Koga, K. *Tetrahedron Lett.* **1996**, *37*, 7377.
- (6) Edwards, A.; Hockey, S.; Mair, F.; Raithby, P.; Snaith, R.; Simpkins, N. *J. Org. Chem.* **1993**, *58*, 6942.
- (7) Toriyama, M.; Sugasawa, K.; Shindo, M.; Tokutake, N.; Koga, K. *Tetrahedron Lett.* **1997**, *38*, 567.
- (8) a) Sobukawa, M.; Nakajima, M.; Koga, K. *Tetrahedron: Asymmetry* **1990**, *1*, 295. b) Izawa, H.; Shirai, R.; Kawasaki, H.; Kim, H-D.; Koga, K. *Tetrahedron Lett.* **1989**, *30*, 7221.
- (9) a) Bunn, B.; Cox, P.; Simpkins, N. *Tetrahedron* **1993**, *49*, 207. b) Newcombe, N.; Simpkins, N. *J. Chem. Soc., Chem. Comm.* **1995**, 831.
- (10) a) Majewski, M.; Irvine, N.; MacKinnon, J. *Tetrahedron: Asymmetry* **1995**, *6*, 1837. b) Majewski, M.; Lazny, R. *J. Org. Chem.* **1995**, *60*, 5825.
- (11) Honda, T.; Kimura, N.; Tsubuki, M. *Tetrahedron: Asymmetry* **1993**, *4*, 1475.
- (12) a) Honda, T.; Kimura, N.; Sato, S.; Kato, D.; Tominaga, H. *J. Chem. Soc., Perkin Trans. 1* **1994**, 1043. b) Smith, A.B.; Nolen, E.; Shirai, R.; Blase, F.; Ohta, M.; Chida, N.; Hartz, R.; Fitch, D.; Clark, W.; Sprengler, P. *J. Org. Chem.* **1995**, *60*, 7837. c) Wild, H. *J. Org. Chem.* **1994**, *59*, 2748. d) MaGee, D.; Setiadji, S.; Martin, R. *Tetrahedron: Asymmetry* **1995**, *6*, 639.
- (13) Thummel, R.; Rickborn, B. *J. Am. Chem. Soc.* **1970**, *92*, 2064.
- (14) Whitsell, J.; Felman, S. *J. Org. Chem.* **1980**, *45*, 755.
- (15) a) Asami, M. *Chem. Lett.* **1984**, 829. b) Asami, M. *Bull. Chem. Soc. Jpn.* **1990**, *63*, 721. c) Asami, M. *Bull. Chem. Soc. Jpn.* **1990**, *63*, 1402.
- (16) a) Bhuniya, D.; Singh, V. *Synth. Comm.* **1994**, *24*, 1475. b) Bhuniya, D.; Datta-Gupta, A.; Singh, V. *J. Org. Chem.* **1996**, *61*, 6108.
- (17) O'Brien, P.; Poumellec, P. *J. Chem. Soc., Perkin Trans. 1* **1998**, 2435.
- (18) Milne, D.; Murphy, P. *J. Chem. Soc., Chem. Comm.* **1993**, 884.
- (19) Mordini, A.; Ben Rayana, E.; Margot, C.; Schlosser, M. *Tetrahedron* **1990**, *46*, 2401.
- (20) a) Asami, M.; Ishizaki, T.; Inoue, S. *Tetrahedron: Asymmetry* **1994**, *5*, 793. b) Asami, A.; Suga, T.; Honda, K.; Inoue, S. *Tetrahedron Lett.* **1997**, *38*, 6425.
- (21) a) Hilmersson, G.; Davidsson, O. *J. Org. Chem.* **1995**, *60*, 7660. b) Hilmersson, G.; Arvidsson, P.; Davidsson, O.; Hakansson, M. *Organometallics* **1997**, *16*, 3352. c) Hilmersson, G.; Arvidsson, P.; Davidsson, O.; Hakansson, M. *J. Am. Chem. Soc.* **1998**, *120*, 8143.
- (22) a) Asami, M.; Takahashi, J.; Inoue, S. *Tetrahedron: Asymmetry* **1994**, *5*, 1649. b) Hodgson, D.; Witherington, J.; Moloney, B. *J. Chem. Soc., Perkin Trans. 1* **1994**, 3373.
- (23) a) Asami, M.; Ishizaki, T.; Inoue, S. *Tetrahedron Lett.* **1995**, *36*, 1893. b) Mori, K.; Murata, N. *Liebigs Ann.* **1995**, 2089. c) Hodgson, D.; Gibbs, A. *Synlett.* **1997**, 657. d) Hayes, R.; Wallace, T. *Tetrahedron Lett.* **1990**, *31*, 3355.

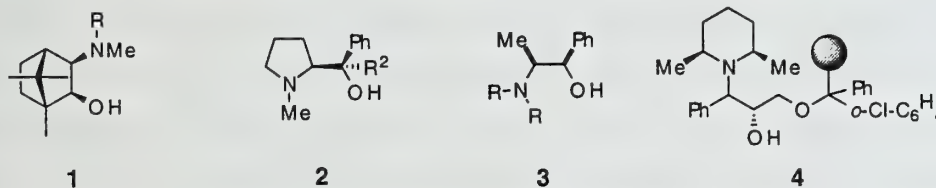
INTRODUCTION

Asymmetric methodologies are being developed for the enantio- and stereo- controlled construction of a wide variety of species. Approaches based on covalently bound chiral auxiliaries to effect control require removal from the substrate after the reaction is complete. The use of catalysts with chiral ligands is more efficient, although the catalyst must then be separated from the product. Polymer-bound chiral ligands afford a very attractive alternative; the ligands are easy to remove from the reaction and can be recycled. However, polymeric catalyst systems present significant technical challenges. The micro-environment surrounding the catalytic site can be affected by the polymer support. This may lead to yields and enantioselectivities which are generally lower than for the small molecule counterparts. Additionally, the heterogeneous nature of many of the polymer supports leads to diffusion limited rates of reaction; hence, longer reaction times are typically required to achieve total conversion.

Four asymmetric reactions have been investigated in the context of polymeric catalyst systems. These include the asymmetric alkylation reaction of aldehydes with diethylzinc, the Sharpless asymmetric dihydroxylation of olefins, the epoxidation of olefins, and the Diels-Alder reaction. The development of each of these systems is discussed in this report.

ASYMMETRIC ALKYLATION

In the late 1980's, the asymmetric alkylation of benzaldehyde by diethylzinc was studied extensively. Noyori¹ investigated (-)-3-*exo*-(dimethylamino)isoborneol (DAIB) (**1**, R = Me), providing a great deal of insight into the mechanism of the alkylation reaction. A non-linear effect was observed.^{1b}



This observation was rationalized by invoking the formation of dimeric complexes. The *R,R'* and *S,S'* homo-dimers were suspected to be less stable than the *R,S'* *meso*-compound or hetero-dimer. The homo-dimer can dissociate to form the catalytically active monomeric species, but the hetero-dimer remains associated and catalytically inactive. Placing these ligands on polymer support would reduce dimer formation and promote the formation of catalytically active species.

Fréchet and Itsuno examined polymer-bound DAIB ligand **1** attached to the polymer via the amine position (R = Merrifield's resin; 1% crosslinked chloromethylated polystyrene. Unless otherwise specified, the polymer supports in this paper are Merrifield's resin.).² Aromatic aldehydes were converted to product efficiently; benzaldehyde was converted to (*R*)-1-phenylpropanol in over 90% yield with an enantiomeric ratio (er) of 96:4. The reaction required 73 h with 5% ligand (based on aldehyde) to achieve these results, while Noyori's system gave slightly better yield and enantioselectivity, and required only 6 h with 2% ligand. This illustrates the decreased reaction rate often encountered with heterogeneous polymeric catalysts. The polymeric nature of the catalyst results in diffusion limited rates of reaction. When the *N*-methyl group was removed from **1**, the selectivity of the ligand plummeted to an er of 55:45, and the (*S*) enantiomer was produced. This illustrates the importance of a fully substituted amine in the ligand. The importance of a symmetrically di-substituted amine was established in free molecule studies,³ indicating the need to attach the ligand to the polymer support through a different linkage.

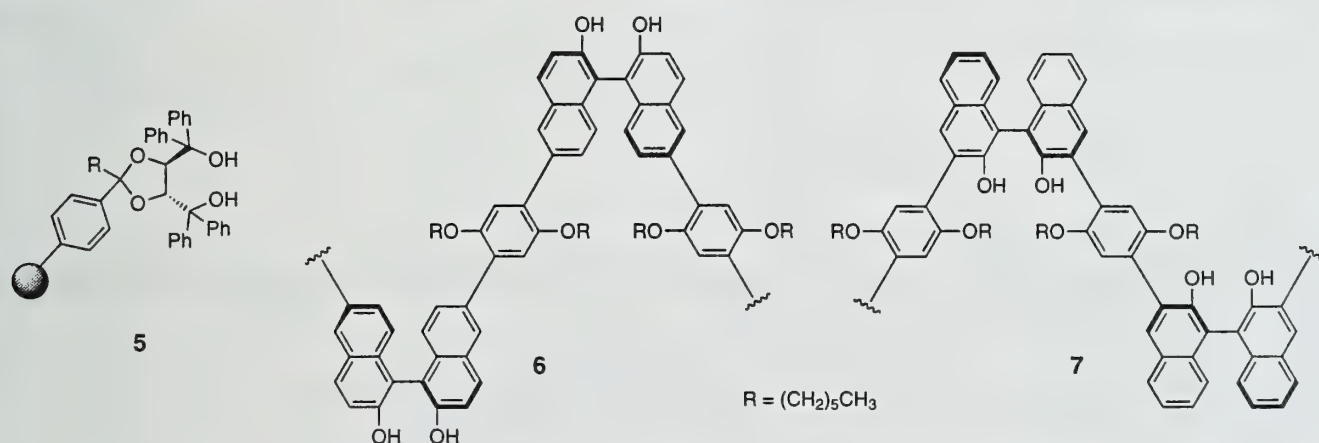
Soai examined **2** and **3** for the diethylzinc reduction of aldehydes. Compound **2** was used to demonstrate that the lithium alkoxide could also be used to catalyze the diethylzinc alkylation.⁴ With ephedrine **3** attached to the polymer support,⁵ Soai demonstrated that, as observed previously, aromatic aldehydes gave better yields and selectivity. Yields of up to 83% with an er of 94:6 were obtained. Long reaction times were again required, in excess of 100 h in some cases. The durability of the system was also probed with *p*-chlorobenzaldehyde. Throughout three runs, the system showed only slight drops in yield and selectivity, proving the polymeric catalysts could be reused to a limited extent.

Soai postulated that the reduced efficacy of the ligands towards aliphatic aldehydes was a function of reduced mobility of the ligand anchored directly at the nitrogen of the ephedrine unit. A series of *N*-butyl ephedrines with variable linker lengths were tested with benzaldehyde and nonanal.⁶ A six methylene unit spacer was found to be optimal in terms of enantioselectivity with benzaldehyde. Compared to the directly attached *N*-butyl ephedrine, the chemical yield was increased to 79% from 64%, and the er increased to 86:14 from 58:42. The linked catalyst was effective for aliphatic aldehydes, converting nonanal to 3-(*S*)-undecanol in 80% yield with an er of 85:15. The methylene spacer was believed to reduce interactions between the substrate and the support, and to enhance the enantioselectivity of the catalyst by acting as a large substituent upon the nitrogen. Soai also evaluated the effect of solvent upon the polymeric catalyst system, and found that hydrocarbon solvents, which did not swell the polymer support, were the best solvents.

The most recent work on the use of amino alcohol ligands such as **4**, was evaluated upon both Merrifield resin and Barlos resin.⁷ The Barlos resin has the same backbone of PS-1%DVB, but possesses

a 2-chlorotrityl anchor instead of Merrifield's chloromethyl group. The Barlos resin was shown to be superior to Merrifield's; benzaldehyde was converted in 24 hours to 1-phenylpropanol in 98% yield with an er of 97:3. It is impressive to note that the small molecule analogue of **4** demonstrated an er of 98:2. Thus, it appears that the ether linkage provided sufficient mobility to allow the ligand almost unencumbered conformational freedom. Pericás also showed that the degree of functionalization on the backbone affects enantioselectivity. A critical density of ligands on the Merrifield's resin generated optimal enantioselectivity, which decreased as additional ligand was immobilized on the backbone. The cause was hypothesized to be the formation of intrachain dimeric species. The additional steric bulk of Barlos resin is postulated to prevent this dimerization, providing the enhanced catalytic activity. If this assertion is correct, it would provide an opportunity to explore non-linear effects of polymer-supported ligands.

A second type of novel ligand for the diethylzinc reaction was recently developed by Seebach and coworkers. The $\alpha, \alpha, \alpha', \alpha'$ -tetraaryl-1,3-dioxolane-4,5-dimethanols, or TADDOLs, were anchored to a variety of supports and were then used to catalyze the diethylzinc addition to aldehydes.⁸ It is also important to note that the TADDOLs generate the catalytically active species by complexing with titanium instead of zinc. The Merrifield bound **5** ($R = H$) generated the alcohol from benzaldehyde in a yield of 97% with an er of 99:1 in only 16 hours. While the yield and selectivity are impressive, the rate can be attributed to the 20 mol % loading of the catalytic TADDOL. The enantiomer of **5** could also generate the enantiomeric alcohol in a yield of 92% with an er of 2:98. While TADDOLs were also investigated in the context of dendrimer support, that is outside the scope of this review.⁹



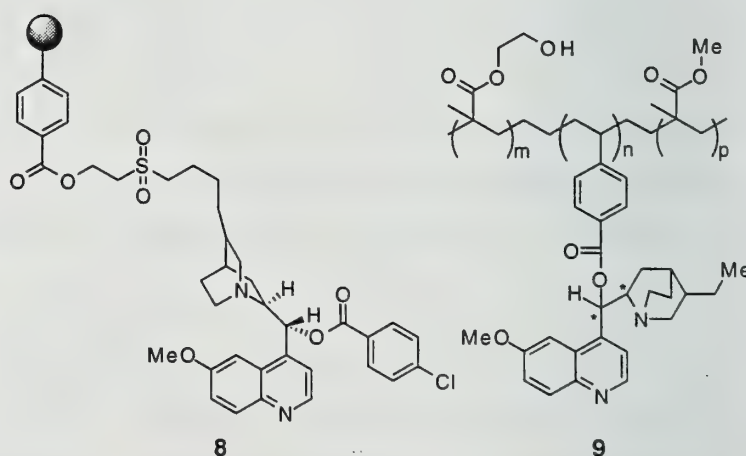
Recently, Pu has introduced a polymeric catalyst for the diethylzinc reaction which derives its chirality from the polymer backbone instead of from side-chain attached ligands.¹⁰ The polybinaphthyls are referred to as the major groove polybinaphthyl **6**, while **7** is designated as the minor groove structure. The minor groove catalyst has been shown to be a much more effective catalyst. This can be rationalized by the position of the two oxygen substituents of **7** which are capable of chelating a

transition metal at two planar chelation sites per monomer. The main chain catalyst **7** demonstrated remarkable efficacy towards both aromatic and aliphatic aldehydes. Polymer **7** was capable of converting aromatic aldehydes to the alcohol quantitatively with an er of 96:4, in only 12 hours. Aliphatic aldehydes were converted in 45 hours with 91% yield and an er of 99:1. A new analogue to **7** has recently been reported^{10b} that cut the reaction time to 5 h, maintained high yields of 88% and er of 98:2. The numerous hexyl ethers also granted these polybinaphthyls solubility in normal organic solvents. A large degree of the effectiveness of this system can be attributed to the homogeneous nature of this polymer.

ASYMMETRIC DIHYDROXYLATION OF OLEFINS

In the early 1980's, Sharpless introduced the use of cinchona alkaloid derivatives based upon quinine and quinidine to effect asymmetric dihydroxylation of olefins with stoichiometric OsO_4 .¹¹ The toxicity and expense of OsO_4 spurred further development, until a catalytic system was developed utilizing the cinchona alkaloid derivatives.¹² Polymeric catalysts have been developed to further increase the safety and economy of this reaction.

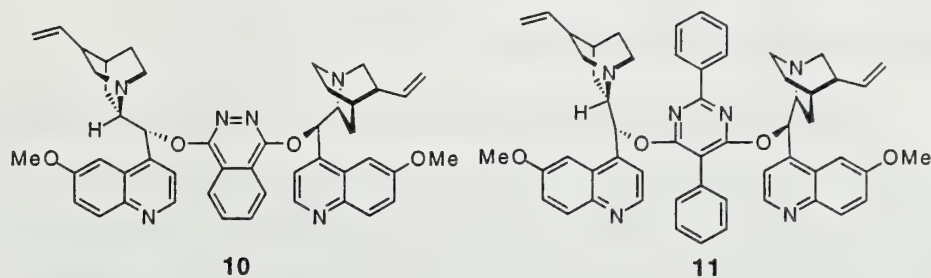
Salvadori found quinine derivative **8** attached to solid support gave moderate chemical yields with widely variable enantioselectivity.¹³ In general, the use of N-Methylmorpholine-N-oxide (NMO) as a secondary oxidant offered higher chemical yields, while the use of potassium ferricyanide provided poorer chemical yields but enhanced stereoselectivity. Song and



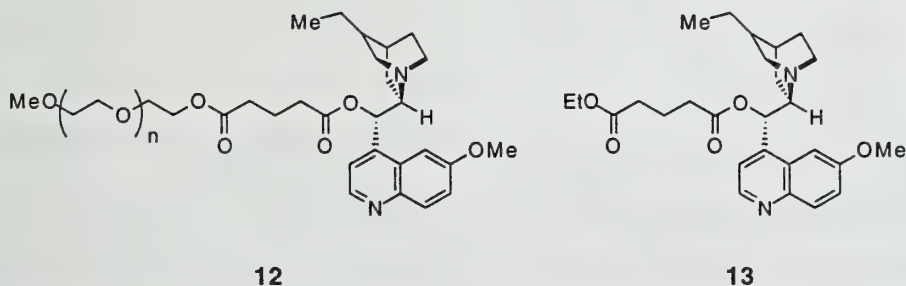
coworkers then examined the effects of polymer backbone polarity with two systems represented by **9**.¹⁴ The methyl methacrylate (MMA)-**9** copolymer was studied ($m = 0$, n and p variable), as was the 2-hydroxyethyl methacrylate (HEMA)-**9** copolymer ($p = 0$, m and n variable). The polarity of the backbone was found to have great impact upon the efficacy of the catalyst. The polarity of the solvents used in dihydroxylation would cause most non-polar polymers such as Merrifield's resin, to collapse, reducing available active sites. The more polar backbone increases compatibility with the solvent, and the active sites are more accessible.

Bis-cinchona derivatives linked by phthalazine or pyrimidine bridges were also investigated, following the discovery that they were better ligands in solution.¹⁵ The phthalazine linker shown in **10**

was most effective for 1,1-disubstituted, 1,2-*trans*-disubstituted, trisubstituted, terminal, and aromatic olefins. The pyrimidine linker shown in **11** was most useful for terminal olefins with branching in the chain. Song and coworkers investigated the utility of **10**¹⁶ and Ravindranathan explored **11**.¹⁷ Both attempted to form copolymers with the bis-cinchona derivative and MMA via free radical polymerization. While Ravindranathan reported moderate yields and



enantioselectivity, and Song reported moderate to excellent yields with er's better than 99:1, Canali's careful repetition of Song's work¹⁸ indicates that the ligands were not incorporated into the polymer backbone. The reactions were being catalyzed by free ligand entrapped in the polymer. Salvadori found similar results when co-polymerizing **10**¹⁹ and ethylene glycol dimethacrylate (EGDMA). Repeated extractions of the polymer examined via UV-Vis spectroscopy indicated that **10** was not covalently incorporated into the copolymer. This example not only points out the difficulties encountered in incorporating ligands into the polymer backbones, but also illustrates the ease with which an entire field may be discredited if care is not taken to conduct the necessary experiments properly.



Soluble polymeric catalysts of the cinchona alkaloid derivatives²⁰ have been developed by Janda. By attaching polyethylene glycol off of the cinchona derivative, as in **12**, a linear polymer capped with a ligand has been formed. Compared with the analogous model compound **13**, both exhibited the same yields and enantioselectivities. The soluble catalyst showed less than a 2% decrease in chemical and stereochemical yield through 5 recycles.

Another recent advance involves a multi-polymer asymmetric dihydroxylation. Janda utilized various solid-phase synthesis resins to support the olefin substrate, and then utilized a phthalazine linked bis-cinchona alkaloid on soluble polymer support to catalyze the asymmetric dihydroxylation reaction.^{20c} Slightly greater catalyst concentration was required to allow total conversion, but the er was 99:1. The

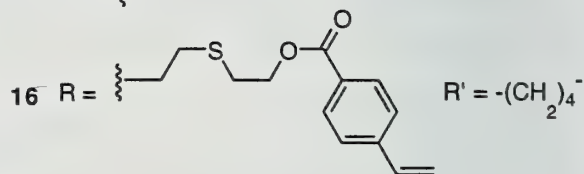
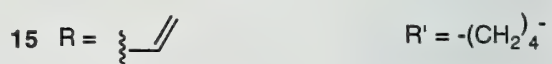
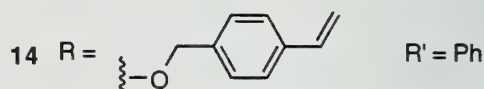
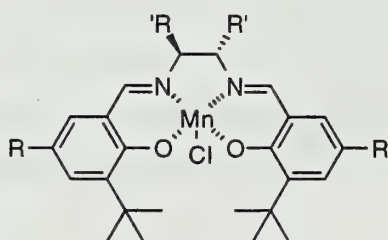
easy separation of both supported product (by filtration) and catalyst (by precipitation and filtration) from the reaction mixture is obviously an advantage offered by this system.

ASYMMETRIC EPOXIDATION

The application of polymeric catalysts to the directed epoxidation of olefins has proven quite troublesome. The majority of the systems are centered upon the Mn(III)-salen catalyst which has proven very useful in free molecule applications. The chemical yields of the polymeric catalysts have remained respectable, but the degree of stereoselectivity has degraded considerably. Representative structures for selected chiral monomers are shown below.

Monomer **14** has been investigated by Dhal and coworkers,²¹ and was polymerized with EGDMA. Chemical yields have consistently been reported in the range of 60-80%, but enantiomeric ratios are very nearly

50:50 with the exception of *cis*-substituted olefins, such as dihydronaphthalene, where the er can climb to 64:36. The small molecule analogue,



where R = benzyl ether, generated the epoxide of dihydronaphthalene in an er of 87:13. Clearly the polymeric backbone here does not provide the correct environment for efficient stereoselectivity. The polymer did demonstrate exceptional stability; it was recycled 5 times and maintained its catalytic activity. Additionally, isolation of the Mn(III)-salen complex on solid support prevents formation of the inactive μ -manganese Mn(IV)-O-Mn(IV) dimer. This helps to extend the life of the catalyst, reducing the amount required for each reaction.

Salvadori studied systems such as **15** and **16** with highly cross-linked PS-DVB resins.²² The constrained monomer **15** was moderately effective, catalyzing *cis*-olefin epoxidation with modest yields and ers up to 80:20. The spaced linker of **16** catalyzed some olefins in yields up to 97%, though enantioselectivity remained low. It is interesting to note that dihydronaphthalene, which proved most effective for Dhal's system, was plagued by the formation of 50% side products in this system.

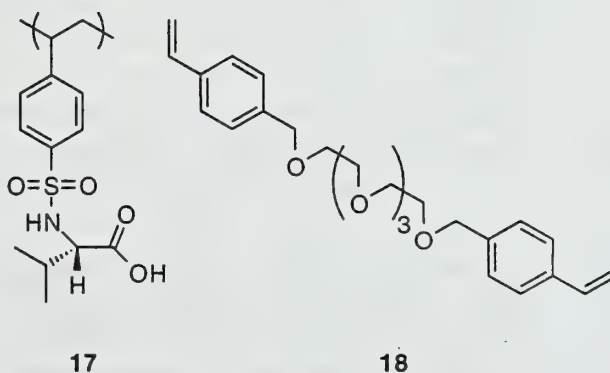
Recently Laibinis approached the synthesis of these complexes on a solid support.²³ The rationale behind this approach was that it would allow the generation of asymmetric complexes and

synthesis on the support would give an accurate number for the degree of functionalization. The yields and enantioselectivities reported were comparable to or lower than reported polymer supported systems. However, the possibility of tailoring the two halves of the Mn(III)-salen complex promise greater utility in the future.

DIELS-ALDER CATALYSTS

The Diels-Alder reaction is a widely known method for the construction of six membered rings. It can proceed in both the *exo* and *endo* fashion, directed by the reaction environment and substrate. Seebach has applied the Ti-TADDOL ligands (**5**) to this reaction.^{8,24} The TADDOL attached to Merrifield resin showed no activity for Diels-Alder catalysis. When co-polymerized with styrene and divinylbenzene into a cross-linked matrix, however, the Diels-Alder reaction of cyclopentadiene with 3-crotonoyloxazolidinone proceeded smoothly. The *endo* product was favored in all cases by at least an 80:20 ratio. The enantioselectivity was moderate, ranging from 70:30 to 85:15, depending on the functionality of the TADDOL. The catalyst also demonstrated good durability, surviving multiple recycles.

Itsuno studied boron complexes of ligands of **17**. When copolymerized with PS and DVB, the resulting polymer showed exceptional catalytic activity. The polymer catalyzed the Diels-Alder reaction between cyclopentadiene and methacrolein with an *endo:exo* ratio of 1:99.²⁵ The product had an er of 82:18. The system was then improved by the use of **18** as the cross-linking agent,²⁶ which increased the enantioselectivity to 96:4. The polymeric catalyst in this instance was superior to the small molecule analogue. Perhaps even more impressive is that Itsuno applied this catalyst to a constant flow reactor. The results were essentially the same as the batch experiments. This demonstrates the applicability of polymeric catalysts to flow systems, which is important because flow systems are not as damaging to polymer supports as stirring.



CONCLUSION

The field of polymeric catalysts has shown considerable growth in the past few years, though in many respects it is still within its infant stages. The advantages of easy recovery and recycling have

been realized, though reduced reaction rates and enantioselectivities remain major problems. With continued work it is possible that both soluble and insoluble supports will be able to serve a wide range of catalytic functions.

REFERENCES

- (1) (a) Kitamura, M.; Suga, S.; Noyori, R. *J. Am. Chem. Soc.* **1986**, *108*, 6071. (b) Kitamura, M.; Okada, S.; Suga, S.; Noyori, R. *J. Am. Chem. Soc.* **1989**, *111*, 4028.
- (2) Itsuno, S.; Fréchet, J.M. J. *J. Org. Chem.* **1987**, *52*, 4142.
- (3) Soai, K.; Yokoyama, S.; Hayasaka, T. *J. Org. Chem.* **1991**, *56*, 4264.
- (4) Soai, K.; Ookawa, A.; Kaba, T.; Ogawa, K. *J. Am. Chem. Soc.* **1987**, *109*, 7111.
- (5) (a) Soai, K.; Niwa, S.; Watanabe, M. *J. Org. Chem.* **1988**, *53*, 927. (b) Soai, K.; Niwa, S.; Watanabe, M. *J. Chem. Soc. Perkin Trans. I.* **1989**, 109.
- (6) (a) Soai, K.; Watanabe, M. *Tetrahedron: Asymmetry* **1991**, *2*, 97. (b) Watanabe, M.; Soai, K. *Eur. Pol. J.* **1995**, *31*, 193.
- (7) Vidal-Ferran, A.; Bampos, N.; Moyano, A.; Pericás, M. A.; Riera, A.; Sanders, J. K. *J. Org. Chem.* **1998**, *63*, 6309.
- (8) Seebach, D.; Marti, R. E.; Hintermann, T. *Helv. Chim. Acta.* **1996**, *79*, 1710.
- (9) Rheiner, P. B.; Sellner, H.; Seebach, D. *Helv. Chim. Acta.* **1997**, *80*, 2027.
- (10) (a) Hu, Q-S.; Huang, W-S.; Vitharana, D.; Zheng, X-F.; Pu, L. *J. Am. Chem. Soc.* **1997**, *119*, 12454. (b) Hu, Q-S.; Huang, W-S.; Pu, L. *J. Org. Chem.* **1998**, *63*, 2798.
- (11) Hentges, S. G.; Sharpless, K. B. *J. Am. Chem. Soc.* **1980**, *102*, 4263.
- (12) (a) Jacobsen, E. N.; Markó, I.; Mungall, W. S.; Schröder, G.; Sharpless, K. B. *J. Am. Chem. Soc.* **1988**, *110*, 1968. (b) Wai, J. S. M.; Markó, I.; Svendsen, J. S.; Finn, M. G.; Jacobsen, E. N.; Sharpless, K. B. *J. Am. Chem. Soc.* **1989**, *111*, 1123.
- (13) (a) Pini, D.; Petri, A.; Salvadori, P. *Tetrahedron* **1994**, *50*, 11321. (b) Pini, D.; Petri, A.; Salvadori, P. *Tetrahedron: Asymmetry* **1993**, *4*, 2351.
- (14) Song, C. E.; Roh, E. J.; Lee, S.; Kim, I. O. *Tetrahedron: Asymmetry* **1995**, *6*, 2687.
- (15) Sharpless, K. B.; Amberg, W.; Bennani, Y. L.; Crispino, G. A.; Hartung, J.; Jeong, K-S.; Kwong, H-L.; Morikawa, K.; Wang, Z-M.; Xu, D.; Zhang, X-L. *J. Org. Chem.* **1992**, *57*, 2768.
- (16) Song, C. E.; Yang, J. W.; Ha, H. J.; Lee, S. *Tetrahedron: Asymmetry* **1996**, *7*, 645.
- (17) Nandan, E.; Sudalai, A.; Ravindranathan, T. *Tetrahedron Lett.* **1997**, *38*, 2577.
- (18) Canali, L.; Song, C. E.; Sherrington, D. C. *Tetrahedron: Asymmetry* **1998**, *9*, 1029.
- (19) Petri, A.; Pini, D.; Salvadori, P. *Tetrahedron Lett.* **1995**, *36*, 1549.
- (20) (a) Han, H.; Janda, K. D. *J. Am. Chem. Soc.* **1996**, *118*, 7632. (b) Han, H.; Janda, K. D. *Tetrahedron Lett.* **1997**, *38*, 1527. (c) Han, H.; Janda, K. D. *Angew. Chem. Int. Ed. Engl.* **1997**, *36*, 1731.
- (21) De, B. B.; Lohray, B. B.; Sivaram, S.; Dhal, P. K. *J. Pol. Sci. Part A. Pol. Chem.* **1997**, *35*, 1809.
- (22) (a) Minutolo, F.; Pini, D.; Salvadori, P. *Tetrahedron Lett.* **1996**, *37*, 3375. (b) Minutolo, F.; Pini, D.; Petri, A.; Salvadori, P. *Tetrahedron: Asymmetry* **1996**, *7*, 2293.
- (23) Angelino, M. D.; Laibinis, P. E. *Macromolecules.* **1998**, *31*, 7581.
- (24) Seebach, D.; Dahinden, R.; Marti, R. E.; Beck, A. K.; Plattner, D. A.; Kühnle, F. N. M. *J. Org. Chem.* **1995**, *60*, 1788.
- (25) Itsuno, S.; Kamahori, K.; Watanabe, K.; Ito, K. *Macromol. Symp.* **1996**, *105*, 155.
- (26) Kamahori, K.; Ito, K.; Itsuno, S. *J. Org. Chem.* **1996**, *61*, 8321.

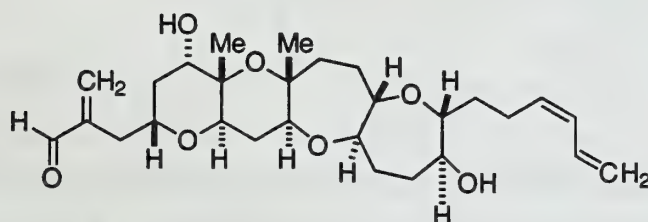
FUSED TETRAHYDROPYRAN AND OXEPANE SYNTHESIS TOWARDS HEMIBREVETOXIN B

Reported by Stephen Thorn

November 12, 1998

Hemibrevetoxin B (**1**), was isolated in 1989 from the marine dinoflagellate *Gymnodinium breve*.¹ It is the smallest member of the brevetoxin family, containing a ring skeleton less than half the size of the previously isolated Brevetoxin A and Brevetoxin B.² Biological interest in this family of compounds has been sparked since the brevetoxins were found to be the active agents in "red tide" outbreaks which have been responsible for massive fish kills and human intoxications.³

Hemibrevetoxin B is a potent lipid soluble neurotoxin which is active in concentrations as low as 0.5 μ M. The brevetoxins' neurotoxicity lies in their ability to activate cell membrane sodium channels and cause unchecked neuron firing.⁴



Hemibrevetoxin B (1)

Figure I. Structure of Hemibrevetoxin B

Structurally, **1** is extremely interesting and synthetically challenging. The polycyclic ether core is comprised of a 6,6,7,7 trans-fused ring system, which contains 10 stereogenic centers, including two quaternary centers. All of the polycyclic ether oxygen atoms possess a β relationship to the oxygen of the adjacent cyclic ether. Such polycyclic ether cores are rarely encountered in nature, appearing most often in marine products. As a result of its compact highly functionalized nature, Hemibrevetoxin B has been selected as a target for new methods of tetrahydropyran and oxepane ring synthesis.

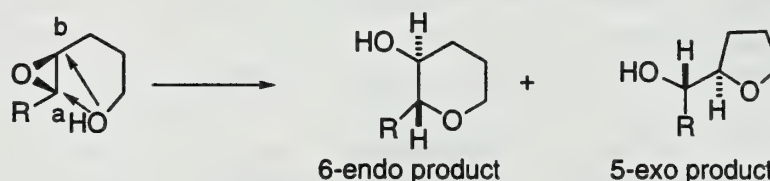
Synthesis

Successful synthetic efforts toward **1** have focused primarily on a linear approach to the polycyclic

core.^{2,3,5,6} Nucleophilic opening of epoxides has been used extensively to generate the trans-fused tetrahydropyran rings, although methods for generating these epoxides have varied dramatically. A wide array of methods have been applied to oxepane ring formation including expansion of existing tetrahydropyran rings, lactonization and reduction, as well as addition of an allylstannane to an aldehyde. Each of these methods confer certain advantages and limitations for the syntheses.

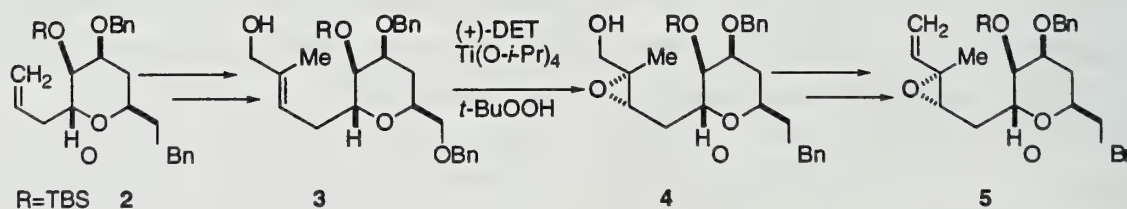
Tetrahydropyran Ring Synthesis

Tetrahydropyran synthesis towards **1** has been accomplished primarily by 6-endo trig cyclization of hydroxy epoxides. Several aspects of this ring closure were addressed to insure high selectivity. A 6-endo trig cyclization (Pathway a) must be activated over the more favored 5-exo trig mode of cyclization (Pathway b).⁷ In addition, an E-olefin must be used for epoxidation and that reaction must occur on the correct face for subsequent trans-fused oxacycle synthesis.



Nicolaou completed the first total synthesis of **1** in 1992.³ His synthetic approach relied upon the Sharpless asymmetric epoxidation to provide the desired epoxide in high yield and excellent selectivity.⁸ The synthesis began with the conversion of D-mannose to allyl tetrahydropyran **2** in 11 steps (Scheme 1). Then **2** was converted to the allylic alcohol, **3**, which, with the appropriate tartrate catalyst, was oxidized to the epoxide **4**. To activate the acid catalyzed 6-endo trig epoxide opening, **4** was converted to the allylic activated system **5**.⁹

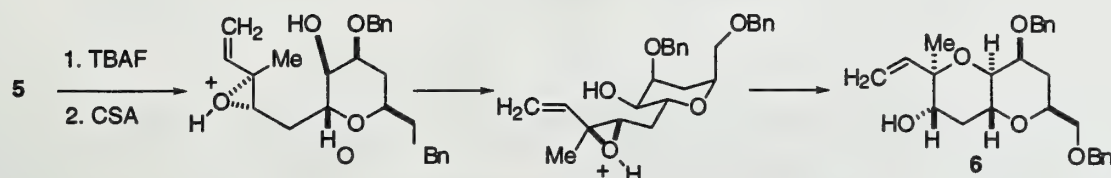
Scheme 1.



It was anticipated that as the reaction progressed the developing electron deficient orbital would be stabilized by the adjacent π electrons of the olefin and thus promote 6-endo trig cyclization (Scheme 2). Removal of the TBS ether and camphor sulfonic acid (CSA) induced cyclization simultaneously provided the trans-fused tetrahydropyran **6** and set the quaternary center. In addition, the bicyclic tetrahydropyran

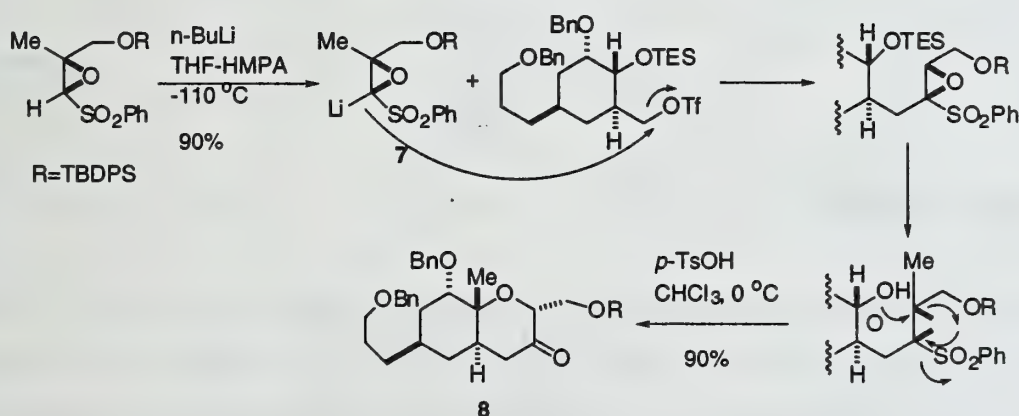
product **6** contained a trans oriented vinyl and hydroxy group which offered the potential for further ring synthesis. While the alcohol is ideally located to form the next oxacycle, the vinyl moiety has limited potential for tetrahydropyran ring synthesis. Conversion of the vinyl moiety to a but-2-en-4-ol is required to allow the use of Sharpless asymmetric epoxidation. An efficient method to affect this transformation is not apparent.

Scheme 2.



Epoxides are usually employed as electrophiles; however, Mori, in his 1998 formal synthesis of Hemibrevetoxin B, demonstrated that a nucleophilic sulphonyl stabilized oxiranyl anion could be used to install chiral epoxides (Scheme 3).⁵ The sulphonyl substituted epoxide can be deprotonated at the sulphonyl bearing carbon to yield the highly reactive anion **7**. However, the oxiranyl anion must be generated and used immediately, in the presence of HMPA, at very low temperatures to avoid decomposition and rearrangement.¹⁰ The active nucleophile **7** freely engaged in substitution reactions to yield hydroxy epoxide products. Hence, deprotection of the secondary alcohol and the preferred 6-endo cyclization afforded **8**.

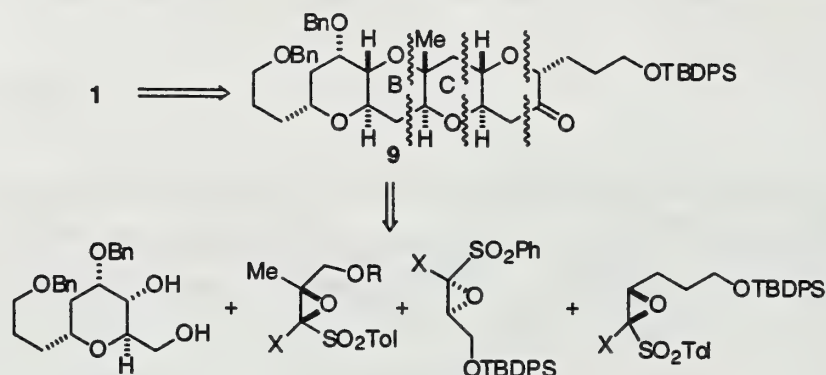
Scheme 3.



It was anticipated that the oxepane rings would be created by ring expansion of tetrahydropyran rings, and thus **9** was chosen as the target. It was envisioned that **9** would be synthesized from an initial tetrahydropyran ring and three sulphonyl stabilized oxiranyl anions as shown in the retrosynthetic analysis in Scheme 4. The ability to repeatedly use the oxiranyl anion for the synthesis of fused polycyclic ethers is

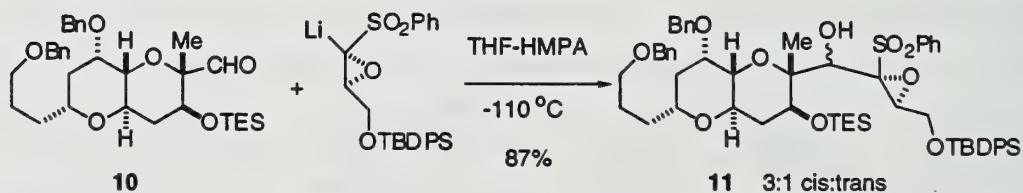
very appealing. Not only does the approach offer the ability to simplify the synthesis, but it increases the convergent nature of the sequence.

Scheme 4.



However, the oxiranyl anion is a relatively large nucleophile and requires an unhindered approach to the electrophile. Formation of the ring fusion quaternary center of rings B and C by this approach was not observed. Apparently, the added steric bulk of the methyl group prevented the oxiranyl anion from displacing a triflate. Use of a more electrophilic aldehyde **10** afforded an 87% yield of **11**, but at the expense of a 3:1 mixture of diastereomers (Scheme 5). The development of quaternary centers by the use of this type of oxiranyl anions appears to be an inefficient method.

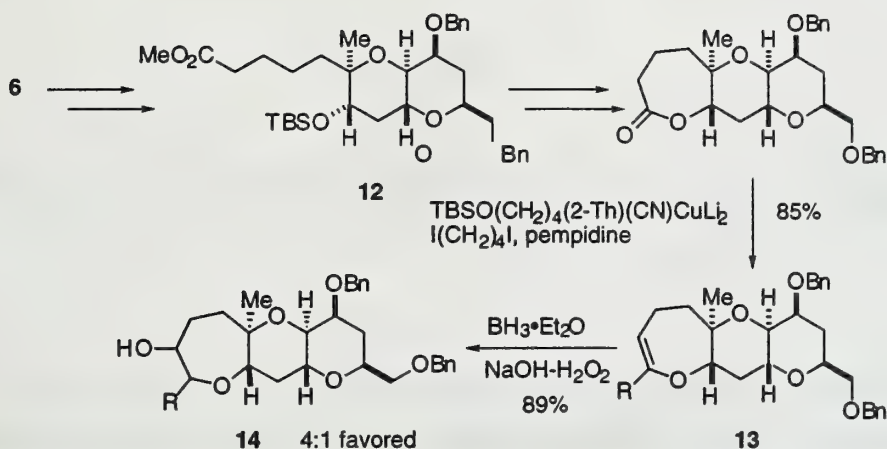
Scheme 5.



Oxepane Ring Synthesis

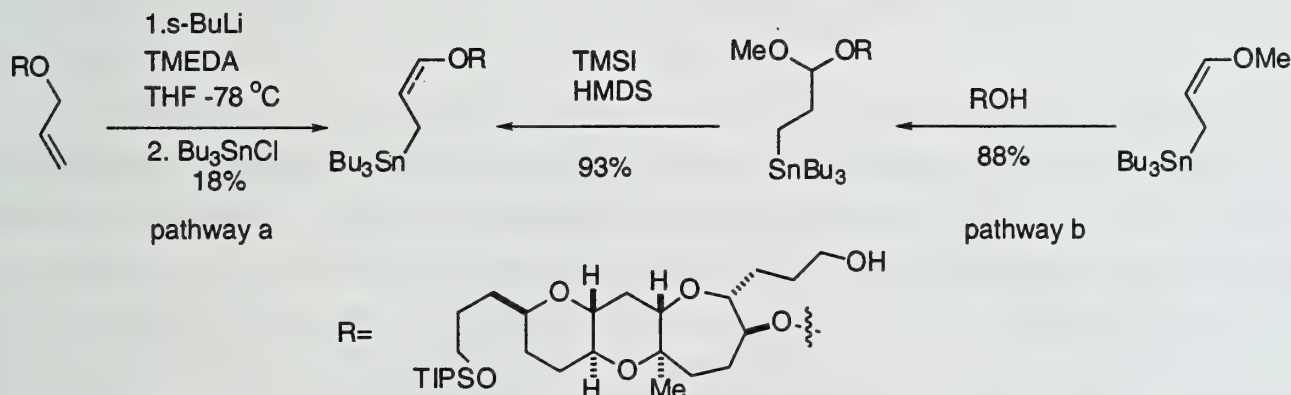
Lactonization to form medium-sized rings is a facile process; hence, Nicolaou investigated the synthesis of oxepane rings from their γ -lactone analogs (Scheme 6).¹¹ Protection of the secondary alcohol and conversion of the terminal alkene to a terminal ester yielded the lactonization precursor **12**, which undergoes ring closure under mild conditions. Lawesson's reagent^{12a,b} produced the thionolactone and the ensuing copper lithium addition and reductive desulfurization provided **13**. Hydroboration afforded the desired diol **14** in a 4:1 mixture of diastereomers. In fact, hydroboration appears to be substrate dependant. This lack of selectivity late in the synthetic process is a serious shortcoming of this method of oxepane synthesis.

Scheme 6.



The addition of allylstannanes to aldehydes provides another avenue for the construction of oxepane rings.⁶ Investigations by Yamamoto began with the bicyclic ether previously constructed by Nicolaou. Unfortunately, standard procedures for the conversion of allylic ethers to γ -alkoxy allyl stannanes were extremely inefficient (16% yield) and undermined the value of this technique (Scheme 7, pathway a).¹³ It was hypothesized that deprotonation at the sterically hindered allylic position is highly disfavored. However, Yamamoto has recently developed new methodology that circumvents the previously encountered problems and provides the desired γ -alkoxy allyl stannanes in high yields (Scheme 7, pathway b).¹⁴

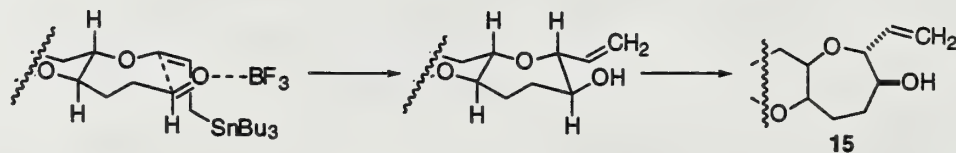
Scheme 7.



The reaction between the γ -alkoxy allyl stannane and the substituted aldehyde, which is known to occur via an open transition state in the presence of Lewis acids,¹⁵ was subjected to extensive investigation by Yamamoto. The product was predicted to be the desired oxepane ring with trans-related exo-cyclic alcohol and vinyl moieties (Scheme 8). Indeed this is the case, selectively forming the desired **15** in 94%

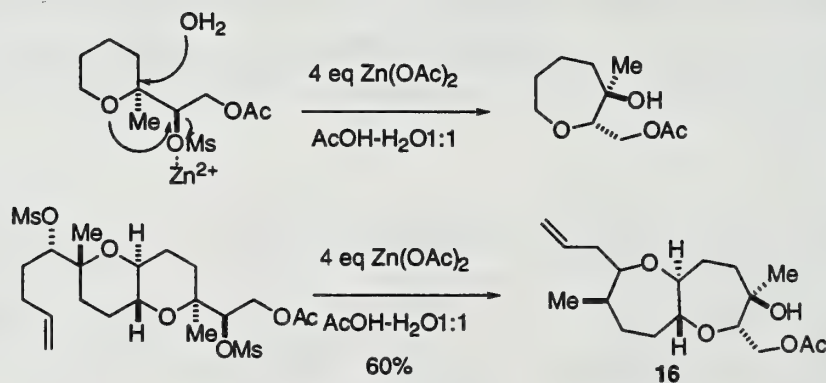
yield. The exocyclic functionality is identical to that generated by the tetrahydropyran synthesis used by Nicalaou. While not suitable for further tetrahydropyran synthesis, this approach does allow further allylstannane additions to aldehydes.

Scheme 8.



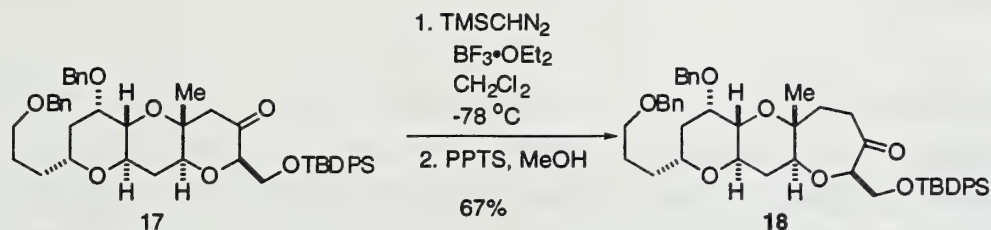
One of the more elegant solutions of the synthesis of oxepane rings has been the ring expansion of existing tetrahydropyran rings. Mori and Nakata have developed different solutions to affect this conversion. Nakata relied on the nucleophilicity of the ethereal oxygen to displace an exocyclic mesylate (Scheme 9).¹⁶ Moreover, double ring expansion was achieved to simultaneously derive the bis-oxepane structure **16** from a fused bis-tetrahydropyran system in moderate yield.

Scheme 9.



Mori's work on ring expansion is an extension of his efforts on tetrahydropyran synthesis.¹⁷ Epoxide opening and ring closure provided the tetrahydropyran structure **17** (Scheme 10). It was anticipated that diazomethane would insert adjacent to the carbonyl to render the required oxepane ring **18** as these additions preferentially occur on the less substituted side of the carbonyl. In trial experiments it was found that diazomethane adds preferentially, but not exclusively on the desired side. Greater selectivity was obtained with the more sterically encumbered trimethylsilyl diazomethane. Subsequent removal of the TMS moiety was trivial and thus ring expansion was affected in two steps. Moreover, no stereocenters were affected and further rings synthesis could proceed unabated.

Scheme 10.



CONCLUSIONS

Synthesis of the polycyclic ether core of Hemibrevetoxin B has served as a test scenario for a wide array of methodologies. Specific challenges have arisen in controlling the mode of ring closure, developing the trans-fusion, and effectively constructing tertiary centers.

The work of Nicolaou presents an efficient means of constructing tetrahydropyran rings. Sharpless asymmetric epoxidation creates the necessary epoxide precursors in excellent yield and selectivity. However preparation of the allylic alcohol precursors and installation of the required electron rich element is achieved in a laborious manner.

The metamorphosis of lactones to the oxepane analogs as developed by Nicolaou suffers from low selectivity. The lactones were simultaneously reduced and functionalized to yield the oxepane ring. This process necessitated a poorly selective hydroboration step. The selectivity of the hydroboration is substrate dependent. This lack of selectivity is unacceptable in the latter stages of a synthesis.

Nakata has provided a highly effective method for generating trans-fused oxepane rings. To date this methodology has only been employed with bicyclic compounds and it is uncertain if it is compatible with additional rings. If not, it is a means to bis-oxepane systems alone and is not applicable to molecules with internal oxepane rings.

Oxepane rings are formed efficiently and selectively by allyl-stannane aldehyde condensation. The major obstacle, γ -alkoxy allyl stannane formation, has been recently been surmounted by Yamamoto. As a result this approach holds the greatest potential for oxepane synthesis.

Synthesis of the epoxides prior to coupling makes Mori's synthesis decidedly more convergent than those previously conceived. The immediate product of cyclization confers multiple synthetic advantages. The potential exists for the synthesis of additional trans-fused rings by repetition of the sequence. The expansion of the tetrahydropyran ring to the oxepane equivalent is a relatively simple process. The major drawbacks are that the oxiranyl anions are relatively unstable and require immediate consumption after production even in the presence of low temperatures. A crowded environment around the electrophile can block the approach of the oxiranyl anion. Overall, the oxiranyl method is a relatively

simple and short method of generating addition rings. The longest linear sequence in the synthesis of the fully functionalized core was 26 steps.

REFERENCES

- (1) Krishna Prasad, A. V.; Shimizu, Y. *J. Am. Chem. Soc.* **1989**, 111, 6476.
- (2) Morimoto, M.; Matsukura, H.; Nakakta, T. *Tetrahedron Lett.* **1996**, 37, 6365.
- (3) Nicolaou, K. C.; Reddy, K. R.; Skokotas, G.; Sato, F.; Xiao, X.-Y.; Hwang, C.-K. *J. Am. Chem. Soc.* **1993**, 115, 3558.
- (4) Hwang, J. M. C.; Wu, C. H.; Badan, D. G. *J. Pharmacol. Exp. Ther.* **1984**, 229, 615.
- (5) Mori, Y.; Yaegashi, K.; Furukawa, H. *J. Org. Chem.* **1998**, 63, 6200.
- (6) Kadota, I.; Yamamoto, Y. *J. Org. Chem.* **1998**, 63, 6597.
- (7) Nicolaou, K. C.; Prasad, C. V. C.; Hwang, C.-K.; Duggan, M. E.; Veale, C. A. *J. Am. Chem. Soc.* **1989**, 111, 5321.
- (8) Katsuki, Sharpless, K. B. *J. Am. Chem. Soc.* **1980**, 102, 5976.
- (9) Nicolaou, K. C.; Prasad, C. V. C.; Somers, P. K.; Hwang, C.-K.; *J. Am. Chem. Soc.* **1989**, 111, 5330.
- (10) Ashwell, M.; Jackson, R. F. W. *J. Chem Soc. Chem. Commun.* **1988**, 645
- (11) Nicolaou, K. C.; McGarry, D. G.; Somers, P. K.; Veale, C. A.; Furst, G. T. *J. Am. Chem. Soc.* **1987**, 109, 2504.
- (12) (a) Sheibye, S.; Pederson, B. S.; Lawesson, S.-O. *Bull. Soc. Chim. Belg.* **1978**, 87, 229.
(b) Cava, M. P.; Levinson, M. I. *Tetrahedron* **1985**, 41, 5061.
- (13) Kadota, I.; Park, J.-Y.; Koumura, N.; Pollaud, G.; Matsukawa, Y.; Yamamoto, Y. *Tetrahedron Lett.* **1995**, 36, 5777.
- (14) Kadota, I.; Sakaihara, T.; Yamamoto, Y. T. *Tetrahedron Lett.* **1996**, 37, 3195.
- (15) Nishigaichi, Y.; Takuwa, A.; Naruta, Y.; Maruyama, K. *Tetrahedron* **1993**, 34, 7395.
- (16) Nakata, T.; Nomura, S.; Matsukura, H. *Tetrahedron Lett.* **1996**, 37, 213.
- (17) Mori, Y.; Yaegashi, K.; Furukawa, H. *Tetrahedron* **1997**, 53, 12917.

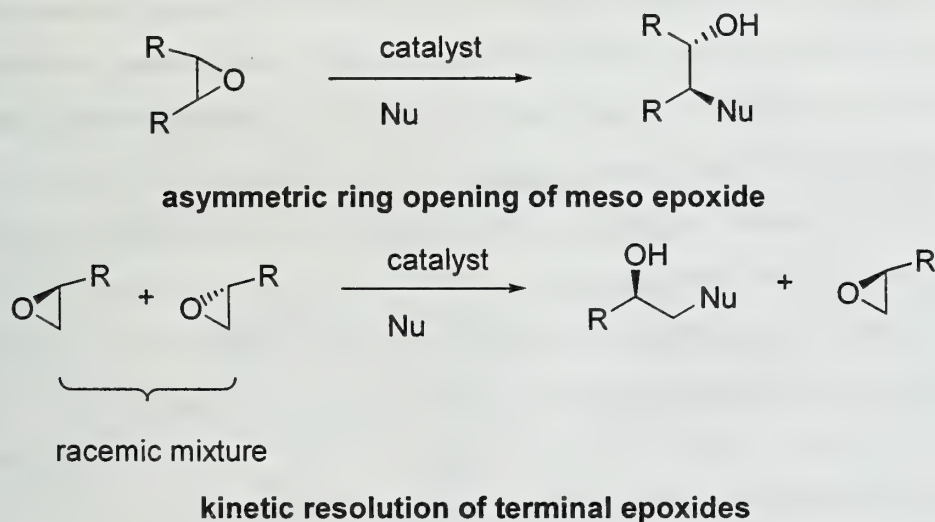
CATALYTIC ASYMMETRIC NUCLEOPHILIC RING OPENING OF MESO EPOXIDES AND KINETIC RESOLUTION OF TERMINAL EPOXIDES

Reported by Sung H. Lim

November 16, 1998

INTRODUCTION

Increasing demand for practical strategies for the preparation of enantiomerically pure compounds has resulted in considerable progress in catalytic asymmetric reactions.^{1,2} Consequences of this work include the development of two approaches to prepare enantioenriched compounds from epoxides: catalytic asymmetric ring opening (ARO) of meso epoxides and kinetic resolution of racemic terminal epoxides through nucleophilic ring openings.^{3,4} Each approach provides an efficient route to enantioenriched products. This report reviews recent developments in these strategies with an emphasis on (salen)metal complex mediated asymmetric catalysis.



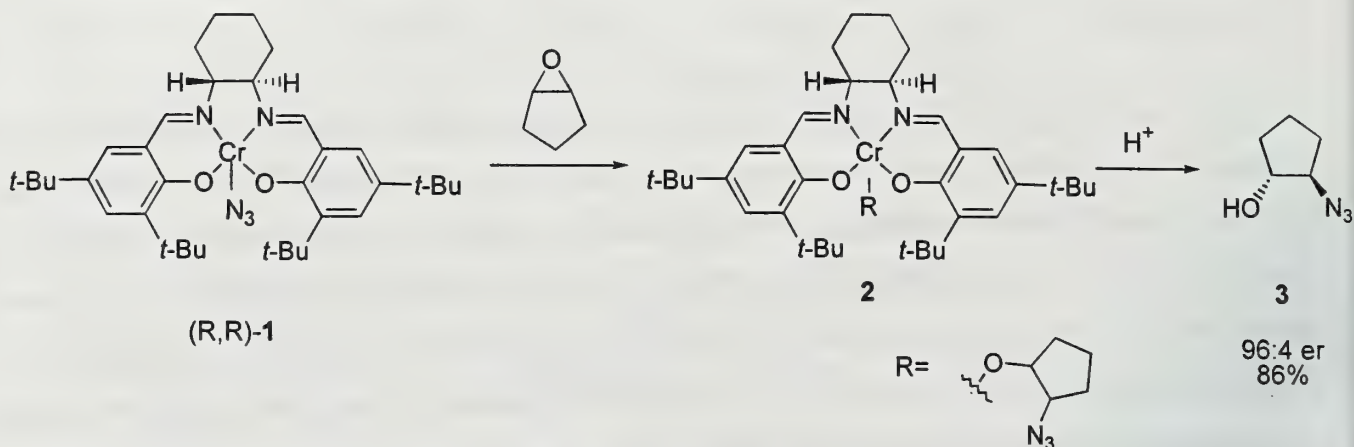
ASYMMETRIC RING OPENING OF MESO EPOXIDES

Mechanism of ARO of epoxides with TMSN_3 in the presence of (salen)Cr complex

The asymmetric ring opening of cyclic and acyclic meso epoxides catalyzed by the chiral (salen)Cr complex **1** affords products with high enantioselectivities.³ An illustrative example is the nucleophilic ring opening of cyclopentene oxide with (R,R)-**1** to afford the azido alcohol **3** with an enantiomeric ratio (er) of 96:4 as seen in Scheme 1. The reaction of cyclopentene oxide was studied in detail to establish the mechanism.⁵ The (salen)CrN₃ complex **1** reacts stoichiometrically with cyclopentene oxide to form a complex **2**. Exposing the solution of **2** to HN₃, methanol, or silica gel

generated azido alcohol **3** with the same enantiomeric ratio as the product from the catalytic reaction. Reaction of **2** with TMSN_3 in the presence of water also provided **3** in addition to regenerating the catalyst **1**. On the basis of these results **1** was identified as an active catalyst.

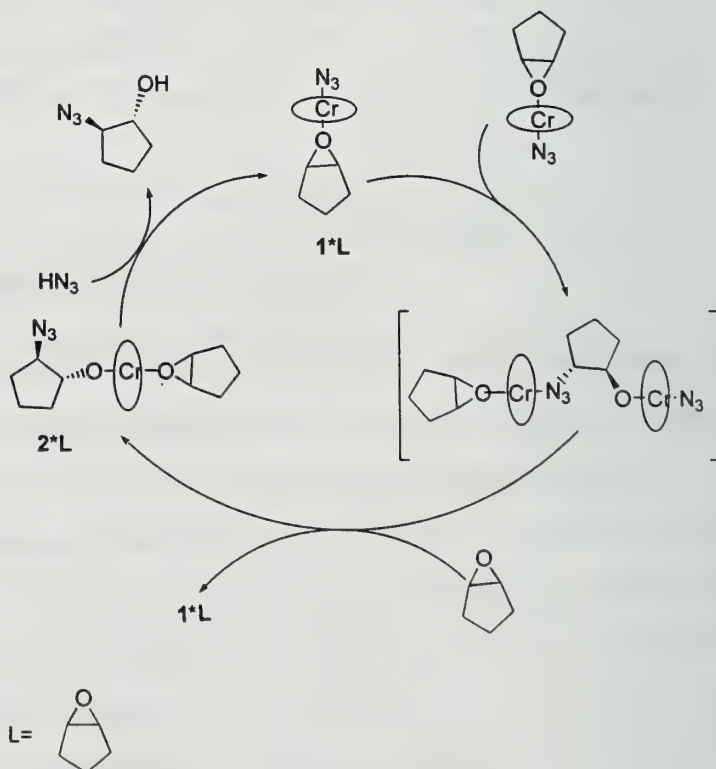
Scheme 1.



Structural studies of the catalyst **1** suggest that both the azide and the oxygen from the epoxide coordinate to the chromium metal in the salen complex.⁴ The catalyst **1** is insoluble in non-coordinating solvents, such as *tert*-butyl methyl ether (TBME), but it is soluble in coordinating solvent THF. The salen complex **1** in THF has an IR stretching frequency at 2053 cm^{-1} which is close to that of other chromium azide complexes. Furthermore, an

X-ray structure of **1**·THF shows that the axial coordination site of chromium is occupied by THF. Addition of epoxides to the insoluble catalyst **1** in TBME leads to a homogeneous solution with an azide IR absorbance at 2053 cm^{-1} . Based on these studies, the epoxide was assumed to be coordinated to chromium via Lewis acid complexation like THF. Kinetic studies showed that these reactions did not depend on the concentration of the free azide nucleophile, but have a second-order dependence on the concentration of **1**. This finding is consistent with a mechanism in which both the epoxide and the nucleophile

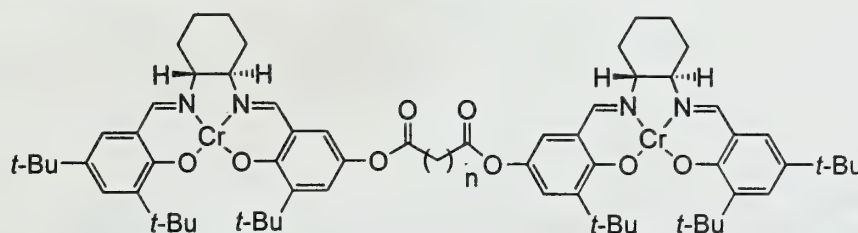
Scheme 2.



are activated by the catalyst in the enantio-determining step. These observations have led to the elucidation of the mechanism as seen in Scheme 2. Coordination of epoxide to the salen complex **1** is followed by azide delivery from the second salen complex to afford a dimeric alkoxide complex. Nucleophilic addition of epoxide to the dimeric complex results in the monomeric complex **2***L, which reacts with azide to give azido alcohol.

Dimeric Salen Catalysts

Elucidation of the salen mechanism for the asymmetric ring opening of cyclopentene oxide with azide revealed an important principle for designing an improved catalyst. Since two salen complexes activate both the epoxide and the nucleophile, covalently bound dimeric complexes such as **4** were envisioned to potentially promote a rate increase through intramolecular reaction.⁶ Various dimeric salen complexes were synthesized and screened for their reactivity and enantioselectivity. The dimeric catalysts **4** were found to catalyze the ARO reaction of cyclopentene oxide at higher reaction rates than the original catalyst **1** without diminished enantioselectivity with an optimal value of $n=5$. Kinetic



4

studies showed that the observed rate of product formation for dimeric catalysts had a strong dependence on the length of the tether linking the two salen units. When the tether was too short, $n=2$, the observed rate constant was decreased. This was assumed to be caused by inaccessibility of the optimal transition state geometry for the ARO reaction. When the length of the tether was too long $n=10$, an increase in entropic cost of the intramolecular reaction also led to a decrease in reactivity.

Nitrogen Nucleophiles

The principle of asymmetric ring opening of epoxides was established in the early 1980's. However, products with only moderate levels of enantioenrichment, 58:42-81:19, were obtained with TMSN_3 .^{7,8} Efficient catalysts yielding ring-opened products with up to 99:1 er from meso epoxides have been developed in recent years.^{9,10,11} Among these catalysts, the best method to date uses Jacobsen's salen metal complexes which are effective at less than 2 mol%.³

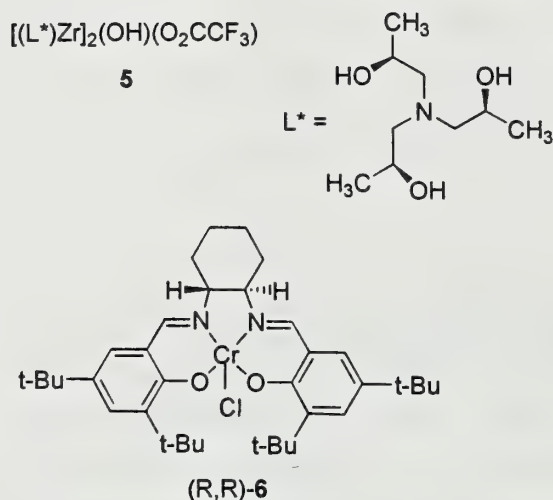
Both Nugent and Jacobsen have developed highly effective catalysts for the ARO reactions of meso epoxides using silyl azide.^{3,9} Although Nugent's Zr(IV) catalyst **5** is highly stereoselective in opening epoxides fused to six-membered rings and acyclic substrates, five membered rings are opened less effectively.^{12,13} However, Jacobsen's precatalyst **6** is more effective for five membered substrates, and works well with other nucleophiles in addition to azide. A comparison of **5** and **6** is shown in Table

1. Neither catalyst is inhibited by a Lewis basic functional group on the epoxides. Since olefin, ether and carbonyl groups are all tolerated under the reaction conditions, these methodologies can be applied to a variety of different substrates. These catalysts not only provide the ring-opened products in good



Table 1. Comparison of **5** and **6**

Substrate	Catalyst	Yield (%)	er (%)
	5	86	96:4
	6	80	94:6
	5	59	93:7
	6	65	91:9
	5	79	94:6
	6	72	90:10
	5	—	—
	6	90	97:3
	5	64	91:9
	6	80	97:3

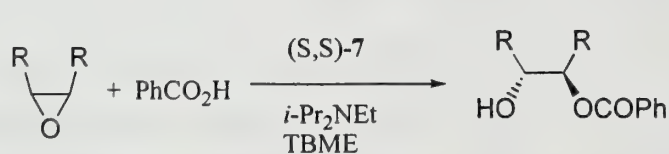


yields with high enantioselectivities, but are also highly efficient catalysts requiring less than 2 mol%.

Oxygen Nucleophiles

The search for oxygen nucleophiles for asymmetric ring opening reactions led to the discovery that carboxylic acids are effective nucleophiles.¹⁴ The first non-enzymatic ARO of meso epoxides with an oxygen-based nucleophile was demonstrated by Jacobsen and co-workers. Using carboxylic acids, ARO technology provides direct and efficient syntheses of the 1,2-diols **8-10** with the (salen)Co catalyst **7**. Additionally, a noncoordinating base such as *i*-Pr₂NEt improved the reaction rate, enantioselectivity and yield (Scheme 3). The mechanistic basis for the beneficial effects of amine base has not been elucidated, but the base was shown to improve the solubility of benzoic acid in TBME.

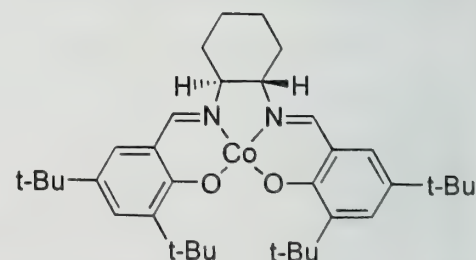
Scheme 3.



8; R=-(CH₂)₄-, 98%, 88:12 er

9; R= Ph, 92%, 96:4 er

10; R= , 95%, 85:15 er



7

Sulfur nucleophiles

In 1997, using the gallium complex **11** and *tert*-butylthiol, Shibasaki achieved ARO of meso epoxides with enantiomeric ratios ranging from 91:9 to 99:1 (Scheme 4).¹¹ Jacobsen has also applied (salen)Cr catalyzed ARO technology to alkanethiols which yielded the desired products¹⁵. A wide range of thiols was screened, and benzyl

mercaptan was identified as the best substrate for this reaction.

However, only moderate ers of up to 79:21 were observed in these

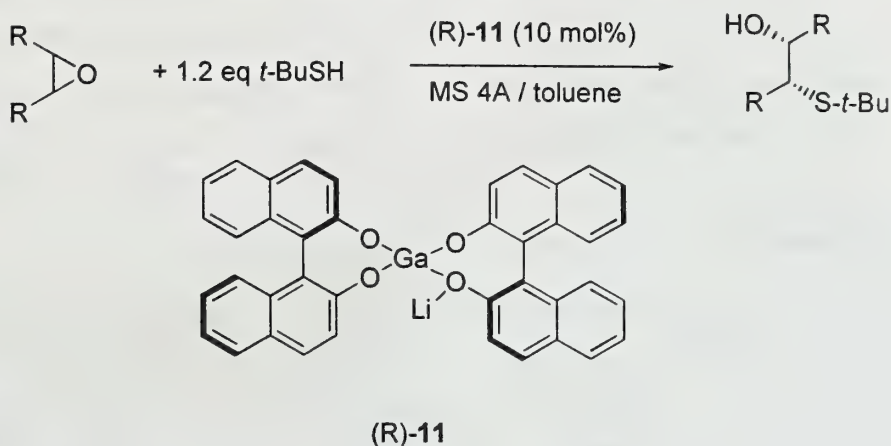
reactions. The problem of low enantioselectivity was resolved by

using a dithiol and 2 equivalents of epoxide, which afforded chiral and

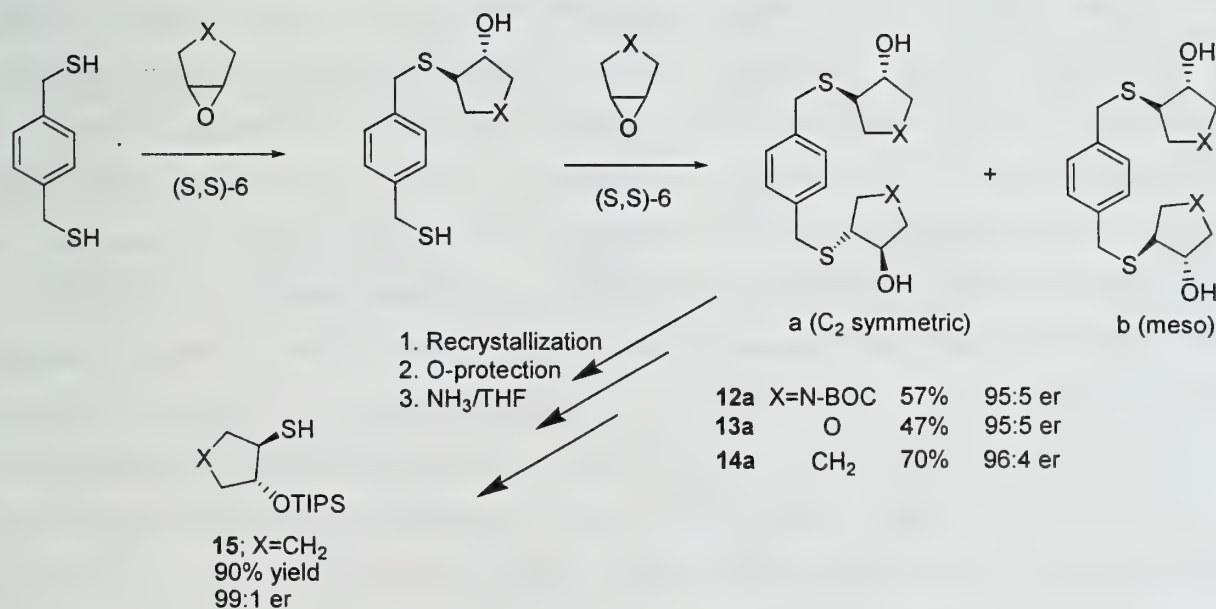
meso bis-adducts. Assuming there is no diastereoselectivity in the

second ring opening event, a reaction with dithiols should improve the enantiomeric ratio from $x:(1-x)$ to $x^2:(1-x)^2$. For example, using a dithiol enantiomeric ratio of the product should improve from 79:21 to 79²:21² (93:7). After separation of the chiral bis-product **14a** from the meso product **14b**, it can be cleaved to release free thiol **15** with a 99:1 er. Although this method is not very efficient with respect to overall yields, enantiopure products can be easily obtained from meso epoxides (Scheme 5).

Scheme 4.



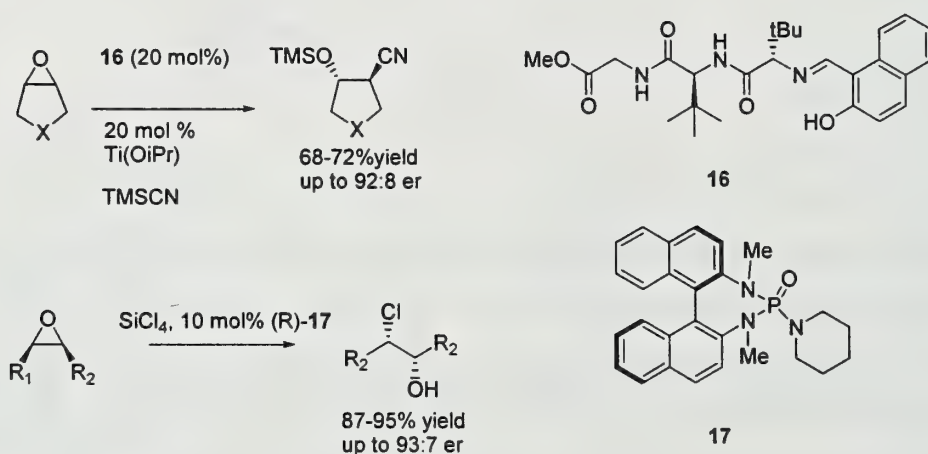
Scheme 5.



Halide and Carbon Based Nucleophiles

The asymmetric nucleophilic ring opening of meso epoxides with TMSCl or TMSCN in the presence of chiral salen-metal complexes gives products with *ers* of less than 61:39.¹⁶ However, Hoveyda and co-workers have used TMSCN to open meso epoxides with Ti(*i*OPr)₄ in the presence of Schiff base **16** to yield products with enantiomeric ratio as high as 93:7 (Scheme 6).¹⁷ Denmark and co-workers have recently reported an alternative strategy for the ARO of meso epoxides with SiCl₄ in the presence of a chiral Lewis base **17**.¹⁸ Although acyclic epoxides were opened with good enantioselectivity of up to 93:7, cyclic epoxides afforded corresponding chlorohydrins in low enantiomeric ratios of 51:49-75:25 (Scheme 6).

Scheme 6.

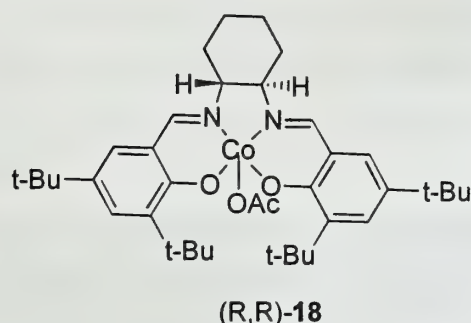
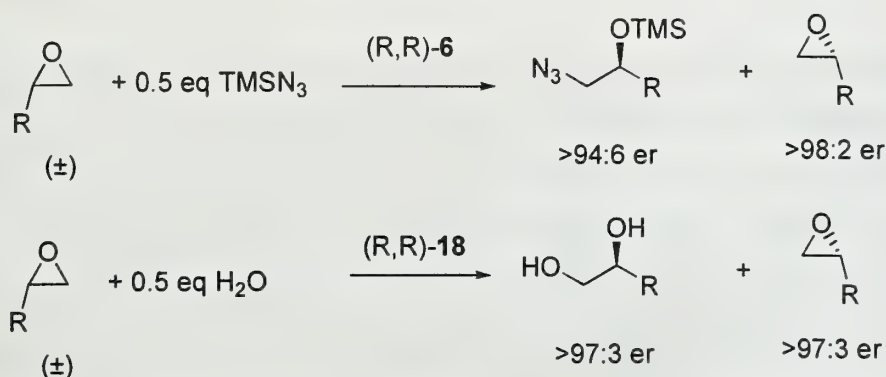


KINETIC RESOLUTION OF TERMINAL EPOXIDES

No simple method for the catalytic asymmetric synthesis of terminal epoxides exists.¹⁹ However, application of kinetic resolution to terminal epoxides with salen complexes provides a valuable strategy to prepare virtually enantio-pure epoxides and ring opened products. Jacobsen has applied this methodology to kinetic resolution of terminal epoxides using (salen)CrN₃ (**1**).²⁰ Since a wide variety of terminal epoxides are available in racemic form,²¹ the application of a kinetic resolution of racemic terminal epoxides with salen complexes should be a valuable strategy. Using TMSN₃ as a nucleophile, unreacted epoxides and ring-opened products are obtained as seen in scheme 7. Although the kinetic resolution strategy with TMSN₃ is synthetically valuable, it is limited in industrial applications due to the hazard and cost of the nucleophile. A search for an alternative nucleophile led to the discovery of hydrolytic kinetic resolution (HKR) of terminal epoxides. Jacobsen and co-workers have discovered efficient ways to prepare enantiopure terminal epoxides and 1,2 diols using hydrolytic

kinetic resolution (Scheme 7).²² Since HKR uses water as a nucleophile, this strategy has the advantage of using safe and inexpensive reagents. Low loading and recyclability of the catalyst (<0.5 mol%) are other attractive features of this approach.

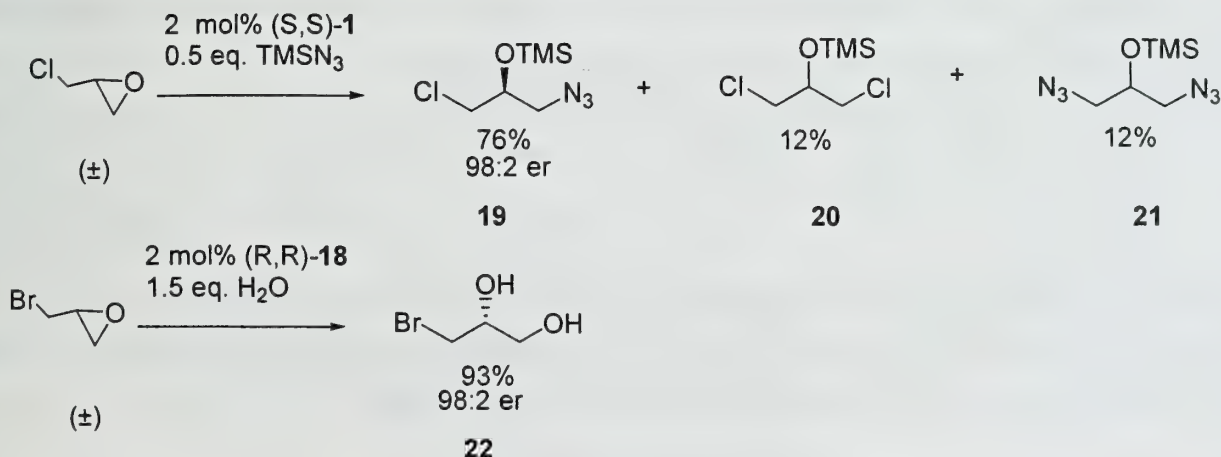
Scheme 7.



Dynamic Kinetic Resolution

During the kinetic resolution of epichlorohydrin, it was found that the epoxide racemized rapidly relative to the ring opening reaction. Thus a dynamic kinetic resolution was applied using salen catalysts to afford the ring-opened product **19** in 76% yield with 98:2 enantiomeric ratio.²³ In addition to the desired product, 1,3-dichloro and 1,3-diazide products were also isolated (Scheme 8). The identities of these byproducts were used to elucidate the mechanism of racemization. Although the amounts of **20** and **21** could not be suppressed, this procedure provides an efficient method for generating the desired

Scheme 8.



enantioenriched products in good yields. This dynamic kinetic resolution strategy was also applied under hydrolytic conditions. Although epichlorohydrin had relatively slow rate of racemization in the presence of water, epibromohydrin racemized quickly to give the diol **22** in 93% yield with 98:2 enantiomeric ratio.²¹

CONCLUSION

The asymmetric nucleophilic ring opening of meso epoxides is a powerful strategy for creating two contiguous stereogenic centers. The salen metal complexes and others have proven to be effective catalysts for ARO of meso epoxides. These catalysts are not only efficient, but also provide products with high enantioselectivity and good yields. By the use of different nucleophiles, various organic building blocks, including diols and aminoalcohols, can be synthesized. Using the kinetic resolution technique, inexpensive terminal epoxides can be resolved to give virtually enantiopure epoxides and ring-opened products. Despite the considerable progress in asymmetric ring opening of epoxides, applications of this technology are still limited to small number of nucleophiles. Development of more general strategy for asymmetric ring opening of epoxides will be of great synthetic value.

REFERENCES

- (1) Tombo, G. M. R.; Bellus, D. *Angew. Chem., Int. Engl.* **1991**, *30*, 1193.
- (2) Nugent, W. A.; RajanBabu, T. V.; Burk, M. J. *Science* **1993**, *259*, 479.
- (3) Marinez, L. E.; Leighton, J. L.; Carsten, D. H.; Jacobsen, E. N. *J. Am. Chem. Soc.* **1995**, *117*, 5897.
- (4) Larrow, J. F.; Schaus, S. E.; Jacobsen, E. N. *J. Am. Chem. Soc.* **1996**, *118*, 7420.
- (5) Hansen, K. B.; Leighton, J. L.; Jacobsen, E. N. *J. Am. Chem. Soc.* **1996**, *118*, 10924.
- (6) Konsler, R. G.; Karl, J.; Jacobsen, E. N. *J. Am. Chem. Soc.* **1998**, *120*, 10780.
- (7) Hodgson, D. M.; Gibbs, A. R.; Lee, G. P. *Tetrahedron* **1996**, *52*, 14361.
- (8) Yamashita, H.; Mukaiyama, T. *Chem. Lett.* **1985**, 1643.
- (9) Nugent, W. A. *J. Am. Chem. Soc.* **1992**, *114*, 2768.
- (10) Hoveyda, A. H. *Chem. & Bio.* **1998**, *5*, R187.
- (11) Iida, T.; Yamamoto, N.; Sasai, H.; Shibasaki, M. *J. Am. Chem. Soc.* **1997**, *119*, 4783.
- (12) McClelland, B. W.; Nugent, W. A.; Finn, M. G. *J. Org. Chem.* **1998**, *63*, 6656.
- (13) Nugent, W. A.; Licini, G.; Bonchio, M.; Bortolini, O.; Finn, M. G.; McClelland, B. W. *Pure & Appl. Chem.* **1998**, *70*, 1041.
- (14) Jacobsen, E. N.; Kakiuchi, F.; Konsler, R. G.; Larrow, J. F.; Tokunaga, M. *Tetrahedron Lett.* **1997**, *38*, 773.
- (15) Wu, M. H.; Jacobsen, E. N. *J. Org. Chem.* **1998**, *63*, 5252.
- (16) Martinez, L. E. Ph.D. Thesis, Harvard, Aug. 1997.
- (17) Cole, B. M.; Shimizu, K. D.; Krueger, C. A.; Harrity, J. P.; Snapper, M. L.; Hoveyda, A. H. *Angew. Chem. Int. Ed. Engl.* **1996**, *35*, 1668.
- (18) Denmark, S. E.; Barsanti, P. A.; Wong, K. T.; Stavenger, R. A. *J. Org. Chem.*, **1998**, *63*, 2428.
- (19) Leighton, J. L.; Jacobsen, E. N. *J. Org. Chem.* **1996**, *61*, 389.
- (20) Schaus, S. E.; Larrow, J. F.; Jacobsen, E. N. *J. Org. Chem.* **1997**, *62*, 4197.
- (21) Tokunaga, M.; Larrow, J. F.; Kakiuchi, F.; Jacobsen, E. N. *Science*, **1997**, *277*, 936.
- (22) Furrow, M. E.; Schaus, S. E.; Jacobsen, E. N. *J. Org. Chem.* **1998**, *63*, 6776.
- (23) Schaus, S. E.; Jacobsen, E. N. *Tetrahedron Lett.* **1996**, *37*, 7937.

ORGANIC SYNTHESIS BY ELECTROCHEMICAL METHODS

Reported by Jiping Fu

November 23, 1998

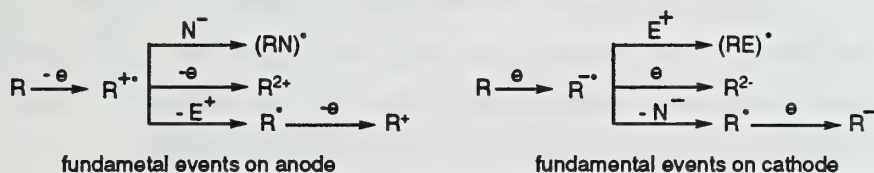
INTRODUCTION

Electroorganic synthesis involves organic reactions which are carried out by passing faraday current through a reaction solution. Electrochemistry is an interface science involving organic chemistry, physical chemistry and analytical chemistry. In the last three decades, many advances have been made on electroorganic synthesis, which enhance synthetic organic chemistry.¹ At present, a variety of organic transformations can be carried out by electrochemical methods very efficiently in good yields, with the advantages few by-products, low costs, no exposure to toxic reagents. There are a number of transformations that can only be carried out by electrochemical methods. Despite the advantages of electroorganic synthesis, organic chemists have not fully utilized this powerful method. This review will show that electrochemical methods provide excellent ways to carry out organic reactions.

GENERAL MECHANISM²

Electrolysis is carried out in an electrocell with a cathode and an anode, and a reference electrode. In the reaction solution, electrolyte usually ammonium salt is needed for conducting the electricity. In electrochemistry, the primary step is the electron transfer between the substrate and the electrode. A radical ion is usually the first formed species, and it can react directly or be further reduced or oxidized to anion or cation (Scheme 1). The reactive species depends on the specific reaction system.

Scheme 1



The electron transfer occurs in a highly structured region which is the electrochemical double layer. It consists of a complex of solvent, substrate, electrolyte molecular. Unlike usual chemical methods in which the reactive species is uniformly dispersed in the reaction system, in electrochemical reactions the reactive species is generated on the surface of electrodes. Because the generation and environment of the reactive species is different from usual chemical methods, a variety of novel reactions may be realized.

CATHODIC REDUCTIONS

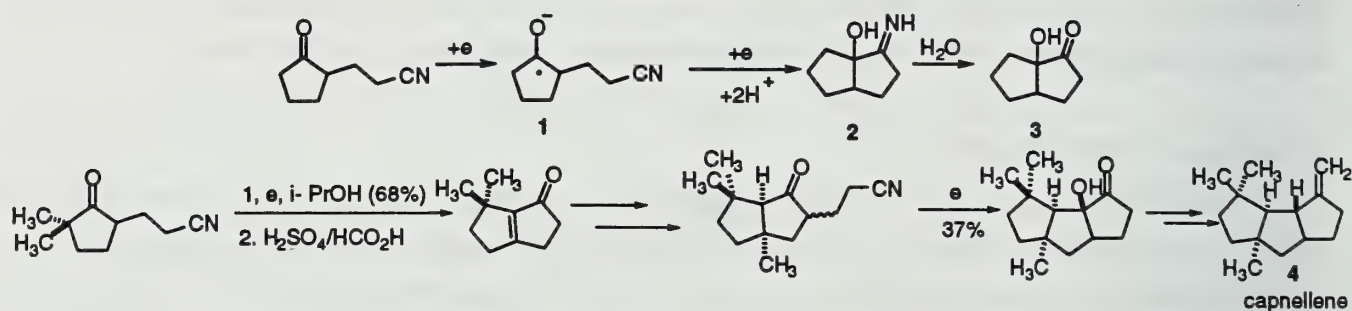
Reductive Coupling

On the cathode, electron accepting functional groups can be reduced to generate radical anions. Reductive couplings can lead to the formation of a σ -bond between two formally electron-deficient centers.³ An industrial scale electrohydrodimerization of acrylonitrile developed by the Monsanto

Company is illustrative.³ Acrylonitrile upon direct one electron reduction, undergoes homocoupling to give adiponitrile, a starting material for Nylon-6,6. Every year, 90,000 tons of adiponitrile is synthesized by this method which is the largest known electroorganic industrial process in the world today.

The carbonyl function is a good electron accepting group. The ketal radical which is generated by reduction, can couple with alkenes,⁴ alkynes,⁵ nitriles,⁵ and aromatic rings.⁶ Intramolecular reaction can occur before the reactive species diffuses into the reaction solution. Reductive carbonyl initiated cyclizations have been extensively studied by Shono and coworkers. Couplings between a ketone and a nitrile are very useful because the resulting carbonyl group allows further functionalization. The ketal radical attacks the nitrile group to form cyclized intermediate **2**, which upon hydrolysis gave cyclized ketone **3**. This transformation has been employed extensively in preparing precursor to a number of natural products. As an example capnellene **4** was synthesized by using the electroreductive cycloaddition from simple starting material (Scheme 2).

Scheme 2



The closure of a ketone onto an aromatic ring, a transformation which might appear to be thermodynamically unfavorable, can also be achieved by electroreductive methods.⁶ The ketone **5** undergoes reductive cycloaddition to give **6** as a single diastereomer (Scheme 3). The repulsion between the electrons of benzene ring and the negative charge on oxygen leads to the preferred stereochemistry. The table compares the results of this method to other chemical methods. With the exception of sodium (HMPA/THF), all other reducing reagents failed to give cyclized product.

Scheme 3

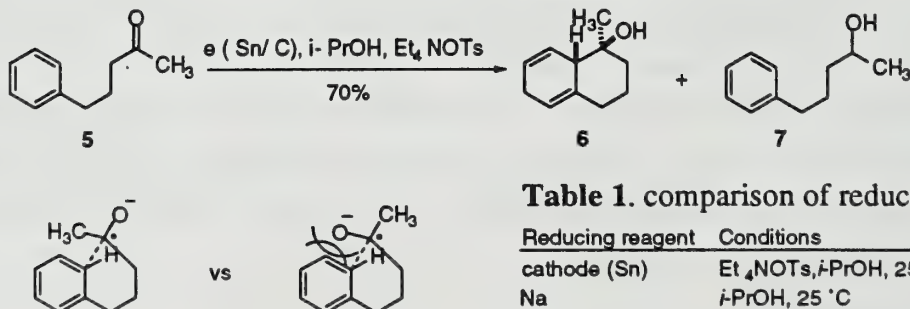
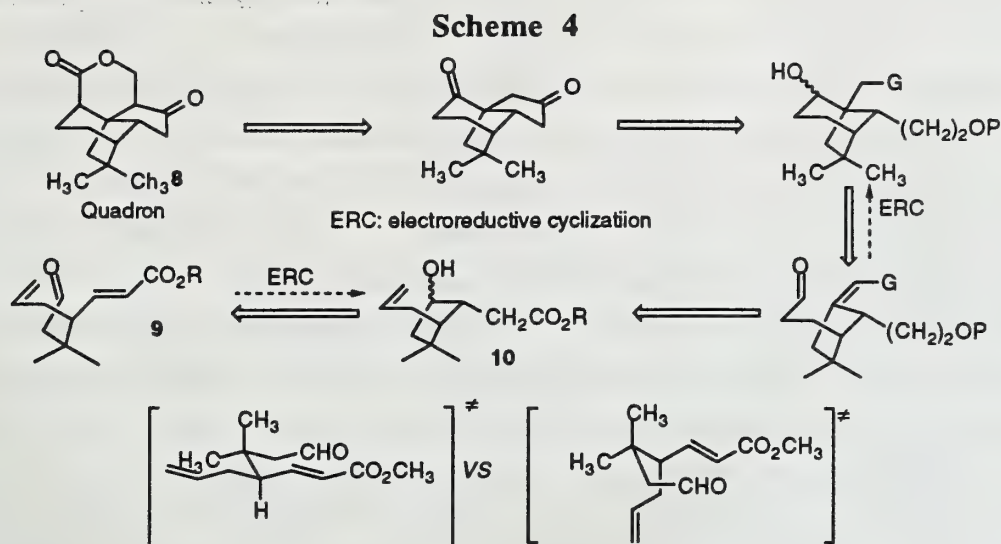


Table 1. comparison of reducing reagent

Reducing reagent	Conditions	% 6	% 7
cathode (Sn)	Et ₄ NOTs, <i>i</i> -PrOH, 25 °C	70	7
Na	<i>i</i> -PrOH, 25 °C	0	90
SmI ₂	<i>t</i> -BuOH/ HMPA/THF, 0 °C	0	trace
Na	HMPA/ THF (2:1), 0 °C	42	17

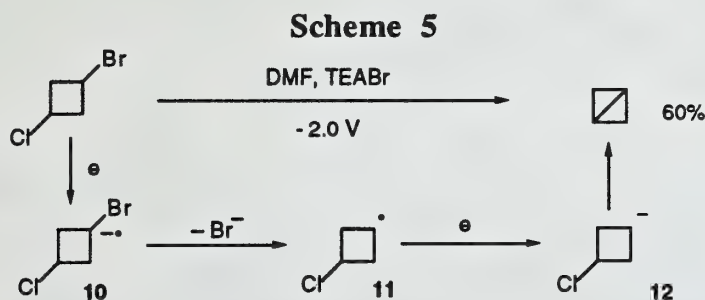
Coupling between an α,β -unsaturated esters and a carbonyl has been well studied by Little⁷. The reductive coupling has been applied to the total synthesis of quadrone **8** using electrochemistry as the key

steps (Scheme 4).⁸ The stereochemistry of the cyclization product can be explained by the preference of allyl group to occupy the equatorial position.



Bond cleavages

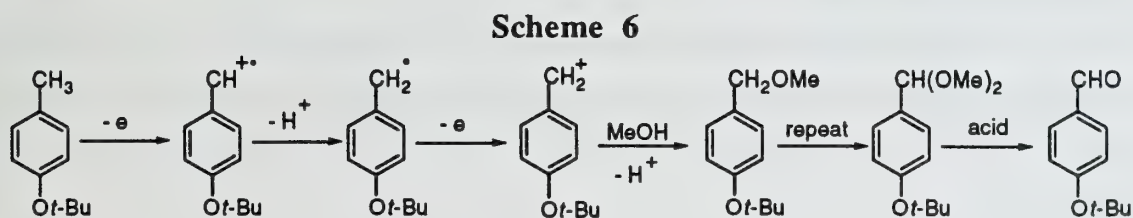
Cathodic reductions provide very good methods for cleavage of carbon-heteroatom single bonds. The reduction of organohalides has been widely studied. It is generally accepted that the reduction of alkyl halogen bonds take place according to a two step mechanism (scheme 5).² The radical anion **10** ejects the halide anion to generate radical **11** which can be quickly reduced to anion **12**. Reduction of organohalide is one of the most powerful method of constructing strained ring system such as bicyclobutane (Scheme 5).⁹



ANODIC OXIDATION

Oxidation of Electron Rich Aromatic Rings and Olefins

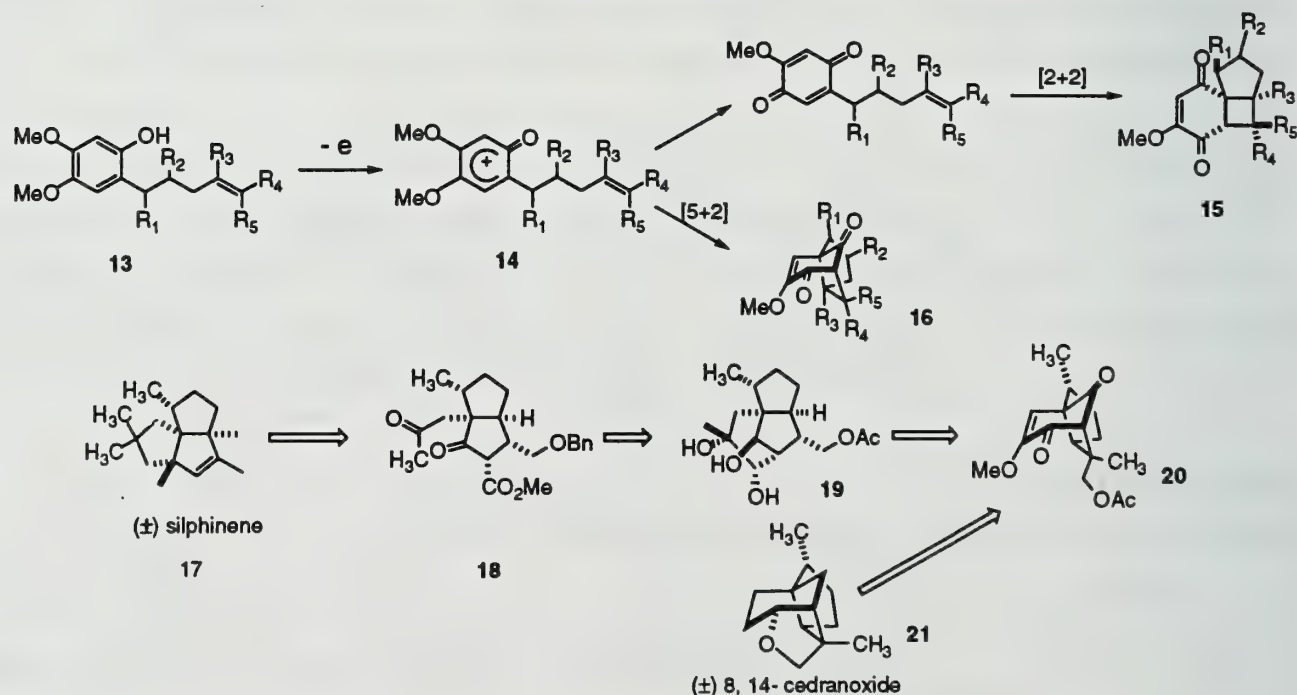
Electrolysis at the anode provides a powerful way for functionalization by oxidation. An important example of electrochemical functionalization involves anodic cleavage of carbon-hydrogen bond.² An example from the industry is the oxidation of the substituted toluene is oxidized to corresponding aldehyde (Scheme 6).¹⁰



Recently, oxidative cyclization has been received considerable attention, because compared to the free radical cyclization, these reaction can lead to highly functionalized products, which simplify further functionalization. Though several chemical methods exist for accomplishing these functionalization, these methods are limited by the acidic nature of oxidizing reagents. The electrochemical methods offer a mild oxidation since most functional groups can be oxidized at neutral conditions. Early success included the intramolecular coupling of phenyl ring to synthesize alkaloids.^{1d} Recently, work has been reported on the coupling between aromatic ring and olefin.^{11, 12} or between electron rich olefins.¹³ One common merit of those reactions is that the resulting product is highly functionalized.

The oxidation of the benzene ring of **13** results in a highly reactive intermediate **14**, which can undergo intramolecular [2+2] and [5+2] cycloaddition to give **15** and **16** depending on the substituents on the olefin (scheme).¹¹ This transformation has been used in many natural product syntheses. As an example, the [5+2] cycloaddition product **20** has been used as precursor for two natural products, silphene **17** and 8,14-cedranoxide **21** as shown in Scheme 7. The six membered ring of **19** can be opened to form fused bicyclic compound **18** with two carbonyl groups, which close to form angular tricyclic silphene **17**. The 8, 14-cedranoxide **21** can be synthesized by simple functional group manipulation. Clearly the success of these syntheses relies on the highly functionalized precursor available from the oxidative cycloaddition.

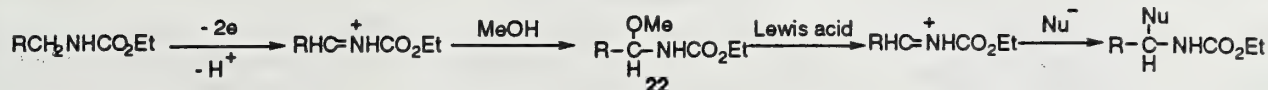
Scheme 7



Oxidation of Heteroatoms

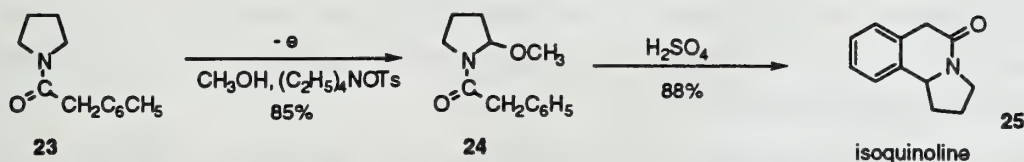
The oxidation of amides and carbamates is the one of the most efficient and useful functionalization by electrochemical methods. After oxidation, the primary intermediate N-acyliminium ion can be trapped by methanol, to afford α -methoxyamides **22**, which is a very useful substrate in alkaloid and amino acid synthesis.

Scheme 8



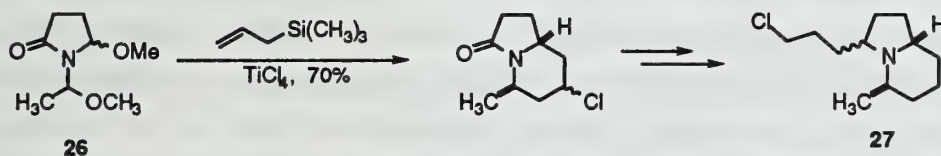
A wide variety of nucleophiles have been used for addition to the imium ion, including alcohols, water, silyl enol ethers, activated methylenes such as malonic ester, acetoacetic acid, furan, phosphorus derivatives. Shono and coworker have synthesized a series of alkaloids based on this method. A typical example is the oxidation of carbomethoxypyrrolidine **23** in methanol to afford the methyl ether **24**, which can be converted into isoquinoline **25** (Scheme 9).¹⁴ A similar reaction with piperidine derivatives has been used in the synthesis of piperidine alkaloids.¹⁵ In addition, optically active alkaloids can be synthesized by diastereoselective introduction of a substituent to the carbon.¹⁶

Scheme 9



Another useful application for preparing piperidine skeletons uses a unique [3+3] type reaction between allyltrimethylsilane and the dimethoxylated amides **26**, which can be prepared by dimethoxylation of N, N' dialkylamides. The synthesis of pharaoh ant trail pheromone **27** is shown as a typical example (Scheme 10).¹⁷

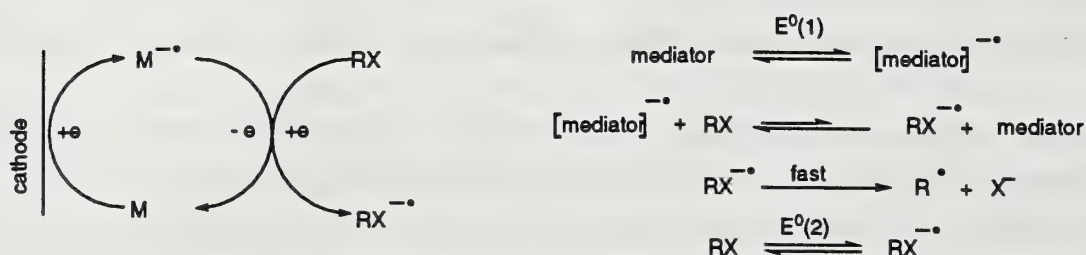
Scheme 10



INDIRECT ELECTROLYSIS

The examples discussed so far involve the reactions of intermediates produced directly at the electrode by heterogeneous electron transfer. But not all substrates are electroreactive, for example, very high potential is needed to oxidize alcohol, which makes the application of direct electroorganic synthesis limited. Another problem with this approach is that the reaction can be inhibited by the non-conducting film on the electrode. For a given conversion, the electrode potential required may be greater than that expected from theory. As an example, during the oxidative coupling of 2-naphthol, a non-conducting film is formed on the electrode and it inhibits further reaction. In recent years, attention has been paid to the indirect electrolysis in which the electrode is used to generate and regenerate a mediator reagent (Scheme 11). The mediator is generated reversibly at the electrode, and carried into solution to react. Typically, mediators are generated at potentials ($E^{\circ}1$) that are lower than that required for the corresponding direct electron transfer ($E^{\circ}2$) with the unfavorable equilibrium driven forward by a rapid and chemically irreversible follow up reaction.¹⁸

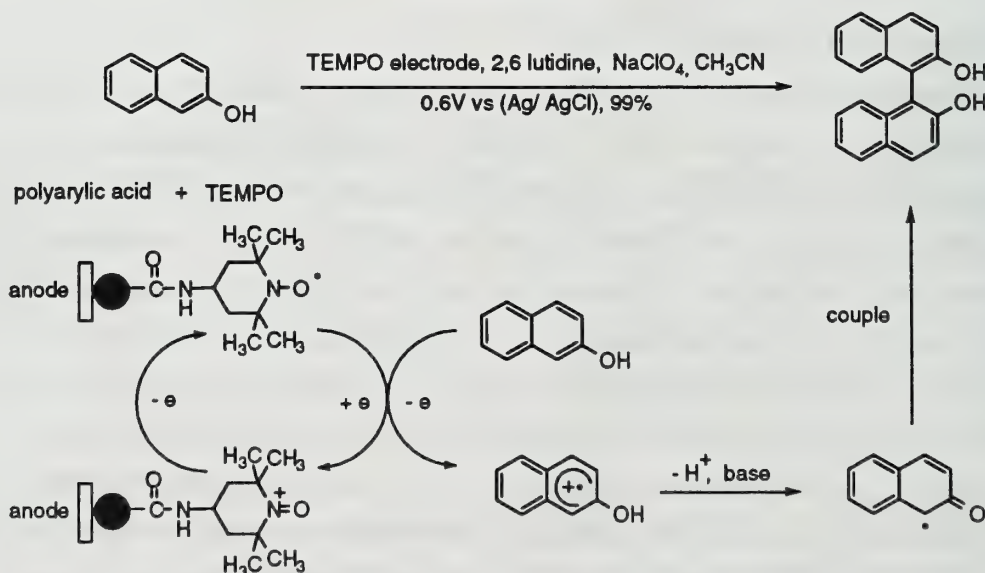
Scheme 11



Using indirect electrolysis, the electron transfer is homogenous between the substrates and mediators. Here the actual reduction or oxidation potential is constant. High selectivity is possible by choosing appropriate ion pair. As compared to chemical methods, a catalytic amount of mediator can be used instead of stoichiometric amount therefore simplifying the workup and the waste disposal. Since most of the reducing or oxidizing reagents are poisonous, this is advantageous. A lots of successful redox systems have been devolped in industry. As a typical example, the $\text{Mn}^{3+}/\text{Mn}^{2+}$ was used by Monsanto Company to synthesize sorbic acid.¹⁹

Halide cations have been used as mediators in oxidation reactions. Iodonium is able to oxidize primary alcohols to esters and secondary alcohols to ketones.²⁰ In industrial uses, benzylbenzoate is produced by oxidizing benzaldehyde in presence of potassium iodide.²¹ Organic compound are also used as mediators in electrolysis. For organic compound to act as mediator, it must be easily reduced or oxidized on the electrodes. TEMPO (2,2,6,6-tetramethylpiperidin-1-yloxy)-modified electrode has been used to oxidize 2-naphthol to give 1,1'-binaphol in excellent yield (Scheme 12).²² The TEMPO electrode was made by coating the graphite felt with a 40 nm thick poly(acrylic acid). The PAA layer was reacted with 4-amino TEMPO (64%), followed by cross-linking with hexamethylenediamine (16%) and butylation with dibutylsulfate to block th remaining carboxylate groups.

Scheme 12

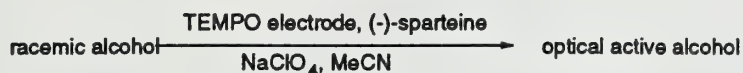


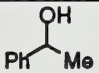
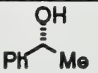
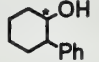
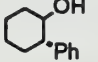
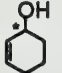
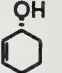
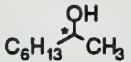
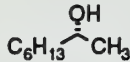
ENANTIOSELECTIVE REACTIONS BY ELECTROCHEMICAL METHODS

The complex nature of the electrochemical double layer makes the reaction mechanism very complicated but also yields the possibility of carrying out highly stereoselective and stereospecific

reactions in this region. Early attempts included using chiral solvents or additives²³ to introduce chiral environment in the electrochemical double layer. But the er generally is low and highly substrate dependent. Recently, using polymer coated electrode and chiral base to effect asymmetric reaction have achieved impressive results. Using TEMPO modified electrode (cross link polymer modified electrode) and (-)-sparteine as chiral base Kashigawagi and coworkers reported kinetic resolution of alcohols up to greater than 99:1 er (Scheme 13).²⁴

Scheme 13

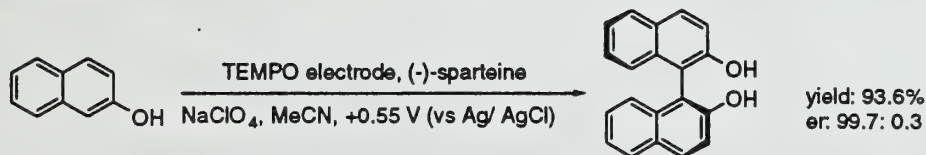


racemic alcohol	product	yield %	er
		46	99.6: 0.4
		45	99.7: 0.3
		48	99.9: 0.1
		47	99.8: 0.2

It is believed that the substrate, the chiral base and the electrode interact with each other strongly in a suitable sized domain which is formed by the cross-linking polymer. The electrons are transferred from the electrode to the substrate *via* the mediator TEMPO. (-)-Sparteine selectively deprotonates the alcohol radical cation which leads to the chiral resolution.

The system has also been used for enantioselective coupling of 2-naphthol. Under similar reaction condition, the oxidative coupling of 2-naphthol gave 1,1'-binaphthol with up to 99.7: 0.3 er and 93.6% yield (Scheme 14).²⁵ This provides the simplest way of making enantiomeric pure binaphthol, which is extensively used in asymmetric syntheses.

Scheme 14



CONCLUSION

Electrochemical methods clearly provide a unique way of effecting oxidative and reductive reactions. From the economic and the environmental point of view, it is cheap, clean. The complicated nature of the electrochemical double layer makes the reaction mechanism very complicated, however it also yields the possibility of carrying out highly enantioselective reactions.

REFERENCE

- (1) (a) *Topics in Current Chemistry* Springer-Verlag: Berlin Heidelberg, 1997, vol. 185 (b) *Topics in Current Chemistry* Springer-Verlag: Berlin Heidelberg, 1994, vol. 170. (c) *Topics in Current Chemistry* Springer-Verlag: Berlin Heidelberg, 1990, vol. 152. (d) *Topics in Current Chemistry* Springer-Verlag: Berlin Heidelberg, 1988, vol. 148.
- (2) (a) Kyriawu, D. *Modern Electroorganic Chemistry* Springer-Verlag: Berlin Heidelberg, 1994. (b) Shono, T. *Electroorganic Chemistry as a New Tool in Organic Synthesis* Springer-Verlag: Berlin, Heidelberg, 1984. (c) Shono, T. *Electroorganic Synthesis* Academic Press: San Diego, 1991. (d) Fry, A. J. *Synthetic Organic Electrochemistry* John Wiley & Sons, Inc., 1989.
- (3) Baizer, M. M. 1969, U. S. Patent, 3193408.
- (4) (a) Shono, T.; Mitani, M. *J. Am. Chem. Soc.* 1971, 93, 5284. (b) Shono, T.; Nishiguchi, I.; Ohmizu, H.; Mitani, M. *J. Am. Chem. Soc.* 1978, 100, 545. (c) Swartz, J.; Mahachi, T.; Miller, K. *J. Am. Chem. Soc.* 1988, 110, 3622. (d) Shono, T.; Kashimura, S.; Mori, Y. *J. Org. Chem.* 1989, 54, 6001.
- (5) Shono, T.; Kise, N.; Fujimoto, T.; Tominaya, N.; Morita, H. *J. Org. Chem.* 1992, 57, 7175.
- (6) (a) Kise, N.; Suzumoto, T.; Shono, T. *J. Org. Chem.*, 1994, 59, 1407. (b) Gorny, R.; Schafer, H.; Frohlich, R. *Angew. Chem. Int. Ed. Engl.* 1995, 34, 2007.
- (7) Fry, A. J.; Little, R. D.; Leonetti, J. *J. Org. Chem.*, 1994, 59, 5017. Kise, N.; Mashiba, S.; Ueda, N. *J. Org. Chem.* 1998, 63, 7931.
- (8) Sowell, C. G.; Wolin, R.L.; Little, R. D. *Tetrahedron Lett.* 1990, 31, 485.
- (9) Rifi, M. *J. Am. Chem. Soc.* 1967, 89, 4442.
- (10) Barl, M.; Degner, D.; Hoffmann Chem. Abstr. 1981, 95, 24556y.
- (11) (a) Maki, S.; Kosemura, S.; Yamamura, S.; Kawano, S.; Ohba, S. *Chem. Lett.* 1992, 652. (b) Maki, S.; Toyoda, K. Kosemura, S.; Yamamura, S. *Chem Lett.* 1993, 1059. (c) Maki, S.; Asaba, N.; Kosemura, S.; Yamamura, S. *Tetrahedron Lett.* 1992, 33, 4169. (d) Maki, S.; Kosemura, S.; Yamamura, S.; Ohba, S. *Tetrahedron Lett.* 1993, 34, 6083. (e) Maki, S.; Toyoda, K.; Mori, T.; Kosemura, S.; Yamamura, S. *Tetrahedron Lett.* 1994, 35, 4839.
- (12) Swenton, J. S.; Callinan, A.; Chen, Y.; Rohde, J. J.; Kerns, M.; Morrow, G. *J. Org. Chem.* 1996, 61, 267.
- (13) (a) Tinao-wooldridge, L.; Moeller, K.; Hunson, C. *J. Org. Chem.* 1994, 54, 2381. (b) Hunds, C.; Moeller, K. *J. Am. Chem. Soc.*, 1994, 116, 3347. (c) New, D.; Tesfai, Z., Moeller, K. *J. Org. Chem.*, 1996, 61, 1578. (d) Moeller, K.; Hudson, C. Tinao-wooldridge, L. *J. Org. Chem.* 1993, 58, 3347.
- (14) Shono, T.; Matsumura, Y.; Tsubata, K. *J. Am. Chem. Soc.* 1981, 103, 1172. Moeller, K.; Beal, L. *Tetrahedron* 1998, 39, 4639.
- (15) Shono, T.; Matsumura, Y.; Uchida, K.; Tsubata, K.; Makino, A. *J. Org. Chem.* 1984, 49, 300.
- (16) Shono, T.; Matsumura, Y.; Tsubata, K.; Uchida, K. *J. Org. Chem.* 1986, 51, 2590
- (17) Shono, T.; Matsumura, Y.; Uchida, K.; Kobayashi, H. *J. Org. Chem.*, 1985, 50, 3243.
- (18) Utley, J. *Chem Soc. Rev.*, 1997, 26, 157.
- (19) Coleman, J.; Hallcher, R.; McMackins, D.; Rogers, T.; Wagenkenchett, J. *Tetrahedron* 1991, 47, 809.
- (20) Shono, T.; Matsumura, Y.; Hayski, J. Mitsoguchi, *Tetrahedron Lett.* 1979, 20, 165.
- (21) Dixit, G.; Rastogi, R.; Zutshi, K. *Electrochim. Acta.* 1982, 27, 561.
- (22) Kashiwagi, Y.; Ono, H.; Osa, T. *Chem. Lett.* 1993, 81.
- (23) Nielsen, M.; Batanero, B.; Lohl, T.; Shafer H. *Chem. Eur. J.* 1997, 3, 12.
- (24) Kashiwagi, Y.; Yanagisawa, Y.; Kurashiwa, F.; Anzai, J.; Osa, T.; Bobbit *J. Chem. Com.* 1996, 2745.
- (25) Osa, T; Kashiwagi, Y.; Yanagisawa, Y.; Bobbit, J. *J. Chem. Soc. Chem. Com.*, 1994, 25, 35.

THE STRUCTURAL AND MECHANISTIC RELATIONSHIP OF ISOPENICILLIN N SYNTHASE AND 2-KETOGLUTARATE-DEPENDENT ENZYMES

Reported by Ellen D. Eberhard Hill

December 3, 1998

INTRODUCTION

Studies of structurally related enzymes can provide understanding of the principles involved in the evolution of catalytic function. Related proteins have significant homology in their primary sequences and tertiary structures. Moreover, the proteins may utilize the same mechanistic strategy to catalyze different overall reactions on a variety of substrates. Investigations into these enzyme relationships have led to a theory of enzymatic evolution: Enzymes evolve by altering their substrate specificity, while maintaining their catalytic machinery. This hypothesis is strengthened by the structural and mechanistic relationship of isopenicillin N synthase (IPNS) and 2-ketoglutarate (2KG)-dependent enzymes.

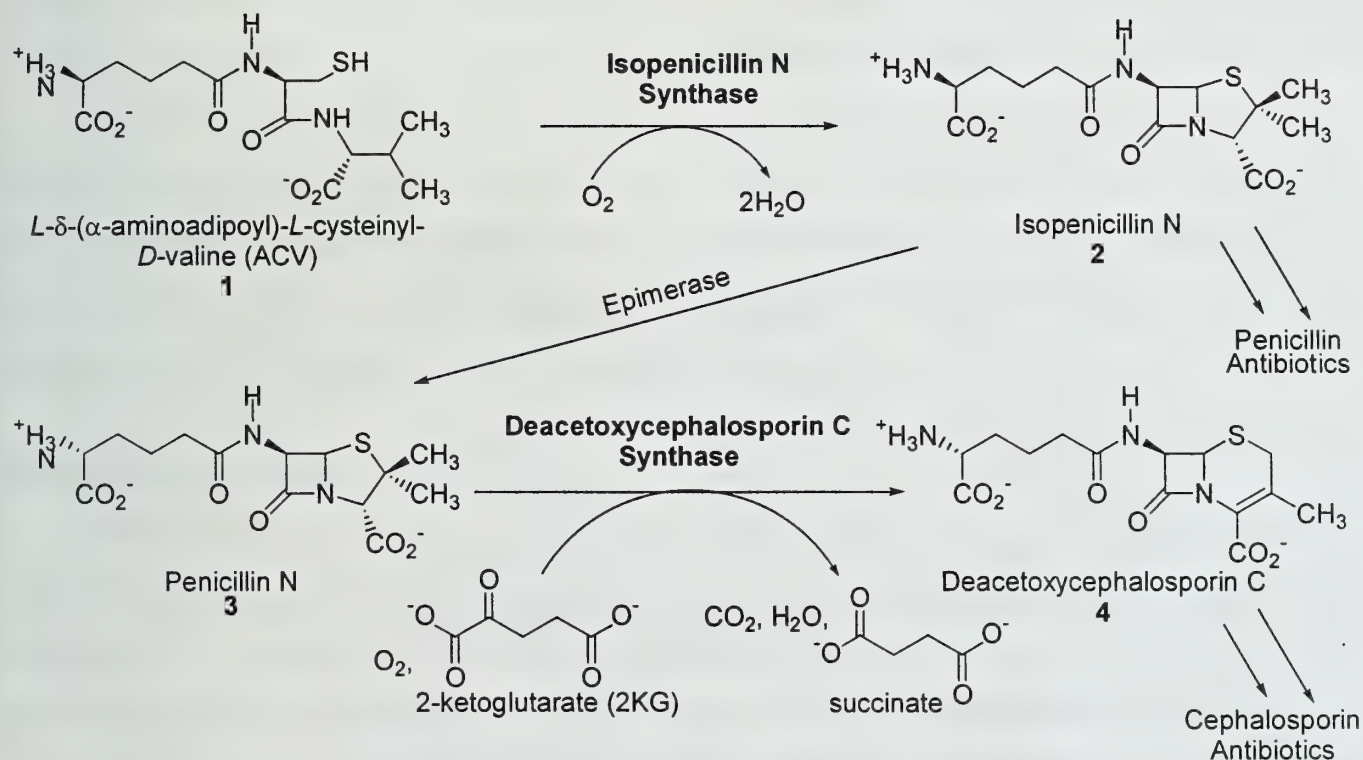


Figure 1. Biosynthetic Pathway of Penicillin and Cephalosporin Antibiotics

The evolutionary relationship of IPNS and 2KG-dependent enzymes was discovered due to the extensive investigations of antibiotic biosynthesis (Figure 1). IPNS catalyzes the last shared step in the biosynthesis of penicillin and cephalosporin antibiotics, the oxidative double cyclization of **1** to **2**. A 2KG-dependent enzyme, deacetoxycephalosporin synthase (DAOCS), catalyzes the oxidative ring

expansion of **3** to **4**, the second step towards the synthesis of cephalosporin antibiotics. Both enzymes use molecular oxygen as the oxidant, but only DAOCS requires 2KG in its mode of oxygen activation. The crystal structure of Mn(II)-bound IPNS identified essential residues which were subsequently found to be conserved in the primary sequences of (DAOCS) and other 2KG-dependent enzymes.¹ The recent crystal structure of DAOCS demonstrated the similarity of its tertiary structure with IPNS.² The active sites of both enzymes are buried within the barrel of a "jelly roll" motif, and the α -helices which frame the jelly roll are also conserved between the two structures.

Because of their structural and reactive similarities, IPNS and 2KG-dependent enzymes may have evolved from a common ancestor to catalyze different reactions. In this abstract, the structural and mechanistic similarity of these enzymes will be examined. Synthetic models, which have been developed to investigate the role of the iron coordination sites in the mechanisms of these enzymes, will also be discussed.

MONONUCLEAR NON-HEME IRON CENTERS

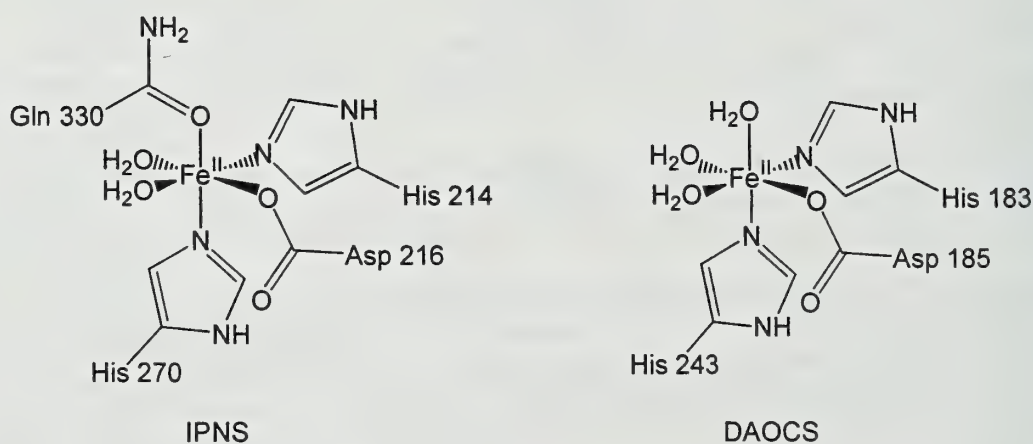


Figure 2. Mononuclear Non-Heme Iron(II) Centers

The iron coordination sites of IPNS and DAOCS are characteristic of enzymes with mononuclear, non-heme iron centers (Figure 2).^{3,4} The octahedral iron is ligated by three protein residues, which are conserved in the primary sequences of this class of enzymes in the motif: His-X-Asp-X_{n=50-70}-His. These endogenous ligands are oriented *cis* to each other, resulting in a tripodal configuration. In the DAOCS structure, water molecules occupy the three remaining binding sites. However, in the IPNS structure, only two of the remaining binding sites are occupied by water molecules. The third is occupied by another endogenous ligand, glutamine 330 (Gln 330).

This fourth endogenous ligand distinguishes IPNS from the 2KG-dependent enzymes. Sequence comparison of 11 available IPNS sequences shows that Gln330 is conserved in all but one sequence, while no homologous ligand is observed in the 2KG-dependent enzymes. Therefore, it is reasonable that the ligand may have a function unique to IPNS. The substrate-bound crystal structure of IPNS:Fe^{II}, indicates that ACV displaces Gln 330 from the iron center upon substrate binding.⁵ Moreover, site-specific mutagenesis indicated that Gln330 is not essential for catalysis.^{6,7} Two functions, which have been proposed for Gln 330 are to prevent 2KG binding or to promote Fe(II) binding.^{7,8}

SUBSTRATE BINDING

The open coordination sites on the non-heme iron center allow the substrate to bind directly to the iron. The structures of **1**-complexed IPNS and 2KG-complexed DAOCS have been determined by X-ray crystallography.^{2,5} It is observed that 2KG binds to Fe(II) in DAOCS in a bidentate fashion with octahedral geometry. In IPNS, **1** binds to Fe(II) in a monodentate fashion with square pyramidal geometry and this has also been observed spectroscopically.⁹⁻¹¹

In both structures, substrate carboxylate groups are stabilized by a conserved arginine-X-serine motif. This motif is also observed in the sequences of other 2KG-dependent enzymes.¹² Site-specific mutagenesis has shown that the arginine residue is involved in binding **1** and 2KG, while the serine residue appears to be critical only in the binding of **1** by IPNS.¹²⁻¹⁵ In prolyl-4-hydroxylase, a 2KG-dependent enzyme, the arginine residue is conserved as a lysine.¹⁶

OXYGEN ACTIVATION

Substrate binding to the iron is considered to activate the iron center towards the binding of oxygen.² The substrate binds through an anionic ligand, reducing the Fe^{II}/Fe^{III} reduction potential. This activates the iron center toward oxygen binding because it occurs with concomitant oxidation of Fe(II) to Fe(III) resulting in the formation of superoxide (Figure 3). This tuning of the iron center's redox properties protects the enzyme from reactive intermediates, such as superoxide, by ensuring that they form only in the presence of substrate.

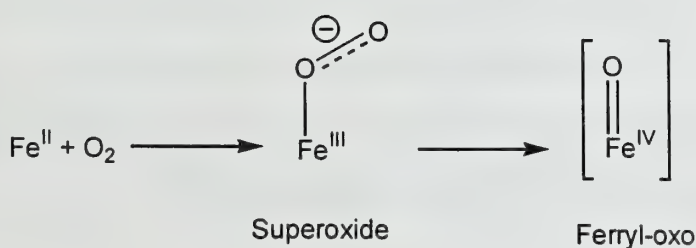


Figure 3. Oxygen Activation

In order to achieve reaction with organic substrates, molecular oxygen must be reduced to superoxide or peroxide.¹⁷ Because there is no definitive proof for which species is active in these non-heme iron enzymes, mechanisms which proceed with either oxygen species have been proposed. Analysis of the crystal structure of IPNS:Fe(II):1:NO prompted the proposal that a superoxide radical abstracts a substrate hydrogen, because the oxygen atom from NO was positioned near the hydrogen to be abstracted.⁵ Model studies also support the participation of a superoxide intermediate in the mechanism.^{18,19}

Oxygen activation is an energetically demanding process which results in formation of a reactive ferryl-oxo intermediate, $[\text{Fe}^{\text{IV}}=\text{O}]$ (Figure 3). In the 2KG-dependent enzymes, the energetic driving force for this process is derived from the oxidative decarboxylation of the 2-ketoglutarate cosubstrate.²⁰ In IPNS the formation of the ferryl-oxo intermediate is coupled with the formation of the beta-lactam ring. It is known that IPNS does not use the 2KG cosubstrate, but the energetic driving force for the formation of the ferryl-oxo intermediate has not been determined.

The ferryl-oxo intermediate has not been spectroscopically observed for the non-heme iron proteins, presumably because it does not accumulate in detectable amounts. The analogous intermediate has been observed spectroscopically in heme proteins, in which the porphyrin is a major stabilizing force for this highly reactive species.^{21,22} In the non-heme enzymes, the oxygen-binding pocket is lined with hydrophobic residues which may help protect the ferryl-oxo from side reactions.²³ Efforts to trap the iron-oxo intermediate for crystallographic characterization are in progress.²⁴

REACTION OF THE FERRYL INTERMEDIATE

The energy stored in the ferryl intermediate is used to catalyze a reaction requiring the activation of an aliphatic C-H bond (Figure 4).³ The overall reactions can be divided into two groups: oxidations and oxygenations. The O_2 -derived oxygen atom in the ferryl-oxo intermediate is either eliminated as water (oxidations) or incorporated into the product (oxygenations).

Oxidation reactions, as catalyzed by IPNS and DAOCS, are oxidative cyclizations. The mechanisms proposed for these reactions begin with the abstraction of a substrate hydrogen by the ferryl-oxo oxygen atom.²⁵⁻²⁹ The alkyl radical undergoes an intramolecular transfer to form the new cycle in the product. The mechanism by which these enzymes avoid recombination of the alkyl radical with the intermediate hydroxyl radical is the topic of model studies.³⁰

Many 2KG-dependent enzymes catalyze oxygenations, such as hydroxylations (Figure 4). These transformations have been shown to proceed with retention of configuration.²⁹ The ferryl-oxo intermediate abstracts a hydrogen from the substrate to form an alkyl radical, which may coordinate to the iron atom before it is transferred back to the hydroxyl radical *via* reductive elimination. This pathway is consistent with an alkyl radical intermediate which does not invert before recombination with the hydroxyl radical.

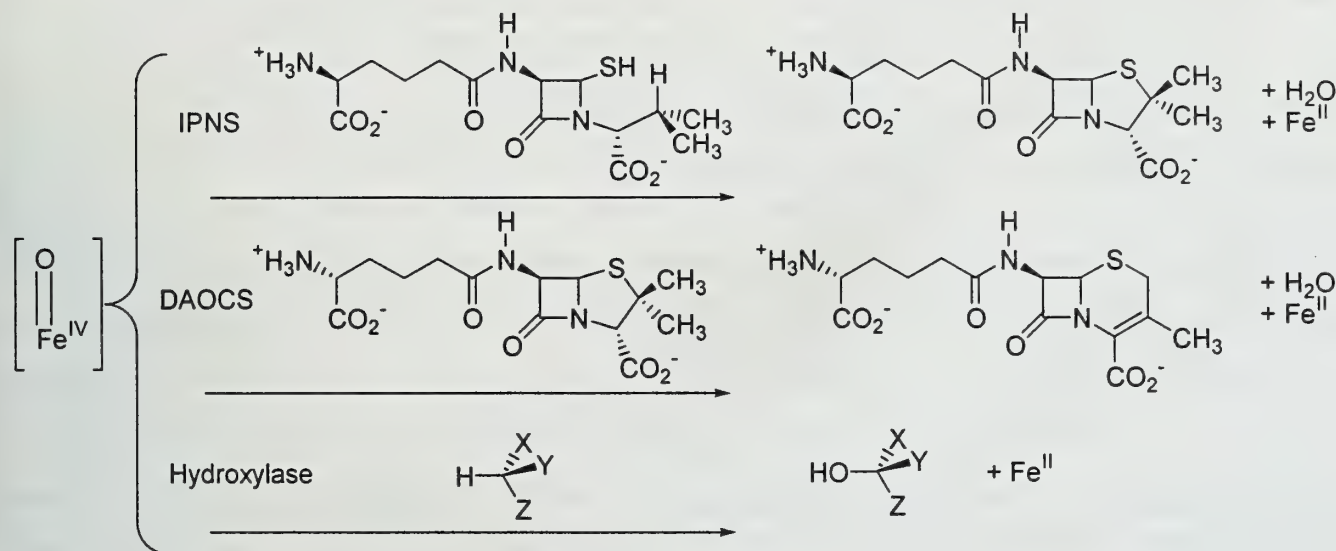


Figure 4. Reactions of the Ferryl Intermediate

MECHANISTIC OVERVIEW

The current understanding of the mechanisms of IPNS and the 2KG-dependent enzymes is based on extensive substrate analog experiments and crystallographic studies.^{1,2,5,31} Overall, these reactions are four-electron reactions, which utilize the full oxidizing power of molecular oxygen. The mechanisms can be considered to proceed in two steps, each requiring two electrons. The first step is the oxygen activation, which produces the high energy ferryl intermediate. For 2KG-dependent enzymes, the oxidative decarboxylation of the cosubstrate provides the driving force for this first step.²⁰ The energetic driving force for this step in the IPNS reaction has not been addressed. In the second step, the energy associated with the ferryl intermediate is used to activate an aliphatic C-H bond to effect hydroxylation, oxidative cyclization, or oxidative ring expansion.

SYNTHETIC MODELS

A better mechanistic understanding of the reactions catalyzed by these non-heme iron enzymes has been approached by studies of the reactivity of ferrous ion in an environment mimicking the protein

environment. The results of these model studies provide support for the proposed enzymatic mechanisms. Complexes which mimic features of the coordination sites of these non-heme iron enzymes and their reactions with molecular oxygen have been investigated (Figure 5).

Que and coworkers have used the tetradentate ligand, tris(2-pyridylmethyl)amine (TPA), in complexes which mimic the tripodal coordination of Fe(II) in the active site (Figure 5). In an IPNS mimic, **5**, the ferrous iron center is complexed with TPA and a thiolate ligand, 2,4,6-trimethylthiophenolate, resulting in a square pyramidal geometry around the iron atom.³² The same geometry is observed in substrate-bound IPNS. At low temperatures, the complex reacts with O₂, and a mechanism involving a ferryl-oxo intermediate was proposed. No intermediates could be observed by EPR or UV-vis spectroscopy, even when cooled to -80 °C.

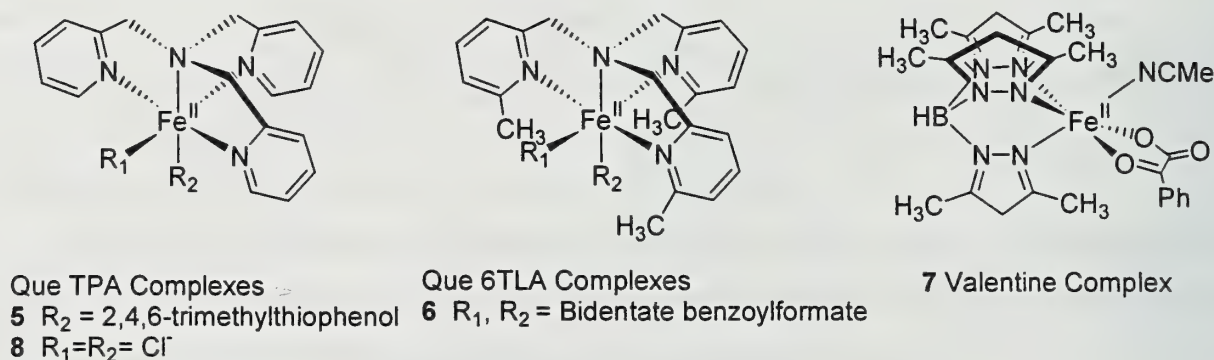


Figure 5. Biomimetic Complexes

The 2-oxoacid dependence of the 2KG-dependent enzymes has been modeled in two separate systems. Que and coworkers utilized another tetradentate ligand, tris[(6-methyl-2-pyridyl)methyl]amine (6TLA), while Valentine and coworkers applied the tridentate (3,5-dimethyl-1-pyrazolyl)borohydride ligand (Figure 5).^{18,19} Both systems were complexed with benzoylformate (BF) to yield complexes **6** and **7**. The crystal structure and spectroscopic data indicated that BF bound in a bidentate fashion, corresponding to the bidentate binding of the 2KG cosubstrate in the enzymes. Upon exposure to oxygen, the benzoylformate undergoes quantitative decarboxylation, producing carbon dioxide, benzoic acid, and two additional oxidizing equivalents. The most likely mechanism of decarboxylation is coupled to the nucleophilic attack of the superoxide on the 2-oxo group in 2KG.

In the enzymatic decarboxylation, the two oxidizing equivalents produced by oxidative decarboxylation are proposed to take the form of the ferryl-oxo intermediate. Attempts to identify the intermediate oxygen species in the model studies have not been successful, but the oxidizing equivalents have been trapped by indirect methods. Que and coworkers incubated **6** with O₂ and 2,4-di-*tert*-butylphenol and recovered near stoichiometric amounts of the corresponding biphenol. A radical

mechanism is proposed for this reaction. Labeling experiments showed that after incubation of **6** and PPh_3 with $^{18}\text{O}_2$, the oxygen label had been incorporated into the benzoic acid and the PPh_3O product. Finally, Valentine and coworkers observed an epoxidation reaction when **7** was incubated with O_2 and *cis*-stilbene. While these results are consistent with the involvement of a ferryl intermediate, direct observation of the intermediate must still be pursued.

Que and coworkers have attempted to mimic the oxidative ligand transfer that is catalyzed by IPNS and DAOCS by utilizing another TPA complex, **8**.^{30,33} In the enzymatic mechanisms, the intermediate alkyl radical undergoes an intramolecular transfer rather than recombining with the hydroxyl radical. Reaction of **8** with *tert*-butylhydroperoxide and cyclohexane, produced greater than 70% yield of the corresponding halo-cyclohexane, indicating that a halide was transferred to the alkyl substrate in preference over the hydroxyl radical. The mechanism was proposed to shuttle between Fe(III) and Fe(V) and included a high-valent oxo intermediate. However, it has since been shown that this reaction most likely proceeds by freely diffusing radicals, not via the proposed oxidative ligand transfer.^{34,35}

The model studies have contributed to the fundamental understanding of the reactivity of the non-heme iron centers. Additional evidence is needed to validate the mechanisms proposed for the observed reactions.

CONCLUSION

The relationship of IPNS and the 2KG-dependent enzymes lends validity to the theory that enzymes evolve by altering substrate specificity while maintaining the same mechanistic strategy. The members of this family of enzymes utilize a non-heme iron center in a common mechanism of dioxygen activation. The energy profiles along the reaction coordinate may be similar for the reactions catalyzed by these enzymes: oxygen is activated, resulting in the formation of a high energy intermediate, which then drives an energetically "downhill" transformation, involving the abstraction of an aliphatic hydrogen atom. Thus, while the overall reactions (hydroxylation, oxidative cyclization, or oxidative ring expansion) are different, they can all proceed by a similar mechanistic strategy. This illustrates how conserved structural scaffolds can be used to catalyze different reactions in nature. Future work investigating these mechanistic proposals will solidify the evolutionary relationship of these enzymes.

REFERENCES

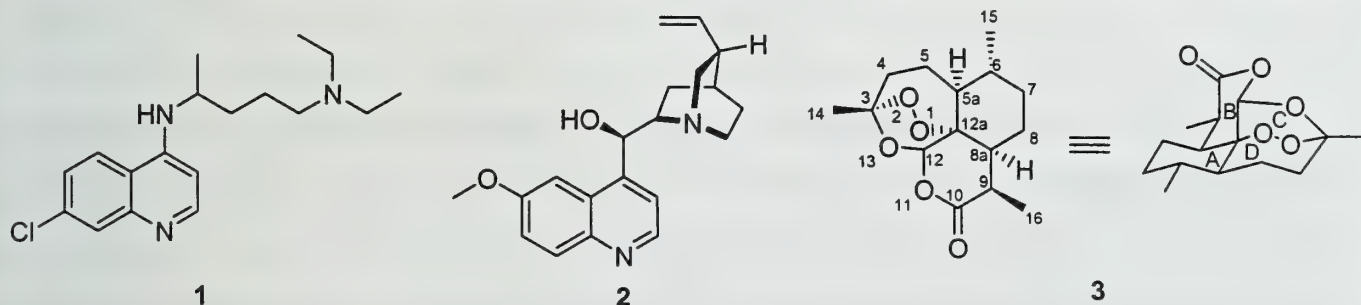
- 1) Roach, P. L.; Clifton, I. J.; Fülöp, V.; Harlos, K.; Barton, G. J.; Hajdu, J.; Andersson, I.; Schofield, C. J.; Baldwin, J. E. *Nature* **1995**, *375*, 700-704.
- 2) Valegård, K.; Terwisscha van Scheltinga, A. C.; Lloyd, M. D.; Hara, T.; Ramaswamy, S.; Perrakis, A.; Thompson, A.; Lee, H.-J.; Baldwin, J. E.; Schofield, C. J.; Hajdu, J.; Andersson, I. *Nature* **1998**, *394*, 805-809.
- 3) Que, L.; Ho, R. Y. N. *Chem. Rev.* **1996**, *96*, 2607-2624.
- 4) Hegg, E. L.; Que, L. *Eur. J. Biochem.* **1997**, *250*, 625-629.
- 5) Roach, P. L.; Clifton, I. J.; Shibata, N.; Schofield, C. J.; Hajdu, J.; Baldwin, J. E.; Hensgens, C. M. H. *Nature* **1997**, *387*, 827-830.
- 6) Landman, O.; Borovok, I.; Aharanowitz, Y.; Cohen, G. *FEBS Letters* **1997**, *405*, 172-174.
- 7) Sami, M.; Brown, T. J. N.; Roach, P. L.; Schofield, C. J.; Baldwin, J. E. *FEBS Letters* **1997**, *405*, 191-194.
- 8) Rowe, C. J.; Shorrock, C. P.; Claridge, T. D. W.; Sutherland, J. D. *Chemistry & Biology* **1998**, *5*, 229-239.
- 9) Chen, V. J. *J. Biol. Chem.* **1989**, *264*, 21677-21681.
- 10) Orville, A. M. *Biochemistry* **1992**, *31*, 4602-4612.
- 11) Randall, C. R. *Biochemistry* **1993**, *32*, 6664-6673.
- 12) Passoja, K.; Myllyharju, J.; Pirskanen, A.; Kivirikko, K. I. *FEBS Letters* **1998**, *434*, 145-148.
- 13) Lukacin, R.; Britsch, L. *Eur. J. Biochem.* **1997**, *249*, 748-757.
- 14) Loke, P.; Sim, T.-S. *FEMS Microbiology Letters* **1998**, *164*, 107-110.
- 15) Loke, P.; Sim, T.-S. *FEMS Microbiol. Lett.* **1998**, *165*, 353-356.
- 16) Myllyharju, J.; Kivirikko, K. I. *EMBO J.* **1997**, *16*, 1173-1180.
- 17) Feig, A. L.; Lippard, S. J. *Chem. Rev.* **1994**, *94*, 759-805.
- 18) Chiou, Y.-M.; Que, L. *J. Am. Chem. Soc.* **1995**, *117*, 3999-4013.
- 19) Ha, E. H.; Ho, R. Y. N.; Kisiel, J. F.; Valentine, J. S. *Inorg. Chem.* **1995**, *34*, 2265-2266.
- 20) Salowe, S. P.; Marsh, E. N.; Townsend, C. A. *Biochemistry* **1990**, *29*, 6499-6508.
- 21) Ortiz de Montellano, P. R., Ed. *Cytochrome P450: Structure, Mechanism, and Biochemistry*; Plenum: New York, 1985.
- 22) Dawson, J. H.; Sono, M. *Chem. Rev.* **1987**, *87*, 1255-1276.
- 23) Rétey, J. *Angew. Chem. Int. Ed. Engl.* **1990**, *29*, 355-361.
- 24) Rutledge, P. J.; Adlington, R. M.; Baldwin, J. E.; Clifton, I. J.; Roach, P. L. *FASEB J.* **1998**, *11*, A884.
- 25) Baldwin, J. E.; Adlington, R. M.; Marquess, D. G.; Pitt, A. R.; Porter, M. J.; Russell, A. T. *Tetrahedron* **1996**, *52*, 2537-2556.
- 26) Cooper, R. D. G. *Bioorg. Med. Chem.* **1993**, *1*, 1-17.
- 27) Salowe, S. P.; Krol, W. J.; Iwata-Reuyl, D.; Townsend, C. A. *Biochemistry* **1991**, *30*, 2281-2292.
- 28) Townsend, C. A.; Basak, A. *Tetrahedron* **1991**, *47*, 2591-2602.
- 29) Basak, A.; Salowe, S. P.; Townsend, C. A. *J. Am. Chem. Soc.* **1990**, *112*, 1654-1656.
- 30) Kojima, T.; Leising, R. A.; Yan, S.; Que, L. *J. Am. Chem. Soc.* **1993**, *115*, 11328-11335.
- 31) Baldwin, J. E.; Bradley, M. *Chem. Rev.* **1990**, *90*, 1079-1088.
- 32) Zang, Y.; Que, L. *Inorg. Chem.* **1995**, *34*, 1030-1035.
- 33) Leising, R. A.; Zang, Y.; Que, L. *J. Am. Chem. Soc.* **1991**, *113*, 8555-8557.
- 34) MacFaul, P. A.; Ingold, K. U.; Wayner, D. D. M.; Que, L. *J. Am. Chem. Soc.* **1997**, *119*, 10594-10598.
- 35) MacFaul, P. A.; Ingold, K. U.; Wayner, D. D. M. *Acc. Chem. Res.* **1998**, *31*, 159-162.

Reported by Justin Shey

10 December 1998

INTRODUCTION

Malaria is the cause of death for about one million people annually and infects up to 3 million.^{1,2} Four species of parasitic protozoa in the genus *Plasmodium* are responsible for malaria, and the strain *P. falciparum* leads to the most deaths by causing cerebral malaria. Chloroquine (1) and other synthetic quinoline alkaloids of quinine (2) have been the traditional treatment for malaria. While 2 is an effective antimalarial drug, it causes adverse side effects in some patients. Normally, the parasite in the blood phase thrives by hemoglobin digestion and polymerization of released heme to hemozoin, which is then stored in their food vacuoles. Antimalarial quinoline alkaloids are believed to kill malarial cells by binding to the released heme preventing polymerization. The resulting accumulation of heme due to drug treatment apparently causes parasitic membranes to burst and also inactivates hemoglobin proteases that are necessary for the survival of the parasite.



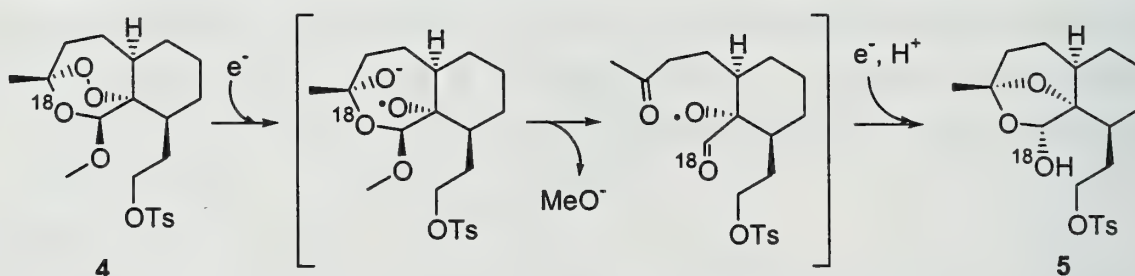
Unfortunately, certain malarial parasites have developed resistance to chloroquine and other related alkaloids. This fact led researchers in China to search for the identity of the active compound present in ancient malarial cures. In 1972, they discovered artemisinin (qinghaosu, 3) in the extracts of the leaves of the plant *Artemisia annua*. Artemisinin was found to be a potent antimalarial compound, and much research has been conducted on understanding its mode of action. This report will focus on chemical experiments performed to elucidate the mechanism of action of artemisinin and other related trioxanes.

MECHANISTIC RATIONAL BASED ON A CARBON CENTERED RADICAL

To gain molecular understanding of the mechanism of artemisinin activity, Posner and coworkers synthesized the peroxy tosylate 4, a known antimalarial compound, 50% enriched with ¹⁸O at

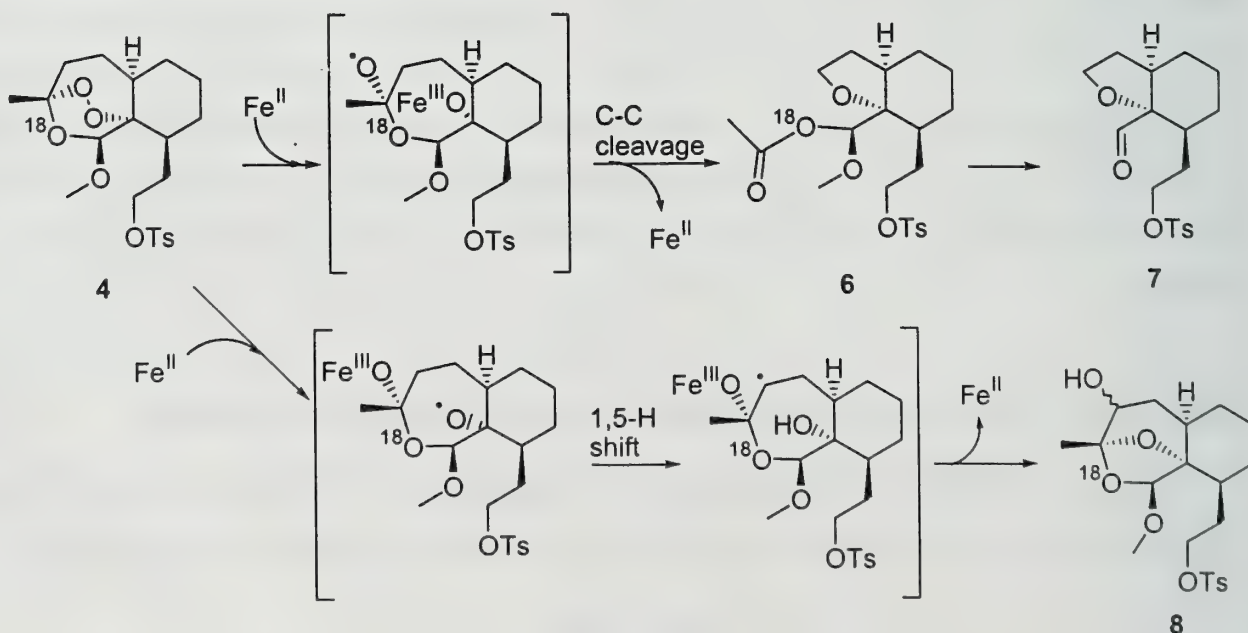
the 13 position.³ Treatment of **4** with reducing agents samarium diiodide, zinc, Ph_3CLi , or Bu_3SnH in the presence of AIBN produced **5** as shown in Scheme 1. When **4** was treated with the peroxide cleaving reagents Me_2S , PPh_3 , or sodium dithionite, there was no reaction. To more closely match the biological situation, **4** was also treated with Fe^{II} bromide or with hemin, the Fe^{III} form of heme, and benzyl mercaptan. The products obtained were **6**, **7**, and **8** as shown in Scheme 2. The formation of **6** and **7** were rationalized by Fe^{II} induced cleavage of the peroxide bond leaving Fe^{III} bound to O-1, followed by C-C bond cleavage to form **6** which can then decompose to the aldehyde **7**. The pathway leading to **8** is rationalized by an iron-oxo bond that forms initially on O-2, and is followed by a 1,5-hydrogen shift to afford a secondary carbon centered radical at position 4. Subsequent steps yield dioxolane alcohol **8**. These results were taken to show that Fe^{II} reaction with **4** proceeds via a different pathway than other reducing agents.

Scheme 1

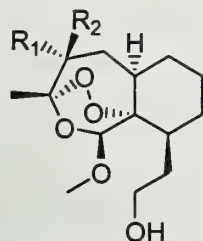


Posner's lab performed studies that support the importance of the proposed carbon centered radical for the formation of alcohol **8** when they synthesized the C-4 methyl and C-4 dimethyl analogs **9a**, **9b**, and **9c** of artemisinin.⁴ Only the 4 β -methyl trioxane **9a** exhibited antimalarial activity when these compounds were incubated with strains of *Plasmodium falciparum*. In fact, this compound was

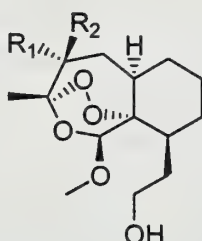
Scheme 2



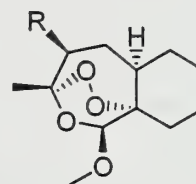
more active than artemisinin. It was suggested that a tertiary radical was more potent for antimalarial activity than a secondary radical. When **9a** was treated with Fe^{II} bromide in THF, the products were a 4:1 ratio of compounds analogous to **6** and **8** in Scheme 2. Also, the benzyl ether of **9c**, which did not display any antimalarial activity, was reacted with hemin and benzyl mercaptan. The result showed that a ring-contracted product analogous to **7** was formed. These results are consistent with the proposal that a 1,5-hydrogen shift (Scheme 2) is important in the antimalarial activity of artemisinin.



9a $\text{R}_1 = \text{H}, \text{R}_2 = \text{Me}$
9b $\text{R}_1 = \text{Me}, \text{R}_2 = \text{H}$
9c $\text{R}_1 = \text{Me}, \text{R}_2 = \text{Me}$



10a $\text{R}_1 = \text{H}, \text{R}_2 = \text{Bn}$
10b $\text{R}_1 = \text{Bn}, \text{R}_2 = \text{H}$
10c $\text{R}_1 = \text{H}, \text{R}_2 = \text{CH}_2\text{TMS}$
10d $\text{R}_1 = \text{CH}_2\text{TMS}, \text{R}_2 = \text{H}$



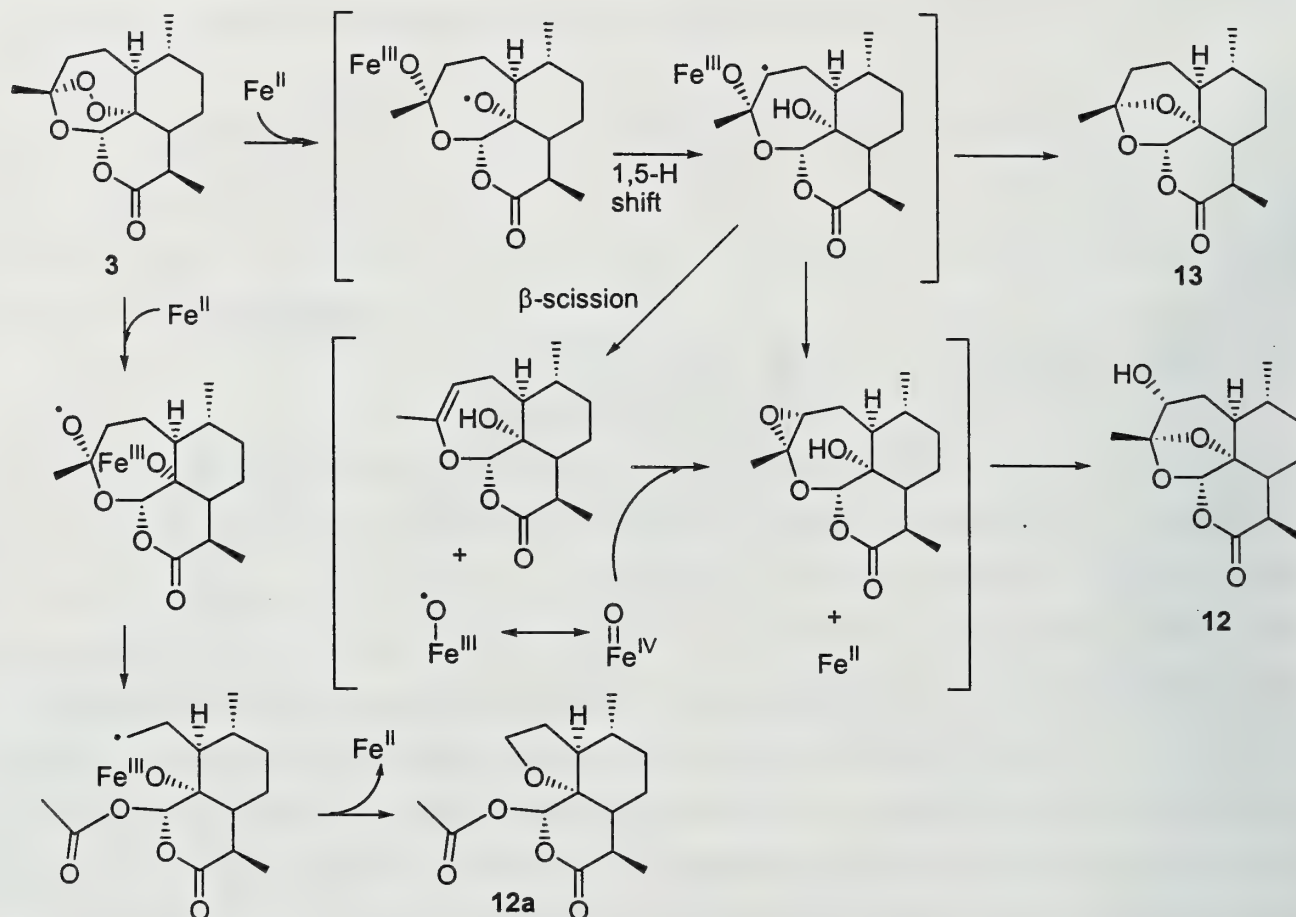
11a $\text{R} = \text{Bn}$
11b $\text{R} = \text{Ph}$

To further probe the structure-activity relationship substrates **10a-10d**, with different substitutions at the C-4 position, were synthesized.⁵ The 4 β -substituted substrates **10a** and **10c** again had much higher antimalarial activity than the analogous 4 α -substrates **10b** and **10d**. However, the trimethylsilyl (TMS) group on **10c**, which should better stabilize the C-4 radical, exhibited lower antimalarial activity than **10a**. Molecular models orient the TMS group away from the peroxide so it is not likely to interfere with the approaching iron. Trioxane **11b** had very low antimalarial activity, and reaction of **11b** with Fe^{II} bromide yielded almost exclusively the ring contracted product presumably from C-C cleavage. These results are interpreted to show that substrates that can form a stabilized radical at C-4 shunts the 1,5-hydrogen shift, which is believed to be important for antimalarial activity, in favor of the C-C cleavage pathway.

In search of the reactive intermediate that causes oxidative stress seen by other researchers, Posner and coworkers performed tests that are believed to support the existence of a high valent Fe^{IV} oxide, which has been shown to cause oxidative damage to biological macromolecules.⁶ Addition of hexamethyl Dewar benzene (HMDB) to artemisinin and Fe^{II} bromide produced the isomerized hexamethylbenzene (HMB) with a ~10% decrease in the hydroxylated product **12**. Under the same reaction conditions, methyl phenyl sulfide was converted to the oxidized sulfoxide, and tetralin was converted to hydroxytetralin. Control reactions showed that deoxygenated solvents produced the same products and both Fe^{II} and artemisinin were required for the oxidations. Posner and coworkers postulated that only a high valent Fe^{IV} oxide could perform these conversions. Reaction of artemisinin and Fe^{II} bromide provided products **12**, **13**, and **12a** in a 1:6:3 ratio (Scheme 3). The yield of the reduced

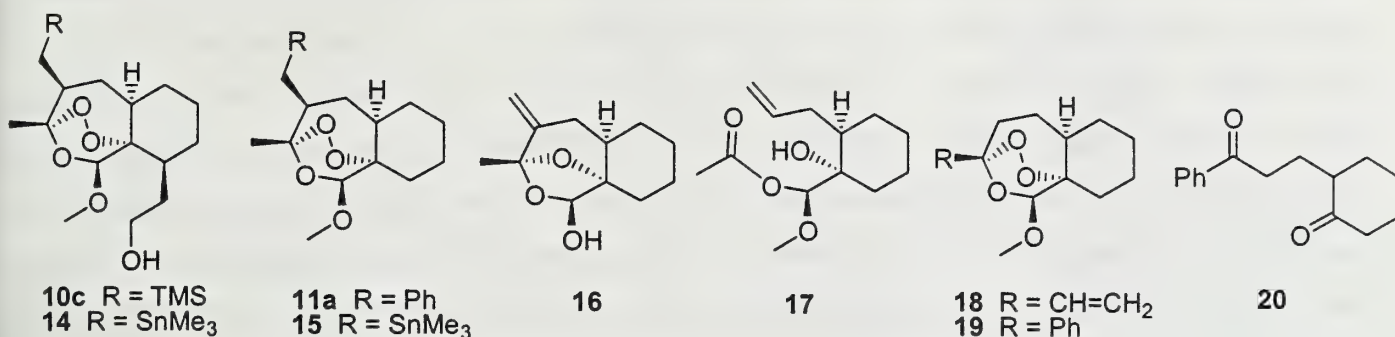
product **13** could be increased with the addition of 1,4-cyclohexadiene, which is a good hydrogen atom donor. These results led to the proposed mechanisms for artemisinin degradation shown in Scheme 3. In addition, the epoxide that is proposed to form in Scheme 3 is believed to be the intermediate that causes alkylation products seen by other researchers.

Scheme 3



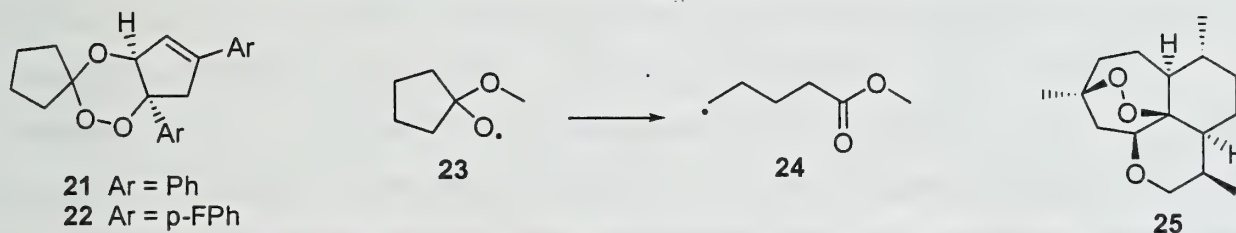
Further support for the importance of a high valent Fe^{IV} oxide was obtained by studies of substrates **14** and **15**, radical scavengers at the C-4 position.⁷ Unlike the silicon analog **10c** and the benzyl analog **11a**, these substrates displayed no antimalarial activity. Compound **15** did not produce HMB (<0.1%) from HMDB when reacted with Fe^{II} bromide suggesting that a high valent iron-oxo compound was not formed. The products of Fe^{II} bromide reaction with **15** are **16** and **17** at 15% and 71% yields, respectively. Formation of **16** can be rationalized by the existence of a radical at C-4. Compounds **18** and **19** were synthesized to facilitate β-scission because the olefinic bond formed by β-scission could be stabilized by conjugation. As expected, both **18** and **19** had significant antimalarial activity. However, when **18** and **19** were treated with Fe^{II} bromide, only **18** produced HMB from HMDB. Reaction of **19** yielded the ring contracted product related to **12a** in 48% and the diketone **20** in 18%. Interestingly, **20** exhibited some antimalarial activity. The authors postulated that the

endoperoxide substrate **19** could act as a prodrug, a compound that would release the activity of the diketone **20** inside malarial cells.



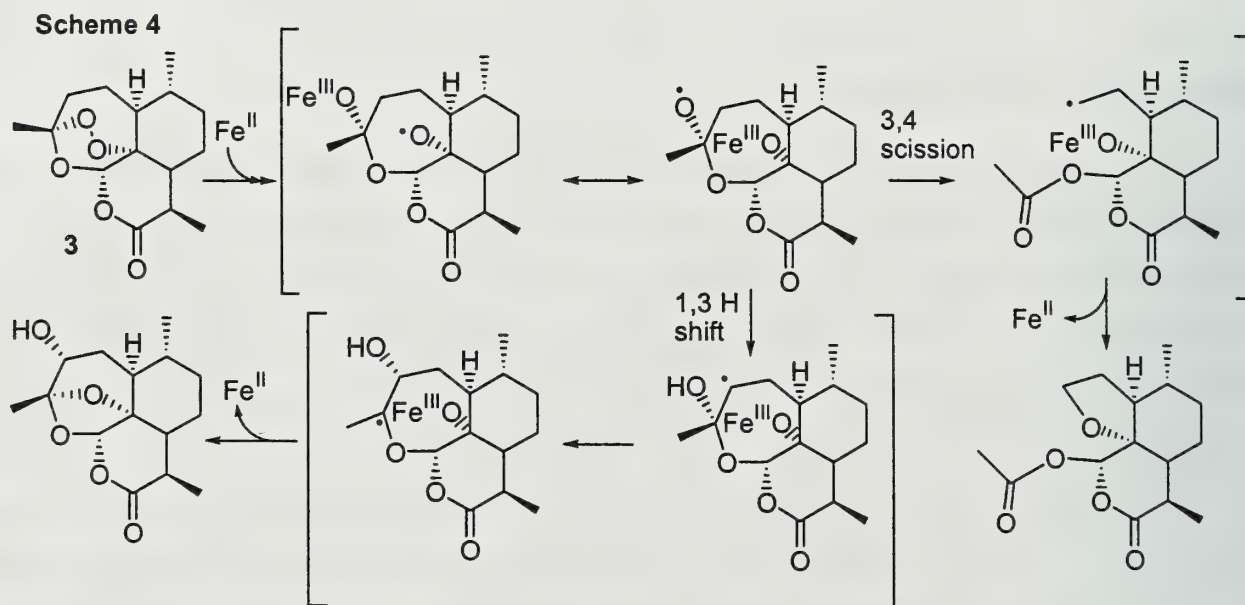
ALTERNATIVE MECHANISM

Early work by Jefford and coworkers showed that the lactone functionality and the tetrahydropyran ring of artemisinin are not essential to the activity of artemisinin; however, O-11 and the trioxane ring are important.⁸ These preliminary studies led them to synthesize **21** and **22** to further understand the involvement of the trioxane ring.^{9,10} Despite their predictions of the (*S,S*) enantiomers of **21** and **22** being more active, racemic mixtures of **21** or **22** showed the same high antimalarial activity as their enantiomerically pure counterparts. This was rationalized by the achiral nature of the heme complex. The proposed mechanism of activity for **21** and **22** is analogous to the 3,4 scission pathway in Scheme 4. Jefford and coworkers performed semi-empirical unrestricted Hartree-Fock calculations using to the PM3 method to show that the isomerization from the oxygen centered radical **23** to the carbon centered primary radical **24** is an exothermic process driven by the formation of an ester. This was taken to suggest that the antimalarial activity arises from a carbon centered radical that alkylates within malarial cells.



In an attempt to further understand the mechanism of artemisinin action, Jefford and coworkers treated **3** with zinc in acetic acid and found the exclusive product to be deoxyartemisinin **13**.¹¹ Since **13** had been isolated from patients treated with **3**, it seems that **13** may be a metabolite of **3** formed within the parasite or host. Reaction of **3** with Fe^{II} chloride gave the hydroxylated product **12** and the ring contracted product **12a**. In the presence of cyclohexene, cyclohexene oxide was not observed which led them to conclude that a high valent iron was not formed in the reaction. The ring contracted product **12a**

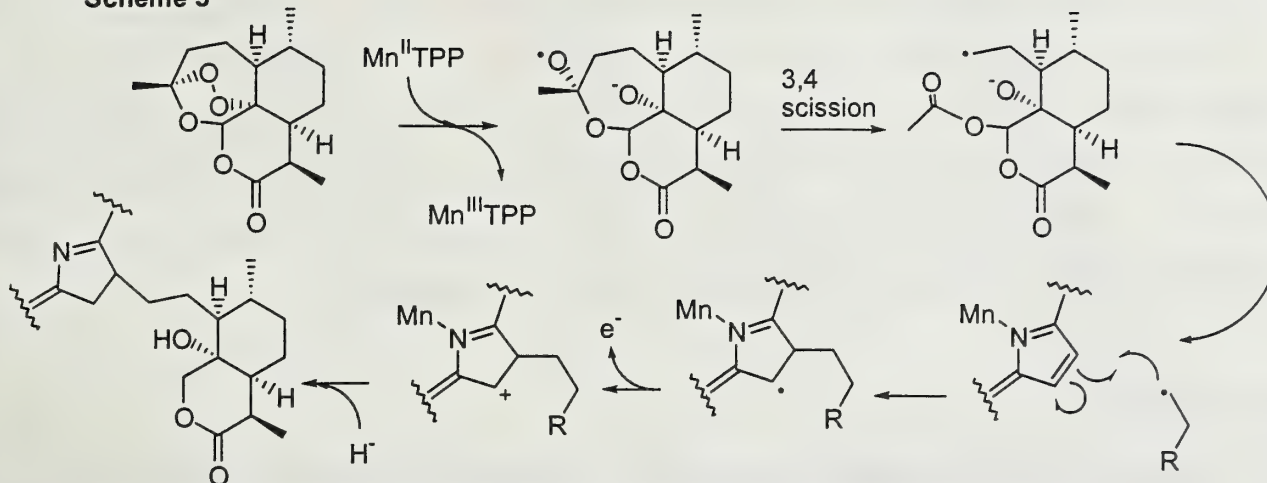
was produced in >75% yield, and hydroxylated product **12** was formed in <20% yield. From their data, Jefford and coworkers believe that the major product arises from a 3,4 scission as shown in Scheme 4. Calculations showed that for a 1,5-hydrogen shift (Scheme 3) to occur, the compound must be in a boat-like transition state. A 1,3-hydrogen shift might actually occur instead, leading to the observed minor product. Posner's results with Fe^{II} bromide in THF were rationalized by proposing bromide anion as a reducing species. Jefford and coworkers also believe that oxidation of methyl phenyl sulfide, tetralin, and the aromatization of HMDB can result from workup and need not involve a high valent Fe^{IV} oxide. As a result, it is postulated that the parasite is killed by the alkylation of proteins with a primary radical.



ALKYLATION BY ARTEMISININ

Mass spectroscopy has shown that alkylation of heme by artemisinin occurs *in vivo*; however, full characterization of the product complex proved challenging. Robert and Meunier were able to isolate an alkylated heme structure *in vitro*.¹²⁻¹⁴ Reaction of $\text{Fe}^{\text{III}}(\text{TPP})\text{Cl}$ (TPP = *meso*-tetraphenylporphyrin dianion) with borohydride produced $\text{Fe}^{\text{II}}\text{TPP}$ which when reacted with artemisinin resulted in a chlorin-type product. Since Fe^{III} is strongly paramagnetic and removing it from the heme requires harsh conditions, the intact compound could not be characterized by NMR. Next, $\text{Mn}^{\text{III}}(\text{TPP})\text{OAc}$ was used because manganese can be removed under milder conditions. $\text{Mn}^{\text{II}}\text{TPP}$ incubation with artemisinin formed an alkylated product in 25% yield that was studied by a variety of methods. NMR showed that C_4 symmetry of the porphyrin was lost and the ring current was decreased. The formation of the product can be explained by the mechanism shown in Scheme 5.

Scheme 5



Robert and Meunier also searched for a high valent manganese complex that would oxidize cyclohexene to cyclohexene oxide from the reaction with artemisinin. An epoxide product was not observed suggesting no metal-oxo species exists in the decomposition of artemisinin. Therefore, one of the major modes of artemisinin activity is considered to involve the alkylation of hemoglobin proteases or histidine rich proteins that polymerize heme to hemozoin. Protein inactivation by alkylation could then lead to the death of the parasite.

STRUCTURE-ACTIVITY RELATIONSHIPS

Avery and coworkers have modified different positions of artemisinin hoping to acquire quantitative structure-activity relationships. Results from heteroatom substitution at O-11 showed that this group can not be too large, otherwise antimalarial activity suffers.¹⁵ Phenyl substitution at this position generally improved activity. Substitution of a carbon for the oxygen at the 13 position resulted in lower activities.¹⁶ Derivative **25**, which has significant antimalarial activity, formed an epoxide (analogous to Scheme 3) in 20% yield when treated with Fe^{II} bromide, partially supporting Posner's proposed mechanism; however, this epoxide did not have antimalarial activity. Substitution at C-3 and studies of 10-deoxoartemisinin substituted at C-3 and C-9 did not provide quantitative structure-activity relationships.^{17,18} As before, removal of the lactone functionality increased antimalarial activity.

CONCLUSIONS

Posner's research has provided support for the importance of a carbon-centered radical formed by a 1,5-hydrogen shift in the antimalarial activity of artemisinin and other trioxanes. It is plausible that artemisinin acts in multiple pathways that involve both Posner and Jefford's proposals. Meunier has

shown that alkylation of heme by artemisinin can probably occur in vivo, and alkylation of proteins by a C-4 radical is a definite possibility. Avery's studies did not show quantitative structure-activity relationship with a variety of compounds. However, π -interactions between heme and the substrate could be the reason for improved antimalarial activity of some phenyl substituted artemisinin derivatives. Further research with more mechanistic probes will be invaluable for complete understanding of the mechanism of artemisinin in killing malarial parasites.

REFERENCES

- (1) Cumming, J. N.; Ploypradith, P.; Posner, G. H. *Adv. Pharmacol.* **1997**, *37*, 253-297.
- (2) Meshnick, S. R.; Taylor, T. E.; Kamchonwongpaisan, S. *Microbiol. Rev.* **1996**, *60*, 301-315.
- (3) Posner, G. H.; Oh, C. H. *J. Am. Chem. Soc.* **1992**, *114*, 8328-8329.
- (4) Posner, G. H.; Oh, C. H.; Wang, D.; Gerena, L.; Milhous, W. K.; Meshnick, S. R.; Asawamahasadka, W. *J. Med. Chem.* **1994**, *37*, 1256-1258.
- (5) Posner, G. H.; Wang, D.; Cumming, J. N.; Oh, C. H.; French, A. N.; Bodley, A. L.; Shapiro, T. A. *J. Med. Chem.* **1995**, *38*, 2273-2275.
- (6) Posner, G. H.; Cumming, J. N.; Ploypradith, P.; Oh, C. H. *J. Am. Chem. Soc.* **1995**, *117*, 5885-5886.
- (7) Posner, G. H.; Park, S. B.; Gonzalez, L.; Wang, D. S.; Cumming, J. N.; Klinedinst, D.; Shapiro, T. A.; Bachi, M. D. *J. Am. Chem. Soc.* **1996**, *118*, 3537-3538.
- (8) Jefford, C. W.; Velarde, J. A.; Bernardinelli, G.; Bray, D. H.; Warhurst, D. C.; Milhous, W. K. *Helv. Chim. Acta* **1993**, *76*, 2775-2788.
- (9) Jefford, C. W.; Favarger, F.; Vicente, M. G. H.; Jacquier, Y. *Helv. Chim. Acta* **1995**, *78*, 452-458.
- (10) Jefford, C. W.; Kohmoto, S.; Jaggi, D.; Timari, G.; Rossier, J.-C.; Rudaz, M.; Barbuzzi, O.; Gerard, D.; Burger, U.; Kamalaprija, P.; Mareda, J.; Bernardinelli, G. *Helv. Chim. Acta* **1995**, *78*, 647-662.
- (11) Jefford, C. W.; Vincente, M. G. H.; Jacquier, Y.; Favarger, F.; Mareda, J.; Millasson-Schmidt, P.; Brunner, G.; Burger, U. *Helv. Chim. Acta* **1996**, *79*, 1475-1486.
- (12) Robert, A.; Meunier, B. *J. Am. Chem. Soc.* **1997**, *119*, 5968-5969.
- (13) Robert, A.; Meunier, B. *Chem. Soc. Rev.* **1998**, *27*, 273-279.
- (14) Robert, A.; Meunier, B. *Chem. Eur. J.* **1998**, *4*, 1287-1296.
- (15) Avery, M. A.; Bonk, J. D.; Chong, W. K. M.; Mehrotra, S.; Miller, R.; Milhous, W.; Goins, D. K.; Venkatesan, S.; Wyandt, C.; Khan, I.; Avery, B. A. *J. Med. Chem.* **1995**, *38*, 5038-5044.
- (16) Avery, M. A.; Fan, P. C.; Karle, J. M.; Bonk, J. D.; Miller, R.; Goins, D. K. *J. Med. Chem.* **1996**, *39*, 1885-1897.
- (17) Avery, M. A.; Mehrotra, S.; Bonk, J. D.; Vroman, J. A.; Goins, D. K.; Miller, R. *J. Med. Chem.* **1996**, *39*, 2900-2906.
- (18) Avery, M. A.; Mehrotra, S.; Johnson, T. L.; Bonk, J. D.; Vroman, J. A.; Miller, R. *J. Med. Chem.* **1996**, *39*, 4149-4155.



UNIVERSITY OF ILLINOIS-URBANA



3 0112 037723803

ORGANIC SEMINAR ABSTRACTS

1998-99, SEMESTER II

University of Illinois

**Department of Chemistry
600 South Mathews Avenue
271 Roger Adams Laboratory
Urbana, IL 61801**

JUNE 1999

NOTICE: Return or renew all Library Materials! The *Minimum Fee* for each Lost Book is \$50.00.

The person charging this material is responsible for its return to the library from which it was withdrawn on or before the **Latest Date** stamped below.

Theft, mutilation, and underlining of books are reasons for disciplinary action and may result in dismissal from the University.
To renew call Telephone Center, 333-8400

UNIVERSITY OF ILLINOIS LIBRARY AT URBANA-CHAMPAIGN

 LIBRARY

MAY 13 2002

FEB 13 2002

MAY 19 2002

JAN 30 2002

SEMINAR TOPICS

SEMESTER II

SPRING 1999

	<u>PAGE</u>
RATIONAL DESIGN OF L-375,378: AN ORALLY ACTIVE ANTI-THROMBOTIC SHANNA MCGOVERN	1
RECENT DEVELOPMENTS IN THE MCMURRY REACTION HAO ZHOU	9
SYNTHETIC TEMPLATES THAT FACILITATE THE FORMATION OF ARTIFICIAL β -SHEETS SARA ADAMSKI	17
POLYMER-ASSISTED SOLUTION-PHASE CHEMICAL LIBRARY SYNTHESIS AND PURIFICATION LYNNE A. MILLER	25
METALLOCENE CATALYSTS FOR OLEFIN POLYMERIZATION SURESH R. SRIRAM	33
ATOM TRANSFER RADICAL POLYMERIZATION QING YU	41
ASYMMETRIC SYNTHESIS OF AMINE DERIVATIVES VIA CHIRAL SULFINIMINES STEPHEN G. JARBOE	49
SYNTHESIS OF THE BICYCLIC CORE OF CP-225,917 AND CP-263,114..... JANNINE HABERMAN	57

MEMORY OF CHIRALITY AND SELF-REGENERATION OF STEREOGENIC CENTERS.....	65
Ji-YOUNG KIM	
CATALYTIC ANTIBODIES: RECENT ADVANCES IN C-C BOND FORMATIONS	73
LAURA G. SCHULTZ	
SOFT LITHOGRAPHY: METHODS AND APPLICATIONS FOR ORGANIC SURFACE CHEMISTRY	81
MATTHEW J. MIO	
MECHANISTIC ASPECTS OF MONOAMINE OXIDASES.....	89
KYLE HURTH	
INVESTIGATIONS OF THE CYTOCHROME P450 CATALYZED HYDROXYLATION OF HYDROCARBONS.....	97
JENNIFER M. VRTIS	
OSMIUM-CATALYZED ASYMMETRIC AMINOHYDROXYLATION (AA) REACTION	105
YONG-JAE KIM	
C ₂ -SYMMETRIC BIS(OXAZOLINE)-COPPER COMPLEXES IN CATALYTIC ASYMMETRIC SYNTHESIS	113
LIQIANG ZHOU	
POLYMERIZATION OF PRE-ORDERED MONOMERS IN LIQUID CRYSTALLINE PHASE	121
YUGUO MA	
STRATEGIES TOWARD THE SYNTHESIS OF CARBOHYDRATE LIBRARIES.....	129
JENNIFER R. COSTERSON	
SYNTHESIS AND COMPLEXATION PROPERTIES OF BRIDGED 2, 2':6',2" TERPYRIDINES	137
JEFFREY T. VESSELS	

RATIONAL DESIGN OF L-375,378: AN ORALLY ACTIVE ANTI-THROMBOTIC

Reported by Shanna M^cGovern

January 28, 1999

INTRODUCTION

Although the mechanisms of blood clotting were elucidated several years ago, the development of an arsenal of sophisticated anti-clotting agents has just begun. There is a plethora of theories about the most effective place in the clotting cascade to inhibit clotting without causing serious side effects. Anti-clotting agents, who may act at any point in the clotting cascade, are used by 48 million people annually for prevention of clot formation, or thrombosis. These agents are required to prevent clotting during and after surgical procedures and acute myocardial infarction. Anti-coagulant therapies are also used as long-term prevention of a second myocardial infarction. Currently, anti-coagulant therapies are costly, often require intravenous administration, and are difficult to predict the dose required for optimal anti-clotting activity. Several potential inhibitors have been developed, however, they often bind covalently, and permanently inhibit the enzyme. This is clinically contraindicated, as it would result in induced hemophilia. Thus, an effective inhibitor with ability to predictably inhibit clotting and provide oral bioavailability is the goal of many research groups. Several research groups at Merck recently used the rigid active site of thrombin to rationally design L-375,378, a potent, orally bioavailable anti-thrombotic.

CURRENT THROMBOLYTIC THERAPIES

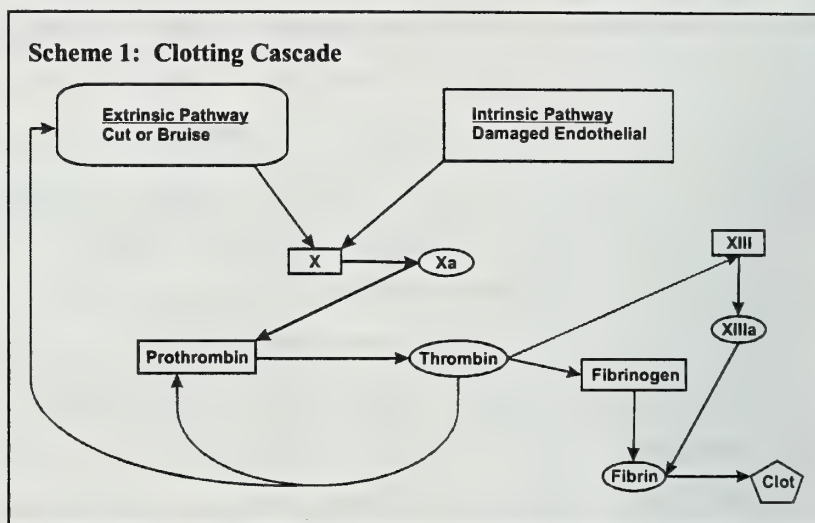
There are three current anti-clotting therapies in clinical use: 1) Heparin, 2) Warfarin, and 3) Hirudin. Known since the early 1930's, heparin is a glucosaminopolysaccharide produced, in small quantities, by the mast and basophil cells in the liver and lungs of humans and broken down by heparinase in the blood after 2 hours.^{1,2} Heparin is obtained as natural product and administered intravenously. Heparin inhibits clotting by enhancing anti-thrombin III's binding to and deactivation of free thrombin.³ Warfarin was first synthesized in 1955, and is FDA approved for oral and intravenous use. This long lasting anti-thrombotic is dosed as the warfarin sodium salt racemate. Both isomers exert the effect of inhibiting a vitamin K dependent enzyme that performs the Glu → γ -carboxy Glu post-translational modification of prothrombin. This dicarboxy amino acid chelates the calcium(II) ions required in the activation of prothrombin.⁴ Hirudin is a naturally occurring 65 amino acid protein found in the saliva of the medicinal leech, *Hirudo medicinalis*. The leech's medical usage dates back to 1500 B.C.,⁵ but it was not until hirudin's successful purification by Markwardt in 1957⁶ that the possibility of a new anti-coagulant

treatment became available. Hirudin binds to the active site of thrombin with a K_i of 0.22 fM,⁷ effectively slowing the clotting response. In July 1998, recombinant hirudin was approved for use in the US to treat heparin-induced thrombocytopenia (HIT). HIT is a potentially fatal complication of full dose heparin therapy, however, intravenously dosed hirudin provides an alternative therapy to heparin, and treats HIT concurrently.

A critical problem with current clotting therapies is that thrombin bound to fibrin is not inhibited. The relatively large peptide inhibitors, anti-thrombin III and hirudin, cannot fit through the fibrin framework to inhibit the bound thrombin. However, small tripeptide structures have the potential to directly inhibit both free and bound thrombin.¹¹

THE CLOTTING CASCADE

The clotting cascade, Scheme 1, is greatly simplified to demonstrate thrombin's critical role

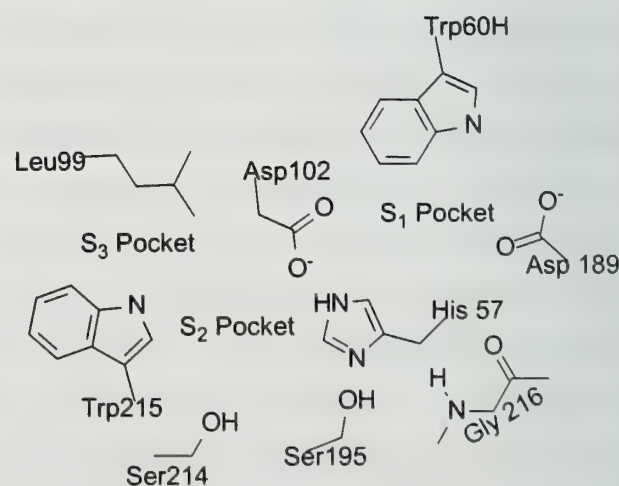


in the clotting mechanism.⁸ Although the intrinsic pathway begins when there is damage to the blood vessel and the extrinsic pathway is activated by a breach in the blood vessel wall they both culminate at factor X activation of thrombin. Thrombin, in turn, catalyzes the cross-link of fibrin strands to form a frame-work for the platelets to bind. Active thrombin binds to these platelets, and continues to catalyze the expression of the clotting cascade. With its key role in the clotting cascade proliferation, thrombin is an excellent target for clotting inhibition.

THE ACTIVE SITE OF THROMBIN

Thrombin (EC 3.4.21.5) is a zymogenic serine protease with a catalytic triad (His 57, Ser 195, Asp 102). Prothrombin binds Ca(II) ions and is cleaved to form the α and β subunits of

Figure 1: Thrombin Active Site



performed a systematic study of modifications to the Me-D-Phe-Pro-Arg-H peptide.¹¹ They concluded that C-terminus hydrophobic groups increased binding, only proline interacted effectively in the second amino acid position, and the tethered amino functionality of the Arg increased binding. Finally, studies with N-terminus substituents demonstrated that α -keto amides and Boc groups were able to increase inhibitory effect. At this time, work with Cyclotheonamide A suggested a novel functionality that might enhance the potency of the tripeptide inhibitors.

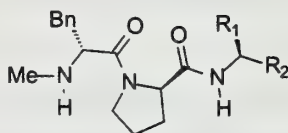
In the early 1990's Cyclotheonamide A (CyA) was isolated from *Theonella swalali* and was found to effectively inhibit thrombin with a K_i of 1 nM after equilibration in solution.¹¹ The subsequent X-ray crystal structure shows the Arg tail in the S_1 binding pocket, suggesting several hydrogen bonds to the α -keto arginine.¹²

With this information, **1** and **2** were synthesized utilizing the α -keto Arg functionality of CyA as a lead. In 1996, Stauffer *et al* reported enhancing the selectivity of **2** by substituting a structurally constrained amine for the Arg group. This was accomplished by utilizing *trans*-4-aminocyclohexylalanine, which was used in previous work with somatostatin. The resulting inhibitor,

L-370,518, exhibited an increase in selectivity and a decrease in K_i ,¹³ thus demonstrating the hydrophobic selectivity of the S_1 pocket of thrombin over trypsin.

Although L-370,518 is a potent inhibitor, there is significant concern about the reactive α -keto amide, *in vivo*.¹⁴ Additionally, like the

Table 1: CyA Analogs



Compound	R ₁	R ₂	K _i , pM	Trypsin
Me-D-Phe-Pro-Arg-H	(CH ₂) ₃ NHC(NH ₂) ₂ ⁺	H	770000	-
1	(CH ₂) ₃ NHC(NH ₂) ₂ ⁺	(CO) ₂ NHMe	90	+
2	(CH ₂) ₃ NHC(NH ₂) ₂ ⁺	(CO) ₂ NH ₂	250	+
L-370,518	4-NH ₂ Cy	(CO) ₂ NH ₂	90	+
L-371,912 *	4-NH ₂ Cy	H	5000	+

+/-, Good/poor selectivity against trypsin;
 *, Orally bioavailable in murine model

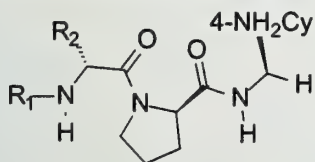
CyA precursor, the α -keto amine compounds are slow binding and the reported K_i is only exhibited after a lengthy equilibration period, which is clinically contraindicated. Lyle's group at Merck synthesized L-371,912 to investigate the difference in potency of L-370,518 without the α -keto amide moiety.¹⁵ Although there was a reduction in potency, this modification suggested that the core peptide was of the

correct structure to interact with the active site. In addition, its slight oral bioavailability suggested that this was an excellent lead compound from which to probe additional regions in the active site. From this point, two groups at Merck developed proline backbone and acetamide backbone analogs of L-371,912 towards the discovery of an ideal anti-thrombotic.

PROLINE BACKBONE ANALOGS

In the 1990's the Thrombosis Research Institute substituted D-diphenylalanine for D-Phe on other potential thrombin inhibitors, and observed 3-10 fold increases in potency. In 1997, Tucker and

Table 2: Proline Backbone Analog Inhibitors



Compound	R ₁	R ₂	K _i , pM	Trypsin	Murine (oral)
L-371,912	Me	Bn	5000	+	10%
3	H	CHPh ₂	5000	--	--
4	Me	CHPh ₂	100	+	--
5	MeSO ₂	CHPh ₂	3000	--	--
6	BnSO ₂	CHPh ₂	2.5	+	--
7	BnSO ₂	Bn	400	--	--
8	H	CHCy ₂	56	+	2%
9*	Boc	CHCy ₂	100	+	90%

--, Not reported; +/-, Good/poor selectivity against trypsin; *, Orally bioavailable in canine model

associates at Merck proposed that the addition of lipophilic groups to the C-terminus would further interact with the aryl binding pocket, S₃, of thrombin and increase binding affinity.¹⁶ This unnatural amino acid was substituted for the Phe of L-371,912, and induced a 30 fold increase in **3**. In addition, they investigated capping the C-terminus with sulfonamides, and found that **7**, the benzylsulfonamide, demonstrated the greatest increase in potency, as it was better able to interact hydrophobically with the Trp 60H, directly above the catalytic triad. Molecular modeling programs and X-ray crystal

structures of **5** and **7**, each with thrombin, suggested that a hybrid structure with diphenylalanine and benzylsulfonamide substitutions could create a more effective inhibitor. Compound **6** was synthesized and it confirmed their hypothesis. The X-ray crystal of **6** with thrombin revealed that the reason for the increased binding was due to **6** using open space in the rigid active site. The Tucker *et al* named this as the N-terminus binding site, created by the inhibitor wrapping back on itself in a hairpin like manner. The benzyl ring of the N-terminus lays parallel to the active site bounded on one side by the

cyclohexane of the inhibitor. Although **6** has promising inhibition action, its bioavailability was not reported¹⁶.

The final modification to proline backbone inhibitors originated from the reduction of the diphenylalanine to dicyclohexylalanine in the anticipation that it would have better oral bioavailability, due to its increased lipophilicity.¹⁷ Compound **3** was tested for oral bioavailability and found to be poor possibly due to its polar nature. In addition to reduction of the diphenylalanine, boc substitution of the N-terminus was re-investigated and **9** was much more orally bioavailable than **8**. The increase is potentially due to a greater interaction of the boc group with the S₃ pocket. Although much information about the active site of thrombin was obtained from this study, none of the reported inhibitors fulfilled the potency criteria for an orally bioavailable anti-thrombotic.

ACETAMIDE BACKBONE ANALOGS

In 1997, Philip Sanderson's group at Merck began with L-371,912 and chose to re-investigate the substitution of various proline analogs and their effectiveness as thrombin inhibitors. In an analogous search for a peptide inhibitor of human leukocyte elastase, it was found that 3-amino-2-pyridinone or 5-amino-6-pyrimidinone acetamides were adequate replacements for the glycylproline amide backbone.¹⁸ In order to determine which proline analog had the best potential for correct non-covalent interaction with the S₂ pocket of thrombin, molecular modeling was employed. The results suggested that the 3-amino-2-pyridinone analog had the highest potential, by maintaining hydrogen bonds with Gly 216, Trp 215, and Ser 214. Since this analog lacked the phenyl ring of the Phe component, various tethered phenyl analogs were synthesized to determine which interacted best with the S₃ pocket. In addition, it was found that a 6-methyl substitution on the pyridinone would allow for interaction with the hydrophobic S₂ pocket. Concurrently, they investigated the use of an amidinopiperidine as a replacement for the *trans*-4-aminocyclohexyl alanine.¹⁹ The systematic study resulted in L-373,890, which exhibited a potency analogous to that of the class 1 inhibitors and good selectivity over trypsin.

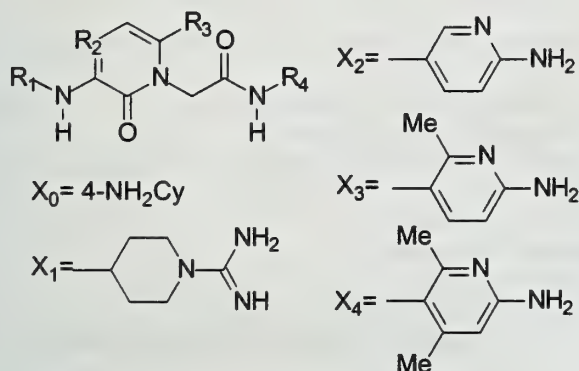
Although L-373,890 is a potent inhibitor, it contains the polar guanidine group that decreases the oral bioavailability. An aminopyridine was chosen based on its similarity to the aminopiperidine, and was found to enhance the potency of the inhibitor. Additionally, methyl substitutions on the piperidine ring showed a significant increase in potency, as they were able to interact favorably with the hydrophobic amino acids in the S₁ pocket, as shown by L-374,087. Further clinical experimentation with L-374,087 showed it had poor pharmacokinetics in murine, canine, and mammalian models.

In the X-ray crystal of L-374,087, hydrogen bonding was not observed between thrombin and the sulfonyl group.²⁰ Thus, the sulfonyl group was presumed to be a conformational analog of a methylene group, and subsequent tests with phenethyl substituents revealed this. However, these analogs revealed that the sulfonyl group stabilizes the pyridinone, as demonstrated by **13**, which readily decomposes in air. It was theorized that the electrophilic sulfonyl group stabilized the aminopyridinone moiety, and this stability could be restored with an electron-withdrawing group placed in the *para* position of the aminopyridinone ring.²¹ L-375,378 was synthesized and the additional heteroatom on the piperidine ring

stabilized the molecule. This compound exhibited high efficacy and excellent pharmacokinetics.

An additional methyl on the aminopyridine was proposed to increase inhibition. This appears to be correct with the data given. However, Sanderson states that when compound **15** is modeled with thrombin it approximates the same conformation as L-374,087, with equal contacts to the rigid active site. Thus, all pharmacokinetic studies performed with L-374,087 presumably approximate **15**. Therefore, only L-375,378 exhibits the high oral activity and efficacy required of an anti-thrombotic in this study of acetamide backbone analogs of L-371,912.

Table 3: Acetamide Backbone Analog Inhibitors



Compound	R ₁	R ₂	R ₃	R ₄	K _i , pM	Trypsin
10	BnCH ₂	CH	Me	X ₀	47000	d. air
11	BnSO ₂	CH	Me	X ₀	4600	-
12	PhEtCO	CH	Me	X ₁	166000	+
L-373,890	BnSO ₂	CH	Me	X ₁	500	+
L-374,087*	BnSO ₂	CH	Me	X ₃	500	+
13	BnCH ₂	CH	Me	X ₃	d. Air	--
L-375,378*	BnCH ₂	N	Me	X ₃	800	+
14	BnCH ₂	N	H	X ₃	Poor	--
15	BnCH ₂	N	Me	X ₄	350	+
16	BnCH ₂	N	Me	X ₂	11000	+

--, Not reported; +/-, Good/poor selectivity against trypsin; *, Orally bioavailable in murine, canine, and primate models

CONCLUSION

Chemists at Merck proposed that there could be a small molecule, orally administered anti-thrombin agents for long-term therapy, with better dosability than warfarin, based on CyA and L-371,912. After synthesizing many compounds, and investigating their SAR's with thrombin, L-375,378 was created. Along with its high clinical activity, L-375,378 has an efficient eight step synthesis with a 26% overall yield. On the basis of these observations, Merck selected L-375,378 for further preclinical and clinical development. In sum, the rigid active site of thrombin allowed for the rational design of L-375,378, a highly potent, orally bioavailable anti-thrombotic.

REFERENCES

- ¹ *Physicians' Desk Reference*, 53rd ed.; Medical Economics, Montvale, NJ, 1999, pp 3305-3307.
- ² *Physiology*; Berne, R. M. and Levy, M. N., Eds.; Mosby: St. Louis, MO, 1998; Chapter 20.
- ³ *Textbook of Medical Physiology*, 9th ed.; Guyton, A. C. and Hall, J. E., Eds.; W.B. Saunders: Philadelphia, PA, 1996; Chapter 36.
- ⁴ Stryer, L. *Biochemistry*, 4th ed; W. H. Freeman: New York, 1995; pp 252-257.
- ⁵ Hoechst Marion Roussel the pharmaceutical company of Hoechst, USA website. <http://www.hmri.com/newsroom/presskits/index.html> (accessed Jan 1999).
- ⁶ Seegers, W. H. *Prothrombin*; Harvard University: Cambridge, MA, 1962; p 363.
- ⁷ Pavone, V.; De Simone, G.; Nastri, F.; Galdiero, S.; Staliano, N.; Lombardi, A.; Pedone, C. *Biol. Chem.* **1998**, *379*, 987-1006.
- ⁸ For a complete diagram see: Di Cera, E. *Trends Cardiovasc. Med.* **1998**, *8*, 348.
- ⁹ 1AD8 and 1HXF; Brookhaven Protein Data Bank Website. <http://pdb.pdb.bnl.gov/> (accessed Jan 1999).
- ¹⁰ He, G-X.; Williams, J. P.; Postich, M. J.; Swaminathan, S.; Shea, R. G.; Terhorst, T.; Law, V. S.; Mao, C. T.; Sueoka, C.; Coutré, S.; Bischofberger, N. *J. Med. Chem.* **1998**, *41*, 4224-4231.
- ¹¹ Bajusz, S.; Szell, E.; Bagdy, D.; Barbas, E.; Horvath, G.; Dioszegi, M.; Fittler, Z.; Szabo, G.; Juhasz, A.; Tomori, E.; Szilagyi, G. *J. Med. Chem.* **1990**, *33*, 1729-1735.
- ¹² Brady, S.F.; Sisko, J.T.; Stauffer, K.J.; Colton, C. D.; Qiu, H.; Lewis, S. D.; Ng, A. S.; Shafer, J. A.; Bogusky, M. J.; Veber, D. F.; et al. *Bioorg. Med. Chem.* **1995**, *3*, 1063-1078.
- ¹³ Brady, S.F.; Lewis, S.D.; Colton, C.D.; Stauffer, K. J.; Sisko, J. T.; Ng, A. S.; Homnick, C. F.; Bogusky, M. J.; Shafer, J. A.; Veber, D. F.; Nutt, R. F. *Proc. 14th Amer. Peptide Symp.* **1995**, 331-333.
- ¹⁴ Cutrona, K. J.; Sanderson, P. E. J. *Tetrahedron Lett.* **1996**, *37*, 5045-5048.
- ¹⁵ Lyle, T.A.; Chen, Z.; Appleby, S.D.; Freidinger, R. M.; Gardell, S. J.; Lewis, S. D.; Li, Y.; Lyle, E. A.; Lynch Jr., J. J.; Mulichak, A. M.; et al. *Bioorg. Med. Chem. Lett.* **1997**, *7*, 67-72.
- ¹⁶ Tucker, T.J.; Lumma, W.C.; Mulichak, A.M.; Chen, Z.; Naylor-Olsen, A.M.; Lewis, S. D.; Lucas, R.; Freidinger, R. M.; Kuo, L. C. *J. Med. Chem.* **1997**, *40*, 830-832.
- ¹⁷ Tucker, T. J.; Lumma, W. C.; Lewis, S. D.; Gardell, S. J.; Lucas, B. J.; Baskin, E. P.; Woltmann, R.; Lynch, J. J.; Lyle, E. A.; Appleby, S. D.; et al. *J. Med. Chem.* **1997**, *40*, 1565-1569.
- ¹⁸ Sanderson, P. E. J.; Dyer, D. J.; Naylor-Olsen, A. M.; Vacca, J. P.; Gardell, S. J.; Lewis, S. D.; Lucas Jr., B. J.; Lyle, E. A.; Lynch Jr., J. J.; Mulichak, A. M. *Bioorg. Med. Chem. Lett.* **1997**, *7*, 1497-1500.
- ¹⁹ Feng, D-M.; Gardell, S. J.; Lewis, S. D.; Bock, M. G.; Chen, Z.; Freidinger, R. M.; Naylor-Olsen, A. M.; Ramjit, H. G.; Woltmann, R.; Baskin, E. P.; et al. *J. Med. Chem.* **1997**, *40*, 3726-3733.
- ²⁰ Sanderson, P. E. J.; Cutrona, K. J.; Dorsey, B. D.; Dyer, D. L.; McDonough, C. M.; Naylor-Olsen, A. M.; Chen, I-W.; Chen, Z.; Cook, J. J.; Gardell, S. J.; et al. *Bioorg. Med. Chem. Lett.* **1998**, *8*, 817-822.
- ²¹ Sanderson, P. E. J.; Lyle, T. A.; Cutrona, K. J.; Dyer, D. L.; Dorsey, B. D.; McDonough, C. M.; Naylor-Olsen, A. M.; Chen, I.; Chen, Z.; Cook, J. J. *J. Med. Chem.* **1998**, *41*, 4466-4474.

RECENT DEVELOPMENTS IN THE McMURRY REACTION

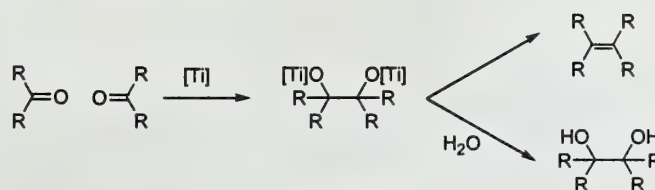
Reported by Hao Zhou

February 1, 1999

INTRODUCTION

Since its simultaneous discovery by three groups¹⁻³ (Mukaiyama, Tyrlik, and McMurry) in the 1970's, the McMurry reaction⁴ has proven to be a very useful tool in synthetic organic chemistry. In this reaction, aldehydes and/or ketones can be reductively coupled to afford alkenes with the help of a low-valent titanium species (Scheme 1). The intramolecular variant, which can be used to synthesize almost any size cycloalkene, is especially important. This abstract will cover the recent investigations of the mechanism, reagents, scope, and applications of the McMurry reaction.

Scheme 1



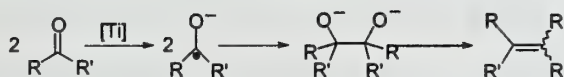
REAGENTS AND MECHANISM

Classical Reagents and Accepted Mechanism

The classical McMurry reaction is generally performed in two consecutive steps: first, preparation of the active titanium species by reduction of TiCl_n (n=3, 4) with a strong reducing agent in an ethereal solvent, then addition of the carbonyl substrate to the above slurry. The most commonly used reagents are TiCl₃/LiAlH₄/THF, TiCl₃-(DME)_{1.5}/Zn-Cu, TiCl₃/Mg/THF and TiCl₃/Li/THF.

Although the mechanism of the McMurry reaction is not fully understood, it is believed that a low valent titanium species first reduces the carbonyl substrate by a single electron transfer. The newly generated ketyl radicals then dimerize to form a carbon-carbon bond. Subsequent deoxygenation of the pinacolate intermediate liberates the alkene products (Scheme 2). Low-valent titanium (LVT) works well in this reaction due to its reducing ability and oxophilicity. The alkene is produced by performing the reaction at 66 °C in THF, however, the intermediate pinacolates can be trapped as the pinacols and isolated from the reaction mixture in high yield if the reaction is performed at 0 °C.

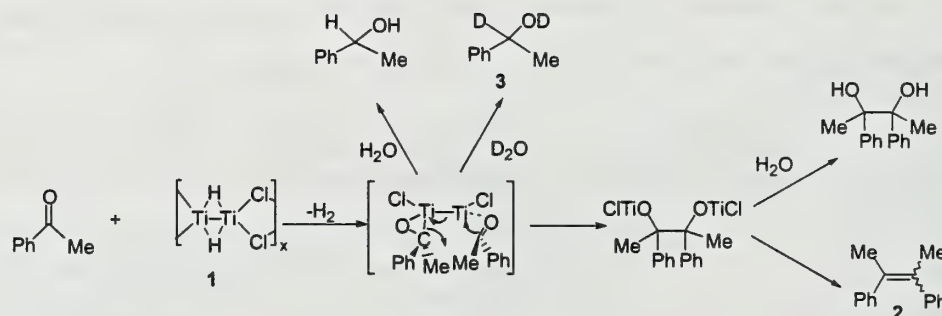
Scheme 2



Recent Studies of the Oxidation State of the Active Species

In the pioneering studies, a Ti^0 species was assumed to be the active species. However, in 1994, Bogdanovic et al. have proposed that the active species generated by the combination of TiCl_3 and LiAlH_4 in THF is $[\text{HTiCl}(\text{THF})_{\sim 0.5}]_x$ (**1**) (see structure in Scheme 3).⁵ An authentic sample of titanium complex **1** was prepared from the reaction of $[\text{TiCl}_3(\text{THF})_3]$ with MgH_2 . The structure of compound **1** was characterized by alcoholysis, IR spectroscopy, and X-ray absorption spectroscopy. Complex **1** could also be isolated from the solution of TiCl_3 and LiAlH_4 in THF in 46% yield. When mixed with carbonyl compounds, this compound gave the same products as those obtained in the McMurry reaction in comparable yields.

Scheme 3



It was found that in the $\text{TiCl}_3(\text{DME})_{1.5}\text{-Zn}(\text{Cu})$ system,⁶ no reduction of Ti^{3+} to Ti^0 species by Zn could be detected until the addition of carbonyl substrate. The solids obtained after refluxing $\text{TiCl}_3(\text{DME})_{1.5}$ and zinc in THF were postulated to be a mixture of $\text{TiCl}_3(\text{DME})_{1.5}$ with zinc by data from X-ray diffraction patterns, electron microscopy, IR spectroscopy and Far IR spectra. IR data indicated that the carbonyl substrate was coordinated to the Ti^{3+} . This coordination was proposed to lower the reduction potential of Ti^{3+} . As a result, Ti^{3+} can be reduced to Ti^{2+} by a mild reducing agent such as Zn, or even Fe, or Sn whose standard potentials are lower than that of Zn. The existence of Ti^{2+} was supported by a stoichiometry study.

In addition, Clive et al.⁷ have reported that titanium-graphite prepared by using 2 equiv of C_8K per TiCl_3 (forming a Ti (I) species) gave a higher yield on the McMurry reaction than titanium-graphite prepared by using 3 equiv of C_8K per TiCl_3 (forming a Ti (0) species).

In summary, a diversity of reagents with the formal oxidation states 0, +1, and +2 can all mediate the reductive McMurry coupling.

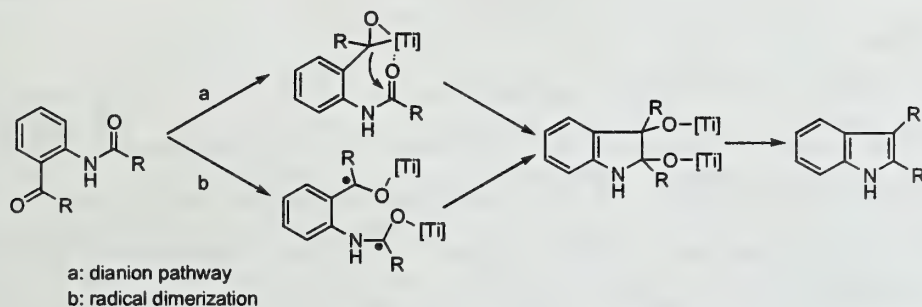
Nucleophilic Mechanism

Bogdanovic et al. proposed that the reaction of acetophenone with titanium complex **1** proceeded through a nucleophilic mechanism. Acetophenone and complex **1** in the molar ratio of 1:2 in THF (-70

^0C to $66\text{ }^0\text{C}$), afforded 2,3-diphenyl-2-butene (**2**) in 70% yield (Scheme 3). A “side-on” coordinated ketone intermediate was proposed based on the formation of dideutero 1-phenylethanol (**3**) when the reaction mixture was deuterolyzed at low temperature. Thus, a nucleophilic mechanism, not a radical dimerization mechanism was postulated. This mechanism was also supported by Frenking et al.⁸ using quantum mechanical calculations.

Fürstner et al.^{9,10} proposed a dianion mechanism for the intramolecular McMurry reaction of a ketone and an amide (Scheme 4). Amides do not easily form radical anions with active low valent titanium. Thus the probability of dimerizing a ketyl radical and an amide radical to form the heterocycle is not very high. However, the ketyl radical could be further reduced to the dianion, which could readily carry out a nucleophilic attack on the adjacent amide group to form the carbon-carbon bond. Moreover, the formation of indole product at high concentration of reagents without any intermolecular coupling contradicts the radical dimerization.

Scheme 4

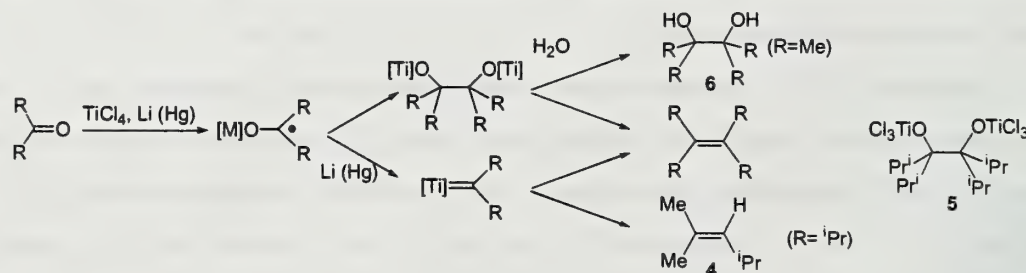


Dualistic Aspects of the Mechanism

Ephritikhine et al.¹¹ recently reported that some McMurry type reactions could follow two different pathways, leading to either the metalpinacol product or the tetraalkylethylene product (Scheme 5). In the reaction of $^i\text{Pr}_2\text{CO}$ with TiCl_4/Li (Hg) amalgam system, $^i\text{Pr}_2\text{C}=\text{C}^i\text{Pr}_2$ and a large amount of 2,4-dimethylpent-2-ene (**4**) was produced. However, no pinacol compound was observed. The reaction of the lithium pinacolate with TiCl_4 and Li (Hg) only produced alkene in a 5% yield. Such control experiments showed that $^i\text{Pr}_2\text{C}=\text{C}^i\text{Pr}_2$ did not result from a metalpinacol intermediate. Moreover, it was found that compound **5** prepared from the corresponding lithium pinacolate with TiCl_4 was not stable, readily decomposing to a mixture of TiCl_3 and $^i\text{Pr}_2\text{CO}$. This finding led to the proposal that the reductive coupling of $^i\text{Pr}_2\text{CO}$ might involve carbenoid intermediates. However, in the reaction of acetone with TiCl_4/Li (Hg), $\text{Me}_2\text{C}=\text{CMe}_2$ and 2,3-dimethylbutane-2,3-diol (**6**) were the major products in accordance with the classical McMurry reaction results. Therefore, acetone might react by the ketyl radical mechanism or dianion mechanism proposed by Fürstner and Bogdanovic. Such a

different result between acetone and diisopropylketone can be explained by steric interactions. More sterically hindered radicals lead to a more difficult dimerization. In addition, steric hindrance could also destabilize the pinacolate intermediate.

Scheme 5



Finely Tuned Reagents

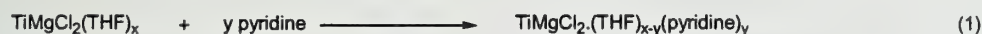
Several attempts to tune the activity of LVT reagents have been made. Banerji et al.¹² reported that when I_2 (0.25 eq) was added as an external redox reagent to $TiCl_3/Li$ in THF system, reductive coupling of carbonyl compounds to form alkene occurred at lower temperature ($\sim 0^\circ C$) in a shorter amount of time (Table 1). This design was based on the effect of redox reagents on organometallic electron transfer processes. Ti^0 was believed to be produced by the reaction of $TiCl_3$ with Li . After the addition of iodine, Ti^0 can be oxidized to TiI_2 which can then disproportionate with Ti^0 to TiI . The TiI formed is proposed to initiate the McMurry reaction even at low temperatures. The $TiCl_3/Li/THF/I_2$ system works well for aliphatic carbonyl couplings as well as aromatic carbonyl couplings. It offers excellent chemoselectivity and diastereoselectivity.

Table 1 Reductive coupling of acetonephenone using $TiCl_3/Li/THF/I_2$

reagents	time (h)	temp ($^\circ C$)	2,3-diphenylbutane-2,3-diol (% yield)	stilbene (%yield)	E/Z ratio
$TiCl_3/Li/THF$	16	reflux	0	89	75/25
$TiCl_3/Li/THF$	16	0-5	87	trace	
$TiCl_3/Li/THF/I_2$	2	0-5	0	90	80/20
$TiCl_3/Li/THF/I_2$	2	-40	trace	75	92/8

Tyrlik's system ($TiCl_3/Mg/THF$) was used to explore the influence of external ligands and auxiliaries on the McMurry reaction.¹³ An inorganic Grignard reagent $[Ti(MgCl_2) \cdot nTHF]$ was assumed to be the active species in this system.¹⁴ When pyridine, a π -acceptor and σ -donor ligand, was added to the $TiCl_3/Mg$ mediated McMurry reaction, less alkene and more pinacol were formed. Complete formation of the diol required the addition of about 10 equiv of pyridine to $TiCl_3/Mg/THF$. The addition

of PPh_3 provided a similar result. The proposed origin of this effect is a reduced electron density of the Ti^0 center by the coordination of pyridine or PPh_3 instead of coordination to THF (eq. 1). Hydroxy auxiliaries (such as menthol, 2,2-dimethyl-1,3-propanediol, and catechol) have been used as external auxiliaries to control the reactivity of LVT by changing the oxidation state of the titanium (eq. 2). High yields of pinacol were achieved with these auxiliaries, most notably with catechol. The catechol-LVT reagent (1:1), upon reaction with benzaldehyde at reflux, produced pinacol as the only product. In contrast, in the absence of catechol the alkene was the sole product. These studies were only carried out with aromatic carbonyl compounds.



New Reagents and Simple Methods

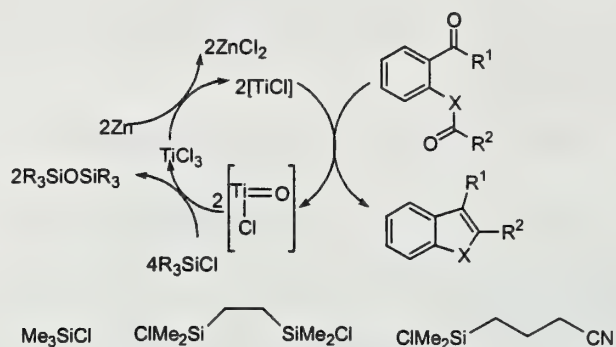
Some simple methods for performing the McMurry reaction have recently been developed. Fürstner et al.¹⁰ reported an “instant method”¹⁰ that involved a TiCl_3/Zn reagent. The studies discussed previously suggest that Ti^0 is not necessary to perform the McMurry reaction. Thus, strong reducing agents such as Li, LiAlH_4 , K, Mg, Na and the stepwise procedure associated with them can be avoided. For instance, a mixture of the appropriate substrate, TiCl_3 (2 equiv), and Zn dust (5 equiv) is refluxed in an ethereal solvent. Presumably during the reaction, TiCl_3 is coordinated to the substrate, and is then reduced by Zn to the proper oxidation state that induces the reductive coupling of the carbonyl groups. This procedure was the first example in which the active species could be prepared in the presence of the substrate, although very acid sensitive substrates may not be suitable for this method. Its power has been demonstrated in the synthesis of indoles, benzofurans and alkenes (Table 2). Oxo amide cyclizations using this method have excellent chemoselectivity and regioselectivity. This “instant method” can also be carried out in nonethereal solvents such as DMF, ethyl acetate, or acetonitrile, and is compatible with many functional groups, thus, extending the scope of the McMurry reaction.

Table 2 Reductive cyclization by using TiCl_3/Zn

substrate	product	yield (%)	substrate	product	yield (%)
		98			76
		87			90

Further improvements on the “instant method” have been reported in the format of a catalytic procedure.¹⁵⁻¹⁶ The carbonyl groups can be coupled using only a catalytic amount of TiCl_3 (Scheme 6). TMSCl , $\text{ClMe}_2\text{SiCH}_2\text{CH}_2\text{SiMe}_2\text{Cl}$ and $\text{ClMe}_2\text{Si}(\text{CH}_2)_3\text{CN}$ were selected as additives due to their pronounced oxophilicity. The mixture of carbonyl substrate, Zn dust, 2–10 mol % of TiCl_3 , and excess additive in MeCN or DME was refluxed in order to yield the desired product.

Scheme 6



In 1995, Fürstner et al.¹⁵ reported that the coupling reaction could be carried out as either a one pot procedure, or in consecutive steps of heating commercial titanium powder with the additive for ≥ 40 h before the addition of substrate. Commercial titanium powder alone was inert to the McMurry reaction due to a compact oxide coating on its surface, but this oxide coating can be removed by treatment with the additives. Electron microscopic studies revealed that the additives not only clean the oxide layer on the surface, but also change the inner structure of the titanium powder.¹⁷

The scope of the McMurry has been extended to the synthesis of aromatic heterocycles by the intramolecular coupling of esters or amides with aldehydes and ketones. The McMurry reaction can also form substituted 1,2-bis(trimethylsilyl)ethene derivatives by the intermolecular or intramolecular reaction of aryltrimethylsilanes.¹⁸ The $\text{Na}/\text{Al}_2\text{O}_3/\text{TiCl}_3$ LVT system is well suited for this reaction. In this case, sodium was deposited on Al_2O_3 , an inorganic support, in order to increase the surface area of the sodium and to decrease the time for completely reducing TiCl_3 . Other compounds, such as TiO_2 , NaCl , and graphite can also serve as good inorganic supports. This was the first example of the reductive coupling of acyl silanes. Some nanostructured titanium clusters have also been shown to be well suited for the McMurry reaction.¹⁹

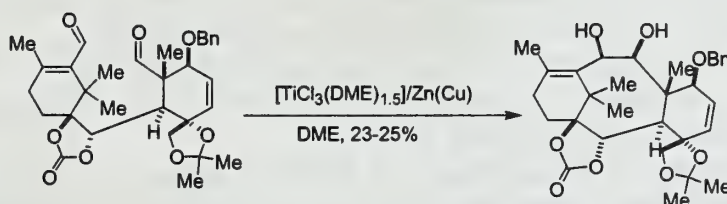
RECENT APPLICATIONS

The formation of titanium-oxygen bonds provides the driving force for the synthesis of sterically hindered tetrasubstituted double bonds. Many syntheses of cycloalkenes using the McMurry reaction

have been reported. One example is the synthesis of tetra-cyclohexylethene,²⁰ from dicyclohexyl ketone by using $\text{TiCl}_3/\text{K}/\text{THF}$. Ferrocifen,²¹ a derivative of the breast cancer drug tamoxifen, was synthesized from the cross-coupling of 4-MeO- $\text{C}_6\text{H}_4\text{COPh}$ and ferrocenyl ethyl ketone in an overall yield of 41%. An alternate approach starting from ferrocenyl acetic acid gave a 5.6% overall yield. The McMurry reaction was also a crucial step for the final macrocyclization in the total synthesis of archaeal 72-membered tetraether lipids.²²

One of the most well-known applications of the McMurry reaction is Nicolaou's total synthesis of taxol.²³ The 8-membered B-ring in its structure was formed by a titanium-mediated cyclization. Using $\text{TiCl}_3\text{-(DME)}_{1.5}/\text{Zn(Cu)}$, the desired pinacol product was afforded from the starting dialdehyde in a 23-25% yield (Scheme 7). This method was also used in the synthesis of various taxol analogs.

Scheme 7



The McMurry reaction had been confined to aldehydes and ketones as the substrates for a long period of time. Only recently it was found that various other functional groups, which were considered to be inert to this reaction, readily undergo intramolecular cross-coupling reactions. This allowed the conversion of easily accessible oxo-amide, oxo-ester, and oxo-carbonate compounds to aromatic heterocycles using Fürstner's "instant method". The syntheses of secofascaplysin, lukianol A, (+)-aristoteline, camalexin and various indole and pyrrole alkaloids demonstrate the usefulness of the McMurry reaction.²⁴⁻²⁶

CONCLUSION

Significant improvements in reagents and understanding of mechanism have been made in the McMurry reaction. The McMurry reaction has been extended to include the synthesis of indoles and pyrroles, as well as cycloalkenes, and has been employed in natural product syntheses. The mechanism of the reaction is much more complex than was previously thought. The structure of the intermediates, pinacolate or carbenoid species, is strongly dependent on the nature of the carbonyl substrate, the titanium compound, and the reducing agent. Future work might focus on further investigations of the mechanism and development of new reagents.

REFERENCES

1. Mukaijama, T.; Sato, T.; Hanna, J. *Chem. Lett.* **1973**, 1041.
2. Tyrlik, S.; Wolochowicz, I. *Bull. Soc. Chim. Fr.* **1973**, 2147.
3. McMurry, J. E.; Fleming, M. P. *J. Am. Chem. Soc.* **1974**, 96, 4708.
4. (a) McMurry, J. E. *Chem. Rev.* **1989**, 89, 1513. (b) Fürstner, A.; Bogdanovic, B. *Angew. Chem., Int. Ed. Engl.* **1996**, 35, 2442.
5. Aleandri, L. E.; Becke, S.; Bogdanovic, B.; Jones, D. J.; Roziere, J. *J. Organomet. Chem.*, **1994**, 472, 97.
6. Frenking, G.; Stahl, M.; Pidun, U. *Angew. Chem., Int. Ed. Engl.* **1997**, 36, 2234.
7. Clive, D. L.; Zhang, C.; Murthy, K. S.; Hayward, W. D.; Daingneault, S. *J. Org. Chem.* **1991**, 56, 6447.
8. Bogdanovic, B.; Bolte, A. *J. Organomet. Chem.*, **1995**, 502, 109.
9. Fürstner, A.; Jumbam, D. *Tetrahedron*, **1992**, 48, 5991.
10. Fürstner, A.; Hupperts, A.; Ptock, A.; Janssen, E. *J. Org. Chem.* **1994**, 59, 5215.
11. Villiers, C.; Ephritikhine, M. *Angew. Chem., Int. Ed. Engl.* **1997**, 36, 2380.
12. Talukdar, S.; Najak, S. K.; Banerji, A. *J. Org. Chem.* **1998**, 63, 4925.
13. Balu, N.; Kayak, S. K.; Banerji, A. *J. Am. Chem. Soc.* **1996**, 118, 5932.
14. Aleandri, L. E.; Bogdanovic, B.; Gaidies, A.; Jones, D. J.; Liao, S.; Michalowicz, A.; Roziere, J.; Schott, A. *J. Organomet. Chem.*, **1993**, 459, 87.
15. Fürstner, A.; Hupperts, A. *J. Am. Chem. Soc.* **1995**, 117, 4468.
16. Fürstner, A. *Pure & Appl. Chem.* **1998**, 70, 1071.
17. Fürstner, A.; Tesche, B. *Chem. Mater.*, **1998**, 10, 1968.
18. Fürstner, A.; Seidel, G.; Gabor, B.; Kopiske, C.; Kruger, C.; Mynott, R. *Tetrahedron*, **1995**, 50, 8875.
19. Reetz, M. T.; Quaiser, S. A.; Merk, C. *Chem. Ber.* **1996**, 129, 741.
20. Columbus, I.; Biali, S. E. *J. Org. Chem.* **1994**, 59, 3402.
21. Top, S.; Dauer, B.; Vaissermann, J.; Jaouen, G. *J. Organomet. Chem.*, **1997**, 541, 355.
22. Eguchi, Y.; Ibaragi, K.; Kakinuma, K. *J. Org. Chem.* **1998**, 63, 2689.
23. (a) Nicolaou, K. C.; Yang, Z.; Liu, J. J.; Ueno, H.; Nantermet, P. G.; Guy, R. K.; Claiborne, C. F.; Renaud, J.; Couladouros, E. A.; Paulvannan, K.; Sorensen, E. J. *Nature*, **1994**, 367, 630. (b) Nicolaou, K. C.; Liu, J. J.; Yang, Z.; Ueno, H.; Sorensen, E. J.; Claiborne, C. F.; Guy, R. K.; Hwand, C. K.; Nakada, M.; Nantermet, P. G. *J. Am. Chem. Soc.* **1995**, 117, 634. (c) Nicolaou, K. C.; Yang, Z.; Liu, J. J.; Nantermet, P. G.; Claiborne, C. F.; Renaud, J.; Guy, R. K.; Ahibayama, K. *J. Am. Chem. Soc.* **1995**, 117, 645.
24. Fürstner, A.; Ptock, A.; Weintritt, H.; Goddard, R.; Kruger, C. *Angew. Chem., Int. Ed. Engl.* **1995**, 34, 678.
25. Fürstner, A.; Weintritt, H.; Hupperts, A. *J. Org. Chem.* **1995**, 60, 6637.
26. Fürstner, A.; Ernst, A.; Krause, H.; Ptock, A. *Tetrahedron*, **1996**, 52, 7329.

SYNTHETIC TEMPLATES THAT FACILITATE THE FORMATION OF ARTIFICIAL β -SHEETS

Reported by Sara L. Adamski-Werner

February 4, 1999

INTRODUCTION

β -Sheets consist of nearly fully extended polypeptide chains that interact with one another through intermolecular hydrogen bonds (Figure 1). Antiparallel β -sheets contain 10 and 14 membered alternating hydrogen bonded rings, while parallel β -sheets contain repeating 12-membered hydrogen bonded rings. Proteins that consist of primarily β -sheet regions include constitutive proteins of silk as well as pectate lyase. Since the proposal of the detailed structures for parallel and antiparallel β -sheets by Pauling,¹ researchers have worked toward understanding the mechanisms behind protein folding, including the mechanism of β -sheet formation. Determination of this mechanism is important for the rational design of pharmaceuticals as well as the basic study of biological processes. Researchers

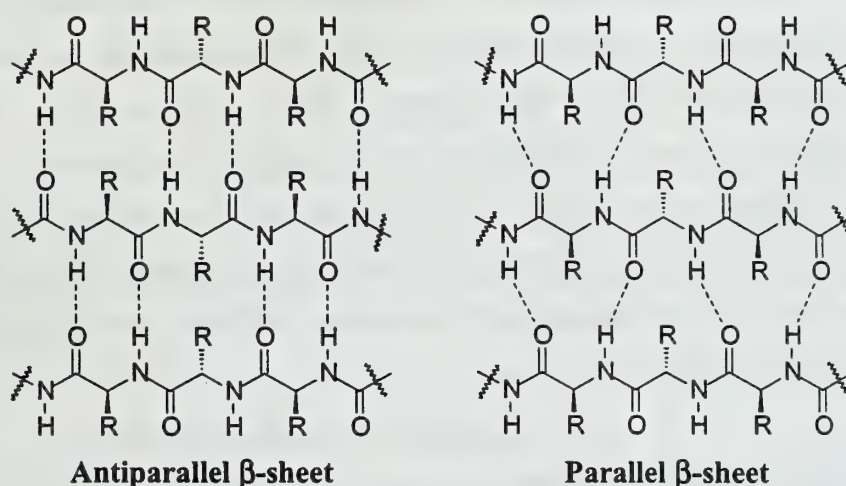


Figure 1

examining the mechanism of amyloid fibril formation in Alzheimer's disease have found a special interest in the study of β -sheets, specifically the investigation of small peptidic analogs as model systems.^{2,3} The analysis of such small peptide models proved difficult because of the propensity of β -sheets to form large, insoluble aggregates through hydrophobic, electrostatic, and hydrogen bonding interactions. These large self-assemblies are difficult to characterize via conventional means including 1D and 2D ^1H NMR, FTIR, circular dichroism, and x-ray diffraction.

The recent development of rigid synthetic templates that facilitate the formation of β -sheet structures has allowed the potential for the design and characterization of model β -sheet analogs, referred to as artificial β -sheets. Many of these rigid templates can be considered β -turn mimics because

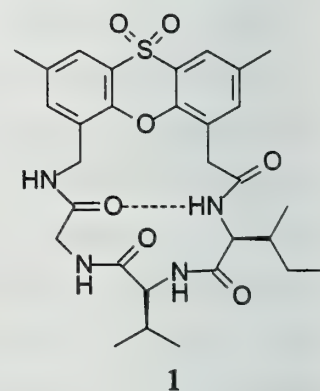
they hold two peptide strands in close proximity, while at the same time reversing the direction of the peptide chain. This allows for interstrand hydrogen bond formation and in some cases, hydrophobic cluster formation.

The use of one and two dimensional ^1H NMR spectroscopy can lend great insight into the structure and behavior of β -sheets.⁴ Specifically, nuclear Overhauser effect spectroscopy (NOESY), deconvolution of coupling constant data, and variable temperature experiments have been implemented to determine the degree of hydrogen bond formation or the lack thereof in artificial β -sheets.

TEMPLATES THAT EMPLOY INTERSTRAND HYDROGEN BONDING

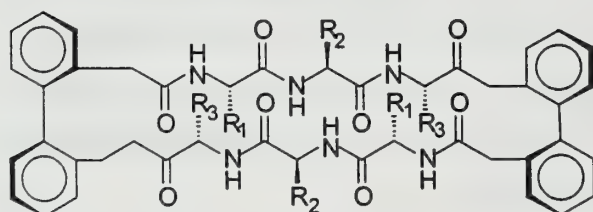
Feigel's Historical *S*-dioxide Template

The Feigel laboratory was one of the first to synthesize and characterize an artificial β -sheet incorporating a synthetic template in 1986.⁵ The incorporation of isoleucine, glycine, and valine into a 2,8-dimethyl-4-(carboxymethyl-6-aminomethyl) phenoxathiin *S*-dioxide template produced (**1**), which exhibited characteristics consistent with those of hydrogen bonded β -sheets. Characterization of **1** by variable temperature NMR, NOESY, and coupling constant analysis showed that the dihedral angles, NOE enhancements and temperature coefficients consistent with a β -sheet-like structure were present.



Feigel's Biphenyl Template

More recently, Feigel and coworkers developed a 2'-(aminomethyl) biphenyl-2-carboxylic acid scaffold, which when attached to peptide strands including phenylalanine and glycine (**2**), also possessed characteristics consistent with β -sheet formation.⁶ NMR analysis of **2**



2

showed evidence for the presence of three atropisomers: the (*R,R*)- (*R,S*)- and (*S,S*)- diastereomers. The major isomer by NMR was a C2 symmetric species, implying that either the (*R,R*)- or (*S,S*)- isomer was the dominant material present. Molecular modeling as well as low temperature NMR of **2** suggested that the major isomer was the (*R,R*)-

diastereomer. The hydrogen bonding in **2** was investigated by NOE experiments and by coupling constant analysis. Both of these tools provided evidence for the existence of an artificial β -sheet.

Kemp's Biphenyl Acetylene Template

Shortly following Feigel's biphenyl template, Kemp and coworkers reported an artificial β -sheet containing valine and glycine and incorporating a 2-amino-2'-carboxydiphenylacetylene template (3).⁷ NOESY spectra of 3 showed NOE enhancements characteristic of β -sheet formation. In addition, CD spectra exhibited absorption minima and maxima consistent with the formation of an artificial β -sheet. Proline is considered to be an amino acid with low propensity for β -sheet formation due to the fact that it "kinks" the pleated sheet and disrupts the interstrand hydrogen bonding distances.⁸ In spite of proline being disfavored for the formation of β -sheets, Kemp and coworkers incorporated it into an artificial β -sheet (4).⁹ They observed that the strands were able to bend by 90° without disturbing the hydrogen bonds in the molecule. Because of the uniqueness of proline, both an *s-cis* and an *s-trans* isomer may be present. NMR of 4 in DMSO showed the existence of both isomers; however, NMR in CD_2Cl_2 only showed evidence for the existence of one isomer. NOE experiments of 4 confirmed that the isomer present in CD_2Cl_2 was *trans*.

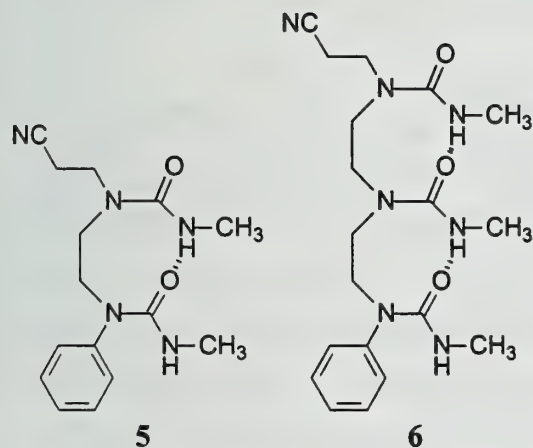
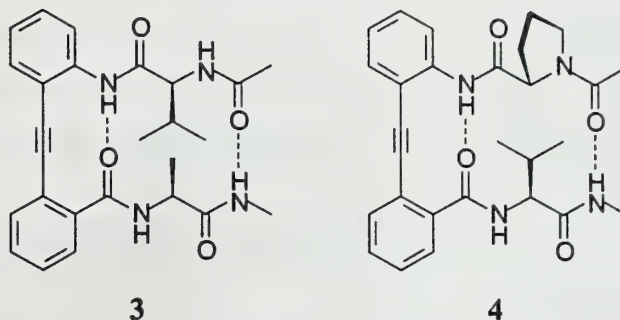


Figure 2

Nowick's Oligourea Templates

Since 1992, Nowick and coworkers have reported the development of artificial β -sheets utilizing several oligourea templates¹⁰ (Figure 2). Bisurea 5 was studied intensively to determine its ability to form a rigid template.¹¹ It has been shown that when one of the urea nitrogens was substituted with both a phenyl and alkyl substituent, the phenyl group and the carbonyl group preferred to occupy *anti* positions (Figure 3). In this

conformation, the carbonyl oxygen was hydrogen bonded to the amide proton of the second urea nitrogen. Molecular dynamics calculations agreed with this analysis, showing that the *anti* conformation was preferred over

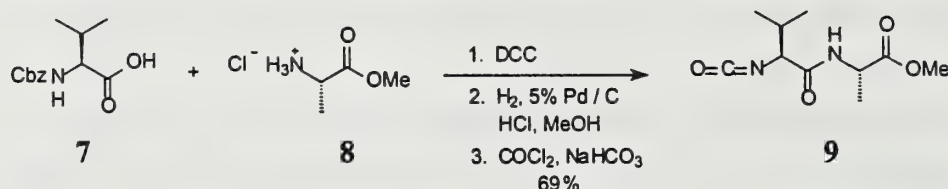


Figure 3

the *syn* conformation by 2 to 7 kcal/mol. IR and ^1H NMR characterization of **5** supported the proposed hydrogen bonding scheme in the bisurea template.

Recently, Nowick and coworkers reported the synthesis of a two-stranded artificial β -sheet beginning with the coupling of the amino acids valine and alanine (Scheme 1). Standard amino acid

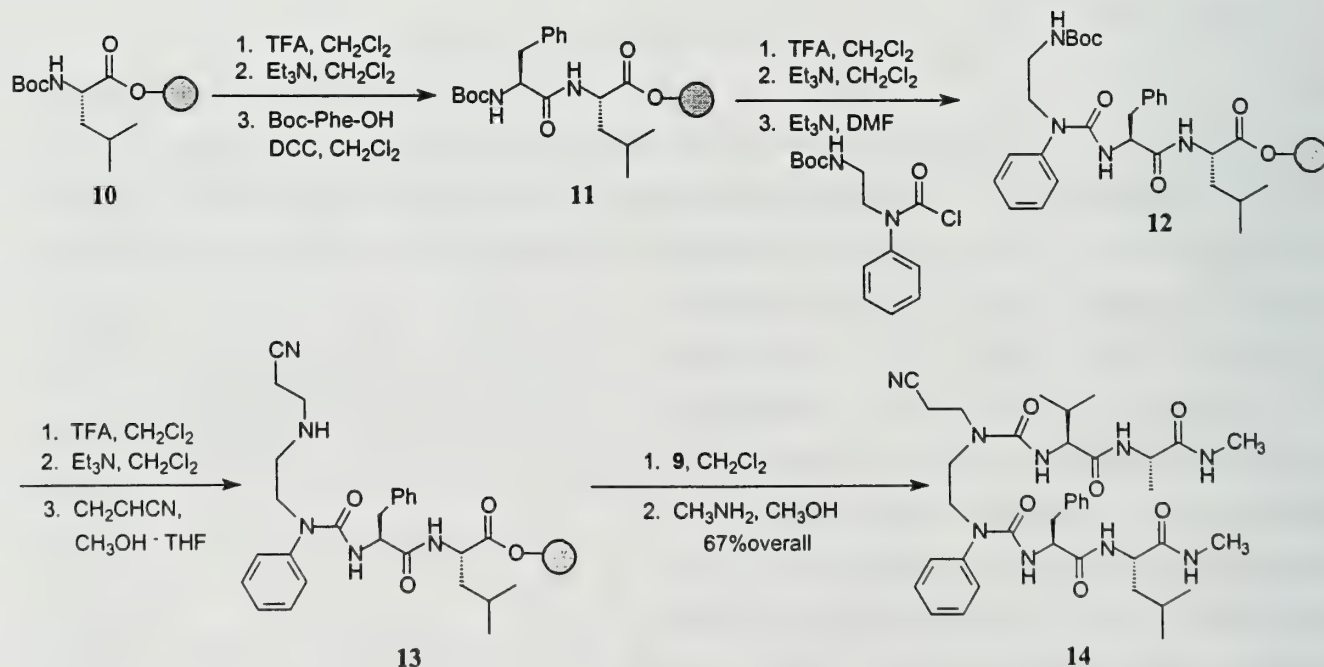
Scheme 1



coupling conditions using DCC, followed by subsequent addition of phosgene in sodium bicarbonate yielded the peptide isocyanate **9** in 69% yield.¹² Artificial β -

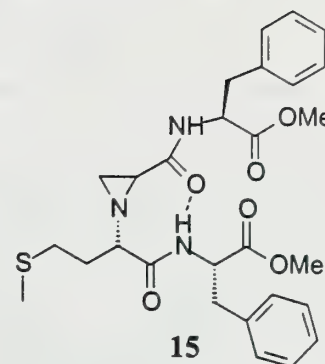
sheet **14** was synthesized in a 67% overall yield using solid phase techniques (Scheme 2).¹³ The final product was examined using amide proton chemical shift analysis and NOE enhancements.¹⁴ The amide protons in the artificial β -sheet were shifted significantly downfield compared to amides of the same amino acids in control peptide strands, suggesting the presence of hydrogen bonding. Furthermore, NOE enhancements were indicative of β -sheet formation.

Scheme 2



Taddei's Aziridine Templates

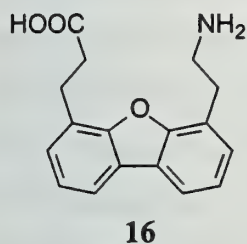
Taddei and coworkers recently reported the preparation of artificial β -sheets using an aziridine scaffold (**15**).¹⁵ Characterization of these artificial β -sheets included a ^1H NMR concentration dependence experiment. Spectra taken in 0.1 M CDCl_3 revealed the amide proton chemical shift at 7.30 ppm. A decrease in concentration to 1 mM resulted in a downfield shift to 7.69 ppm. This result supported the formation of intramolecular hydrogen bonds.



TEMPLATES THAT EMPLOY HYDROPHOBIC CLUSTER FORMATION

Kelly's Dibenzofuran Template

One of the first artificial β -sheet templates synthesized by Kelly and coworkers incorporated a dibenzofuran skeleton (**16**).^{16,17} Extensive studies of this template incorporating lysine, valine, and alanine led to the important notion that hydrophobic cluster formation between the dibenzofuran and hydrophobic amino acid side chains was imperative for the formation of β -sheet structures.¹⁸ Subsequently, Kelly and coworkers have developed and reported several other aromatic templates that give rise to hydrophobic clusters, as discussed below.



Kelly's Biphenyl Template

Kelly's 2,3'-substituted biphenyl-based template was reported to induce similar hydrophobic cluster formation as that of the dibenzofuran template, as well as interstrand hydrogen bond formation.¹⁹ Analysis of simple diamide derivatives of the template in organic solvent revealed the possibility of forming both a 13-membered hydrogen bonded ring and a 15-membered hydrogen bonded ring (Figure 4). Variable temperature NMR studies suggested interconversion of the hydrogen bonded rings, during which the 15-membered ring was favored. While IR studies supported that result, X-ray

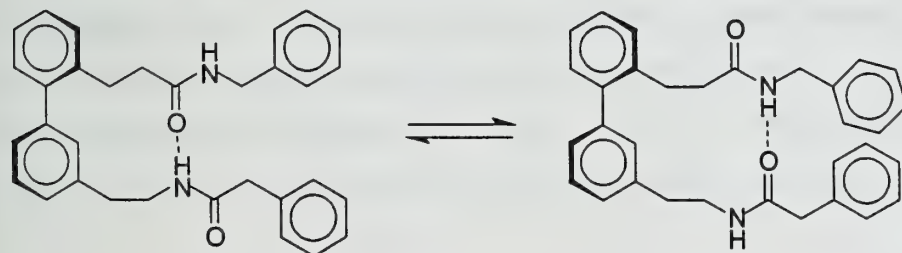
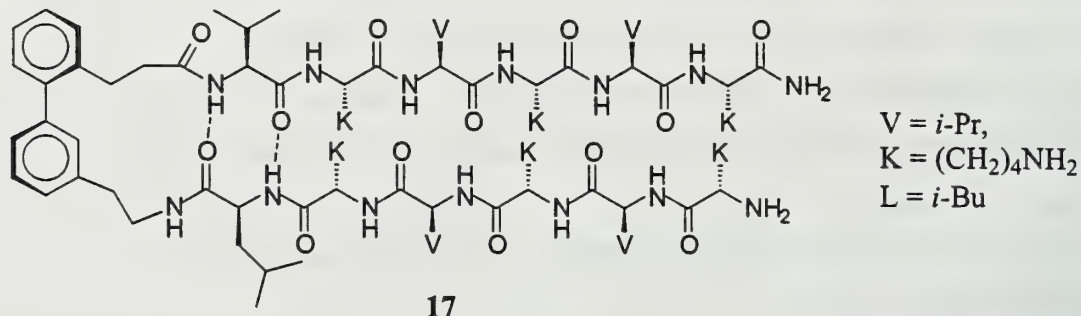


Figure 4

crystallographic analysis suggested that the 13-membered hydrogen bonded ring was favored, possibly due to the influence of crystal packing forces. IR

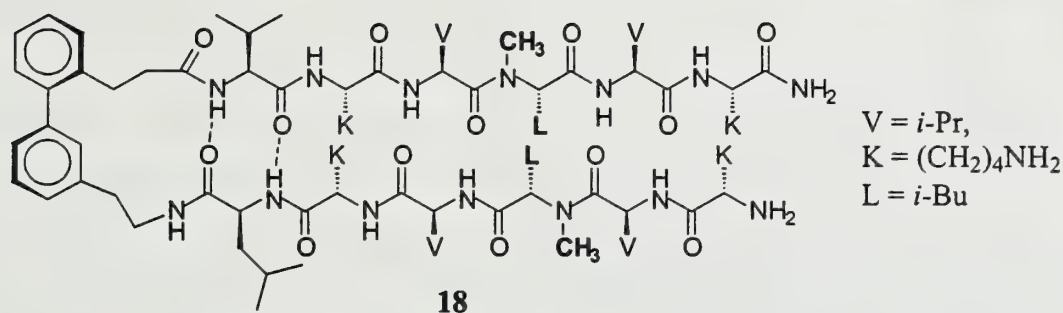
spectra were taken at varying concentrations in CHCl_3 , and the absence of a concentration dependence on the shape or shift of the amide bands suggested the lack of intermolecular interactions.

Incorporation of various peptide strands allowed for the detailed study of the biphenyl template in aqueous solvent.²⁰ Protonation of the lysine side chain in **17**, at low pH, should prevent the formation



of β -sheet structure if hydrophobic cluster formation is an important factor. Conversely, deprotonation of the lysine side chain should allow folding to occur. Circular dichroism studies of this tridecapeptide revealed that between pH 8.6 and 9.0, a transition from random coil structure to β -sheet structure occurred. The presence of a concentration dependence in the CD spectrum implied that intermolecular interactions, specifically hydrogen bonding, were occurring along with the intramolecular interactions. Removal of the ethylene linker between the template and the peptide strand showed the absence of β -sheet structure by CD from pH 4.0 to 9.8. This observation was presumably due to decreased flexibility in the peptide chains and inability of the flanking valine and leucine to interact with the hydrophobic biphenyl template, thus supporting the theory of hydrophobic cluster formation. NOE studies were consistent with the formation of a hydrophobic cluster and the presence of interstrand hydrogen bonding. Amide proton–deuterium exchange rates for the leucine and valine residues flanking the biphenyl template in **17** indicated that the exchange rates for the valine and leucine amide protons were approximately an order of magnitude slower than the other amides in the molecule with measurable rates. Finally, equilibrium ultracentrifugation resulted in observation of self-assembled β -sheets, supporting the presence of intermolecular hydrogen bonding interactions as seen by circular dichroism.

Methylation of amide groups that do not participate in hydrogen bonding should eliminate the formation of intermolecular hydrogen bonding. Indeed, substitution of two of the lysines with *N*-methyl leucine (i.e. **18**) resulted in the absence of any observations consistent with intermolecular β -sheet formation.



Kelly's Dimethylxanthene Template

More recently, Kelly and coworkers reported a 9,9-dimethylxanthene-based amino acid template.²¹ Similar to the biphenyl template, the xanthene template is capable of forming either a 13-membered hydrogen bonded ring or a 15-membered hydrogen bonded ring (Figure 5). Studies of this template in organic solvent

reveal the presence of puckering due to the isopropylidene functionality.

This puckering could prove useful in the formation of hydrophobic clusters due to the accessibility of

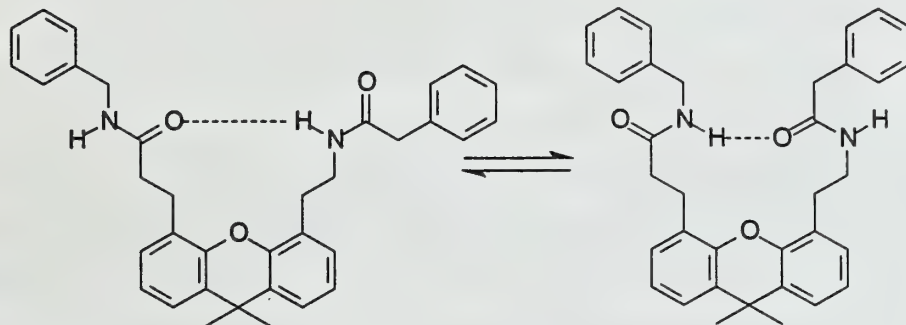


Figure 5

conformations not accessible with the other β -sheet nucleating templates. IR and COSY experiments suggested that the formation of the 13-membered ring was favored, and intermolecular interactions were absent at room temperature.

CONCLUSION

The synthesis and characterization of synthetic template-facilitated artificial β -sheets is a relatively young area of research. Understanding the mechanism behind protein folding, specifically β -sheet formation and aggregation, may allow development of treatments for amyloid diseases, specifically Alzheimer's disease.

REFERENCES

- 1) Pauling, L.; Corey, R. *Proc. Natl. Acad. Sci. U.S.A.* **1951**, *37*, 729.
- 2) Maeda, H.; Ooi, K. *Biopolymers* **1981**, *20*, 1549.
- 3) Nowick, J.; Smith, E.; Pairish, M. *Chem. Soc. Rev.* **1996**, *25*, 401.
- 4) Wüthrich, K. *NMR of Proteins and Nucleic Acids*; Wiley & Sons; New York, 1986.
- 5) Feigel, M. *J. Am. Chem. Soc.* **1986**, *108*, 181.
- 6) Brandmeier, V.; Sauer, W.; Feigel, M. *Helv. Chim. Acta.* **1994**, *77*, 70.
- 7) Kemp, D.; Li, Z. *Tetrahedron Lett.* **1995**, *36*, 4175.
- 8) Chou, P.; Fasman, G. *Biochemistry* **1974**, *13*, 211.
- 9) Kemp, D.; Li, Z. *Tetrahedron Lett.* **1995**, *36*, 4179.
- 10) Nowick, J.; Powell, N.; Martinez, E.; Smith, E.; Noronha, G. *J. Org. Chem.* **1992**, *57*, 3763
- 11) Nowick, J.; Abdi, M.; Bellamo, K.; Love, J.; Martinez, E.; Noronha, G.; Smith, E.; Ziller, J. *J. Am. Chem. Soc.* **1995**, *117*, 89.
- 12) Nowick, J.; Holmes, D.; Noronha, G.; Smith, E.; Nguyen, T.; Huang, S. *J. Org. Chem.* **1996**, *61*, 3929.
- 13) Holmes, D.; Smith, E.; Nowick, J. *J. Am. Chem. Soc.* **1997**, *119*, 7665.
- 14) Nowick, J.; Smith, E.; Noronha, G. *J. Org. Chem.* **1995**, *60*, 7386.
- 15) Filigheddu, S.; Taddei, M. *Tetrahedron Lett.* **1998**, *39*, 3857.
- 16) Díaz, H.; Espina, J.; Kelly, J. *J. Am. Chem. Soc.* **1992**, *114*, 8316.
- 17) Bekele, H.; Nesloney, C.; McWilliams, K.; Zacharias, N.; Chitnumsub, P.; Kelly, J. *J. Org. Chem.* **1997**, *62*, 2259.
- 18) Tsang, K.; Díaz, H.; Graciani, N.; Kelly, J. *J. Am. Chem. Soc.* **1994**, *116*, 3988.
- 19) Nesloney, C.; Kelly, J. *J. Org. Chem.* **1996**, *61*, 3127.
- 20) Nesloney, C.; Kelly, J. *J. Am. Chem. Soc.* **1996**, *118*, 5836.
- 21) McWilliams, K.; Kelly, J. *J. Org. Chem.* **1996**, *61*, 7408.

POLYMER-ASSISTED SOLUTION-PHASE CHEMICAL LIBRARY SYNTHESIS AND PURIFICATION

Reported by Lynne A. Miller-Deist

February 8, 1999

INTRODUCTION

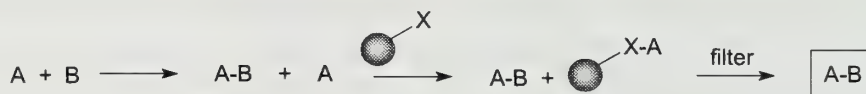
In the past decade, the generation and use of combinatorial chemistry libraries has emerged as a powerful method for pharmaceutical drug discovery and synthesis.¹⁻⁶ While traditional organic chemistry requires a labor-intensive synthetic process to produce a single purified target molecule, combinatorial chemistry can generate a large library of structurally diverse compounds simultaneously. The massive interest in the utilization of such libraries for the production of small organic molecules has prompted the development of new, general methodologies to accomplish the rapid purification, isolation and manipulation of the compounds therein.

Many of the early chemistry libraries were prepared by substrate-linked, polymer-supported synthesis using beads,⁷ pins,⁵ chips,⁸ and other solid supports. This strategy enabled the separation of reagents, starting materials and solvents from the desired product by a simple filtration. Therefore, excess reactants could be used to drive a reaction to completion without complicating the isolation and purification of the final product. Unfortunately, this simple purification came at a price. The cost and loading capacity of the commercially available solid-phase resins restricted the quantity of material that could be produced. In addition, the lack of techniques for monitoring reaction progress and analyzing products made the development of solid-phase synthetic techniques slow and inefficient. In an effort to eliminate these shortcomings, solution-phase combinatorial chemistry was offered as a second approach to chemical library synthesis.

Solution-phase combinatorial methods hold several advantages when compared to their solid-phase counterparts. For example, the multiplicity of solution-phase reactions that have been optimized and documented in the literature far surpasses the number of those utilizing solid-phase. Furthermore, in the solution-phase, reaction progress and the identity and purity of products can be analyzed by well-established chromatographic and spectroscopic means. Solution-phase techniques also eliminate the need for resin attachment and cleavage steps, and the large number of relatively affordable reagents and solvents makes scale-up simple and inexpensive. Regrettably, the methods traditionally utilized for the purification of individual compounds (e.g. crystallization, extraction and chromatography)⁹ do not lend themselves well to the purification of large libraries of structurally-diverse products.

In 1996, Kaldor and Siegel¹⁰ of Lilly Research Laboratories set out to develop a hybrid method of chemical library purification combining the chemical versatility associated with solution-phase synthetic techniques with the ease of purification associated with the solid-phase. The concept was a simple one—to perform a reaction in the solution-phase from which unreacted excess starting materials could be removed via a subsequent “quenching” step which would covalently bind them to a “scavenger” molecule linked to a solid support (Scheme 1). This approach theoretically would provide products of high purity by simple filtration and evaporation. Techniques such as these have collectively become known as polymer-assisted solution-phase (PASP) chemistry.

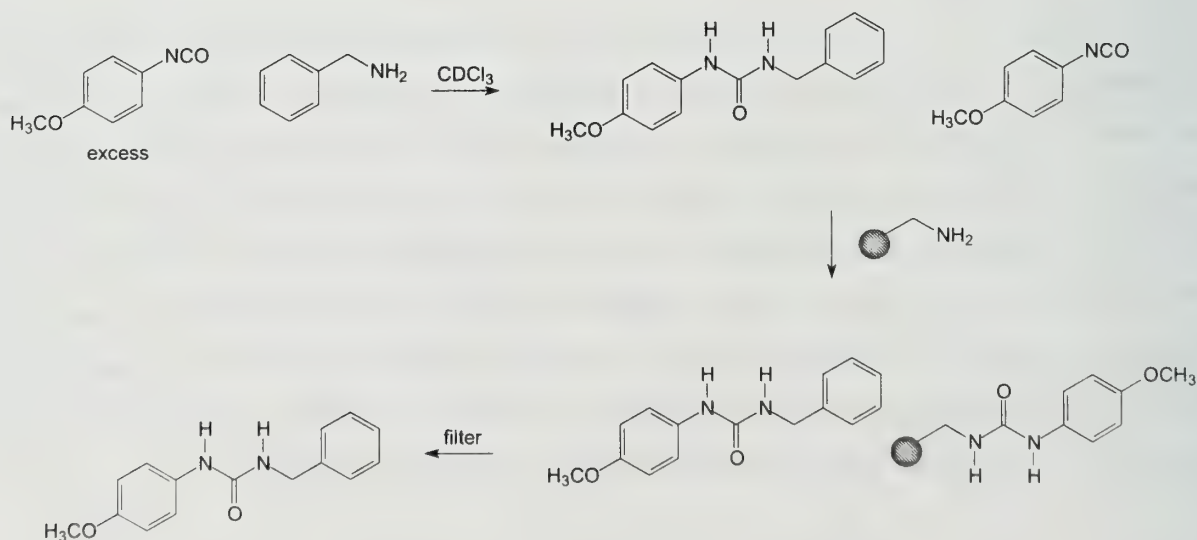
Scheme 1



SOLID-PHASE SCAVENGING

The concept of scavenging reagents in organic chemistry was not a new one. In 1981, Fréchet and co-workers¹¹ reported the use of a solid-supported amine to remove exo-methylene lactone contaminants from natural oils. In 1983, Carpino and co-workers¹² reported the use of solid-supported piperazine as a scavenger of dibenzofulvene. Kaldor and Siegel first chose to investigate the addition of excess *p*-methoxyphenyl isocyanate to benzylamine in CDCl_3 with aminomethylpolystyrene added as a scavenger (Scheme 2). The benzylamine and the isocyanate were allowed to stir at room temperature

Scheme 2



for one hour, at which point excess aminomethyl polystyrene was added, the reaction filtered, and the resulting CDCl_3 solution analyzed by ^1H NMR. Only the desired urea product was observed, with no evidence of excess isocyanate. After this initial success, Kaldor and Siegel went on to utilize electrophilic and nucleophilic scavengers in the synthesis of ureas, thioureas, amides, sulfonamides and carbamates, as well as in the alkylation of both primary and secondary amines.

POLYMER-SUPPORTED QUENCH (PSQ)

The Kaldor and Siegel results were published at the same time as a second landmark paper in the area of polymer-assisted solution-phase chemistry. In 1997, Hodges and Booth⁹ of Parke-Davis reported their independent development of polymer-supported quench (PSQ) reagents for the purification of parallel solution-phase combinatorial libraries. Three polymeric reagents (Figure 1) structurally similar to those utilized by Kaldor and Siegel were readily synthesized in one step from commercially available polymers.

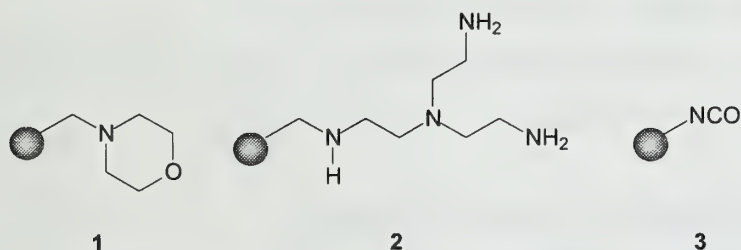
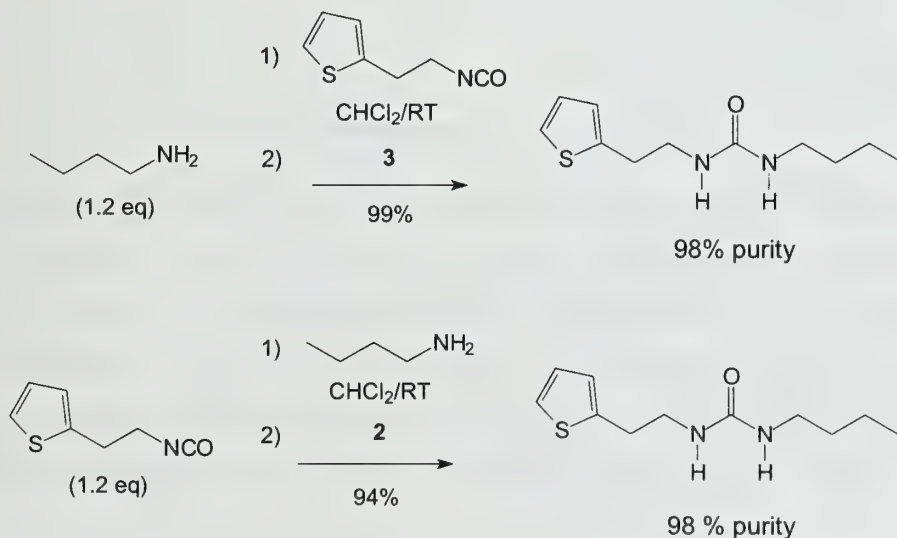


Figure 1. Polymeric reagents utilized by Hodges and Booth⁹.

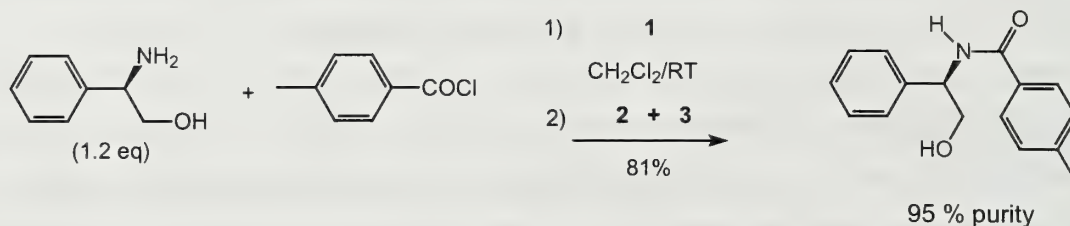
Scheme 3 shows selected examples in which these polymeric reagents were employed for

Scheme 3



synthesis and purification. Two very important advantages of polymer-assisted solution-phase techniques could be ascertained from these results. First, it was shown that product formation and

Scheme 4

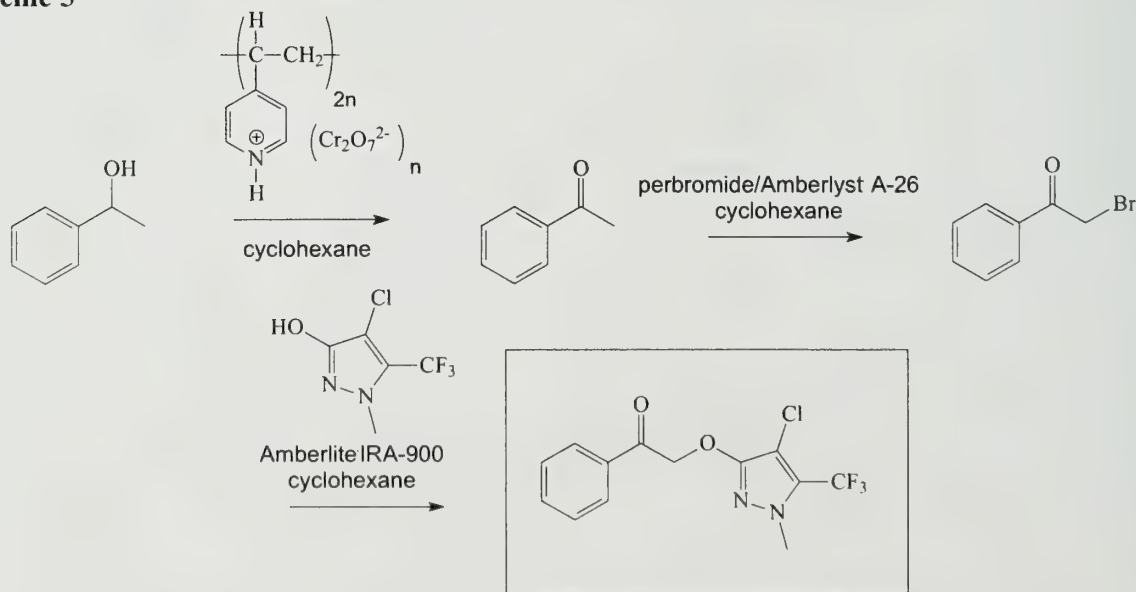


purification could be optimized by choosing one reagent to use in excess and adjusting the quenching resin accordingly. This was nicely illustrated by the complementary synthetic routes utilized in Scheme 3. Second, the purification of the amino alcohol in Scheme 4 also determined that a variety of quenching reagents could be added simultaneously to a reaction mixture for the purpose of removing impurities and excess starting materials. This result supported those presented in a paper by Parlow¹³ in 1995 regarding what would prove to be a valuable contribution to the field of solution-phase library purification: simultaneous multistep synthesis using polymeric reagents.

POLYMERIC REAGENTS AND MULTISTEP SYNTHESIS

In 1995, Parlow of Monsanto Company reported on the synthesis shown in Scheme 5. This synthesis was initially performed using three different polymeric reagents in a sequential fashion to obtain a 42% yield of desired product. The same synthesis was then performed utilizing all three

Scheme 5

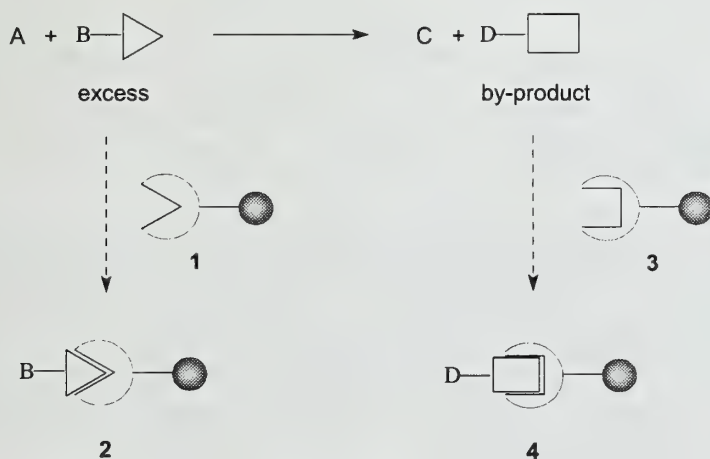


polymeric reagents simultaneously in a single reaction vessel. Upon filtration, a 48% yield of the desired product was obtained. This result was of fundamental importance, as the incompatibility of the soluble counterparts of these reagents in a homogeneous solution would never have resulted in the formation of the desired product. This simple yet significant study helped pave the way toward the third strategy developed for the polymer-assisted purification of solution-phase chemical libraries. This strategy utilizes sequestering resins, polymer-supported reagents, sequestration-enabling-reagents (SER), and soluble, bifunctional tagged reagents for solution-phase chemical library purification and has become known as complementary molecular reactivity and recognition (CMR/R).

COMPLEMENTARY MOLECULAR REACTIVITY/RECOGNITION (CMR/R)

In 1997, Parlow and Flynn¹⁴ of Monsanto's Searle Discovery Research independently reported a modification of polymer-supported quench methodology known as complementary molecular reactivity and recognition. This approach relied on the inherent or artificially-imparted molecular recognition and/or molecular reactivity as the basis for product purification and isolation. Scheme 6 illustrates the CMR/R approach for a system containing excess reactants and byproducts.

Scheme 6



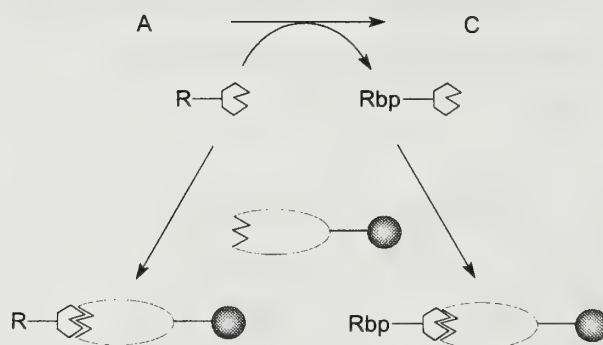
Excess reactant B would drive the solution-phase reaction toward completion by complete consumption of limiting reactant A. Once A had been consumed, the excess reactant B could be removed from solution by a complementary molecular reactivity resin **4**, so that simple filtration would give a purified solution of product C. If byproduct D should be produced along with product C, and D contained an inherently accessible molecular recognition functionality, a second complementary molecular reactivity resin **6** could be utilized to chemoselectively sequester D from the product. In this

way, simple filtration and concentration would afford purified product C. Parlow and co-workers successfully applied CMR/R technology to the rapid purification of parallel amine acylation reactions.

They found that mass recovery of greater than 88% generally was obtained with purities of 94% or greater by HPLC, MS and NMR analysis. This methodology was then applied successfully to the solution-phase work-up of organometallic reactions in an effort to show the inherent applicability of polymer-assisted solution-phase techniques to rapid, automated industrial processes. While the CMR/R reactant and byproduct resins were successfully implemented to purify these solution-phase libraries, the need for a general methodology for use with entities lacking an inherently-sequestrable functionality remained.

Scheme 7 illustrates the design proposed by Parlow and co-workers for the use of artificially-imparted molecular recognition in polymer-assisted solution-phase technology. In this case, soluble

Scheme 7



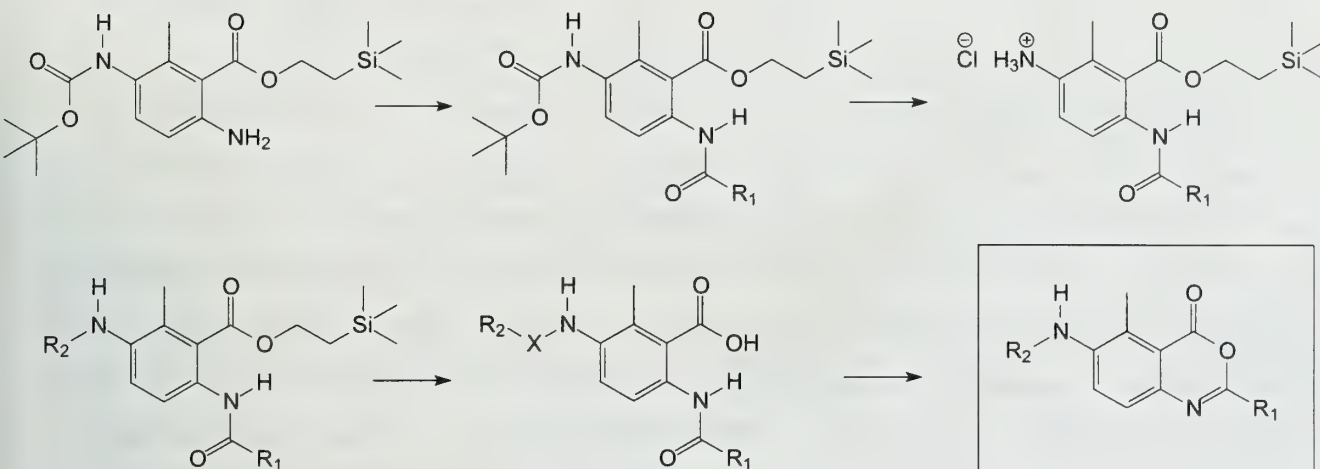
bifunctional tagged reagents would contain artificially-imparted molecular recognition functionality designed to interact specifically with a complementary molecular recognition tag on a resin. The resulting byproduct would lend itself to sequestration by the tagged resin to afford a purified solution of product C after incubation and filtration. This methodology was applied successfully to the parallel Moffatt oxidations of secondary alcohols to ketones.

PASP AND MULTISTEP SYNTHESSES

A recent example of the application of CMR/R technology to multistep library synthesis was the parallel preparation and purification of a solution-phase library of benzoxazinones (Scheme 8) by Parlow and co-workers.¹⁵ In general, compounds in which R₁ is described as an alkyl or alkoxy functionality exhibited good to excellent purities ranging from 82-99%. Only three compounds exhibited HPLC purities less than 50%. When one considers the goal of producing 35 complex

molecules with differing functionalities and sufficient purity for further experimentation and screening, the yields obtained utilizing this five-step synthesis (average: 49%) are quite respectable and deem this purification strategy highly amenable to use with automation processes in the future.

Scheme 8



CONCLUSION

It has been shown that PASP techniques can be used to simplify the synthesis and purification of solution-phase chemical libraries. Furthermore, the use of polymer-supported reagents in conjunction with this methodology has led to the development of more versatile protocols amenable to a wide variety of solution-phase syntheses. These processes show great promise for use with the automated standard operating protocols utilized in industrial settings for the preparation and purification of large numbers of structurally diverse compounds for experimentation and screening. These and related methodologies have recently been applied to the solution-phase syntheses of a number of valuable classes of compounds, including heterocyclic carboxamides,¹⁶ acyl-aminopiperidines¹⁷ and perhydrooxazin-4-ones.¹⁸ In addition, a number of new applications have been seen with regard to the use of chemically-tagged reagents for use in solution-phase chemical library synthesis. Noteworthy examples of these reagents are newly-designed Mitsunobu reagents¹⁹ and in-situ chemical tagging of tetrafluorophthalic anhydride as a "sequestration-enabling-reagent"²⁰ in the synthesis and purification of solution-phase combinatorial libraries.

REFERENCES

- 1) Gallop, M. A.; Barrett, R. W.; Dower, W. J.; Fodor, S. P. A.; Gordon, E. M. *J. Med. Chem.* **1994**, 37, 1233.
- 2) Janda, K. D. *Proc. Natl. Acad. Sci. U.S.A.* **1994**, 91, 10799.
- 3) Tenet, N. K.; Gardner, M.; Gordon, D. W.; Kobylecki, R. J.; Steele, J. *Tetrahedron* **1995**, 51, 8135.
- 4) Bunin, B. A.; Ellman, J. A. *J. Am. Chem. Soc.* **1992**, 114, 10997.
- 5) Geysen, M. H.; Meloen, R. H.; Barteling, S. J. *Proc. Natl. Acad. Sci. U.S.A.* **1984**, 81, 3998.
- 6) Houghton, R. A. *Proc. Natl. Acad. Sci. U.S.A.* **1985**, 82, 2149.
- 7) Merrifield, R. B. *J. Am. Chem. Soc.* **1963**, 85, 2149.
- 8) Fodor, S. P. A.; Read, J. L.; Stryer, L.; Lu, A. T.; Solas, D. *Science* **1991**, 251, 767.
- 9) Booth, R. J.; Hodges, J. C. *J. Am. Chem. Soc.* **1997**, 119, 4882.
- 10) Kaldor, S. W.; Siegel, M. G.; Fritz, J. E.; Dressman, B. A.; Hahn, P. J. *Tetrahedron Lett.* **1996**, 37, 7193.
- 11) Cheminat, A.; Benezra, C.; Farrall, M. J.; Fréchet, J. M. J. *Can. J. Chem.* **1981**, 59, 1405.
- 12) Carpino, L. A.; Mansour, E. M. E.; Knapczyk, J. *J. Org. Chem.* **1983**, 48, 666.
- 13) Parlow, J. J. *Tetrahedron Lett.* **1995**, 36, 1395.
- 14) Flynn, D. L.; Crich, J. Z.; Devraj, R. V.; Hockerman, S. L.; Parlow, J. J.; South, M. S.; Woodard, S. *J. Am. Chem. Soc.* **1997**, 119, 4874.
- 15) Parlow, J. J.; Flynn, D. L. *Tetrahedron* **1998**, 54, 4013.
- 16) Parlow, J. J.; Mischke, D. A.; Woodard, S. S. *J. Org. Chem.* **1997**, 62, 5908.
- 17) Creswell, M. W.; Bolton, G. L.; Hodges, J. C.; Meppen, M. *Tetrahedron* **1998**, 54, 3983.
- 18) Panunzio, M.; Villa, M.; Missio, A.; Rossi, T.; Seneci, P. *Tetrahedron Lett.* **1998**, 39, 6585.
- 19) Starkey, G. W.; Parlow, J. J.; Flynn, D. L. *Bioorg. & Med. Chem. Lett.* **1998**, 8, 2385.
- 20) Parlow, J. J.; Naing, W.; South, M. S.; Flynn, D. L. *Tetrahedron Lett.* **1997**, 38, 7959.

METALLOCENE CATALYSTS FOR OLEFIN POLYMERIZATION

Reported by Suresh R. Sriram

February 15, 1999

INTRODUCTION

In 1975, it was predicted that by the 21st century the growth in the utilization of commodity plastics such as polystyrene (PS), polyvinylchloride (PVC), polypropylene (PP), and polyethylene (PE) would diminish to a small percentage and that the utility of engineering plastics and high performance liquid crystalline polymers would increase significantly.¹ However, development of superior catalysts and better process engineering for the production of these commodity polymers has completely changed this scenario. With growing environmental concerns with regard to waste materials, the use of a single polymer that can be recycled and utilized in a wide range of applications is gaining popularity. Metallocene catalysts have provided the opportunity to tailor polymers for suitable applications utilizing raw materials such as olefins obtained from petroleum. Petroleum and polyolefins are hydrocarbons with similar energy content, therefore, once the product life of the polyolefin has been fully utilized it can be recycled into the parent low molecular weight hydrocarbons by thermal degradation.² This report will focus on the design and development of metallocene catalysts for polymerizing olefins with unique microstructures.

METALLOCENE CATALYSTS

Stereoregular polyolefins have traditionally been synthesized by heterogeneous Ziegler-Natta catalysts.³ Due to the heterogenous nature of the Ziegler-Natta catalysts it was difficult to understand the mechanism and the origin of stereoregularity. Metallocenes belonging to group IVA in the periodic table have proven useful in understanding the mechanism of olefin polymerization and the observed control over stereoregularity.

Activation of Metallocene Catalysts

In 1977, Kaminsky and coworkers discovered that hydrated forms of $(\text{CH}_3)_3\text{Al}$ yielded oligomeric species called methylalumoxanes (MAO), which in conjunction with metallocenes accelerated the polymerization of ethene and propene by a factor of 10,000.⁴ MAO is a mixture of fluxional cage and cluster type compounds formed from AlMe_2O and

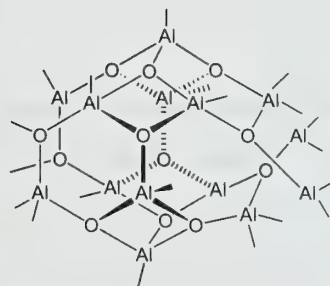
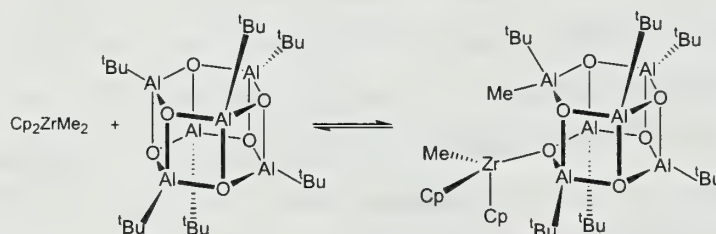


Figure 1. Possible structure of methylalumoxane clusters.

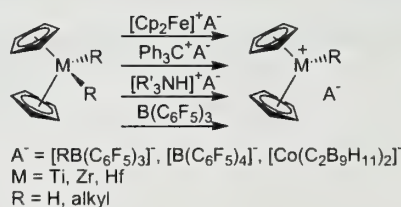
$\text{Me}_2\text{AlOAlMeOAlMe}_2$ species (Figure 1). Aluminum (tri and tetra coordinate) and oxygen atoms are arranged alternately, and the free valencies are satisfied by the methyl groups. Recently Sinn⁵ and Barron⁶ have independently studied the structure and function of MAO. Spectroscopic and theoretical studies suggest that MAO behaves as a Lewis acid.³ In order to understand the role of MAO, Barron and coworkers, synthesized a number of non fluxional alumoxane cage compounds, $[(^t\text{Bu})_2\text{Al}\{\text{OAl}(^t\text{Bu})_2\}]_2$ and $[(^t\text{BuAlO})_n]$ where n is 6-9. The closed cage compound $[(^t\text{BuAlO})_6]$ reacts reversibly to give the ion pair complex $[\text{Cp}_2\text{ZrMe}][^t\text{Bu}_6\text{Al}_6\text{O}_6\text{Me}]$, which is a very active catalyst for the polymerization of ethene (Scheme 1). Barron and coworkers attribute this enhanced reactivity of cage alumoxanes to a new concept, 'latent Lewis acidity'.⁶

Scheme 1



Cp_2ZrCl_2 in the presence of MAO as a cocatalyst polymerizes ethene with a very high activity of 40,000 kg of PE / g Zr / h. A high excess ($\text{Al/Zr} = 5,000\text{--}10,000$) of MAO is needed to obtain high polymerization activity. The functions of MAO as a cocatalyst are the methylation of metallocenes, stabilization of the cationic active center, and reactivation of inactive metallocene species formed by α -hydrogen transfer between the active methylated metallocene and MAO.⁷ A number of cationic metallocene systems have been generated without the use of MAO (Scheme 2) and these species have proven effective in polymerizing ethene and propene.³

Scheme 2

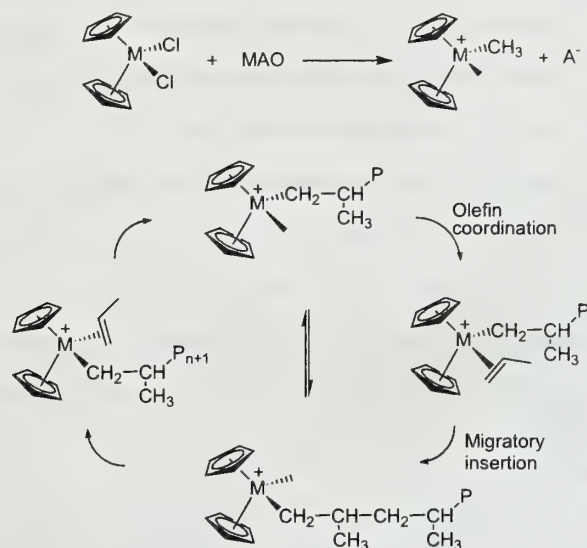


Mechanism of Olefin Polymerization Using Metallocene Catalysts

The widely accepted mechanism for olefin polymerization is illustrated in Scheme 3. The cocatalyst MAO activates the metallocene after complexation, followed by a methyl transfer to provide a vacant coordination site. The olefin coordinates to the vacant site and undergoes a migratory insertion. This step leads to the creation of a vacant coordination site for olefin coordination, and allows for

continued chain growth.³ The orientation of the olefin during coordination to the metal at the vacant site can be controlled by the chirality of the metallocene catalysts which can be prepared by using conformationally constrained ligands.

Scheme 3



STEREOREGULAR POLYMERS

The orientation of the incoming monomer during coordination can be controlled by the ligands on the metallocene.

Based on the enantioface (Re or Si) from which insertion occurs, there are three possibilities, isotactic, syndiotactic, or atactic. Using polypropylene as an example, tacticity can be illustrated as shown in Figure 2.

When the chirality of the metal center controls the enantioface selection of the prochiral monomer, the stereoregularity is under the catalyst site control. When the stereogenic center of the last inserted monomer in the growing chain directs the stereochemical course of α -olefin insertion, the stereoregularity is under chain end control. The microstructure and the extent of stereoregularity can be determined by ^{13}C NMR.

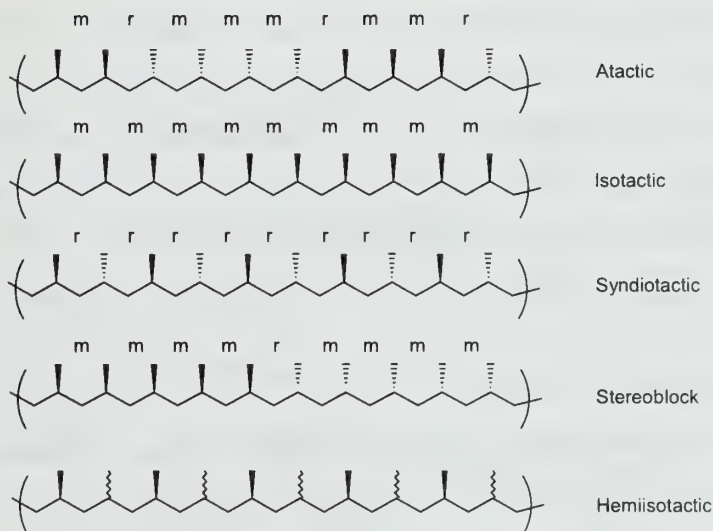


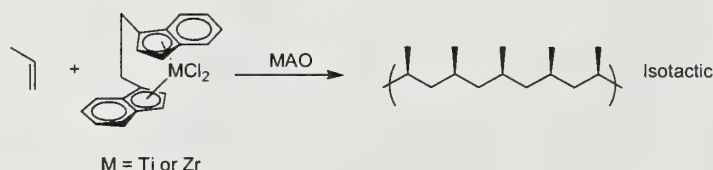
Figure 2. Illustration of various polymer microstructures.

When the stereogenic center of the last inserted monomer in the growing chain directs the stereochemical course of α -olefin insertion, the stereoregularity is under chain end control. The microstructure and the extent of stereoregularity can be determined by ^{13}C NMR.

Isotactic Polymers

Ewen was able to obtain highly isotactic PP using chiral metallocene (\pm)Et[Ind]₂TiCl₂ with MAO as cocatalyst (Scheme 4).⁸ The PP resulting from this catalyst is 63% isotactic and 37% atactic. It should be noted that the actual catalyst is a mixture of 56% of the chiral (\pm)Et[Ind]₂TiCl₂ and 44% of the achiral (meso)-Et[Ind]₂TiCl₂. Kaminsky and coworkers discovered that zirconocene catalysts are superior to the Ti and Hf analogs in generating stereoregular polymer chains and possess higher catalytic activity. Isotactic PP synthesized by metallocenes are superior to the isotactic PP produced by conventional Ziegler-Natta catalysts because of narrow polydispersity indices, leading to greater stiffness and increased tensile strength.²

Scheme 4



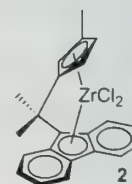
Syndiotactic Polymers

The synthesis of syndiotactic polymers using metallocenes was also first reported by Ewen and coworkers in 1988.⁹ They synthesized the C_s symmetric zirconocene **1**, which is effective in generating syndiotactic polymers. The racemic pentad content of the polymer was 81% for the polymerization carried out at 50 °C. Stereodefects of the type *rmmr* were observed indicating the polymerization was under catalyst site control. The regularly alternating insertion of olefins at the heterotopic sites in the C_s symmetric complex **1** results in a syndiotactic polymer. It should be noted that reliable and efficient synthesis with narrow polydispersity indices of syndiotactic polyolefins has not yet been achieved by heterogeneous Ziegler-Natta catalysts.



Hemiisotactic Polymers

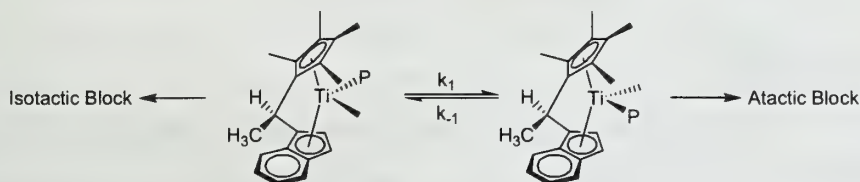
Ewen noted that subtle changes to catalyst symmetry resulted in polymers with unique microstructures. A hemiisotactic polymer is defined as one in which every other stereocenter possesses the same configuration, while adjacent stereocenters have random stereochemistry. Ewen developed catalyst **2**, a subtle modification of catalyst **1**, that polymerizes propene to hemiisotactic PP.¹⁰



Elastomeric Polypropylene

Natta and coworkers first identified rubbery PP obtained by fractionation of the PP obtained using traditional Ziegler-Natta catalyst. They attributed these elastomeric properties to the presence of blocks of crystallizable isotactic sequences and amorphous atactic sequences in the polymer chain.¹¹ Collete and coworkers utilized group IV transition metal alkyls supported on alumina as the catalysts to produce elastomeric PP.¹² The material showed no plastic yield and possessed an elastic recovery characteristic of elastomers. In 1990, Chien and coworkers reported the synthesis of elastomeric PP using a stereorigid titanocene catalyst.¹³ Chien proposed that the polymerization yielded stereoblocks due to polymerization occurring at sterically unhindered (aspecific) and hindered (isospecific) coordination sites (Scheme 5). The maximum percentage of the isotactic pentad in the elastomeric PP polymerized at ambient temperature was 38%, and the percentage decreased with increasing temperature.

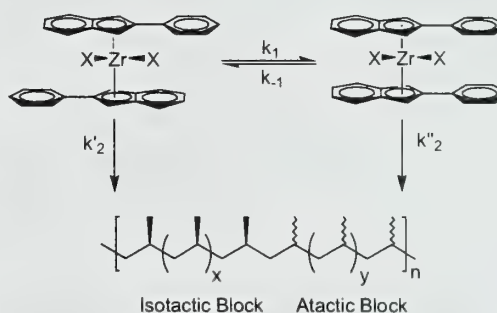
Scheme 5



To study the impact of modifications on the stereorigid metallocene developed by Chien, Collins and coworkers performed a series of systematic changes on the bridging group and the metal in the metallocene.¹⁴ Collins and coworkers emphasize that the availability of two inequivalent sites on the catalyst for monomer coordination is not sufficient to prepare elastomeric PP. It was observed that high molecular weights must be achieved in order for the material to possess good elastomeric properties. Collins cautions that the distinction between elastomeric PP and isotactic PP can not be simply assigned to the block like microstructure of the elastomeric PP.

Waymouth and coworkers devised an ingenious method for effecting dynamic stereocontrol in the polymerization of α -olefins (Scheme 6).¹⁵ The unique strategy involved the design of a catalyst that can isomerize between a chiral and an achiral geometry to produce stereoblocks of isotactic sequences and atactic sequences, respectively. Dynamic isomerization provides a very

Scheme 6



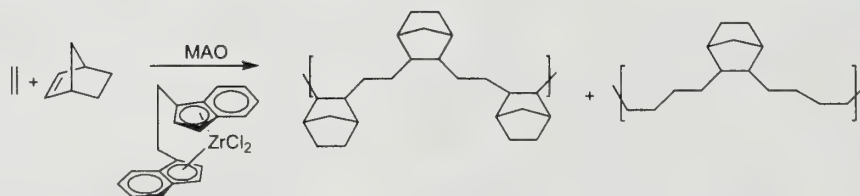
powerful strategy to control the block size and distribution of stereoblocks. They were successful in obtaining the crystal structures of the chiral and achiral form of the catalyst in the same unit cell, suggesting that the rotomers are energetically similar.

The isotactic pentad content increases with increase in propylene pressure.¹⁵ They also performed a number of ligand modifications.¹⁶ When positions 3 and 5 on the phenyl group in the 2-phenylindene were substituted by methyl and trifluoromethyl groups, the trifluoromethyl substituted complex gave higher isotactic pentad content when compared to polymers synthesized by the methyl substituted complex, which indicates that subtle changes in the electronic character affect the catalyst structure which results in a change in the microstructure of polymer.¹⁶ The change in the metal center from Zr to Hf in the unbridged 2-phenylindene metallocene yields PP with lower isotacticities, which is postulated to result from a change in the dynamics of propagation relative to isomerization.¹⁶ The change in the symmetry of the catalyst from C_{2v} to C_1 symmetry in unbridged metallocenes did not provide a truly elastomeric PP.¹⁶

Polymerization of Cycloolefins

Metallocene based catalysts are also capable of polymerizing cycloolefins without ring opening side reactions. Kaminsky and coworkers first reported the successful homopolymerization of cycloolefins using zirconocene activated with MAO.¹⁷ The resulting polycycloolefins have very high melting points and crystallinity. The melting temperature of polycyclobutenes, polycyclopentenes and polynorbornenes are 485 °C, 395 °C, and 600 °C, respectively. This leads to difficulties in polymer processing, but this difficulty has been overcome by the copolymerization of cycloolefins with ethene. The structure of norbornene and ethene copolymers can be alternating or random but most metallocene catalyzed cycloolefin polymers possess a statistical microstructure (Scheme 7). Preparation of copolymers with greater than 50 mol % of norbornene has not yet been achieved. These copolymers are being utilized for their unique properties of optical clarity, stiffness, and light weight.¹⁸

Scheme 7



NEW POLYMERIZATION CATALYSTS

Single Site Catalysts

High density PE (HDPE) can be produced by both Ziegler-Natta catalysts as well as metallocene catalysts. Due to its crystalline nature, HDPE suffers from poor processibility. However, the incorporation of small amounts of long chain α -olefins improves the processibility and properties. Traditional metallocene catalysts are not able to incorporate higher α -olefins effectively under industrial production conditions.

Based on the ligand developed by Bercaw¹⁹ and the synthesis of the corresponding titanium complex by Okuda,²⁰ new metallocene analogs of *ansa*-monocyclopentadienyl amido (CpA) group IV catalysts have been developed (Figure 3). These catalysts have been found to be more robust and versatile than the conventional metallocenes in their ability to synthesize ethene, ethene-propene and ethene-styrene polymers and copolymers, and have been successfully incorporated into large scale production.²¹ Since polymer chain growth occurs at one type of active site leading to polymers with narrow polydispersity ($M_w/M_n \sim 2$), when compared to Ziegler-Natta catalysts ($M_w/M_n > 5$), these are called single site catalysts.

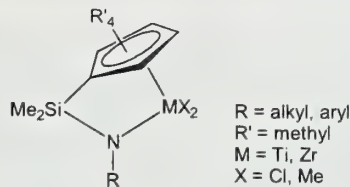
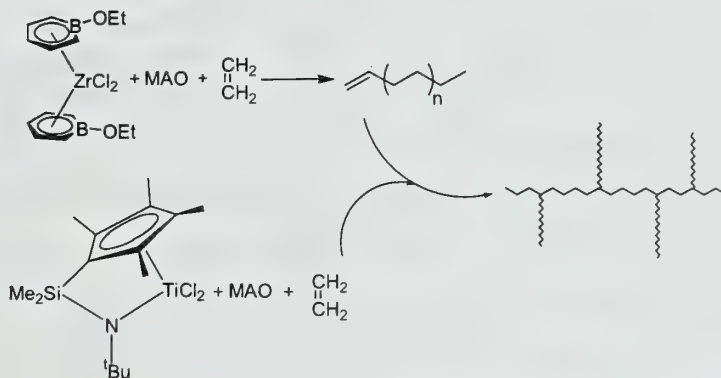


Figure 3. General representation of a single site catalyst.

Polyolefins Using Metallocene Mimics

Bazan and coworkers have tuned the activity of metallocenes by incorporating changes in the electronic character of the ligands.²² These metallocene mimics, which possess boratabenzene ligands instead of cyclopentadienyl ligands, specifically yield 1-alkenes (Scheme 8). The authors postulate that the boratabenzene ligands enable tuning of the electron density and the reactivity of the electrophilic metal center. In an effort to obtain branched high molecular weight polyethylene they used a mixture of the metallocene mimic and standard single site catalyst to perform a tandem in situ polymerization. The polymerization yielded branched, processible polyethylene similar to linear low density polyethylene (LLDPE). The standard method for obtaining

Scheme 8



LLDPE involves the use of two monomers (ethylene and 1-octene), but in this case a single monomer (ethene) is used.

CONCLUSIONS AND FUTURE PROSPECTS

There still exists an enormous number of avenues for tailoring new catalysts to produce polyolefins having new architectures and/or special properties which may provide solutions to special challenges. There is more fundamental science to be learned in terms of changes in the type of ligands, electronic properties, sterics, and the nature of the transition metal in order to develop the next generation of catalysts.

REFERENCES

1. Barghoorn, P.; Stebani, U.; Balsam, M. *Acta Polym.* **1998**, *49*, 266.
2. Kaminsky, W. *J. Chem. Soc., Dalton Trans.* **1998**, 1413.
3. Brintzinger, H. H.; Fischer, D.; Mulhaupt, R.; Rieger, B.; Waymouth, R. M. *Angew. Chem., Int. Ed. Engl.* **1995**, *107*, 1255.
4. Sinn, H.; Kaminsky, W.; Vollmer, H. J.; Woldt, R. *Angew. Chem., Int. Ed. Engl.* **1980**, *92*, 396.
5. Sinn, H. *Macromol. Symp.* **1995**, *97*, 27.
6. Harlan, C. J.; Bott, S. G.; Barron, A. R. *J. Am. Chem. Soc.* **1995**, *117*, 6465.
7. Kaminsky, W. *Macromol. Symp.* **1995**, *97*, 79.
8. Ewen, J. A. *J. Am. Chem. Soc.* **1984**, *106*, 6355.
9. Ewen, J. A.; Jones, R. L.; Razavi, A.; Ferrara, J. P. *J. Am. Chem. Soc.* **1988**, *110*, 6255.
10. Ewen, J. A. *Makromol. Chem., Macromol. Symp.* **1991**, *48*, 253.
11. Natta, G. *J. Polym. Sci.* **1959**, *34*, 531.
12. Collete, J. W.; Tullock, C. W.; MacDonald, R. N.; Buck, W. H.; Su, A. C. L.; Harrell, J. R.; Mulhaupt, R.; Anderson, B. C. *Macromolecules* **1989**, *22*, 3851.
13. Mallin, D. T.; Rausch, M. D.; Lin, Y. G.; Dong, S.; Chien, J. C. W. *J. Am. Chem. Soc.* **1990**, *112*, 2030.
14. Gauthier, W. J.; Corrigan, J. F.; Taylor, N. J.; Collins, S. *Macromolecules* **1995**, *28*, 3771.
15. Coates, G. W.; Waymouth, R. M. *Science* **1995**, *267*, 217.
16. a) Maciejewski Petoff, J. L.; Bruce, M. D.; Waymouth, R. M.; Masood, A.; Lal, T. K.; Quan, R. W.; Behrend, S. J. *Organometallics* **1997**, *16*, 5909. b) Hauptman, E.; Waymouth, R. M.; Ziller, J. W. *J. Am. Chem. Soc.* **1995**, *117*, 11586. c) Lin, S.; Hauptman, E.; Waymouth, R. M.; Lal, T. K.; Quan, R. W.; Ernst, A. B. *J. Mol. Catal. A: Chem.* **1998**, *136*, 23. d) Kravchenko, R.; Masood, M. A.; Waymouth, R. M.; Myers, C. L. *J. Am. Chem. Soc.* **1998**, *120*, 2039.
17. Kaminsky, W.; Bark, A.; Arndt, M. *Makromol. Chem., Macromol. Symp.* **1991**, *47*, 83.
18. McCoy, M. *Chem. Eng. News* **1998**, *78*, 15.
19. Shapiro, P. J.; Bunel, E.; Schaefer, W. P.; Bercaw, J. E. *Organometallics* **1990**, *9*, 867.
20. Okuda, J. *Chem. Ber.* **1990**, *123*, 1649.
21. McKnight, A. L.; Waymouth, R. M. *Chem. Rev.* **1998**, *98*, 2587.
22. Barnhart, R. W.; Bazan, G. C.; Mourey, T. *J. Am. Chem. Soc.* **1998**, *120*, 1082.

ATOM TRANSFER RADICAL POLYMERIZATION

Reported by Qing Yu

February 18, 1999

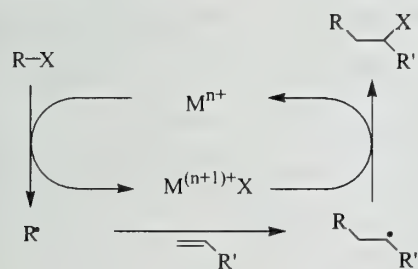
INTRODUCTION

Since the discovery in the 1950s of the first living polymerization that exhibited a termination-free chain growth process, many new polymerization methods with similar "living" modes of propagation have been developed, including anionic, cationic, coordination and ring-opening metathesis. Living radical polymerization, however, was considered difficult to achieve due to inherent side reactions such as radical coupling and disproportionation. The discovery of TEMPO-based persistent radicals,¹ which minimize termination by reducing the stationary concentration of the reacting radicals, proved that living radical polymerization could be achieved. The subsequent renaissance in the field of radical polymerization led to the discovery of atom transfer radical polymerization (ATRP) in 1995.^{2,3} As a promising new controlled radical polymerization method, ATRP has rapidly become one of the preferred methods in polymer synthesis.⁴

FROM ATRA TO ATRP

Atom transfer radical addition (ATRA), also known as the Kharasch reaction, has been used by organic chemists for many years as an efficient method for carbon-carbon bond formation.⁵⁻⁷ The mechanism of ATRA involves a transition metal catalyst which acts as a halogen atom carrier (Scheme 1). The three main steps in ATRA include: 1) abstraction of a halogen atom X from the organic halide R-X by the transition metal catalyst M^{n+} to form the active radical R^\bullet and the oxidized transition metal catalyst $M^{(n+1)+}X$, 2) inter- or intramolecular addition of the reactive radical R^\bullet to an alkene species $CH_2=CHR'$ to form a new radical, $RCH_2-CH^\bullet R'$, 3) halogen atom back-transfer from $M^{(n+1)+}X$ to radical $RCH_2-CH^\bullet R'$, forming a new organic halide $RCH_2-CHR'X$ as the addition product and regenerating the reduced form of the transition metal catalyst, M^{n+} .

Scheme 1

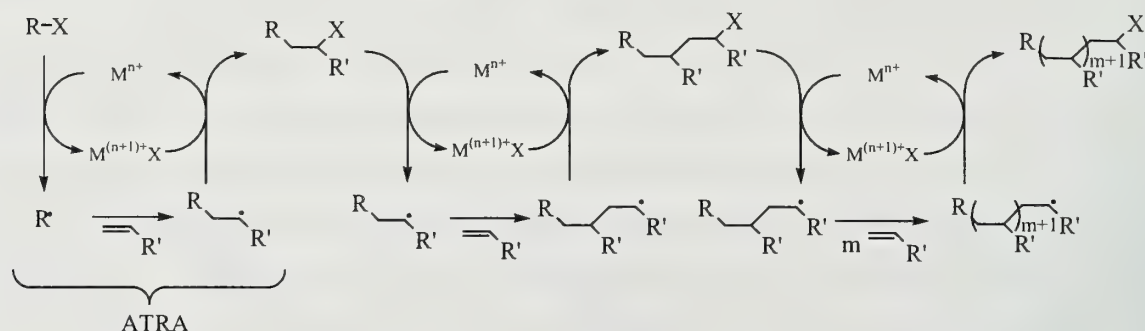


ATRA usually provides excellent yields, and side reactions such as radical coupling are rarely observed. This suggests that the concentration of reactive radicals in ATRA is low enough to suppress bimolecular coupling. In addition, ATRA adds one monomer to the starting organic halide in a similar fashion to the chain propagation during a radical

polymerization. Most importantly, the addition product still bears the halogen atom, making another cycle of radical addition possible (Scheme 2). Thus, the promising potential of extending ATRA to controlled radical polymerization was recognized.

In 1995, Sawamoto and Matyjaszewski independently discovered a new type of controlled radical polymerization mediated by transition metals. Sawamoto reported the living polymerization of

Scheme 2

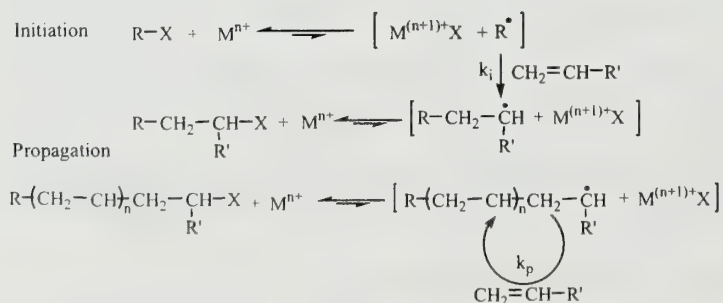


methyl methacrylate (MMA) catalyzed by $\text{RuCl}_2(\text{PPh}_3)_3$ with $\text{MeAl}(\text{ODBP})_2$ as an activator.³ Matyjaszewski utilized CuCl with a 2,2'-bipyridine ligand to polymerize styrene.² Alkyl halides were used by both groups to initiate the polymerization. Because this controlled polymerization is an extension of ATRA such that the product is reincorporated into the catalytic cycle as starting material, the reaction is referred to as atom transfer radical polymerization (ATRP).

MECHANISM OF ATOM TRANSFER RADICAL POLYMERIZATION

Since ATRP is a direct extension of ATRA to polymer chemistry, a similar mechanism was proposed for ATRP which involves an atom transfer pathway with a low concentration of radical intermediates (Scheme 3). During the initiation step, the transition metal catalyst M^{n+} reversibly abstracts a halogen atom from initiator R-X to form an active radical R^\bullet and oxidized catalyst $\text{M}^{(n+1)+}\text{X}$.

Scheme 3



After the addition of the active radical R^\bullet to the monomer $\text{CH}_2=\text{CHR}'$, a new active radical is generated which reversibly forms the dormant species $\text{RCH}_2\text{-CHR}'\text{X}$ by halogen atom back transfer from $\text{M}^{(n+1)+}\text{X}$. In the following propagation steps, monomers add to the propagating radical repeatedly to elongate the polymer chain.

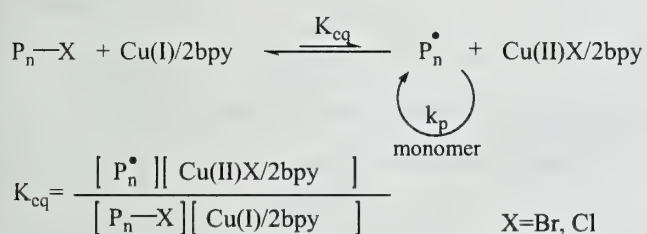
An alternative mechanism was also proposed where the propagation involves an insertion step rather than radical addition. In this mechanism, oxidative addition of the organic halide R-X to catalyst M^{n+} forms complex $R-M^{(n+2)+}-X$, followed by an insertion of the alkene into the carbon- $M^{(n+2)+}$ bond. In the subsequent step, reductive elimination gives an extended organic halide as the addition product as well as the active catalyst M^{n+} .

Since both proposed mechanisms are plausible under some polymerization conditions for ATRP, it is important to establish whether radical species are indeed involved. Although the free radical concentration in ATRP is too low for EPR detection,⁸ the propagating species in ATRP is believed to be a free radical based on several pieces of evidence. First, radical inhibitors such as TEMPO or galvinoxyl were found to terminate polymerization instantly, while the addition of cationic and anionic inhibitors showed no significant effect.⁹ Second, the tacticity of the polymers obtained from ATRP is very similar to that found in polymers prepared under conventional radical polymerization conditions, suggesting a similar free radical intermediate.^{2,3} In addition, reactivity ratios in copolymerization also support that ATRP proceeds via radical type propagation.¹⁰

KINETICS OF ATOM TRANSFER RADICAL POLYMERIZATION

In a radical polymerization, the rate of propagation and the rate of termination by radical coupling are first order and second order in radical concentration, respectively. Therefore, when the radical concentration is sufficiently low, termination becomes negligible compared to propagation, and the polymerization is termed "living" or controlled. It has been shown that to achieve near termination-free radical polymerization, active radical concentrations as low as 10^{-7} to 10^{-8} M are required. In ATRP, adequate control of the radical concentration requires two conditions to be met. First, the equilibrium between the active radical and the dormant species must be such that the formation of dormant species is strongly favored. Second, the inter-conversion between the active and the dormant species must be kinetically fast.

Scheme 4



Matyjaszewski and coworkers investigated the kinetics of ATRP through polymerization of styrene, methacrylate (MA) and methyl methacrylate (MMA) initiated by 1-phenethyl halides with copper(I) catalysts and 4,4'-dialkyl substituted 2,2'-bipyridine ligands (Scheme 4).^{11,12}

Their results showed that the equilibrium strongly favors the dormant species, with $K_{eq} = 3.9 \times 10^{-8}$ ($X = Br$) and $K_{eq} = 2.1 \times 10^{-8}$ ($X = Cl$) for the

polymerization of styrene at 110 °C. The radical concentrations in bulk polymerization at 130 °C were found to be 0.22×10^{-7} M for MA, 0.58×10^{-7} M for styrene, and 1.84×10^{-7} M for MMA. Percec and coworkers studied ATRP of several monomers in different solvents initiated by arenesulfonyl halides and reported similar equilibrium constants between active radicals and dormant species, along with a similar trend in radical concentration, except that the radical concentrations were lower ($\sim 10^{-9}$ M) due to lower initiator concentration utilized.¹³

It should be noted that ATRP is not absolutely termination-free. At the beginning of the polymerization, when the concentration of $\text{XM}^{(n+1)+}$ is low and the equilibrium between active radicals and dormant species is not fully established, termination by radical coupling does occur, which builds up $\text{XM}^{(n+1)+}$ concentration and helps to establishing the equilibrium. Therefore, it has been shown that adding a small amount of $\text{XM}^{(n+1)+}$ species at the beginning of the polymerization helps to control molecular weight distribution. At high monomer conversion, the rate of polymerization becomes slower due to the lower monomer concentration, and termination also becomes significant because the rate of radical coupling remains the same. One way to overcome this type of termination at high monomer conversion is to add a fresh feed of monomers at higher conversion.

MAJOR COMPONENTS OF ATRP

In most of the ATRP systems reported to date, the molecular weight of the polymers increases linearly with monomer conversion, suggesting a constant number of growing chains through the entire polymerization process. In addition, the theoretical molecular weight, which can be calculated based on the initial concentrations of initiator and monomer, agrees well with the experimental values, suggesting high initiator efficiency. The polydispersity index (PDI) usually remains in the range from 1.05 to 1.50 up to 90% monomer conversion. All these results show that by choosing proper initiators and catalyst systems, ATRP truly has a “living” character and good control over molecular weight distribution can be achieved.

General Polymerization Conditions

ATRP reactions are generally conducted at elevated temperatures either in bulk or with solvents under inert gas protection. Bulk polymerization has the advantages of faster reaction rate and lack of interference from the solvent, but it is not applicable to the situation where the polymers formed are not soluble in their monomers. Common solvents used in ATRP include toluene, benzene, and diphenyl ether. Solvents such as pyridine significantly effect the polymerization due to interactions with the transition metal catalysts. The reaction temperature depends on the individual system with a common

range from 60 °C to 130 °C. The polymerization usually takes from several hours to three days to reach high conversion. This relative slow rate is due to the low concentration of active radicals, especially towards the end of the polymerization when monomer concentration becomes lower.

Initiators

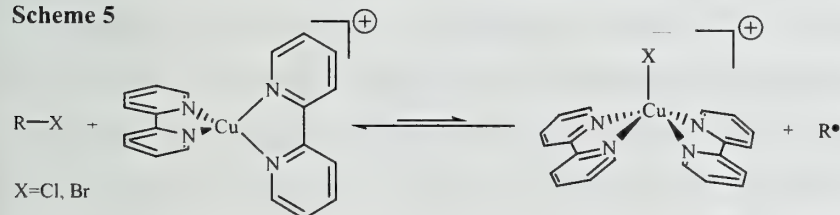
The role of initiators in ATRP is to dictate the number of propagating chains by efficiently forming active radicals at the beginning of the polymerization. Therefore, high initiation efficiency and a fast initiation rate compared to propagation are required to obtain low PDI. Initiators are usually alkyl halides with structural similarity to the monomers, such as 1-phenethyl bromide for the polymerization of styrene, but other types of initiators have also been successfully used.¹⁴ Substituted phenylsulfonyl chlorides have been shown to be universal functional initiators for the polymerization of a variety of monomers with excellent PDI control.¹⁵⁻¹⁷ Since the carbon-chloride bonds are weaker in phenylsulfonyl chlorides than in the dormant growing polymer chains, the rate constant of initiation is several orders of magnitude higher than that of propagation with 100% initiation efficiency.¹³

Catalysts and Ligands

To catalyze ATRP, the transition metal catalysts should be able to induce homolytic cleavage of the carbon-halide bond during initiation and propagation, and undergo one electron oxidation without the occurrence of oxidative addition. So far, the reported successful examples of transition metals include Ru(II),³ Cu(I),^{2,18} Ni(II),¹⁹ and Fe(II).²⁰

Suitable ligands in ATRP are very important. First, proper choice of ligands can significantly improve the solubility of many catalyst systems. It has been shown that when 2,2'-bipyridine is functionalized with alkyl chains to form the more organic-phase soluble 4,4'-bis-(5-nonyl)-2,2'-bipyridine in the Cu(I) catalytic system, the initially heterogeneous polymerization becomes homogeneous, providing improved molecular weight control.¹² In addition, ligands can modify the

Scheme 5



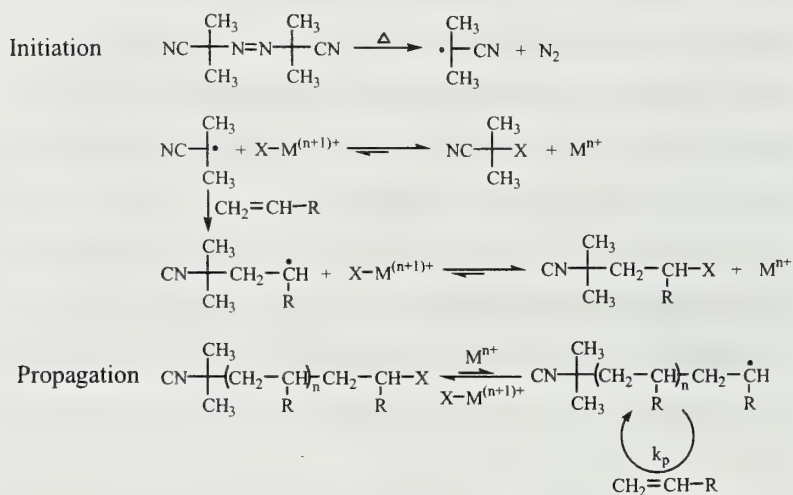
electric and steric nature of the catalyst complexes.²¹ For example, the 2,2'-bipyridine ligand not only stabilizes Cu(I) by π -electron back donation from

the metal, but also helps the interchange between tetrahedral Cu(I) and distorted square based pyramidal Cu(II) (Scheme 5).²² The active species in other ATRP catalyst systems are still under investigation.

REVERSE ATOM TRANSFER RADICAL POLYMERIZATION

Matyjaszewski and coworkers have extended normal ATRP to a reversed ATRP based on the equilibrium between active radical and dormant species (Scheme 6).^{23,24} The only difference between normal ATRP and reverse ATRP is the initiation step. In reverse ATRP, a common radical initiator such as AIBN is used in conjunction with the oxidized transition metal catalysts in normal ATRP, such

Scheme 6



as $\text{Cu(II)X}_2(\text{bpy})_2$ complexes. After the formation of active radicals by the initiator, oxidized catalyst $\text{X-M}^{(n+1)+}$ rapidly establishes the equilibrium between the radicals and the dormant species by halogen atom back-transfer. Thus, low radical concentration is maintained, and the propagation proceeds in the same fashion as normal ATRP. Under proper conditions, good PDI control can be

achieved,²⁵ and end-group analysis of the polymer obtained shows that the polymerization is indeed initiated by AIBN. As an interesting extension of ATRP, reverse ATRP can change some conventional radical polymerizations into controlled polymerization simply by adding transition metal catalysts without changing initiators.

APPLICATIONS OF ATRP IN THE SYNTHESIS OF NEW MATERIALS

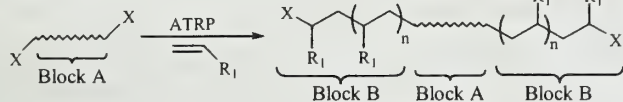
ATRP has shown many advantages as an efficient method to control PDI, such as easy initiation and easy end-group control. In addition, a variety of monomers with different functional groups can be polymerized, and polymerization conditions are not very stringent. Recent applications of ATRP in polymer synthesis have proved that ATRP is a convenient method to obtain polymers with different architecture (Scheme 7). Many interesting polymeric materials, including block copolymers,^{26,27} star polymers,²⁸ and hyperbranched polymers,^{29,30} have been successfully synthesized using ATRP. Other novel structures have also been obtained, such as the dendritic-linear block copolymers reported by Frechet and coworkers.³¹

ADVANTAGES AND DISADVANTAGES OF ATRP

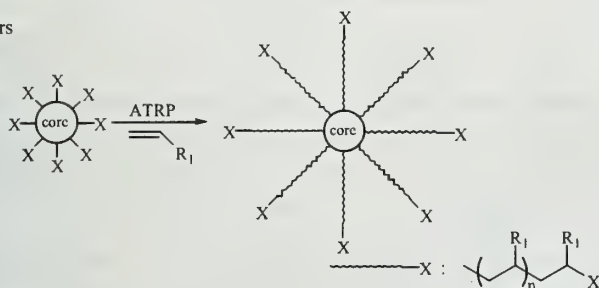
Unlike TEMPO-based controlled radical polymerization, ATRP can be used to polymerize a variety of monomers, such as styrene, MA, MMA, acrylonitrile, etc. In theory, any monomers that can

Scheme 7

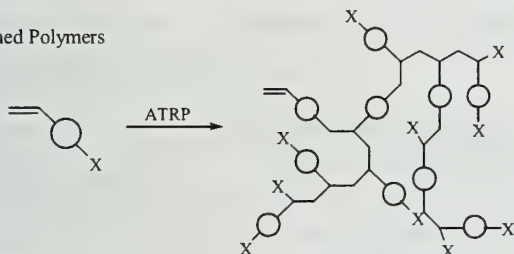
Block Copolymers



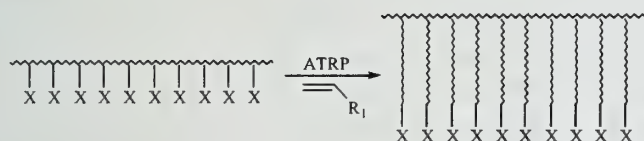
Star Polymers



Hyperbranched Polymers



Comb Polymers



be polymerized using radical propagation can be polymerized with ATRP by choosing proper transition metals, ligands, solvents, temperature and other conditions. The polymerization can be simply initiated by a carbon-halogen bond with proper bond strength, and the halogen end-groups leave lots of room for further modification of the polymeric products.

ATRP also has its disadvantages. Like other types of free-radical polymerizations, ATRP does not provide stereocontrol over the polymers obtained. In addition, the polymerization rate is relatively slow due to the low radical concentration, making it improper for the situations where fast polymerization rates are important.

CONCLUSION

The recent discovery and development of ATRP has greatly expanded the scope of controlled radical polymerization. By establishing the equilibrium between reacting radicals and dormant species with transition metal catalysts, the radical concentration becomes low enough to suppress termination. The method is compatible with a variety of monomers, and polymers with low PDI can be easily synthesized with molecular weights up to 180,000.¹⁶ It also provides a powerful method in the control of polymer topology and synthesis of polymers with novel structures.

REFERENCES

- (1) Beckwith, A. L. J.; Bowry, V. W.; O'Leary, M.; Moad, G.; Rizzardo, E.; Solomon, D. H. *J. Chem. Soc., Chem Commun.* **1986**, 1003-1004.
- (2) Wang, J.-S.; Matyjaszewski, K. *J. Am. Chem. Soc.* **1995**, *117*, 5614-5615.
- (3) Kato, M.; Kamigaito, M.; Sawamoto, M.; Higashimura, T. *Macromolecules* **1995**, *28*, 1721-1723.
- (4) Patten, T. E.; Matyjaszewski, K. *Adv. Mater.* **1998**, *10*, 901.
- (5) Curran, D. P. *Comprehensive Organic Synthesis*; Pergamon, Oxford, **1991**; Vol. 4.
- (6) Nagashima, H.; Ozaki, N.; Ishii, M.; Seki, K.; Washiyama, M.; Itoh, K. *J. Org. Chem.* **1993**, *58*, 464-470.
- (7) Udding, J. H.; Tuijp, K. J. M.; Zanden, M. N. A. v.; Hiemstra, H.; Speckamp, W. N. *J. Org. Chem.* **1994**, *59*, 1993-2003.
- (8) Kajiwar, A.; Matyjaszewski, K.; Kamachi, M. *Macromolecules* **1998**, *31*, 5695-5701.
- (9) Nishikawa, T.; Ando, T.; Kamigaito, M.; Sawamoto, M. *Macromolecules* **1997**, *30*, 2244-2248.
- (10) Haddleton, D. M.; Crossman, M. C.; Hunt, K. H.; Topping, C.; Waterson, C.; Suddaby, K. G. *Macromolecules* **1997**, *30*, 3992-3998.
- (11) Wang, J.-S.; Matyjaszewski, K. *Macromolecules* **1995**, *28*, 7901-7910.
- (12) Matyjaszewski, K.; Patten, T. E.; Xia, J. *J. Am. Chem. Soc.* **1997**, *119*, 674-680.
- (13) Percec, V.; Barboiu, B.; Kim, H.-J. *J. Am. Chem. Soc.* **1998**, *120*, 305-316.
- (14) Matyjaszewski, K.; Shipp, D. A.; J-L, W.; Grimaud, T.; Patten, T. *Macromolecules* **1998**, *31*, 6836-6840.
- (15) Percec, V.; Barboiu, B. *Macromolecules* **1995**, *28*, 7970-7972.
- (16) Grimaud, T.; Matyjaszewski, D. *Macromolecules* **1997**, *30*, 2216-2218.
- (17) Percec, V.; Barboiu, B.; Sluis, M. v. d. *Macromolecules* **1998**, *31*, 4053-4056.
- (18) Patten, T. E.; Xia, J.; Abernathy, T.; Matyjaszewski, K. *Science* **1996**, *272*, 866.
- (19) Uegaki, H.; Kotani, Y.; Kamigaito, M.; Sawamoto, M. *Macromolecules* **1997**, *30*, 2249-2253.
- (20) Ando, T.; Kamigaito, M.; Sawamoto, M. *Macromolecules* **1997**, *30*, 4507.
- (21) Haddleton, D. M.; Shooter, A. J.; Morsley, S. R. *Controlled Radical Polymerization*; Matyjaszewski, K., Ed.; ACS Symposium Series, **1998**; Vol. 685, pp 284.
- (22) Haddleton, D. M.; Jasieczek, C. B.; Hannon, M. J.; Shooter, A. J. *Macromolecules* **1997**, *30*, 2190-2193.
- (23) Wang, J.-S.; Matyjaszewski, K. *Macromolecules* **1995**, *28*, 7572-7573.
- (24) Xia, J.; Matyjaszewski, K. *Macromolecules* **1997**, *30*, 7692-7696.
- (25) Moineau, G.; Dubois, P.; Jerome, R.; Senninger, T.; Teyssie, P. *Macromolecules* **1998**, *31*, 545-547.
- (26) Shipp, D. A.; Wang, J.-L.; Matyjaszewski, K. *Macromolecules* **1998**, *31*, 8005-8008.
- (27) Moineau, G.; Minet, M.; Dubois, P.; Teyssie, P.; Senninger, T.; Jerome, R. *Macromolecules* **1999**, *32*, 27-35.
- (28) Angot, S.; Murthy, K. S.; Taton, D.; Gnanou, Y. *Macromolecules* **1998**, *31*, 7218-7225.
- (29) Gaynor, S. G.; Edelman, S.; Matyjaszewski, K. *Macromolecules* **1996**, *29*, 1079-1081.
- (30) Matyjaszewski, K.; Pyun, J.; Gaynor, S. G. *Macromol. Rapid Commun.* **1998**, *19*, 665-670.
- (31) Leduc, M. R.; Hawker, C. J.; Dao, J.; Frechet, J. M. J. *J. Am. Chem. Soc.* **1996**, *118*, 11111-11118.

ASYMMETRIC SYNTHESIS OF AMINE DERIVATIVES VIA CHIRAL SULFINIMINES

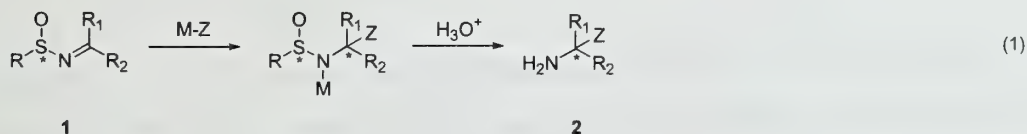
Reported by Stephen G. Jarboe

February 22, 1999

INTRODUCTION

The myriad of natural products and biologically active compounds that contain an amine functionality have made the stereoselective synthesis of chiral amine derivatives of great interest.¹ From a simple retrosynthetic approach, the stereoselective addition of a nucleophile to an imine appears to be a straightforward path to a wide variety of chiral amino compounds. However, stereoselective additions to imines are complicated by low electrophilicity, ease of enolization, and existence of *syn/anti* imine conformers.²

Methodologies that incorporate a chiral auxiliary on the imine, specifically an optically pure sulfur(IV) center, have recently emerged as a solution to these problems. The use of enantiopure sulfinimines **1** (thiooxime *S*-oxides) as electrophiles for a number of organometallic additions allows the stereocontrolled synthesis of amine derivatives **2** (eq 1).³ This review details the synthesis of enantiomerically pure sulfinimines and highlights their use in the stereoselective synthesis of a number of amine derivatives.



GENERAL METHOD

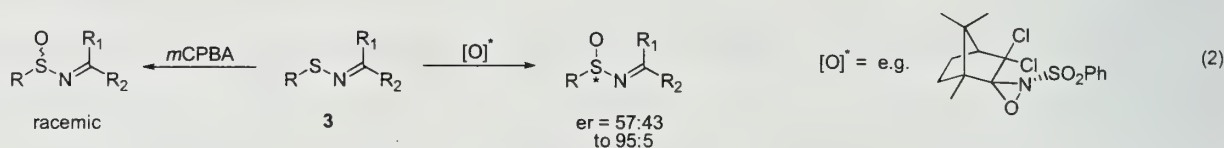
The sulfoxide moiety is considered to serve a dual role in mediating organometallic additions to sulfinimines. First, it acts as an imine activator, increasing electrophilicity and thus reactivity toward nucleophilic additions. Second, the chiral center provides an asymmetric directing group near the reaction site.³ These factors, coupled with the ease with which this auxiliary can be removed without epimerization of the newly formed stereogenic center, combine to make this methodology a powerful approach to asymmetric amine synthesis.

Numerous complementary methods exist for the preparation of optically pure sulfinimines.

These methods provide sulfinimines with a range of reactivities, and thus allow access to a broad range of amine derivatives (*vide infra*). Simple addition of various nucleophiles, notably hydride and metallo-carbanions, to appropriately substituted sulfinimines affords enantioenriched amines upon acid-catalyzed hydrolysis.³ Nucleophilic additions to sulfinimines are generally straightforward, and require neither elevated temperatures nor special catalysis. The auxiliary can be removed under mild conditions or derivatized into a sulfonamide protecting group for further synthesis.⁴

PREPARATION OF SULFINIMINES

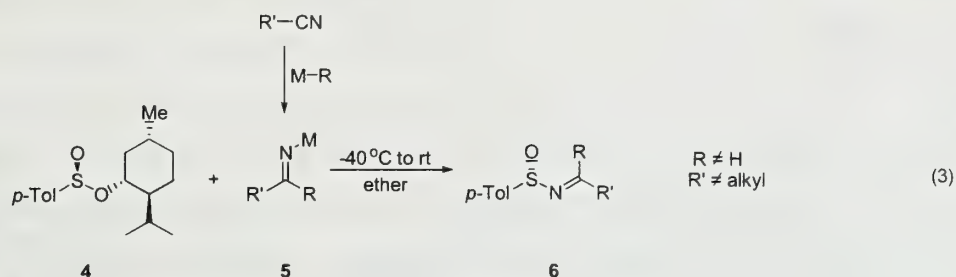
In 1974, Davis reported the racemic oxidation of sulfenimines **3** with *m*-CPBA to provide the first synthesis of the sulfinimine functionality.⁵ Attempts at direct asymmetric oxidation have proven to be generally unsuccessful for the efficient preparation of optically pure sulfinimines.³ For example, Davis reported that the oxidation of sulfenimine **3** by a chiral oxaziridine (eq 2) gave enantiomeric ratios which ranged from 57:43 to 95:5.^{2,3} Inefficient crystallizations were required to achieve enantiomeric purity, and thus the methodology was limited to amines derived from crystalline sulfenimine precursors.



A more successful route to enantioenriched sulfinimines involves introduction of the imine functionality to an enantiomerically enriched sulfur(IV) center. Such enriched centers are available through asymmetric oxidation of corresponding sulfides.⁶ Alternatively, a number of commercially available compounds contain set stereogenic sulfinyl centers.

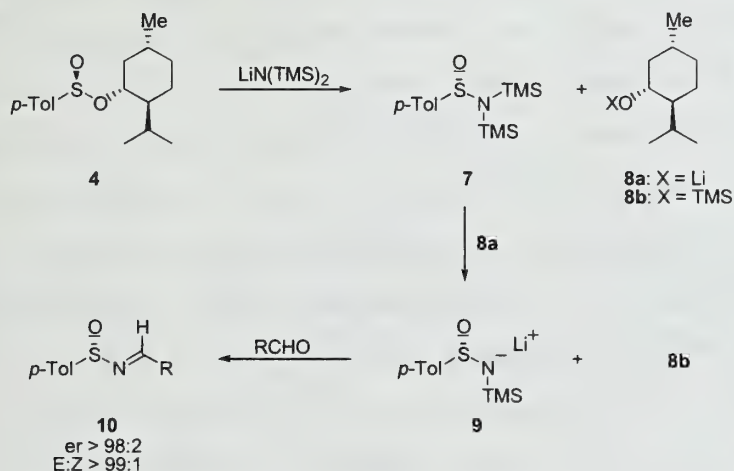
Because of its versatility and commercial availability in both enantiomeric forms, Andersen's reagent **4** has become popular for the introduction of the chiral stereodirecting *para*-toluenesulfinyl group. Cinquini and coworkers used this reagent in the first reported synthesis of enantiomerically enriched sulfinimines (eq 3).⁷ Since substitution at sulfur(IV) occurs stereospecifically with inversion,⁸ metal ketimines **5** react with Andersen's reagent to provide enantioenriched sulfinimines **6**. The organometallic nucleophile in this approach is limited, however, to ketimines which can be formed by addition of organolithium or Grignard reagents to aromatic nitriles. Although Davis has reported² that addition of 1 equivalent of methyl lithium to the DIBAL reduction of benzonitrile in the presence of Andersen's reagent did produce the corresponding *N*-sulfinyl aldimine, these reactions were in moderate

yields at best. The failure of this approach for aliphatic sulfinimines severely limits the scope of this method for chiral amine synthesis.



Progress toward more efficient and general syntheses of sulfinimines has led to two complementary methodologies developed by Davis and Ellman.^{2,4} Davis has made procedural modifications which expand the utility of Andersen's reagent. The menthol portion of **4** is displaced by lithium bis(trimethylsilyl)amide (LiHMDS) to produce the sulfonamide **7**, which provides the mono-desilated *N*-anion **9**. This anion can in turn undergo a Peterson-type olefination with a variety of aldehydes, affording the corresponding *N*-sulfinyl aldimines **10**.² (Scheme 1)

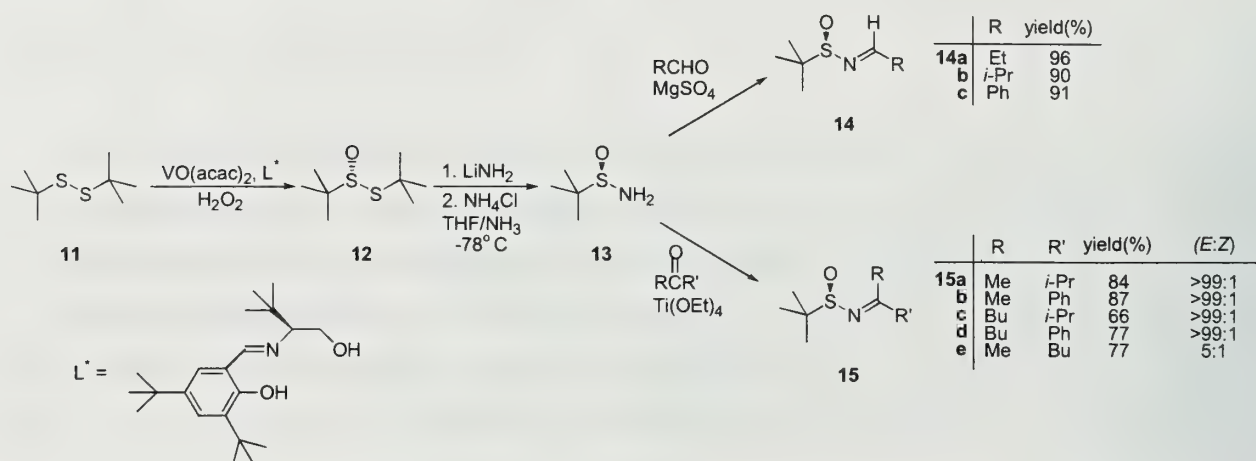
Scheme 1



Ellman and coworkers developed the first alkyl-based sulfinyl auxiliary for sulfinimines.⁹ Their efforts were guided by analogy to asymmetric aziridine reactions in which the *tert*-butyl sulfinyl group has proven to afford better stereoselectivities than the corresponding aryl auxiliaries.¹⁰ The *tert*-butanesulfonamide **13** was envisioned as a versatile intermediate which would condense with a variety of carbonyl compounds to produce the sulfinimines directly. Catalytic asymmetric oxidation of *tert*-butyl disulfide¹¹ **11** affords the sulfinyl thiosulfinate **12** with an *er* of 96:4.⁹ Stereospecific nucleophilic

substitution at sulfur then provides the desired sulfinamide **13** (Scheme 2).⁹ Ellman has shown that **12** reacts with a number of other organometallic reagents, including primary lithioamines, carbon nucleophiles, and metallo-imines to afford enantioenriched primary sulfinamides, sulfoxides, and sulfinimines respectively.⁹

Scheme 2



In the initial work, it was found that displacement by the lithium amide afforded the desired product in high yields, but with complete loss of enantiointegrity. The lithium thiolate byproduct was proposed to be responsible for this racemization at room temperature. The racemization process was found to be slow at -78°C , while substitution by the lithium amide is rapid; thus quenching the reaction at -78°C gave **13** in good yields (71-78%) and without loss of enantiomeric purity.⁹ A single recrystallization provides the enantiopure sulfinamide **13** that condenses with a number of aryl and alkyl aldehydes and ketones to afford a variety of *N*-sulfinyl aldimines **14** and *N*-sulfinyl ketimines **15**.^{9,12}

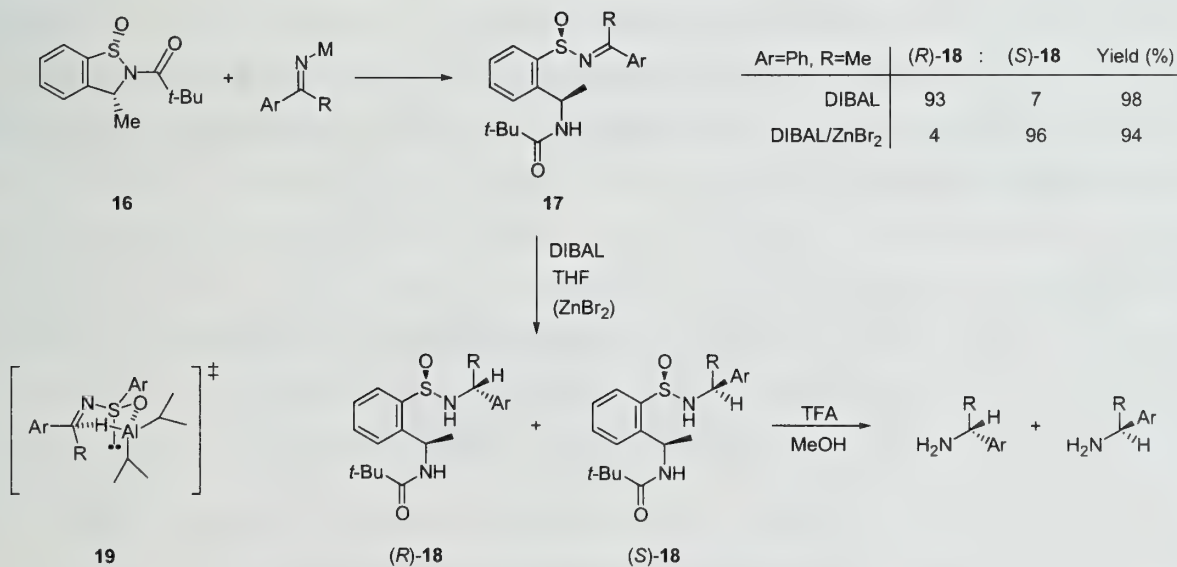
The geometry about the imine functionality of these sulfinimines is critical in the asymmetric nucleophilic addition reactions. For aldimine cases (e.g. **14a-c**), only one *E/Z* isomer is present as determined by NMR spectroscopy. This isomer is assumed to have the *E* configuration based on analogy to systems characterized in the solid state by X-ray crystallography.² When sterically similar ketones are used to provide **15e**, both *E* and *Z* may be present, thus affecting the subsequent additions.¹²

SYNTHESIS OF AMINE DERIVATIVES

α -Substituted Amines

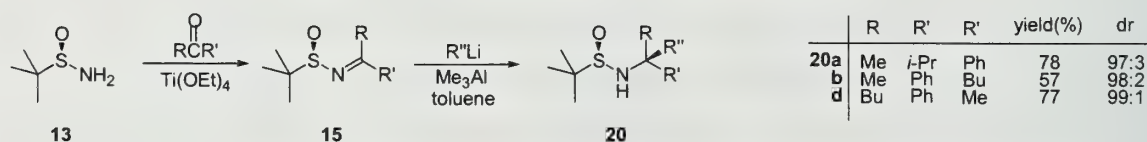
The activation of the imine functionality by the electron withdrawing sulfoxide allows a range of nucleophiles to be added, providing a variety of chiral, enantioenriched amines. α,α -Disubstituted amines can be produced from either hydride reduction of ketimine-type sulfinimines **6**, or by the addition of organometallics to sulfinimines derived from aldehydes **10** and **14**.³ Amines that contain an aryl substituent are efficiently synthesized by a sulfinimine reduction method developed by Wills and coworkers,¹³ as shown in Scheme 3. This hydride addition to sulfinimines **17** derived from aromatic ketimines proceeds with higher yields and greater selectivities than those in similar experiments reported by Davis.² Although limited to aromatic nitriles, this system is mechanistically noteworthy. DIBAL reduction of **17** stereoselectively affords the sulfinimine (*R*)-**18** in 98% yield and with a dr of 93:7. This selectivity can be rationalized by a proposed six-membered chair-like transition state **19**.¹³ However the addition of zinc(II) bromide to this reaction affords (*S*)-**18** with a dr of 96:4.¹³ No clear mechanistic reason for this reversal is known, although a similar selectivity reversal has been seen in the reduction of β -ketosulfoxides.¹⁴ Thus, from a single enantiomer of the starting cyclic sulfonamide **16**, reaction conditions can be tuned to add hydride to either face of the imine with high levels of asymmetric induction.

Scheme 3



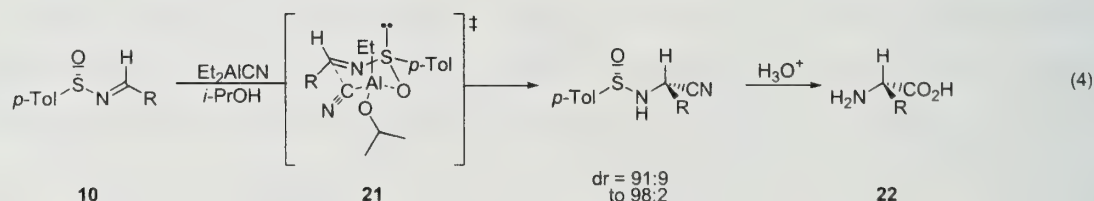
The methods developed by both Davis and Ellman provide α,α -disubstituted amines from aldehyde-derived sulfinimines upon addition of organometallic nucleophiles. However, the *tert*-butyl sulfinamide **13** provides a variety of di-alkyl derivatives which are unavailable through the aryl-based **10**.^{3,5} Nucleophilic addition to *N*-sulfinyl arylketimines **6** produced by Cinquini's method (eq 3) provides α,α,α -trisubstituted amines; however, Ellman has recently shown a more general path to this class of compounds. (Scheme 4) Titanium tetraethoxide mediated condensation of sulfinamide **13** with a variety of ketones affords **15** in good to excellent yields, which provide these amines upon organometallic nucleophilic addition.¹²

Scheme 4



Amino Acids

The Strecker synthesis, first reported in 1850, has evolved as a powerful tool in the synthesis of amino acids. Davis has shown that reactions between cyanide anions and sulfinimines under pseudo-Strecker conditions afford enantiomerically enriched α -substituted amino acids **22** upon simultaneous hydrolysis of auxiliary and nitrile (eq 4).¹⁵ Alcohol additives are used to facilitate the stereoselective addition of Et_2AlCN to sulfinimines. The stereoselectivity and role of the alcohol have been rationalized by a proposed six-membered chair-like transition state structure **21**. Alternatively, Hua has reported the use of orthoesters as acid equivalents on a sulfinimine substrate.¹⁶ More directly, Zanda and coworkers have used carboxylic ester substituted sulfinimines to afford an α -trifluoromethyl- α -benzyl amino ester after benzyl Grignard addition.¹⁷

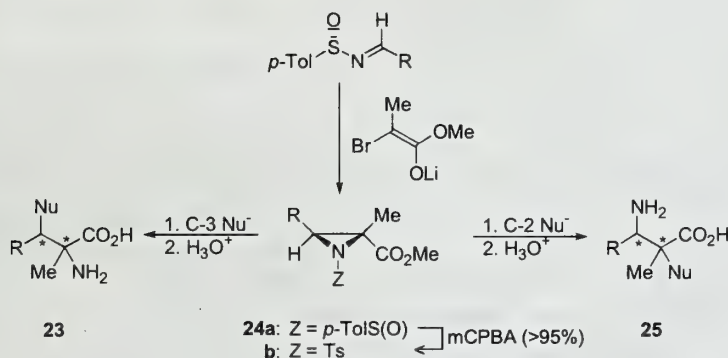


The simple addition of enolates can afford β -amino acids in both high yields and stereoselectivities.^{4,18} Similar to some α -amino acid approaches, masked acids can be introduced into

the β -position, most notably by the oxidative conversion of allyl units. Allyl Grignard addition provides the desired β -amino acids upon ozonolysis, oxidative workup, and hydrolysis.¹⁹ Mikolajczyk and coworkers showed the use of α -phosphonate carbanions to afford β -aminophosphonate and β -aminophosphonic acids.²⁰ The optimized system gave only 91:9 er, although with high yields. The low facial selectivities may be attributed to a proposed loose eight-membered ring transition state structure.

Davis has also developed a stereoselective Darzen-type addition of α -bromoester enolates to afford *N*-sulfinylaziridine-2-carboxylic esters **24**.²¹ Regioselective nucleophilic ring opening at either C-3 or C-2 and subsequent hydrolysis affords enantioenriched α - or β -amino acids **23** and **25** respectively. (Scheme 5)

Scheme 5



UTILITY

Addition to various sulfinimines has been explored as the key asymmetric step in a number of syntheses. Davis has reported the syntheses of members of the 3-substituted-1(2H)-isoquinone alkaloid family.²² Similarly, the stereocenter formed from this methodology has been used to synthesize both 2-substituted and 2,6-disubstituted piperidines upon amine cyclizations.²³ This methodology has been used by Hassner in his reported synthesis of (*S*)-anatabine.²⁴ Davis has also shown the sulfinimine's utility to afford (*R*)-(3,4,5-trihydroxyphenyl)glycine, the central amino acid core of the antibiotic vancomycin.²⁵ Finally, enolate addition to sulfinimines has been used to synthesize the C-13 side chain of taxol in 62% yield.¹⁸ Efficient asymmetric synthesis of these amine derivatives is provided via the chiral sulfinimines.

CONCLUSION

The large number of amine derivatives in synthetically and biologically interesting compounds calls for the development of synthetic organic methodology. Complete proficiency in this field requires predictable, rational, and efficient stereoselectivity in reactions. Although there is room for improvements and further mechanistic understanding, the use of chiral sulfinimines has begun to show promise as a practical methodology in this endeavor.

REFERENCES

- (1) (a) Blouch, R. *Chem. Rev.* **1998**, 1407. (b) Enders, D.; Reinhold, U. *Tetrahedron: Asymmetry* **1997**, 8, 1895. (c) Johansson, A. *Contemp. Org. Chem.* **1995**, 2, 393.
- (2) Davis, F. A.; Reddy, R. R.; Szewczyk, J. M.; Reddy, G. V.; Portonovo, P. S.; Zhang, H.; Fanelli, D.; Reddy, R. T.; Zhou, P.; Carroll, P. J. *J. Org. Chem.* **1997**, 82, 2555.
- (3) Davis, F. A.; Zhou, P.; Chem, B. *Chem. Soc. Rev.* **1998**, 27, 13.
- (4) Tang, T. P.; Ellman, J. A. *J. Org. Chem.* **1999**, 64, 12.
- (5) Davis, F. A.; Friedman, A. J.; Kluger, E. W. *J. Am. Chem. Soc.* **1974**, 96, 5000.
- (6) Carreno, M. C. *Chem. Rev.* **1995**, 95, 1717.
- (7) Annunziata, R.; Cinquini, M.; Cozzi, F. *J. Chem. Soc. Perkin Trans. 1* **1982**, 339.
- (8) Kishi, M.; Ishihara, S.; Komeno, T. *Tetrahedron* **1974**, 30, 2135.
- (9) Cogan, D. A.; Liu, G.; Kim, K.; Backes, B. J.; Ellman, J. A. *J. Am. Chem. Soc.* **1998**, 120, 8011.
- (10) Ruano, J. L. G.; Fernandez, I.; Catalina, A. A. *Tetrahedron: Asymmetry* **1996**, 7, 3407.
- (11) Bolm, C.; Bienewald, F. *Angew. Chem. Int. Ed. Engl.* **1995**, 34, 2640.
- (12) (a) Cogan, D. A.; Ellman, J. A. *J. Am. Chem. Soc.* **1999**, 121, 268. (b) Liu, G.; Cogan, D. A.; Owens, T. D.; Tang, T. P.; Ellman, J. A. *J. Org. Chem.* Submitted.
- (13) Hose, D. R. J.; Mahon, M. F.; Molloy, K. C.; Raynham, T.; Wills, M. J. *Chem. Soc. Perkin Trans. 1* **1996**, 691.
- (14) Carreno, M. C.; Ruano, J. L. G.; Martin, A. M.; Pedregal, C.; Rodriguez, J. H.; Rubio, A.; Sanchez, J.; Solladie, G. *J. Org. Chem.* **1990**, 55, 2120.
- (15) Davis, F. A.; Portonovo, P. S.; Reddy, R. E.; Chiu, Y.-H. *J. Org. Chem.* **1996**, 61, 440.
- (16) Hua, D. H.; Lagneau, N.; Wang, H.; Chem, J. *Tetrahedron: Asymmetry* **1995**, 6, 349.
- (17) Bravo, P.; Crucianelli, M.; Vergani, B.; Zanda, M. *Tetrahedron Lett.* **1998**, 39, 7771.
- (18) Davis, F. A.; Reddy, T. R.; Reddy, R. E. *J. Org. Chem.* **1992**, 57, 6387.
- (19) Hua, D. H.; Miao, S. W.; Chem, J. S.; Iguchi, S. *J. Org. Chem.* **1991**, 56, 4.
- (20) Mikolejczyk, M.; Lyzwa, P.; Drabowicz, J.; Wieczorak, M. W.; Blaszczyk, J. *Chem. Commun.* **1996**, 1503.
- (21) (a) Davis, F. A.; Reddy, G. V.; Liange, C. *Tetrahedron Lett.* **1997**, 38, 5139. (b) Davis, F. A.; Zhou, P.; Reddy, G. V. *J. Org. Chem.* **1994**, 59, 3243.
- (22) Davis, F. A.; Andemichael, Y. W. *Tetrahedron Lett.* **1998**, 39, 3099.
- (23) Davis, F. A.; Szewczyk, J. M. *Tetrahedron Lett.* **1998**, 39, 5951.
- (24) Balasubramanian, T.; Hassner, A. *Tetrahedron: Asymmetry* **1998**, 9, 2201.
- (25) Davis, F. A.; Fanelli, D. L. *J. Org. Chem.* **1998**, 63, 1981.

SYNTHESIS OF THE BICYCLIC CORE OF CP-225,917 AND CP-263,114

Reported by Jannine Haberman

February 25, 1999

INTRODUCTION

CP-225,917 (**1**) and CP-263,114 (**2**) (Figure 1) were discovered during a screening for inhibitors of squalene synthase and Ras farnesyl transferase and isolated from an unidentified fungus.^{1,2} Inhibitors of these enzymes are of interest because of their potential pharmaceutical applications as cholesterol reducing³ and antitumor agents.⁴ The relative configurations of CP-225,917 and CP-263,114 were elucidated by Kaneko and coworkers from extensive NMR experiments; however, the absolute configurations have not yet been determined.¹ The biosynthesis of these natural products has been proposed based on the biosynthetic pathway of the related nonadrides, glauconic acid and rubratoxins A and B.¹ Among the interesting structural features of **1** and **2** are the bicyclo[4.3.1]deca-1(9)-ene ring system, containing a bridgehead double bond and a quaternary carbon center; the bridging lactone, which comprises the hemiketal of **1** and the ketal of **2**; the anti alkyl substituents at C(9) and C(17); and the maleic anhydride moiety. Currently, the syntheses of CP-225,917 and CP-263,114 are under investigation in several research laboratories.⁵⁻¹³ This review will highlight the progress made in the construction of **1** and **2**.

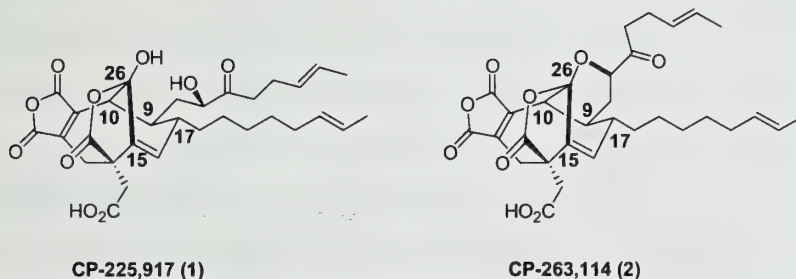
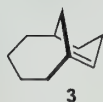


Figure 1. Structures of CP-225,917 and CP-263,114.

SYNTHETIC STRATEGIES

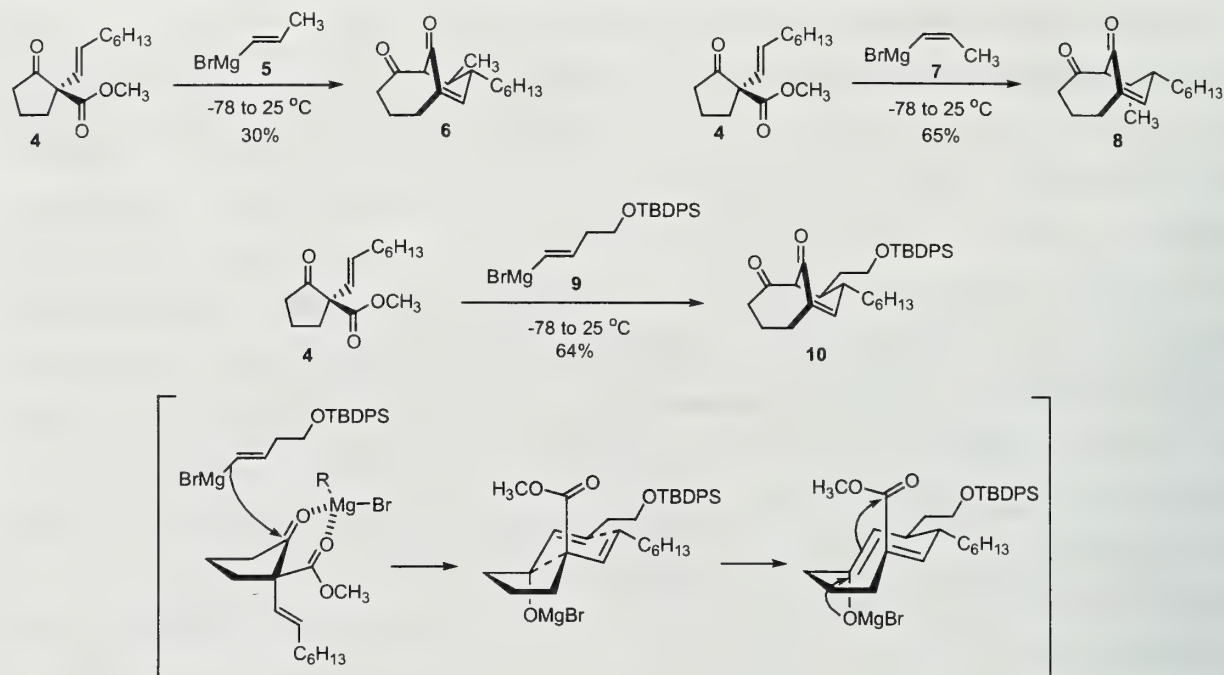
The primary focus of the synthetic efforts reported thus far has been on the assembly of the bicyclo[4.3.1] core structure **3**, which is a common motif in CP-225,917 and CP-263,114. The strategies developed for the formation of this bicyclic ring system include anion-accelerated oxy-Cope rearrangement,^{5,6} intramolecular Diels-Alder reaction,^{7,8} divinylcyclopropane rearrangement,^{9,10} and aldol condensation,^{11,12} as discussed below.



Anion-Accelerated Oxy-Cope Rearrangement

Synthesis of the bicyclo[4.3.1] core structure via a tandem anion-accelerated oxy-Cope rearrangement and transannular cyclization (Scheme 1) was achieved by Shair and coworkers.⁵

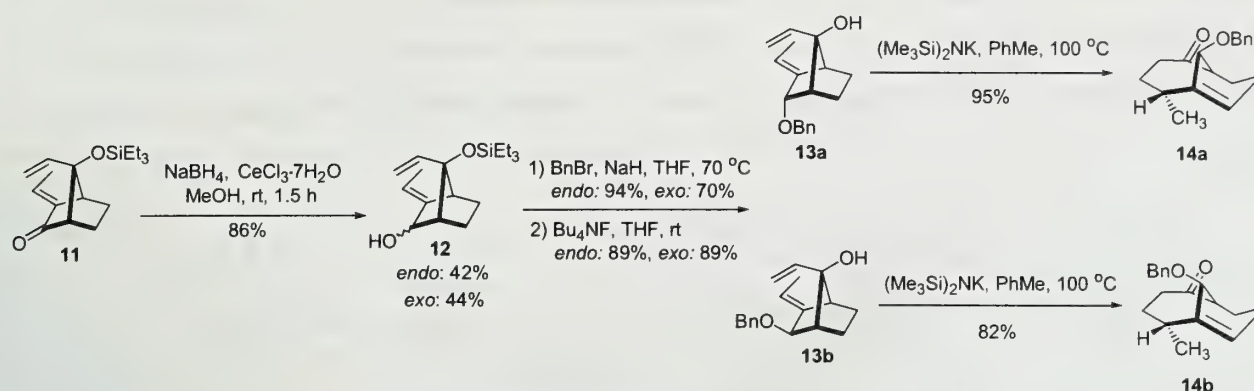
Scheme 1



This transannular cyclization parallels the proposed C(10)-C(26) biosynthetic cyclization.¹ Reaction of 2-alkyl-β-ketoester **4** with (E)-1-propenylmagnesium bromide **5** afforded enedione **6** in 30% yield. The anti orientation of the C(9) and C(17) alkyl substituents of **6** was consistent with the known relative configuration of CP-225,917 and CP-263,114. Addition of (Z)-1-propenylmagnesium bromide **7** to ketone **4** gave the bicyclic core **8**, with its two alkyl substituents oriented syn in 65% yield. As a result of the above model studies, vinyl Grignard **9** was used to prepare for the formation of the C(9) sidechain of **1** and **2**. The core structure **10** was obtained in 64% yield, once again exhibiting the anti orientation observed in CP-225,917 and CP-263,114. Shair has proposed that this stereospecific bicyclization proceeds via a chelation-controlled addition of the vinyl Grignard to the β-ketoester, followed by anion-accelerated oxy-Cope rearrangement through a chair transition state. The chair transition state controls the stereochemistry at C(9) and C(17), the configuration of the bridgehead double bond, and the geometry of the (Z)-enolate, which promotes the C(10)-C(26) transannular cyclization. The success of this cyclization reaction supports the analogous cyclization that has been proposed for the biosynthesis of **1** and **2**.

Another strategy for assembling the bicyclic ring system, utilizing an anion-accelerated oxy-Cope rearrangement (Scheme 2), was described by Clive.⁶ Enone **11** was prepared in ten steps from

Scheme 2

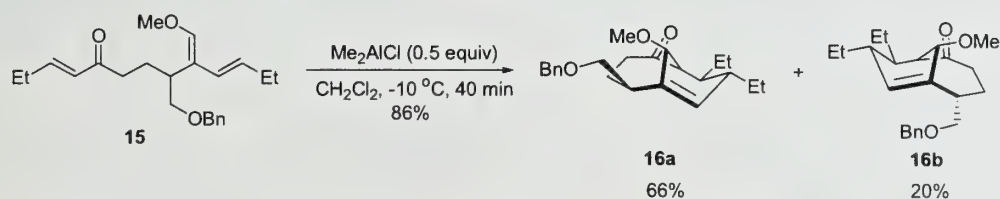


readily available starting material. Luche reduction afforded a 1:1 mixture of *endo* and *exo*-allylic alcohols **12**, which were separated and protected as the corresponding benzyl ethers. Desilylation gave **13a** and **13b**, which were subjected to anionic oxy-Cope rearrangement, affording **14a** and **14b** in 95% and 82% yield, respectively. Similar to Shair's work, this method directly addresses the formation of the C(15)-C(16) bridgehead double bond. In future studies, it is anticipated that capture of the enolates, resulting from rearrangement of **13a** and **13b**, with Mander's reagent¹⁴ will allow for the introduction of the maleic anhydride moiety. It is also hoped that the oxygen functionality at C(26) will allow for the construction of the hemiketal of **1** or the ketal of **2**.

Intramolecular Diels-Alder Reaction

The use of the intramolecular Diels-Alder reaction in the synthesis of bicyclic molecules containing bridgehead double bonds has previously been reported.¹⁵ This method was used by Nicolaou for the construction of bicyclic ring system **16** (Scheme 3).⁷ Treatment of racemic triene **15** with dimethylaluminum chloride in dichloromethane at -10°C afforded cycloadducts **16a** and **16b** in 66%

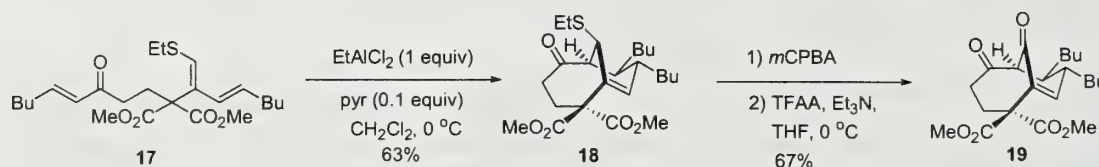
Scheme 3



and 20% yields, respectively.

Fukuyama reported a similar strategy for the assembly of the bicyclic ring system (Scheme 4), in which an intramolecular Diels-Alder reaction afforded the desired product as a single diastereomer.⁸ Reaction of triene **17** in the presence of ethylaluminum chloride and pyridine in dichloromethane at 0 °C afforded Diels-Alder adduct **18** in 63% yield. Oxidation with *meta*-chloroperoxybenzoic acid followed by Pummerer rearrangement in the presence of trifluoroacetic anhydride and triethylamine

Scheme 4



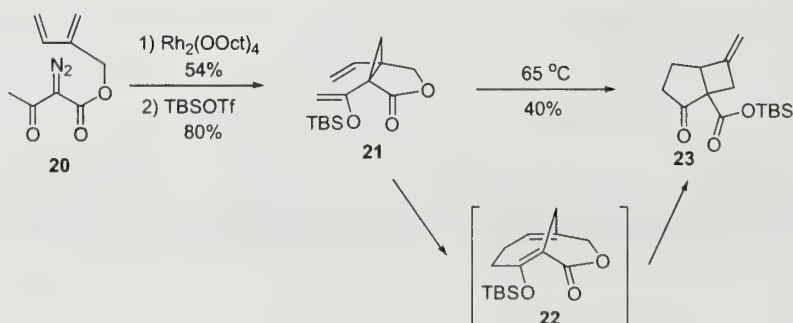
gave **19** in 67% yield over two steps. It was discovered that the use of pyridine increased the yield of **18**. Pyridine attenuated isomerization of **17** to the (*E*)-ethylthio substituted olefin, which was isolated along with cycloaddition product **18**.

Both strategies, which rely on an intramolecular Diels-Alder reaction for the formation of the bicyclic core, establish the anti orientation of the C(9) and C(17) alkyl groups, introduce the C(15)-C(16) bridgehead double bond, and provide functionality at C(26) necessary for the completion of **1** and **2**. In addition, Fukuyama's diester triene **17** also allows for the formation of the quaternary carbon center at C(14).

Divinylcyclopropane Rearrangement

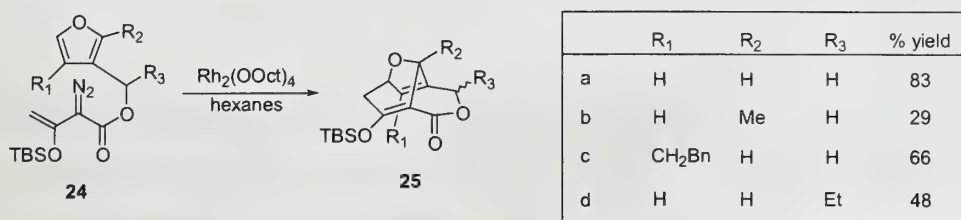
The intramolecular reaction between dienes and vinyl carbenoids has been used for the stereoselective generation of bicyclic ring systems.¹⁶⁻¹⁸ The use of the resulting cyclopropanation/Cope rearrangement in the synthesis of **1** and **2** has been explored by Davies⁹ and Nicolaou.¹⁰ Rhodium(II) octanoate catalyzed decomposition of diazoacetoacetate **20** (Scheme 5), followed by silylation with *tert*-

Scheme 5



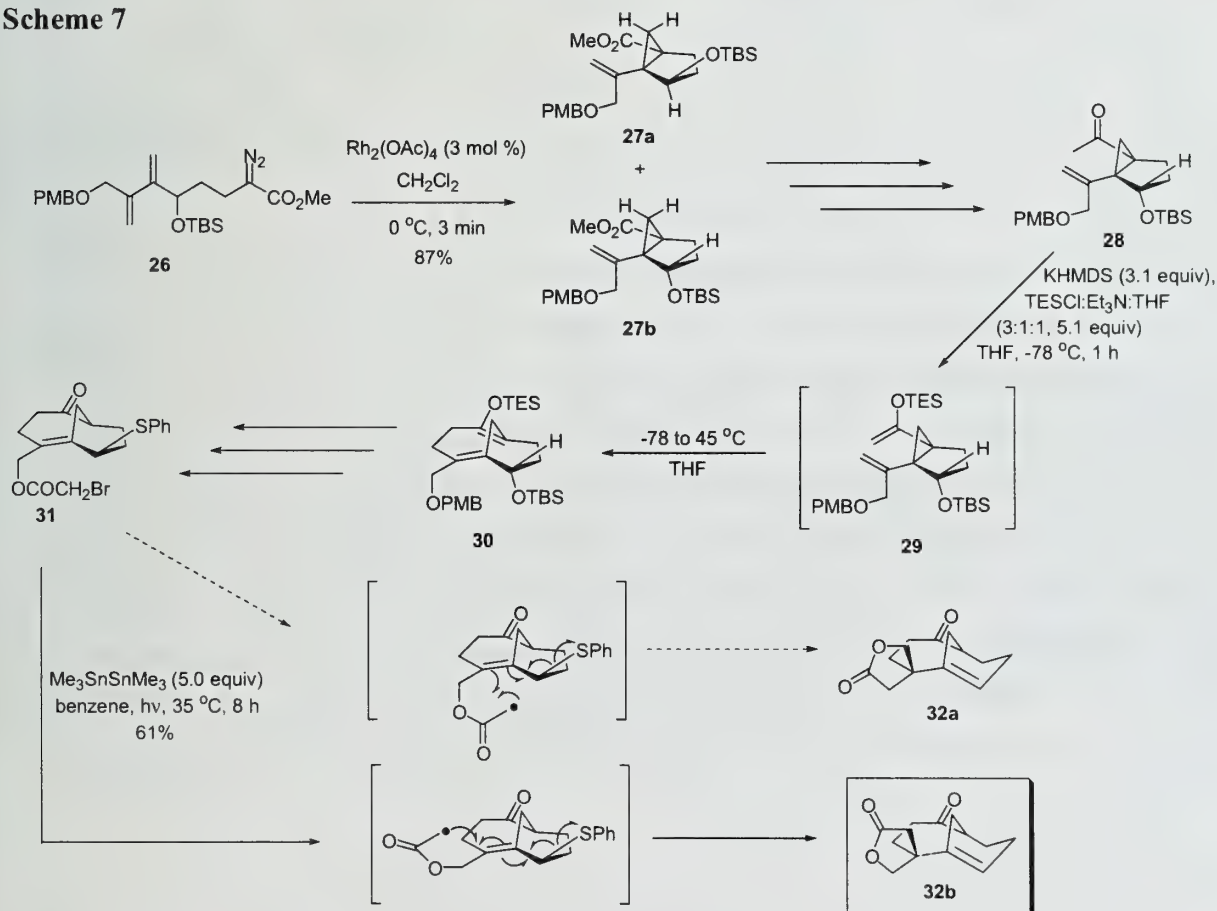
butyldimethylsilyl triflate, afforded divinylcyclopropane **21**. Heating to 65 °C resulted in rearrangement and formation of fused cyclobutane **23** in 40% yield. It has been proposed by Davies⁹ that cyclobutane **23** forms via a transannular rearrangement of the desired [4.3.1]-bicycle **22**, followed by silyl transfer. Diazofuran **24** (Scheme 6) was used to suppress formation of the undesired fused cyclobutane, since the resulting product would be more strained and therefore less likely to form. As expected, rhodium(II) octanoate catalyzed decomposition of diazofurans **24a-24d** provided tricyclic products **25a-25d**. Further investigations are underway to extend this tandem process to the synthesis of **1** and **2**.

Scheme 6



Employing a dicyclopropane rearrangement followed by a radical cyclization (Scheme 7), Nicolaou successfully synthesized the bicyclic core.¹⁰ Rhodium(II) acetate catalyzed decomposition of

Scheme 7

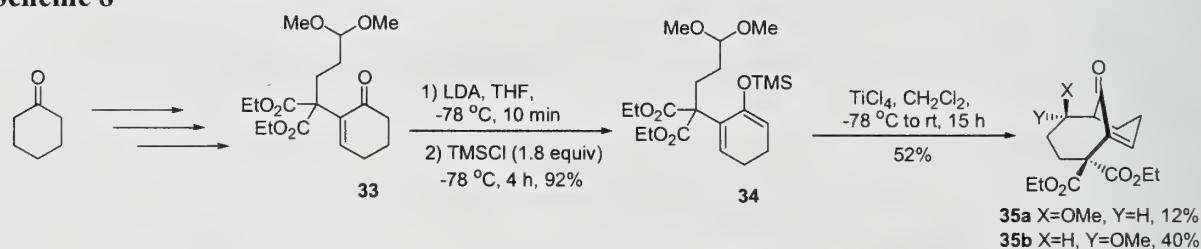


diazoester **26** afforded cyclopropanes **27a** and **27b** in a combined yield of 87%. Conversion to ketone **28** was accomplished in eight steps with an overall yield of 66%. Treatment of **28** with a mixture of TESC/Et₃N/THF (3:1:1) in the presence of KHMDS at -78 °C resulted in the formation of enol ether **29**. Divinylcyclopropane rearrangement, initiated by heating to 45 °C, afforded bicycle **30**, which was converted to phenylsulfide **31** in four steps. Photolysis in the presence of Me₃SnSnMe₃ promoted a radical cyclization, forming the desired [4.3.1]-bicyclic ring system, containing the bridgehead double bond and the quaternary carbon center. However, the configuration at the quaternary carbon center of **32b** was opposite to that of the originally anticipated product **32a**.

Aldol Condensation

Armstrong achieved a six step synthesis of the bicyclo[4.3.1]decenone core, utilizing an aldol condensation in the ring closing step.¹¹ Dimethylacetal **33** (Scheme 8) was prepared in four steps from cyclohexanone in an overall yield of 37%. Conversion to silyl enol ether **34** was

Scheme 8

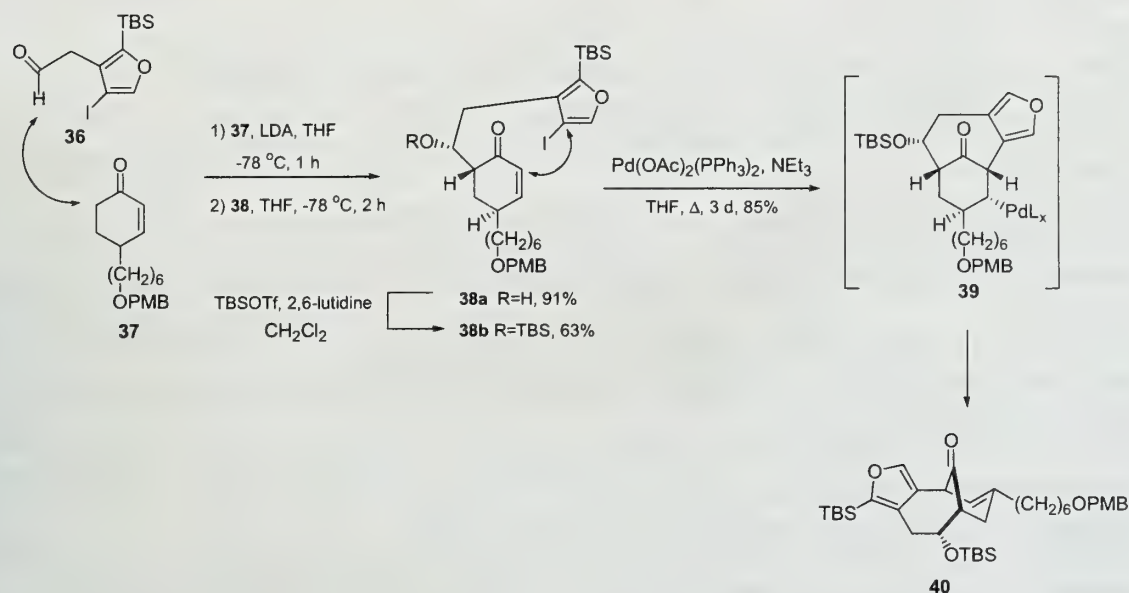


accomplished with TMSCl in 92% yield. Treatment with TiCl₄ in dichloromethane afforded **35a** and **35b** in 12% and 40% yield, respectively. Armstrong's strategy accomplished the formation of both the bicyclic core and the quaternary carbon center. It is anticipated that group differentiation of the diester will allow for installation of the C(14) stereocenter of **1** and **2**.

While other strategies for the construction of the bicyclic core structure directly address the formation of the C(15)-C(16) bridgehead double bond, Danishefsky has recently reported the synthesis of a C(15)-C(16)-dihydro ring system via a sequential aldol condensation and intramolecular Heck ring closure (Scheme 9), which focuses on introducing all of the necessary functionality for the completion of **1** and **2**.¹² Aldol condensation of aldehyde **36** with cyclohexenone derivative **37** afforded β -hydroxy ketone **38a**, which was converted to the corresponding silyl ether **38b** in an overall yield of 57%. The reaction, which occurred anti to the alkyl sidechain of **37**, provided the correct configuration

for the subsequent Heck ring closure to give the desired product. Treatment of **38b** with catalytic $\text{Pd}(\text{OAc})_2(\text{PPh}_3)_2$ produced intermediate **39**, which afforded the desired bicyclic ring system **40** in 85%.

Scheme 9



Bicyclic core **40** was assembled with the functionality necessary for the introduction of the maleic anhydride moiety, the formation of the quaternary carbon center, and the installation of the C(9) alkyl sidechain.¹³

CONCLUSION

The novel structure and biological potential of CP-225,917 and CP-263,114 has resulted in the development of several methods for the assembly of the [4.3.1]-bicyclic core. Anion-accelerated oxy-Cope rearrangement, intramolecular Diels-Alder reaction, divinylcyclopropane rearrangement, and aldol condensation have been utilized in the key cyclization step. The anti orientation of the C(9) and C(17) alkyl sidechains, the formation of the bridgehead double bond, and the introduction of an oxygen functionality at C(26) have been considered in the development of many of these reactions. The total synthesis of these natural products is still under investigation.

REFERENCES

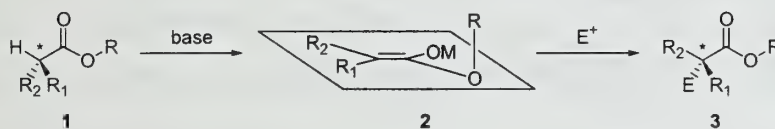
- (1) Dabrah, T. T.; Kaneko, T.; Massefski, W., Jr.; Whipple, E. B. *J. Am. Chem. Soc.* **1997**, *119*, 1594.
- (2) Dabrah, T. T.; Harwood, H. J., Jr.; Huang, L. H.; Jankovich, N. D.; Kaneko, T.; Li, J. -C.; Lindsey, S.; Moshier, P. M.; Subashi, T. A.; Therrien, M.; Watts, P. C. *J. Antibiot.* **1997**, *50*, 1.
- (3) Goldstien, J. L.; Brown, M. S. *Nature* **1990**, 343.
- (4) Buss, J. E.; Marsters, J. C., Jr. *Chem. Biol.* **1995**, *2*, 787.
- (5) Chen, C.; Layton, M. E.; Shair, M. D. *J. Am. Chem. Soc.* **1998**, *120*, 10784.
- (6) Sgarbi, P. W. M.; Clive, D. L. J. *Chem. Commun.* **1997**, 2157.
- (7) Nicolaou, K. C.; Harter, M. W.; Boulton, L.; Jandeleit, B. *Angew. Chem., Int. Ed. Engl.* **1997**, *36*, 1194.
- (8) Waizume, N.; Itoh, T.; Fukuyama, T. *Tetrahedron Lett.* **1998**, *39*, 6015.
- (9) Davies, H. M. L.; Calvo, R.; Ahmed, G. *Tetrahedron Lett.* **1997**, *38*, 1737.
- (10) Nicolaou, K. C.; Postema, M. H. D.; Miller, N. D.; Yang, G. *Angew. Chem., Int. Ed. Engl.* **1997**, *36*, 2821.
- (11) Armstrong, A.; Critchley, T. J.; Mortlock, A. A. *Synlett* **1998**, 552.
- (12) Kwon, O.; Su, D. S.; Meng, D.; Deng, W.; D'Amico, D. C.; Danishefsky, S. J. *Angew. Chem., Int. Ed. Engl.* **1998**, *37*, 1877.
- (13) Kwon, O.; Su, D. S.; Meng, D.; Deng, W.; D'Amico, D. C.; Danishefsky, S. J. *Angew. Chem., Int. Ed. Engl.* **1998**, *37*, 1880.
- (14) Mander, L. N.; Sethi, S. P. *Tetrahedron Lett.* **1983**, *24*, 5425.
- (15) Gwaltney, S. L., II; Sakata, S. T.; Shea, K. J. *J. Org. Chem.* **1996**, *61*, 7438.
- (16) Davies, H. M. L. *Tetrahedron* **1993**, *49*, 5203.
- (17) Davies, H. M. L.; McAfee, M. J.; Oldenburg, C. E. M. *J. Org. Chem.* **1989**, *54*, 930.
- (18) Davies, H. M. L.; Matasi, J. J.; Ahmed, G. *J. Org. Chem.* **1996**, *61*, 2305.

INTRODUCTION

One of the major goals of organic chemists has been to develop strategies for highly stereoselective carbon-carbon bond formation. To achieve this goal, traditional strategies rely on the use of chiral auxiliaries, chiral solvents or chiral catalysts to effect a variety of asymmetric transformations such as enolate alkylations and cycloadditions.^{1,2} Recently, two alternative approaches based on the concepts of "memory of chirality" and "self-regeneration of stereogenic centers" (SRS) have been employed in asymmetric synthesis without using external sources of chirality.^{3,4}

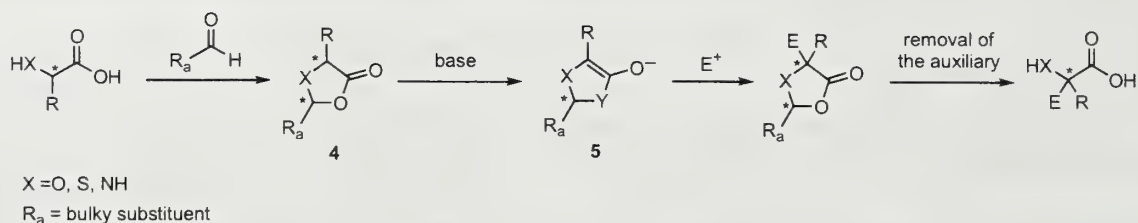
When the sole stereogenic center of a substrate is lost during the formation of an activated intermediate, such as an enolate, the resulting alkylation product is a racemic mixture. Memory of chirality describes a system in which an apparently achiral intermediate reacts stereoselectively to form a carbon-carbon bond in the absence of any external sources of chirality. This concept is illustrated in Scheme 1, in which optically pure ester **1** is alkylated via the ester enolate intermediate **2** to generate an optically active alkylated product **3**. In this process, the configuration at the single stereogenic center is lost as a result of the enolate formation. However, the two faces of the enolate are differentiated due to the position of the enolate substituent R, which is oriented out of the enolate plane due to the inherent structure and configuration of R₁ and R₂ (Scheme 1).³

Scheme 1



As in the example of memory of chirality (Scheme 1), self regeneration of stereogenic centers (SRS) utilizes an optically pure starting material with a single stereogenic center and this substrate is first derivatized with an achiral auxiliary.⁴ In the process of derivatization, a new stereogenic center is created by virtue of the existing stereogenic center in the starting material, to generate **4** (Scheme 2). Formation of enolate **5** destroys the original stereogenic center, yet the stereoselective carbon-carbon bond formation is still achieved due to the facial discrimination resulting from the newly generated stereogenic center. Upon the completion of the stereoselective carbon-carbon bond formation, removal

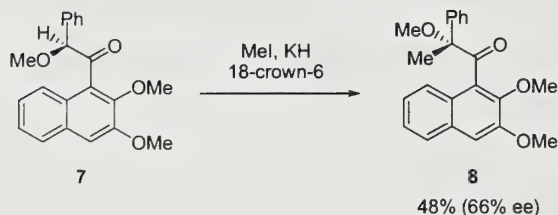
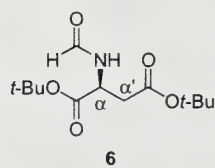
Scheme 2



of the auxiliary is carried out. This report describes several stereoselective reactions utilizing memory of chirality or SRS.

MEMORY OF CHIRALITY

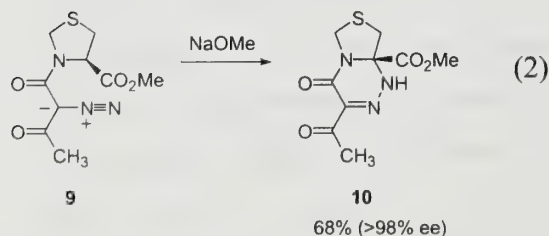
One of the earliest examples involving stereocontrol arising from apparent “memory of chirality” was described by Seebach and co-workers in 1981.⁵ Alkylation of di-*t*-butyl *N*-formyl-aspartate (**6**) in the absence of chiral auxiliaries or catalysts led to α -alkylated product in 15% yield and 60% ee. This phenomenon was also observed by Fuji and coworkers in 1991. In this case the alkylation of ketone **7**, provided **8** in a moderate yield of 48% and 66% ee (eq 1).⁶ The alkylation of **7** in the absence of a chiral environment with



various electrophiles demonstrated that the stereoselectivity of the alkylation is dictated by the configuration of the stereogenic center of **7**. It was proposed that the asymmetric induction arises from either a mixed substrate-enolate aggregate or the axial chirality of the enolate. The investigation carried out to rationalize the mechanism of the

asymmetric induction suggests the axial chirality of the enolate as the mode of the stereoselective alkylation.⁶

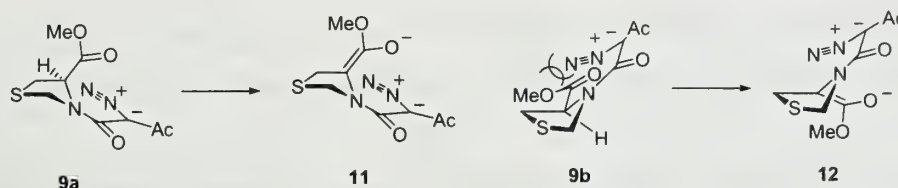
A stereoselective intramolecular reaction involving memory of chirality was observed by



Stoodley and coworkers. The authors found that under basic conditions, diazoacetyl thiazolidine carboxylate **9** reacts to form thiatriazabicyclonone **10** as a single enantiomer (eq 2).⁷ In this reaction, the favored conformation of **9** is believed to be **9a** in which the steric

interactions between the diazo functionality and the methyl ester are minimized relative to **9b** (Figure 1). If the thiazolidine ring conformation in **9a** is retained upon the generation of the enolate **11**, one can rationalize the stereochemical outcome of the product **10**.

Figure 1



In an attempt to utilize the memory of chirality for general application, Fuji and coworkers have investigated alkylation of α -amino acids.⁸ It was found that the protected (*S*)-phenyl alanine derivative **13** could be alkylated in 40% yield and 82% ee. This investigation showed that both enantioselectivity and yield vary with the substituents on the nitrogen. It was also reported that asymmetric induction by axial or planar chirality created by certain substituents on nitrogen could be applied to other amino acids as well, marking the first step toward development of a general synthetic method using the principle of memory of chirality.

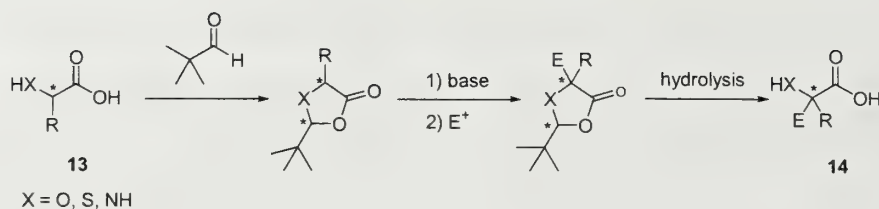
SELF-REGENERATION OF STEREOGENIC CENTERS

General Concept and Stereocontrol Elements

SRS was conceived independently by both Fráter⁹ and Seebach¹⁰ in 1981. Since then it has been greatly utilized in stereoselective alkylation of amino acids^{4,11} and carboxylic acid derivatives⁴ for it provided the key synthetic steps in total syntheses of biologically important compounds such as (*S*)-(+)- α M4CPG,¹² a selective antagonist of metabotropic glutamate receptors, and (+)-lactacystin,^{13,14} the first non-protein neurotrophic factor reported.

Stereoselective alkylations controlled by SRS involve three steps: (1) beginning with a chiral non-racemic starting material, the creation of an additional stereocenter via the derivatization of the chiral starting material with an achiral auxiliary, (2) the formation of the new carbon-carbon bond with the generation of a new stereogenic center, and (3) the removal of the auxiliary.⁴ Although the stereogenic center in the starting material is destroyed, the stereoselective carbon-carbon bond formation is still achieved by the virtue of the stereogenic center generated from the derivatization with an achiral auxiliary. The most common application of SRS involves stereoselective alkylation of compounds such as **13** (Scheme 3). Derivatization of **13** with an achiral auxiliary to introduce the second stereogenic

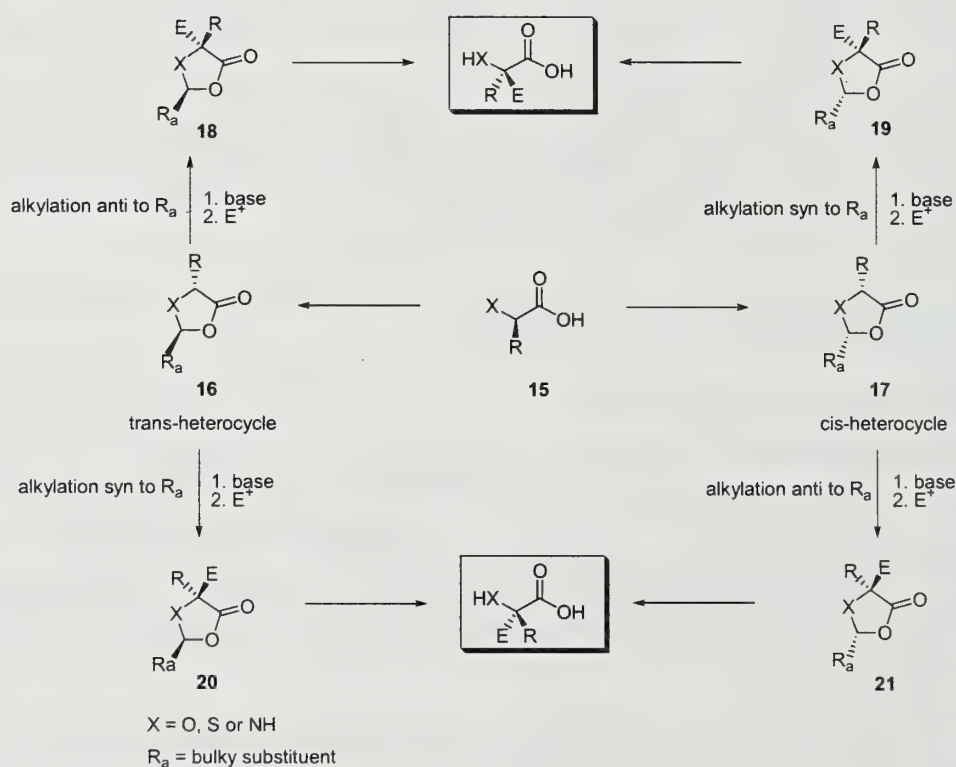
Scheme 3



center is usually achieved by formation of a heterocycle with a bulky aldehyde auxiliary such as pivaldehyde. Subsequent alkylation and the removal of the auxiliary would generate the optically active product, **14**.

Two stereochemical outcomes of stereoselective alkylation by SRS are possible: inversion and retention of the configuration of **15** at α -carbon (Scheme 4). These outcomes are controlled, first during

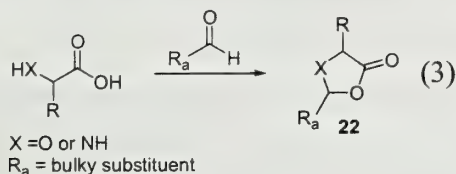
Scheme 4



the formation of the heterocycles **16** and **17** and then by the addition of the electrophile. The cyclization of **15** could result in heterocycle formation with R_a either trans or cis to R. The alkylation of each heterocycle could then result in two diastereomers: an isomer resulting from anti addition of electrophile to produce **18** and **21** and the other from syn addition of electrophile to provide **19** and **20**. By achieving selectivity in these two steps, the final alkylation product of the desired configuration at α -carbon could

be obtained. Thus, two different stereochemical outcomes of the substrate can be accessed via four possible pathways (Scheme 4).

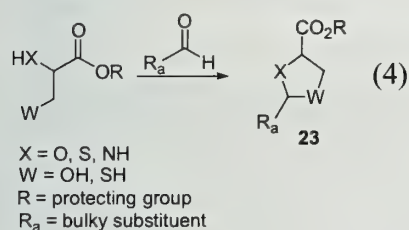
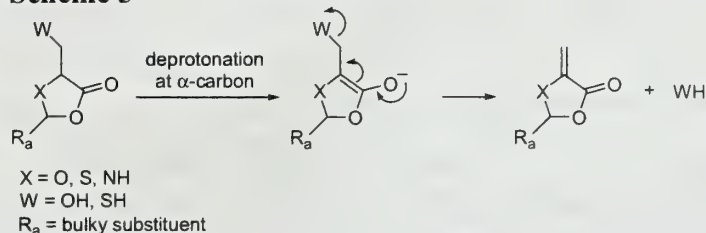
Formation and Stereocontrol over Heterocyclic Intermediates



aldehyde with the α -heteroatom functionality and the carboxylate oxygen of the substrate (eq 3).⁴ The use of such a class of heterocycles is not applicable for compounds substituted

There are two types of heterocycles utilized in SRS: one with an endocyclic carbonyl functionality **22** (eq 3) and the other with an exocyclic carbonyl functionality **23** (eq 4). Heterocycle **22** is produced by condensation of a bulky

Scheme 5

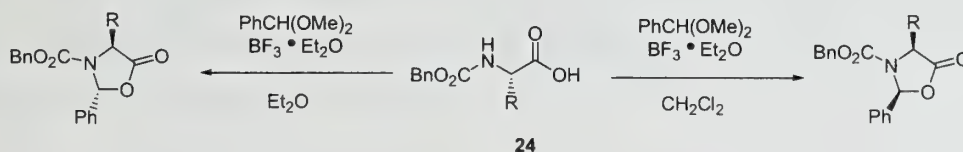


α -heteroatom of the chiral substrate.

The formation of heterocycles results in diastereomeric mixtures of cis and trans-isomers with diastereoselectivities ranging from 20 to 98%, depending on the substituents on the α -carbon.¹⁷ The formation of oxazolidinones, dioxolanones, oxazolidines and dioxolanes takes place with the cis diastereomer as the major product while the formation of imidazolidinones generally results in the trans diastereomer as the major product. The diastereomers are readily separated by recrystallization or chromatography.

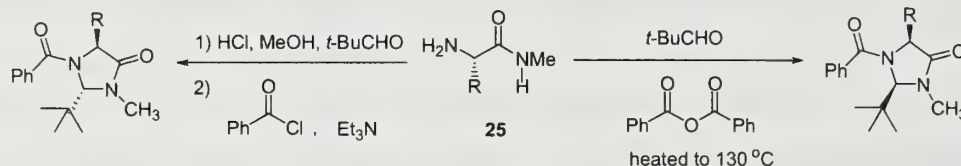
The ability to stereoselectively access either cis or trans heterocycles regardless of the class of heterocycles formed would ultimately improve the scope and generality of SRS. O'Donnell and coworkers have investigated the cyclization of *N*-Cbz protected amino acids such as **24** in order to achieve this goal (Scheme 6).¹⁸ Each diastereomer can be selectively obtained as the major product

Scheme 6



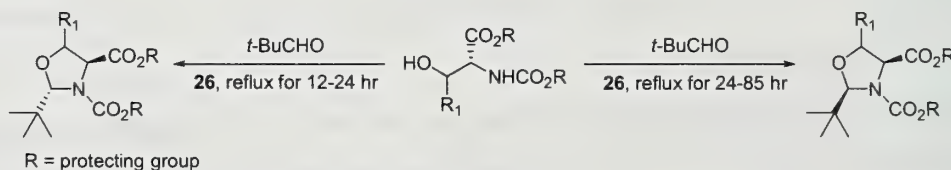
through the use of $\text{BF}_3 \cdot \text{Et}_2\text{O}$ with different solvents. The use of Et_2O as solvent results in the trans oxazolidinone while the use of CH_2Cl_2 yields cis oxazolidinone. Seebach and coworkers have also found that diastereomeric formation of imidazolidinones from *N*-methyamides such as **25** could be achieved by altering the reaction conditions (Scheme 7).¹⁹ Under acidic conditions, the trans isomer is favored while under acylating conditions the cis isomer is formed as the major product. The ability to

Scheme 7



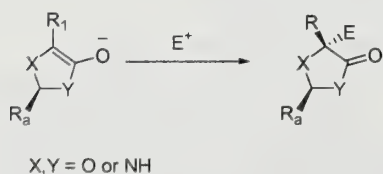
access both diastereomers of heterocycles with an exocyclic carbonyl functionality can be achieved by employing a Rh^{III} catalyst **26**.²⁰ Cyclizations of α -amino- β -hydroxy-carboxylates with pivaldehyde initially lead to trans-oxazolidines as the major products with 62-98% de. However, the more thermodynamically stable cis-oxazolidine isomer, can be obtained as the major product with 50-60% de for some substrates by allowing the reaction to go on 2-6 times longer than required to obtain trans-heterocycles (Scheme 8).

Scheme 8



Stereoselective Alkylation

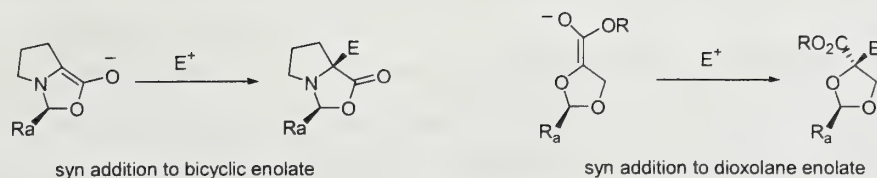
The treatment of the heterocycle with bases such as lithium diisopropylamide (LDA) effects formation of the enolate. With most enolates, electrophiles approach anti to R_a with high



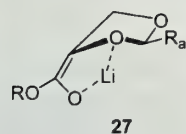
diastereoselectivity (eq 5).⁴ Alkylations of the enolates of proline derived bicyclic heterocycles and dioxolane carboxylates, however, lead to electrophilic addition on the same face as R_a with selectivities ranging from 60 to 95% de (Scheme 9).^{16,17}

The driving force for the syn electrophilic addition observed with the bicyclic enolate is proposed to be the placement of electrophile in a thermodynamically more stable exo position after the addition. It has been proposed that a lithium chelated complex such as **27** leads to electrophilic addition on the same face as R_a for dioxolane enolates. In this complex, the chelation of lithium with the

Scheme 9

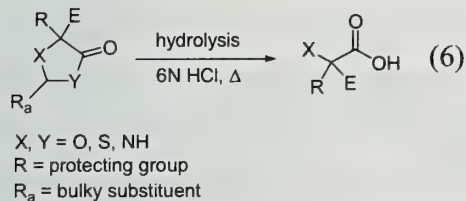


carbonyl oxygen and the endocyclic oxygen attached to α -carbon causes a puckering of the ring. Due to such a puckering of the ring, the face opposite to the acetal substituent becomes a concave face, rendering the side anti to R_a less accessible. In addition, it was proposed that the alkyl group on the enolate ester blocks the face opposite to the acetal substituent, thus, preventing the approach of electrophiles to the *re* face.



Hydrolysis of Heterocyclic Intermediates – a Limitation of SRS

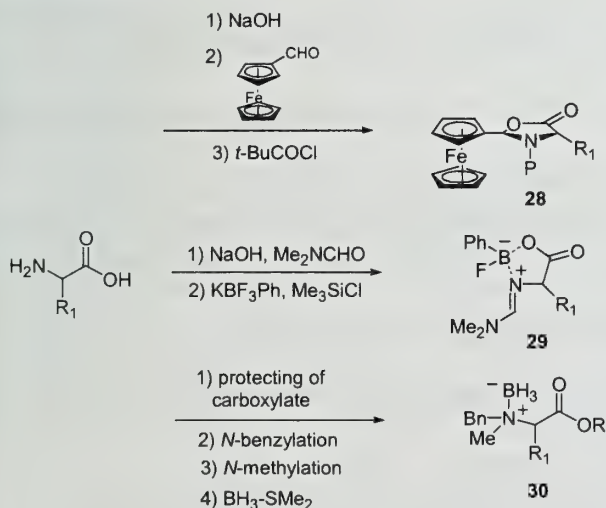
Alkylation of the heterocycles utilized in SRS is highly diastereoselective. This high stereoselectivity makes such a transformation via these heterocycles very attractive. However, some applications of SRS have proven not to be practical, due to the harsh acidic condition required to obtain the free amino acid or the carboxylic acid derivative (eq 6). Generally, hydrolysis of these heterocycles is possible only with a strong acid and at elevated temperatures.¹² Incompatibility of such reaction conditions with many functional groups clearly show the limitation of SRS with the heterocycles discussed above.



applications of SRS have proven not to be practical, due to the harsh acidic condition required to obtain the free amino acid or the carboxylic acid derivative (eq 6). Generally, hydrolysis of these heterocycles is possible only with a strong acid and at elevated temperatures.¹² Incompatibility of such reaction

In search of alternatives to render the principle of SRS more versatile, use of auxiliaries other than the classical organic aldehydes to derivatize the substrate such as ferrocenyl oxazolidinones (28),

Scheme 10



oxazaborolidinones (29), and borane-amine adducts (30), have been investigated (Scheme 10).²¹⁻²³ Alkylation of **28**, **29** and **30** resulted in the formation of the products with good diastereoselectivities ranging from 92-98% de, 60-98% de, and 36-82% de respectively. The removal of the auxiliaries from these derivatives can be achieved under much milder conditions than those required for the heterocyclic intermediates. Hydrolysis of **28** was achieved under acidic conditions with Amberlyst-15. Boron decomplexation from **29** was easily achieved with ethylene diamine in refluxing methanol. Finally, borane-amine adducts **30** were transformed into free amino acid derivatives by treatment with aqueous NH₄Cl.

CONCLUSION

Asymmetric induction can be achieved without the use of classical chiral additives through the use of memory of chirality and self-regeneration of stereogenic centers (SRS). Given the limited number of examples, memory of chirality has yet to be developed for utilization in general synthesis. The foundational work of developing general methods for wide range of applications is ongoing. However, when the development of such methods is realized, they will provide powerful and efficient means for asymmetric induction. The currently more useful concept of SRS is also not without limitations. Difficulty in auxiliary removal and low stereocontrol with the heterocyclic derivatives are yet to be resolved. However, the efficiency of the concept has been proven by numerous examples of synthetic applications.¹²⁻¹⁴

REFERENCES

- 1) Seyden-Penne, J. *Chiral Auxiliaries and Ligands in Asymmetric Synthesis*; Wiley & Sons: New York, 1995.
- 2) Proctor, G. *Asymmetric Synthesis*; Oxford University Press: New York, 1996.
- 3) Fuji, K.; Kawabata, T. *Chem. Eur. J.* **1998**, *4*, 373.
- 4) Seebach, D.; Sting, A. R.; Hoffmann, M. *Angew. Chem., Int. Ed. Engl.* **1996**, *35*, 2709.
- 5) Seebach, D.; Wasmuth, D. *Angew. Chem., Int. Ed. Engl.* **1981**, *20*, 971.
- 6) Kawabata, T.; Yahiro, K.; Fuji, K. *J. Am. Chem. Soc.* **1991**, *113*, 9695.
- 7) Beagley, B.; Betts, M. J.; Pritchard, R. G.; Schofield, A.; Stoodley, R. J.; Vohra, S. *J. Chem. Soc. Perkin Trans. 1* **1993**, 1761.
- 8) Kawabata, T.; Wirth, T.; Yahiro, K.; Suzuki, H.; Fuji, K. *J. Am. Chem. Soc.* **1994**, *116*, 10809.
- 9) Fráter, G.; Müller, U.; Günther, W. *Tetrahedron Lett.* **1981**, 22.
- 10) Seebach, D.; Naef, R. *Helv. Chim. Acta* **1981**, *64*, 2704.
- 11) Catuviela, C.; Díaz-de-Villegas *Tetrahedron: Asymmetry* **1998**, *9*, 3517.
- 12) Ma, D.; Tian, H. *Tetrahedron: Asymmetry* **1996**, *7*, 1567.
- 13) Corey, E. J.; Reichard, G. A. *J. Am. Chem. Soc.* **1992**, *114*, 10677.
- 14) Sunazuka, T.; Nagamitsu, T.; Matsuzaki, K.; Tanaka, H.; Omura, S. *J. Am. Chem. Soc.* **1993**, *115*, 5302.
- 15) Seebach, D.; Boes, M.; Naef, R.; Schweizer, W. B. *J. Am. Chem. Soc.* **1983**, *105*, 5391.
- 16) Seebach, D.; Coquoz, M. *Chimia* **1985**, *39*, 20.
- 17) Seebach, D.; Lamatsch, B.; Amstutz, R.; Beck, A. K.; Dobler, M.; Egli, M.; Fitzi, R.; Gautschi, M.; Herrandon, B.; Hidber, P. C.; Irwin, J. J.; Locher, R.; Maestro, M.; Maetzke, T.; Mourino, A.; Pfammater, E.; Plattner, D. A.; Schickli, C.; Schewizer, W. B.; Seiler, P.; Stucky, G. *Helv. Chim. Acta* **1992**, *75*, 913.
- 18) O'Donnell, M. J.; Fang, Z.; Ma, X.; Huffmann, J. C. *Heterocycles* **1997**, *46*, 617.
- 19) Naef, R.; Seebach, D. *Helv. Chim. Acta* **1985**, *68*, 135.
- 20) Seebach, D.; Sommerfeld, T. L.; Jiang, Q.; Venanzi, L. M. *Helv. Chim. Acta* **1994**, *77*, 1313.
- 21) Alonso, F.; Davies, S. G. *Tetrahedron: Asymmetry* **1995**, *6*, 353.
- 22) Vedejs, E.; Fields, S. C.; Schrimpf, M. R. *J. Am. Chem. Soc.* **1993**, *115*, 11612.
- 23) Ferey, V.; Toupet, L.; Le Gall, T.; Mioskowski, C. *Angew. Chem., Int. Ed. Engl.* **1996**, *35*, 430.

CATALYTIC ANTIBODIES: RECENT ADVANCES IN C-C BOND FORMATIONS

Reported by Laura G. Schultz

March 4, 1999

INTRODUCTION

There has been much interest recently in developing enzyme mimics that can tolerate harsher conditions, have broader substrate specificity, and catalyze non-enzymatic, even disfavored reactions. One such mimic is the catalytic antibody. Catalytic antibodies have been proposed to increase the reaction rate by stabilizing the transition state using complementary interactions.¹

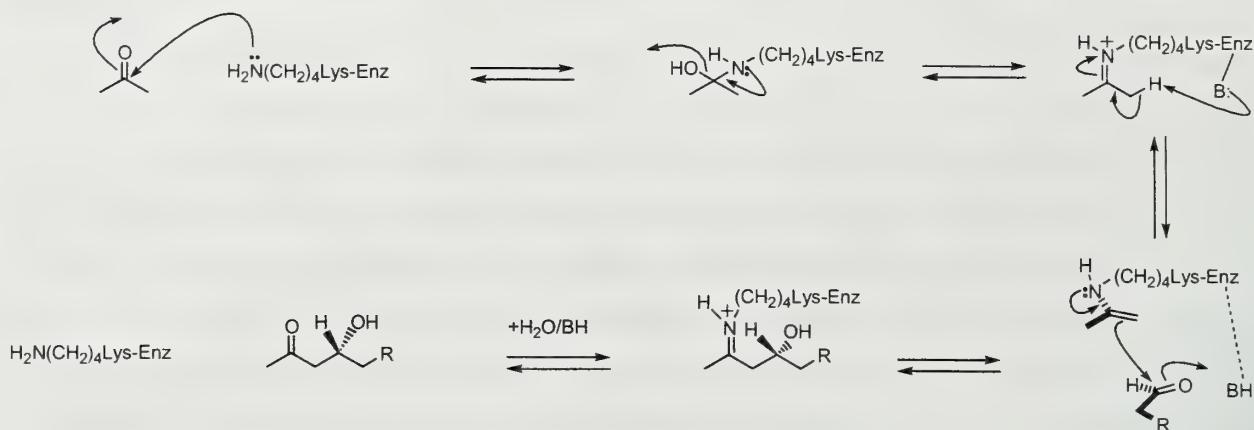
There are two major approaches for producing catalytic antibodies – reactive immunization and transition state hapten design.^{2,3} In the more traditional approach, the hapten, the organic molecule which will bind to the antibody, consists of a stable transition state analog which serves as a template for antibody production.² One problem of this approach involves the similarity of the hapten to either the substrate or the product. Product inhibition can occur if the analog resembles the product too closely; likewise, catalysis will not occur if the antibody binds the substrate too tightly. Reactive immunization uses a moderately reactive hapten to trap a transition state analog in the binding site of the antibody as antibody production occurs. In this strategy, the antibody actually participates in the reaction mechanism.³ It is difficult to generate a substrate molecule of the correct reactivity. Either the substrate will be so reactive that product forms prior to antibody binding or product will not form until after antibody production. Both hapten design approaches require monoclonal hybridoma technology developed by Kohler and Milstein, allowing the selection of monoclonal antibodies.⁴

Numerous transformations, from hydrolysis reactions to rearrangements, have been catalyzed by antibodies elicited using both immunization techniques. Perhaps the most synthetically useful reactions involve formation of carbon-carbon bonds. This review will highlight recent advances in the catalysis of aldol condensations and Diels-Alder reactions by antibodies.

ALDOL AND RELATED REACTIONS

The aldol reaction involves the coupling of enolate donors with aldehyde or ketone acceptors to produce β -hydroxycarbonyl compounds or their subsequent elimination products. Type I aldolases catalyze this reaction using an enamine mechanism depicted in Scheme 1.⁵ An active site lysine residue attacks the carbonyl producing a carbinolamine which dehydrates to the iminium ion. The iminium ion then is transformed to the more stable enamine which adds to the aldehyde or ketone. Product release

Scheme 1

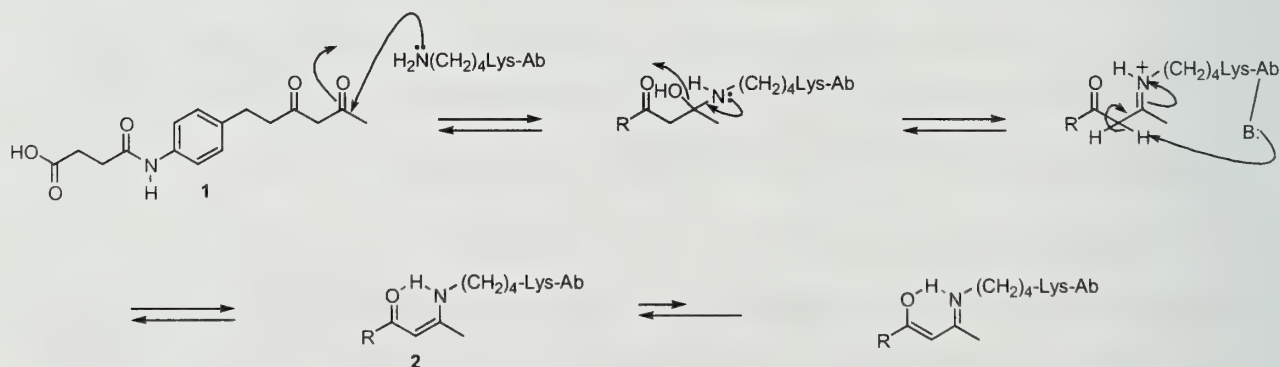


occurs after hydrolysis of the resulting iminium ion. Aldolases use either dihydroxyacetone phosphate, pyruvate, acetaldehyde, or glycine derivatives as donors.⁶ Thus, the potential exists for catalysts with broader substrate specificity. The application of catalytic antibodies to aldol and related reactions is discussed below.

Lerner's and Barbas' Catalytic Antibodies As Enamine Mimics

Lerner, Barbas, and co-workers used reactive immunization to produce antibodies with high catalytic activity for the aldol reaction.^{5,7-8} They designed a diketone hapten **1** which could be trapped in the antibody binding site as the stable enamine **2** depicted in Scheme 2.⁵ Two catalytic antibodies with

Scheme 2

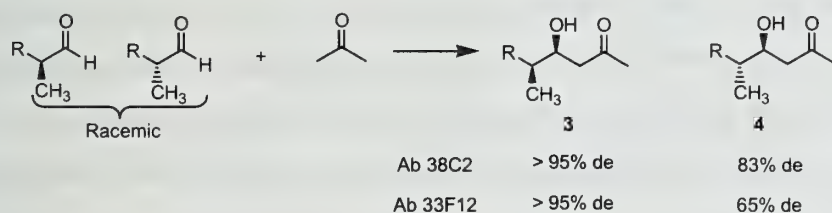


aldolase activity, 38C2 and 33F12, were isolated with broad substrate specificity. A variety of functionalized and nonfunctionalized aliphatic open chain and cyclic ketones could be used as donors in cross aldol reactions; in general, acceptors were limited to hydrophobic compounds.⁵ Self-aldol reactions and Baldwin-favored intramolecular condensations also were catalyzed by these antibodies.⁸ The kinetics of antibody catalysis were examined using Michaelis-Menten analysis. The values of k_{cat}

ranged from $3.0 \times 10^{-4} \text{ min}^{-1}$ to 5.0 min^{-1} , corresponding to rate enhancements of $10^6 - 10^9$ over the uncatalyzed reaction; K_m values ranged from 17 to 125 μM , indicating varied degrees of substrate affinity. Mechanistic studies suggest that antibody catalysis uses the enamine mechanism.⁵ For example, absorption at 316 nm indicates formation of the stable enamine **2** by the hapten. A crystal structure of the antigen binding fragment of the antibody revealed a lysine residue at the base of the hydrophobic binding pocket.⁷ Addition of acetone and sodium borohydride to the antibody resulted in loss of catalysis.⁵ The authors hypothesize that reduction of the imine of acetone traps the lysine as isopropylamine, preventing further activity. Furthermore, the antibody showed a pH optimum for enamine formation between pH 6.0 and 7.0. Since the pK_a of lysine is 10.5, it should be protonated and non-nucleophilic within the optimal pH range. The authors suggest that the lysine pK_a is reduced due to its hydrophobic environment, since the binding pocket is lined with several hydrophobic amino acid residues, including valine, leucine, isoleucine, and tryptophan.

The next goal of Lerner, Barbas, and co-workers was to determine whether the antibody could control the stereochemical outcome of the reaction.⁵ The reaction of α -methyl-substituted aldehydes with acetone, depicted in Scheme 3, produced the corresponding (4*S*)-hydroxyketones **3** and **4** with diastereoselectivities ranging from 65% to 95%. The acetone enamine added to the *si* face of the aldehyde, providing both Felkin-Anh (**3**) and anti-Felkin-Anh (**4**) products.⁵ Subsequent investigation

Scheme 3



revealed that hydroxyacetone showed reversed selectivity, adding to the *re* face of the aldehyde or ketone. Both *si* and *re* face addition occurred with high enantioselectivities for a variety of substrates, with up to 99% ee. The enantioselectivity was improved for acceptors with sterically hindered or unsaturated substituents. Lerner's and Barbas' aldolase antibodies also catalyzed the retro-aldol reaction with a K_m value of approximately 270 μM and k_{cat} of 1.4 min^{-1} .⁹ Kinetic resolution of aldol products resulted in compounds with high enantioselectivities, above 90% ee in most cases. The ability to achieve high enantioselectivities with these catalytic antibodies motivated Lerner, Barbas, and co-workers to apply this catalyst to natural product syntheses. Epothilone is a cytotoxic compound with anti-cancer activity.¹⁰ Three stereocenters of epothilone and brevicomin¹¹ (Figure 1), a pheromone of

the bark beetle, were resolved kinetically in precursor fragments using antibody 38C2 resulting in high enantioselectivity of the product. Lerner, Barbas, and co-workers also applied the catalytic antibodies to

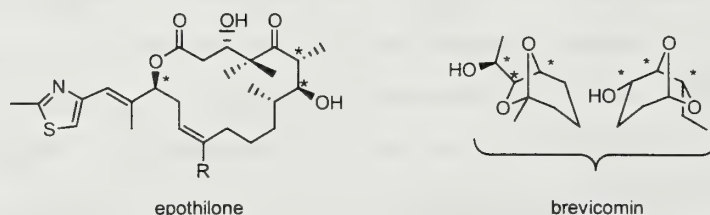


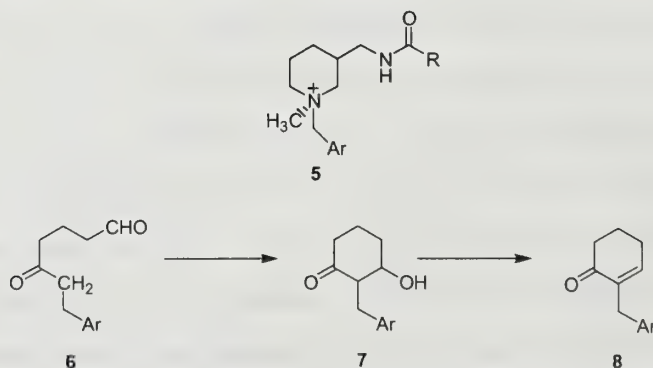
Figure 1 Structures of Epothilone and Brevicomins

other reactions that may involve enamine mechanisms, including β -keto acid decarboxylation¹² and the Robinson annulation.¹³ Both reactions resulted in large rate enhancements with high enantioselectivity obtained in the Robinson annulation.

Reymond's Catalytic Antibodies as Both Enolate and Enamine Mimics

Type II aldolases use enolate donors instead of enamine donors.⁶ A catalytic histidine residue accelerates enolate formation by removing a proton from the donor α -carbon. A zinc (II) cofactor helps stabilize the enolate donor-acceptor complex. Using the more traditional immunization approach, Reymond, Koch, and Lerner hoped to stimulate the production of a general base in the antibody active site using positively charged hapten **5**. The binding site is usually complementary in charge distribution to the hapten and, thus, a positively charged hapten was believed to be stabilized by a negatively charged amino acid residue in the antibody binding site. Antibody deprotonation of the donor α -hydrogen by this negatively charged residue would catalyze the intramolecular aldol reaction of **6** to yield product **7** or **8**, as depicted in Scheme 4.¹⁴ Previous work by Hilvert and co-workers demonstrated

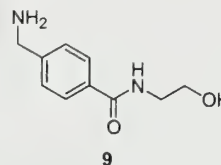
Scheme 4



this concept.¹⁵ Ultimately, both enolate formation and subsequent elimination were catalyzed by antibody 78H6, yielding product **8** with k_{cat} equal to $2.4 \times 10^{-6} \text{ min}^{-1}$. No stereochemical control was

observed during the aldol addition; however, trans elimination of only the (2*S*, 3*S*) diastereomer occurred.

Many enzymes use co-factors to aid in the catalytic mechanism of a reaction. Reymond and co-workers discovered that amine co-factor **9** and antibody 72D4, elicited using hapten **5**, catalyzed intermolecular aldol additions of acetone to aldehydes with maximal rate accelerations of 950-fold.¹⁶ The authors hypothesize that the amine co-



factor serves the same catalytic role as the lysine residue in both natural aldolases and Lerner's catalytic antibodies (*vide infra*).¹⁷ Formation of an antibody-amine complex places the substrate in a hydrophobic, structured environment. The values of k_{cat} ranged from 1.6×10^{-6} to $1.2 \times 10^{-5} \text{ s}^{-1}$ with variations in K_m from 0.73 to 4.9 mM. Antibody 72D4 catalyzed the addition of acetone to the *si* face of the aldehyde forming the (4*S*)-hydroxyketones with diastereoselectivities of 65% – 95%. Reymond and co-workers then examined the catalysis of retro-aldol reactions, which also exhibited stereochemical control by the antibody/amine complex.¹⁸ *S*-Hydroxyketones underwent retro-aldol reactions while *R*-hydroxyketones readily eliminated to form α,β -unsaturated ketones. Reymond hypothesizes that anti-elimination of the *R*-hydroxyketone occurs due to a favorable conformation.

DIELS-ALDER REACTIONS

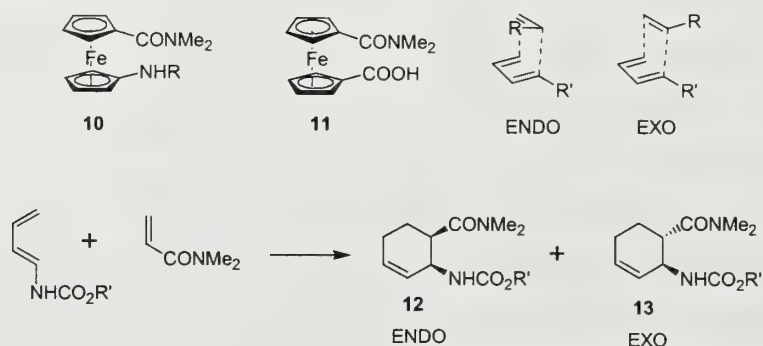
The Diels-Alder reaction involves a very high entropic cost, since two substrate molecules must align with the correct orbital overlap for the reaction to occur.¹⁹ The goal of a catalyst will be to pre-organize the substrates and stabilize the transition state, counteracting the energy cost. Several major research groups have developed antibody catalysts for the Diels-Alder reaction, as described below.

Janda's Diels-Alder Catalytic Antibodies

In order to create a highly organized, specific binding pocket within the antibody, traditional hapten design has emphasized rigid structures with defined stereochemistry. Janda's approach was counter- intuitive, using ferrocene hapten **10**.¹⁹ The two aromatic rings of ferrocene were envisioned to mimic the exo and endo orbital overlap of diene/dienophile as depicted in Scheme 5. Two antibodies, 13G5 and 4D5, were isolated showing vastly different stereochemical control. Antibody 13G5 catalyzed the exo pathway yielding **13** with greater than 98% de and 95% ee. However, antibody 4D5 yielded the endo product **12** with the same diastereoselectivity and enantioselectivity. The crystal structure of antibody 13G5 with inhibitor **11** was recently solved showing the formation of three important antibody-inhibitor hydrogen bonds: tyrosine-carbonyl amide, aspartate-carboxylic acid, and

asparagine-carboxylic acid. These interactions correctly orient the diene and dienophile but result in only moderate catalysis rates.²⁰

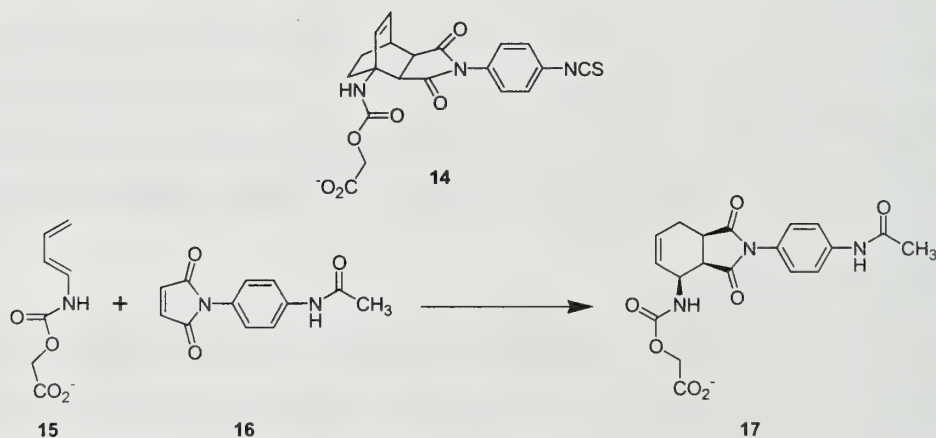
Scheme 5



Schultz's Diels-Alder Catalytic Antibodies

Schultz and co-workers adhered to the more traditional, rigid hapten design for antibody production. Their goal was to pre-organize the substrates into reactive conformations to control both rate and stereochemistry. Schultz focused on the reaction of diene **15** with a substituted maleimide dienophile **16**.²¹ Bicyclic hapten **14** was designed to constrain the orientation of the substrates into a boat conformation, as depicted in Scheme 6. Antibody catalysis did yield formation of **17**. Pseudo-first

Scheme 6

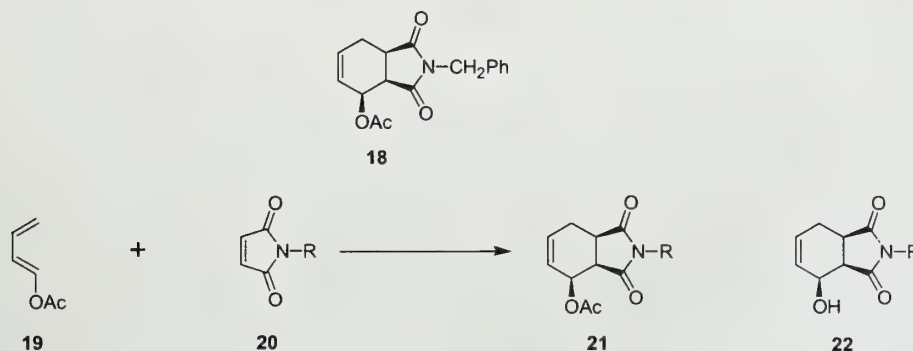


order kinetics revealed a K_m of 1130 μM for diene **15** and 740 μM for dienophile **16**. X-ray crystallography of the antibody-hapten complex indicates that the hapten resides in a deep, hydrophobic binding pocket.²² π - π Interactions between a tryptophan residue and the succinimide carbonyl moieties and specific hydrogen bonds to asparagine and water determine substrate orientation and, thus, product stereochemistry.

Suckling's Diels-Alder Catalytic Antibodies

Suckling and co-workers also studied the reaction of substituted butadiene with maleimide derivatives, shown in Scheme 7.²³ Despite the similarity of hapten **18** and product **21**, no product inhibition was observed. In fact, H11 showed catalytic proficiency with rate enhancements of 1700-

Scheme 7



fold. However, alcohol **22** was isolated instead of acetate ester **21**.²⁴ Crotonaldehyde was an observed side product formed by antibody-catalyzed hydrolysis of **19** with rate enhancements of 7000-fold. Although the antibody catalyzes the slow hydrolysis of **21**, Suckling and co-workers believe that the acetate ester is not formed during the cycloaddition. The authors postulate that the antibody-catalyzed cycloaddition of the crotonaldehyde enol to **20** occurs. In the absence of antibody, the crotonaldehyde tautomerization of enol to aldehyde is complete within two minutes, indicating that the cycloaddition in solution probably does not occur. The authors speculate that the enol must exist within the active site, consistent with the failure to trap the enol.

CONCLUSION

There has been much debate regarding whether catalytic antibodies are truly specific catalysts with controlled binding site geometry. In 1996, Kirby and co-workers were able to catalyze the eliminative ring-opening of benzisoxazole using bovine serum albumin (BSA), an "off the shelf protein."²⁵ The same rate enhancement observed with Kirby's protein had been seen previously using a catalytic antibody. A lysine residue of BSA and a carboxylate of the catalytic antibody served as general bases promoting deprotonation and subsequent elimination. Both merely provided hydrophobic environments for the reaction. This questions the importance of catalytic antibodies as potential catalysts. In the catalysis of the aldol reaction and the Diels-Alder reactions, catalytic antibodies certainly have caused rate enhancements and defined stereochemistry; control experiments with "off the shelf proteins" show no rate enhancements. Catalysts which can control both the stereochemistry and

rate of chemical reactions would be advantageous. Whether catalytic antibodies can perform these functions with the efficiencies of enzymes still remains to be seen. There are still many problems with scalability, substrate specificity, and expense.

REFERENCES:

- 1) Brady, P.A.; Sanders, J.K.M. *Chem. Soc. Rev.* **1997**, 26, 327 – 336.
- 2) Kirby, A.J. *Angew. Chem., Int. Ed. Engl.* **1996**, 35, 707 – 724.
- 3) Wirshling, P.; Ashley, J.A.; Lo, C.-H. L.; Janda, K.D.; Lerner, R.A. *Science* **1995**, 270, 1775 – 1782.
- 4) Rott, I. *Essential Immunology*; Blackwell Scientific: London, 1994, pp 120 – 127.
- 5) Lerner, R.A.; Barbas, C.F., III. *Acta. Chem. Scand.* **1996**, 50, 672 – 678.
Wagner, J.; Lerner, R.A.; Barbas, C.F., III. *Science* **1995**, 270, 1797 – 1800.
- 6) Faber, K. *Biotransformations in Organic Chemistry*, Springer: New York, **1997**, 243 – 258.
- 7) Barbas, C.F., III.; Heine, A.; Zhong, G.; Hoffmann, T.; Gramatikova, S.; Björnstedt, R.; List, B.; Anderson, J.; Stura, E.A.; Wilson, I.A.; Lerner, R.A. *Science* **1997**, 278, 2085 – 2092.
- 8) Hoffmann, T. Zhong, G.; List, B.; Shabat, D.; Anderson, J.; Gramatikova, S.; Lerner, R.A.; Barbas, C.F., III. *J. Am. Chem. Soc.* **1998**, 120, 2768 – 2779.
- 9) Zhong, G.; Shabat, D.; List, B.; Anderson, J.; Sinha, S.C.; Lerner, R.A.; Barbas, C.F., III. *Angew. Chem. Int. Ed. Engl.* **1998**, 37, 2481 – 2484.
- 10) Sinha, S.C.; Barbas, C.F., III; Lerner, R.A. *Proc. Natl. Acad. Sci. U.S.A.* **1998**, 95, 14603 – 14607.
- 11) List, B.; Shabat, D.; Barbas, C.F., III; Lerner, R.A. *Chem. Eur. J.* **1998**, 4, 881 – 885.
- 12) Björnstedt, R.; Zhong, G.; Lerner, R.A.; Barbas, C.F., III. *J. Am. Chem. Soc.* **1996**, 118, 11720 – 11724.
- 13) Zhong, G.; Hoffmann, T.; Lerner, R.A.; Danishefsky, S.; Barbas, C.F., III. *J. Am. Chem. Soc.* **1997**, 119, 8131 – 8132.
- 14) Koch, T.; Reymond, J.-L.; Lerner, R.A. *J. Am. Chem. Soc.* **1995**, 117, 9383 – 9387.
Reymond, J.-L. *J. Mol. Cat. B: Enz.* **1998**, 5, 331 – 337.
- 15) Thorn, S.N.; Daniels, R.G.; Auditor, M.-T.M.; Hilvert, D. *Nature* **1995**, 373, 228 – 230.
- 16) Reymond, J.-L.; Chen, Y. *Tetrahedron Lett.* **1995**, 36, 2575 – 2578.
- 17) Reymond, J.-L.; Chen, Y. *J. Org. Chem.* **1995**, 60, 6970 – 6979.
- 18) Reymond, J.-L. *Angew. Chem., Int. Ed. Engl.* **1995**, 34, 2285 – 2287.
- 19) Yli-Kauhaluoma, J.T.; Ashley, J.A.; Lo, C.-H.; Tucker, L.; Wolfe, M.M.; Janda, K.D. *J. Am. Chem. Soc.* **1995**, 117, 7041 – 7047.
- 20) Heine, A.; Stura, E.A.; Yli-Kauhaluoma, J.T.; Gao, C.; Deng, Q.; Beno, B.R.; Houk, K.N.; Janda, K.D.; Wilson, I.A. *Science* **1998**, 279, 1934 – 1940.
- 21) Braisted, A.C.; Schultz, P.G. *J. Am. Chem. Soc.* **1990**, 112, 7430 – 7431.
- 22) Romesberg, F.E.; Spiller, B.; Schultz, P.G.; Stevens, R.C. *Science* **1998**, 279, 1929 – 1933.
- 23) Suckling, C.J.; Tedford, M.C.; Bence, L.M.; Irvine, J.I.; Stimson, W.H. *J. Chem. Soc., Perkin Trans. I* **1993**, 1925 – 1929.
- 24) Pitt, A.R.; Stimson, W.H.; Suckling, C.J.; Marrero-Tellado, J.J.; Vazzana, C. *Isr. J. Chem.* **1996**, 36, 171 – 175.
- 25) Hollfelder, F.; Kirby, A.J.; Tawfik, D.S. *Nature* **1996**, 383, 60 – 63.

SOFT LITHOGRAPHY: METHODS AND APPLICATIONS FOR ORGANIC SURFACE CHEMISTRY

Reported by Matthew J. Mio

March 8, 1999

INTRODUCTION

There is little doubt that the development of microelectronic technology has led the world into the computer information age. The ability to miniaturize circuitry, processors, and devices has revolutionized the electronics industry by contributing greater portability, a reduction in energy usage, and a myriad of new technological innovations.¹ Microfabrication, the design and construction of microelectronics, is central to this industry. Often overlooked is the *chemistry* used in microfabrication: *patterning* a surface to impart upon it a designed *form*, and in turn, endowing it with a specific *function*. Since its inception in the late 1950s, photolithography has dominated microfabrication as the main technique used to pattern surfaces for microelectronics.^{2,3} Employing chrome masks to introduce patterns and photo-reactive polymers as resists, traditional photolithography has become the standard industrial method for device construction on planar substrates. Sub-micrometer devices and features on surfaces call for comparable wavelengths of light to be used in photolithography, however, the optical diffraction and opacity of lenses and photomasks are limited.¹ With these and other difficulties (e.g. expense, necessity of clean room conditions, inability to pattern curved substrates) in mind, many groups have proposed new complementary techniques for lithography and pattern transfer.

The most active area of research concerning lithographic alternatives has been in the field of soft lithography - "soft" meaning that it does not involve "harsh" UV radiation to effect patterning.^{1,4} In the last five years, soft lithography has achieved high resolution, high fidelity, versatility, and rapidity for patterning surfaces through the use of three basic processes: molding, embossing, and printing. This abstract shall begin with a short summary of five major approaches considered as soft lithographic techniques. The flexibility of these methods will then be illustrated by applications of each in the realm of organic surface chemistry.

MOLDING, EMBOSSING AND PRINTING

General Concepts

The main advantage of soft lithography is its use of the elastomeric polymer poly(dimethylsiloxane) or PDMS, as either mold, embosser, or stamp.¹ This polymeric tool is cast from

a master mold that contains the desired patterned features. PDMS easily conforms to substrates over a large, nonplanar surface area, does not swell in most solvents, shrinks by less than 1% upon curing, is chemically inert, has a low interfacial free energy, and is quite durable. Such benefits display soft lithography's accessibility and economy.

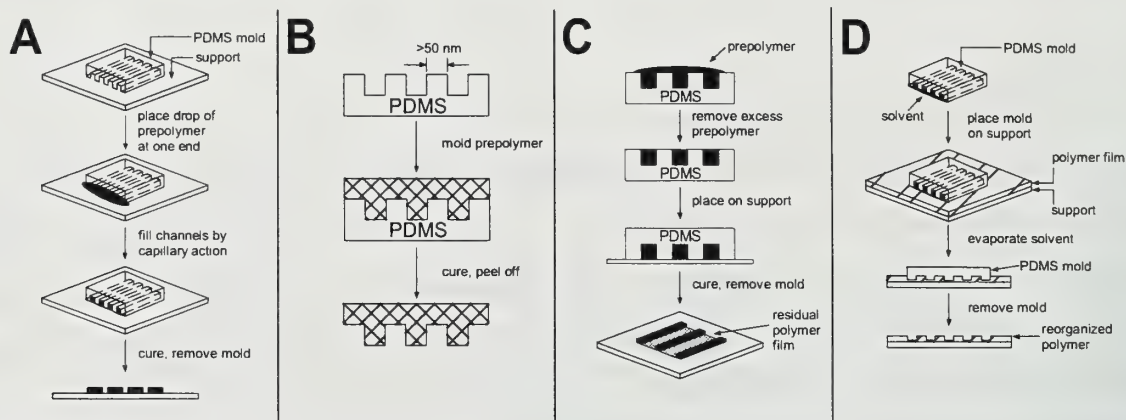


Figure 1. Soft lithographic molding and embossing techniques: A) MIMIC,⁶ B) REM,⁷ C) μ TM,⁷ and D) SAMIM.⁸

Molding

Micromolding in capillaries (MIMIC) was the first technique to employ soft lithographic molding.⁶ In this method, the PDMS master mold is specifically designed to have a continuous network of channels, with holes leading from the outside edge into the pattern (Fig. 1A). The mold is then inverted and placed in contact with a support. By placing a drop of prepolymer (uncrosslinked polymer) at the “entrance” to the pattern, the liquid spontaneously fills the channels by capillary action. After a proper filling time, the prepolymer is either thermally or photochemically cured (crosslinked), and the mold is released. A second technique for soft lithographic molding is replica molding (REM), a method which supports casting of non-planar surfaces (Fig. 1B),⁷ due to mold flexibility. As a result, topologically complex surfaces such as blazed diffraction gratings can be molded. The inability to pattern multi-layer structures with MIMIC or REM led to the development of another technique, microtransfer molding (Fig. 1C).⁸ In μ TM, liquid prepolymer is applied to the PDMS mold as if to cast, but then the excess prepolymer is scraped off, followed by an inversion of the mold and placement onto a substrate. After curing, the mold is removed and the resulting structure is maintained by the substrate. Multi-layered structures can be rendered by repeating the process and reorienting the mold. The soft lithographic procedures detailed above regularly pattern features between 100 μ m to 1 μ m; however, REM has resulted in 200 nm features.⁷

Embossing

Soft lithographic embossing techniques came to the fore with the report of solvent-assisted micromolding (SAMIM).⁹ Much like its predecessors, SAMIM uses a PDMS mold and a polymer as the cast, but in this case, the polymer is pre-spun onto a wafer support (Fig. 1D). Embossing occurs when the patterned PDMS is wetted with a solvent that is known to dissolve the cast polymer. After wetting, the mold is placed face down on the polymer-coated support. The solvent from the mold partially dissolves or swells the spun polymer resist into the negative image of the patterned mold. SAMIM has been shown to cover a broad range of feature sizes between 100 μm and <100 nm.

Printing

The third, most widely used soft lithographic technique is microcontact printing (μCP).⁴ This procedure entails the "printing" of long-chain organic molecules onto a specific surface using PDMS as a "stamp" (Fig. 2). Organic molecules are physisorbed onto the stamp, which in turn delivers the molecules to the surface upon contact via chemisorption. In the first report of this technique, alkanethiols were used as the "ink" and Au was used as the surface to be patterned.¹⁰ Self-assembled monolayers (SAMs) of this type are the most robust and well-understood,¹¹ though there are reports of alkanethiol printing capabilities on Ag¹² and alkylsiloxane printing on SiO₂.¹³ By utilizing thiols with the formula $X-(\text{CH}_2)_n-\text{SH}$, where $11 \leq n \leq 16$, SAM thickness and terminal functionality can be tuned. Microcontact printing can also be used to pattern curved substrates, an impossibility in traditional photolithography.¹⁴ While μCP can only pattern surface features in the 100 μm to $\sim 1 \mu\text{m}$ range, the applications presented below will demonstrate its versatility.¹

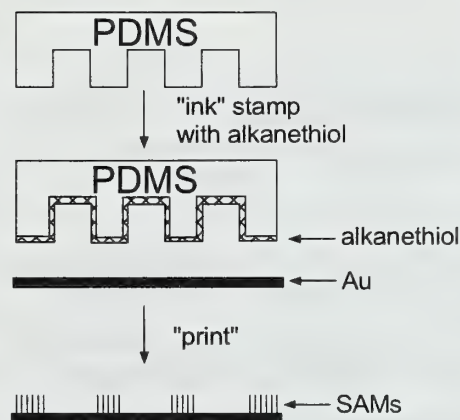


Figure 2. Microcontact printing of SAMs onto a gold substrate.¹⁰

APPLICATIONS OF SOFT LITHOGRAPHY IN ORGANIC SURFACE CHEMISTRY

Functionalizing SAMs

An immediate extension of μCP using SAMs lies in the functionalization of the terminus of the applied organic molecule, thus determining surface chemical properties. The wealth of possible functionality is quite large, but methyl-terminated SAMs have been shown to organize with the fewest

number of defects.¹¹ Such defects have made it difficult in the past to pattern SAMs of different functionalities on the same surface, and have impeded research in surface-anchored reactions. Yet, soft lithographic methods to achieve such surface functionality are straightforward.

An example of extending μ CP for SAM functionalization is pictured in Fig. 3.¹⁵ After printing of mercaptohexadecanoic acid on Au, the patterned substrate was washed with a basic solution of

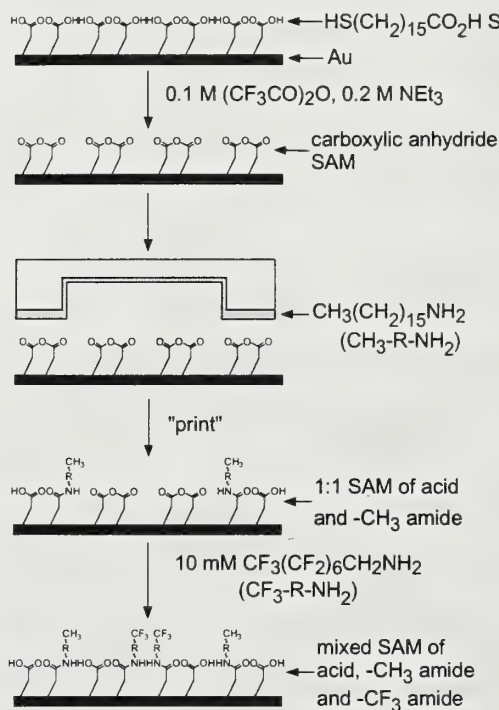
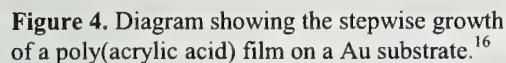


Figure 3. Diagram depicting the patterning of two different N -alkyl amide SAMs using μ CP.¹⁵

comparing patterned surfaces to the thickness and fluorine signal of unpatterned control films. Both methods indicate a high degree of reaction. This example has also been utilized to pattern thiol-terminated SAMs by reacting anhydrides as above with cysteamine ($\text{HSCH}_2\text{CH}_2\text{NH}_2$).

Another example of patterning reactive SAMs, reported by Crooks and coworkers, explored the building of a highly branched polymer superstructure as a stable, covalently-bound thick-film for possible use in chromatography, chemical sensing, or as a resist (Fig. 4).¹⁶ Microcontact printing of hexadecanethiol onto a gold substrate, and subsequent exposure to mercaptoundecanoic acid (MUA) led to a surface patterned with hydrophobic and hydrophilic SAMs. Activation of the acids via a mixed anhydride followed by reaction with α,ω -diamino-terminated poly(*tert*-butylacrylate) yielded a grafted polymer layer. The *tert*-butyl esters were then hydrolyzed with methanesulfonic acid, and the cycle was repeated. To monitor polymer growth, FTIR-external reflectance spectroscopy, ellipsometry, and tapping-mode atomic force microscopy (TM-AFM) measurements were taken after each level of growth.

trifluoroacetic anhydride to generate "paired-chain" anhydrides. The same surface was then printed upon by a PDMS stamp inked with n -hexadecylamine (R^1NH_2). The anhydride groups selectively reacted only over the contact area to generate a 1:1 mixture of acids and amides over the printed area. The remaining anhydride groups in the unpatterned area were then quenched by immersing the substrate in a fluorinated alkyl amine solution (R^2NH_2). Unstamped areas now presented trifluoromethyl groups and acids in a 1:1 ratio. Characterization via scanning electron microscopy (SEM) and secondary ion mass spectrometry (SIMS) showed a high contrast edge resolution between printed and non-printed regions on the order of 100 nm. Ellipsometric and X-ray photoelectron spectroscopy (XPS) data aided in approximating the yield of the reactions by

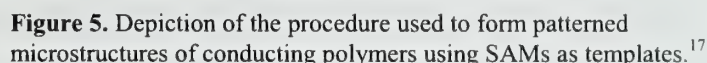


The lack of polymer growth in unpatterned regions was tracked by a constant ellipsometric measurement of 1.8 nm of thickness in the methyl-terminated SAM regions. In comparison, MUA-patterned regions grew linearly to a thickness of 11.2 nm after three cycles. TM-AFM measurements show an edge resolution of approximately 500 nm. These experiments, while primitive, detail the beginnings of the manipulation of μ CP as a SAM functionalization technique.

In another effort to broaden the scope of microcontact printing, noncovalent interactions have been employed. Examples involve the selective deposition of polymers onto a patterned substrate. Development of such methods has lead to selective templating of polymer thin films.

MacDiarmid, Whitesides, and coworkers reported the use of microcontact printing as a method to design a simple liquid crystal display (LCD).¹⁷ Using μ CP, hydroxyl-terminated glass was patterned with octadecylsiloxane SAMs (Fig. 5). Upon placement of the surface in monomer baths of pyrrole or aniline, polymerization occurred faster in adherence to the hydrophobic SAM pattern (as measured by ellipsometry). Because the polymerization on the hydroxylated surface proceeded at a slower rate compared to the hydrophobic surface, conditions for selective polymer deposition were obtained. Due to the conductive nature of these polymers, the conformation of the molecules in the deposited films was investigated to characterize their electronic structure. UV-

Figure 5. Depiction of the procedure used to form patterned microstructures of conducting polymers using SAMs as templates.¹⁷



vis-near-IR spectroscopy of polymers deposited on the hydrophobic SAM showed a characteristic “free-carrier-tail” in the near IR region. This band is characteristic of the mobility of conductive electrons, arising because polymer molecules are in an extended conformation. Polymers deposited in hydrophilic regions showed no such near-IR band, suggesting a more compact conformation. It was reasoned that while SAMs may impart their high level of organization to polymer molecules they are in contact with,

this order may cascade down the polymer chain and fully extend the molecule farther from this interface. In an attempt to support this idea of conductivity, a poly(pyrrole)-patterned surface was coated with polymer dispersed liquid crystals (PDLC) and sandwiched between two glass slides. After affixing Cu wire, application of a current transformed the PDLC matrix near the deposited polymer pattern from opaque to transparent as the electric field oriented the LC dispersion and altered its refractive index. These data demonstrate the flow of current over the hydrophobic SAMs, but not the hydrophilic surface.

Hammond and co-workers have also reported the use of microcontact printing to selectively deposit polymer films.¹⁸ Gold surfaces were first patterned with carboxylic acid-presenting SAMs and

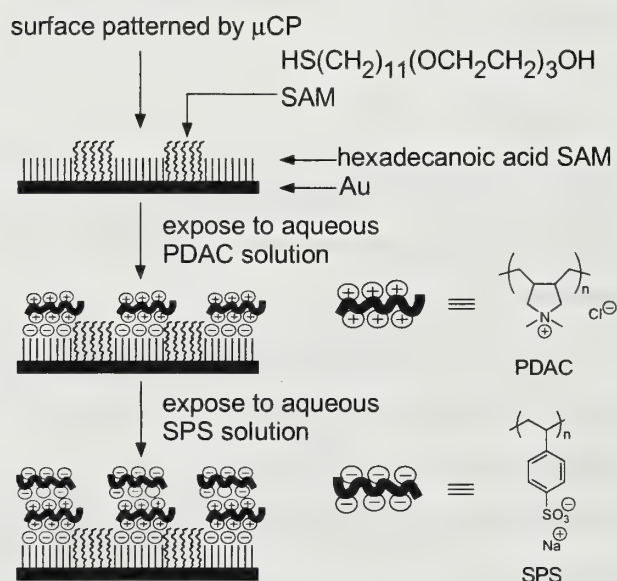


Figure 6. Diagram depicting the selective deposition of polyelectrolytes using SAMs as templates.¹⁸

oligo(ethylene glycol)-functionalized (EG) SAMs via μ CP (Fig. 6). Polymer solutions of poly(diallyl dimethyl ammonium chloride) (PDAC) and sodium poly(styrene sulfonate) (SPS) were then adsorbed onto the substrate. By immersing the substrate in the PDAC solution first, then PDS and repeating this procedure, multilayer electrostatic polymer films were generated. Interestingly, one of the main factors that influenced polymer deposition was the ionic strength (NaCl concentration) of the polymer bath. It was found that at higher salt concentrations,

deposition could be completely reversed onto the EG SAMs. This effect was due in part to

competition between the Na^+ cations and those of the PDAC. Patterned SAMs of this type demonstrate the tunability of μ CP as a method for templated surface adsorption.

3D Microstructures

Microelectromechanical systems (MEMS) have been predicted to be the next great leap in micro- and nano-scale technology in the next century.¹⁹ MEMS are devices which imitate "macro-scale" devices such as gears, switches, and locks. While being orders of magnitude smaller than their visible-world counterparts, MEMS are made of the same types of patterned parts. As a result, microfabrication of such parts becomes of utmost importance.

Soft lithographic methods have been used to order structures on the micrometer and sub-micrometer scale.^{20,21} The level of control and accessibility in such reports may result in more rapid

implementation for future structures. MIMIC has been used in initial experiments to investigate crystalline arrays of poly(styrene) (PS) microspheres. As discussed previously, MIMIC relies on capillary action to draw solutions of prepolymers into PDMS molds for final curing. In these experiments, a 2.5 wt % aqueous latex suspension of PS microspheres was used as the prepolymer. After sufficient time was allowed for capillary action, the PDMS mold was removed to reveal crystalline arrays of microspheres in a hexagonally closest-packed arrangement. A report in 1998 confirmed the use of this microsphere crystallization in generating hierarchically-ordered oxides.²² Samples were not removed from the PDMS mold after MIMIC. Instead, another liquid was allowed to pass through the capillaries - a sol-gel block copolymer and tetraethoxysilane mixture. The resulting structure was then removed from the mold and calcinated in air. The outcome was a highly ordered silica pattern with ordering on the 10, 100, and 1000 nm scale.

In a more classical mechanical motif, microcontact printing in conjunction with electroplating was utilized to produce free-standing three-dimensional metallic microstructures.²³⁻²⁵ These examples truly exhibit μ CP's power to pattern curved or round substrates (Fig. 7). Layers of Ti and Ag were evaporated onto a glass capillary. Once the surface was prepared, the capillary was microcontact printed by rolling it over a PDMS stamp inked with hexadecanethiol. Dipping the capillary into successive wet-etch solutions removed all Ag and Ti not protected by the SAMs. Electroplating with silver was then accomplished by immersion of the substrate into a commercially available plating bath to thicken the protected silver by a few hundred micrometers. The capillary was placed into a concentrated HF bath to dissolve the glass and free the rigid microstructure. This process was used to form stents for potential use in maintaining artery shape after angioplasty,²³ folded tetrahedra,²⁵ and frame cubes measuring 2 mm on a side.²⁴ These examples illustrate the patterning of planar, two-dimensional design ideas into three-dimensional, noncylindrically-symmetrical microstructures. Such technology, with its speed and adaptability may soon find its place in the MEMS industry.

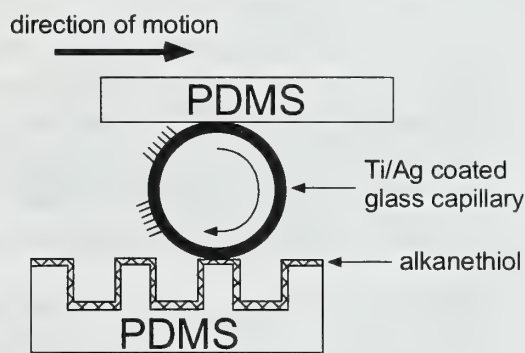


Figure 7. Diagram depicting the use of μ CP to pattern SAMs on round substrates.²⁴

CONCLUSION

The techniques and applications of soft lithography have undergone considerable expansion since their inception in the mid-1990s. Although current technology utilizes photolithography, it is precarious

to believe that its processes will satisfy every need of surface patterning for the next century due to its expense, requirement of clean room conditions, inability to pattern curved substrates, and use of only a limited amount of polymeric photoresists. Soft lithography on the other hand, is an inexpensive, versatile, high resolution, and rapid tool, that complements photolithographic shortcomings in the unfolding field of micro- and nanometer-scale chemistry and technology.

REFERENCES

- (1) Xia, Y.; Whitesides, G. M. *Angew. Chem., Int. Ed. Engl.* **1998**, *37*, 550-575.
- (2) Ito, H. In *Desk Reference of Functional Polymers: Syntheses and Applications*; Arshady, R., Ed.; American Chemical Society: Washington, DC, 1997; pp.311-339.
- (3) Ito, H. In *Desk Reference of Functional Polymers: Syntheses and Applications*; Arshady, R., Ed.; American Chemical Society: Washington, DC, 1997; pp.341-369.
- (4) Zhao, X.-M.; Xia, Y.; Whitesides, G. M. *J. Mater. Chem.* **1997**, *7*, 1069-1074.
- (5) Qin, D.; Xia, Y.; Whitesides, G. M. *Adv. Mater.* **1996**, *8*, 917-919.
- (6) Kim, E.; Xia, Y.; Whitesides, G. M. *Nature* **1995**, *376*, 581-584.
- (7) Xia, Y.; Kim, E.; Zhao, X.-M.; Rogers, J. A.; Prentiss, M.; Whitesides, G. M. *Science* **1996**, *273*, 347-349.
- (8) Zhao, X.-M.; Xia, Y.; Whitesides, G. M. *Adv. Mater.* **1996**, *8*, 837-840.
- (9) Kim, E.; Xia, Y.; Zhao, X.-M.; Whitesides, G. M. *Adv. Mater.* **1997**, *9*, 651-654.
- (10) Kumar, A.; Biebuyck, H. A.; Whitesides, G. M. *Langmuir* **1994**, *10*, 1498-1511.
- (11) Dubois, L. H.; Nuzzo, R. G. *Annu. Rev. Phys. Chem.* **1992**, *43*, 437-463.
- (12) Xia, Y.; Venkateswaran, N.; Qin, D.; Tien, J.; Whitesides, G. M. *Langmuir* **1998**, *14*, 363-371.
- (13) Xia, Y.; Mrkisch, M.; Kim, E.; Whitesides, G. M. *J. Am. Chem. Soc.* **1995**, *117*, 9576-9577.
- (14) Jackman, R. J.; Wilbur, J. L.; Whitesides, G. M. *Science* **1995**, *269*, 664-665.
- (15) Yan, L.; Zhao, X.-M.; Whitesides, G. M. *J. Am. Chem. Soc.* **1998**, *120*, 6179-6180.
- (16) Lackowski, W. M.; Ghosh, P.; Crooks, R. M. *J. Am. Chem. Soc.* **1999**, *121*, 1419-1420.
- (17) Huang, Z.; Wang, P.-C.; MacDiarmid, A. G.; Xia, Y.; Whitesides, G. M. *Langmuir* **1997**, *13*, 6480-6484.
- (18) Clark, S. L.; Montague, M. F.; Hammond, P. T. *Macromolecules* **1997**, *30*, 7237-7244.
- (19) Service, R. F.; Amato, I. *Science* **1998**, *282*, 396-405.
- (20) Kim, E.; Xia, Y.; Whitesides, G. M. *Adv. Mater.* **1996**, *8*, 245-247.
- (21) Kim, E.; Xia, Y.; Whitesides, G. M. *J. Am. Chem. Soc.* **1996**, *118*, 5722-5731.
- (22) Yang, P.; Deng, T.; Zhao, D.; Feng, P.; Pine, D.; Chemlka, B. F.; Whitesides, G. M.; Stucky, G. D. *Science* **1998**, *282*, 2244-2246.
- (23) Rogers, J. A.; Jackman, R. J.; Whitesides, G. M. *Adv. Mater.* **1997**, *9*, 475-477.
- (24) Jackman, R. J.; Brittain, S. T.; Adams, A.; Prentiss, M. G.; Whitesides, G. M. *Science* **1998**, *280*, 2089-2091.
- (25) Jackman, R. J.; Brittain, S. T.; Adams, A.; Wu, H.; Prentiss, M. G.; Whitesides, S.; Whitesides, G. M. *Langmuir* **1999**, *15*, 826-836.

MECHANISTIC ASPECTS OF MONOAMINE OXIDASES

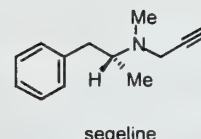
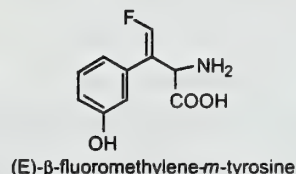
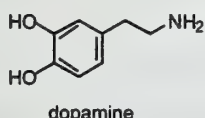
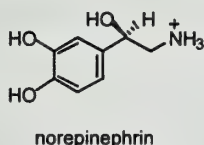
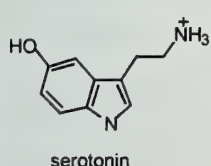
Reported by Kyle Hurth

March 12, 1999

INTRODUCTION

Monoamine Oxidases A and B (MAO A, MAO B) [EC 1.4.3.4] are membrane-bound mitochondrial flavoproteins which catabolize biogenic and xenobiotic amines. These isozymes share 70% homology and may have arisen through chromosomal recombination followed by gene duplication.

¹ MAO A metabolizes the biogenic amines serotonin and norepinephrin; whereas, MAO B is selective for dopamine. This discrimination has led to the development of subtype specific inhibitors such as the MAO A inhibitor prodrug (E)- β -fluoromethylene-*m*-tyrosine, and the MAO B inhibitor segeline (L-deprenyl). These compounds, in combination with aromatic-L-amino acid decarboxylase inhibitors, have proved particularly useful in treating depression and Parkinson's Disease. ^{2,3} A lack of understanding of MAO active site structure and mechanism has hampered the further development of useful compounds such as these. The following discussion will highlight some aspects of the mechanism of the MAO catalyzed oxidation of amines.

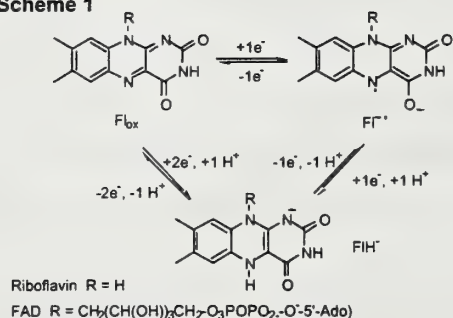


BACKGROUND

Flavin

Scheme 1 depicts the oxidized flavin isoalloxazine ring system (Fl_{ox}) which may undergo reduction by two single-electron transfer (SET) steps, or by one two-electron transfer to produce reduced flavin hydroquinone (FlH^-).⁴ Both MAO A and MAO B require flavin adenine dinucleotide (FAD) to accept electrons from amines during oxidation.⁵ In the form of free oxidized riboflavin, the conjugated isoalloxazine ring system has a reduction potential of -0.25 V. This is very low when compared to the 1.2 V—1.5 V peak oxidation potential for a primary amine in acetonitrile. Nevertheless, oxidation may proceed for several reasons. In the MAO active site, the reduction potential of FAD may be increased by bending the tricyclic ring system towards the bent conformation preferred for FlH^- . This bending reduces antiaromaticity, which may lower the energy of the Fl_{ox} LUMO. Furthermore, active site - substrate interactions may induce strain and distortion in amine bonds. This would raise the energy of the amine substrate, thus facilitating movement along the reaction coordinate and lowering the potential energy

Scheme 1

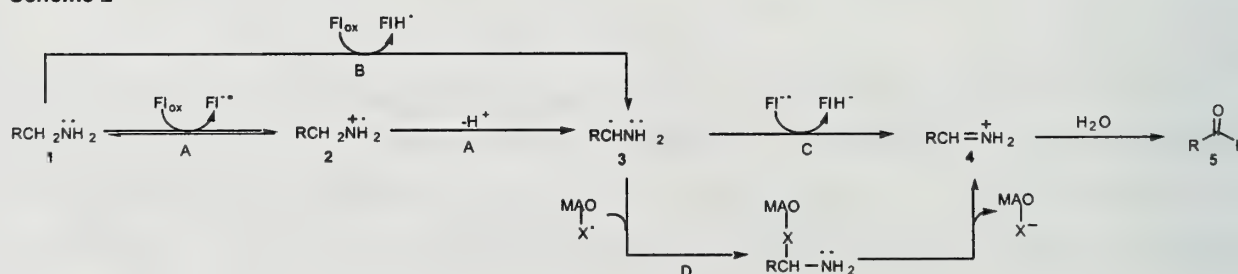


may be overestimated by about 500 mV.⁷

Mechanism

MAO catalyzed oxidation of an amine **1** generates the corresponding imine **4**, which undergoes non-enzymatic hydrolysis to its respective aldehyde **5** (Scheme 2). This reaction is believed to proceed through either a mechanism involving SET to produce an aminium radical cation **2**, followed by hydrogen ion abstraction to produce the α -amino radical **3** (path A), or a mechanism involving hydrogen atom transfer (HAT) from the amine to flavin (path B) producing **3** directly from **1**.⁸ Some authors favor a mechanism involving HAT over SET, because there is no spectroscopic evidence for the existence of reduced flavin semiquinone (Fl $^{\bullet-}$). However, lack of observable Fl $^{\bullet-}$ may be the result of an equilibrium which strongly favors amine **1**, because of the unfavorable potential for oxidation of an amine by flavin. In both of these mechanisms, **3** is produced and may subsequently undergo either a second SET from flavin (path C), or radical recombination with either an active site amino acid radical or a very short-lived Fl $^{\bullet-}$ species (path D). It is postulated that an active site amino acid radical, such as cysteine, could be formed from electron transfer to Fl $^{\bullet-}$.

Scheme 2



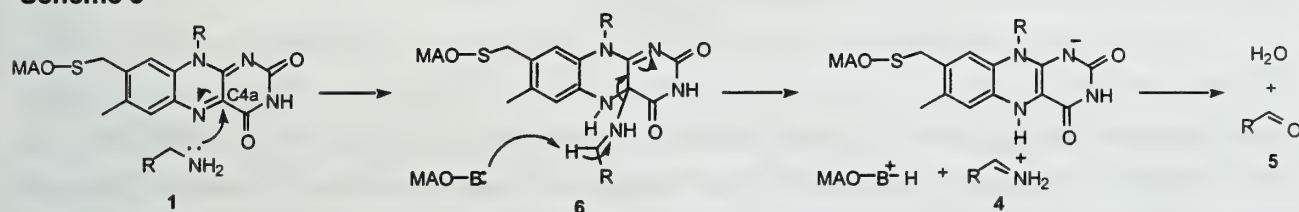
It is of particular interest that studies using rapid-scan stopped flow and magnetic techniques have failed to detect **2**.⁹ These experiments used stopped-flow, with a 1 ms time resolution, combined with external magnetic fields of between 10 and 6500 G. If a SET mechanism is involved, a pair of radical intermediates should form (i.e. **2** and Fl $^{\bullet-}$). When a magnetic field is applied, the rate of singlet to triplet interconversion of the radical ion pair would be altered, effecting enzymatic rates. This

phenomena has been documented for a different enzyme, ethanolamine ammonia lyase, which when placed into a 500 - 1500 G magnetic field experiences a 60% rate decrease.

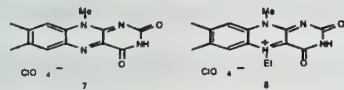
Edmondson and co-workers have made arguments based on competitive (k_H/k_T and k_D/k_T) kinetic isotope effects (KIEs) seen for benzylamine oxidation¹⁰ in support of a HAT mechanism with a late transition state and significant tunneling.¹¹ However, more recently, attenuated KIEs seen for the oxidation of benzyl-1-(aminomethyl)cyclopropane-1-carboxylate in D_2O have been rationalized by a SET mechanism.¹² Thus, KIE studies have proven controversial in determining the mechanism of MAO.

A third proposed mechanism for the MAO catalyzed oxidation of amines involves nucleophilic addition of amine to flavin and has been referred to as a polar mechanism (Scheme 3).¹³ This mechanism begins with direct attack at C4a of the Fl_{ox} isoalloxazine ring by amine **1**, producing the C4a amine-flavin adduct **6**, followed by elimination to yield the corresponding imine **4** and FlH^- . Though this mechanism has been advanced for MAO catalysis of primary and secondary amines, it does not appear to be applicable to MAO catalyzed oxidation of sterically hindered tertiary amines.

Scheme 3



Mariano and co-workers recent observation of C4a-adducts between amines and two model compounds, 3-methylumiflavin perchlorate **7**¹⁴ and 3-methyl-5-ethylumiflavin perchlorate **8**,¹⁵ has reopened debate as to this mechanism's feasibility. It has been suggested that the relatively harsh conditions (H_2O -MeCN, 10 mM HCl, 80 °C, 7 days) required to oxidize benzylamine by **7** are unrepresentative of the enzyme catalyzed reaction.¹⁶ Furthermore, arguments have been made that **8** is strongly predisposed toward nucleophilic addition. Thus, both of these compounds may be inappropriate as models for MAO, as they may be overestimating the plausibility of a polar mechanism.



Regeneration of Flavin

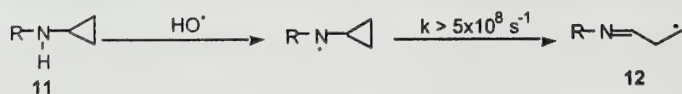
MAO uses O_2 as an electron acceptor, converting O_2 to H_2O_2 , in order to regenerate Fl_{ox} from FlH^- . Regeneration of Fl_{ox} from FlH^- is essential for sustained enzymatic activity (Scheme 4). The mechanism for FlH^- oxidation is believed to proceed through the C4a-hydroperoxide intermediate **10**. Initial SET (path B) is most likely, since molecular oxygen exists in a triplet ground state and would require a spin flip for electrophilic addition (path A). On the other hand SET to generate **9**, followed by radical coupling (path C) could form **10**, which would eliminate to give Fl_{ox} . Alternatively a second SET may directly produce Fl_{ox} (path D).²

The reaction scheme illustrates the proposed mechanism for the formation of the 10-methyl-10H-phenothiazine-11-one derivative. The starting material is 10-methyl-10H-phenothiazine-11-one, which reacts with MAO-B⁺H and O=O. Path A involves the formation of intermediate 10, which then loses H₂O₂ to yield the final product. Path B involves the formation of intermediate 9, which then loses H⁺ to yield the final product.

In spite of the fact that an aminyl radical cation (**2**, Scheme 2) remains undetected, much indirect evidence for its existence has been reported by Silverman and co-workers. This work has utilized cyclopropylamine and cyclobutylamine mechanism-based inhibitors. A mechanism-based inhibitor is an initially inactive compound which is transformed into a species which may divert the normal chemistry of the enzyme and lead to its inactivation.¹⁷ In the following examples, cyclopropylamine and cyclobutylamine ring-opened radical products inactivated MAO through covalent attachment to either flavin or an active site amino acid. In both the cyclopropylamine and cyclobutylamine studies, the lack of an α -proton in these substrates implies that MAO catalyzed oxidation cannot proceed by HAT.

Secondary aminyl radical cations have been observed by flash-photolysis experiments using low temperature EPR, but in work with cyclopropylamine **11**, only ring-opened radical **12** could be detected (Scheme 5).¹⁸ Opening to produce **12** was estimated to proceed at a rate greater than $5 \times 10^8 \text{ s}^{-1}$. Based on these findings, a series of cyclopropylamine-containing mechanism-based inactivators were incubated with MAO in the hopes of generating a reactive primary radical species **12** at a rate which could compete with enzymatic catalysis.¹⁹

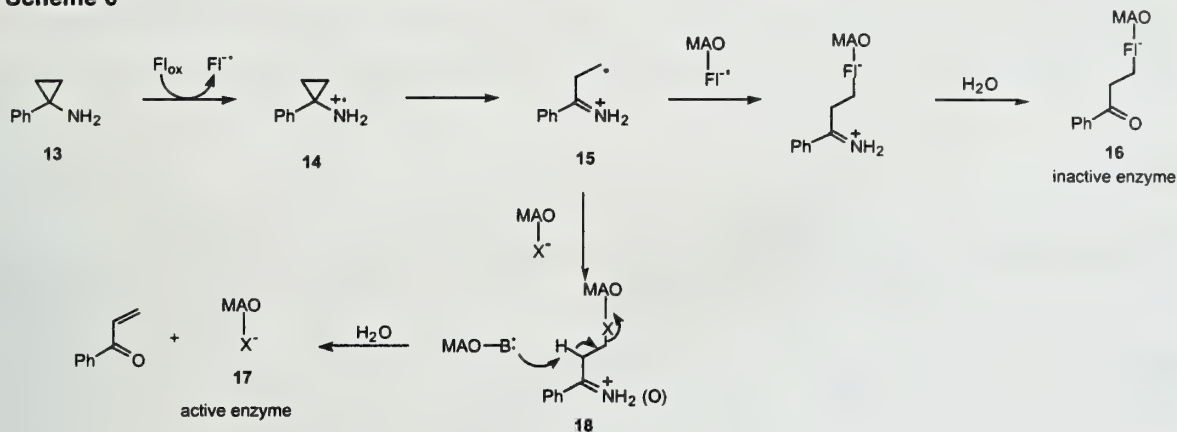
Scheme 5



92

mechanism for enzyme activation begins with a SET to Fl_{ox} from 1-phenylcyclopropylamine **13**, resulting in production of an aminyl radical cation **14**, which undergoes ring opening to generate the primary radical species **15** (Scheme 6). Radical **15** may either undergo coupling with Fl^{•+}, leading to substrate-labeled inactive enzyme **16**, or may combine with a nearby amino acid residue, eventually leading to active enzyme **17** after β-elimination of **18**. In this proposed mechanism the amino acid residue should be a good leaving group for active enzyme to be recovered.

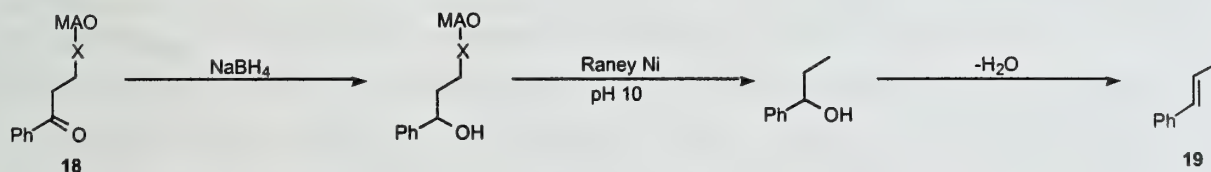
Scheme 6



¹⁴C-labeling was employed so that the fate of substrate and of substrate-labeled enzyme could be followed. Evidence for attachment to flavin came from gel filtration of proteolytic digests, which showed comigration of radioactivity and reduced flavin. Additionally, treatment of inactive enzyme with tritiated NaBH₄ showed incorporation of 1 eq. of tritium into the protein.

Attachment to an active site cysteine residue was deduced by reduction of the imine (or corresponding ketone) with NaBH₄, and by treatment with Raney-Nickel (Scheme 7). Reduction of **18** inhibits enolization and subsequent loss of substrate from enzyme. Raney-Nickel was employed to selectively reduce C-S bonds, resulting in the production of trans-β-methylstyrene **19** and enzyme lacking a cysteine sulfhydryl - as determined by 5,5'-dithiobis(2-nitrobenzoic acid) titration. Proteolysis/MALDI-TOF experiments have confirmed alkylation of the active site cysteine residue as Cys³⁶⁵ in bovine liver MAO B, which corresponds to Cys³⁷⁴ and Cys³⁶⁵ in human MAO A and MAO B respectively.²⁰

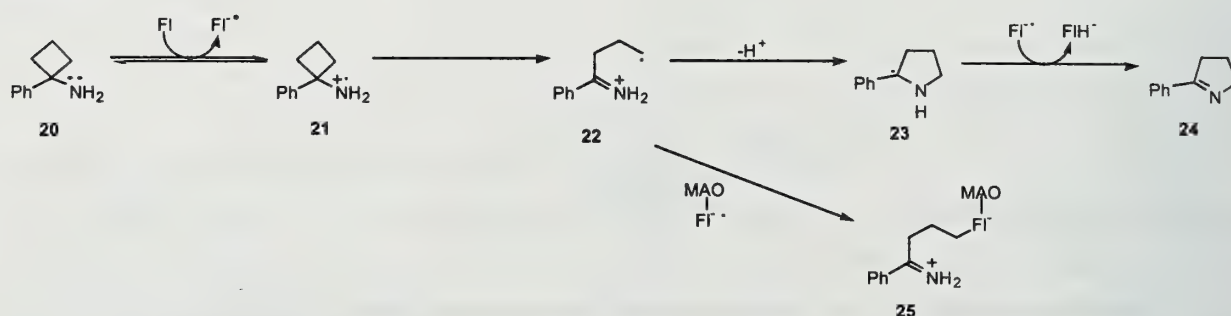
Scheme 7



1-Phenylcyclobutylamine

It was proposed that if SET from 1-phenylcyclobutylamine **20** to Fl_{ox} produced the aminyl radical cation **21**, rapid ring-opening would lead to the formation of compound **22**, containing an imine that may function as an intramolecular radical trap (Scheme 8). Based on literature precedence, intramolecular trapping was predicted to lead to the pyrrolidiny radical **23**.²¹ Subsequent SET to Fl^{\bullet} was expected to produce **24**. Following incubation of MAO with **20**, Silverman and co-workers observed time-dependent enzyme inactivation along with the production of **24**.²² Inactivation may be rationalized by radical combination of Fl^{\bullet} and the primary radical cation **22** to give inactivated enzyme **25**. Incubations containing the radical spin-trap, α -phenyl *N*-tert-butyl nitron, resulted in the generation of a triplet of doublets upon in the EPR spectrum, indicative of the presence of a stable nitroxyl species.

Scheme 8



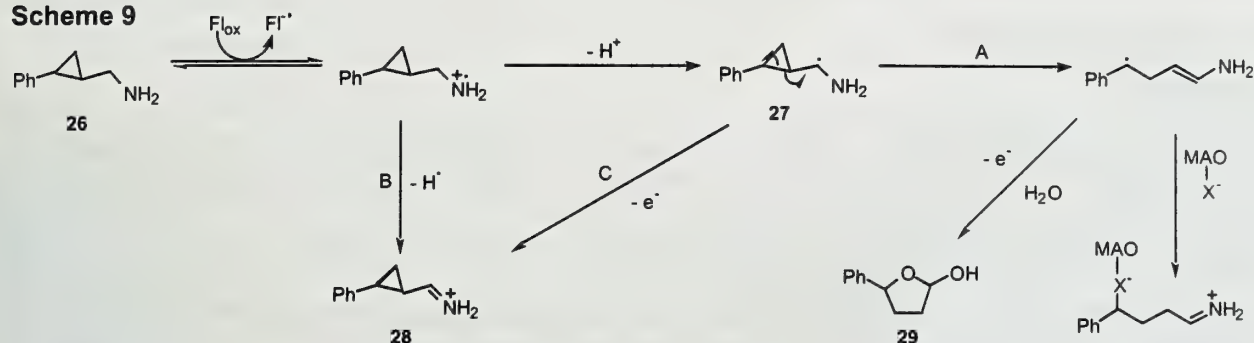
EVIDENCE IN SUPPORT OF AN α -AMINORADICAL

Initial investigations into the existence of an α -aminoradical (**3**, Scheme 2) involved studies with *trans*-1-(aminomethyl)-2-phenylcyclopropane **26**. However, these studies were inconclusive in differentiating among SET, HAT, or nucleophilic addition mechanisms (Scheme 9). MAO catalyzed oxidation of **26** was expected to produce the lactol **29**; however, imine **28** was formed exclusively.²⁴ It was concluded that cyclopropyl ring-cleavage (path A) did not occur because of poor orbital overlap between the cyclopropyl ring system and the radical.²⁵ This may have been the result of frozen rotation of the substrate while enzyme bound. It was further postulated that a second SET from α -aminoradical **27** (path C) led to product formation. However, HAT after formation of the aminyl radical cation (path B) could also have been responsible for these results and would have precluded the formation of α -aminoradical **27**. Thus these studies were inconclusive. A follow up study with (aminomethyl)cubane gave indirect support for the existence of α -aminoradical **3**.

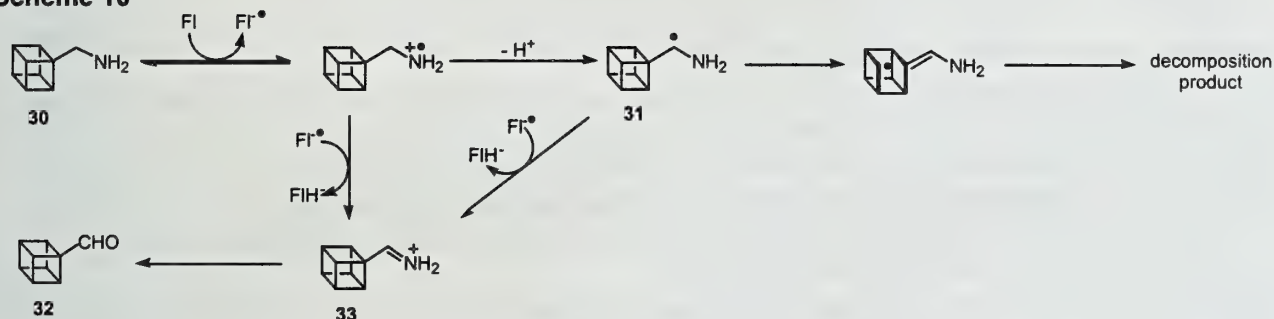
In order to test the orbital overlap hypothesis, (aminomethyl)cubane (**30**) was incubated with MAO (Scheme 10). If the α -aminoradical **31** were produced, its radical orbital should overlap with one of the three adjacent bonds of the cubane ring structure. As such, it was predicted that cubane ring-cleavage should proceed with a rate of about $3 \times 10^{10} \text{ s}^{-1}$. MAO catalyzed oxidation of **30** produced aldehyde **32** and an unidentifiable decomposition product with aromatic NMR resonances. Decomposition products were not believed to have come from the iminium cation **33**, since

cubylcarbonyl cations have been shown to undergo exclusive rearrangement to homocubanes. Furthermore, it was not believed that decomposition products arose from an anionic species, based on studies arguing against carbanion intermediates in MAO catalyzed oxidations. The presence of an unidentifiable decomposition product was interpreted as evidence that the cubane structure had undergone ring-cleavage that proceeded from α -aminoradical **31**, supporting a SET mechanism.²⁶

Scheme 9



Scheme 10



RECENT DEVELOPMENTS/CONCLUSION

There are good arguments in favor of both a SET and a HAT mechanism for MAO-catalyzed oxidation of amines. Unfortunately, much of the evidence supporting a SET mechanism is indirect, and arguments for a HAT mechanism rely heavily on the fact that Fl^\bullet has not been detected. Though KIE experiments may help to distinguish between these two mechanisms, the results from two studies have been rationalized by opposing mechanisms. Additionally, Jencks reports that "there is no evidence that isotope effects can be useful in helping distinguish between mechanisms which involve proton, hydrogen atom, or hydride ion transfer," arguing that proton and hydrogen atom transfer show a wide range of KIEs with little generalizability.²⁷ KIEs may reveal information about certain mechanistic issues, such as the rate limiting step; however, their utility for differentiating between SET and HAT mechanisms may not be so clear.

Though roughly 70 years of research has been conducted since the discovery of MAO in 1928, current and future work may prove to be the most promising for defining the mechanistic aspects of MAO. Recent investigations have found that a redox-active disulfide may couple to FlH^\bullet , which may explain why its detection is problematic.²⁸ Silverman has recently found evidence that MAO-catalyzed oxidations may be completely reversible and has proposed a novel mechanism for flavin reoxidation.²⁹

Catalytic MAO is suspected to exist as a dimer. Since flavin is covalently attached to each monomer, there has been confusion as to the role of the second flavin molecule. According to Silverman's interpretation of spectroscopic data, the second flavin may play a significant role in re-oxidizing flavin at the active site. Others have focused on investigating active site structure, discovering that mutations of residues²⁰⁸ may produce either MAO A-type selectivity (residue = Phe, Tyr) or MAO B-type selectivity (residue = Ile, Val, Ala).³⁰ Further investigations such as these should help define the enzymatic details and mechanism of MAO.

REFERENCES

1. Grimsby, J.; Chen, K.; Wang, L.J.; Lan, N.C.; Shih, J.C. *Proc. Natl. Acad. Sci. USA* **1991**, *88*, 3637.
2. Silverman, R.B. In *The Organic Chemistry of Drug Design and Drug Action*; Academic Press: San Diego, **1992**, p 352.
3. Cohen, G.; Farooqui, R.; Kesler, N. *Proc. Natl. Acad. Sci. USA* **1997**, *94*, 4890.
4. Silverman, R.B. *Acc. Chem. Res.* **1995**, *28*, 335.
5. Zhou, B.P.; Lewis, D.A.; Kwan, S.W.; Abell, C.W. *J. Biol. Chem.* **1995**, *270*, 23653.
6. Breinlinger, E.; Niemz, A.; Rotello, V.M. *J. Am. Chem. Soc.* **1995**, *117*, 5379.
7. Tomilov, A.P.; Maironovskii, S.G.; Fioshin, M.Y.; Smirnov, V.A. *Electrochemistry of Organic Compounds*; Halsted Press: New York, **1972**.
8. Castagnoli, N.J.; Rimoldi, J.M.; Bloomquist, J.; Castagnoli, K.P. *Chem. Res. Toxicol.* **1997**, *10*, 924.
9. Miller, R.J.; Edmondson, D.E.; Grissom, C.B. *J. Am. Chem. Soc.* **1995**, *117*, 7830.
10. Walker, M.C.; Edmondson, D.E. *Biochemistry* **1994**, *33*, 7088.
11. Jonsson, T.; Edmondson, D.E.; Klinman, J.P. *Biochemistry* **1994**, *33*, 14871.
12. Silverman, R.B.; Lu, X.; Blomquist, G.D.; Ding, C.Z.; Yang, S. *Bioorg. Med. Chem.* **1997**, *5*, 297.
13. Hamilton, G.A. *Prog. Bioorg. Chem.* **1971**, *1*, 83.
14. Kim, J.M.; Bogdan, M.A.; Mariano, P.S. *J. Am. Chem. Soc.* **1993**, *115*, 10591.
15. Hoegy, S.E.; Mariano, P.S. *Tetrahedron* **1997**, *53*, 5027.
16. Silverman, R.B.; Lu, X. *J. Am. Chem. Soc.* **1994**, *116*, 4129.
17. Zhong, B.; Lu, X.; Silverman, R.B. *Bioorg. Med. Chem.* **1998**, *6*, 2405.
18. Maeda, Y.; Ingold, K.U. *J. Am. Chem. Soc.* **1980**, *102*, 328.
19. Silverman, R.B.; Cesarone, J.M.; Lu, X. *J. Am. Chem. Soc.* **1993**, *115*, 4955.
20. Zhong, B.; Silverman, R.B. *J. Am. Chem. Soc.* **1997**, *119*, 6690.
21. Tanner, D.D.; Rahimi, R.M. *J. Org. Chem.* **1979**, *44*, 1674.
22. Silverman, R.B.; Zieske, P.A. *Biochemistry* **1986**, *25*, 341.
23. Yelekci, K.; Lu, X.; Silverman, R.B. *J. Am. Chem. Soc.* **1989**, *111*, 1138.
24. Silverman, R.B.; Zelechonsky, Y. *J. Org. Chem.* **1992**, *57*, 6373.
25. Lu, X.; Yang, S.; Silverman, R.B. *J. Org. Chem.* **1996**, *61*, 8961.
26. Silverman, R.B.; Zhou, J.P.; Eaton, P.E. *J. Am. Chem. Soc.* **1993**, *115*, 8841.
27. Jencks, W.P. In *Catalysis in Chemistry and Enzymology*; McGraw-Hill: New York, **1969**, p 273.
28. Sablin, S.O.; Ramsay, R.R. *J. Biol. Chem.* **1998**, *273*, 14074.
29. Lu, X.; Silverman, R.B. *J. Am. Chem. Soc.* **1998**, *120*, 10583.
30. Tsugen, Y.; Ito, A. *J. Biol. Chem.* **1997**, *272*, 14033.

INVESTIGATIONS OF THE CYTOCHROME P450 CATALYZED HYDROXYLATION OF HYDROCARBONS

Reported by Jennifer M. Vrtis

March 22, 1999

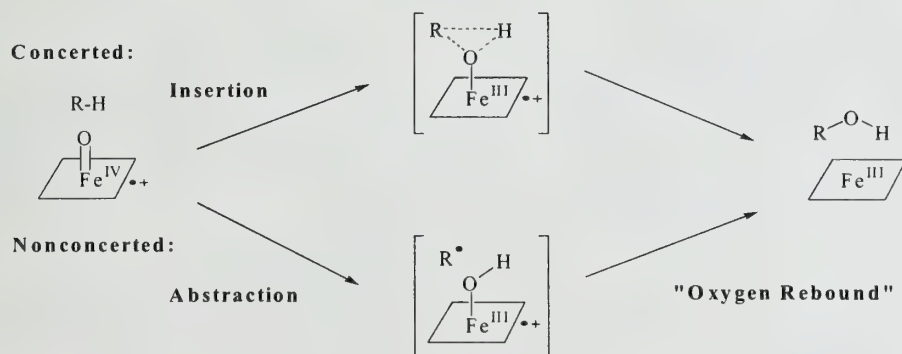
INTRODUCTION

The heme containing cytochrome P450 "super family" of enzymes is prevalent in many types of organisms including plants, animals, and yeasts. These enzymes are essential for the oxidation and production of biological compounds such as fatty acids, amino acids, and hormones.¹ Prior to understanding the function of these enzymes, the term P450 was originally coined because of the characteristic absorption band at 450 nm from the ferrous – carbon monoxide complex of cytochrome P450.² Cytochrome P450 enzymes were later determined to be oxygenases, enzymes that incorporate oxygen atoms from molecular oxygen into an organic molecule.³ Examples of reactions catalyzed by P450 "oxygenases" include alkene epoxidations, aromatic hydroxylations, alcohol and aldehyde oxidations, and hydroxylations of hydrocarbons.⁴ The latter is one of the most remarkable reactions, as it is usually viewed as a difficult challenge in synthetic chemistry. Recent investigations and proposed mechanisms of the hydrocarbon hydroxylation by cytochrome P450 will be the focus of this review.

CONCERTED VERSUS NONCONCERTED PATHWAY

Despite the fact that thorough investigations of the mechanism for the hydroxylation of hydrocarbons by P450 have been carried out for over twenty years, many issues are still unresolved. However, there is general consensus that there are two possible pathways by which a hydrocarbon can become oxidized by the putative high valent iron-oxo species, of cytochrome P450. These differ by their proposed mode of oxygen insertion, involving either a concerted or nonconcerted, "oxygen rebound"⁵ mechanism (Scheme 1).

Scheme 1

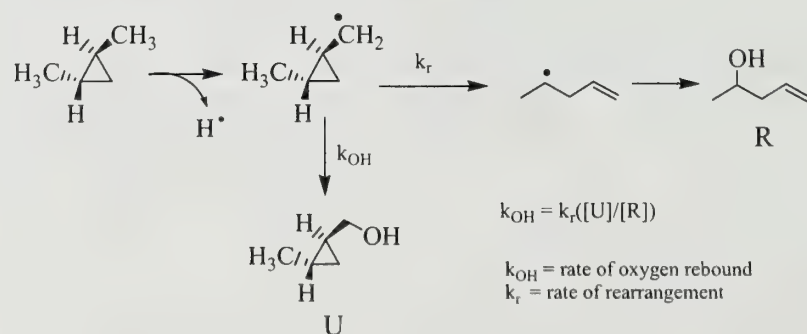


Early investigations of P450 catalyzed reactions implicated a concerted mechanism. These included studies indicated retention of stereochemistry at the hydroxylated carbon and small kinetic isotope effects (KIE), $k_H/k_D < 2$.^{6,7} However, later KIE studies reported a large $k_H/k_D > 11$ and were taken as evidence for a nonconcerted pathway.^{5,8} The initial KIEs, however, were non-informative because the intermolecular k_H/k_D values were determined by comparing the overall reaction rate for deuterated versus nondeuterated substrates. These experiments assumed that the rate-determining step is the cleavage of the C-H bond in the substrate, however, this may not be the case. To avoid the uncertainties in the interpretations for intermolecular KIE, an intramolecular KIE study was carried out. In this study, the rates were measured for the hydroxylation of the deuterated and protonated site of a symmetrical molecule, [1,1-²H₂]-1,3-diphenylpropane).⁹ This study showed large isotope effects, $k_H/k_D > 6$ and was reported to reflect the true isotope effect because the only step of the catalytic cycle that would be isotope sensitive is the breaking of the C-H (or C-D) bond. Thus, the high intramolecular KIE observed suggested a nonconcerted mechanism for the hydroxylation of this substrate. Further evidence for a nonconcerted mechanism included studies in which the stereochemistry of certain substrates was lost^{5,10} and studies involving radical clocks as discussed below.¹¹⁻¹⁶

RADICAL CLOCKS

Radical clocks have been employed to determine the existence of a radical in the P450 catalyzed hydroxylation reaction. Radical clocks contain a highly strained carbocyclic structure¹⁷ such as *trans*-1,2-dimethylcyclopropane, which upon formation of a radical on an adjacent carbon would rearrange to an acyclic product¹² (Scheme 2). The rate of the oxygen rebound (k_{OH}) can be estimated from the ratio of unrearranged (U) to rearranged (R) hydroxylated products and a previously calibrated rate for ring opening, k_r .

Scheme 2

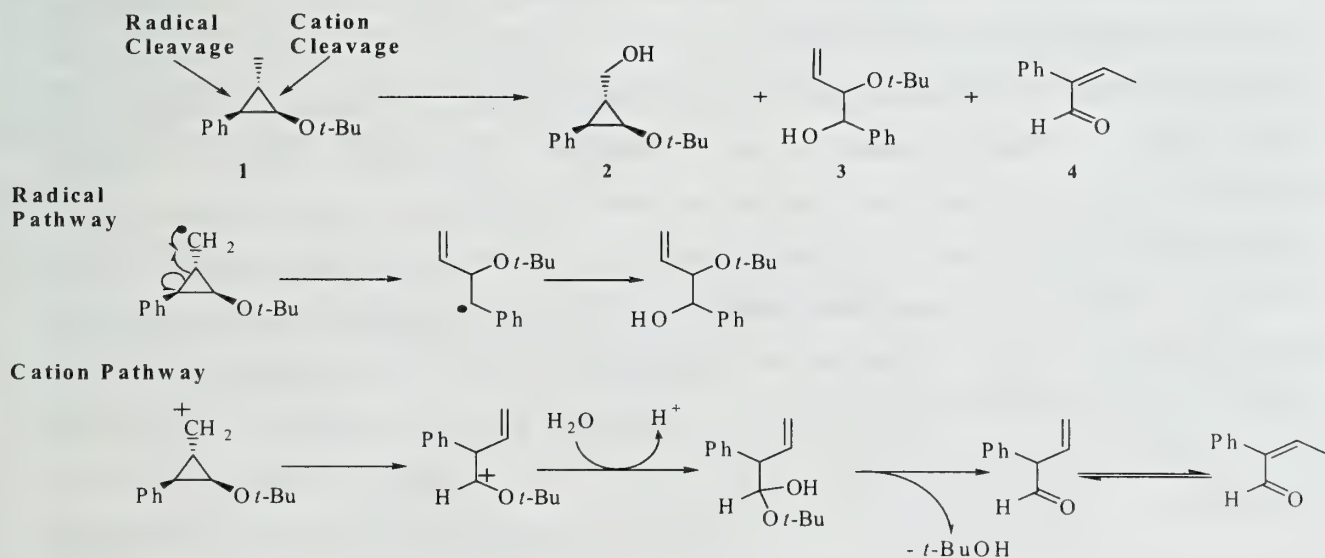


Numerous radical probe studies have been performed to investigate the existence of a radical mechanism in P450. The oxygen rebound rate (k_{OH}) was typically determined to be between $1 \times 10^{10} \text{ s}^{-1}$ to $1 \times 10^{13} \text{ s}^{-1}$. Some authors have argued that the difference of three orders of magnitude in k_{OH} values can be attributed to steric effects within the enzyme, which may slow the rate of the ring opening reaction (k_r) of the substrates and seemingly increase the k_{OH} . Another explanation was the possibility that the acyclic radical could react with the enzyme providing inaccurate ratios of [U] to [R].¹² However, as emphasized by Newcomb, the inconsistencies in k_{OH} could also arise from competing reactions in a pathway other than the competition between the rearrangement of a radical intermediate and oxygen rebound.¹⁶ One example is the competition between the formation of a radical versus cationic intermediate as described below.

Newcomb's Radical Clocks¹⁴⁻¹⁶

A potential flaw in the previously used radical probes is that both radical and carbocation intermediates of the nonconcerted hydroxylation may afford the same products. To address this issue, Newcomb has developed^{15,16} a calibrated hypersensitive radical probe (*trans,trans*-2-*tert*-butoxy-3-phenylcyclopropyl) methane (**1**) that may distinguish between radical and cationic intermediates (Scheme 3).¹⁴ A radical intermediate at the methyl position of the radical probe **1** was expected to rearrange to afford product **3** after oxygen rebound. A carbocation intermediate would rearrange to the homoallyl cation,¹⁸ and upon hydrolysis and subsequent isomerization would provide the aldehyde **4** and *t*-butanol. Under P450 catalyzed hydroxylation reaction conditions **1** afforded three products **2**, **3**, and **4**, in a ratio of 22:1:5.

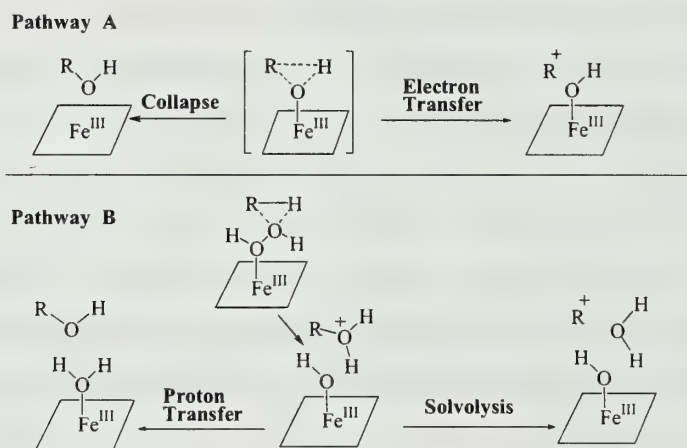
Scheme 3



MODE OF CATION FORMATION

As discussed for radical probe **1**, the incongruous values of k_{OH} can be attributed to the existence of both radical and carbocation intermediates. Newcomb proposed two possible modes for the formation of the carbocation intermediates (Scheme 4).¹⁴⁻¹⁶ It was envisioned that an electron transfer (ET) could occur to give the carbocation intermediate, which upon hydrolysis would rearranged and unrearranged hydroxylated products. Collapse of the transition structure would compete with ET to generate unrearranged hydroxylated products. In pathway B, an active oxidant iron complexed with hydrogen peroxide, would form the protonated alcohol via insertion of OH^+ into a C-H bond of the substrate. Solvolysis of the protonated alcohol or deprotonation would give a carbocation intermediate or unrearranged products, respectively.

Scheme 4



To investigate the two pathways, the hypersensitive radical probes **5** - **10** were developed and subjected to hydroxylation by P450 (Figure 1).¹⁶ The results of these studies were claimed to be inconsistent with pathway A (Scheme 4). An increase in the methyl substitution at the radical center would decrease its oxidation potential due to the stabilities of a primary, secondary, or tertiary carbocation. This would be expected to lead to more products derived from a cationic pathway for the more substituted radicals. However, the results do not agree with this rationalization (Figure 1). Only unrearranged hydroxylated products were observed for the tertiary radical probe **8** which should have been oxidized most efficiently to afford the rearranged products. Therefore, it was suggested that the ET mechanism was an incorrect depiction of cation formation. Further evidence that discredits pathway A is the inconsistent results between probe **9** vs. **5** and **10** vs. **6**. The *p*-trifluoromethyl group was expected to destabilize a cyclopropylcarbinyl cationic intermediate and therefore the amount of unrearranged

hydroxylated products of **9** and **10** should exceed that of **5** and **6**, respectively. However, the ratio of the products reported is opposite as would be expected for pathway A, Scheme 4.


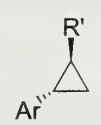
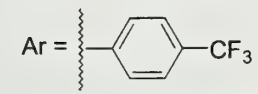
Radical Probes	Probe	R'	UOH / ROH
	5	Me	4.3
	6	Et	25
5 - 8	7	Pr	26
9, 10	8	<i>i</i> -Pr	>100
	9	Me	4
	10	Et	12

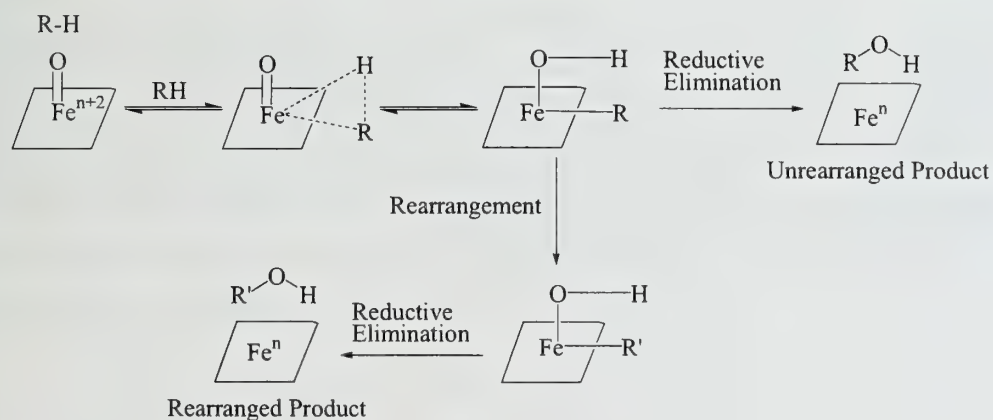
Figure 1: Hypersensitive radical probes

The results of the hypersensitive probes also do not support pathway B. The *p*-trifluoromethyl group should disfavor aryl assisted solvolysis due to the electron withdrawing effect. However, as stated above the opposite results were observed for probe **9** vs **5** and **10** vs **6**. These results therefore suggest that the competition pathways of carbocation formation, as shown in scheme 4, are not an explanation for the anomalous k_{OH} values.

AGOSTIC COMPLEX

Collman, Brauman, and coworkers proposed an alternative explanation to the formation of the unrearranged and rearranged products.¹⁹ As seen in Scheme 5, an “agostic substrate – catalyst complex” was proposed as the key intermediate. The agostic interactions from this complex were suggested to increase the Brønsted acidity of the hydrogen, causing the C-H bond to become more polarized and lead to proton migration to the iron-oxo species. Reductive elimination would lead to unrearranged hydroxylated products. In some cases, rearrangement to a more stable alkyl metal complex could precede reductive elimination and yield rearranged products.

Scheme 5



Evidence for this model was the inhibition of cyclohexane oxidation by a protoporphyrin, iron model catalyst in the presence of H₂, D₂, and CH₄. It was rationalized that the observed decrease in rates of cyclohexanol production can be attributed to the stronger agostic complexes of H₂, D₂, or CH₄ with the iron-oxo species that would inhibit the formation of the substrate-catalyst complex. However, one flaw in this model is that larger probes (i.e., phenyl substituted cyclopropane groups) would be unlikely to reach the iron due to steric interactions between the substrate and the protoporphyrin ring.

MULTI- STATE REACTIVITY MODEL

The hypersensitive probes brought forth by Newcomb seem to confirm that the proposal for hydrogen abstraction, followed by oxygen rebound is incomplete. In addition, the results provide evidence for a cation intermediate though the mechanism of its formation and conversion to product is still unclear. Newcomb's results however, concur with a multi-state reactivity model, for hydroxylation as proposed by Shaik, Schwartz, and coworkers (Scheme 6).²⁰ The model relates the FeO⁺ cation in the gas phase²¹ to that of the iron-oxo complex in cytochrome P450. Even though the reactivity of the ferryl complex of P450 with a hydrocarbon will not be completely similar to the gaseous FeO⁺, the correlation provides new insight into the unresolved issue of the P450 catalyzed hydroxylation reactions. The multistate reactivity paradigm offers an explanation based on the spin-state of the iron-oxo species in cytochrome P450. A competition exists between two reaction manifolds. Reaction of the high spin (H.S.), "spin-unpaired" state will proceed by a radical mechanism and consequently result in the loss of stereochemistry of substrates and rearrangements as expected for radical reactions. The low spin (L.S.), "spin-paired" state can undergo an insertion type of mechanism and retain stereochemistry of substrates.

Scheme 6



The key point to this model is that the probability of spin inversion (SI) from the high spin to the low spin surface is probe dependent. Better electron donor groups are reported to aid in the stabilization of the LS state, and therefore result in an earlier crossing point for SI (Figure 2A). A later SI increases the probability of the reaction proceeding at the H.S. surface, that is the reaction would proceed via hydrogen atom abstraction and afford more rearranged products.

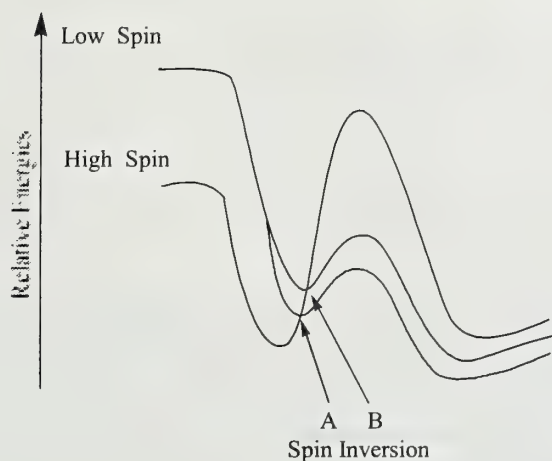


Figure 2: Qualitative potential energy surfaces for the reaction of high spin and low spin states of FeO^+ with R-H

This model is consistent with the probes studied by Newcomb. The increasing donor properties from the primary probe **5** up to the tertiary probe **8** result in earlier SI and subsequent decrease in the amount of rearranged product. In fact, only unrearranged products were observed for probe **8**. In addition the *p*-trifluoromethyl group would slightly reduce the donor ability and thereby result in a later SI with less chance to crossover to the LS surface and therefore afford more rearranged hydroxylated products. This is observed for both probes **9** and **10** which gave more rearranged products relative to **5** and **6**, respectively.

The multistate reactivity model is an attractive model to explain the anomalies of the cytochrome P450 hydroxylation reaction. However, further experimental evidence must be provided to validate this mechanism. To investigate their model, Shaik and Schwartz suggested that the ligand to the ferryl species could be altered which would affect the energy difference between the initial L.S. and H.S. energy surfaces. In addition, the affect of the donor properties could be studied by development of other hypersensitive radical probes. Lastly, the probablity of SI could also be altered and monitored in the presence of an external magnetic field.²²

CONCLUSIONS

Hydroxylation of unactivated hydrocarbons by cytochrome P450s proves to be a remarkable feat by Nature which has fascinated scientists for many years. Numerous investigations have been undertaken to obtain support for or against the concerted or nonconcerted pathway of hydroxylation. The most recent investigations and proposed mechanisms by Newcomb, Shaik and Schwarz, and Collman and Brauman provide new insight into the mechanism. However, further studies will need to be carried out to test these models.

REFERENCES

- 1) Kaim, W.; Schwederski, B. *Bioinorganic Chemistry: Inorganic Elements in the Chemistry of Life*; John Wiley & Sons Ltd.: West Sussex, England, 1994.
- 2) Omura, T.; Sato, R. *J. Biol. Chem.* **1964**, *239*, 2370-2378.
- 3) Hamilton, G. A. *Molecular Mechanisms of Oxygen Activation*; Academic: New York, 1974.
- 4) Sono, M.; Roach, M. P.; Coulter, E. D.; Dawson, J. H. *Chem. Rev.* **1996**, *96*, 2841-2887.
- 5) Groves, J.; McClusky, G. *Biochem. Biophys. Res. Commun.* **1978**, *81*, 154-160.
- 6) McMahon, R. E.; Sullivan, H. R.; Craig, J.; Pereira, W. *Arch. Biochem. Biophys.* **1969**, *132*, 575-576.
- 7) Shapiro, S.; Piper, J. U.; Caspi, E. *J. Am. Chem. Soc.* **1982**, *104*, 2301-2305.
- 8) Kadkhodayan, S.; Coulter, E. D.; Maryniak, D.; Bryson, T. A.; Dawson, J. *J. Biol. Chem.* **1995**, *270*, 28042-28048.
- 9) Hjelmeland, L.; Aronow, L.; Trudell, J. *Biochem. Biophys. Res. Commun.* **1977**, *76*, 541-549.
- 10) Heimbrook, D.; Sligar, S. *Biochem. Biophys. Res. Commun.* **1981**, *99*, 530-535.
- 11) Ortiz de Montellano, R.; Stearns, R. *J. Am. Chem. Soc.* **1987**, *109*, 3415-3420.
- 12) Bowry, V.; Ingold, K. U. *J. Am. Chem. Soc.* **1991**, *113*, 5669-5707.
- 13) Atkinson, J.; Ingold, K. U. *Biochemistry* **1993**, *32*, 9209-9214.
- 14) Newcomb, M. L. T., M.; Chestney, D.; Roberts, E.; Hollenberg, P. *J. Am. Chem. Soc.* **1995**, *117*, 12085-12091.
- 15) Toy, P.; Dhanabalasingam, B.; Newcomb, M.; Hanna, I.; Hollenberg, P. *J. Org. Chem.* **1997**, *62*, 9114-9122.
- 16) Toy, P.; Newcomb, M.; Hollenberg, P. *J. Am. Chem. Soc.* **1998**, *120*, 7719-7729.
- 17) Griller, D.; Ingold, K. U. *Acc. Chem. Res.* **1980**, *13*, 317-323.
- 18) Wiberg, K.; Shobe, D.; Nelson, G. *J. Am. Chem. Soc.* **1993**, *115*, 10645-10652.
- 19) Collman, J.; Chien, A.; Eberspacher, T.; Brauman, J. *J. Am. Chem. Soc.* **1998**, *120*, 425-426.
- 20) Shaik, S.; Filatov, M.; Schroder, D.; Schwarz, H. *Chem. -Eur. J.* **1998**, *4*, 193-199.
- 21) Fiedler, A.; Schroder, D.; Shaik, S.; Schwartz, H. *J. Am. Chem. Soc.* **1994**, *116*, 10734-10741.
- 22) Grissom, C. *Chem. Rev.* **1995**, *95*, 3-24.

OSMIUM-CATALYZED ASYMMETRIC AMINOHYDROXYLATION (AA) REACTION

Reported by Yong-Jae Kim

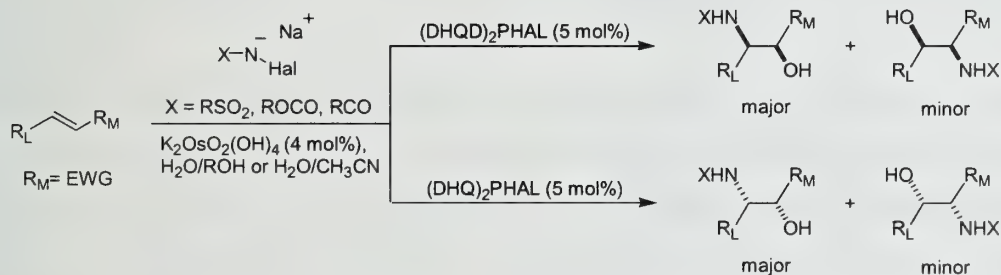
March 29, 1999

INTRODUCTION

Various methods have been developed for the efficient formation of β -aminoalcohols due to their abundance in natural products, as well as their potential use as synthons. Common methodologies involve the use of Pd to promote functionalization of olefins,¹ or the use of nucleophilic nitrogen sources to open epoxides,² cyclic carbamates or sulfites.³ Although these reactions afford good yields and regioselectivities, each method possesses certain limitations. Such limitations include the use of stoichiometric amounts of metal or strongly nucleophilic N-sources such as azides which could be problematic with sensitive functionalities.

Asymmetric aminohydroxylation (AA) of olefins was recently developed by Sharpless and coworkers for synthesizing β -aminoalcohols under mild conditions.^{4,5} This procedure utilizes a catalytic amount of an osmium source with a chloramine as the oxidant/N-source (Scheme 1). In the 1970s, an earlier version of this reaction employed a stoichiometric or catalytic amount of osmium tetroxide in a one pot procedure,^{6,7} but improvements in the regio- and stereoselectivity have been recently made in the presence of a catalytic amount of chiral ligand. This report highlights some of the recent advances of the catalytic AA process in the formation of β -aminoalcohols.

Scheme 1

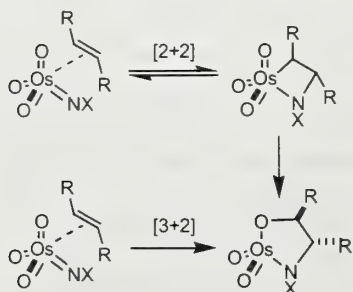


MECHANISM

Oxygen transfer from a metal oxide to organic functional groups, such as olefins, has received much attention due to its general applicability.⁸ For instance, functionalization of olefins to 1,2-diols using osmium(VIII) tetroxide in the asymmetric dihydroxylation reaction (AD) has been developed into a synthetically useful procedure.⁹ It is proposed that the mechanism of the AA reaction is similar to the

AD reaction, where two separate catalytic cycles are suggested to be operative (Scheme 3).^{10,11} The

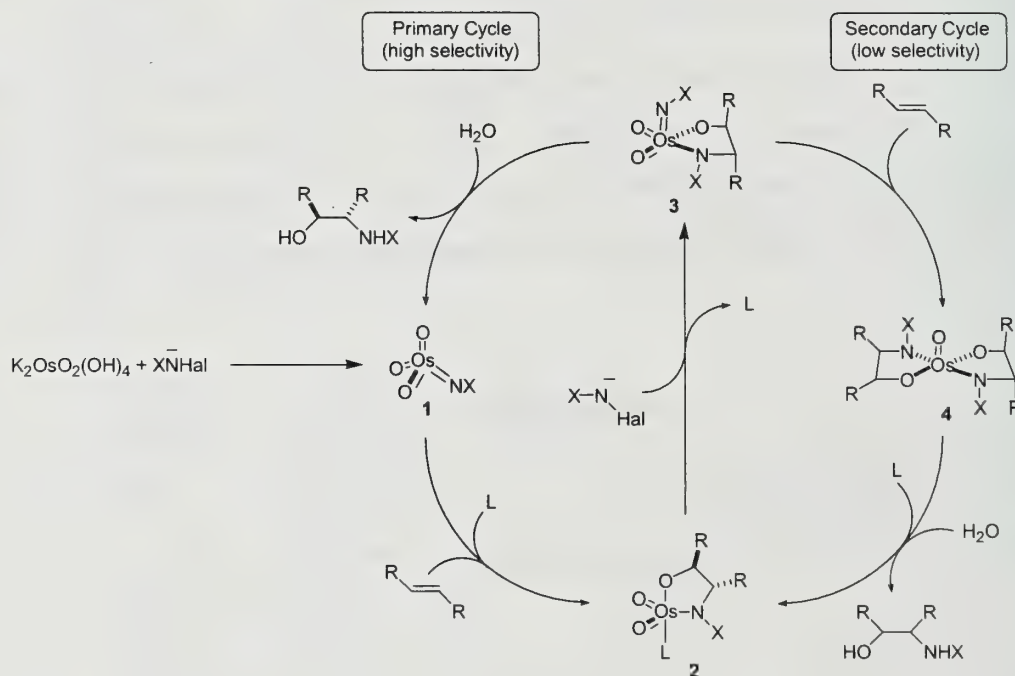
Scheme 2



trioxoimido osmium(VIII) complex (1), which is the presumed reactive intermediate, is formed from a catalytic amount of potassium osmate(VI) dihydrate ($K_2OsO_2(OH)_4$) and the oxidant/N-source. Addition of the ligand and the olefin to 1, by either a [3+2] mechanism or a [2+2] mechanism followed by rearrangement (Scheme 2), affords an osmium(VI) azaglycolate complex (2) which is subsequently oxidized by the chloramine to the dioxoimido osmium(VIII) azaglycolate 3. Hydrolysis with water yields the aminoalcohol and regenerates the

catalyst. Erosion of the enantioselectivity is proposed to occur due to a secondary cycle, in which 3 reacts with another olefin to give the osmium(VI) bisazaglycolate 4. Subsequent hydrolysis of 4 affords the aminoalcohol in a racemic form.

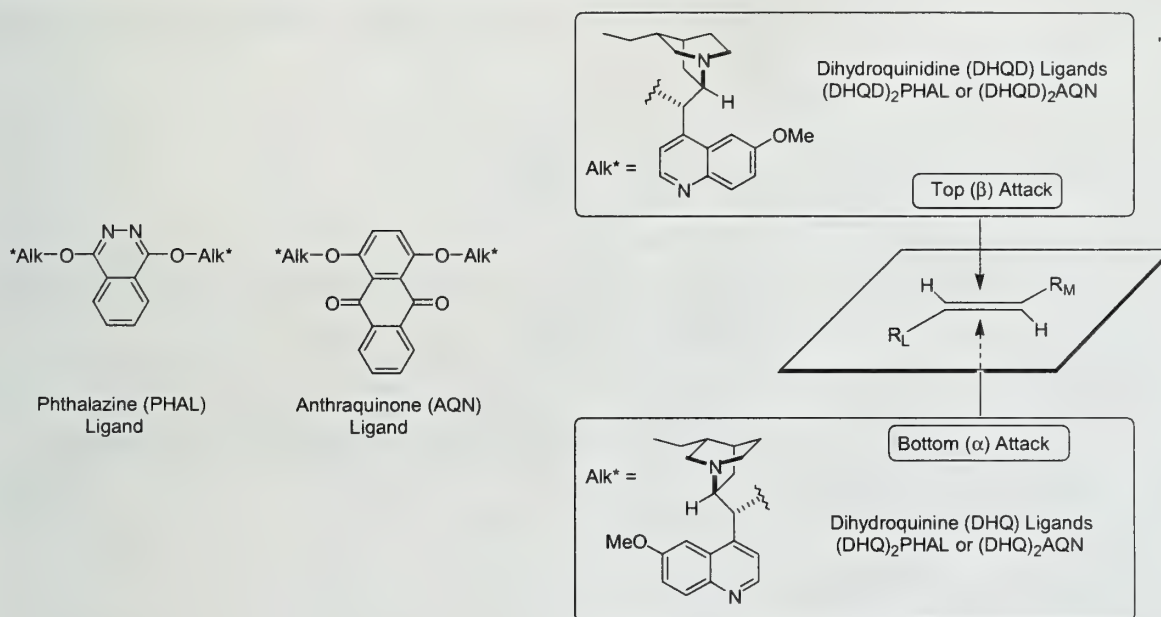
Scheme 3



To prevent the intrusion of the secondary cycle, a high concentration of water is used to accelerate the catalyst turnover, thus suppressing bis-azaglycolate formation. The reaction is run in a 1:1 mixture of water and a polar organic solvent, such as acetonitrile or *n*-propanol, in order to achieve high enantioselectivity. Rate enhancements are normally observed in acetonitrile while an increase in regio- and enantioselectivity as well as efficiency are observed in alcoholic solvents.

The ligands used to affect the stereoselectivities are composed of either phthalazine (PHAL) or anthraquinone (AQN) attached to two identical chiral cinchona alkaloids such as dihydroquinidine (DHQD) or dihydroquinine (DHQ) (Scheme 4). The osmium-ligand complex forms a “binding pocket” which provides facial discrimination for the delivery of the heteroatoms to the enantiotopic faces of the olefin. Similar to the facial selectivity observed in the AD reaction, the osmium-ligand complex delivers the heteroatoms to the top (β) face of the olefin with the use of dihydroquinidine ligands such as (DHQD)₂PHAL or (DHQD)₂AQN and to the bottom (α) face with dihydroquinine ligands such as (DHQ)₂PHAL or (DHQ)₂AQN, as shown in the empirical mnemonic device in Scheme 4.

Scheme 4



In addition to its influence on the face selectivity of approach by the olefin, the ligand also affects the regioselectivity.¹²⁻¹⁴ The nitrogen atom generally prefers the position distal to the most electron withdrawing group with PHAL ligands, but with AQN the opposite regioisomer is observed. Although the mechanism is not fully understood, the optimal choice of solvent and N-source can provide regioselectivities of more than 20:1.¹²

SCOPE AND UTILITY

The ability to utilize N-sources with a variety of protecting groups on the amine makes the AA reaction a powerful tool in synthesizing β -aminoalcohols. Another advantage is the generality of the conditions in which a variety of reactions can be performed. General reaction conditions are as follows:

3 equivalents of oxidant/N-source, a catalytic amount of $K_2OsO_2(OH)_4$ (4 mol%) and ligand (5 mol%) in a 1:1 solution of water to acetonitrile or an alcohol at temperatures between 0 °C and room temperature.

Sulfonamides

Initial investigation of the AA reaction incorporated Chloramine-T as the oxidant/N-source.¹⁵ Olefins were converted to their C-3 sulfonamides in ratios of greater than 5:1 with respect to their C-2 regioisomers (Table 1). Improved rates and selectivities were observed when sodium *N*-chloro-*N*-methanesulfonamide (Chloramine-M) was used.¹¹ It was proposed that steric factors enable the olefin to fit into the osmium-ligand “binding pocket” better with the smaller substituent on the sulfonamide. Rate enhancement due to faster hydrolysis governed by electronic effects provide another explanation for these results.¹¹

Table 1. Catalytic AA reaction with sulfonamides

Substrate	Product	Yield (%) Chloramine-T (M)	ee (%), DHQ Chloramine-T (M)	ee (%), DHQD ^a Chloramine-T (M)	t (h) Chloramine-T (M)
		64 (65)	81 (95)	71 (95)	3 (3)
		65 (76)	77 (94)	50 (82)	2 (1.5)
		52 (71)	62 (75)	50 (82)	14 (16)
		64 (49)	45 (66)	36 (63)	6 (18)

^aThe ee values are for products that are enantiomeric to those in the product column

Although the use of the sulfonamides showed promising yields and enantioselectivities, the limited range of substrates (no styrene type olefins presented) and the harsh conditions for removal of the nitrogen protecting groups (HBr/HOAc for toluenesulfonamide; Red-Al, toluene reflux for methanesulfonamide) has led to the investigation of alternative N-sources.

Carbamates

Carbamate based N-sources have greatly enhanced the scope of the AA reaction by providing Cbz,^{13,16} BOC,^{13,17} and Teoc¹⁸ protected amines, which allow for orthogonal deprotection strategies (reductive, acidic, and nucleophilic respectively).

In the carbamate experiments, styrene type olefins, absent from the sulfonamide study, show good to excellent yields and selectivities (Table 2). Regioselectivities of more than 10:1 with enantioselectivities of up to 99% were achieved. Cinnamates, fumarates, and crotonates also showed improved selectivities using carbamate N-sources.

Table 2. Catalytic AA reaction with carbamates

$\text{Ph}-\text{CH}=\text{CH}-\text{CO}_2\text{CH}_3 \xrightarrow[\text{H}_2\text{O}/\text{ROH or H}_2\text{O}/\text{CH}_3\text{CN}]{\text{ZNCINa (3 equiv)}} \text{Ph}-\text{CH}(\text{NHZ})-\text{CH}(\text{OH})-\text{CO}_2\text{CH}_3$ <p style="text-align: center;">K₂OsO₂(OH)₄ (4 mol%) (DHQ)₂PHAL (5 mol%) Z = Cbz, BOC, Teoc, EtOCO</p>					
Substrate	Product	Z	Yield (%)	ee (%), DHQ	ee (%), DHQD ^a
		EtOCO	78	99	99
		Cbz	65	94	97
		Cbz	55	84	87
		Cbz	92	91	88
		Cbz	73	93	90
		Cbz	70	99	99
		BOC	80	98	97
		Teoc	88	97	96
		Cbz	91	91	98
		BOC	87	99	96
		Teoc	90	99	99

^aThe ee values are for products that are enantiomeric to those in the product column

The fastest turnover rates of the carbamates were observed with the Teoc groups. As seen with the sulfonamides, shorter reaction times were generally observed with smaller and less hydrophobic N-sources.

One further advantage of the carbamate based N-sources is the influence of the ligand and solvents on the regioselectivities.^{13,14} Reactions with PHAL backbone ligands in *n*-propanol/water favored the benzylic amines (**A**), whereas with AQN backbone ligands with acetonitrile/water, the benzylic alcohols (**B**) were preferred. The best results were achieved with benzyl carbamates with yields between 40-67% and enantioselectivities around 90%. Similar trends were seen with an alternative N-source, acetamide, as summarized in Table 3. Although further improvement in yield is desired, reversal of regioselectivity furnishes a practical route to benzylic alcohols.

Table 3. Control of regioselectivity with different ligands and solvents

$\text{R-CH=CH}_2 \xrightarrow[\text{Ligand (5 mol\%), H}_2\text{O/ROH or H}_2\text{O/CH}_3\text{CN}]{\text{ZNHaI}^- (1-3 \text{ equiv}), \text{K}_2\text{OsO}_2(\text{OH})_4 (4 \text{ mol\%})} \text{R-CH(NHZ)-CH}_2\text{OH (A)} + \text{R-CH(OH)-CH}_2\text{NHZ (B)}$

Z = Cbz, Ac

Substrate	Product	Solvent	Ligand	Cbz		Ac	
				A:B	ee (%) A, B	A:B	ee (%) A, B
		<i>n</i> -PrOH	(DHQ) ₂ PHAL	3 : 1	93, N/A	1.1 : 1	91, 83
		CH ₃ CN	(DHQ) ₂ PHAL			1 : 6.1	N/A, 88
		<i>n</i> -PrOH	(DHQ) ₂ AQN	1 : 4	N/A, 95		
		CH ₃ CN	(DHQ) ₂ AQN			1 : 13	N/A, 88
		<i>n</i> -PrOH	(DHQ) ₂ PHAL	3 : 1	93, N/A	2.5 : 1	96, 62
		CH ₃ CN	(DHQ) ₂ PHAL			1 : 2.4	85, 84
		<i>n</i> -PrOH	(DHQ) ₂ AQN	1 : 4	N/A, 94		
		CH ₃ CN	(DHQ) ₂ AQN			1 : 9	N/A, 86

Acetamide

Acetamide is another practical oxidant/N-source for the AA reaction, thus providing mild cleavage conditions for the deprotection of amines.¹² Cinnamates produce β -aminoalcohols with yields above 70% and high regio- and enantioselectivities compared to other N-sources (Table 4). Substituted styrenes prove to be an interesting class due to their regioselectivity dependence on the choice of solvent and ligand. Reversal of regioselection (**A** < **B**) is observed with use of acetonitrile/water or if the backbone ligand is changed from PHAL to AQN, similar to the results observed for the benzyl carbamate (Table 3). The decrease in yield in acetonitrile/water and with use of AQN ligand is a drawback, but a significant increase in enantioselectivity is observed.

Table 4. Catalytic AA reaction with amide

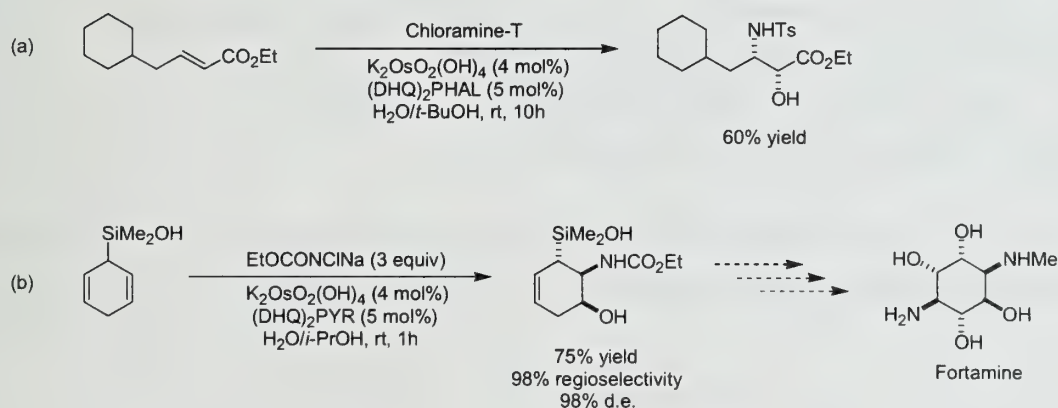
$ \begin{array}{c} \text{R}_L\text{---CH=CH---R}_M \xrightarrow[\text{K}_2\text{OsO}_2(\text{OH})_4 \text{ (4 mol\%)}]{\text{AcNBrLi (1 equiv)}} \\ \text{(DHQ)}_2\text{PHAL (5 mol\%)} \\ \text{H}_2\text{O/ROH or H}_2\text{O/CH}_3\text{CN} \end{array} \rightarrow \begin{array}{c} \text{NHAc} \\ \\ \text{R}_L\text{---CH---CH---R}_M \\ \\ \text{OH} \end{array} $					
Substrate	Product	Regio-selectivity	Yield (%)	ee (%), DHQ	ee (%), DHQD ^a
		> 20:1	81	99	99
		> 20:1	71	99	99
			50	94	93
		1.1:1	38	91	N/A

^aThe ee values are for products that are enantiomeric to those in the product column

SYNTHETIC APPLICATIONS

The AA reaction has been successfully applied in recent syntheses. The side chains of the anticancer drugs taxol and taxotere were synthesized in high enantioselectivity on a 120 g scale through AA of a cinnamate using only 1.5% of the osmium catalyst and 1% of (DHQ)₂PHAL.^{12,19} Various α -arylglycinols obtained by the AA of styrenes as described above were oxidized with TEMPO, which furnished numerous α -arylglycines with no loss of enantioselectivity by epimerization.¹³ Also cyclohexylnorstatine, a key component of a renin inhibitor, was synthesized using the AA reaction

Scheme 5



(Scheme 5a),²⁰ and desymmetrization of dieny silanes has been shown to proceed with complete diastereo- and regioselectivity to provide the precursor for amino-cytosols as shown in Scheme 5b.^{21,22}

CONCLUSION

It has been demonstrated that the catalytic asymmetric aminohydroxylation (AA) reaction is a powerful tool in synthesizing various aminoalcohols from simple olefins. The highest selectivities and yields are seen with the *trans*-olefins where regio- and enantioselectivities are dependent on the ligand and solvent used. Although the AA reaction is still being developed, the scope and application have already shown that its use will soon match the powerful AD reaction.

REFERENCES

- (1) Backväll, J. E.; Björkman, E. E. *J. Org. Chem.* **1980**, *45*, 2893.
- (2) Martinez, L. E.; Leighton, J. L.; Carsten, D. H.; Jacobsen, E. N. *J. Am. Chem. Soc.* **1995**, *117*, 5897.
- (3) Chang, H. T.; Sharpless, K. B. *Tetrahedron Lett.* **1996**, *37*, 3219.
- (4) Reiser, O. *Angew. Chem., Int. Ed. Engl.* **1996**, *35*, 1308.
- (5) O'Brien, P. *Angew. Chem., Int. Ed. Engl.* **1999**, *38*, 326.
- (6) Sharpless, K. B.; Patrick, D. W.; Truesdale, L. K.; Biller, S. A. *J. Am. Chem. Soc.* **1975**, *97*, 2305.
- (7) Herranz, E.; Biller, S. A.; Sharpless, K. B. *J. Am. Chem. Soc.* **1978**, *100*, 3596.
- (8) Jørgensen, K. A.; Schiøtt, B. *Chem. Rev.* **1990**, *90*, 1483.
- (9) Kolb, H. C.; VanNieuwenhze, M. S.; Sharpless, K. B. *Chem. Rev.* **1994**, *94*, 2483.
- (10) Wai, J. S. M.; Marko, I.; Svendsen, J. S.; Finn, M. G.; Jacobsen, E. N.; Sharpless, K. B. *J. Am. Chem. Soc.* **1989**, *111*, 1123.
- (11) Rudolph, J.; Sennhenn, P. C.; Vlaar, C. P.; Sharpless, K. B. *Angew. Chem., Int. Ed. Engl.* **1996**, *35*, 2810.
- (12) Bruncko, M.; Schlingoff, G.; Sharpless, K. B. *Angew. Chem., Int. Ed. Engl.* **1997**, *36*, 1483.
- (13) Reddy, K. L.; Sharpless, K. B. *J. Am. Chem. Soc.* **1998**, *120*, 1207.
- (14) Tao, B.; Schingloff, G.; Sharpless, K. B. *Tetrahedron Lett.* **1998**, *39*, 2507.
- (15) Li, G.; Chang, H.-T.; Sharpless, K. B. *Angew. Chem. Int. Ed. Engl.* **1996**, *35*, 451.
- (16) Li, G.; Angert, H. H.; Sharpless, K. B. *Angew. Chem. Int. Ed. Engl.* **1996**, *35*, 2813.
- (17) O'Brien, P.; Osborn, S. A.; Parker, D. D. *Tetrahedron Lett.* **1998**, *39*, 4099.
- (18) Reddy, K. L.; Dress, K. R.; Sharpless, K. B. *Tetrahedron Lett.* **1998**, *39*, 3667.
- (19) Li, G.; Sharpless, K. B. *Acta Chem. Scand.* **1996**, *50*, 649.
- (20) Upadhyay, T. T.; Sudalai, A. *Tetrahedron: Asymmetry* **1997**, *8*, 3685.
- (21) Landais, Y. *Chimia* **1998**, *52*, 104.
- (22) Angelaud, R.; Landais, Y. *Tetrahedron Lett.* **1997**, *38*, 1407.

C₂-SYMMETRIC BIS(OXAZOLINE)-COPPER COMPLEXES IN CATALYTIC ASYMMETRIC SYNTHESIS

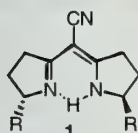
Reported by Liqiang Zhou

April 1, 1999

INTRODUCTION

An important goal of organic synthesis is the design of catalysts for asymmetric reactions that provide high diastereo- and enantioselectivity. Most current synthetic catalysts are metal complexes bound to chiral ligands. The chirotopic environment around the substrate upon complexation to the metal center is thought to provide enantioselective induction in product formation.

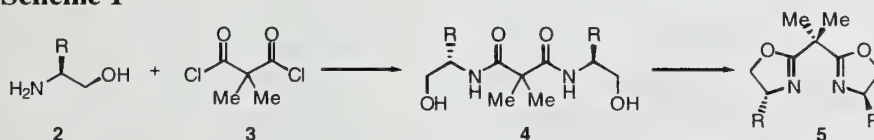
C₂-symmetric bis(oxazoline) complexes have been designed and applied successfully to a variety of asymmetric reactions.¹ Bis(oxazoline) ligands are structurally related to semicorrins **1** developed by Pfaltz and co-workers,² and their C₂-symmetry minimizes the number of possible stereoisomeric transition states.³ Although structural diversity has been introduced into the bis(oxazoline) ligands, the general motif is constant: the planar π -system and the two five-membered rings afford the ligand conformational rigidity, and the substituents on the ring are close to the coordination site, affording a well defined chiral environment around the metal. This review focuses on C₂-symmetric bis(oxazoline)-Cu complexes in asymmetric synthesis.



CYCLOPROPANATION

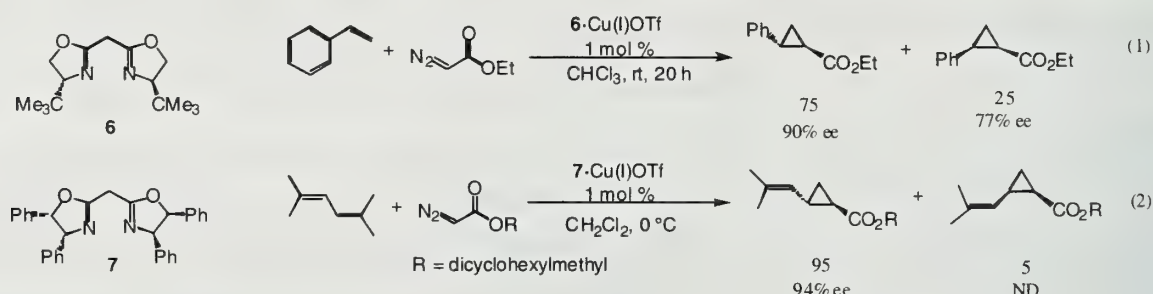
Bis(oxazoline) ligands are usually synthesized in two steps (Scheme 1). First, condensation of malonic acid derivatives **3** with optically active amino alcohols **2** gives dihydroxymalondiamides **4**. This is followed by activation of the hydroxyl groups and cyclization to form bisoxazolines **5**. Various activation agents have been used to effect the ring closures.^{2,4}

Scheme 1



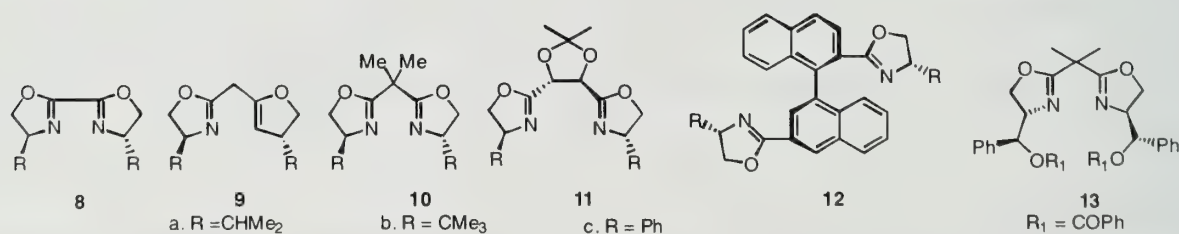
Masamune et al.^{5a} demonstrated the utility of bis(oxazoline)-Cu complexes in the cyclopropanation of styrene with ethyl diazoacetate (eq 1). Among several complexes evaluated, **6** gave

the best results. Enantioselectivities were also affected by the diazoacetate substituents. (–) – Menthyl diazoacetate gave better results than ethyl or *t*-butyl diazoacetates. Catalysts derived from **6** afforded good diastereo- and enantioselectivity for a variety of mono-substituted, *trans*-disubstituted and terminal disubstituted olefins. Masamune et al. subsequently further modified the bisoxazoline ligand for enantioselective cyclopropanation of trisubstituted and unsymmetrical *cis*-disubstituted olefins.^{5b} For instance, a chrysanthemate derivative was synthesized from 2,5-dimethyl-2,4-hexathene in the presence of **7**•Cu(I)OTf with excellent stereoselectivity (eq 2).



In these transformations, the catalyst is believed to react with the alkyl diazoacetate to form a metal-carbene complex, and subsequent olefin attack results in product formation. Steric interactions between the substituents of the ligand and the carboxy group of the carbenoid intermediate determine the approach of the olefin and hence the stereochemical outcome of the reaction.^{2a}

Evans et al. treated **8**, **9**, and **10** with CuOTf to prepare complexes for cyclopropanation catalysis.^{6,7} Poor enantioselectivity was obtained for Cu(I)•**8**, which suggested that six- rather than five-membered chelates are preferred for effective catalysis. The geminal methyl groups in **10** prevented enolization, and ligand **10b** afforded the best selectivities. Reaction of styrene with diazoacetate in the presence of 1 mol% Cu(I)•**10b** afforded the *trans*- and *cis*- isomers in a ratio of 74 : 26, with >99% ee for each isomer.

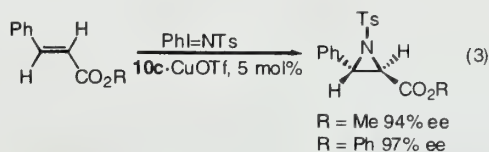


A variety of other bis(oxazoline) ligands have also been developed. Andersson et al.⁸ designed a series of bisoxazoline ligands **11** that form seven-membered chelation complexes with Cu(I). It was found that **11a** gave better asymmetric induction than **10a**, but was inferior to **10b**. Hayashi et al.⁹

prepared ligands **12**, which possess both axial chirality and carbon centered chirality. Catalysts derived from **12a** afforded 2-(phenyl)cyclopropanecarboxylate in up to 97% ee. Balavoine et al.¹⁰ introduced asymmetric centers on the side chains of bisoxazoline rings **13**, however stereoselectivity did not improve significantly.

AZIRIDINATION

Evans et al. first demonstrated that C₂-symmetric (bisoxazoline)-Cu complexes catalyzed the aziridination of olefins with (*N*-(*p*-toluenesulfonyl)imino)phenyliodinane,



PhI=NTs (eq 3).¹¹ Aryl-substituted olefins were found to be

suitable substrates. Complexes based on phenyl-substituted ligand **10c** catalyzed the aziridination of cinnamate esters with good enantioselectivity (up to 97% ee) in benzene. Reactions mediated by bis(oxazoline) complexes of CuCl and CuBr were very slow and poorly enantioselective. Counterions such as OTf⁻ and SbF₆⁻ were necessary for efficient asymmetric induction. Jacobsen et al. studied the aziridination of imines with diazocarbonyl compounds catalyzed by C₂-symmetric bis(oxazoline)-Cu complexes.¹² In general the yields and enantioselectivities were low.

DIELS-ALDER REACTIONS

Corey et al. first demonstrated that Fe(III) and Mg(II) complexes with C₂-symmetric bis(oxazoline) ligands are promising chiral Lewis acid catalysts for the Diels-Alder reaction of unsubstituted acrylimides.¹³ Subsequently, Evans et al. reported the utility of C₂-symmetric bis(oxazoline)-Cu(II) complexes as Lewis acids in enantioselective Diels-Alder reactions.¹⁴ Catalysts derived from ligand **10b** (*t*-Bu-Box) gave the best stereoselectivity (Table 1). A square-planar bis(oxazoline)-Cu(II)-dienophile complex **15** was proposed to rationalize the observed stereoselectivity.

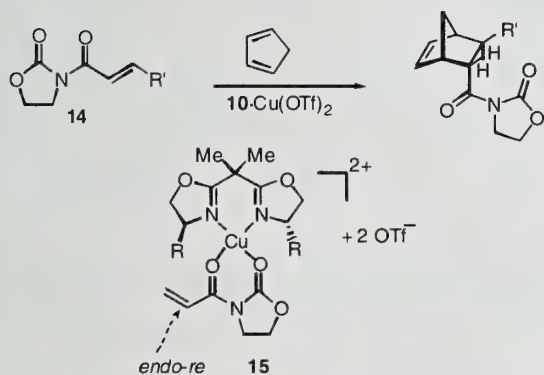


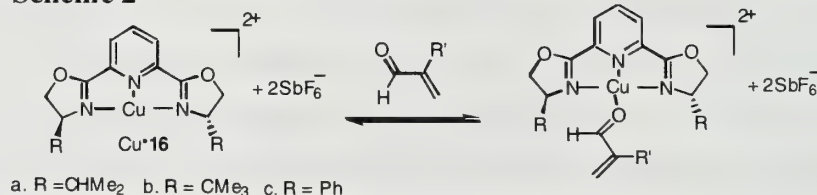
Table 1. Enantioselective Diels-Alder Reactions of Imides with Cyclopentadiene

14, R'	10, R	yield (%)	endo : exo	endo ee (%)
H	Ph	92	95 : 5	30
H	CHMe ₂	93	96 : 4	58
H	CMe ₃	86	98 : 2	>98
Me	CMe ₃	85	96 : 4	97
Ph	CMe ₃	85	90 : 10	90
CO ₂ Et	CMe ₃	92	94 : 6	95

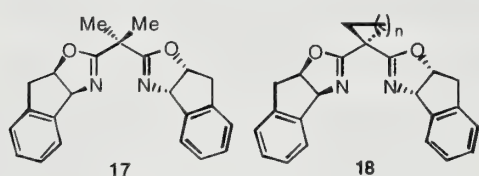
Double stereodifferentiating experiments using the enantiomeric chiral imides were performed.¹⁴ In the stereochemically matched case, the reaction proceeded to completion with undiminished stereoselectivity, while in the mismatched case the reaction proceeded slowly with very low diastereoselectivity. These results supported the square-planar geometry of the metal center.

The tridentate bis(oxazoliny)pyridine ligands **16** (pybox) were developed and applied to Diels-Alder reaction.¹⁵ Cu(II)(pybox) complexes were thought to adopt a square-planar coordination geometry with a single accessible coordination site for carboxyl-derived dienophiles such as α,β -unsaturated aldehydes (Scheme 2). The cycloaddition of methacrolein with cyclopentadiene catalyzed by (pybox)Cu(OTf)₂ afforded good diastereoselectivity (*exo* : *endo* = 96 : 4) and enantioselectivity (*exo* product: 85% ee). Counterion effect was observed and the SbF₆⁻ counterion gave the best results.

Scheme 2



Evans compared the cationic Lewis acidic Cu(II) and Zn(II) catalysts derived from box and pybox ligands.¹⁶ X-ray crystal structures demonstrated that the Cu(II)(box) and Zn(II)(box) complexes adopted square planar and tetrahedral geometries, respectively. Copper complexes were effective catalysts over a wide range of temperatures and were more effective in both enantioselection (>98% ee vs. 92% ee) and rate acceleration (4 h vs. 8 h for complete conversion).



Gosh et al.¹⁷ and Davies et al.¹⁸ both developed an Inda-box **17** and studied its complex with Cu(OTf)₂ in the Diels-Alder reaction of cyclopentadiene and substituted α,β -unsaturated *N*-oxazolidinones. Good enantioselectivities

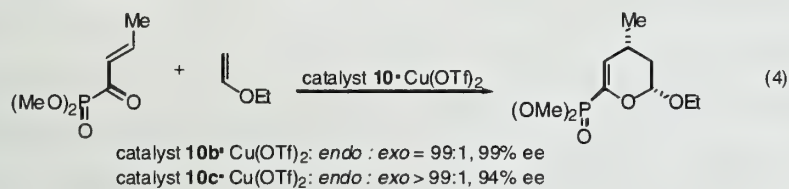
(92-99% ee) were achieved. Davies et al. synthesized spirocyclic bis(oxazoline) ligands **18** and proposed that a larger bite angle (*n* is smaller) gave higher diastereo- and enantioselectivities.¹⁸

HETERO DIELS-ALDER REACTIONS

Chiral Lewis acid catalyzed hetero Diels-Alder reactions between aldehydes and dienes are of particular interest as the resulting cycloadducts are potential synthetic intermediates of a variety of natural products. Jørgensen et al. used C₂-symmetric bis(oxazoline)-Cu(II) complexes to catalyze the

reaction of glyoxylate esters and dienes.²⁰ It was noted that the catalysts derived from (*R,R*)-**10c** and (*S,S*)-**10b** gave the same product. As glyoxylate esters are assumed to form bidentate complexed with both of these bis(oxazoline)-Cu(II) complexes, Jörgenson proposed that (*S,S*)-**10b** adopts square planar geometry at the copper center, while for (*R,R*)-**10c** the geometry is tetrahedral.

Evans et al.²¹ reported that α,β -unsaturated acyl phosphonates undergo enantioselective hetero Diels-Alder reactions with enol ethers in the presence of **10b**•Cu(II) and **10c**•Cu(II) complexes (eq 4). Complexation between the vicinal C=O and P=O was thought to afford the observed asymmetric induction. As observed by Jörgensen, (*R,R*)-**10c**•Cu(OTf)₂ and (*S,S*)-**10b**•Cu(OTf)₂ provided the same stereochemistry of product with high enantioselectivity in both cases. A trigonal pyramidal geometry was proposed for the copper center in **10c**•Cu(OTf)₂ rather than Jörgensen's proposed tetrahedral geometry. According to the authors,²² a tetrahedral Cu(II)-substrate complex is unlikely because there is a high barrier for the square planar to tetrahedral distortion for Cu(II) complexes, while trigonal pyramidal four-coordinate Cu(II) geometry does occur with some frequency.

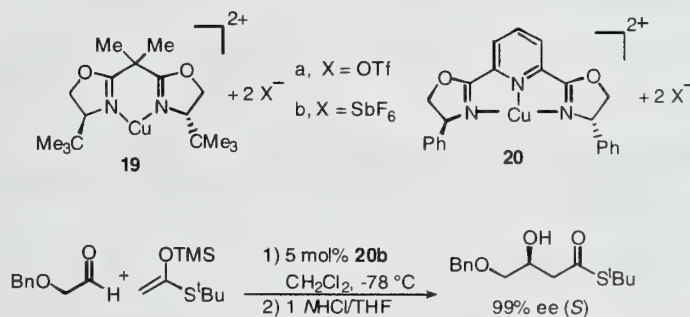


An X-ray structure was obtained for [Cu(OTf)-(H₂O)₂[(*S,S*)-*t*-Bu-box]](OTf).²³ A distorted square pyramidal geometry was revealed, with one of the triflate ligands weakly bound to the metal center in the apical position and the two water molecules occupying the equatorial positions. This observation provided support for the square planar model proposed by Jörgensen and Evans.

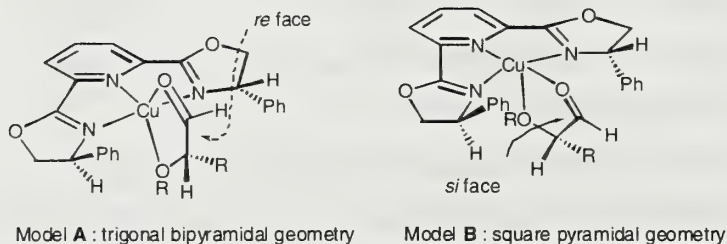
ALDOL ADDITION REACTIONS

Evans et al. applied Cu(II) box and pybox complexes in Mukaiyama aldol reaction of (benzyloxy)acetaldehyde with silylketene acetals (Scheme 3). (*t*-Bu-box)-Cu **19** and (Ph-pybox)-Cu **20** both proved to be highly enantioselective.²⁴ High selectivity was restricted to (benzyloxy)acetaldehyde, suggesting that chelation with the catalyst is required.

Scheme 3

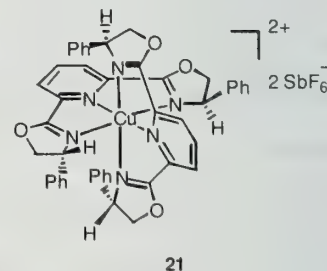


Scheme 4



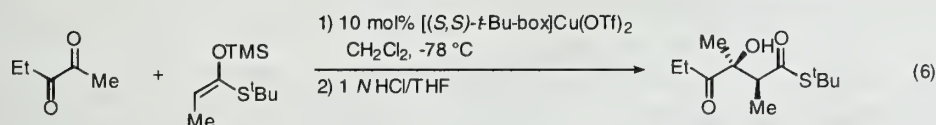
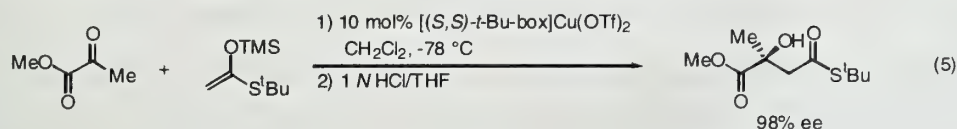
while the *re* face is exposed to nucleophilic attack. In the square pyramidal complex **B**, the *re* face is masked, leaving the *si* face exposed. As the (*S*)-enantiomer of hydroxy esters (*si* facial attack) is preferably obtained, the square pyramidal coordination model **B** is consistent with the observations. Double stereodifferentiating experiments with (*R*)- and (*S*)- α -(benzyloxy)propionaldehyde were conducted and further supported the square pyramidal model. An X-ray crystal structure of (benzyloxy)acetaldehyde bound to the catalyst was obtained and a square pyramidal geometry was observed. A face-to-face π - π interaction was hypothesized to play an important organizational role in the assembly of the catalyst-substrate complex. The ESI spectrum of [Cu(Ph-pybox)-(BnOCH₂CHO)](SbF₆)₂ affirmed the presence of a doubly charged catalyst-substrate complex [Cu(Ph-pybox)-(BnOCH₂CHO)]²⁺ in solution. The EPR spectrum also indicated that the copper geometry is square pyramidal in solution.

Nonlinear effects can provide insight into the enantioselective catalyst systems and the mechanisms of the reactions they mediate.²⁵ In the (Ph-pybox)-Cu complex catalyzed enantioselective aldol additions of enolsilanes to (benzyloxy)acetaldehyde, a positive nonlinear effect was observed.^{24b} For example, employment of a catalyst of 25% ee (*S,S*) afforded the aldol adduct in 74% ee (*S*). It was proposed that the ligands and copper can form both heterodimer [Cu((*S,S*)-Ph-pybox)((*R,R*)-Ph-pybox)](SbF₆)₂ **21** and homodimer [Cu((*S,S*)-Ph-pybox)₂](SbF₆)₂. Crystal structures of heterodimer and homodimer and semiempirical calculations demonstrated that the former was thermodynamically more stable. In a catalyst system that (*S,S*) ligand was in excess, the heterodimer **21** was preferably formed, serving as a catalytically inactive reservoir for the minor (*R,R*)-Ph-pybox ligand and consequently enriching the remaining [Cu((*S,S*)-Ph-pybox)](SbF₆)₂ catalyst.



Evans and co-workers studied the C₂-symmetric bis(oxazoline)-Cu(II) complexes as chiral Lewis acids in the enantioselective aldol addition of enolsilanes to pyruvate esters (eq 5).²⁶ [Cu(*S,S*)-*t*-Bu-

box)](OTf)₂ catalyzed the reaction in 93 to 99% ee. For substituted silylketene acetals, syn diastereoselectivity ranged from 90:10 to 98:2, and enantioselectivity ranged from 93 to 98% ee. A square planar geometry was proposed for the coordination of catalyst and the substrate to explain the observed asymmetric induction. EPR spectroscopic studies of the complexes in solution provided evidence for the assumption. The syn selectivity of the substituted silylketene acetals was rationalized by attack of the acetal on the square pyramidal Cu(II)-aldehyde complex via an open transition state. High levels of carbonyl regioselectivity (98:2), diastereoselectivity (93:7), and enantioselectivity (97% ee) were also observed in the aldol addition to 2,3-pentanedione (eq 6).



CONCLUSION

C₂-symmetric bis(oxazoline)-copper complexes have been applied to a variety of asymmetric reactions with good to excellent diastereoselectivity and enantioselectivity. The unifying motif is that the substrate undergoes activation by chelating to the chiral complexes, which affords a catalyst-substrate geometry that accounts for the asymmetric induction. Further investigation into the mechanism of the catalyzed reactions may pave the way to improve the existing catalytic systems and aid in the search for new catalysts for asymmetric synthesis.

REFERENCES:

- (1) Ghosh, A. K.; Mathivanan, P.; Cappiello, J. *Tetrahedron: Asymmetry* **1998**, 9, 1.
- (2) (a) Pfaltz, A. *Chimia* **1990**, 44, 202; (b) Pfaltz, A. *Acc. Chem. Res.* **1993**, 26, 339.
- (3) Kagan, H. B.; Dang, T.-P. *J. Am. Chem. Soc.* **1972**, 94, 6429.
- (4) (a) Denmark, S. E.; Nakajima, N.; Nicaise, J.-C.; Faucher, A. M.; Edwards, J. P. *J. Org. Chem.* **1995**, 60, 4884. (b) Evans, D. A.; Peterson, G. S.; Johnson, J. S.; Barnes, D. M.; Campos, K. R.; Woerpel, K. A. *J. Org. Chem.* **1998**, 63, 4541.
- (5) (a) Lowenthal, R. E.; Abiko, A.; Masamune, S. *Tetrahedron Lett.* **1990**, 31, 6005. (b) Lowenthal, R. E.; Masamune, S. *Tetrahedron Lett.* **1991**, 32, 7373.
- (6) Evans, D. A.; Woerpel, K. A.; Hinman, M. M.; Faul, M. M. *J. Am. Chem. Soc.* **1991**, 113, 726.
- (7) Evans, D. A.; Woerpel, K. A.; Scott, M. J. *Angew. Chem., Int. Ed. Engl.* **1992**, 31, 430.

- (8) Bedekar, A. V.; Koroleva, E. G.; Andersson, P. G. *J. Org. Chem.* **1997**, *62*, 2518.
- (9) Uozumi, Y.; Kyota, H.; Kishi, E.; Kitayama, K.; Hayashi, T. *Tetrahedron: Asymmetry*, **1996**, *7*, 1603.
- (10) Hoarau, O.; Ait-Haddou, H.; Castro, M.; Balavoine, G. G. A. *Tetrahedron: Asymmetry*, **1997**, *8*, 3755.
- (11) (a) Evans, D. A.; Faul, M. M.; Bilodeau, M. T.; Anderson, B. A.; Barnes, D. M. *J. Am. Chem. Soc.* **1993**, *115*, 5328. (b) Evans, D. A.; Faul, M. M.; Bilodeau, M. T. *J. Am. Chem. Soc.* **1994**, *116*, 2742.
- (12) Hansen, K. B.; Finney, N. S.; Jacobsen, E. N. *Angew. Chem., Int. Ed. Engl.* **1995**, *34*, 676.
- (13) (a) Corey, E. J.; Imai, N.; Zhang, H.-Y. *J. Am. Chem. Soc.* **1991**, *113*, 728. (b) Corey, E. J.; Ishihara, K. *Tetrahedron Lett.* **1992**, *33*, 6807.
- (14) Evans, D. A.; Miller, S. J.; Lectka, T. *J. Am. Chem. Soc.* **1993**, *115*, 6460.
- (15) Evans, D. A.; Murry, J. A.; von Matt, P.; Norcross, R. D.; Miller, S. J. *Angew. Chem., Int. Ed. Engl.* **1995**, *34*, 798.
- (16) Evans, D. A.; Kozlowski, M. C. Tedrow, J. S. *Tetrahedron Lett.* **1996**, *37*, 7481.
- (17) Ghosh, A. K.; Mathivanan, P.; Cappiello, J. *Tetrahedron Lett.* **1996**, *37*, 3815.
- (18) (a) Davies, I. W.; Senanayake, C. H.; Larsen, R. D.; Verhoeven, T. R.; Reider, P. J. *Tetrahedron Lett.* **1996**, *37*, 1725. (b) Davies, I. W.; Gerena, L.; Cai, D.; Larsen, R. D.; Verhoeven, T. R.; Reider, P. J. *Tetrahedron Lett.* **1997**, *38*, 1145.
- (19) (a) Evans, D. A.; Johnson, J. S. *J. Org. Chem.* **1997**, *62*, 786. (b) Evans, D. A.; Shaughnessy, E. A.; Barnes, D. M. *Tetrahedron Lett.* **1997**, *38*, 3193.
- (20) Johannsen, M.; Jorgensen, K. A. *J. Org. Chem.* **1995**, *60*, 5757.
- (21) Evans, D. A.; Johnson, J. S. *J. Am. Chem. Soc.* **1998**, *120*, 4895.
- (22) Evans, D. A.; Burgey, C. S.; Paras, N. A.; Vojkovsky, T.; Tregay, W. *J. Am. Chem. Soc.* **1998**, *120*, 5824.
- (23) Evans, D. A.; Olhava, E. J.; Hohnson, J. S.; Janey, J. M. *Angew. Chem., Int. Ed. Engl.* **1998**, *37*, 3372.
- (24) (a) Evans, D. A.; Murry, J. A.; Kozlowski, M. C. *J. Am. Chem. Soc.* **1996**, *118*, 5814. (b) Evans, D. A.; Kozlowski, M. C.; Murry, J. A.; Burgey, C. S.; Campos, K. R.; Connell, B. T.; Staples, R. J. *J. Am. Chem. Soc.* **1999**, *121*, 669.
- (25) Girard, D.; Kagan, H. B. *Angew. Chem., Int. Ed. Engl.* **1998**, *37*, 2922.
- (26) (a) Evans, D. A.; Kozlowski, M. C.; Burgey, C. S.; MacMillan, D. W. C. *J. Am. Chem. Soc.* **1997**, *119*, 7894. (b) Evans, D. A.; Burgey, C. S.; Kozlowski, M. C.; Tregay, S. W. *J. Am. Chem. Soc.* **1999**, *121*, 686.

POLYMERIZATION OF PRE-ORDERED MONOMERS IN LIQUID CRYSTALLINE PHASE

Reported by Yuguo Ma

April 5, 1999

INTRODUCTION

Polymers are commonly understood to be large molecules comprised of repeating units connected by covalent bonds usually formed through polymerization reactions.¹ Polymerization of pre-ordered monomers is a promising new technique to achieve a high degree of control over the polymerization processes and this can result in a suitable rate of polymerization (RP) and degree of polymerization (DP). The pre-ordering of the polymerizable monomers can be achieved by both chemical and physical methods.²⁻⁵ Free-radical polymerization in liquid crystalline (LC) phases⁶ is an important method that has been recently used to achieve this goal.

The liquid crystalline state is a phase between solid and liquid, and has characteristics of both. The four classes of liquid crystals are known as nematic, cholesteric, smectic, and discotic phases. In addition, several sub-classes of the smectic and discotic types are known. The molecules which show nematic, cholesteric and smectic phases are in general rod-shaped, while discogens are plate-like in structure. These phases all show some degree of order in molecular packing and macroscopic anisotropic properties. A representation of the molecular packing of each class of liquid crystals is shown in Figure 1. Another way in which liquid crystals can be classified is according to whether they

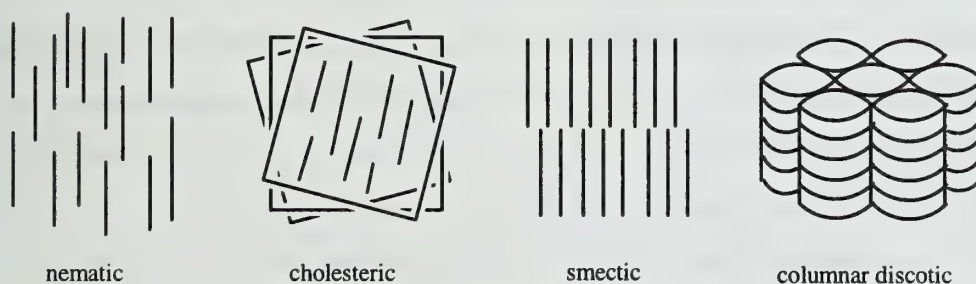


Figure 1. Representation of the molecular shapes and orientations of the major LC phase types.

are thermotropic or lyotropic. Thermotropic liquid crystals are those which show their mesomorphism in response to a change in temperature whereas the lyotropic mesomorphic state is solvent induced.⁷ This report will discuss polymerization of pre-ordered monomers in both thermotropic and lyotropic LC phases.

POLYMERIZATION IN THERMOTROPIC LIQUID CRYSTALLINE PHASE

Kinetic Studies

The mechanism and kinetics of a polymerization may change significantly when it occurs in LC phases because of the changes in diffusion, mobility and packing of monomers and growing polymer chains. Previously, there have been a number of reports describing the kinetics of polymerization of liquid crystalline monomers and reports of monomers dispersed in liquid crystalline media.⁸ However, it is difficult to make simple generalizations about the effects of the liquid crystalline media on factors such as the rate of polymerization or polymer molecular weight. These difficulties may be a consequence of the fact that growing chains can segregate themselves from an ordered host phase beyond a certain point in their polymerization. Further polymerization then occurs in a much more disordered environment.

Because free-radical polymerization is characterized by initiation, propagation, and termination rate processes, any attempt to define the effect of the medium must take into account their individual rate constants as functions of the change in medium and percent conversion. Equation 1 describes the kinetics of a standard free-radical polymerization process:

$$R_p = \frac{k_p}{k_t^{1/2}} [M](R_i/2)^{1/2} \quad (1)$$
 R_p is the rate of polymerization and R_i is the rate of initiation. R_i is assumed not to undergo an apparent change by transferring the reaction from isotropic to anisotropic phase. The terms k_p and k_t are the propagation and termination rate constants, respectively.

Hoyle and coworkers studied the kinetics of the photoinitiated polymerization of a cholesteryl-bearing methacrylate (CMA-10). The phase diagram for CMA-10 and polymers are shown in Figure 2. The effect of the liquid crystalline phase on the polymerization kinetics was evaluated by selecting temperatures at which the polymerization was conducted either completely in a smectic phase (45 °C) or initially in an isotropic phase followed by conversion to a biphasic medium (80 °C) (Figure 2).

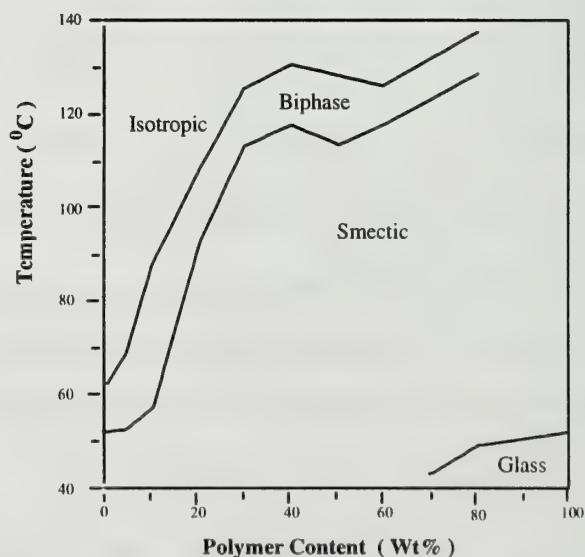
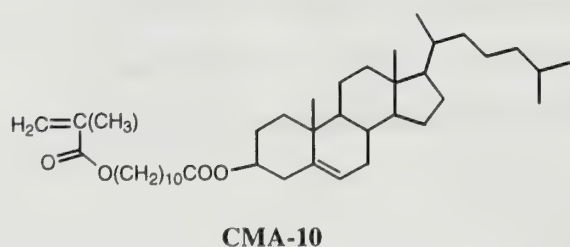
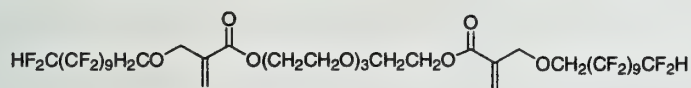


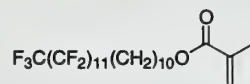
Figure 2. Phase diagram for CMA-10 monomer and CMA-10 polymer.

It was found that the values for k_t are much lower in the smectic phase at 45 °C than in the isotropic phase at 80 °C, but only a modest decrease in k_p in the smectic phase at 45 °C was observed compared to 80 °C. The large drop in k_t compared to k_p results in an enhancement of the rate of polymerization.⁹ The results are in accord with the supposition that LC media can affect the individual kinetic rate constant of polymerization. The accelerated polymerization rate corresponded to the changes in the medium order. Further evidence for a drop in k_t was obtained when the molecular weights were examined for pulse-laser-initiated polymerization of LC monomers.¹⁰ In the case of polymerization in the isotropic phase, the molecular weight and the yield of the generated polymer decreased with a decrease in time between firing of individual laser pulses. However, polymerization in the smectic phase of the monomer was not affected by the laser repetition rate. It is postulated that for pulse-laser-initiated polymerization in the smectic phase, the normally rapid termination process in isotropic solution, involving coupling of primary and short chain oligomeric radicals with growing polymeric radicals is greatly reduced.

In another case of photoinitiated polymerization of a semifluorinated difunctional monomer **1**, the observation that the polymer chain kinetic lifetime was markedly longer in the smectic phase gives further support for decreased termination rates, although the maximum rate attained for photoinitiated polymerization in the smectic phase is lower than that in the isotropic phase.¹¹



1



F12H10MA

Compared with the polymerization of single double bond monomer F12H10MA¹² which has an enhanced R_p , it is postulated that the k_p , just like k_t , is also “diffusion controlled”.¹ Thus the rate constant k_p decreases with an increase in the viscosity of the system. Combined with the highly hindered radical-forming site, k_p decreases faster than k_t . Therefore there is a decrease in R_p . Since compound **1** is a difunctional monomer that has two double bonds in its structure, a “reaction diffusion controlled termination mechanism”¹ which couples the termination and propagation processes in the photoinitiated polymerization of isotropic difunctional monomers,¹³ is also possible.

All of these cases show a drop in k_t and k_p in the LC phase polymerization. When k_t decreases quickly, and k_p decreases only slightly, the overall R_p increases. When k_p decreases faster than k_t , R_p decreases. One might wonder if this is true for all LC phase polymerization? Bowman and coworkers studied the polymerization behavior and its kinetics during the formation of polymer-stabilized ferroelectric liquid crystals,^{6,14,15,18} and their results show that the effects are not always the same. The

chemical structure of the acrylate monomers (HDDA and C6M) and ferroelectric liquid crystals (FLC) that were used as media (1:1 mixture of W7 and W82) are shown in Figure 3. In their studies, polymerization rate profiles and double bond conversions were monitored at different temperatures and in different liquid crystal phases. As the ordering of the media increased, the polymerization rates increased dramatically for all the monomers studied, despite a large decrease in temperature. To understand the mechanism of this behavior, the rate constants of both termination and propagation processes were determined.

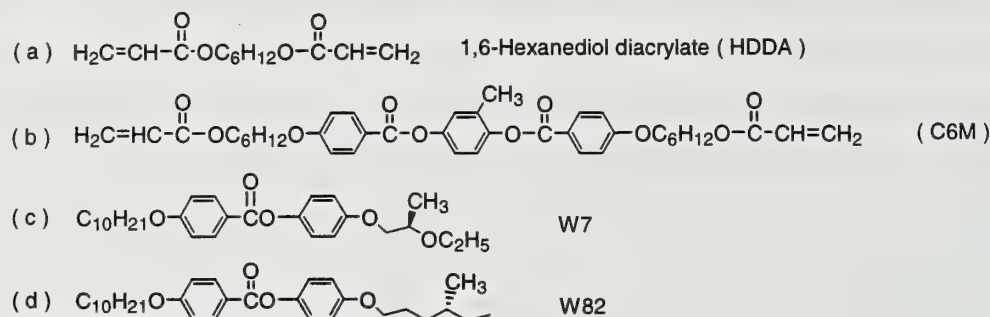


Figure 3. Chemical structure of the acrylate monomers and ferroelectric LCs

Interestingly, for HDDA (Figure 3), termination rates were reduced, whereas for C6M. Both the termination and propagation rates were increased. This altered polymerization behavior was attributed to segregation of the monomer in the liquid crystal. Support for this segregation has been obtained by using polarized infrared spectroscopy and X-ray diffraction. A model was proposed to explain the segregation of the monomers (Figure 4). The HDDA monomers were suggested to segregate between the LC smectic layers giving an increase of layer spacing. The C6M monomers, on the other hand, were proposed to segregate within the smectic layers and align with the LC molecules. In the HDDA case, k_p depended little on the phase or temperature; however, k_t was almost an order of magnitude lower in the Sc^* (a sub-class of smectic) phase. Thus, a reduced k_t leads to higher radical concentrations and a higher polymerization rate. In contrast, for C6M polymerization, k_p and k_t are almost an order of magnitude greater in the Sc^* phase than in the isotropic phase. As the rate of polymerization is dependent on k_p to the first power and only dependent on k_t to the negative one-half power (eq. 1), a similar increase in both constants will result in an increase in the overall rate. The increase in k_p and k_t is probably due to an anisotropic distribution of both radicals and double bonds. If the reactive double bonds are concentrated in a reduced volume such as proposed in Fig. 4, then the effective concentration of the double bonds, as well as the radicals, is much higher than the bulk concentration. This result leads to an increase in the apparent k_p and k_t .

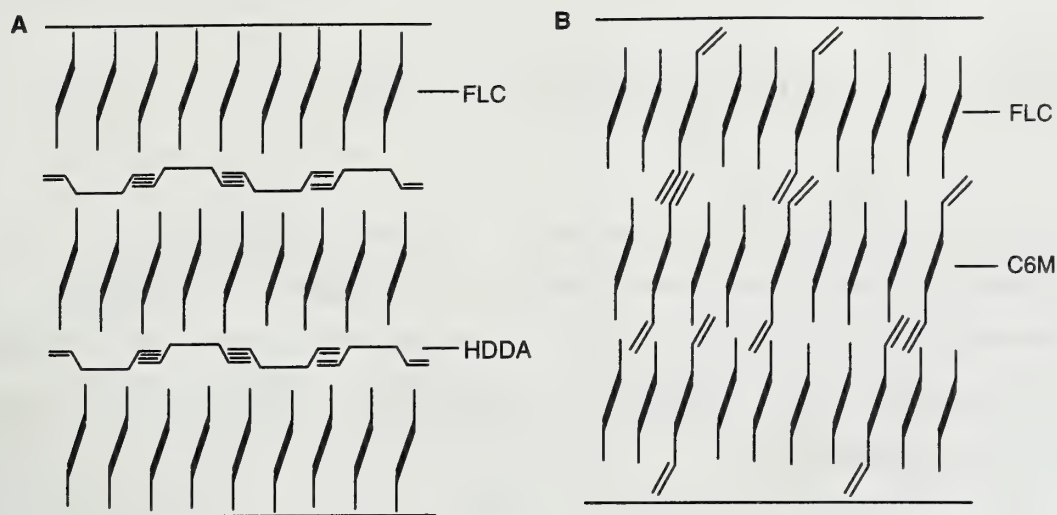


Figure 4. proposed models for the segregation of (A) HDDA and (B) C6M in W7/W82

To further understand the reason for changes in the individual rate constant, Bowman and coworkers developed a kinetic model¹⁵ that correlates the rate constant with the volume reduction caused by monomer segregation. Based on this model, they predicted a change in propagation as well as termination rate constants and modeled the change in overall polymerization rate with time. The predictions agree reasonably well with the experimental results.

Applications

Liquid crystal polymers have many applications resulting from anisotropic physical and optical properties. The pre-orientation of LC monomers, followed by polymerization, can produce materials with improved mechanical properties that can be applied to polymer films. For instance, since the orientation of monomers can be kept after the polymerization, an oriented film can be produced. Hoyle and coworkers prepared thin polymer films by photopolymerization of LC mixtures composed of a difunctional (two double bonds per monomer) and two monofunctional monomers oriented either by contacting with unidirectionally rubbed polyimide films or by application of a low power magnetic field.¹⁶ In both cases, the orientation of the LC monomers was maintained after polymerization.

Another application of polymerization of pre-ordered monomers in LC phases is the production of polymer-LC composites, for example, polymer-stabilized LCs (PSLCs). Hikmet et al¹⁷ and Bowman et al¹⁸ successfully made an "anisotropic gel" by polymerization of monomers in non-reactive ferroelectric LC materials. The orientation of monomers is also maintained to a large extent after polymerization. Furthermore, Hikmet's anisotropic gel does not change the uniaxial orientation of molecules. However, in Hoyle's oriented film, heat changes the orientation.

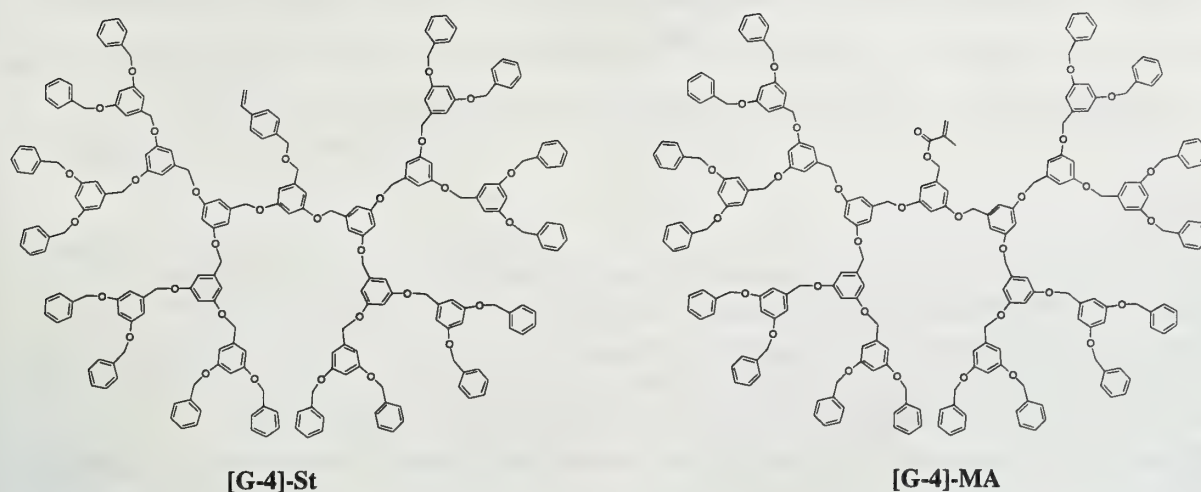
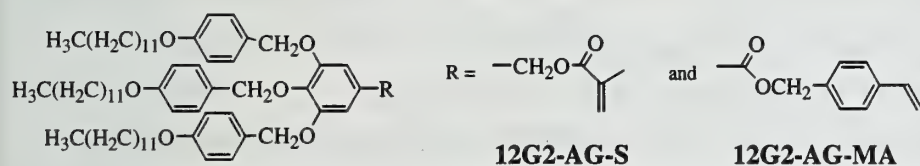


Figure 5. Structure of macromonomers containing styrenyl ([G-4]-St) and methacryloyl groups ([G-4]-MA).²⁰

Recently, Percec and coworkers reported a self-acceleration of the radical polymerization of 12G2-AG-S and 12G2-AG-MA in the self-assembled state.⁵ A sharp increase was observed for the rate of polymerization of 12G2-AG-S initiated with AIBN at 60 °C with increasing concentration ($[M]_0 > 0.2$ M). The quantity $k_p/k_t^{1/2}$ for the polymerization of 12G2-AG-S and of 12G2-AG-MA was compared with their low molar mass models, styrene (S) and methyl methacrylate (MMA). Under the same conditions, $k_p/k_t^{1/2}$ for 12G2-AG-S and 12G2-AG-MA was more than an order of magnitude higher than the values for S and MMA. It was argued that above a critical $[M]_0$, the dendritic monomers self-assemble in spherical supermolecules which provide a *reactor* that increases the concentration of



polymerizable groups. At DP >20, this reactor becomes cylindrical. In both cases, it resembles a capsule or a

cagelike environment in which the polymerizable groups are jacketed by their own dendritic coat.²⁴⁻²⁶ This environment generates a low k_t and a low initiator efficiency. This combination of effects yields high DP values with very high conversion in a short reaction time by using short half-time initiators like AIBN and $[M]_0 > 0.2$ M. Alternatively, long half-time initiators yield a controlled polymerization.

CONCLUSION

Through a series of studies of polymerization rate and kinetic constants, a greater understanding of the influence of liquid crystalline order on the polymerization process has been achieved. The LC

phase provides a good media to study the kinetics and mechanism of free-radical polymerization. It has been shown that the polymerization of pre-ordered monomers in a LC phase is very useful in the formation of oriented patterns in a polymer film,¹⁶ a phenomenon useful for optical imaging or other applications. Furthermore, this is a very useful method to prepare nanoscale materials.²⁷

REFERENCES

- (1) Ravve, A. *Principles of Polymer Chemistry*; Plenum Press: New York, **1995**; Chapter 1.
- (2) Ramamurthy, V. *Tetrahedron* **1986**, *42*, 5753-5839.
- (3) Fuchs, H.; Ohst, H.; Prass, W. *Adv. Mater.* **1991**, *3*, 10-18.
- (4) Baxter, B. C.; Gin, D. L. *Macromolecules* **1998**, *31*, 4419-4425.
- (5) Percec, V.; Ahn, C.-H.; Barboiu, B. *J. Am. Chem. Soc.* **1997**, *119*, 12978-12979.
- (6) Guyman, C. A.; Hoggan, E. N.; Clark, N. A.; Pieker, T. P.; Walba, D. M.; Bowman, C. N. *Science* **1997**, *275*, 57-59.
- (7) Weiss, R. G. *Tetrahedron* **1988**, *44*, 3413-3475.
- (8) Paleos, C. M. *Chem. Soc. Rev.* **1985**, *14*, 45-67.
- (9) Hoyle, C. E.; Watanabe, T. *Macromolecules* **1994**, *27*, 3790-3796.
- (10) Hoyle, C. E.; Chawla, C. P. *Macromolecules* **1995**, *28*, 1946-1951.
- (11) Hoyle, C. E.; Mathias, L. J.; Jariwala, C.; Sheng, D. *Macromolecules* **1996**, *29*, 3182-3187.
- (12) Hoyle, C. E.; Kang, D.; Jariwala, C.; Griffin, A. C. *Polymer* **1993**, *34*, 3070-3075.
- (13) Anseth, K. S.; Kline, L. M.; Walker, T. A.; Anderson, K. J.; Bowman, C. N. *Macromolecules* **1995**, *28*, 2491-2499.
- (14) Guyman, C. A.; Bowman, C. N. *Macromolecules* **1997**, *30*, 1594-1600.
- (15) Guyman, C. A.; Bowman, C. N. *Macromolecules* **1997**, *30*, 5271-5278.
- (16) Hoyle, C. E.; Watanabe, T.; Whitehead, J. B. *Macromolecules* **1994**, *27*, 6581-6588.
- (17) Hikmet, R. A. M.; Michielsen, M. *Adv. Mater.* **1995**, *7*, 300-304.
- (18) Guyman, C. A.; Shao, R.; Holter, D.; Frey, H.; Clark, N. A.; Bowman, C. N. *Liquid Crystal* **1998**, *24*, 263-270.
- (19) Smith, R. C.; Fischer, W. M.; Gin, D. L. *J. Am. Chem. Soc.* **1997**, *119*, 4092-4093.
- (20) Deng, H.; Gin, D. L.; Smith, R. C. *J. Am. Chem. Soc.* **1998**, *120*, 3522-3523.
- (21) Frechét, J. M. J.; Gitsov, I. *Macromol. Symp.* **1995**, *98*, 441-465.
- (22) Draheim, G.; Ritter, H. *Macromol. Chem. Phys.* **1995**, *196*, 2211-2222.
- (23) Chen, Y. M.; Chen, C. F.; Liu, W. H.; Li, Y. F.; Xi, F. *Macromol. Rapid. Commun.* **1996**, *17*, 401-407.
- (24) Balagurusamy, V. S. K.; Ungar, G.; Percec, V.; Johansson, G. *J. Am. Chem. Soc.* **1997**, *119*, 1539-1555.
- (25) Hudson, S. D.; Jung H. T.; Percec, V.; Cho, W. D.; Johansson, G.; Ungar, G.; Balagurusamy, V. S. K. *Science* **1997**, *278*, 449-452.
- (26) Percec, V.; Ahn, C.-H.; Cho, W.-D.; Jamieson, A. M.; Kim, J.; Leman, T.; Schmidt, M.; Gerle, M.; Moller, M.; Prokhorova, S. A.; Sheiko, S. S.; Cheng, S. Z. D.; Zhang, A.; Ungar, G. D.; Yeardley, D. J. P. *J. Am. Chem. Soc.* **1998**, *120*, 8619-8631.
- (27) Gray, D. H.; Hu, S. L.; Juang, E.; Gin, D. L. *Adv. Mater.* **1997**, *9*, 731-736.

GLYCOSYLATION STRATEGIES TOWARD THE SYNTHESIS OF CARBOHYDRATE LIBRARIES

Reported by Jennifer R. Costerison

April 15, 1999

INTRODUCTION

The use of combinatorial chemistry in the production of structurally diverse compounds has revolutionized the drug discovery process. However, the construction of carbohydrate libraries has gained little attention when compared to other small molecule libraries primarily due to their complex functionality and synthesis.¹ The production of oligosaccharides is important for furthering the understanding of biological processes in which they participate.² Carbohydrates are required for cell surface recognition and communication with protein receptors, which are necessary to control bacterial and viral infections, inflammation, and cancer metastasis.³ The study of these processes have fueled the interest in adapting traditional carbohydrate synthesis to a combinatorial approach.

In contrast to small molecule libraries, the synthesis of oligosaccharides is more complex.¹ With the diversity in carbohydrate monomers and a multitude of possible regioisomeric glycosidic linkages, combinatorial chemistry would be attractive for high-throughput production of many different oligosaccharides. This review will cover various glycosylation strategies for synthesizing oligosaccharide libraries.

BACKGROUND

Traditional glycosylation methodologies require a glycosyl donor, which is appropriately functionalized with a leaving group at the anomeric center, and a glycosyl acceptor, which serves as the nucleophile.⁴ Glycosylation can be performed either in two steps, which requires protecting group manipulations, or in a one step direct exchange reaction. Once the glycosidic bond is formed, the configuration at the anomeric center can be axial (α), or equatorial (β).⁵ Anomeric stereocontrol is dependent on many factors such as reaction conditions, donor activation conditions, and the nature of both the donor and acceptor glycoside.⁵ The most common method of stereocontrol involves neighboring group participation by the proper choice of a protecting group on the C(2) hydroxyl through which 1,2-trans products can be obtained.⁴ In addition to neighboring group participation, other means can be used including steric, electronic, chelation, thermodynamic, and kinetic control. Because of the complexity in formation of the glycosidic bond, many different glycosylation strategies have been employed for the generation of oligosaccharides both in solution and on solid phase.⁴

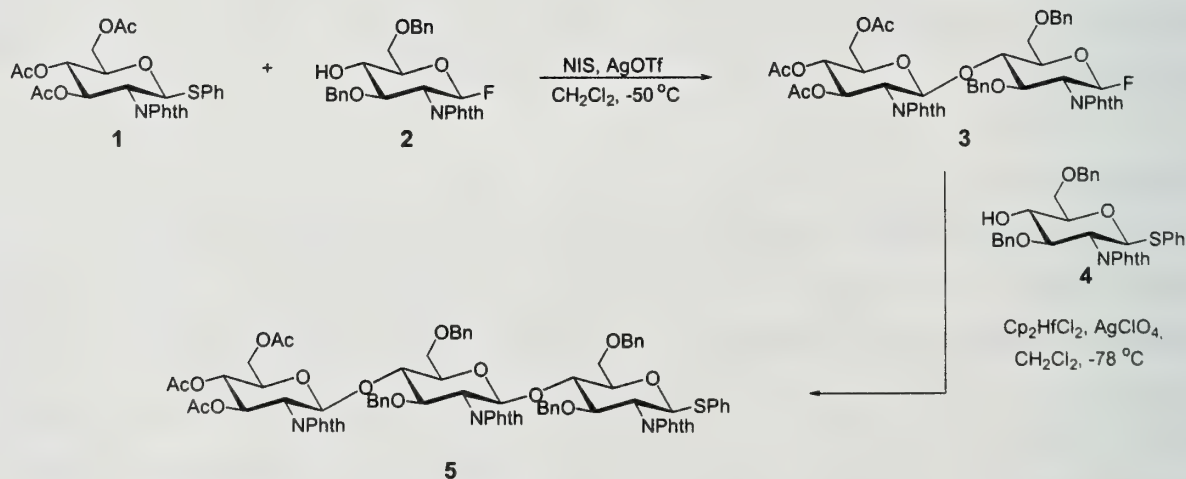
Direct substitution of the free hemiacetal of the glycosyl donor with the desired acceptor using trifluoromethanesulfonic anhydride and diphenyl sulfoxide was reported by Gin and co-workers.⁶ This method allows the *in situ* activation of the glycosyl donor hydroxy group which requires no derivatization prior to glycosylation. This direct dehydrative method of glycosylation is potentially more efficient, but has not been utilized for the synthesis of a carbohydrate library.

The use of glycals as glycosyl donors has been reported by many groups, most extensively by Danishefsky and co-workers.⁷⁻⁹ This methodology has proven successful both in solution and on solid phase. Because the utilization of glycals in glycosylation is an extremely diverse topic, it will not be discussed in this review.

ORTHOGONAL GLYCOSYLATION STRATEGY

One of the most straightforward methods for oligosaccharide synthesis involves the immediate use of glycosylation products as the donor for the next coupling reaction. Such orthogonal glycosylation requires two sets of chemically distinct glycosyl donors and activating conditions that utilize the differential chemical reactivity of the donor sugar, thereby requiring fewer protecting group manipulations.¹⁰

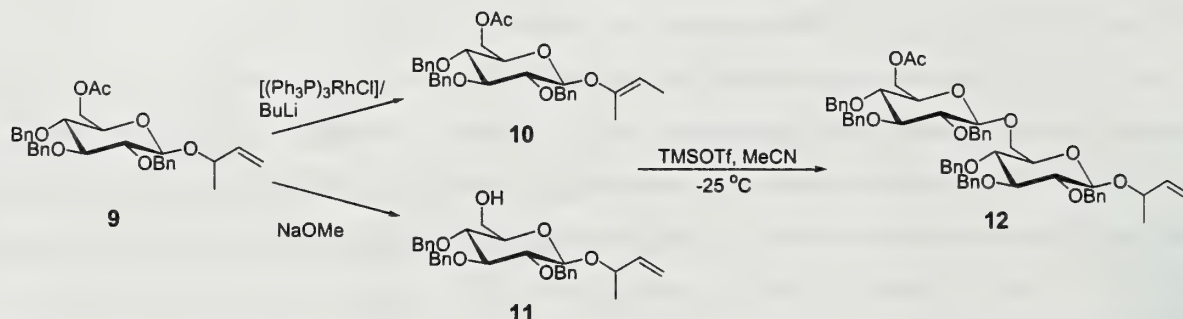
Scheme 1



An example of this strategy was reported by Ito and co-workers (Scheme 1). Thioglycoside **1** was activated by NIS reacted with acceptor **2** to give the disaccharide **3** in 90% yield with no detectable α -anomer produced.¹⁰ To further illustrate the concept of orthogonal glycosylation, disaccharide **3** and another thioglycoside acceptor **4** were coupled to give trisaccharide **5** in 72% yield. To control the configuration at the anomeric center, an *N*-phthaloyl group was employed at the 2-position to induce a 1,2-trans product by neighboring group participation.¹⁰ To substantiate the value of this methodology, a

group was removed and the resulting alcohol was coupled with donor **10** to form the desired trisaccharide.

Scheme 3

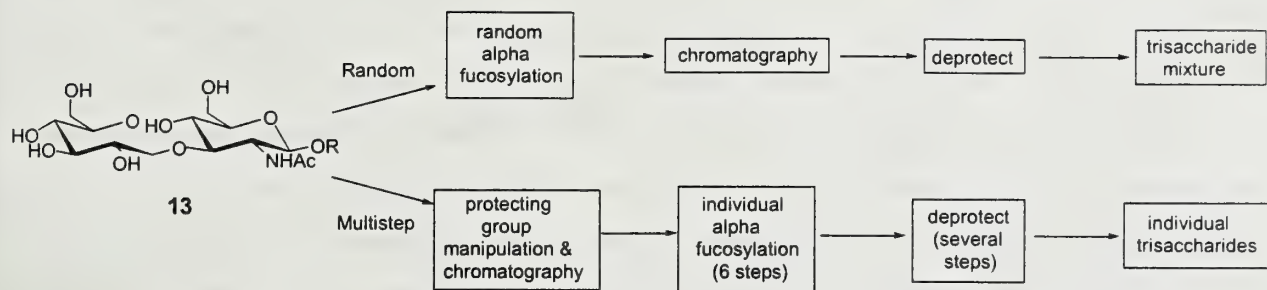


Using the disaccharide mixture, a library of 20 trisaccharides was synthesized after deprotection and coupling as above. The library was purified by gel filtration chromatography and analyzed by FAB MS. The success of this methodology in the generation of a small carbohydrate library suggests that the latent-active glycosylation approach could be applied to the preparation of larger, more diverse libraries.

RANDOM GLYCOSYLATION STRATEGY

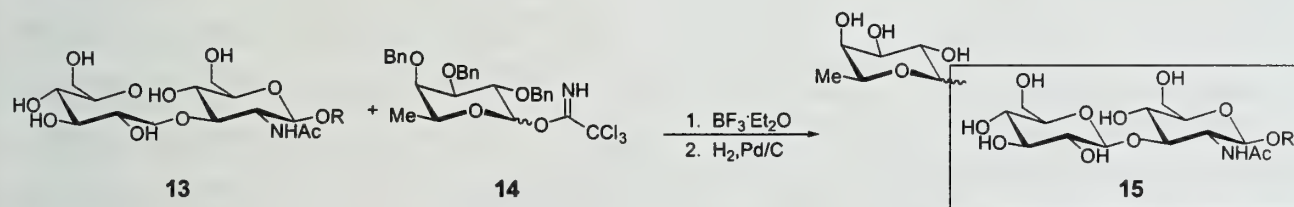
A novel glycosylation strategy involving a fully unprotected glycosyl acceptor was introduced by Hindsgaul.¹⁴ The objective of this approach is to randomly generate large libraries in the solution phase that contain all of the possible trisaccharide products for evaluation in a biological assay. This strategy requires only two steps, glycosylation and deprotection, versus systematic, multistep synthesis involving various protecting group manipulations in parallel synthetic approaches (Figure 1). A product mixture which includes all the possible oligosaccharides in nearly equal amounts must be obtained in order to successfully implement this random methodology.¹⁴ Disaccharide **13** [β Gal(1 \rightarrow *n*) β GlcNAc-OR, where *n* = 3, 4, or 6 and R=(CH₂)₈OC₆H₄*p*-OCH₃] was coupled with tri-*O*-benzylfucopyranosyl trichloroacetimidate (**14**) in DMF in 30% conversion (Scheme 4). After extensive separation, the distribution of trisaccharide products, represented by **15**, was determined by ¹H NMR. The statistical product distribution of the α -fucosylation of trisaccharide **13** is 17% of each disaccharide. The distribution of the isolated isomers was shown to be 12% α (1 \rightarrow 4), 22% α (1 \rightarrow 6), 19% α (1 \rightarrow 2'), 23% α (1 \rightarrow 3'), 8% α (1 \rightarrow 4'), and 16% α (1 \rightarrow 6'). The by-products obtained, which included unreacted disaccharide and over-fucosylated tetrasaccharide, were separated from the desired products using chromatography.

Figure 1



Based on literature precedent,¹⁵ it was assumed that the least hindered primary alcohols, (6-OH or 6'-OH) would be the major glycosylation products, however this was not observed. A possible rationale is since no protecting groups are used on the glycosyl acceptor, no added steric hinderance is observed. Consequently, all the hydroxyl groups show a similar range of reactivity. Random glycosylation offers a direct method which avoids protecting group manipulations.¹ However, there are numerous drawbacks including low conversion, extensive product purification, and substrate-dependent anomer ratios.

Scheme 4

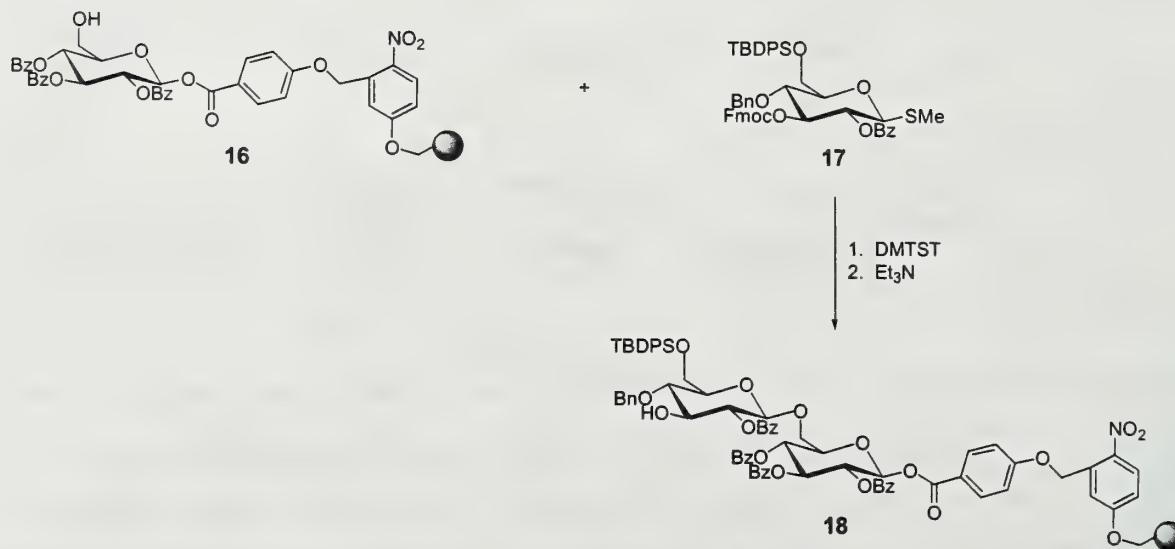


SOLID PHASE SYNTHESIS USING INSOLUBLE POLYMERS

Since the 1970s,¹⁶ there has been much interest in the use of polymer supports generating carbohydrates.⁴ Two distinct methodologies have been developed: use of insoluble polymer supports and soluble polymer supports.¹ Each methodology has advantages, disadvantages, and specific applications.

Many variables can be explored in solid phase synthesis such as the choice of polymer resin, the linker molecules, and the position of the linker. For insoluble polymer synthesis, the most common resin employed is the Merrifield resin and its derivatives. This polystyrene-based resin can be connected directly to the carbohydrate or through a linker molecule.¹

Scheme 5



To demonstrate the solid phase synthesis of an oligosaccharide, Nicolaou and co-workers synthesized a dodecasaccharide using Merrifield resin.¹⁷ The benzoyl protected monosaccharide was attached via a photolabile linker to the resin to afford glycosyl acceptor **16** (Scheme 5). Coupling of **16** to glycosyl donor **17** gave the resin-bound disaccharide **18** in 90% yield with exclusive formation of the β -anomer. In this fashion a 1,3- and 1,6-linked dodecasaccharide was synthesized as a single stereochemical isomer and cleaved from the resin in 10% overall yield from **16**. This relatively high yield results from the addition of excess reagents to drive the reaction to completion. Any excess reagents, byproducts, and impurities can be washed away from the polymer-bound product. Many other authors have used similar strategies for the synthesis of oligosaccharides including Fraiser-Reid,¹⁸ Schmidt,^{19,20} and Kahne.^{21,22}

There are many possible advantages to solid phase strategies such as easy purification and isolation of products, use of coding techniques on the polymer, higher product yields²¹, and high selectivity.²³ The major disadvantage of insoluble polymer resins in carbohydrate synthesis is that glycosylation is extremely substrate specific, which is amplified in the solid phase.¹ Heterogeneous reaction conditions were made more homogeneous through the use of insoluble support covered with soluble material called TentaGel.

Kahne reported a library synthesis using TentaGel resin, which is polyethylene glycol-grafted polystyrene.²⁴ This strategy uses an insoluble support, polystyrene, surrounded by soluble material, polyethylene glycol (PEG), to induce solution phase conditions through better solvation. Kahne and co-workers synthesized approximately 1300 di- and trisaccharides including both α and β anomers. A split and mix strategy was implemented along with chemical tags to encode the reaction history. Six glycosyl

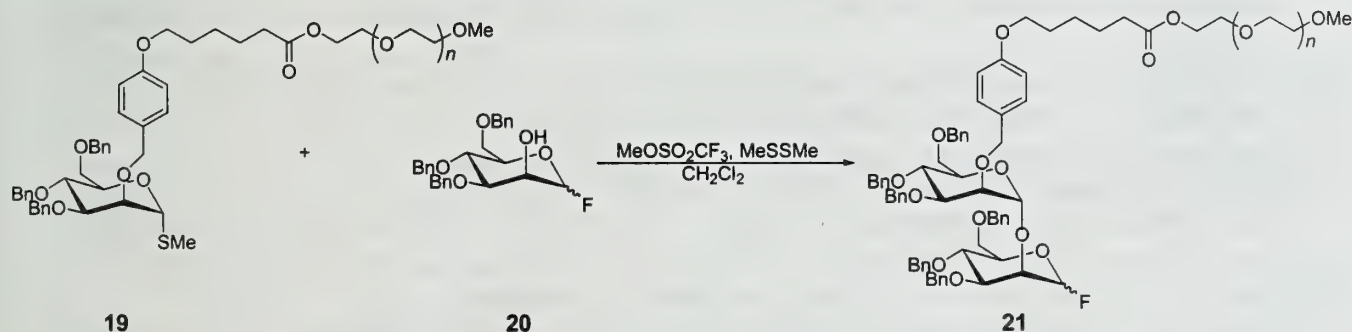
acceptors were attached to TentaGel resin and combined with twelve different sulfoxide donors. The products were *N*-acylated with different acylating reagents to afford the oligosaccharide library. The resin-bound carbohydrate library was screened against *Bauhinia purpurea* lectin and stained with Streptavidin-linked alkaline phosphatase. After a colorimetric assay, the most deeply stained beads were removed and the structure elucidated. It was found that similar core polysaccharides were present which substantiates the specificity of lectin binding and this method of screening. To combine the advantages of both solution and solid phase, a new strategy was implemented using "soluble" solid phase polymers.

SOLID PHASE SYNTHESIS USING SOLUBLE POLYMERS

Polymer-supported solution synthesis involves a reactive substrate bound to a polymer that is soluble in the reaction conditions but insoluble in the work-up conditions.¹ This technique combines the advantages of the solution-like medium of solution phase with the ease of purification and use of coding techniques of solid phase strategies.

An example of this methodology was reported by Ito and co-workers in which PEG was used as soluble support.¹¹ Glycosyl donor **19** was coupled to glycosyl acceptor **20** to give disaccharide **21** in 89% yield with no detectable β -anomer (Scheme 6). Further couplings were used to produce a tetrasaccharide in 42% yield (based on **19**) after cleavage from the resin. All by-products were removed easily by reverse phase chromatography. Slightly different approaches utilizing PEG or MPEG, poly(ethylene glycol) ω -monomethyl ether, support^{25,26} have been reported.

Scheme 6



CONCLUSION

Oligosaccharide synthesis has become an important area because of the many biological processes in which they participate.⁵ The synthesis of carbohydrates is complicated because of the lack of stereo- and chemoselectivity inherent in glycosylation. To further the field of carbohydrate synthesis,

many different approaches to glycosylation that include fewer protecting group manipulations, have been investigated. Random glycosylation achieves the generation of large and diverse carbohydrate libraries in a quick and direct manner. This diversity is beneficial if a biological assay is utilized to screen for protein binding in pharmacological applications. The adaptation of solid phase techniques to carbohydrate synthesis allows for the generation of large libraries of compounds. The use of these resin-bound approaches results in the facile purification and potential on-bead screening, known to be benefits of solid-phase synthesis. More work is needed to further apply a general glycosylation strategy to the solid phase.

REFERENCES

- (1) Wang, Z. G.; Hindsgaul, O. *Glycoimmunology* 2; 1 ed.; Plenum Press: New York, 1998; Vol. 435.
- (2) Ito, Y.; Manabe, S. *Curr. Opin. Chem. Biol.* **1998**, *2*, 701-708.
- (3) Arya, P.; Ben, R. N. *Angew. Chem., Int. Ed. Engl.* **1997**, *36*, 1280-1282.
- (4) Boons, G. J. *Tetrahedron* **1996**, *52*, 1095-1121.
- (5) Sofia, M. J. *Mol. Div.* **1998**, *3*, 75-94.
- (6) Garcia, B. A.; Poole, J. L.; Gin, D. Y. *J. Am. Chem. Soc.* **1997**, *119*, 7597-7598.
- (7) Seeberger, P. H.; Danishefski, S. J. *Acc. Chem. Res.* **1998**, *31*, and references therein.
- (8) Zheng, C.; Seeberger, P. H.; Danishefski, S. J. *J. Org. Chem.* **1998**, *63*, 1126-1130.
- (9) Danishefski, S. J.; McClure, K. F.; Randolph, J. T.; Ruggeri, R. B. *Science* **1993**, *260*, 1307-1309.
- (10) Kanie, O.; Ito, Y.; Ogawa, T. *J. Am. Chem. Soc.* **1994**, *116*, 12073-12074.
- (11) Ito, Y.; Kanie, O.; Ogawa, T. *Angew. Chem., Int. Ed. Engl.* **1996**, *35*, 2510-2512.
- (12) Mootoo, D. R.; Konradsson, P.; Udodong, U.; Fraser-Reid, B. *J. Am. Chem. Soc.* **1988**, *110*, 5583-5584.
- (13) Boons, G.; Heskamp, B.; Hout, F. *Angew. Chem., Int. Ed. Engl.* **1996**, *35*, 2845-2847.
- (14) Kanie, O.; Barresi, F.; Ding, Y.; Labbe, J.; Otter, A.; Forsberg, S.; Ernst, B.; Hindsgaul, O. *Angew. Chem., Int. Ed. Engl.* **1995**, *34*, 2720-2722.
- (15) Schmidt, R. R. *Angew. Chem., Int. Ed. Engl.* **1986**, *25*, 212-233.
- (16) Frechet, J. M.; Schuerch, C. *J. Am. Chem. Soc.* **1972**, *94*, 604-609.
- (17) Nicolaou, K. C.; Watanabe, N.; Li, J.; Pastor, J.; Winssinger, N. *Angew. Chem., Int. Ed.* **1998**, *37*, 1559-1561.
- (18) Rodebaugh, R.; Joshi, S.; Fraser-Reid, B.; Geysen, H. M. *J. Org. Chem.* **1997**, *62*, 5660-5661.
- (19) Rademann, J.; Schmidt, R. R. *J. Org. Chem.* **1997**, *62*, 3650-3653.
- (20) Rademann, J.; Schmidt, R. R. *Tetrahedron Lett.* **1996**, *37*, 3989-3990.
- (21) Liang, R.; Loebach, J.; Horan, N.; Ge, M.; Thompson, C.; Yan, L.; Kahne, D. *Proc. Natl. Acad. Sci. U.S.A.* **1997**, *94*, 10554-10559.
- (22) Yan, L.; Taylor, C. M.; Goodnow, J., R.; Kahne, D. *J. Am. Chem. Soc.* **1994**, *116*, 6953-6954.
- (23) Hunt, J. A.; Roush, W. R. *J. Am. Chem. Soc.* **1996**, *118*, 9998-9999.
- (24) Liang, R.; Yan, L.; Loebach, J.; Ge, M.; Uozumi, Y.; Sekanina, K.; Horan, N.; Gildersleeve, J.; Thompson, C.; Smith, A.; Biswas, K.; Still, W. C.; Kahne, D. *Science* **1996**, *274*, 1520-1522.
- (25) Jiang, L.; Hartley, R.; Chan, T. *Chem. Commun.* **1996**, 2193-2194.
- (26) Douglas, S. P.; Whitfield, D. M.; Krepinsky, J. J. *J. Am. Chem. Soc.* **1995**, *117*, 2116-2117.

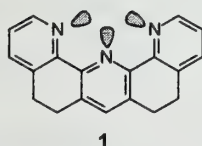
Synthesis and Complexation Properties of Bridged 2,2':6',2'' Terpyridines

Reported by Jeff Vessels

May 6, 1999

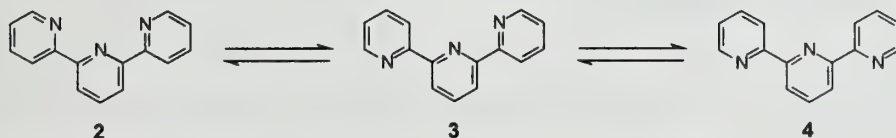
Introduction

Communication in biological systems is performed through molecular recognition. Central to this process are hydrogen bonding arrays in the host and guest molecules. Bridged 2,2':6',2'' terpyridines (**1**) are one class of molecules utilized for the investigation of hydrogen bonding in the field of host-guest chemistry. The importance of these terpyridines is due, in part, to the rigidity of the molecule and the presence of three convergent nonbonding pairs of electrons. As with many investigations of structure-property relationships, the synthesis of the target molecules is a limiting factor. The synthesis of bridged terpyridines and complexation of bridged terpyridines to phosphoric acid diesters, cyclitols, guanine derivatives as well as alkali metals and ruthenium will be discussed in this abstract.



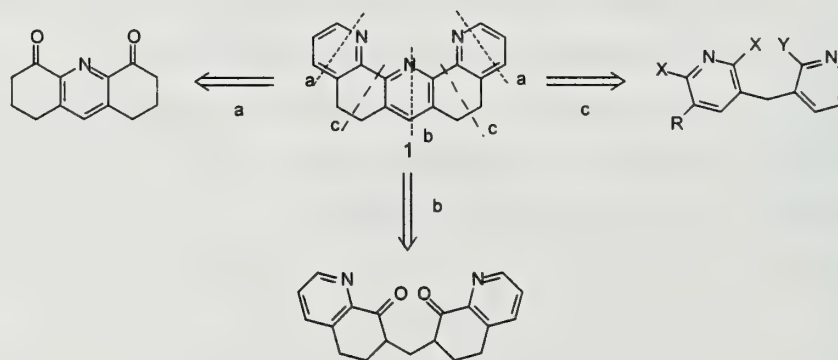
Conformation

The three major conformations of 2,2':6',2'' terpyridine are the syn-syn **2**, syn-anti **3**, and anti-anti **4**. The predominate conformation is determined to be **4** based on solution NMR studies, UV studies, as well as by analogy to 2,2'-bipyridine.^{1,2,3,4} However, the syn-syn conformation **2** is required for complexation of the 2,2':6',2'' terpyridine to an exogenous guest. To overcome the thermodynamic preference for **4** in solution, the pyridine rings can be bridged with ethylene linkers giving rise to **1**. By varying the bridging element, the angle between the distal pyridines can be modified resulting in the modification of the complexation properties of the host.



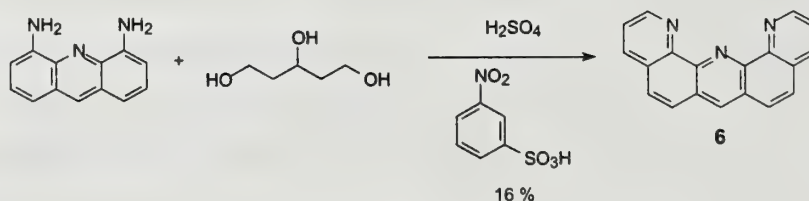
Retrosynthetic Analysis

Three primary retrosynthetic disconnections are envisioned for the formation of the ethylene bridged terpyridine **1**. The first **a** is the formation of the distal pyridine rings which could be performed via a Friedländer condensation from a diketone.^{4,5,12,13} The second **b** could be performed by the formation of the central pyridine ring which could be achieved via the condensation of a 1,5 diketone.^{4,6,7,8,9,10,11,12,13,14} The third **c** involves the coupling of the two distal pyridine rings to the central pyridine ring which could be achieved by an Ulmann coupling. Of the syntheses reported to date, **a** and **b** are the major approaches; no synthesis utilizing **c** as the key step in formation of the terpyridine has been reported.



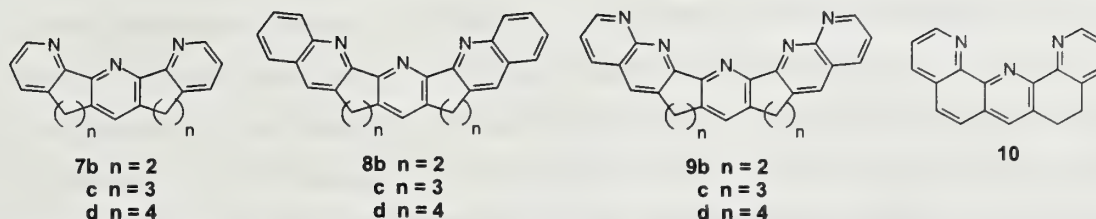
First Bridged Terpyridine

The first reported synthesis of a bridged terpyridine was by Koft and Case in 1962.⁵ Koft and Case performed a double Skraup reaction on 4,5-diaminoacridine with glycerol to afford the quino[8,7-b][1-10]phenanthroline (**6**) in 16 % yield.



Thummel's Bridged Terpyridines

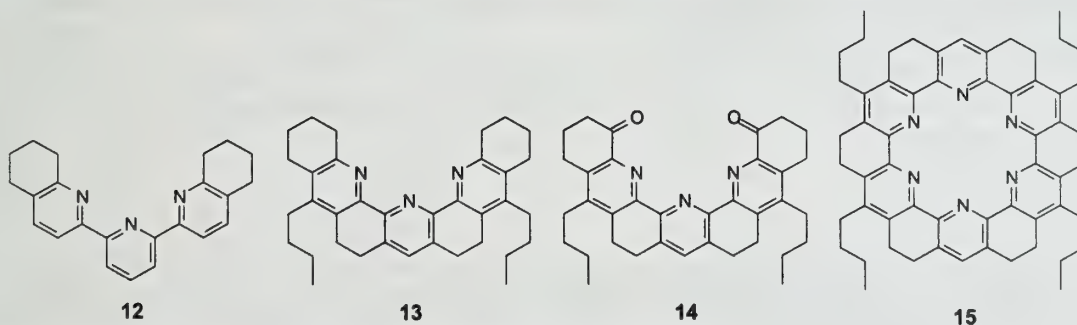
Thummel and co-workers have investigated several families of bridged terpyridine Ruthenium complexes as a function of methylene linker **7b-d**, **8b-d**, and **9b-d** in hopes of increasing the excited state lifetime of the complex.¹⁵ They believed that by decreasing the difference between the excited and ground states of the metal-to-ligand charge transfer (MLCT),



the nonradiative decay rate constant would increase, resulting in an increase in the excited state lifetime. Structures **7b-d**, **8b-d**, and **9b-d** were expected to give rise to different degrees of planarity about the ruthenium with concomitant differences in the UV λ_{max} .^{4,12,13} Contrary to their expectations, no dramatic differences were observed in the absorption spectra of **7b-d**, **8b-d**, and **9b-d**. These results suggest that across the family, the ligands in the ruthenium complexes, independent of linker length, adopted a similar conformation. The crystal structure of $\text{Ru}(\mathbf{7d})_2(\text{PF}_6)_2$ showed that the bridging butylene in **7d** distorts to enforce an octahedral coordination to the ruthenium. Additionally, the UV λ_{max} of the ruthenium complexes of **7b**, **10**, to **6** show incremental increases in the wavelength, which support an increase in the delocalization within the ligands.^{16,14} Although Thummel and co-workers had believed that a decrease in the π^* would increase the nonradiative decay constant, significant changes were not observed in the nonradiative decay between **10** and **6**.

Metal Complexation of Heptacyclic Terpyridine

Fast reactions of complexation are needed for metal ligand binding to have analytical and preparative applications.¹⁷ One way to achieve a fast reaction is to employ open chain ligands, albeit normally with a reduction in stability constant and in selectivity toward alkali metals. To increase the stability constant of an open chain ligand, the ligand can be preorganized by cyclization. Preorganization of the ligand as illustrated for **13** and **14** can be used to increase the



stability constant without affecting the kinetics of complexation.

The stability constants of hosts **13-17** and alkali metal picrates were determined (Table 1). The stability constants for the flexible host **12** could not be determined under the experimental conditions due to the low concentration of the picrate. Thus, the stability constant cannot exceed 10^3 M^{-1} . Host **14** displays some selectivity towards Na^+ and K^+ relative to Li^+ , Rb^+ , and Cs^+ . By contrast, host **13** shows a slight selectivity towards Li^+ . In comparison, torand **15** shows no selectivity between Na^+ and K^+ , and the stability constants are approximately five orders of magnitude greater than **14**. Since the selectivity of crown ethers is based on the radius of the metal, a host that encapsulates the guest may be needed for selectivity between alkali metals. The poor selectivities of **13**, **14**, and **15** may be attributed to their planar geometries. Kinetic studies of complexation should be performed to determine if the kinetics depend on whether the host is open as in **13**, **14** or closed as in **15**.

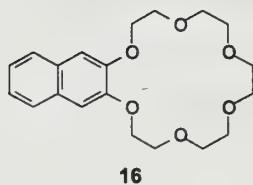
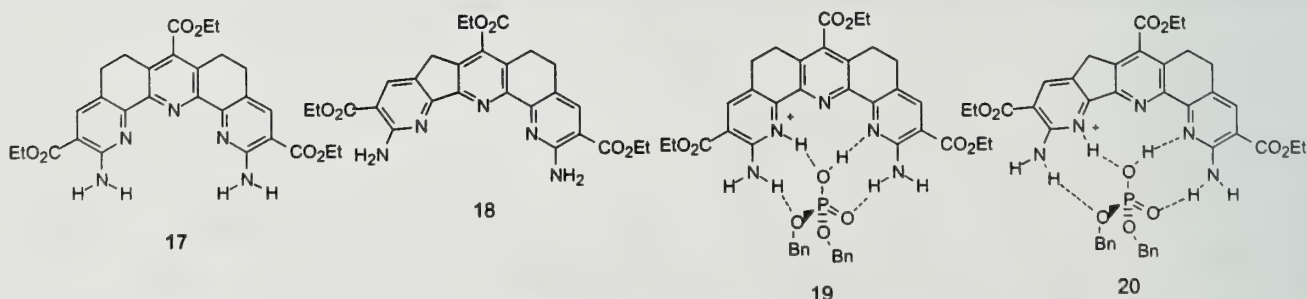


Table 1: Stability Constants ($\log K_a$)

	Li	Na	K	Rb	Cs
12	<3	<8	<3	<3	<3
13	5.2	4.7	4.7	4.3	4.1
14	8.3	9.7	9.5	8.9	8.1
15	--	14.7	14.3	--	--
16	4.4	6.1	7.9	7.1	6.1

Complexation to Phosphoric Acid Diesters

Anslyn and co-workers investigated terpyridines **17** and **18** as model receptors for transport of phosphoric acid diesters through dielectric media via complexes **19** and **20**.¹⁸ Hosts **17** and **18** should each have four hydrogen bonds and should shield the phosphoric acid diesters

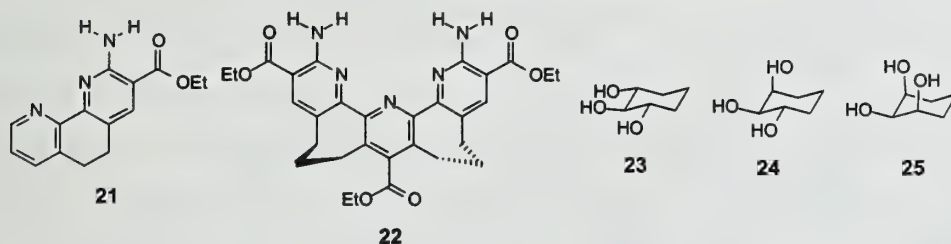


from the surrounding solvent. The use of phosphate anions was avoided in an effort to eliminate any ion association which might otherwise prevent the study of the smaller hydrogen bonding interactions.

Complexation studies were performed to determine the ability of hosts **17** and **18** to aggregate at different concentrations. Additional, studies sought to determine the extent of dimerization of the phosphoric acid diester upon complexation to the host. The stability constants of complexes **19** and **20** were $7.8 \times 10^3 \text{ M}^{-1}$ and $8.9 \times 10^4 \text{ M}^{-1}$ respectively. A molecular mechanics calculation showed that the hydrogen bonds for **20** are more linear than the hydrogen bonds for **19**, therefore contributing to a high stability constant. Anslyn claimed that the cleft of the terpyridine will encapsulate the phosphoric acid diester and shield it from solvent; however, the cleft is almost planar and his molecular mechanics calculations suggest that a majority of the phosphoric acid diester would be exposed to solvent.¹⁹ In order to transport a phosphoric acid diester through dielectric media a host with the ability to shield more of the phosphoric acid diester from the solvent should be designed.

Molecular Recognition of Cyclitols

Anslyn and co-workers also investigated bridged terpyridines in an effort to develop receptors that transport sugars through dielectric media.²⁰ They decided to use a series of di- and tri-cyclitols **23**, **24**, and **25** to mimic some of the interactions between sugars and bridged terpyridines. Anslyn and co-workers have also examined the binding constants of receptors **17**, **21**, and **22** to cyclohexane diols and triols **23**, **24**, and **25**. The calculated dihedral angle between



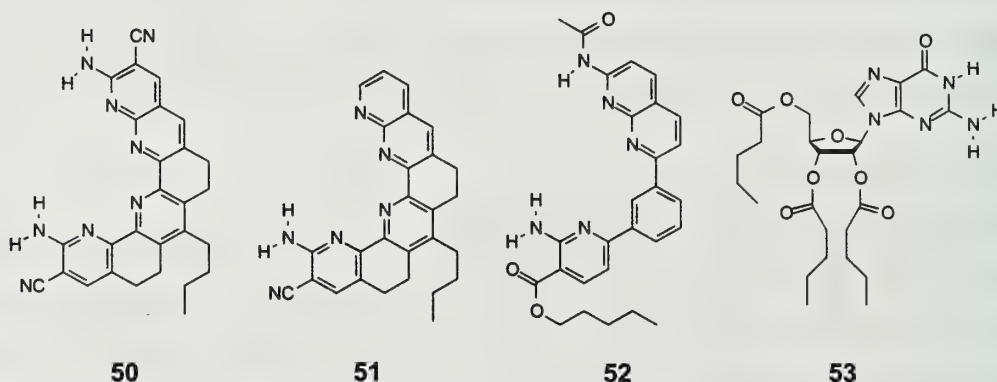
the two peripheral pyridine rings are 24° and 80° in terpyridines **17** and **22**.²¹ The binding constants are listed in **Table 2**. It should be noted that the binding constants for

Table 2: Binding Constant for Complexation of Receptors

	17 $K(\text{M}^{-1})$	22 $K(\text{M}^{-1})$	21 $K(\text{M}^{-1})$
<i>trans</i> -1,2-diol	5	17	2
<i>cis</i> -1,2-diol	7	12	
23	39	39	14
24	35	47	12
25	80	110	36

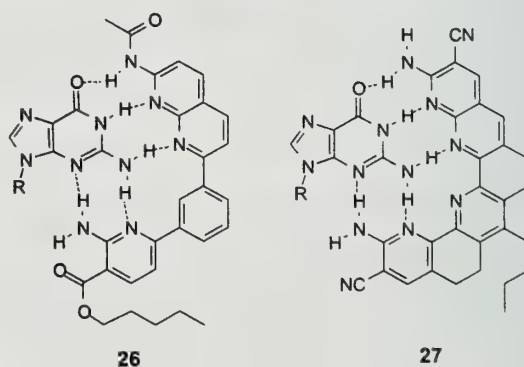
26 are higher than those for the other hosts. In host-guest complexes with **22**, there appears to be a correlation between binding constant and the number of *trans*-hydroxyls in the guest. As the number of *trans*-hydroxyls increases so does the binding constant. Anslyn and co-workers also performed experiments which indicate that the intramolecular hydrogen bond for a *cis*-diol is

stronger than that for a *trans*-diol. The authors postulate that a portion of the difference in binding is due to the energy needed to break an intramolecular *cis*-hydrogen bond upon complexation, versus that required to break a *trans* hydrogen bond. Binding studies were also performed with β -dodecyl-D-glucoside and **22** which resulted in a binding constant of 190 M^{-1} . Conclusions as to the interactions which contribute to the binding are difficult because of the number of structural variations from **23**. Other sugars should be investigated, varying the number of *trans*-hydroxyls to determine if the pattern seen for the tri-hydroxyl cyclitols is preserved.



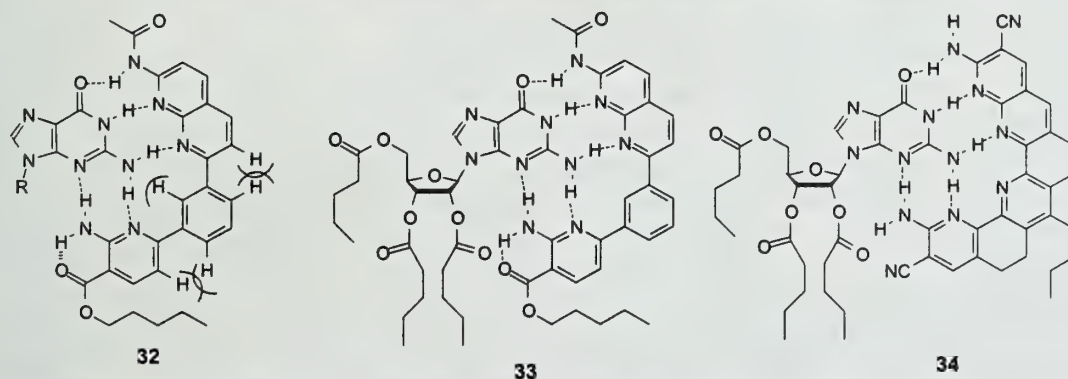
Hydrogen-Bonding Receptors for Guanine Derivatives

Zimmerman and Bell and co-workers designed a receptor with the ability to hydrogen bond to guanine derivatives.²² Guanine contains seven sites capable of forming hydrogen bonds. Zimmerman and Thiessen designed a flexible receptor **52**, whereas Bell and Hou designed rigid receptors **28** and **29**. The predicted complexes **26** and **27** both have five hydrogen bonds to guanine. The greatest structural difference between receptors **28** and **30** is their flexibility. The stability

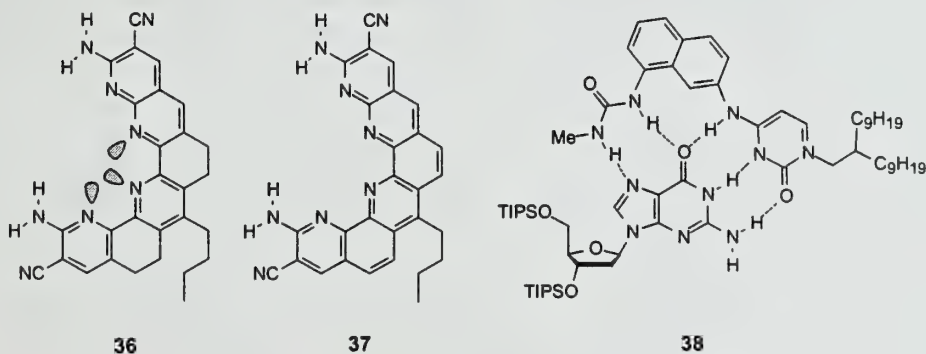


constants for **28**•**31**, **29**•**31**, and **30**•**31** were >190000 , 19000 , and 170 . **28** and **29** are better hosts for **31** than for **30**. One of the factors contributing to the lower stability of the **30**•**31** complex is the two degrees of rotation lost upon complexation. Upon complexation there is also a steric interaction **32** which does not occur in the **28**•**31** and **29**•**31** complexes. The third

contribution to the lower stability of the **30•31** is the lack of three convergent lone pairs that could result in desolvation in the terpyridine cleft. This would increase the strength of the hydrogen bonds. Calculations performed by Anslyn and co-workers showed that there is a 24° angle between the distal pyridines in a similar system **17**.²¹ One way to test the energy contribution of the convergent lone pairs to binding is to raise the enthalpy of the system by forcing the terpyridine to be planar. The planar terpyridine complexed to **37** should show an improved stability constant. In addition to its ability to bind to a guest, the relative selectivity of a host is also of interest. More binding studies should be performed with other neutral nucleic acid mimics to determine the selectivity of the receptor. Comparing the guanine hosts **28** and **30** to other guanine hosts in the literature is difficult because stability constants cannot be directly compared when different solvent systems are used. In addition, the guanine hosts **28** and **29**



were designed only to use hydrogen bonding for binding, while other host used solvophobic effects, electrostatics, and π -stacking to increase the association constant.²³ As a result, only one direct comparison can be made between complexes **38** and **29•31**.²⁴ Both have five hydrogen bonds to guanine, and both are flexible. Assuming the methods for determining the association constants are comparable between laboratories, **38** and **29•31** both have an association constant of 170 M^{-1} in a 1:4 mixture of DMSO:CDCl₃. For **28** to be a viable receptor in aqueous media, additional solvophobic, electrostatic, or π stacking effects will be needed to enhance binding of guanine.



Conclusion

It has been shown that derivatives of bridged terpyridines can be synthesized by a number of different methods. The condensation of the 1,5 diketone is the best method for the formation of a bridged terpyridine. The bridged terpyridines have been used effectively to complex some triols, phosphoric acid diesters, alkali metals, and guanine derivatives. The preorganization of these systems and the three convergent nonbonding lone pairs are key elements in determining the complexation properties of 2,2':6',2'' terpyridines.

References

- ¹ Elsbernd, H.; Beattie, J. K. *J. Inorg. Nucl. Chem.* **1972**, *34*, 771.
- ² Lytle, F. E.; Petrosky, L. M.; Carlson, L. R. *Anal. Chim. Acta.* **1971**, *57*, 239.
- ³ Nakamoto, K. *J. Phys. Chem.* **1960**, *64*, 1420.
- ⁴ Thummel, T. P.; Jahng, Y. *J. Org. Chem.* **1985**, *50*, 2408-2412.
- ⁵ Koft, E.; Case, F. H. *J. Org. Chem.* **1962**, *22*, 865-868.
- ⁶ Bell T. W.; Firestone, A. *J. Org. Chem.* **1986**, *51*, 764-765.
- ⁷ Bell T. W.; Firestone, A. *J. Am. Chem. Soc.* **1986**, *108*, 8109-8111.
- ⁸ Bell T. W.; Liu, J. *Angew. Chem. Int. Ed. Engl.* **1990**, *29*, 923-925.
- ⁹ Bell, T. W.; Heiss, A. M.; Ludwig, T. T.; Xiang, C. *Synlett* **1996**, 79-81.
- ¹⁰ Keuper, R.; Risch, N.; Flörke, F.; Haupt, H. *Liebigs Ann.* **1996**, 705-715.
- ¹¹ Keuper, R.; Risch, N. *Liebigs Ann.* **1996**, 717-723.
- ¹² Thummel R. P. *Tetrahedron* **1991**, *47*, 6851-6886.
- ¹³ Thummel, T. P. *Synlett* **1991**, 1-12.
- ¹⁴ Riesgo, E. C.; Jin, X.; Thummel, T. P. *J. Org. Chem.* **1996**, *61*, 3017-3022.
- ¹⁵ Thummel R. P.; Jahng, Y. *Inorg. Chem.* **1986**, *25*, 2527-2534.
- ¹⁶ Hung, C.; Wang, T.; Jang, Y.; Kim, W. Y.; Schmehl, F. H.; Thummel, R. P.; *Inorg. Chem.* **1996**, *35*, 5953-5956.
- ¹⁷ Bell T. W.; Cragg, P. J.; Firestone, A.; Kwok, A. D.-I.; Liu, J.; Ludwig, R.; Sodoma, A.; *J. Org. Chem.* **1998**, *63*, 2232-2243.
- ¹⁸ Chu, F.; Flatt, L. S.; Anslyn, E. V. *J. Am. Chem. Soc.* **1994**, *116*, 4194-4204.
- ¹⁹ Huang, C.; Cabell, L. A.; Anslyn E. V. *Tetra. Lett.* **1990**, *31*, 51.
- ²⁰ Huang, C.; Cabell, L. A.; Anslyn, E. *J. Am. Chem. Soc.* **1998**, *116*, 2778-2792.
- ²¹ Huang, C. Y.; Lynch, V.; Anslyn, E. V. *Angew. Chem., Int. Ed. Engl.* **1992**, *31*, 1244.
- ²² Bell, T. W.; Hou, Z.; Zimmerman, S. C.; Thiessen, P. A. *Angew. Chem. Int. Ed. Engl.* **1995**, *34*, 2163-2165.
- ²³ Thiessen, P. A. Ph.D. Thesis, University of Illinois at Urbana-Champaign, 1998.
- ²⁴ Amemiya, S.; Bühlmann, P.; Umezawa, Y. *Chem. Comm.* **1997**, 1027-1028.



UNIVERSITY OF ILLINOIS-URBANA



3 0112 037709083

Q.547
I6s
1999/00:I

ORGANIC SEMINAR ABSTRACTS

1999-00, SEMESTER I

University of Illinois

**Department of Chemistry
600 South Mathews Avenue
271 Roger Adams Laboratory
Urbana, IL 61801**

January 2000

LIBRARY U. OF I. URBANA-CHAMPAIGN
CHEMISTRY LIBRARY

NOTICE: Return or renew all Library Materials! The Minimum Fee for each Lost Book is \$50.00.

The person charging this material is responsible for its return to the library from which it was withdrawn on or before the **Latest Date** stamped below.

Theft, mutilation, and underlining of books are reasons for disciplinary action and may result in dismissal from the University.
To renew call Telephone Center, 333-8400

UNIVERSITY OF ILLINOIS LIBRARY AT URBANA-CHAMPAIGN

CHEMISTRY LIBRARY

MAY 19 2002

FEB 13 2001

L161—O.

SEMINAR TOPICS

SEMESTER I

FALL 1999

	<u>PAGE</u>
TITANIUM (II) PROMOTED ENE AND METALLO-ENE REACTIONS OF ENYNES LARRY G. HUFFMAN, JR.	1
MOLECULAR EVOLUTION: SELF-REPLICATING SYSTEMS NEIL O.L. VIERNES	9
CYTOMIMETIC VESICLES: BEHAVIOR AND APPLICATIONS β -SHEETS MARY L. KRAFT	17
NON-ENZYMATIC KINETIC RESOLUTION OF SECONDARY ALCOHOLS DWIGHT D. KIM	25
DEAROMATIZATION OF ARENES BY TRANSITION METAL COMPLEXES MATT GIESELMAN	33
ORGANOLANTHANIDES AND CATALYTIC HYDROAMINATION GREGORY L. BEUTNER	41
TRANSITION-METAL CATALYZED [4+1] CYCLOADDITIONS RAMZI F. SWEIS	49

ZIRCONIUM-CATALYZED ASYMMETRIC ADDITION OF GRIGNARD REAGENTS TO OLEFINS.....	57
HIEN M. NGUYEN	
STRATEGIES FOR COMBATING β -LACTAMASE INDUCED ANTIOTBIOTIC RESISTANCE	65
ERIKA A. TAYLOR	
UNNATURAL AMINO ACIDS IN PROTEINS VIA A BIOSYNTHETIC APPROACH	73
JAISREE MOORTHY	

TITANIUM (II) PROMOTED ENE AND METALLO-ENE REACTIONS OF ENYNES

Reported by Larry G. Huffman Jr.

September 2, 1999

INTRODUCTION

Cyclization reactions of enynes provide useful methods for the synthesis of carbocyclic and heterocyclic compounds from simple, acyclic precursors.¹ Such reactions have proven to be valuable transformations for the synthesis of many substituted cycloalkanes and their corresponding natural products.² Applications of the thermally-promoted reaction to the synthesis of complex structures have been severely limited due to extreme reaction conditions and substrate limitations. Use of transition-metals, both catalytically and stoichiometrically, allows the cyclization to proceed under much milder conditions, often with enhanced selectivity and substrate compatibility. Until recently, only late transition-metals (i.e., Ni,³ Pd⁴) have been used for catalytic cycloisomerizations while both late (i.e., Co⁵) and early transition-metals (i.e., Zr,⁶ Ti⁷) have been used for stoichiometric reductive cyclizations. This report highlights the most recent advances of enyne cyclizations using Ti(II) promoters, including a highly effective chiral auxiliary approach for an intramolecular asymmetric metallo-ene reaction and the first early transition-metal catalyzed cycloisomerization of enynes.

BACKGROUND

Reductive Cyclizations of Enynes

The first metal-promoted cyclizations of enynes were reductive titanocene-mediated reactions.⁷ Negishi subsequently developed the zirconocene-mediated reaction. Sometimes called a Negishi cyclization,⁸ the transformation results in the formation of a zirconacyclopentene **1** (Scheme 1). This

Scheme 1. Zirconocene-Promoted Reductive Cyclization of Enynes.

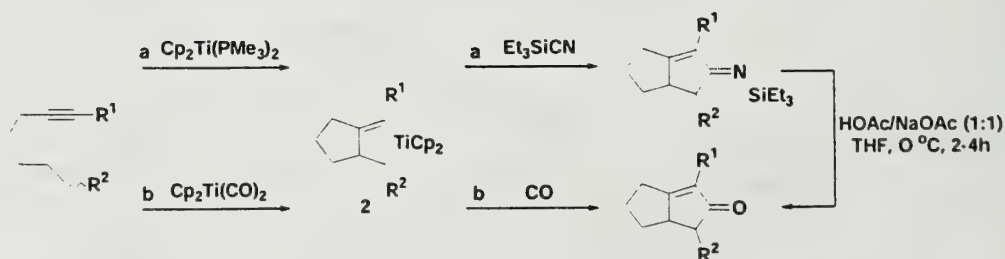


organometallic species is usually hydrolyzed to provide the reductive cyclization product (path a); however, it can also be trapped by electrophiles (e.g., I_2 , $RCHO$, path b) or converted to a cyclopentenone (path c) via carbonylative insertion (a Pauson-Khand type reaction).⁹ The zirconocene-mediated reaction provides an excellent method for the formation of carbocyclic moieties, but the cyclization does not work for substrates containing allylic ethers. Substrates containing esters are also incompatible and oxygen functionalities attached to the latent carbocyclic ring are only tolerated with bulky protective groups (e.g., TBDMS). While Waymouth has reported a zirconium-catalyzed reductive cyclomagneziation of dienes,¹⁰ there have been no reports of a zirconium-catalyzed cyclization of enynes.

Reductive cyclizations using titanocene mediators¹¹ show complementary selectivities and compatibilities to the zirconocene-mediated processes. Notably, titanium-mediated processes show enhanced substrate compatibility with oxygen containing functional groups including esters, ethers and carbamates.¹² One drawback to titanium-mediated processes is that substrates with bulky alkyne substituents are not cyclized by titanocene equivalents but are cyclized with zirconocene equivalents. This difference in reactivity is probably due to the smaller ionic radius of titanium causing a more congested coordination environment of the metallocene. Less hindered titanium (II) metal sources (i.e., non-metallocene) can be used for more bulky substrates.¹³

A major advantage of the use of titanium in preference to zirconium is that titanium can be used catalytically.^{14,15} Several titanocene-catalyzed cyclizations of enynes have been reported. Buchwald and coworkers have developed two key catalytic processes outlined in Scheme 2. Isocyanide equivalents can be inserted into 2 to yield iminocyclopentenenes (path a).¹⁴ A catalytic Pauson-Khand type reaction has also been accomplished by running the reaction under an atmosphere of CO (path b).¹⁵

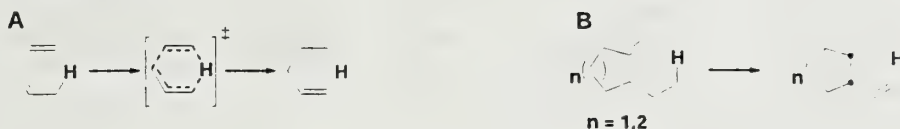
Scheme 2. Titanium-Catalyzed Reductive Cyclizations of Enynes.



Ene Reaction

An ene reaction is the concerted addition of a π -bond containing species (enophile) to a species containing an allylic hydrogen (ene) with transfer of the allylic hydrogen (Scheme 3).¹⁶ The reaction is

Scheme 3. Ene Reaction.

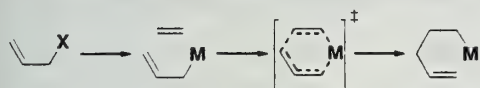


a six electron thermally-allowed suprafacial pericyclic reaction. The reaction is favored enthalpically because the net result is the conversion of a π -bond into a σ -bond. When conducted intramolecularly, the ene reaction is a cycloisomerization that can be used to construct carbocyclic frameworks.¹⁷

Metallo-Ene Reaction

The addition of an allyl metal species to a π -bond with transfer of the metal has been called a metallo-ene reaction by Oppolzer.¹⁸ The transformation is analogous to the ene reaction but the allylic hydrogen has been replaced by a metal (Scheme 4). The allyl metal species are usually formed by either

Scheme 4. Metallo-Ene Reaction.



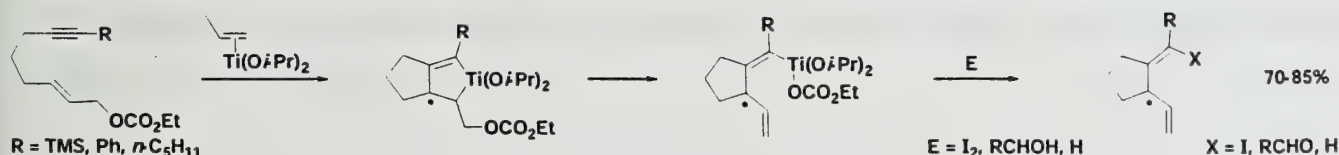
metallation of an allylic carbon halogen bond (e.g., lithiation), oxidative addition to a carbon halogen bond (e.g., Grignard formation) or displacement of an allylic leaving group to form a

π -allyl metal species (e.g., Pd catalysis). The final organometallic species are usually worked up hydrolytically, resulting in a net reduction of the starting material(s). Palladium and nickel have been used successfully to effect metallo-ene cycloisomerizations.¹⁹ These reactions are especially advantageous because they effect the cyclization of the substrate without decreasing the functionality by reduction.

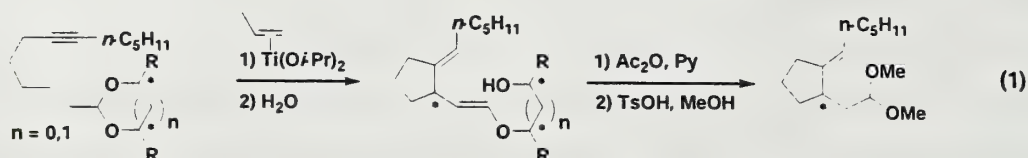
TITANIUM-MEDIATED ASYMMETRIC METALLO-ENE TYPE REACTIONS

Sato and coworkers discovered that $(\eta^2\text{-CH}_3\text{CHCH}_2)\text{Ti}(\text{O}i\text{Pr})_2$, prepared in situ from $\text{Ti}(\text{O}i\text{Pr})_4$ and two equiv of $i\text{PrMgBr}$, can promote the synthetic equivalent of a metallo-ene reaction (Scheme 5).²⁰ A stereogenic center is generated during the metallo-ene reaction of an enyne. Asymmetric generation of the stereogenic center has previously been achieved in only moderate to poor

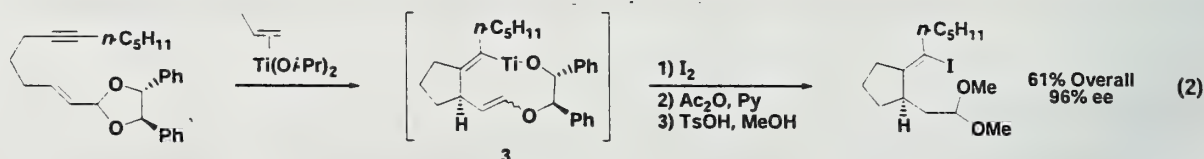
Scheme 5. Sato's Titanium-Mediated Reductive Cyclization of Enynes.



enantioselectivities.²¹ Sato and coworkers recently reported a chiral auxiliary approach that provides substituted cyclopentanes in enantiomeric ratios as high as 98:2 (eq 1).²²



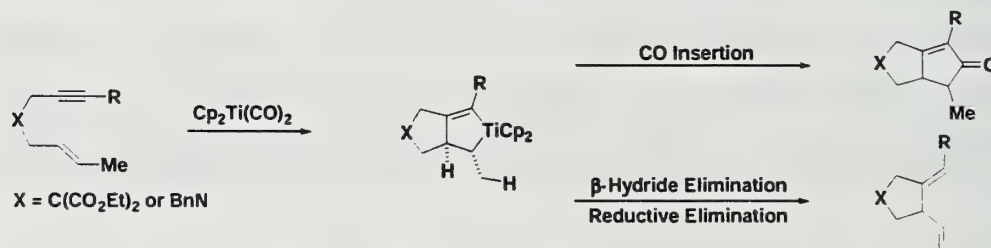
The authors note that the intermediate organotitanium species **3** can be trapped by iodine, providing the synthetically useful vinyl iodide (eq 2).



TITANOCENE-CATALYZED INTRAMOLECULAR ENE REACTION OF ENYNES

During their studies on the titanocene-catalyzed Pauson-Khand reaction, Buchwald and coworkers noticed that $\text{Cp}_2\text{Ti}(\text{CO})_2$ ²³ could cycloisomerize enynes¹⁵ (Scheme 6). The net

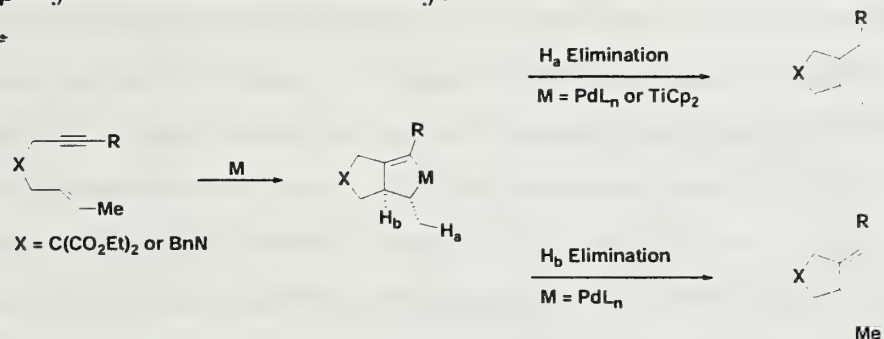
Scheme 6. Discovery of Titanocene Catalyzed Ene Reaction.



transformation is a catalytic intramolecular ene reaction of the substrate. While such reactions were known to be catalyzed by late transition-metals,²⁴ this was the first report involving an early transition-metal catalyzed process.²⁵ As noted above, only reductive cyclizations had been previously carried out with early transition-metals.

Palladium has been used most extensively for the cycloisomerization of enynes. The palladium catalysts for the cycloisomerization reactions are much more expensive than the titanium catalyst. The palladium-catalyzed process also suffers from competitive formation of the thermodynamically more stable 1,3-dienes in mixtures with the desired 1,4-dienes expected from an ene reaction (Scheme 7).

Scheme 7. β -Hydride Elimination Pathways.



As shown in Table 1, the titanium-catalyzed cycloisomerization proceeds with a variety of substrates forming exclusively 1,4-dienes as products. The isomeric 1,3-dienes are not competitively

Table 1 Titanocene Catalyzed Ene Cycloisomerization of Enynes.

Entry	Substrate ^a	Product	% Yield	Entry	Substrate	Product	% Yield
1			97	5			79
2			82	6			88
3			79	7			89
4			85	8		No Reaction	0

^a E = CO_2Et

formed as with the palladium-catalyzed process. The only reported case of isolating a 1,3-diene was with the nitrogen containing substrate (Table 1, entry 4). Heating this substrate with catalyst at 95 °C in toluene for 4 h yielded exclusive formation of the 1,4-diene yet heating for an additional 8 h resulted in isomerization to the 1,3-diene. Methyl, *n*-propyl and phenyl substituted alkynes are all acceptable substrates. Interestingly, the cyclohexyl substituted alkene (entry 5) results in selective hydride elimination between two tertiary carbons to form only the 1,4-diene. The substrate with a substituent in the γ position to the alkyne resulted in complete diastereoselectivity to yield only the *trans*-cyclopentane (entry 7). Substrates with substituents in the α - or β -positions exhibited little or no diastereoselectivity. These results are in accord with stereoselectivities previously observed for reductive cyclizations using titanocene and zirconocene mediators.²⁶

One striking result is that *trans*-alkenes are isomerized yet *cis*-alkenes are not. A substrate containing both a *cis*- and *trans*-alkene resulted in completely selective cycloisomerization of the *trans*-alkene (Table 1, entry 6). The reason for this selectivity can be explained by examining models of *trans*- and *cis*-metallacycles (formed stereospecifically from *trans*- or *cis*-alkenes respectively) (Figure

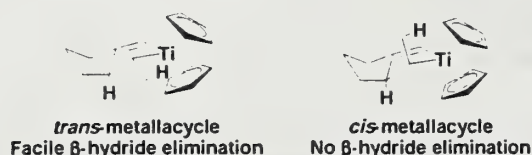


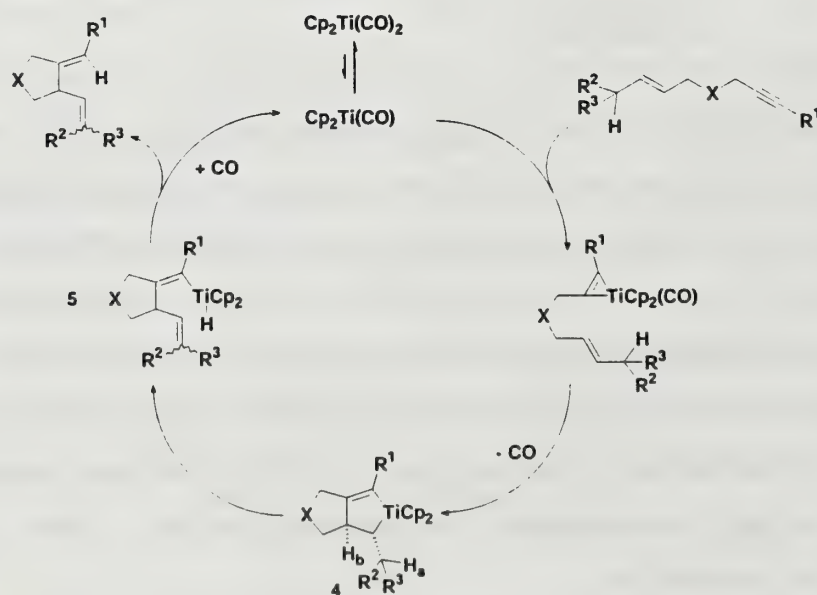
Figure 1. *Trans* and *Cis*-Metallacycles.

1). In order for the hydride elimination to occur, the hydrogen must overlap with the LUMO of the titanocene (*vide infra*). The LUMO of the titanocene is oriented perpendicular to the plane defined by the titanium and the centroids of the two cyclopentadienyl ligands.²⁷ β -

hydride elimination is facile from the *trans*-metallacycle because the requisite carbon-hydrogen bond is aligned with the LUMO. This is not the case for the *cis*-metallacycle in which the β -hydrogen does not have the proper geometry for elimination. The stereoelectronic requirements of the hydride elimination explain the absolute selectivity for 1,4-dienes instead of 1,3-dienes. It was reported that *cis*-alkene containing substrates were partially converted to cyclopentenones (through the Pauson-Khand type process).

The proposed catalytic cycle for the ene reaction is shown in Figure 2. Initial loss of CO allows binding of the substrate. Loss of the other CO allows metallacycle 4 to form with concomitant oxidation of Ti(II) to Ti(IV). Exclusive β -hydride elimination of H_a results in the titanocene hydride intermediate 5. Reductive elimination, induced by CO binding,²⁸ results in product diene and regeneration of the presumed catalytic Ti(II) species.

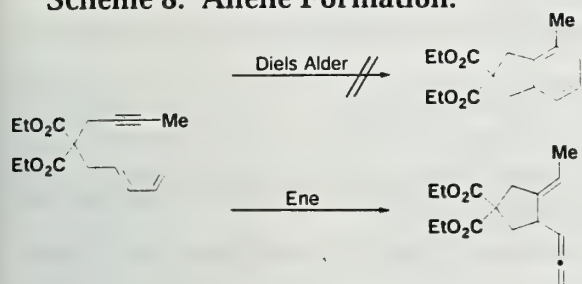
Figure 2. Proposed catalytic cycle for the titanocene catalyzed ene reaction of enynes.



It was reported that lower catalyst loading could be used if catalyst concentration was decreased. The more dilute reactions required increased reaction times and temperature. This effect could be due to limiting a catalyst dimerization process as well as a greater proportion of dissociated titanocene dicarbonyl at lower concentrations.

Interestingly, cyclization of substrates containing a 1,3-diene proceeded to give allene containing products (Scheme 8). Substrates of this kind are known to undergo Diels-Alder cyclizations with late transition-metal catalysts.²⁹ This marks the first report of

Scheme 8. Allene Formation.



a transition-metal catalyzed process that forms an allene from a 1,3-diene and highlights the selectivity of the titanocene to exclusively eliminate the proximal β -hydride leading to formation of a 1,4 diene.

CONCLUSIONS

Development of a reliable and highly stereoselective cyclization of enynes allows for the efficient formation of enantiomerically enriched cyclopentanes. At present, substrate scope of the transformation seems rather limited. Exploring and expanding substrate compatibility should be a focal point of future research. Developing the reaction into a catalytic process would be greatly advantageous because of the reduction in the amount of expensive enantiopure reactant necessary. The catalytic ene reaction developed by Buchwald and coworkers provides a useful and cheaper alternative to previous palladium-catalyzed reactions. Again, substrate scope seems limited for the reaction and future research efforts should be carried out to define and expand the scope of the reaction. Asymmetric induction via the catalytic ene reaction may be possible using *ansa*-bridged tetrahydroindenyl titanocenes. Such catalysts have been shown to effect asymmetric Pauson-Khand type reactions³⁰ and are an obvious avenue to be explored.

References

- 1) Trost, B. M.; Krische, M. J. *Synlett* **1998**, 1-16.
- 2) Trost, B. M. In *Studies in Natural Products Chemistry*; Atta-ur-Rahman, Ed.; Elsevier: Amsterdam, 1991; Vol. 8; pp 277-282.
- 3) Trost, B. M.; Tour, J. M. *J. Am. Chem. Soc.* **1987**, *109*, 5268-5270.
- 4) Trost, B. M.; Romero, D. L.; Rise, F. *J. Am. Chem. Soc.* **1994**, *116*, 4268-4278.
- 5) Krafft, M. E.; Wilson, A. M.; Dasse, O. A.; Bonega, L. V. R.; Cheung, Y. Y.; Fu, Z.; Shao, B.; Scott, I. L. *Tetrahedron Lett.* **1998**, *39*, 5911-5914.
- 6) Negishi, E.; Holmes, S. J.; Tour, J. M.; Miller, J. A. *J. Am. Chem. Soc.* **1985**, *107*, 2568-2569.
- 7) Nugent, W. A.; Calabrese, J. C. *J. Am. Chem. Soc.* **1984**, *106*, 6422-6424.
- 8) Negishi, E. In *Comprehensive Organic Synthesis*; Trost, B. M., Fleming, I., Eds.; Pergamon: Oxford, U. K., 1991; Vol. 5, pp 1163-1184.
- 9) Khand, I. U.; Knox, G. R.; Pauson, P. L.; Watts, W. E.; Foreman, M. I. *J. Chem. Soc. Perkin Trans. 1* **1973**, 977-981.
- 10) Knight, K. S.; Wang, D.; Waymouth, R. M.; Ziller, J. *J. Am. Chem. Soc.* **1994**, *116*, 1845-1854.
- 11) Grossman, R. B.; Buchwald, S. L. *J. Org. Chem.* **1992**, *57*, 5803-5805.
- 12) Zr-O bonds are ~15 kcal/mol stronger than Ti-O bonds. Conner, J. A. *Top. Curr. Chem.* **1977**, *71*, 71-110.
- 13) Urabe, H.; Hata, T.; Sato, F. *Tetrahedron Lett.* **1995**, *36*, 4261-4264.
- 14) Berk, S. C.; Grossman, R. B.; Buchwald, S. L. *J. Am. Chem. Soc.* **1994**, *116*, 8593-8601.
- 15) Hicks, F. A.; Kablaoui, N. M.; Buchwald, S. L. *J. Am. Chem. Soc.* **1996**, *118*, 9450-9451.
- 16) Hoffman, H. M. R. *Angew. Chem., Int. Ed. Engl.* **1969**, *8*, 556-577.
- 17) Taber, D. F. *Intramolecular Diels-Alder and Alder-Ene Reactions*; Springer-Verlag: Berlin, 1984, pp 61-94.
- 18) Oppolzer, W. *Angew. Chem., Int. Ed. Engl.* **1989**, *28*, 38-52.
- 19) Oppolzer, W. In *Comprehensive Organic Synthesis*; Trost, B. M., Fleming, I., Eds.; Pergamon: Oxford, U. K., 1991; Vol. 5, pp 29-61.
- 20) Takayama, Y.; Gao, Y.; Sato, F. *Angew. Chem., Int. Ed. Engl.* **1997**, *36*, 851-853.
- 21) Oppolzer, W.; Kuo, D. L.; Hutzinger, M. W.; Leger, R.; Durand, J.-O.; Leslie, C. *Tetrahedron Lett.* **1997**, *38*, 6213-6216. Goeke, A.; Sawamura, M.; Kuwano, R.; Ito, Y. *Angew. Chem., Int. Ed. Engl.* **1996**, *35*, 622-623. Trost, B. M.; Czeskis, B. A. *Tetrahedron Lett.* **1994**, *35*, 211-214.
- 22) Takayama, Y.; Okamoto, S.; Sato, F. *J. Am. Chem. Soc.* **1999**, *121*, 3559-3560.
- 23) Commercially available from Strem Chemicals. Also readily synthesized from Cp₂TiCl₂. Sikora, D. J.; Moriarty, K. J.; Rausch, M. D. In *Inorganic Synthesis*; Angelici, R. J. Ed.; John Wiley and Sons, Inc: New York, 1990; Vol. 28, pp 248-256.
- 24) Trost, B. M.; Lautens, M.; Cham, C.; JeBaratnam, D. J.; Mueller, T. *J. Am. Chem. Soc.* **1991**, *113*, 636-644.
- 25) Sturla, S. J.; Kablaoui, N. M.; Buchwald, S. J. *J. Am. Chem. Soc.* **1999**, *121*, 1976-1977.
- 26) Rajanbabu, T. V.; Nugent, W. A.; Taber, D. F.; Fagan, P. J. *J. Am. Chem. Soc.* **1988**, *110*, 7128-7135. Pagenkopf, B. L.; Lund, E. L.; Livinghouse, T. *Tetrahedron* **1995**, *51*, 4421-4438.
- 27) Lauher, J. W.; Hoffmann, R. *J. Am. Chem. Soc.* **1976**, *98*, 1729-1742.
- 28) Gell, K. I.; Schwartz, J. *J. Am. Chem. Soc.* **1981**, *103*, 2687-2695.
- 29) Rh: Jolly, R. S.; Leudtke, G.; Sheehan D.; Livinghouse, T. *J. Am. Chem. Soc.* **1990**, *112*, 4965-4966. Ni: Wender, P. A.; Jenkins, T. E. *J. Am. Chem. Soc.* **1989**, *111*, 6432-6434. Pd: Kumar, K.; Jolly, R. S. *Tetrahedron Lett.* **1998**, *39*, 3047-3048.
- 30) Hicks, F. A.; Buchwald, S. L. *J. Am. Chem. Soc.* **1996**, *118*, 11688-11689.

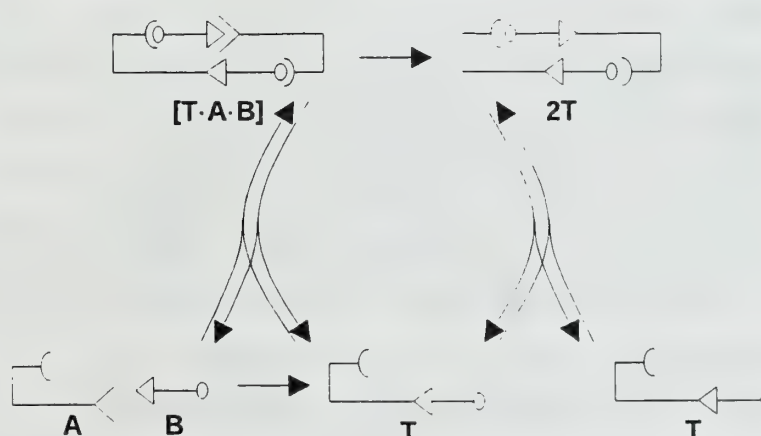
INTRODUCTION

Symbiotic and competitive relationships are prevalent throughout nature. DNA and proteins work in a cooperative fashion where peptides are involved in DNA replication and DNA acts as a template for peptide synthesis. This symbiotic relationship between DNA and proteins is believed to be the product of evolution. Scientists investigating molecular evolution have suggested that originally, one of these two systems performed all the functions essential to life. The discovery that RNA can function as a catalyst has led to the hypothesis that RNA could have been the original system from which life was derived. Through evolution, DNA and enzymes eventually usurped most of the duties from RNA.¹ One problem proponents of the 'RNA world' have is that, unlike peptides, scientists have not yet been able to synthesize nucleosides under prebiotic conditions. Even so, little emphasis has been placed on peptide systems as the first biomolecule. One of the primary reasons is that DNA and RNA systems have shown the ability to self-replicate, while prior to 1996 peptide systems had not. Great strides have been made in the study and understanding of self-replication and recent reports of self-replicating peptides have been published. The study of self-replication has been pursued in hopes of understanding the chemical, physical and biological factors necessary for molecular evolution and life.

SMALL MOLECULE SELF-REPLICATING SYSTEMS

The simplest replicating system involves molecules that are self-complementary. Scheme 1 shows a self-complementary catalytic cycle. Covalently linking molecules A and B forms a self-complementary template molecule T that is able to form the dimer 2T. Template T is able to sequester its fragments A and B and place them within close proximity to promote its reproduction $[T \cdot A \cdot B]$.

Scheme 1



Rebek and coworkers first successful self-complementary replicating small molecule system involved the use of the adenosine derivative **1** and a pentafluorophenyl ester containing imide derivative **2a**.² The resulting self-complementary template molecule **3a** is able to dimerize (**4**) through both Watson-Crick and Hoogsteen hydrogen bonding (Figure 1).

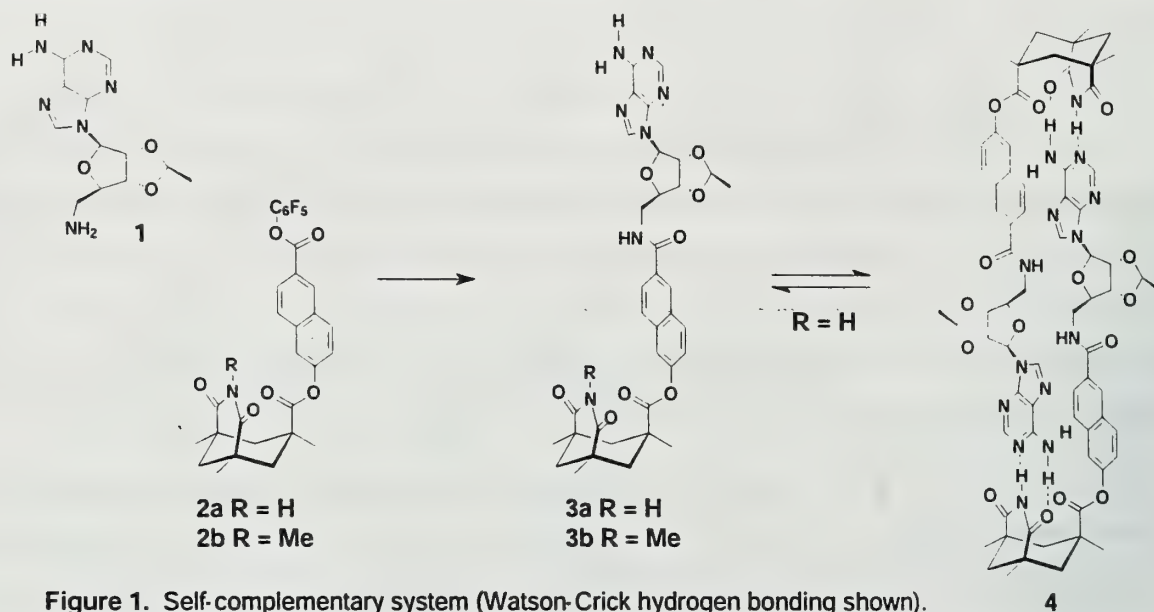


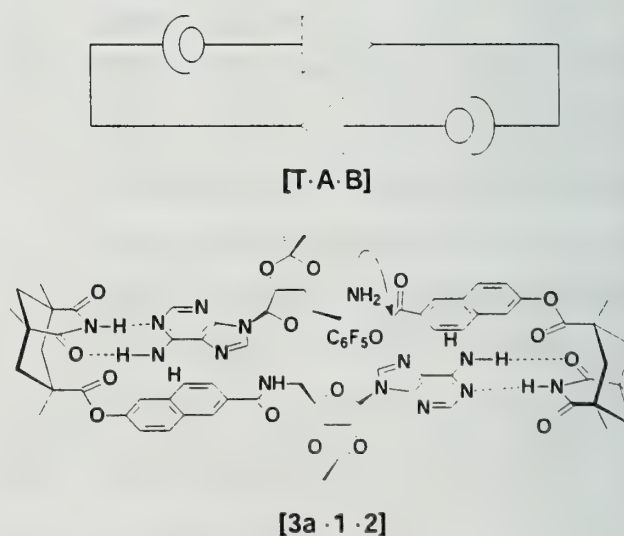
Figure 1. Self-complementary system (Watson-Crick hydrogen bonding shown).

Template **3a** catalyzes amide bond formation between **1** and **2** (Scheme 2). The rate has been found to be dependent on the initial concentration of template added. Increasing the initial template concentration results in a rate enhancement proportional to the square root of $[\text{template}]_0$. This adherence to the 'square root law' initially observed in von Kiedrowski's self-replicating DNA systems is characteristic of replicating systems.³

Control experiments were performed to show that the source of the autocatalysis was a template effect instead of chemical autocatalysis by functional groups within the template itself.³⁻⁵ The addition of diacylaminopyridines resulted in a reduction in the rate of formation of **3a**, indicating a need for base pairing in the autocatalysis. Results also showed that the imide, amide and purine functionalities alone did not autocatalyze the reaction. Template autocatalysis by **3a** remained the only reasonable mechanism for rate enhancement.

This conclusion, however, has been a source of debate within the community.

Scheme 2.



Carbazole Systems

The carbazole-diimide 5 provided a molecular skeleton that would simultaneously bind the adenine unit via Hoogsteen and Watson-Crick hydrogen bonding.⁶ The rigidity of the assembly also prevented the intramolecular pathway from occurring (7, Figure 2).

A dramatic increase in rate was not observed as rates were comparable to the original naphthoyl replicators 3a. The increase in binding strength of the diimide prevents the template from

disassociating. Control reactions similar to those done in the first system discussed eliminated the possibility of chemical modes of autocatalysis. The most reasonable explanation for autocatalysis is that the product of the coupling 6 acts as a template to bring together the reactants in a termolecular complex. The close proximity of functional groups then enhances the rate of reaction.

Reciprocal Template Self-Replication

Nucleic acid replication is not self complementary. One strand of DNA acts as a template for the other's formation. Two complementary molecules, T_{AB} and T_{CD} , whose termini form a heterodimer $[T_{AB} \cdot T_{CD}]$, will be able to act as templates for the synthesis of their complementary molecules, T_{CD} and T_{AB} respectively. Fragmenting these molecules into either A and B or C and D creates a reciprocal system in which the complementary template T_{CD} or T_{AB} , is able to bind the units of the other system and catalyze their coupling (Scheme 3).

Utilizing the carbazole-diimide moiety, Rebek and coworkers began exploration of reciprocal systems.⁷ Two carbazole-diimide functionalities were covalently linked to form a dicarbazole unit with four imide functionalities 9. The complementary α,ω -adenine molecule 8 was synthesized similarly (Figure 3).

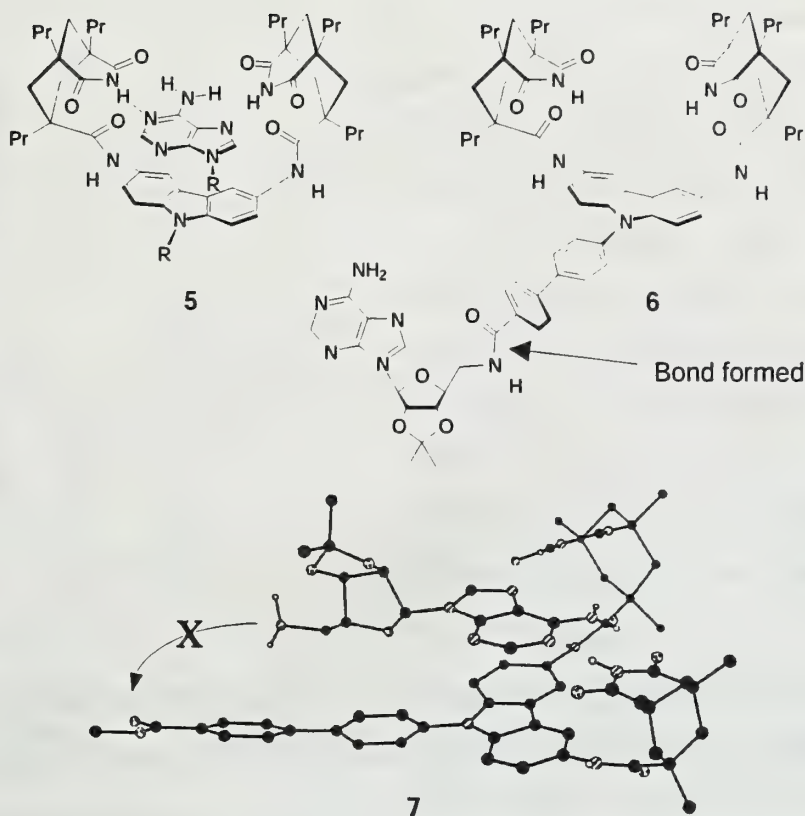
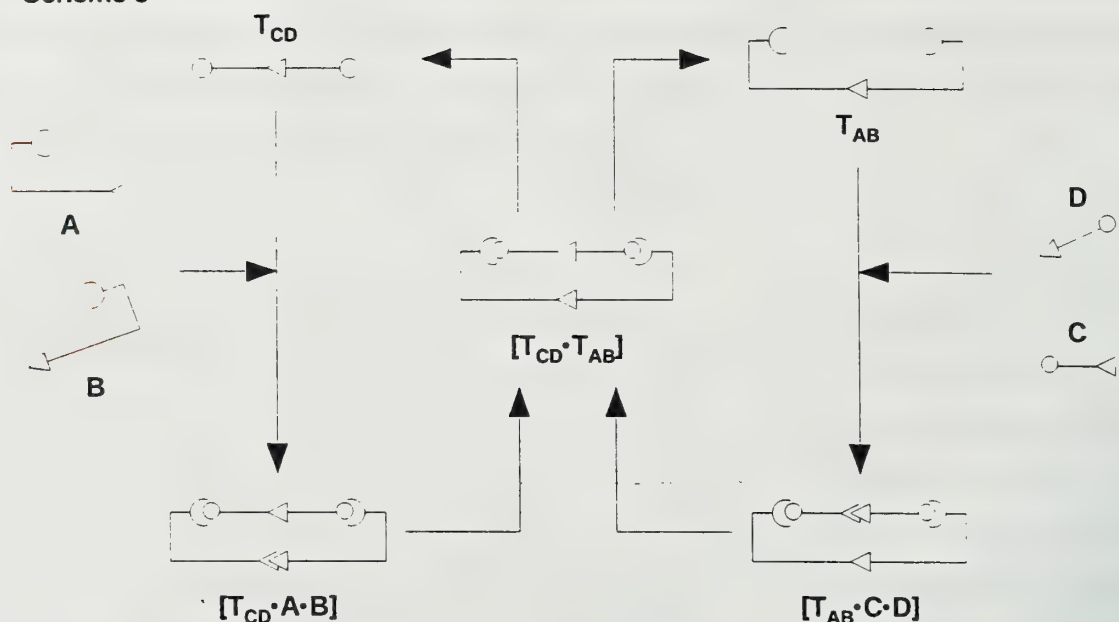


Figure 2. Adenosine binding to the carbazole-diimide (5), carbazole-diimide template (6), model of intramolecular reaction of aminadenosine and biphenyl diimide (7).

Scheme 3



Template 8 catalyzed the synthesis of 9 and reciprocity was achieved as 9 catalyzed the synthesis of 8. Catalytic activities of the reciprocal systems were greater than that of the self-complementary systems.⁸

SELF-REPLICATING PEPTIDE CHAINS

In the 1950's Stanley L. Miller conducted experiments where current was passed through a mimic prebiotic 'soup.' A group of complex molecules including amino acids were synthesized. Nucleobases, however, were not produced.⁹ This result led to the hypothesis that peptides played a large role in molecular evolution although nucleic acids have received much of the attention. Unlike

oligonucleotides, self-replicating peptide systems had not been reported prior to 1996.¹⁰⁻¹² Peptide systems by Ghadiri and Chmielewski have recently been shown to self-replicate, thus adding renewed interest in peptides as the first biomolecule.

Using the coiled-coil leucine-zipper homodimerization domain of the yeast transcription factor GCN4, Ghadiri and coworkers have demonstrated a self-replicating peptide system.¹³ The peptide sequence consists of a repeating heptad ((*abcdefg*)_n, Figure 4a) where residues *a* and *d* form the

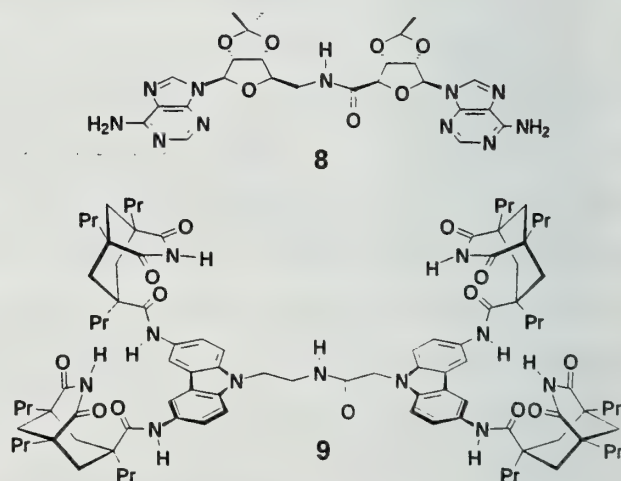


Figure 3. Reciprocal systems

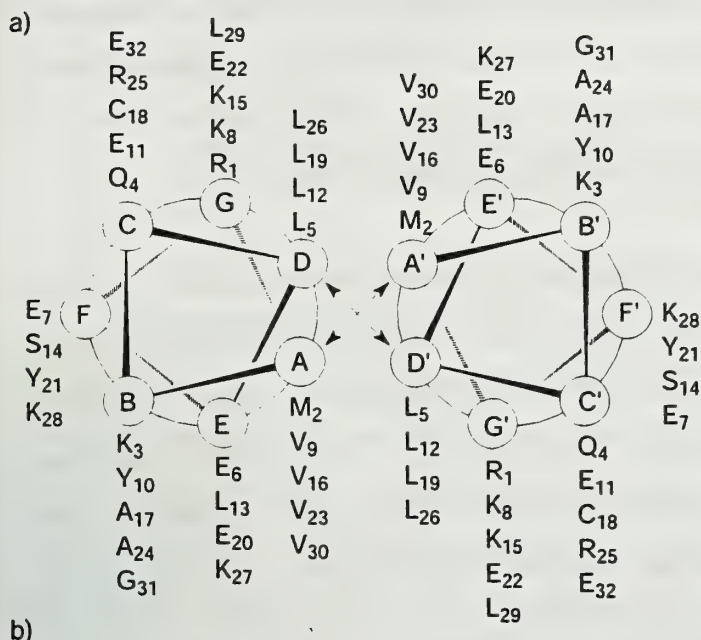


Figure 4. Helical wheel diagram of template peptide in dimeric a-helical coiled-coil conformation b) Amino acid sequence of template T, Electrophile E, and Nucleophile N (ligation site).

hydrophobic face of the helix. Comprised of leucine and valine, the hydrophobic face acts as a template for dimerization with a second helix.

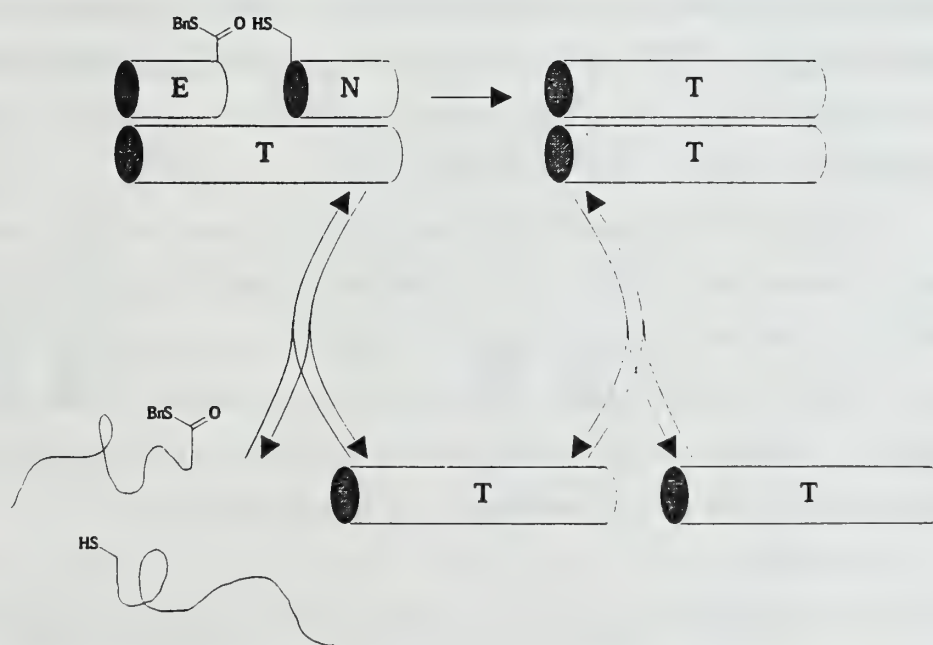
The template peptide T was cleaved at Ala₁₇-Cys₁₈. Using the coupling scheme of Kent et al. to reform the template, the electrophilic C-terminal fragment E was preactivated as a thiobenzyl ester and the nucleophilic N-terminal fragment N was unmodified (Figure 4b).¹⁴

Self-replication is achieved when the hydrophobic face of the helical peptide template T is able to interact with the hydrophobic face of fragments E and N. The nucleophilic

fragment N is within proximity to react with the electrophilic fragment E creating another template peptide to catalyze further reproduction (Scheme 4).

Initial rates of formation increased as the initial concentration of template to the reaction increased, indicating autocatalysis. Experimental data followed the square-root profile characteristic of synthetic replicators. Control experiments showed that the autocatalysis was template-assisted.¹⁵ No catalysis is observed when the reaction is run in the presence of a denaturing solution of guanidinium hydrochloride (2.5M), indicating the crucial

Scheme 4.



role conformation plays in catalysis. Mutations on the hydrophobic face of the peptide template were made to prevent binding of either the E or N peptide chains. Addition of the mutant templates showed product formation profiles similar to reactions without template T addition. These mutations were thus found to be non-catalytic. This data is consistent with the template-assisted mechanism.

Response to Environmental Change

Utilizing a similar tertiary coiled-coil structure, Chmielewski and coworkers modified the *e* and *g* peptide residues with glutamic acid.¹⁶ Under acidic conditions the protonated Glu side chains should promote the formation of the α -helical structure, and at pH = 7.5 the negatively charged Glu chains should destabilize the α -helix and adopt a random coil conformation. The template E1E2 was fragmented into two peptides at the Ala₁₇-Cys₁₈ bond and the end groups modified. Peptide bond formation utilizing the strategy developed by Kent produced the template E1E2 (Figure 5). It was believed that at low pH the peptide would form a helix and act as an active template for its self-replication, and at higher pH the peptide would denature into the random coil conformation. As a result, the reaction would go from autocatalytic to bimolecular and a reduction of product formation would be observed.

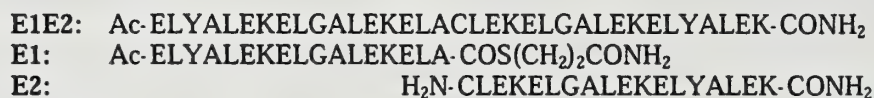


Figure 5. Peptide sequence of template E1E2, electrophile E1, and nucleophile E2.

Circular dichroism (CD) spectroscopy revealed a pH dependent transition from a random coil to a helical structure for E1, E2 and E1E2, with a maximum helical content at pH 4.0. CD indicated the tertiary coiled-coil structure of the template E1E2 at pH 4.0. Kinetic studies were then conducted at pH levels ranging from pH 3.0 to 7.5. Low rates of template formation were observed at higher pH. Only at low pH did the reaction rate increase significantly. Maximum product formation at pH 4.0, corresponds to the pH at which the peptide has maximum helicity.

An increase in rate as the initial concentration of template E1E2 was increased demonstrated the systems' autocatalytic activity. The initial rate of product formation followed the square root law indicative of self-replicating systems. At pH 7.5, no catalysis was observed. Addition of 50% trifluoroethanol (a known coiled-coil denaturant) to the reaction at pH 4.0 showed inhibition of product formation. Chmielewski and coworkers were able to show a peptide that is able to alter or control its self-replication as the pH environment around the peptide changes.

Modification of the *e* and *g* side chains with lysine provided Chmielewski with a peptide template that would form a helix at highly basic conditions or at neutral pH in the presence of NaClO₄.¹⁷

The peptide was again fragmented at Ala₁₇ and Cys₁₈ and bond formation occurred though the Kent route (Figure 6).

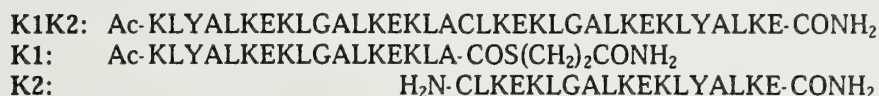


Figure 6. Peptide sequence of template K1K2, electrophile K1, and nucleophile K2.

CD showed that the maximum helical content of the template K1K2 and fragments K1 and K2 was at 2.5M NaClO₄. Product formation at varying NaClO₄ (0.0 – 2.0M) concentrations was measured. A significant increase in rate was observed at 1.0 and 2.0M NaClO₄. Autocatalysis was shown at varying amounts of initial template K1K2. Initial rates of product formation followed the square root law indicative of self-replicating systems.

Molecular Evolution: Auto- and Cross-Catalysis

Utilizing the peptide templates K1K2 and E1E2, Chmielewski and coworkers began to probe the cross-catalytic nature of these peptides.¹⁸ Two hybrid peptide templates K1E2 and K2E1 were also synthesized. Auto- and cross-catalytic activities were measured at pH 7.5. Not surprisingly, templates E1E2 and K1K2 did not display autocatalysis. All templates, however, displayed cross-catalysis with at least one other sequence.

Equimolar amounts of peptide fragments E1, E2, K1 and K2 reacted at pH 7.5 produced nearly equimolar amounts of templates E1E2, K1K2 and E2K1 along with a preference for E1K2. In subsequent experiments each template was added to the mixture and the product distribution measured. Template K1K2 and E1E2 displayed the most dramatic results producing majority fragments E1E2 and K1K2 respectively (Figure 8a). Next, the reaction environment was altered. An acidic medium promoted the catalysis of peptide E1E2 (>95%), while reaction at pH 7.5 and 2M NaClO₄ exhibited a

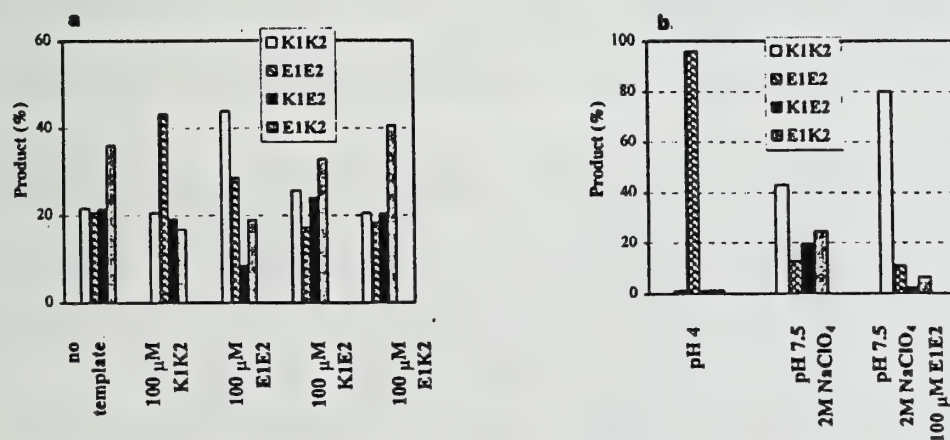


Figure 8. a) Product distribution from mixed fragment reaction (E1 + E2 + K1 + K2) at pH 7.5
 b) Product distribution from mixed fragment reaction when reaction conditions are changed.

preference for K1K2. Addition of template E1E2 to the reaction mixture increased the preference for K1K2 (>80%) (Figure 8b). This example demonstrated a symbiotic relationship formed between two peptides E1E2 and K1K2.

CONCLUSION

While scientists have yet to discover a peptide or DNA/RNA system that is able to self-replicate from its monomeric components, significant strides have been made toward the understanding of self-replication. So far, research has been able to provide examples of systems that respond to environmental change as well as cooperate to promote formation of other molecules. As more complex systems are studied, perhaps it will one day be possible to realize chemical systems that better mimic living systems.

REFERENCE

- (1) Joyce, G. F. *Nature* 1989, 338, 217-224.
- (2) Tjivikua, T. B., P.; Rebek, J., Jr. *J. Am. Chem. Soc.* 1990, 112, 1249-1250.
- (3) Nowick, J. S., Feng, Q., Tjivikua, T., Ballester, P., Rebek, J., Jr. *J. Am. Chem. Soc.* 1991, 113, 8831-8839.
- (4) Wintner, E. A. C., M.M.; Rebek, J., Jr. *Acc. Chem. Res.* 1994, 27, 198-203.
- (5) Conn, J. M., Wintner, E.A., Rebek, J., Jr. *J. Am. Chem. Soc.* 1994, 116, 8823-8824.
- (6) Conn, M. M., Wintner, E.A., Rebek, J., Jr. *Angew. Chem. Int. Ed. Engl.* 1994, 33, 1577-1579.
- (7) Pieters, R. J. H., I.; Rebek, J., Jr. *Angew. Chem. Int. Ed. Engl.* 1994, 33, 1579-1581.
- (8) Pieters, R. J. H., I.; Rebek, J., Jr. *Tetrahedron* 1995, 51, 485-498.
- (9) Miller, S. L. *Science* 1953, 117, 528-529.
- (10) von Kiedrowski, G. *Angew. Chem. Int. Ed. Engl.* 1986, 25, 932-935.
- (11) Sievers, D. von Kiedrowski, G. *Nature* 1994, 369, 221-224.
- (12) von Kiedrowski, G. W., B.; Helbing, J.; Matzen, M., Jordan, S. *Angew. Chem. Int. Ed. Engl.* 1991, 30, 423-428.
- (13) Lee, D. H., Granja, J.R., Martinez, J.A., Severin, K., Ghadiri, M.R. *Nature* 1996, 382, 525-528.
- (14) Dawson, P. E., Muir, T.W., Clark-Lewis, I., Kent, S.B.H. *Science* 1994, 266, 776-779.
- (15) Severin, K. L., D.H.; Martinez, J.A.; Ghadiri, M.R. *Chem. Eur. J.* 1997, 3, 1017-1024.
- (16) Yao, S. G., I.; Zutshi, R.; Chmielewski, J. *J. Am. Chem. Soc.* 1997, 119, 10559-10560.
- (17) Yao, S. G., I.; Zutshi, R.; Chmielewski, J. *Angew. Chem. Int. Ed. Engl.* 1998, 37, 478-481.
- (18) Yao, S. G., I.; Zutshi, R.; Chmielewski, J. *Nature* 1998, 396, 447-450.

CYTOMIMETIC VESICLES: BEHAVIOR AND APPLICATIONS

Reported by Mary L. Kraft

September 20, 1999

INTRODUCTION

Vesicles are spherical assemblies with an aqueous interior separated from the outside by an amphiphilic bilayer (Figure 1). They are capable of imitating cell like processes such as fission, fusion, endocytosis and exocytosis. Since vesicles mimic cell processes, they are referred to as cytomimetic and can be used as simple models for biological cells.

Like biological cells, vesicle bilayers are composed of amphiphilic lipids. These bilayers create a semipermeable barrier between the external media and the interior of the vesicle. The lipids are impermeable to most ionic or polar compounds. However, water can pass through the bilayers due to its small size.¹

Vesicles form spontaneously when suitable amphiphiles are placed in aqueous solutions. The bilayer assembles with the amphiphiles' hydrophobic tails towards the middle of the bilayer, and the polar head groups facing the aqueous interior or exterior of the vesicle. Several methods have been used to prepare vesicles. When amphiphiles are mixed with aqueous buffers, they self assemble into vesicles that are actually encased by multiple lipid bilayers. This type of vesicle is referred to as multilamellar. Sonicating the multilamellar vesicles results in vesicles with a single bilayer. These unilamellar vesicles are called liposomes.¹ Other methods utilized to induce liposome formation include freeze-thaw, drying-rehydration, dialysis, and solid hydration.² Vesicles made by these methods range in size from several hundred Å to hundreds of μm. Vesicles are characterized by DSC, TEM, SEM, and for larger vesicles, light or phase contrast microscopy.

TEMPERATURE AND CHEMICALLY-INDUCED SHAPE CHANGES

Shape transitions in vesicles are important because they mimic cellular processes. Understanding the physical foundations of how these events occur provides information about cellular surface changes such as endocytosis, budding and exocytosis. Several researchers have observed shape alterations in simple vesicles arising from temperature variations, or from polymerizing part of the lipid bilayer. Accounts of these transformations and theories that explain this phenomenon follow.

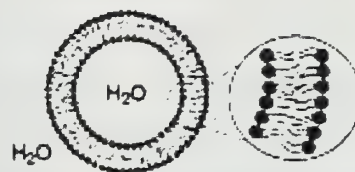


Figure 1. Diagram of a vesicle in aqueous media. The enlarged portion shows the lipid bilayer.²

Temperature-Induced

Temperature-induced shape transitions in vesicles were studied by J. Kas and E. Sackmann.³ Vesicles were made of dimyristoylphosphatidylcholine (DMPC) (**1**) were placed in deionized Millipore water and heated to 41.0 °C. The vesicles were initiated as spherical at 27.2 °C and became ellipsoidal at 36.0 °C. Further heating induced a variety of different pear or bowling pin shaped vesicles between the temperatures of 37.5–40.9 °C. Finally at 41.0 °C, a small bud appears. A schematic of these conversions is exhibited in Figure 2.

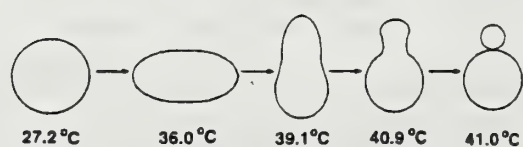


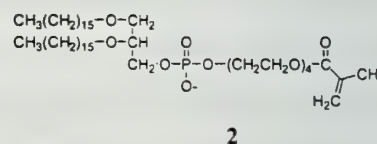
Figure 2. Vesicle shape changes according to temperature.²

These shape changes can best be explained by the Svetina and Zeks bilayer coupling hypothesis.⁴ This hypothesis explains shape transformations in terms of differential changes in area changes for the inner and outer monolayers, or leaflets. The asymmetry that results from

an increase or decrease in area for one leaflet relative to the other promotes curvature, causing the vesicle to pucker. Increases in the area of the outer leaflet result in bud like formation, while increases in the inner leaflet of the bilayer result in an invagination. The various shape changes can result from environmental variations such as temperature fluctuations.

Chemically-Induced

Sackmann et al. performed another experiment on vesicles composed of **1** and a polymerizable lipid, bis-(hexadecyloxy)propyl-12-methacrylyl-3,6,9,12-tetraoxa-dodecyl-phosphate (4,16-POMECY) (**2**) in a 4:1 ratio³. Prior to photopolymerization, the vesicles existed as pear shaped entities in a 55 millimolar mannitol solution at 29 °C. After two minutes of irradiation from a mercury lamp to photoinduce polymerization, a pocket, which resembled the vesicle within a vesicle structure shown in Figure 3, was induced in the vesicle.



This transformation can be explained in terms of Svetina and Zeks coupled bilayer model. When the 4,16-POMECY lipids are incorporated into the bilayer, they have a tendency to accumulate in the outer leaflet of the bilayer due to steric repulsion of the large head groups. This idea is supported by small angle neutron scattering experiments.³ Polymerizing these head groups leads to a reduction in the

area of the outer leaflet relative to the inner leaflet. As a result, the outer leaflet shrank creating an invagination in the vesicle.

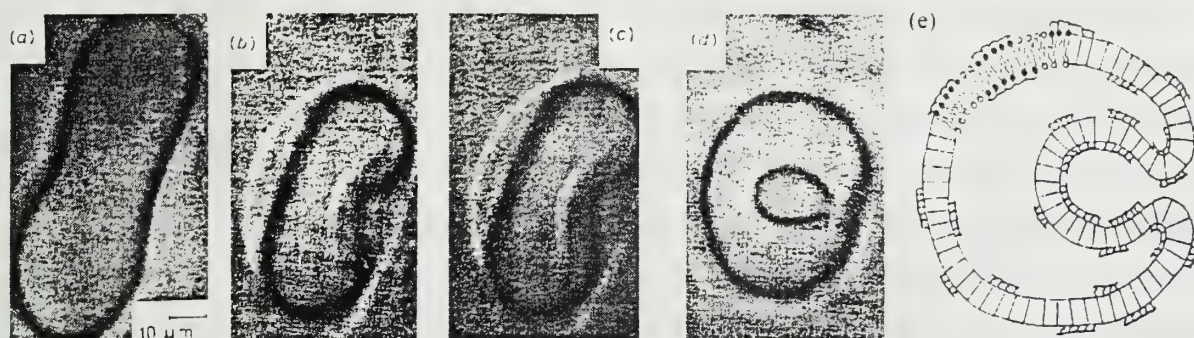
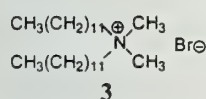
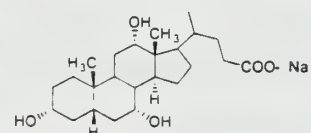


Figure 3. Shape changes due to polymerization of the outer bilayer. a) Vesicle before polymerization. b) and c) Vesicles after initiation by UV radiation. d) Final transformation of vesicle. e) Diagram of a polymerized vesicle.⁴



Surfactant-triggered vesicle-vesicle interactions, such as fusion, the merging of two vesicles, have also been extensively studied. Menger and Gabrielson examined the foraging of DDAB (3) vesicles triggered by the addition of sodium cholate (4).⁵ (Foraging is a very fast series of fusion reactions.) Sodium cholate was added to a solution of vesicles, producing a chain reaction of fusion events. A single vesicle progressively grew as it absorbed a cluster of nearby smaller vesicles. When there were no longer any vesicles to be consumed, the large vesicle began to fall apart. Lipid molecules were expunged from the bilayer, as though the bilayer space was unzipping. Even more surprising was the observation that the vesicle maintained its spherical shape during this progression as illustrated in Figure 4d.



4

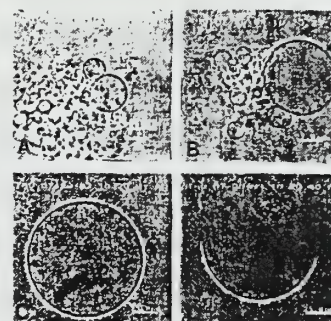


Figure 4. Micrographs of foraging. (A). A vesicle, indicated with the arrow, before foraging activity. (B) Vesicle foraging. Note how the indicated vesicle has grown. (C). The vesicle after foraging. (D) The vesicle unzipping.⁵

The interaction of surfactants on vesicles is another area of significant importance. Surfactants are typically used as soaps since they are capable of solvating the hydrophobic components of materials, including the lipid layers in biomembranes. Surfactants, with a hydrophilic head group and a single nonpolar tail, are be classified as anionic, cationic, or non-ionic according to the charge on the surfactant's head group. At the critical micelle concentration (cmc) surfactants form micelles in aqueous solutions.⁸ Jones has explained the effect of surfactants on biomembranes.⁸ When a vesicle is exposed to a surfactant the lipid layer becomes saturated with surfactant molecules disrupting bilayer packing. If a high enough concentration

of surfactant is added to the vesicle, the bilayer begins to eject micelles composed of surfactant and lipid.

Menger and Gabrielson studied the effects of octyl glucoside on giant unilamellar vesicles.⁵ They added octyl glucoside to the vesicles at a concentration lower than the cmc. This low concentration did not result in vesicle disintegration, but rather resulted in a “birthing process” in which a smaller vesicle was able to force its way through the bilayer of a larger vesicle. The hole created in the parent vesicle was capable of instantaneously resealing, as displayed in Figure 5. It was proposed the surfactant disrupted the bilayer enough to momentarily part the lipid molecules, allowing the smaller vesicle to push its way through.

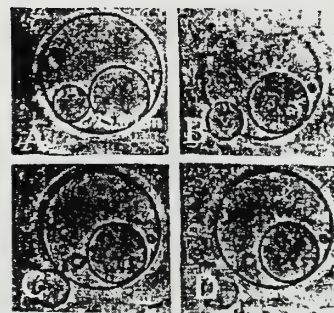


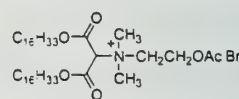
Figure 5. (A). A vesicle with two smaller vesicles trapped inside. (B) One of the smaller vesicles pushes its way through the bilayer (C) and reaches the outer medium. (D) The membrane of the outer vesicle is completely healed.⁵

APPLICATIONS OF CYTOMIMETIC VESICLES

Drug Delivery

Attempts to use vesicles for applications other than cell models have also been made. The ability of a vesicle to entrap substances within its interior, coupled with the cell-like nature of its membrane (ensuring their biodegradability and biocompatibility in animals) makes vesicles prime candidates for use as drug delivery agents.

Menger et al. explored using vesicles as drug delivery agents.^{9,10} Menger et al. created vesicles that were ruptured when exposed to acetylcholinesterase (AcE), an enzyme that is overproduced by neuroblastoma.¹¹ A 7-hydroxyquinolinium salt, which is fluorescent after hydrolysis, was encapsulated inside vesicles composed of amphiphile (5).

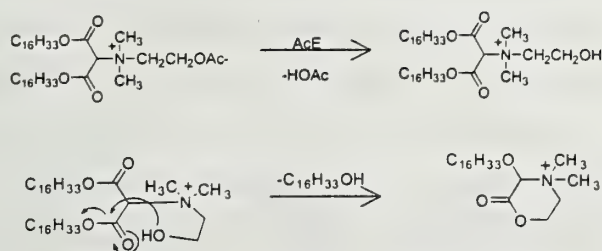


5

The vesicles were put into a buffered solution (pH = 6.8, phosphate buffer) and 1.1×10^{-8} M of AcE was added. The observed fluorescence suggested the indicator molecules escaped from the vesicles whereupon they were hydrolyzed by the AcE. The AcE also ruptured vesicles by indirectly catalyzing the hydrolysis of one of the lipid tails (Scheme 1). Because single tailed amphiphiles usually do not form bilayers,¹⁰ the bilayer was destabilized and the vesicles ruptured. This discovery is significant because it demonstrates the prospective release of vesicle contents near a neuroblastoma cell.

Zalipsky and coworkers have developed vesicles for drug delivery which exhibit a long lifetime in the body.^{13,14} Cellular clearance of liposomes from the body before reaching the target delivery site can be minimized by the addition of methoxypolyethylene glycol (mPEG) to the surface of the liposomes. These longer-lifetime liposomes are referred to as sterically stabilized liposomes, or SSLs.¹³

Scheme 1.



of this linker severs the PEG chain from the liposome and allows the vesicle to destabilize, releasing its entrapped contents.

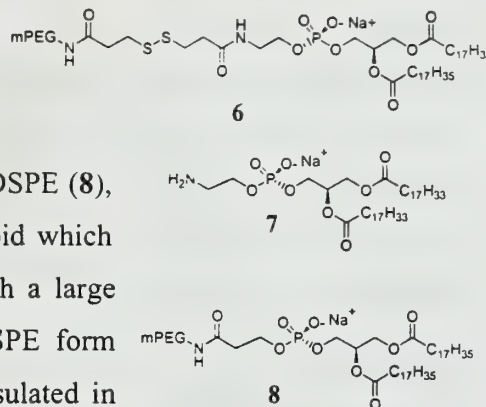
Liposomes were made from 3 mol % of disulfide-linked mPEG-DTP-DSPE (6) and 97 mol % dioleoylphosphatidylethanolamine (DOPE) (7). Control

vesicles were also formed with DOPE and 3 mol % of mPEG-DSPE (8), which lacks a disulfide bond. DOPE is a fusion-assisting lipid which only forms bilayers when accompanied by an amphiphile with a large hydrophilic portion. Both mPEG-DTP-DSPE and mPEG-DSPE form bilayers with DOPE. When fluorescent molecules were encapsulated in

these vesicles, very little leakage occurred. However, when dithiothreitol (DTT), a thiolytic agent, was added to media containing the PEG-DTP-DSPE molecules, the fluorescent molecules were released from the liposomes. This indicated that the loss of PEG side chains from the liposomes resulted in destabilization of the lipid bilayers, inducing the disintegration of the vesicles. There was no corresponding effect when DTT was added to the control vesicles. These results show that the mimetic secretory cells can successfully release drugs when triggered by a thiolytic agent.

Needham and coworkers have also invented liposomes for drug delivery.¹² They created a lipid-enclosed microgel that is analogous to a secretory cell. Spherical microgel cores were prepared from methylene-bis-acrylamide and methacrylic acid in a 1:4 mole ratio. This resulted in anionic, pH sensitive microgels that were loaded with a cationic form of doxorubicin (DX), a red, fluorescent anticancer drug, at a concentration of approximately 1 M. Next the microgels were shrunk in a low pH solution, and coated with a lipid bilayer in order to prevent the enlargement of the vesicles in physiological environments. The microgels were mixed with a 4:1:5 ratio of dipalmitoylphosphatidylcholine, dipalmitoylphosphatidylglycerol, and cholesterol. A green fluorescent dye was added to the liposome bilayer in order to designate the presence of lipid bilayer encasing the microgel. The resulting liposomes were examined by differential interference contrast micrography, producing an image of a red ball with green edges. This indicated the lipid bilayer encapsulated the

Although these vesicles have extra stability in the body, the PEG chains grafted to the bilayer actually overstabilize the liposome preventing either fusion or drug release. To solve this problem, Zalipsky and coworkers created a cleavable linker between the vesicle bilayer and the PEG chain.¹⁴ Cleavage



microgel. The final step was to induce the release of the drug from the vesicle which necessitated rupturing the vesicle. The bilayer was disrupted electromechanically by applying voltage to the liposome. Upon vesicle rupture the resulting exposure to the more basic surrounding media caused the microgel to swell to 160% its original size within four seconds. The deterioration of the lipid bilayer allowed Na^+ in the surrounding media to diffuse into the microgel and the DX and remaining protons to diffuse out. Monitoring by bright-field microscopy showed the gradual loss of the DX until

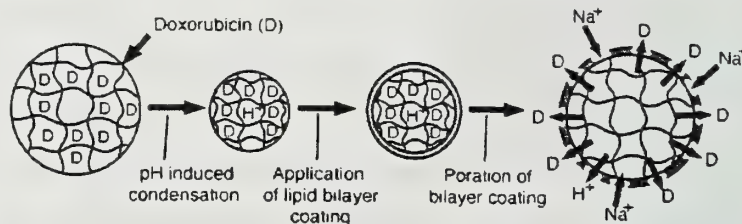
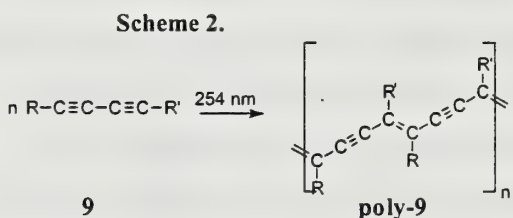


Figure 6. Application and release of doxorubicin (D) from the lipid encased microgel. D is loaded into the microgel, followed by pH induced-volume shrinkage. Microgels were encased with lipid bilayers. Finally, drug release results from poration of the lipid bilayer.¹⁴

the microgel became clear. The entire process is illustrated in Figure 6. By modifying this method to use the selective destruction of the liposome bilayers by ultrasound, this process can be potentially utilized for the release of drugs within body.¹²

Biosensors



The application of vesicles as biosensors has also been explored. Charych et al. have utilized modified polydiacetylenes (**poly-9**) as biosensors by modifying the surface of the vesicle formed from the amphiphiles with biologically active molecules.¹⁵⁻¹⁹ Diacetylene (**9**) photopolymerizes by 1,4-addition of the triple bonds (Scheme 2). By modifying the R groups on (**9**), an amphiphilic polymer that assembles into vesicle bilayer can be made. The π -conjugation of the polymerized amphiphiles result in colored vesicles. When a pathogen binds to a receptor on the polymer containing vesicle, a color change occurs. Before binding solutions containing the unbound vesicles are purple or blue. When pathogens bind to the receptors the solutions turn red, pink, or orange. This color change, termed biochromism, results from a disturbance in the bilayer's membrane packing. This may possibly be from changes in the side chain conformations, or from the insertion of the attached pathogen's membrane into the vesicle's bilayer.

In one example, Charych and coworkers^{15,18} modified a diacetylene monomer with sialic acid. Sialic acid was chosen because it binds to hemagglutinin (HA) lectin, which is the receptor of the influenza virus. The C-glycoside of sialic acid was coupled to 10,12-pentacosadiynoic acid (**10**) resulting in the functionalized monomer (**11**). Then 1-10% of **11** was mixed with **10**, and hydrated to

form vesicles. The vesicles were irradiated for either 5 to 10 minutes to form solutions of blue polymerized vesicles, or 10 to 30 minutes to form purple vesicle solutions. The addition of

HA to these solutions resulted in a color change from blue to pink, or purple to orange. The color transitions are observable both visually and by UV-vis spectroscopy. Both vesicles have a maximum absorption at 630 nm and a smaller peak at 550 nm. After addition of the virus, the maximum at 630 nm decreases in relation to the absorption at 550 nm. Graphs of these UV spectra are pictured in Figure 7. Vesicles without sialic acid did not exhibit a color change when exposed to influenza virus particles. Likewise, no color change was observed when

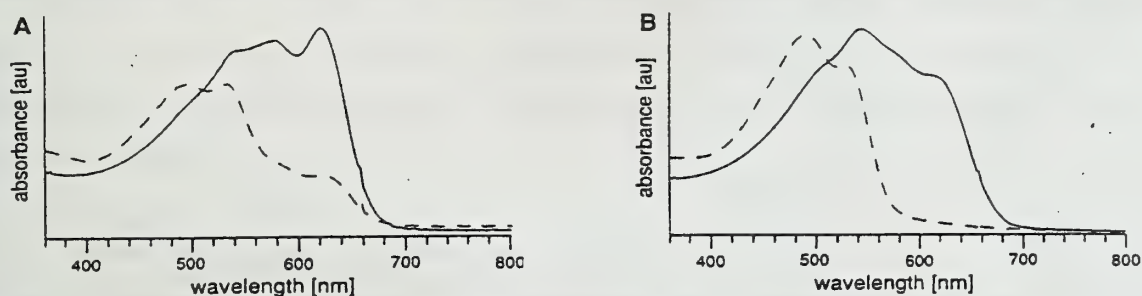
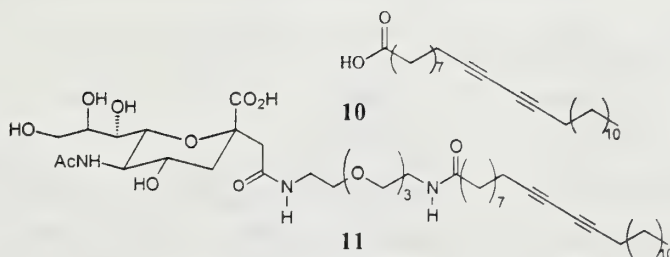


Figure 7. Absorption spectra of solutions of (A) blue vesicles after 8 minutes of irradiation, and (B) purple vesicles 24 minutes of irradiation. The solid line represents the vesicles before exposure to HA and the dashed line is after one hour of exposure.¹⁸

bovine serum albumin was added to sialic acid functionalized vesicles. This experiment has significance because the cytomimetic vesicles quickly and easily indicate whether or not a particular ligand efficiently binds a particular pathogen.

CONCLUSION

Vesicles mimic cell membranes. In the lab, researchers have demonstrated that they are capable of inducing, as well as explaining shape transformations on these self assembled amphiphiles. Progress has also been made on using these cytomimetic devices in medical applications. In the future, other achievements in the use of these materials are sure to come.

REFERENCES

- (1) Voet, D.; Voet, J. G. *Biochemistry*, 2nd Edition; John Wiley & Sons: New York, 1995.
- (2) Menger, F. M.; Angelova, M. I. *Acc. Chem. Res.* **1998**, *31*, 789-797.
- (3) Sackmann, J. K. *Biophys. J.* **1991**, *60*, 825-844.
- (4) Hoekstra, D. *Biochemistry* **1982**, *21*, 2833-2840.
- (5) Menger, F. M.; Gabrielson, K. *J. Am. Chem. Soc.* **1994**, *116*, 1567-1568.
- (6) Cowley, A. C.; Fuller, N. L.; Rand, R. P.; Parsegian, V. A. *Biochemistry* **1978**, *17*, 3163-3168.

- *
- (7) McIntosh, T. J.; Magid, A. D.; Simon, S. A. *Biochemistry* **1987**, *26*, 7325-7332.
 - (8) Jones, M. N. *Chem. Soc. Rev.* **1992**, *21*, 127-136.
 - (9) Menger, F. M.; Johnston, J. J. *Am. Chem. Soc.* **1991**, *113*, 5467-5468.
 - (10) Menger, F. M.; Nelson, K. H.; Guo, Y. *Chem. Commun.* **1998**, *18*, 2001-2002.
 - (11) Kimhi, Y.; Mahler, A.; Saya, D. *J. Neurochem.* **1980**, *34*, 554.
 - (12) Kiser, P. F.; Wilson, G.; Needham, D. *Nature* **1998**, *394*, 459-461.
 - (13) Zalipsky, S.; Brandeis, E.; Newman, M. S.; Woodle, M. C. *FEBS Letters* **1994**, *353*, 71-74.
 - (14) Kirpotin, D.; Hong, K.; Mullah, N.; Papahadjopoulos, D.; Zalipsky, S. *FEBS Letters* **1996**, *388*, 115-118.
 - (15) Okada, S.; Peng, S.; Spevak, W.; Charych, D. *Acc. Chem. Res.* **1998**, *31*, 229-239.
 - (16) Charych, D.; Cheng, Q.; Reichert, A.; Kuziemo, G.; Stroh, M.; Nagy, J. O.; Spevak, W.; Stevens, R. C. *Chem. Biol.* **1995**, *3*, 113-120.
 - (17) Spevak, W.; Nagy, J. O.; Charych, D. H. *Adv. Mater.* **1995**, *7*, 85-89.
 - (18) Reichert, A.; Nagy, J.; Spevak, W.; Charych, D. *J. Am. Chem. Soc.* **1995**, *117*, 829-830.
 - (19) Pan, J. J.; Charych, D. *Langmuir* **1997**, *13*, 1365-1367.

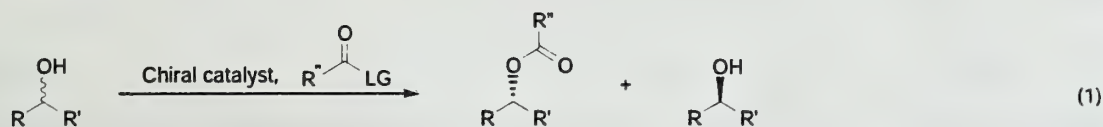
NON-ENZYMATIC KINETIC RESOLUTION OF SECONDARY ALCOHOLS

Reported by Dwight D. Kim

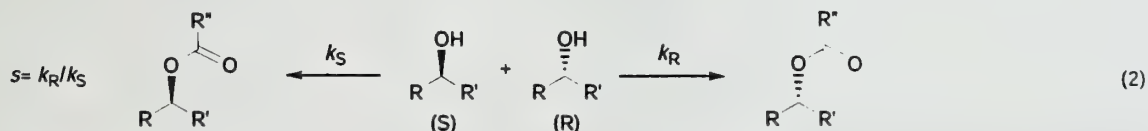
September 27, 1999

INTRODUCTION

Chiral, non-racemic, secondary alcohols are important intermediates in many synthetic sequences. These substrates have historically been prepared by stereoselective reduction of ketones, by resolution through enzymatic acylation of racemates,¹⁻³ or by resolution with stoichiometric chiral acylating reagents.^{4,5} More recently, discoveries of catalytic, non-enzymatic kinetic resolution of racemic mixtures provide elegant examples of catalytic development, and offer practical routes to these molecules.⁶ In a kinetic resolution each enantiomer of a racemic mixture reacts with an enantioenriched chiral reagent at a different rate.⁷ If the rates are sufficiently different, significant enantioenrichment of the product and the reactant can be achieved. In the case of racemic secondary alcohols, kinetic resolution is typically accomplished by selective reaction of an achiral acylating reagent under the influence of a chiral catalyst.



The relative rates of reaction for the R enantiomer and the S enantiomer are used to define the selectivity of a kinetic resolution. The selectivity factor, s , which expresses the rate of reaction of one enantiomer with respect to the other, is defined by $s = k_R/k_S$. Using the convention that the faster rate is k_R , if the s value is high, both product and unreacted starting material will be highly enantioenriched after 50% conversion. For example, if $s > 49$, then alcohol with an enantiomeric ratio (er) $> 99:1$ can be obtained at $< 55\%$ conversion.⁸ It is to be noted that the er obtained is a function of the extent of reaction.



If the selectivity factor s is not very high, enantioenriched alcohols can be recovered by driving the reaction to greater conversions at the expense of yield. As a general rule, the er of the alcohol starting material increases with conversion, while that of the acylated product decreases.

GENERAL MECHANISM AND CHIRAL REAGENTS

The proposed mechanism for the kinetic resolution of secondary alcohols begins with acylation

Copyright © 1999 by Dwight D. Kim

of the chiral catalyst as shown in Figure 1. The activated chiral intermediate next reacts selectively with one enantiomer of the alcohol. Recognition of the acylated catalyst with one enantiomer results from preferential transition state geometry during step (2). Displacement of the catalyst affords enriched acylated product, unreacted alcohol, and regenerated catalyst. An amine base is usually added to promote acylation of the alcohol, and to scavenge the acidic byproduct.

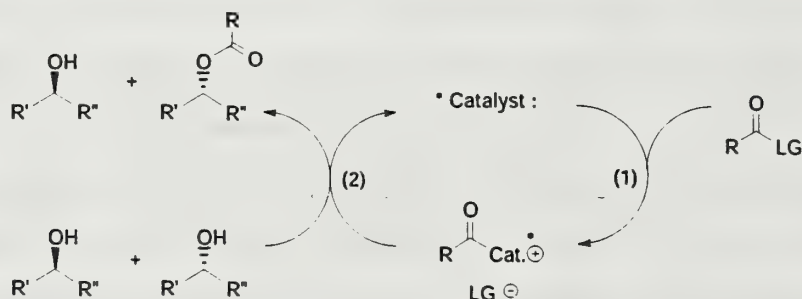
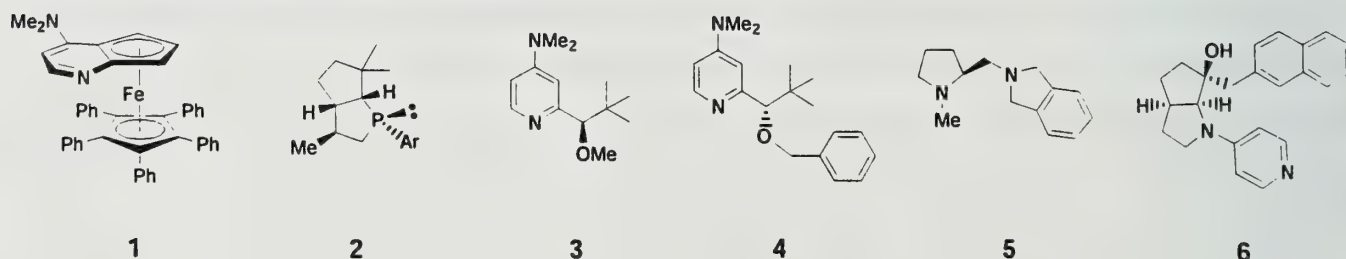


Figure 1. Catalytic cycle of kinetic resolution.

A number of nucleophilic reagents have been utilized to acylate secondary alcohols. These chiral nucleophilic acyl transfer agents, 1-6 which have been developed by a number of groups, are shown in Chart 1. This structurally diverse collection of compounds all contain a stereocenter near the nucleophilic functionality required for catalysis.

Chart 1. Structures of acylating agents.



KINETIC RESOLUTION

Aryl alkyl carbinols

Fu and coworkers have developed the 4-(dimethylamino)pyridine-based catalyst 1 for the kinetic resolution of aryl alkyl carbinols.⁸⁻¹² High enantiomeric ratios in the unreacted alcohols were obtained with just over 50% conversion to the acylated product (Table 1). These results indicate selectivity factors of $s > 43$ for this reaction.

Table 1. Kinetic Resolution of Aryl Alkyl Carbinols with 1.

$ \begin{array}{c} \text{OH} \\ \\ \text{R}^1 - \text{C} - \text{R}^2 \end{array} \xrightarrow[0^\circ\text{C}, 25.5\text{ h.}]{1\% \text{ 1, } t\text{-amyl alcohol, Et}_3\text{N, Ac}_2\text{O}} \begin{array}{c} \text{O}=\text{O} \\ \quad \backslash \\ \text{R}^1 - \text{C} - \text{R}^2 \end{array} + \begin{array}{c} \text{OH} \\ \\ \text{R}^1 - \text{C} - \text{R}^2 \end{array} $					
Entry	R ¹	R ²	% conv.	er (alcohol)	<i>s</i>
1	Ph	Me	55	>99:1	43
2	Ph	<i>t</i> -butyl	51	98:2	95
3	<i>o</i> -MeC ₆ H ₄	Me	53	>99:1	71
4	1-Naph	Me	52	97:3	65

The nucleophilicity of DMAP has been previously characterized, and indicates that the ring nitrogen can readily attack acetic anhydride.¹³⁻¹⁵ A solid state structure of the acylated intermediate 7, was obtained by means of X-ray crystallography; this complex is assumed to be the reactive intermediate in solution (Figure 2).⁹ The crystal structure of the acylated catalyst 7 demonstrates that the dimethylamino, the pyridinyl ring, and the acetyl all lie in the same plane. Support for delocalization of charge is indicated by the bond lengths within the DMAP substructure as shown in Figure 2. The oxygen of the *N*-acetyl group faces the fused cyclopentadienyl ring to minimize steric interactions. In this conformation the bulky phenyl rings effectively block the *Re* face of the acetyl group from the incoming alcohol. The rationale for selective alcohol attack is not well established but is believed to involve a combination of steric minimization, π - π stacking, and minimization of allylic strain in the substrate.

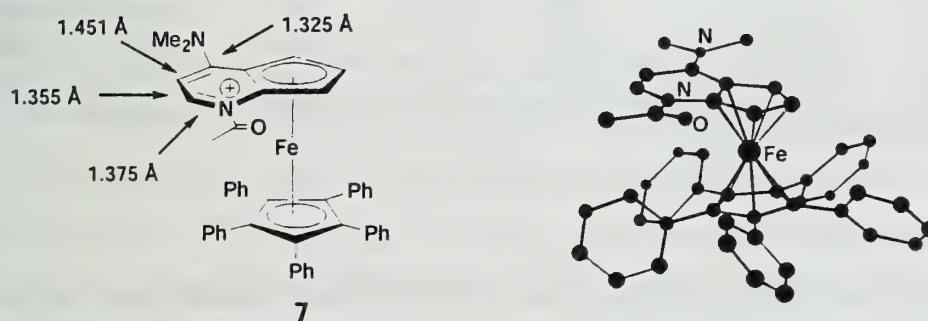
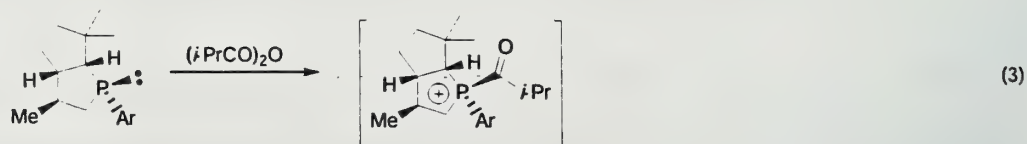


Figure 2. Crystal structure of the acylated DMAP-based catalyst.

The solvent was optimized to obtain the highest *s* values. Reactions in *t*-amyl alcohol gave the best selectivities and rates of reaction; however, it is not clear what role the solvent plays or why it is not

acylated. In contrast, previous DMAP-catalyzed acylation reactions were favored in non-polar solvents as they allowed for the formation of an ion pair of the acylpyridinium salt (Figure 1).

Vedejs and coworkers developed the 2-phospha-bicyclo-[3.3.0]octane-based catalyst **2** for resolution of secondary alcohols.^{5,16-18} Reactions in heptane with (*i*-PrCO)₂O provided the results shown in Table 2. The results demonstrate that *s* values increase with decreasing temperature (*s*= 42 at -20 °C while *s*= 22 at rt), although the rate of reaction decreased by less than a factor of ten. Although no direct evidence was provided, it was inferred that **2** undergoes reversible formation of an acylated intermediate which is preferentially attacked from one face of the carbonyl (Equation 3).



The fused ring and the phosphorus aryl group contribute significant steric hindrance, effectively retarding attack at one face of the carbonyl. Subsequent addition of alcohol to the chiral acylating species results in enantioselective product formation.

Table 2. Kinetic Resolution of Aryl Alkyl Carbinols with **2**.

Entry	R ¹	R ²	Ar (cat.)	T (°C)	Time (h)	% conv.	er (alcohol)	<i>s</i>
1	Ph	Me	3,5-di(<i>t</i> -Bu)Ph	-20	4	29	69:31	42
2	Ph	<i>t</i> -Bu	Ph	-40	65	46	89:11	67 ^a
3	<i>o</i> -MeC ₆ H ₄	Me	3,5-di(<i>t</i> -Bu)Ph	-40	4	50	97:3	145
4	1-Naph	Me	3,5-di(<i>t</i> -Bu)Ph	-40	7	30	71:29	99

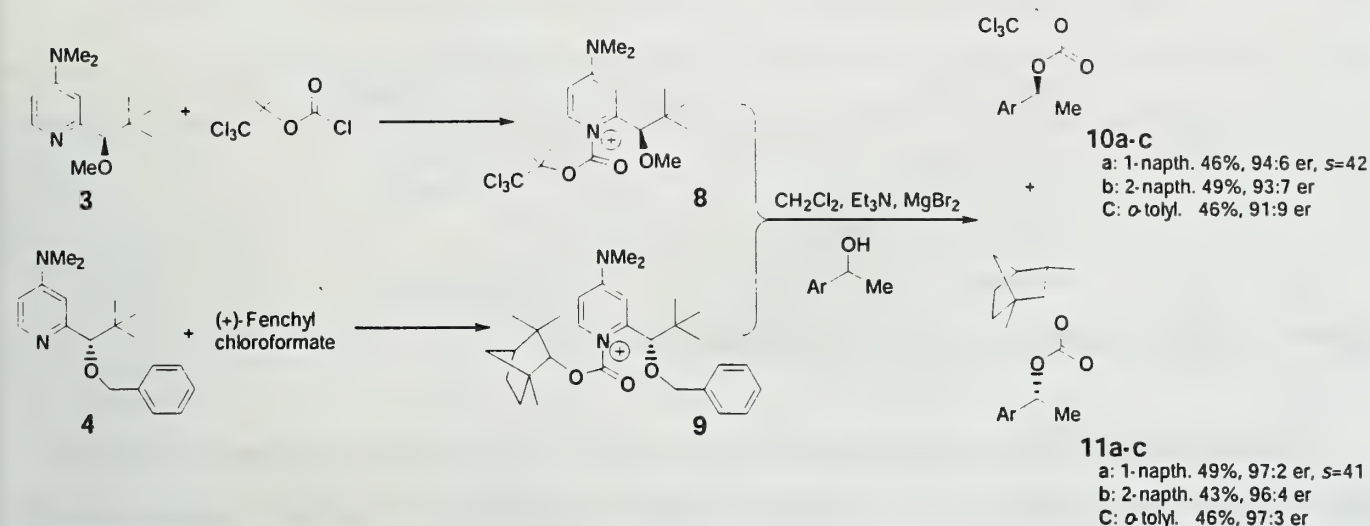
^a Toluene solvent, Bz₂O anhydride

Parallel Kinetic Resolution

Vedejs and coworkers reported a related application of DMAP-derived nucleophilic reagents for parallel kinetic resolution.¹⁹ Previously, reagent **3** was used as a nucleophilic acylating agent, but stoichiometric amounts were needed.⁵ Because of opposite configuration at the stereogenic center, reagents **3** and **4** were utilized for parallel kinetic resolution. In parallel kinetic resolution the enantiomeric alcohols react with structurally different acylating agents. In separate flasks, trichloro-*t*-butylchloroformate reacts with **3**, and fenchyl chloroformate reacts with **4** to form the acylating agents **8** and **9**, respectively (Scheme 1). Intermediates **8**, **9**, and the aryl alkyl carbinol were mixed, and at 98%

conversion, products **10a-c** and **11a-c** were obtained in high yields and with high selectivities. Although fenchyl chloroformate is chiral, both enantiomers of the analogous menthyl chloroformate provided similar selectivities when reacted with racemic alcohols, indicating that the chirality of the acyl chloride does not influence the selectivity of the reaction.

Scheme 1.



Because parallel kinetic resolution of aryl alkyl carbinols allows for the rapid reaction of each enantiomer with different acylating agents, the er's for both products are high, as reflected in the high *s* values. As long as the *s* values of the reaction are similar, the concentration of each enantiomer remains constant as each reacts with its preferred acylating agent.

Cycloalkanols

Cycloalkanols can be enantioselectively acylated in the presence of **5** and **6**. Catalyst **5** is capable of differentiating the enantiomers of various cycloalkanols with *s* values ranging from 27-160.^{20,21} The rationale for selective product formation is analogous to TMEDA-promoted acylations of secondary alcohols.^{22,23} Both sets of methyl and methylene protons exhibit downfield shifts in their ¹H NMR spectra upon addition of benzoyl chloride, suggesting that both nitrogens coordinate to the carbonyl carbon, forming a rigid catalytic acylating agent.

The catalyst developed by Fuji and coworkers, **6**, was observed to utilize a conformational change in order to differentiate the enantiomers.²⁴ Reactions with 5 mol % of **6** in toluene at room temperature, using isobutyric anhydride, afforded low *s* values ranging from 2-12. The remote stereogenic centers of **6** allowed for a catalyst that maintained the catalytic activity of the achiral model, 4-pyrrolidinopyridine (PPY). Solution structure studies of **6** have allowed elucidation of the relationship

between structure and mechanism. NOE ^1H NMR studies of both **6** and the acylated catalyst **12** have given insight into their respective solution structures. The NOE differences between the methylene protons (H_A), the bridgehead proton (H_C), and the ring protons (H_B) suggest that the pyridine ring and the naphthylene rings are not in close proximity. The authors concluded that **6** exists in an "open" conformation (Figure 3).

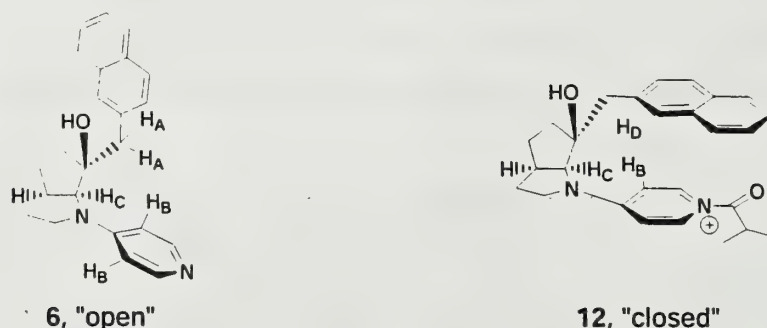


Figure 3. Solution conformations of **6** and its acylated derivative.

When an acylating reagent was added to **6**, chemical shift differences were observed in the NMR spectrum due to the formation of **12**. The pyridine protons of **12** consist of four independent chemical shifts influenced by pyridine-naphthalene π - π stacking. NOE differences between the naphthyl proton (H_D) and the pyridine proton (H_B) also confirmed a "closed" conformation (Figure 3). Therefore, the addition of the acylating agent (*i*-PrCOCl) to form the acylpyridinium adduct causes a conformational change. In the closed conformation **12** effectively has the *Si* face of the carbonyl group blocked from attack, which influences the enantioselectivity of the reaction. The cycloalkanols screened consisted of various ring sizes and had carbonyl functionalities bearing aryl groups (Figure 4). It is believed the aryl group of the cycloalkanol carbonate substrate plays an important role in enantioselectivity, as substituents bearing electron donating groups stabilize π - π interactions with the positively charged PPY portion of **12**. Substrates with stronger electron donating groups yielded reactions with higher *s* values.

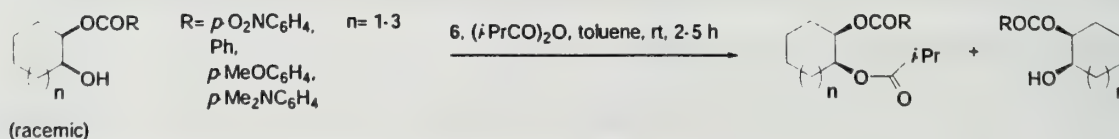


Figure 4. Various cycloalkanols acylated by **6**.

Peptide-Based Catalyst

Catalyst 13 has been designed by Miller and coworkers to mimic the active site of an enzyme.²⁵ The catalyst acylation site is based on *N*-methylimidazole with a proline functionality incorporating a β -turn motif, a key design feature of the chiral backbone (Figure 5). Cycloalkanols with a protected amino group on the adjacent carbon proved to be the best substrates for 13.

Catalyst 14 was developed by modification of 13, and was used in acylations with acetic anhydride, resulting in the structure dependent *s* values given in Table 3.²⁶ The conformation of the chiral backbone is dictated by the proline group, and substitution with L- and D-proline yielded pseudo-

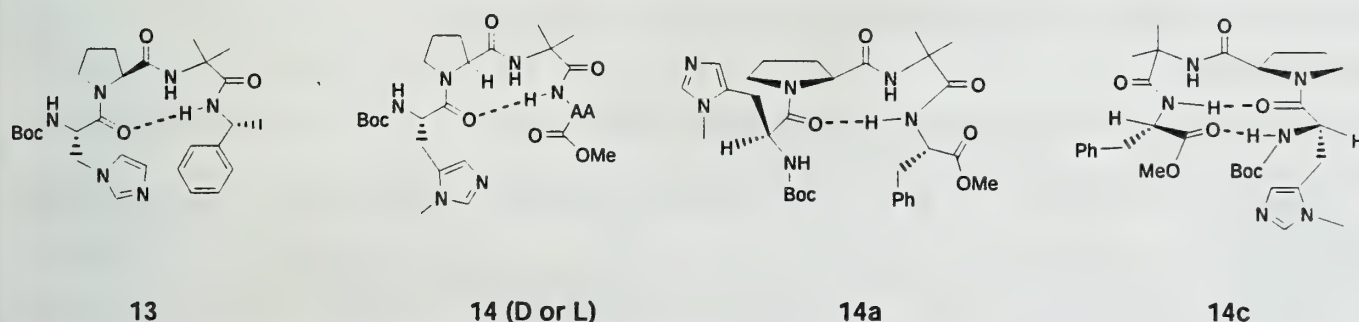
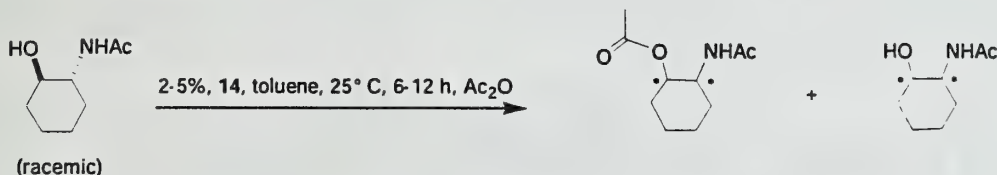


Figure 5. Proline-based catalysts developed by Miller.

enantiomeric catalysts (*vide infra*). It was found that the L- and D-proline catalysts of 14 afforded products of opposite configuration, with D-proline residues giving the higher *s* values. Changes in the amino acid (AA) of 14 affected *s* values, as opposite configurations of proline and amino acid (e.g., D-proline and L-phenylalanine) gave the highest enantioselectivities (Table 3).

Table 3. Kinetic Resolutions Catalyzed by 14



Entry	Catalyst	% conv.	er (alcohol)	<i>s</i>
1	14a, AA= L-Phe (L-Pro)	56	72:28 (R,R)	3.0
2	14b, AA= D-Phe (L-Pro)	71	94:6 (R,R)	5.7
3	14c, AA= L-Phe (D-Pro)	58	99:1 (S,S)	28.0
4	14d, AA= D-Phe (D-Pro)	57	94:6 (S,S)	14.0

AA= Amino acid substitution in 14

The most efficient catalyst 14c, and its diastereomer 14a, were investigated by ^1H NMR to determine their respective solution conformations (Figure 5). In terms of the β -turn structure, 14a and 14c can be rationalized to behave as pseudoenantiomers as acylation preferences give products of opposite configuration, though the selectivity factors are different.

CONCLUSIONS

Kinetic resolution of secondary alcohols, mediated by nucleophilic chiral catalysts, is a developing methodology. It has been shown to be an effective technique for separating racemic mixtures by conversion of one enantiomer to a separable derivative. Of importance for the synthetic applications is the fact that kinetic resolution demonstrates a proof of concept, that specifically designed catalysts are coming closer to achieving the resolving power of enzymes.

REFERENCES

1. Sih, C. J.; Wu, S. H. *Top. Stereochem.* 1989, 19, 63-125.
2. Klivanov, A. M. *Acc. Chem. Res.* 1990, 23, 114-120.
3. Wong, C. H.; Whitesides, G. M. *Enzymes in Synthetic Organic Chemistry*; Ch.2; Pergamon: New York, 1994.
4. Evans, D. A.; Anderson, J. C.; Taylor, M. K. *Tetrahedron Lett.* 1993, 34, 5563-5566.
5. Vedejs, E.; Chen, X. *J. Am. Chem. Soc.* 1996, 118, 1809-1810.
6. Somfai, P.; *Angew. Chem. Int. Ed. Engl.* 1997, 36, 2731-2733.
7. Kagan, H. B.; Fiaud, J. C.; *Top. Stereochem.* John Wiley & Sons: New York, 1988; Vol. 18, pp 249-330.
8. Ruble, J. C.; Tweddell, J.; Fu, G. C. *J. Org. Chem.* 1998, 63, 2794-2795.
9. Tao, B.; Ruble, J. C.; Hoic, D. A.; Fu, G. C. *J. Am. Chem. Soc.* 1999, 121, 5091-5092.
10. Ruble, J. C.; Latham, H. A.; Fu, G. C. *J. Am. Chem. Soc.* 1997, 119, 1492-1493.
11. Ruble, J. C.; Fu, G. C. *J. Org. Chem.* 1996, 61, 7230-7231.
12. Garrett, C. E.; Fu, G. C. *J. Am. Chem. Soc.* 1998, 120, 7479-7483.
13. Scriven, E. F. *Chem. Soc. Rev.* 1983, 12, 129-161.
14. Hofle, G.; Steglich, W.; Vorbruggen, H. *Angew. Chem. Int. Ed. Engl.* 1978, 17, 569-583.
15. Steglich, W.; Hofle, G. *Angew. Chem. Int. Ed. Engl.* 1969, 8, 981.
16. Vedejs, E.; Daugulis, O. *J. Am. Chem. Soc.* 1999, 121, 5813-5814.
17. Vedejs, E.; Bennett, N. S.; Conn, L. M.; Diver, S. T.; Gingras, M.; Lin, S.; Oliver, P. A.; Peterson, M. J. *J. Org. Chem.* 1993, 58, 7286-7288.
18. Vedejs, E.; Diver, S. T. *J. Am. Chem. Soc.* 1993, 115, 3358-3359.
19. Vedejs, E.; Chen, X. *J. Am. Chem. Soc.* 1997, 119, 2584-2585.
20. Sano, T.; Imai, K.; Ohashi, K.; Oriyama, T. *Chem. Lett.* 1999, 265-266.
21. Oriyama, T.; Hori, Y.; Imai, K.; Sasaki, R. *Tetrahedron Lett.* 1996, 37, 8543-8546.
22. Sano, T.; Ohashi, K.; Oriyama, T. *Synthesis* 1999, 7, 1141-1144.
23. Oriyama, T.; Imai, K.; Sano, T.; Hosoya, T. *Tetrahedron Lett.* 1998, 39, 3529-3532.
24. Kawabata, T.; Nagato, M.; Takasu, K.; Fujii, K. *J. Am. Chem. Soc.* 1997, 119, 3169-3170.
25. Miller, S. J.; Copeland, G. T.; Papaioannou, N.; Horstmann, T. E.; Ruel, E. M. *J. Am. Chem. Soc.* 1998, 120, 1629-1630.
26. Copeland, G. T.; Jarvo, E. R.; Miller, S. J. *J. Org. Chem.* 1998, 63, 6784-6785.

DEAROMATIZATION OF ARENES BY TRANSITION METAL COMPLEXES

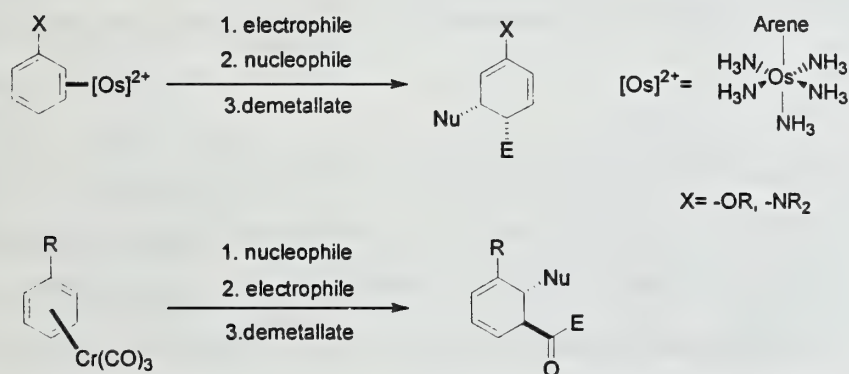
Reported by Matt Gieselman

October 7, 1999

INTRODUCTION

Due to the wide range of commercially available aromatic compounds, the dearomatization of arenes to give functionalized alicyclic rings offers a wealth of attractive intermediates. Examples of dearomatization include asymmetric Birch reductions¹, reductive alkylation,² nucleophilic addition to oxazoline substituted naphthalenes,³ and dihydroxylation by toluene dioxygenase.⁴ In recent years, metal arene complexes that dearomatize arenes have also been developed. The electron withdrawing or donating properties of the metal activate the arene ligand to nucleophilic or electrophilic addition. For synthetic usefulness, ideal complexes are easily prepared with a wide range of arene ligands, react with a wide range of nucleophiles and electrophiles, easily demetallate to give the free product, react with control of regiochemistry, and react with relative and absolute stereocontrol. η^6 -Chromium tricarbonyl complexes and η^2 -pentaammineosmium(II) complexes meet some of these criteria. These metal complexes are complementary with regards to regiochemistry, relative stereochemistry, and chemoselectivity of alkylations on the arene ligand (Scheme 1).

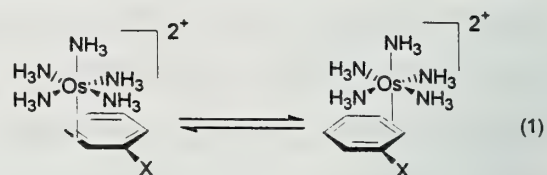
Scheme 1



PROPERTIES OF THE METAL COMPLEXES

The (arene)chromium tricarbonyl complexes are neutral 18 electron complexes, and there is a significant back-bonding interaction from the metal to the carbonyl ligands. This limits the amount of back-bonding into the arene ligand. The electron withdrawing properties of the metal, and this lack of back-bonding make the aromatic ring slightly electrophilic.⁵ Also, the carbonyl ligands adopt eclipsed conformations with the arene ligand. This conformational preference is important when considering the regiochemistry of nucleophilic addition to the complex.

Unlike the η^6 -chromium complex, pentaammineosmium(II) coordinates to an arene ligand in an η^2 fashion to form 18 electron complexes.⁶ In η^2 -osmium complexes, the bond between the osmium and the arene is stabilized by back-bonding of the filled osmium d_{π} orbitals into the π^* orbital of the arene. Even though the osmium center has a formal +2 charge, this back-bonding has such a large effect that the aromatic ring is nucleophilic. The complexation of the arene ligand also causes localization of the π electron density in the arene. The crystal structure of the naphthalene bound complex revealed alternating long and short bonds in the arene ligand. The η^2 -osmium complexes exhibit a type of fluxional behavior. In this process, the osmium moves from one side of the aromatic ring to the other (equation 1). The rate for this process in anisole derivatives is about 1 s^{-1} at 20°C .⁶ In the case of substituted benzene rings, this isomerization makes it difficult to isolate optically pure complexes.⁷ This isomerization becomes important when absolute control of stereochemistry is considered.

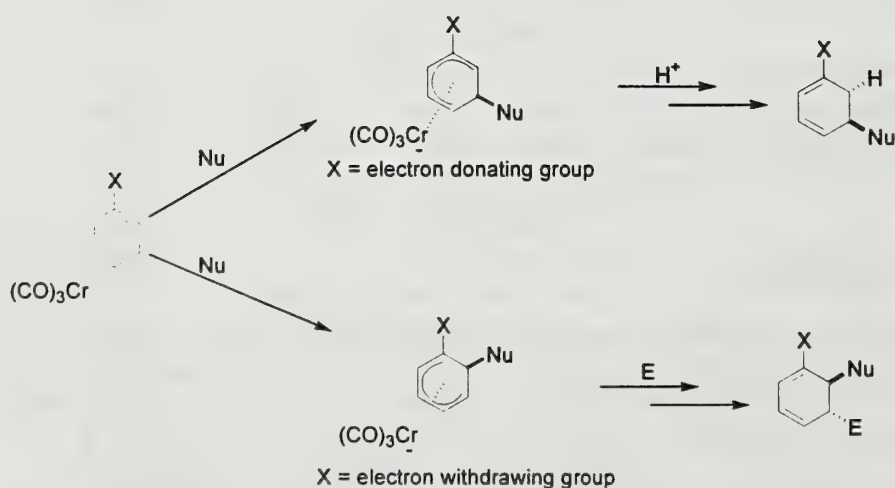


ALKYLATION OF CHROMIUM COMPLEXES

Regioselectivity

Addition of nucleophiles to (arene)chromium tricarbonyl complexes forms an η^5 -coordinated anionic complexes. The regiochemistry of nucleophilic addition depends on several factors including

Scheme 2



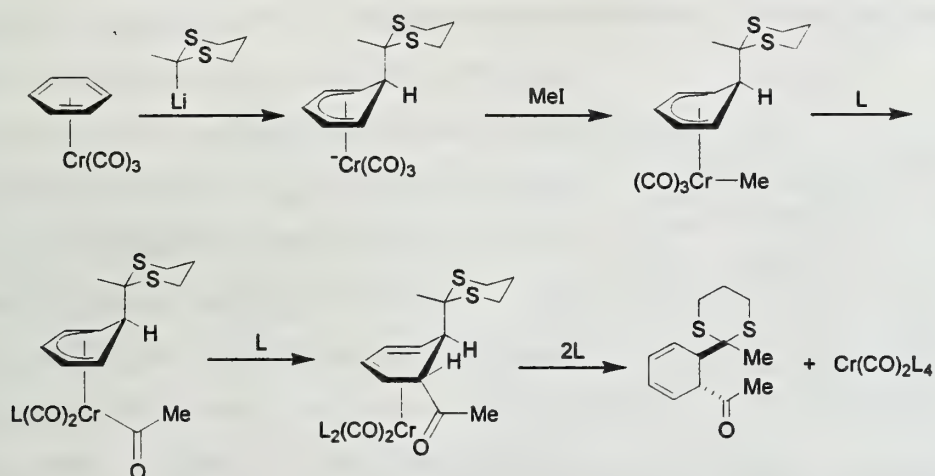
the identity of the substituent on the ring, the conformational preferences of the carbonyl ligands, the steric bulk of the nucleophile, and the reactivity of the nucleophile.^{5,8} In general, for arenes with an electron donating substituent, nucleophiles add to the meta position. On the other hand, when the substituent is an electron withdrawing group,

nucleophiles add ortho or para (Scheme 2). Subsequent addition of an electrophile or proton occurs to the adjacent ortho position in the first case, and to the adjacent meta position in the second.

Stereoselectivity

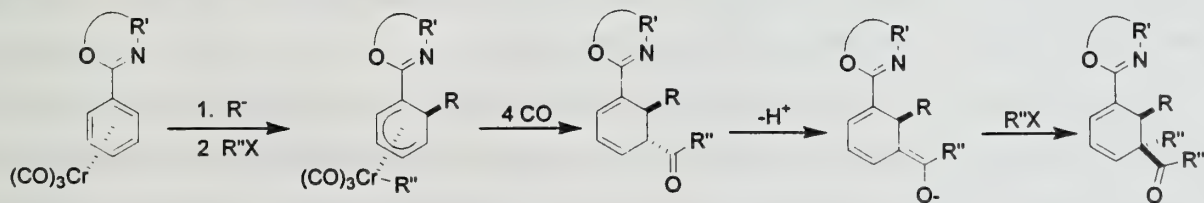
When a nucleophile is added to a chromium-benzene complex, the resulting η^5 -coordinated anion can react with an electrophile (Scheme 1). The initial nucleophilic addition occurs stereospecifically to the side of the ring *exo* to the chromium. The electrophile will then add to the metal. Migratory CO insertion followed by reductive elimination to the *endo* face of the organic ligand gives the *trans*-substituted cyclohexadienyl metal complex. Decomplexation then gives the *trans* cyclohexadiene. Scheme 3 shows an example of this sequence with a dithiane anion as the nucleophile and MeI as the electrophile. This method sets the relative stereochemistry of the new substituents with a high degree of selectivity.⁹ This reaction sequence is general for a variety of halide electrophiles.

Scheme 3



Kundig and coworkers have worked with oxazoline and methanimine substituted arene chromium complexes. In the phenyloxazoline derivatives, the nitrogen in the substituent directs the initial addition to the *ortho* position. An interesting extension of this methodology is shown in Scheme 4. The product of the demetallation step can be enolized and another equivalent of electrophile will add stereoselectively *exo* to the original nucleophile. The result is a tetra-substituted cyclohexadiene with

Scheme 4



the nucleophile and the acyl group *syn* to one another.¹⁰ Even though the addition of nucleophiles and

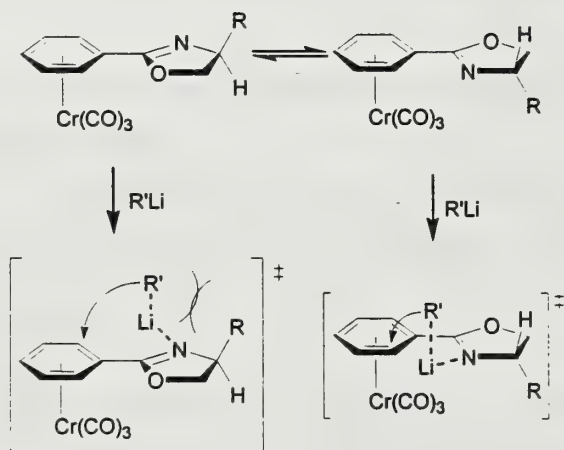
electrophiles occurs with a high degree of relative stereocontrol, all the demetallated organic products are racemic.

On monosubstituted arene ligands, the ortho positions are enantiotopic to one another as are the meta positions. Several different strategies have been conceived to induce asymmetric addition to only one of these positions. First, a chiral nucleophile can be used in the initial addition step. Enantiopure starting complexes where the arene ligand lies in a chirotopic environment can also be used to induce asymmetry,¹¹ or chiral ligands can be placed on the metal center.¹²⁻¹⁴ Finally a chiral auxiliary can be positioned on the arene substituent.^{13,15-18} The highest asymmetric induction has been achieved with chiral auxiliaries.

Kundig and coworkers have made enantiomerically pure phenyloxazoline tricarbonyl complexes. An alkyl lithium nucleophile will be delivered to one of the diastereotopic ortho positions preferentially based on steric interactions of the R group with the nucleophile as shown in Scheme 5.¹⁵ Models and X-

ray crystal structures have shown that in both rotamers in Scheme 5, the alkyl group, R, has no steric interaction with the metal group. Diastereomeric ratios as high as 99:1 have been obtained with this method.

Scheme 5



free cyclohexenone. Moderate enantiomeric ratios up to 74:26 were obtained with this method.

Pearson and coworkers have used bicyclic chiral alcohols as chiral auxiliaries.^{16,18} Addition of 2-lithio-2-methylpropionitrile followed by treatment with acid gave the substituted cyclohexenone similar to Semmalheck's work. The most effective chiral auxiliaries were based on a norbornane skeleton. The absolute stereochemistry was explained by steric approach control, and enantiomeric ratios as high as 96:4 were obtained with these chiral auxiliaries.

It has been shown that the intermediate cyclohexadienyl anion reacts with a variety of halide electrophiles. However, one general weakness to this method is the relatively low electrophilicity of the initial chromium(0) complex, such that the scope of nucleophiles that add to the arene ligand is limited.¹⁹ In general, only strong lithium carbanions add to the arene ligand. A solution to this problem

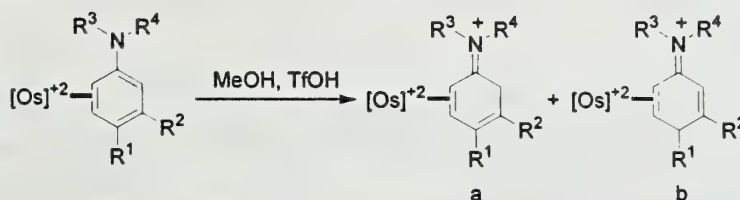
in recent years has been to use cationic manganese-arene complexes.¹⁹⁻²¹ However, this chemistry is presently limited by problems with decomplexing the metal from the arene ligand and by lack of control of absolute stereochemistry.

ALKYLATION OF PENTAAMMINEOSMIUM(II) COMPLEXES

Regioselectivity

Osmium-arene complexes that are substituted with an electron donating group are protonated or alkylated with an electrophile predominantly at the para position under equilibrating conditions.⁶ This is complementary to the η^6 -chromium complex in which a nucleophile adds initially to the meta position. The regiochemistry of the addition depends on the substitution pattern of the ring. For example, the regioselectivity of the protonation of substituted aniline derivatives is shown in Table 1.²² When there is no steric bias from substituents in the ring itself, protonation occurs at the para position (entries 1 and 2). When there is a methyl group at the para position, protonation occurs at the ortho carbon (entry 3).

Table 1. Regioselectivity of Protonation of Aniline Complexes



Entry	R1	R2	R3	R4	a	b
1	H	H	H	H	-	>95
2	H	H	H	Et	15	85
3	Me	H	Me	Me	>95	-

Reasons for this regioselectivity may be thermodynamic in nature. Protonation at the ortho position would disrupt the conjugation of the uncoordinated part of the ring. Also, the substituents on the nitrogen that lie in the plane of the ring may sterically crowd the ortho position.²³ Subsequent nucleophilic addition to the ring generally occurs at the meta position on the opposite side and face of the ring from the osmium. Anisole ligands show the same trends in regioselectivity.²³

Stereoselectivity

Aniline and anisole complexes undergo electrophilic addition at the para position with a number of Michael acceptors.^{22,23} For example, the N-ethyl aniline complex undergoes Lewis acid catalyzed Michael addition with methyl vinyl ketone to give the anilinium intermediate **1** in 89% yield (Scheme 6). The electrophile adds stereoselectively to the side of the ring exo to the osmium.²² In principle, it should be possible to add a nucleophile to the intermediate anilinium complex to give the dearomatized cyclohexadiene. However, the anilinium complexes resist this nucleophilic addition. In contrast, the anisolum counterparts do undergo nucleophilic addition with carbon nucleophiles. In addition, anisole

obtained. While this procedure has not yet been extended to a wide variety of electrophiles and nucleophiles, the method shows promise and is currently being investigated.

CONCLUSION

Coordination of chromium and osmium to arenes makes it possible to regioselectively alkylate the organic ligand to give functionalized cyclohexadienes and cyclohexenones. The two methods are complementary to one another. Coordination of chromium makes the aromatic ring electrophilic and nucleophiles add to the meta or ortho position. Coordination of osmium, on the other hand, partially localizes the π electron density and makes the ring nucleophilic at the para position by back-bonding of the d orbital electrons. When these transformations are carried out with absolute stereocontrol, they can potentially yield a wide range of attractive synthetic intermediates.

REFERENCES

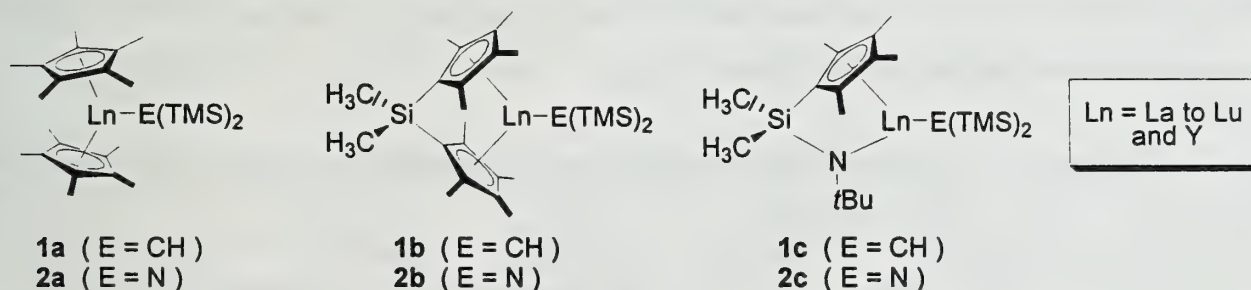
- 1) Schultz, A. G. *Chem. Comm.* **1999**, 1263-1271.
- 2) Schultz, A. G.; Pettus, L. *Tetrahedron Lett.* **1997**, 38, 5433-5436.
- 3) Shimano, M.; Meyers, A. I. *J. Org. Chem* **1995**, 60, 7445-7455.
- 4) Hudlicky, T.; Tian, X.; Konigsberger, K.; Maurya, R.; Rouden, J.; Fan, B. *J. Am. Chem. Soc.* **1996**, 118, 10752-10765.
- 5) Semmelhack, M. F. *Comprehensive Organic Synthesis*; Trost, B. M. and Fleming, I., Ed.; Pergamon Press: Oxford, U.K., 1991; Vol. 8, pp 517-549.
- 6) Harman, W. D. *Chem. Rev.* **1997**, 97, 1953-1978.
- 7) Chordia, M. D.; Harman, W. D. *J. Am. Chem. Soc* **1998**, 120, 5637-5642.
- 8) Semmelhack, M. F.; Garcia, J. L.; Cortes, D.; Farina, R.; Hong, R.; Carpenter, B. K. *Organometallics* **1983**, 2, 467-469.
- 9) Kundig, E. P.; Cunningham, A. F.; Paglia, P.; Simmons, D. P. *Helv. Chim. Acta* **1990**, 73, 386-404.
- 10) Kundig, E. P.; Bernardinelli, G.; Liu, R.; Ripa, A. *J. Am. Chem. Soc.* **1991**, 113, 9676-9677.
- 11) Quattropiani, A.; Anderson, G.; Bernardinelli, G.; Kundig, E. P. *J. Am. Chem. Soc.* **1997**, 119, 4773-4774.
- 12) Kundig, E. P.; Quattropiani, A.; Inage, M.; Ripa, A.; Dupre, C.; Cunningham, A. F.; Bourdin, B. *Pure & Appl. Chem.* **1996**, 68, 97-104.
- 13) Kundig, E. P.; Amurrio, D.; Anderson, G.; Beruben, D.; Khan, K.; Ronggang, A. R. L. *Pure & Appl. Chem.* **1997**, 69, 543-546.
- 14) Amurrio, D.; Khan, D.; Kundig, E. P. *J. Org. Chem* **1996**, 61, 2258-2259.
- 15) Kundig, E. P.; Ripa, A.; Bernardinelli, G. *Angew. Chem. Int. Ed. Engl.* **1992**, 31, 1071-1073.
- 16) Pearson, A. J.; Gontcharov, A. V.; Woodgate, P. D. *Tetrahedron Lett.* **1996**, 37, 3087-3088.
- 17) Semmelhack, M. F.; Schmalz, H. G. *Tetrahedron Lett.* **1996**, 37, 3089-3092.
- 18) Pearson, A. J.; Gontcharov, A. *J. Org. Chem.* **1998**, 63, 152-162.
- 19) Pike, R. D.; Sweigart, D. A. *Synlett* **1990**, 565-571.
- 20) Lee, T. Y.; Kang, Y. K.; Chung, Y. K.; Pike, R. D.; Swiegart, D. A. *Inorg. Chim. Acta* **1993**, 214, 125-134.
- 21) Pearson, A. J.; Gontcharov, A. V.; Zhu, P. Y. *Tetrahedron* **1997**, 53, 3849-3862.
- 22) Kolis, S. P.; Gonzalez, J.; Bright, L. M.; Harman, W. D. *Organometallics* **1996**, 15, 245-259.

- 23) Kolis, S. P.; Kopach, M. E.; Liu, R.; Harman, W. D. *J. Org. Chem.* **1997**, *62*, 130-136.
- 24) Kopach, M. E.; Kolis, S. P.; Liu, R.; Robertson, J. W.; Chordia, M. D.; Harman, W. D. *J. Am. Chem. Soc.* **1998**, *120*, 6199-6204.

INTRODUCTION

Organolanthanide reagents provide novel alternatives to traditional transition metal catalysis.¹ The development of soluble bis(pentamethylcyclopentadienyl) (Cp*) complexes **1a-c** and **2a-c** has expanded the use of lanthanides to a variety of chemical transformations (Chart 1).^{2,3,4} During the past twenty years, the reactivity of these compounds has been probed through studies of catalytic hydrogenation,⁵ polymerization,² hydrosilylation⁶ and hydroboration reactions.⁷ Two general properties emerged: extremely high turnover rate in olefin insertion ($N_t \approx 120,000 \text{ h}^{-1}$) and mildly exothermic hydrolysis of Ln-alkyl bonds in the presence of a number of protic sources. The successful application of these catalysts to intramolecular hydroamination is a direct result of these unique properties. This report will detail the reactivity and structural features of organolanthanides and their application to organic synthesis.

Chart 1. Representative Organolanthanide Catalysts

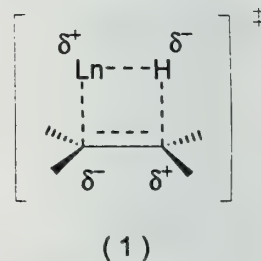


ORGANOLANTHANIDE STRUCTURAL TRENDS

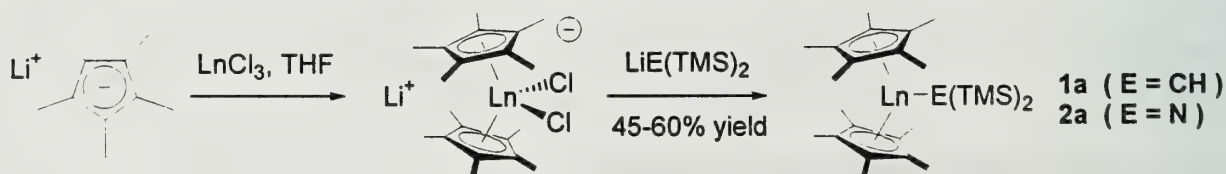
To understand better the use of these catalysts in hydroamination, it is informative to examine the general chemistry of organolanthanides. Elements within the lanthanide series have in common similar reactivities and a thermodynamically stable +3 oxidation state.⁸ Therefore, these metals are interchangeable in most reaction systems. Since ionic radius and Lewis acidity change in a systematic way from lanthanum to lutetium, the reactivity of the catalyst can be modulated to adjust to the demands of individual substrates. Metal choice adds the option of tunability to organolanthanide catalyst design.

Ligand modification, however, is still very important. Extremely bulky ligands are used to limit the maximum coordination number of the complex. In unrestricted systems employing smaller ligands, coordination numbers can often reach as high as 10 or 12. The use of bis(pentamethylcyclopentadienyl) ligands confines coordination to the so-called “equatorial girdle” between the rings.⁹ The size of this space can be adjusted as illustrated in Chart 1. Addition of a silyl tether, as in **1b** or **2b** serves to pull the rings back, opening up the metal’s coordination sphere. Further enlargement is possible by replacement of one of the Cp* rings with a nitrogen ligand as in **1c** or **2c**. These “constrained geometry” catalysts have allowed for the extension of organolanthanide-based catalysis to a wide variety of substrates. Besides obvious steric effects, such ligand modifications have subtle electronic effects. The donor ability of the Cp* rings is reduced by addition of a silyl tether, making the lanthanide ion more electropositive and more reactive.¹⁰ Substitution of a nitrogen ligand as in **1c** further alters the electronics of the metal center. The contributions of these two ligand effects are important factors in understanding the reactivity of different substrates in the hydroamination.

Unlike their transition metal counterparts, lanthanides typically do not undergo the standard oxidative addition / reductive elimination processes. The overwhelming stability of the Ln^{3+} state relative to Ln^{2+} or Ln^{4+} favors transformations through a highly polarized and highly ordered four-membered transition state ($\Delta S \approx -25$ eu).¹¹ Increasing the Lewis acidity of the metal stabilizes the polar transition state, as does appropriate functionalization of substrate (see 1).



Scheme 1. Synthesis of bis(cyclopentadienyl) lanthanide complexes 1a, 2a



Complexes **1a** and **2a** are easily prepared in one pot procedures from commercially available starting materials as shown in Scheme 1. Choice of the bis(trimethylsilyl) ligand is arbitrary since both the nitrogen and carbon analogs show identical reactivities. The one advantage in the synthesis of the nitrogen analog is that it employs commercially available LiHMDS.¹² Purification of the organolanthanides is accomplished by sublimation. While oxygen and moisture sensitivity are major drawbacks, the thermal stability of these complexes is high.

INTRAMOLECULAR HYDROAMINATION CYCLIZATIONS

Hydroamination is the addition of an amine across a double or triple bond, typically in *syn* fashion. It is a desirable process since the intramolecular version would allow easy access to naturally occurring pyrrolizidine and indolizidine skeletons. The reaction has never been popularized due to the harsh conditions and reagents employed in conventional methodologies.¹³ Although the overall reaction is exothermic ($\Delta G \approx -17$ kcal/mol), electrostatic repulsion between the π electrons of the olefin and the lone pair of the nitrogen lead to a prohibitively high activation energy.¹³ Early attempts at transition metal catalysis were unsuccessful due to catalyst poisoning through irreversible binding of the amine substrate to the electrophilic metal center.¹⁴ One procedure that has shown some success in intermolecular hydroaminations, even at catalyst loadings below 1%, has been the Pd^0 system pioneered by Yamamoto.¹⁵

Organolanthanides avoid the problem of catalyst poisoning due to the inherent lability of Ln-X bonds. The high rate of olefin insertion allows one to envision multiple cyclizations before release of the cyclized product. In recent years, organolanthanides have been applied to the cyclization of aminoalkynes,¹⁶ alkenes¹¹ and allenes.¹⁷ Intermolecular hydroamination has also been examined.¹⁸ Aminoalkenes were the first class of substrates to be examined extensively.¹¹ The scope of the cyclization and effect of catalyst structure can be seen in Table 1. Both 5 and 6 membered ring closures are possible. Products could be isolated in greater than 85% yield. Interactions between the alkene

Table 1: Cyclization of aminoalkenes

	Substrate	Product	Catalyst	Ionic radius (\AA)	N_e, h^{-1}	Temp ($^{\circ}\text{C}$)
1			$\text{Cp}^*_2\text{LaCH}(\text{TMS})_2$, 1a	1.106	140	60
2			$\text{Cp}^*_2\text{LaCH}(\text{TMS})_2$, 1a	1.106	5	60
3			$\text{Cp}^*_2\text{LaCH}(\text{TMS})_2$, 1a	1.106	45	25
4			$\text{Cp}^*_2\text{LaCH}(\text{TMS})_2$, 1a	1.106	95	25
5	5	6	$\text{Cp}^*_2\text{SmCH}(\text{TMS})_2$, 1a	1.079	48	60
6	5	6	$\text{Cp}^*_2\text{LuCH}(\text{TMS})_2$, 1a	0.977	<1	80
7	5	6	$\text{Me}_2\text{SiCp}^*_2\text{LuCH}(\text{TMS})_2$, 1b	0.977	75	80

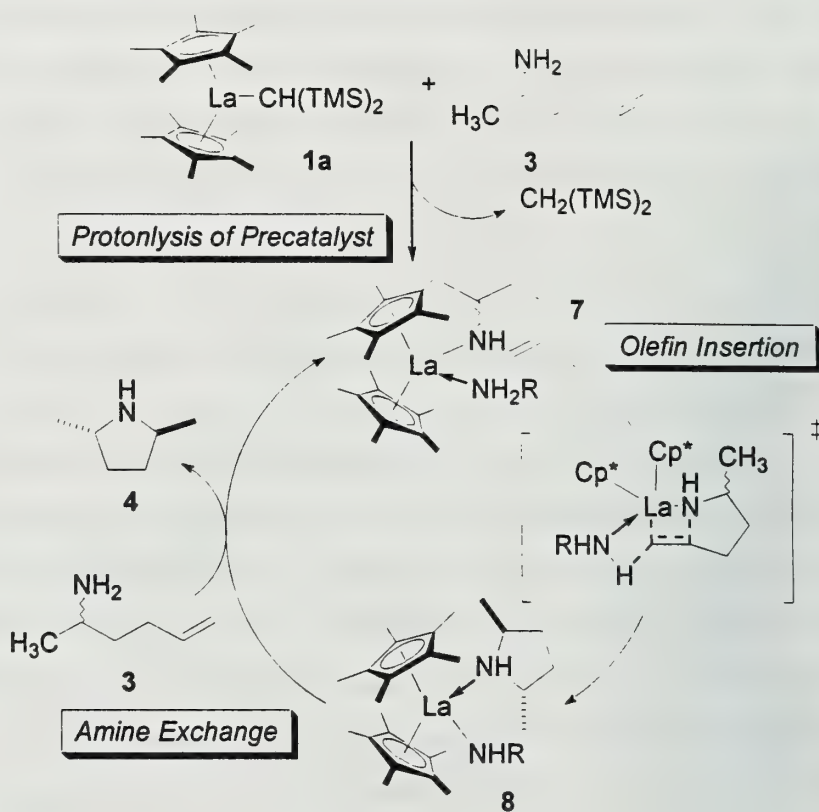
substituents and the Cp* ring favor a less congested catalyst structure: $k_{La} > k_{Sm} > k_{Lu}$. As can be seen in entry 7, the use of “constrained geometry” catalyst **1b** accelerates the reaction by opening up the coordination sphere of the metal.

The general catalytic cycle shown in Scheme 2 was proposed to explain this reactivity.¹¹ It applies equally to aminoalkynes and allenes, since all are presumed to react by the same mechanism. The rate law for these reactions was determined to be first order in lanthanide, suggesting rapid formation of an intermediate amido complex which then undergoes intramolecular olefin insertion in the rate determining step. Initiation of the cycle involves cleavage of the Ln-CH(TMS)₂ bond in the presence of the amine substrate yields the active amine-amido species **7**. The authors

proposed this termolecular structure based on the observation that addition of *n*-propylamine to the reaction increased the *trans:cis* selectivity of the cyclization of **3** by a factor of 10. Additional experiments involving *N*-deuterated **3** revealed a primary isotope effect ($k_H/k_D = 5.2$ (25°C)), indicating that a deuterium must be transferred during the rate determining step. It was proposed that the insertion is assisted by a second, coordinated amine. This suggests that the coordination of a second, unreactive amine influences the orientation of the reactive amine and the diastereoselectivity of the cyclization. The proposed amine-amido species **7** was confirmed to be an intermediate by NMR and X-ray crystallography.¹¹

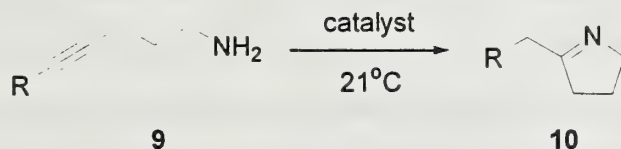
Once **7** forms, insertion of the olefin into the Ln-NHR bond occurs via a amine-assisted, four-centered transition state to yield **8**. Cleavage of the resulting Ln-R bond by a second amine regenerates **7** and liberates the free, cyclized amine. Despite a unified mechanism, the thermodynamics of these transformations are distinct for each class of substrate. The reaction of the alkynyl substrate is approximately 6 kcal/mol more exothermic than the reaction of aminoallenes while it is 22 kcal/mol more exothermic than the equivalent reaction of an aminoalkene.¹⁷ These thermodynamic differences

Scheme 2. Hydroamination Catalytic Cycle



are borne out in experiments where $k_{\text{alkyne}} > k_{\text{allene}} \gg k_{\text{alkene}}$. Due to the unique thermodynamic profile of each reaction, subtle reactivity differences with respect to the catalyst structure and metal are observed.

Table 2: Comparison of cyclization rates for various aminoalkynes



Entry	R	Catalyst	Ln ionic radius (Å)	N_t , h ⁻¹
1	H	Cp* ₂ LaCH(TMS) ₂ , 1a	1.160	135
2	H	Cp* ₂ NdCH(TMS) ₂ , 1a	1.109	207
3	H	Me ₂ SiCp* ₂ NdCH(TMS) ₂ , 1b	1.109	78
4	H	Cp* ₂ SmCH(TMS) ₂ , 1a	1.079	580
5	Me ₃ Si	Cp* ₂ SmCH(TMS) ₂ , 1a	1.079	>7600
6	H	Cp* ₂ LuCH(TMS) ₂ , 1a	0.977	711

The effect of the metal and the ligand on aminoalkyne cyclizations is shown in Table 2.¹⁶ In these representative examples, some trends immediately become clear. In contrast to alkenes, alkynes react most rapidly with the smaller lanthanide ions: $k_{\text{Lu}} > k_{\text{Sm}} > k_{\text{Nd}} > k_{\text{La}}$. The highly exothermic nature of the alkyne insertion ($\Delta H = -35$ kcal/mol) implies an early transition state that is less likely to be influenced by the steric congestion of catalysts formed from the later, smaller lanthanide elements. In the absence of steric controls, electronic effects dominate reactivity. The higher Lewis acidity of the smaller lanthanide stabilizes the growing charges in the transition state. The importance of polarization

Table 3: Comparison of cyclization rates for various aminoallenes^a

Substrate	Product	Catalyst	N_t , h ⁻¹	E / Z ratio
<p style="text-align: center;">11</p>	<p style="text-align: center;">12</p>	Cp* ₂ YCH(TMS) ₂ , 1a	31.4	14:86
11	12	Cp* ₂ LuCH(TMS) ₂ , 1a	7	12:88
	<p style="text-align: center;">(±)</p>	Cp* ₂ LuCH(TMS) ₂ , 1a	>630	20:80

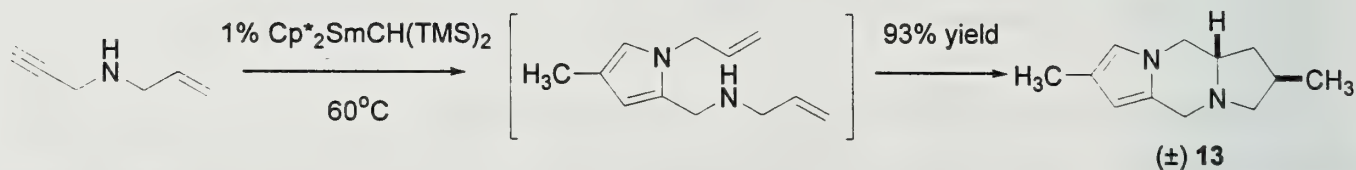
^a: all reactions run at 23°C, yields in excess of 93%

in the four-centered transition state is further emphasized in entry 5. The ability of silyl groups to stabilize α carbanions matches the demands of the transition structure (1).

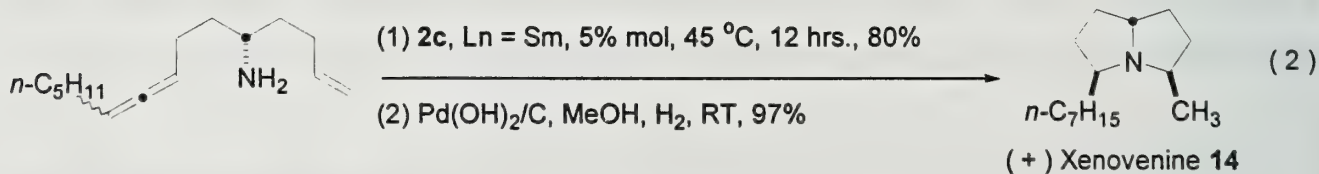
Some representative cyclizations of aminoallenes are shown in Table 3.¹⁶ The rates of this reaction are slightly lower than those of aminoalkynes. An early transition state is still operative as suggested by the low steric demands of the reaction ($\Delta H = -29$ kcal/mol). Lanthanide ions of intermediate size yield the highest rates: $k_Y > k_{Sm} > k_{Lu} \geq k_{La}$. Thus, the demands of a highly ordered transition state ($\Delta S = -16.48$ eu) balance against substrate-catalyst steric interactions, requiring a proper fit in the active complex. The “constrained geometry” catalysts **1b** and **1c** are known to give greatly increased reaction rates in these cyclizations.

Proper catalyst choice is essential for accomplishing multiple cyclizations. The reactivity patterns of the various substrates can be exploited to provide tri-cyclic products in good yields as shown in Scheme 3.^{19,20}

Scheme 3. Tandem hydroamination reaction



The methodology was put into practice in the total synthesis of a pyrrolizidine alkaloid (+)-Xenovenine, **14**.²¹ The synthesis provided enantiopure product in 10 steps with an overall yield of 10%. The key dual-cyclization step occurred in 80% yield, giving a single diastereomer (see 2).

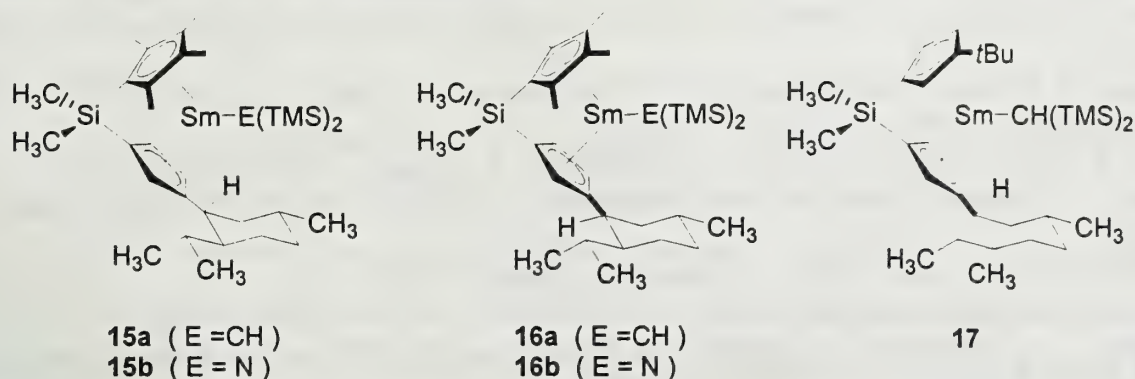


ASYMMETRIC VARIANTS

The bis(cyclopentadienyl) framework provides a scaffold for the construction of a chiral environment around the metal center. Incorporation of a chiral element by attaching it to one of the cyclopentadienyl rings provides a C_1 symmetric complex such as the (-)-menthyl complex **15a-b** (Scheme 4). This enantiopure complex was shown to cyclize aminopent-4-ene in 72% ee at $0^\circ C$.²² This moderate level of enantioselectivity is believed to be a direct result of catalyst epimerization under the reaction conditions. As shown in Scheme 5, steric interactions between the chiral ligand and the

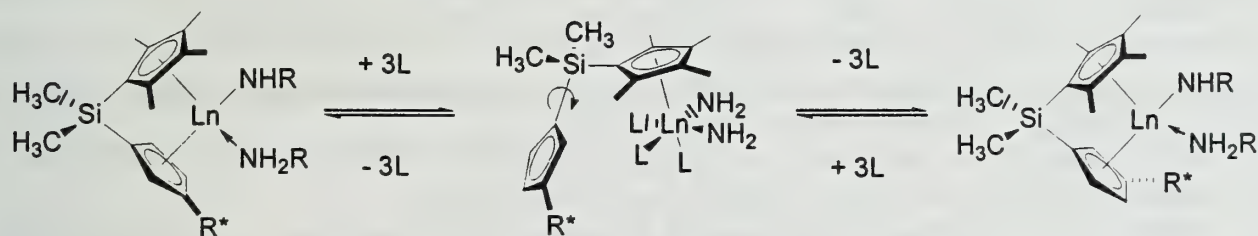
opposing Cp* ring weaken coordination to the metal and favor dissociation / re-association of the ring resulting in racemization.

Scheme 4. Chiral Organolanthanide Catalysts



Configurational changes in the chiral portion, such as in the (+)-neomenthyl complex **16a-b**, increase steric interactions, leading to faster epimerization and lower ee% under the same conditions (58 % ee).

Scheme 5. Epimerization Process of Chiral Lanthanides



OUTLOOK AND FUTURE GOALS

Further application of the intramolecular hydroamination cyclization to alkaloid synthesis may provide a new route into these commonly occurring natural products. However, questions of functional group compatibility will have to be addressed. So far, only chlorides and some ethers have been shown to tolerate the hydroamination conditions.⁶ A better understanding of the mechanism and scope of this transformation will hopefully expand its use in synthesis.

Development of efficient asymmetric catalysts will be another major step for this methodology. Designing a simple ligand which does not rely upon a large, chiral pool adduct for selectivity is desired. Developments involving “pseudo-*meso*” catalysts such as **17** may provide better results in the intramolecular hydroamination.²³ The epimerization issue, although a minor one considering the high ee % obtained, may be a unavoidable downfall. Optimistically the tunability of reactivities present in the lanthanide series may provide a solution to this problem.

REFERENCES

- (1) *Lanthanides: Chemistry and Use in Organic Synthesis*; Kobayashi, S., Ed.; Springer: New York
- (2) Jeske, G.; Schock, L. E.; Swepston, P. N.; Schumann, H.; Marks, T. J. *J. Am. Chem. Soc.* **1985**, *107*, 8103.
- (3) Gagne, M. R.; Brard, L.; Conticello, V. P.; Giardello, M. A.; Stern, C. L.; Marks, T. J. *Organometallics* **1992**, *11*, 2003.
- (4) Tian, S.; Arrendondo, V. M.; Stern, C. L.; Marks, T. J. *Organometallics* **1999**, *18*, 2568.
- (5) Jeske, G.; Lauke, H.; Swepston, P. N.; Schumann, H.; Marks, T. J. *J. Am. Chem. Soc.* **1985**, *107*, 8091.
- (6) Molander, G.A.; Retsch, W. H. *Organometallics* **1995**, *14*, 4570.
- (7) Bijpost, E. A.; Duchateau, R.; Teuben, J. H. *J. Mol. Cat. A: Chem.* **1995**, *95*, 121.
- (8) Cotton, F. A.; Wilkinson, G.; Murillo, C. A.; Bochmann, M. *Advanced Inorganic Chemistry*; John Wiley & Sons, Inc.: New York; p. 1108.
- (9) Bagnall, R. W.; Xing-Fu, L. *J. Chem. Soc. Dalton Trans.* **1982**, 1365.
- (10) Nolan, S. P.; Stern, D.; Hedden, D.; Marks, T. J. In *Bonding Energetics in Organometallic Compounds*, Marks, T. J. Ed.; Am. Chem Soc.; Washington, D.C.
- (11) Gagne, M. R.; Stern, C. L.; Marks, T. J. *J. Am. Chem. Soc.* **1992**, *114*, 275.
- (12) Tilley, T. D.; Anderson, R. A. *Inorg. Chem.* **1981**, *20*, 3267.
- (13) Muller, T. E.; Beller, M. *Chem. Rev.* **1998**, *98*, 675.
- (14) Larock, R. C. *Angew. Chem., Int. Ed. Engl.* **1978**, *17*, 27.
- (15) Kadota, I.; Shibuya, A.; Lutete, L. M.; Yamamoto, Y. *J. Org. Chem.* **1999**, *64*, 4570.
- (16) Li, Y.; Marks, T. J. *J. Am. Chem. Soc.* **1996**, *118*, 9295.
- (17) Arredondo, V. M.; McDonald, F. E.; Marks, T. J. *Organometallics* **1999**, *18*, 1949.
- (18) Li, Y.; Marks, T. J. *Organometallics* **1996**, *15*, 3770.
- (19) Li, Y.; Marks, T. J. *J. Am. Chem. Soc.* **1998**, *120*, 1757.
- (20) Molander, G. A.; Dowdy, E. D. *J. Org. Chem.* **1999**, *64*, 6515.
- (21) Arrendondo, V. M.; Tian, S.; McDonald, F. E.; Marks, T. J. *J. Am. Chem. Soc.* **1999**, *121*, 3633.
- (22) Giardello, M. A.; Conticello, V. P.; Brard, L.; Sabat, M.; Rheingold, A. L.; Stern, C. L.; Marks, T. J. *J. Am. Chem. Soc.* **1994**, *114*, 10212.
- (23) Giardello, M. A.; Conticello, V. P.; Brard, L.; Gagne, M. R.; Marks, T. J. *J. Am. Chem. Soc.* **1994**, *114*, 10241.

TRANSITION-METAL CATALYZED [4+1] CYCLOADDITIONS

Reported by Ramzi F. Sweis

October 18, 1999

INTRODUCTION

The synthesis of 5-membered carbocyclic rings has been the subject of much investigation due to their frequent occurrence in many small molecule drugs. Two of the most widely used approaches involve [3+2] cycloadditions¹ and the Pauson-Khand reaction.² An alternative to these reactions is [4+1] cycloadditions (eq 1). Variations of this have been used throughout the chemical literature to construct pyrazoles,³ pyrrolidines,⁴ pyrrolidinones,⁵ and cyclopentaquinolines.⁶ In addition, the [4+1] approach has been demonstrated in the synthesis of substituted cyclopentenenes⁷ and cyclopentanones.⁸ Recently, reports of transition metal catalysis have enhanced the utility of [4+1] cycloadditions. Two



main catalytic versions of this cycloaddition have been studied. One involves the use of iron carbonyl complexes as the active catalyst, and the other employs a rhodium-based catalyst. Advances in the understanding of the mechanism and scope of these two systems as well as other recent progress in metal catalyzed [4+1] cycloadditions are presented below.

IRON CATALYSTS

2,5-Dialkylidenecyclopentenones

The first example of a transition metal catalyzed [4+1] cycloaddition was reported by Eaton and coworkers.⁹ Treatment of diallene **1** with 10 mole % $\text{Fe}(\text{CO})_5$ and carbon monoxide produced the

Table 1.

entry	R ¹	R ²	R ³	R ⁴
1	Me	Me	Me	Me
2	<i>t</i> Bu	Me	<i>t</i> Bu	Me
3	Ph	Me	Ph	Me
4	<i>t</i> Bu	Me	Me	<i>t</i> Bu

disubstituted cyclopentenone **2** in yields of typically 72% and higher (Table 1). In entries 2 and 3, only one product was observed. The stereoselectivity in the exocyclic vinyl substituents implied that the iron catalyst exerts a π -facial preference in its coordination with the diallene. In addition, entry 4 cyclized at a much lower rate than entries 1-3. This observation was consistent with an η^4 , rather than an η^2 -coordination of the iron catalyst with the diallene since with the meso diallenes (entries 2 and 3), one face of the π -system is free of steric hindrance when coordinated in the η^4 mode. The C_2 -symmetric diallene (entry 4) does not have a sterically unhindered face. Based on this data, the catalytic cycle shown in Scheme 1 was proposed.

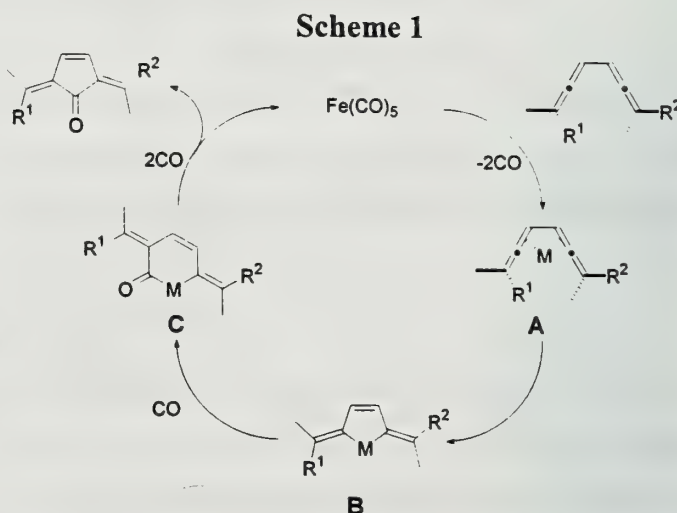
The reaction rate displayed first order dependence on the concentration of the iron carbonyl catalyst and the diallene, and inverse dependence on the concentration of carbon monoxide used. Based on the proposed catalytic cycle, the authors state that the data is consistent with the coordination of iron to the diallene as the rate-determining step. A negative entropy of activation was measured

for this reaction which lent further support to the hypothesis of coordination as the rate-determining step.¹⁰ The data do not rule out, however, that subsequent steps also can be rate determining. The inverse dependence of the reaction rate on CO concentration suggests that the formation of **A** may be reversible process. ¹³C NMR studies established that the diallene effectively promotes ¹³CO exchange into the iron catalyst. In the absence of the diallene, incorporation of the ¹³C label was not observed.

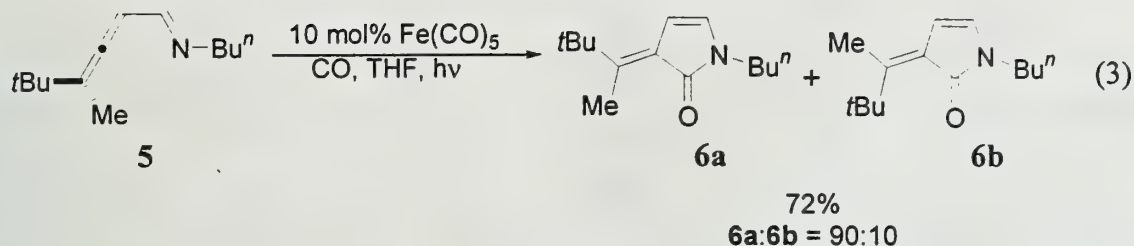
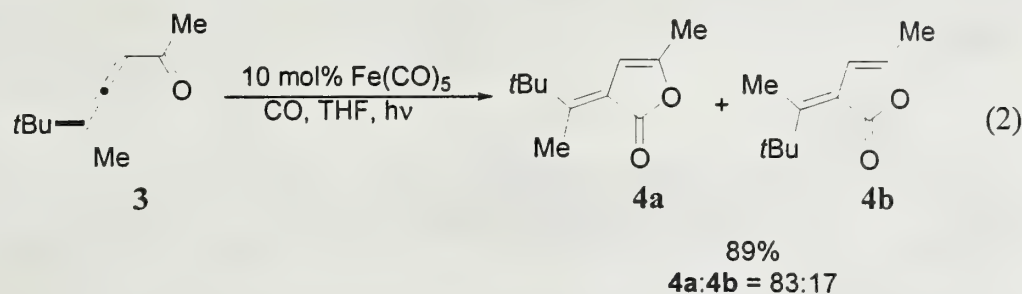
The effect of solvents on the reaction rate was also investigated. It was unclear whether coordinating solvents would assist the formation of **A** or impede it by competitively binding iron. Cyclization in highly coordinating σ -donor solvents such as THF-*d*₈ and CD₃CN was much slower than in the poorly coordinating solvent CD₂Cl₂ and the π -ligand solvent C₆D₆. This data suggests that coordination of the diallene is indeed slowed by competitive binding of solvent to the iron.

Alkylidene butenolides and pyrrolidinones

The iron-catalyzed carbonylative [4+1] methodology has been extended towards the synthesis of heterocyclic ring systems. The cycloaddition of **3** furnishes the α -alkylidenebutenolide **4** in good yields and selectivity (eq 2).¹¹ Allenyl imines also undergo cyclization under similar conditions to afford 3-



alkylidene-4-pyrrolin-2-ones (eq 3).¹² As in the previous case, the selectivity in the products is indicative of π -facial bias in the coordination of iron to the allene.



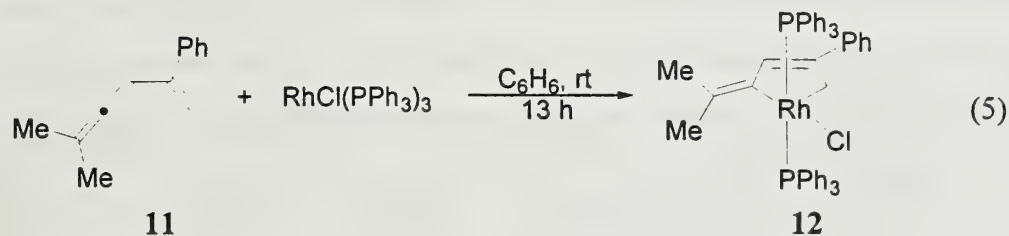
There are several differences between these reactions and the reaction of diallenes using $\text{Fe}(\text{CO})_5$. Fluorescent light is required to initiate the reaction of **3** and **5**. In addition, a rate dependence on the concentration of CO and allene is not observed. Since photochemical activation is required, it was proposed that fluorescent light promoted the displacement of a carbonyl ligand on iron with a solvent molecule. This, in turn, is believed to be the active catalyst. Low temperature IR studies confirmed the existence of such a species.¹³ In accordance with this data, the likely rate-determining step of this reaction is the dissociation of the solvent ligand from the iron before coordination of the catalyst to the allene.

RHODIUM CATALYSTS

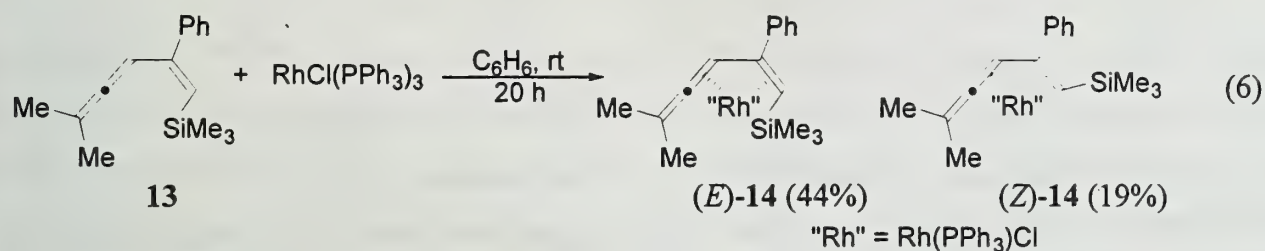
The use of rhodium catalysts for [4+1] cycloadditions has been developed by Ito and coworkers.^{14,15} The cationic DuPHOS-rhodium complex catalyzed the conversion of vinylallene **7** to the alkylidene cyclopentenone **8** with the formation of a new stereogenic center at C₅ (Table 2).¹⁶ The proposed catalytic cycle follows that reported for the iron-catalyzed reaction. Although the enantioselectivities are highly substrate dependent, it is a significant accomplishment to gain stereocontrol over substrates that do not have directing heteroatoms.

The stereoselectivity of this reaction was rationalized on the basis of η^4 -binding between the rhodium metal and the allene substrate. Two models were proposed to explain the absolute stereochemical outcome (Figure 1). The depiction of η^4 -coordination to one face of the vinyl allene in **I**

(eq 4). Substrate **9** does not undergo cycloaddition when subjected to the conditions of Table 2. This supports the notion that only the η^4 -coordinated rhodium intermediate is capable of cycloaddition.¹⁸ In contrast, a planar σ^2 -complex, **12**, is formed when a vinylallene having no substituents on the alkenyl terminus is added to the rhodium metal (eq 5).



When the substituted vinylallene, **13**, was complexed with rhodium, two products, the *E* and *Z* isomers, were obtained in 44% and 19% yields respectively (eq 6). Heating an isolated sample of (*E*)-**14**



gradually led to its isomerization to the *exo* form. This is believed to occur through a ring-flipping mechanism whereby the (*E*)-**14** transforms to the more thermodynamically stable (*Z*)-**14** by going through a planar σ^2 -complex metallacycle. Implication of this planar metallacycle in the isomerization of two η^4 -complexes is supported by the isolation of **12**. This in turn, lends further credence to the existence of a planar σ^2 -metallacycle in the catalytic cycle.

PLATINUM CATALYSTS

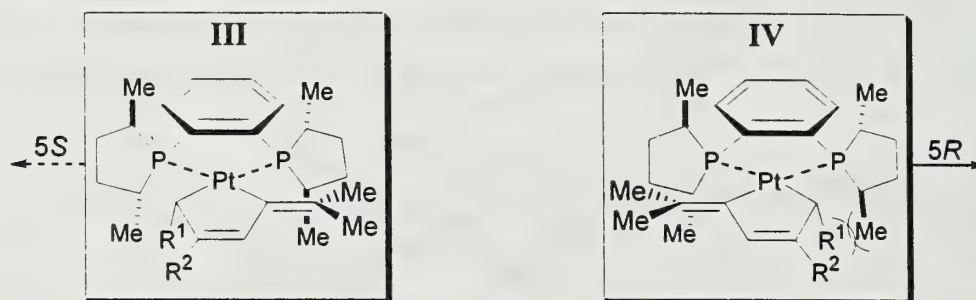
In an identical system to that used for rhodium, Ito and coworkers have found that a reversal of stereoselectivity was observed when the metal was changed to platinum (Table 3). This is a unique

Table 3.

entry	7 $\xrightarrow[\text{CO, DME, 55-60}^\circ\text{C, 6-20h}]{[\text{Pt(cod)}_2]-(R,R)\text{-Me-DuPHOS}}$			8
	R ¹	R ²	yield	e.r. (<i>R</i>):(<i>S</i>)
1	n-Pr	n-Pr	76	87:13
2	-(CH ₂) ₄ -		81	82:18
3	-(CH ₂) ₅ -		96	88:12
4	n-Bu	n-Bu	97	85:15

observation given that there are few published examples whereby induced chirality was reversed by switching the transition metal employed. Unlike in the case with rhodium, the enantioselectivities seem to be substrate independent. The reversal of induced chirality was explained by a change in the stereodetermining step of the catalytic cycle. It was proposed that the selectivity was determined after the establishment of the planar σ^2 -metallacycle of platinum. The two possible diastereomers of the σ^2 -metallacycle are shown in Figure 2. Metallacycle **III** is thermodynamically more stable since it does not

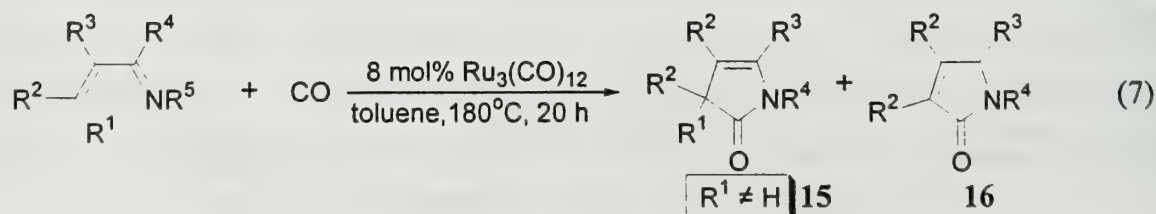
Figure 2.



contain the steric interaction shown in metallacycle **IV**. It is the latter metallacycle, however, that leads to the observed product. Ito and coworkers have rationalized that the unfavorable diastereomer, **IV**, incorporates carbon monoxide with much higher reactivity than **III**. The origin of this higher reactivity remains as of yet, unknown.

RUTHENIUM CATALYSTS

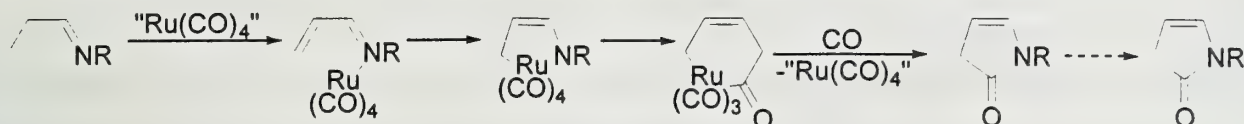
A catalytic version of the [4+1] cycloaddition employing ruthenium-based catalysts has been developed by Murai and coworkers.¹⁹ What is unique in this case is that there is no necessity for allenyl substrates as in previous methodologies. The vinylic substrates used were simple α,β -unsaturated imines (eq 7). Reaction conditions are quite harsh, but generally lead to the γ -lactams in good (>80%)



yields. The identity of the R^1 substituent is crucial in determining the location of the internal double bond. If $R^1=H$, then the initially formed **15** is transferred to the thermodynamically more stable α,β -unsaturated isomer, **16**. The substrates are generally substituted at the R positions by alkyl groups.

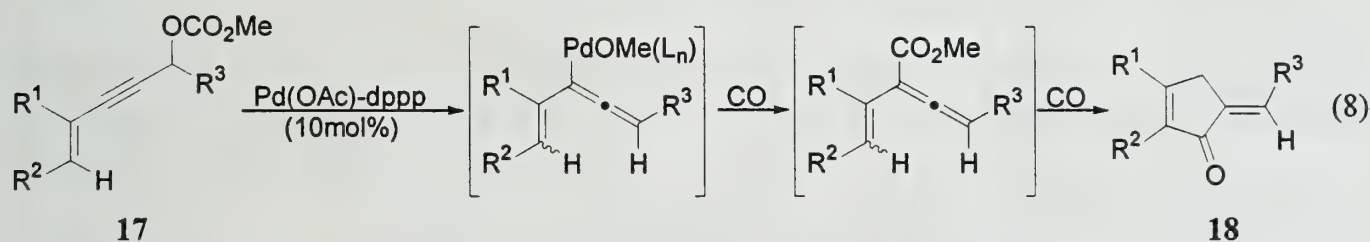
Attempted cycloaddition of aromatic imines led to no cyclization for reasons that remain as of yet unclear. The proposed reaction pathway proceeds by initial coordination of the ruthenium catalyst to the imine (Scheme 2). This initial coordination facilitates conversion to the metallacycle which undergoes subsequent insertion of CO and reductive elimination to regenerate the catalysts and the γ -lactam product.

Scheme 2.



PALLADIUM CATALYSTS

A few interesting palladium-catalyzed [4+1] cycloadditions have also been reported. Vicinal dicarbonylations of enyne carbamates have been shown to proceed through a conjugated enallene system to yield the corresponding α,β -unsaturated cyclopentenones through the use of a bidentate-ligand palladium catalyst (eq 8).^{20,21} The enallene has been detected and shown to carbonylate to the cyclic



product, confirming its existence as an intermediate. The reactions are conducted at room temperature, thereby constituting an extremely mild cycloaddition.

CONCLUSION

Transition metal catalyzed [4+1] cycloadditions can serve as viable alternatives to current methods of constructing 5-membered carbocyclic and heterocyclic rings. The π -facial selectivity of metal coordination is a key factor in the development of asymmetric versions. The unique systems and substrate scope of several metal catalysts shown for this construct demonstrates the potential for applicability in a variety of systems.²² A convenient feature of a [4+1] cycloaddition is that five-membered rings such as cyclopentenones can be synthesized with additional functionality in the form of an external vinylic bond. In addition, the use of rhodium and platinum can enable the incorporation of a stereogenic center into the ring. Only limited examples of conducting these cycloadditions in the presence of other heteroatom functionalities have been shown to date, and this may constitute a

limitation. Much investigation into the use of this reaction, towards syntheses has yet to be demonstrated, but recent advances in the understanding of the mechanism will aid future development.

REFERENCES

- (1) Trost, B. M.; Grese, T. A.; Chan, D. M. T. *J. Am. Chem. Soc.* **1991**, *113*, 7350-7362. and references therein.
- (2) Schore, N. E. In *Comprehensive Organic Synthesis*; Trost, B. M., Ed.; Pergamon Press: Oxford, 1991; Vol. 5, p 1037-1064.
- (3) Imming, P.; Mohr, R.; Muller, E.; Overheu, W.; Seitz, G. *Angew. Chem., Int. Ed. Eng.* **1982**, *4*, 284.
- (4) Padwa, A.; Norman, B. *J. Org. Chem.* **1990**, *55*, 4801-4807.
- (5) Rigby, J. H.; Qabar, M. *J. Am. Chem. Soc.* **1991**, *113*, 8975-8976.
- (6) Curran, D. P.; Liu, H. *J. Am. Chem. Soc.* **1991**, *113*, 2127-2132.
- (7) Padwa, A.; Filipkowski, M. A.; Meske, M.; Murphree, S. S.; Watterson, S. H.; Ni, Z. *J. Org. Chem.* **1994**, *59*, 588-596.
- (8) Colomvakos, J. D.; Egle, I.; Ma, J.; Pole, D. L.; Tidwell, T. T.; Warkentin, J. *J. Org. Chem.* **1996**, *61*, 9522-9527.
- (9) Eaton, B. E.; Rollman, B.; Kaduk, J. A. *J. Am. Chem. Soc.*, **1992**, *114*, 6245-6246.
- (10) Sigman, M. S.; Eaton, B. E. *J. Am. Chem. Soc.*, **1996**, *118*, 11783-11788.
- (11) Sigman, M. S.; Kerr, C. E.; Eaton, B. E. *J. Am. Chem. Soc.*, **1993**, *115*, 7545-7546.
- (12) Sigman, M. S.; Eaton, B. E. *J. Org. Chem.* **1994**, *59*, 7488-7491.
- (13) Sigman, M. S.; Eaton, B. E. *Organometallics* **1996**, *15*, 2829-2832.
- (14) Murakami, M.; Itami, K.; Ito, Y. *Angew. Chem. Int. Ed. Eng.* **1995**, *34*, 2691-2694.
- (15) Murakami, M.; Itami, K.; Ito, Y. *J. Am. Chem. Soc.* **1997**, *119*, 2950-2951.
- (16) Murakami, M.; Itami, K.; Ito, Y. *J. Am. Chem. Soc.* **1999**, *121*, 4130-4135.
- (17) Murakami, M.; Itami, K.; Ito, Y. *J. Am. Chem. Soc.* **1996**, *118*, 11672-11673.
- (18) Murakami, M.; Itami, K.; Ito, Y. *Organometallics* **1999**, *18*, 1326-1336.
- (19) Morimoto, T.; Chatani, N.; Murai, S. *J. Am. Chem. Soc.* **1999**, *121*, 1758-1759.
- (20) Mandai, T.; Tsuji, J.; Tsujiguchi, Y. *J. Am. Chem. Soc.* **1993**, *115*, 5865-5866.
- (21) Darcel, C.; Bruneau, C.; Dixneuf, P. H. *Synlett* **1996**, 218-220.
- (22) Murakami, M.; Itami, K.; Ito, Y. *Angew. Chem. Int. Ed. Eng.* **1998**, *38*, 3418-3420.

ZIRCONIUM-CATALYZED ASYMMETRIC ADDITION OF GRIGNARD REAGENTS TO OLEFINS

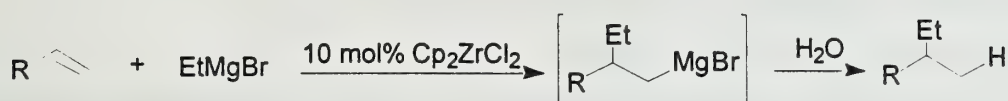
Reported by Hien M. Nguyen

10/25/99

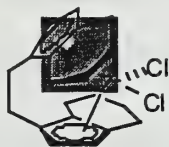
INTRODUCTION

The development of catalytic asymmetric reactions that effect formation of carbon-carbon bonds is an important and challenging task in chemical synthesis.¹ In 1983, Dzhemilev reported that Cp_2ZrCl_2 catalyzed the addition of EtMgCl to unactivated olefins (Scheme 1).² Subsequent investigations have shown Cp_2ZrCl_2 to catalyze the addition of alkylmagnesium halides to a variety of alkenes with high levels of regio- and diastereoselectivity.³⁻⁵

Scheme 1. Dzhemilev Reaction



If the union of an alkylmagnesium halide and an olefin were to be effected in an enantioselective fashion, a useful catalytic asymmetric carbomagnesation reaction would be at hand. This review will highlight the use of the C_2 -symmetric ethylene-bis(tetrahydroindenyl) zirconium dichloride (**1**) in asymmetric carbomagnesation reactions.



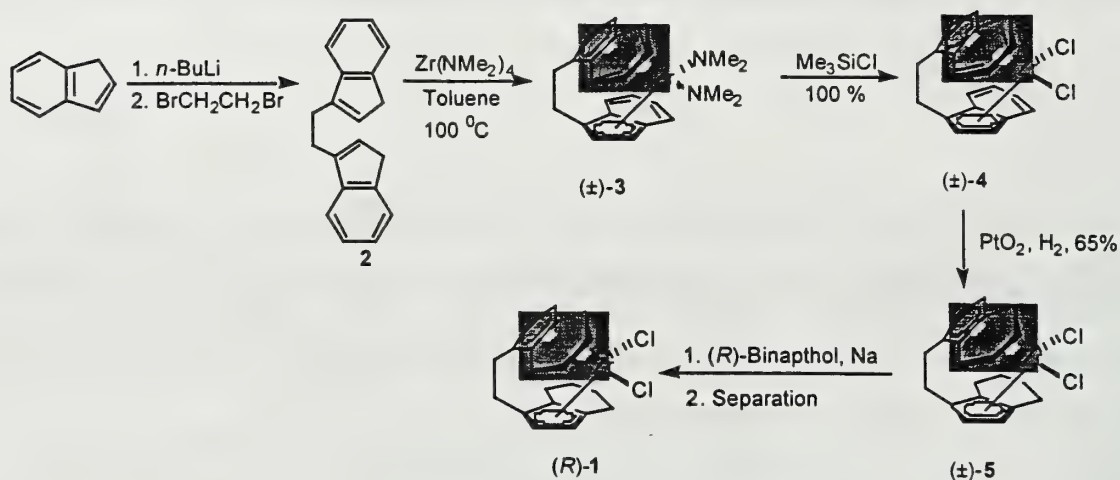
1

SYNTHESIS AND RESOLUTION OF C_2 -SYMMETRIC ZIRCONIUM CATALYST

Zirconium catalyst **1** was first synthesized by Brintzinger and coworkers starting from $\text{ZrCl}_4(\text{THF})_2$ and $(\text{EBI})\text{Li}_2$ (EBI = ethylene 1,2-bis(1-indenyl)).⁶ This strategy was further modified by Collins⁷ and Buchwald;⁸ however, these approaches gave **1** in low yield. Recently, a more efficient synthesis of **1** was reported by Jordan and coworkers (Scheme 2).⁹ The reaction of $\text{Zr}(\text{NMe}_2)_4$ and **2** in toluene at 100 °C afforded **3** as a mixture of diastereomers that rapidly equilibrated.⁹ The initial *rac/meso* ratio of **3** was 2/1 after 2 h but increased to 13/1 after 17 h. Pure (\pm) -**3** could be isolated by recrystallization from toluene. Subsequent treatment of (\pm) -**3** with TMSCl provided (\pm) -**4**, that was subsequently converted to (\pm) -**5** via hydrogenation. The catalyst could be resolved through the formation binaphtholate complexes.¹⁰ Treatment of (\pm) -**5** with 0.5 equiv of nonracemic sodium binaphtholate followed by separation resulted in (R) -**1**.

Copyright © 1999 by Hien Nguyen

Scheme 2. Preparation of (EBTHI)ZrCl₂ (1)

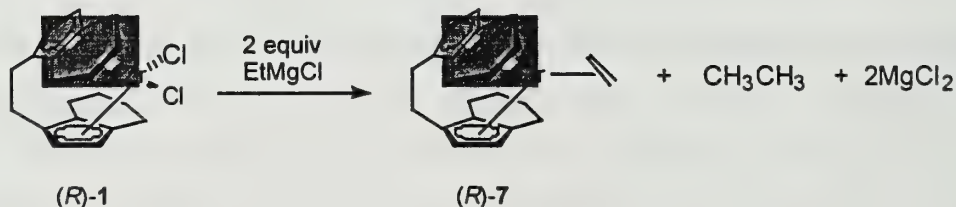


ASYMMETRIC CARBOMAGNESATION REACTION

Formation of Zirconocene-Alkene Complex

Several reports have indicated that zirconocene-alkene complexes such as **7** act as alkylating agents.²⁻⁵ Since there were no reports on the purported complex **7**, Hoveyda and coworkers studied its formation by ¹H NMR spectroscopy (Scheme 3).¹¹ Formation of **7** was not observed when (*R*)-**1** was treated with 5 equiv of EtMgCl in THF-*d*₈ for 2 h at -78 °C. However, when 3 equiv of EtMgCl were used and the mixture was monitored at 50 °C, formation of the coupling product [(EBTHI)Zr(Et)Cl] was observed within 30 min. This intermediate completely converted to **7** upon addition of 3 more equivalents of EtMgCl to the reaction mixture.

Scheme 3. The Transition Metal-Alkene Complex

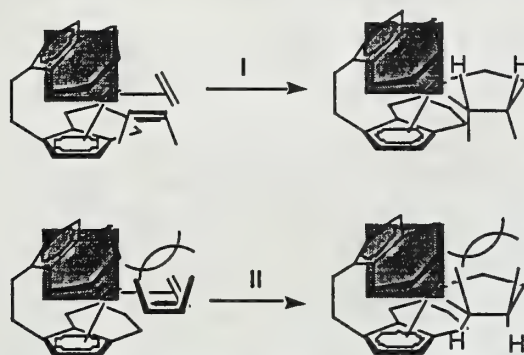


Substrate-Catalyst Interaction

Analysis with molecular models suggests that reaction of cis-disubstituted olefins with (*R*)-**1** should afford high levels of enantioselectivity.¹² Insertion of the alkene substrate into the complex **7** can occur *via* two pathways (Figure 1). Pathway **I** is more favorable because the substrate can approach the metal-alkene complex with a minimum of unfavorable steric interactions, whereas reaction through the alternative pathway **II** is sterically hindered by the cyclohexyl group of the chiral ligand.

Previous mechanistic studies also show that a neighboring heteroatom located α to the olefin can facilitate carbomagnesation reaction. Due to the inductive effect of a neighboring heteroatom, insertion of the olefin substrate into the metal-alkene complex can be facilitated; the electron density developed at the recipient C-Zr bond is stabilized by the electron-withdrawing substituent.^{5b}

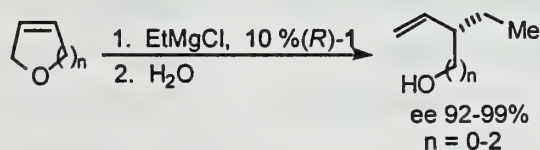
Figure 1. Substrate-Catalyst Interaction



Ethylmagnesation of Unsaturated Cyclic Ethers

Hoveyda and coworkers initially used unsaturated cyclic ethers to study the asymmetric ethylmagnesation reaction. Treatment of cyclic ethers with 5 equiv of EtMgCl in the presence of 10 mol% of (*R*)-1 at 25 °C provided the corresponding alcohols in good yield (65-75%) and excellent enantioselectivity (Scheme 4).¹²

Scheme 4. Ethylmagnesation of Cyclic Ethers

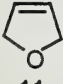
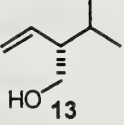
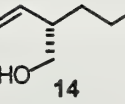
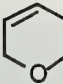
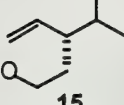
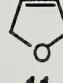
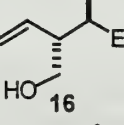
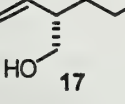
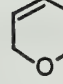
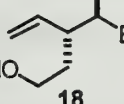


The proposed catalytic cycle for the enantioselective ethylmagnesation is shown in Scheme 5. The reaction is initiated by the formation of (*R*)-7. Insertion of the cyclic alkene substrate into 7 results in zirconacyclopentane 8. Regioselective cleavage of 8 by EtMgCl affords 9. Finally, β -hydride abstraction, along with intramolecular magnesium-alkoxide elimination, results in the ethylmagnesation product and regeneration of (*R*)-7.

For six- and seven-membered rings, it is important to note that the C-Zr bond is preferentially formed at the carbon α to the C-O bond due to the influence of the inductive effect of the neighboring oxygen atom on the formation of zirconacyclopentane 8.

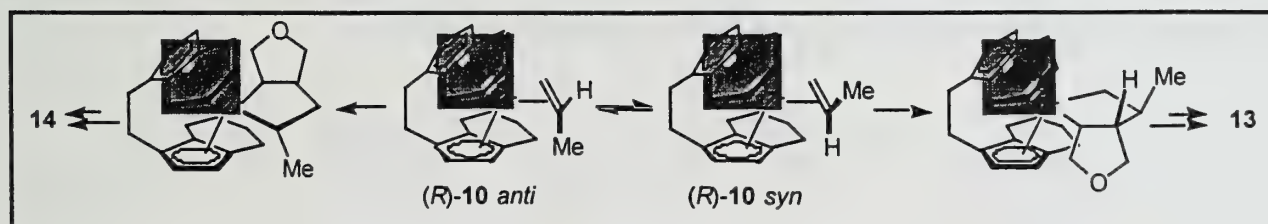
6.28 (2H) and 5.85 (2H) disappeared and four new doublets at δ 6.57, 5.89, 5.85, and 5.78 (1H each) appeared. This new complex could be assigned to the monoalkylating zirconocene chloride (EBTHI)Zr(CH₂CH₂CH₃)Cl. After 45 min at 22 °C the zirconocene alkyl chloride was replaced by the new intermediate, that subsequently reacted with **11** to provide **13** and **14**. As a result, this latter complex may be a 1:1 mixture of (*R*)-**10-syn** and (*R*)-**10-anti**.

Table 1. Zirconium-Catalyzed Carbomagnesation of Dihydrofuran and Pyran

Entry	Substrate	Major Products	Minor Products	Temp (°C)	RMgCl	Product Ratio	Major ee (%)	Minor ee (%)
1				22	<i>n</i> -PrMgCl	2:1	99	99
2				70	<i>n</i> -PrMgCl	20:1	94	
3				22	<i>n</i> -PrMgCl	>25:1	98	
4				22	<i>n</i> -BuMgCl	2:1	99	99
5				70	<i>n</i> -BuCl	20:1	90	
6				22	<i>n</i> -BuMgCl	>25:1	95	

The above observations suggest that both the *anti* and *syn* isomers **10** form in solution, and one of the two isomers reacts faster with the olefin substrate to produce the major product. As shown in Scheme 7, insertion of **11** into (*R*)-**10-syn** on the side proximal to the methyl group affords the zirconacyclopentane intermediate that leads to the major product **13**.^{3e} This mode of addition avoids steric interactions between the protruding cyclohexyl unit of the chiral ligand and **11**. Insertion into (*R*)-**10-anti** on the side distal to the methyl group affords the minor product **14**. At higher temperature the two isomeric complexes (*R*)-**10** equilibrate rapidly, and the one which reacts faster becomes the major product.¹³

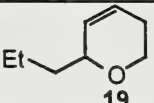
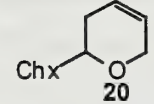
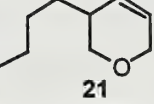
Scheme 7. Propylmagnesation of Dihydrofuran



ZIRCONIUM-CATALYZED KINETIC RESOLUTION

The high levels of enantioselectivity in the asymmetric carbomagnesation reactions (Tables 1 and Scheme 4) imply a highly ordered association between the catalyst and the substrate.^{3e} With substrate enantiomers, the pre-existing stereogenic center should influence the outcome of the reaction,¹⁴ suggesting the possibility of kinetic resolution. As shown in Table 2, when racemic pyrans were treated with 5 equiv of EtMgCl and 10 mol% (*R*)-**1**, the unreacted substrates of pyrans **19** and **21** (entries 1 and 3) were recovered with excellent enantioselectivity.¹⁴ However, pyran **20** (entry 2) could not be efficiently resolved (41% ee).

Table 2. Kinetic Resolution of Pyrans

Entry	Substrate	Conversion (%)	Temp (°C)	Time (h)	Unreacted Sub Config, ee (%) ^a
1		60	25	10	<i>R</i> , 94
		60	70	0.5	<i>R</i> , 99
2		60	25	40	<i>R</i> , 41
3		58	70	6	<i>S</i> , 99

^a The identity of recovered substrates was determined through comparison with authentic enantiomers.

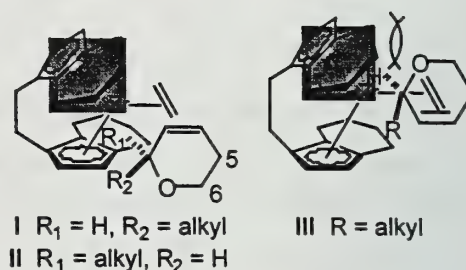
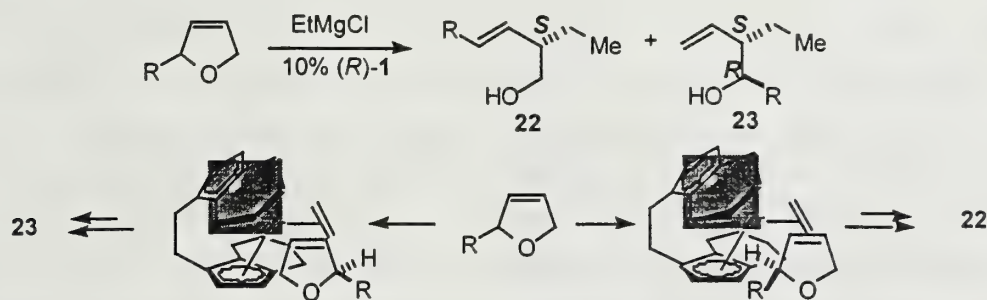


Figure 2. Mode of Addition I-III

With racemic pyran **19**, molecular models indicate that the catalyst-substrate association *via* pathway **I** is more favorable than pathways **II** or **III** (Figure 2). The results from Table 2 are consistent with these models; the unreacted (*R*)-**19** is recovered with excellent enantioselectivity. In addition, at 70 °C faster reaction rate and more effective resolution were observed (94% ee vs >99% ee; $k_{\text{fast}}/k_{\text{slow}} = 13$ and > 20, respectively). As a result, (*R*)-**19** was recovered with higher enantioselectivity. The 5-substituted pyran **21** could be resolved effectively (entry 3), probably due to steric repulsion between the C-5 alkyl group and the zirconocene-bound ethylene.

Unlike racemic pyrans, both enantiomers of dihydrofurans were reactive, through different modes of addition, to afford the two separable products **22** and **23** with excellent enantioselectivity (95-99 % ee).¹⁵ It is important to note that one enantiomer reacts at one end of the double bond, and the other reacts at the other end. As a result, the furan substrate inserts into the metal-alkene complex in such a way that unfavorable steric interactions can be minimized (Scheme 8).

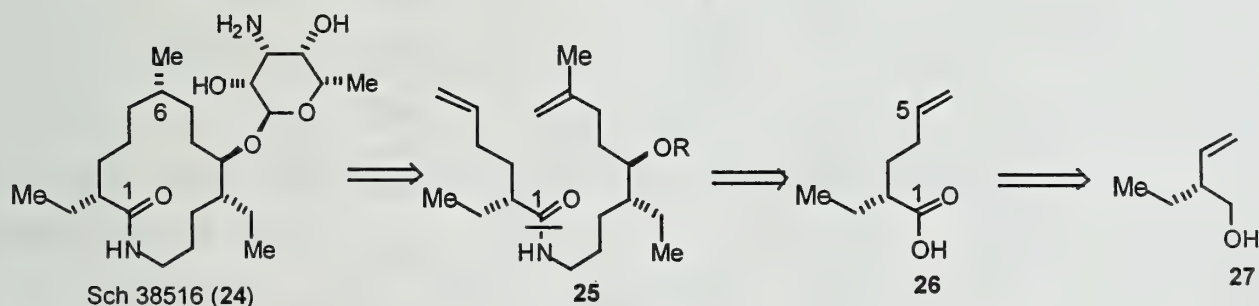
Scheme 8. Zirconium-Catalyzed Kinetic Resolution of Furans



SYNTHETIC APPLICATIONS

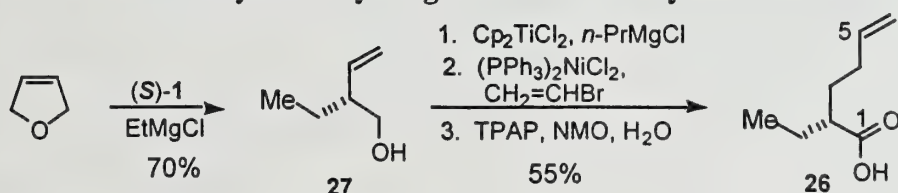
Sch 38516 (**24**), an antifungal agent, was discovered by scientists at Schering-Plough in 1990.¹⁶ Subsequently, it was found to be identical to fluvirucin B₁,¹⁷ an agent against influenza A virus. Because several stereogenic centers exist in the macrolactam structure, compound **24** is attractive target for enantioselective synthesis. Hoveyda and coworkers have recently reported the enantioselective total synthesis of Sch 38516.¹⁸ As shown in Scheme 9, Sch 38516 could arise from ring-closing metathesis of **25** followed by hydrogenation. The zirconium-catalyzed ethylmagnesation reaction of unsaturated dihydrofuran has been used as a key intermediate to provide **26**.

Scheme 9. Retrosynthetic Analysis for Sch 38516



Treatment of dihydrofuran with 5 equiv of EtMgCl in the presence of 0.4 mol% (*S*)-**1** afforded **27** in 99% ee (Scheme 10). Because **27** contains both a hydroxyl group and a double bond, it could be further functionalized through a tandem Ti- and Ni-catalyzed processes to provide **26** in excellent enantioselectivity (> 99% ee).

Scheme 10. Zr-Catalyzed Ethylmagnesation in the Synthesis of Sch 38516



CONCLUSION

Zirconium-catalyzed asymmetric addition of Grignard reagents to unactivated olefins proceeds with high regio- and stereoselectivity under mild conditions. This approach offers a useful method for constructing C-C bonds because the addition of Grignard reagents to nonfunctionalized alkenes usually requires severe reaction conditions. In addition, the products obtained from enantioselective carbomagnesation can be further functionalized and applied to the synthesis of natural products. Nonetheless, the challenge of developing the enantioselective addition of various Grignard reagents (methyl, vinyl, and phenyl) to olefins remains unsolved. Although (*R*)-**1** has proven to be effective at promoting carbomagnesation, its high cost and tedious synthesis will motivate the invention of alternatives.

REFERENCES

1. *Catalytic Asymmetric Synthesis*, Ojima, D., Ed.; Wiley: New York, 1993.
2. (a) Dzhemilev, U. M.; Vostrikova, O. S.; Sultanov, R. M. *Izv. Akad. Nauk. SSSR, Ser. Khim.* **1983**, 218. (b) Dzhemilev, U. M.; Vostrikova, O. S. *J. Organomet. Chem.* **1985**, 285, 43.
3. (a) Hoveyda, A. H.; Xu, J. *J. Am. Chem. Soc.* **1991**, 113, 5079. (b) Hoveyda, A. H.; Xu, Z.; Morken, J. P.; Houri, A. F. *J. Am. Chem. Soc.* **1991**, 113, 8950. (c) Hoveyda, A. H.; Xu, Z.; Houri, A. F. *J. Am. Chem. Soc.* **1992**, 114, 6692. (d) Houri, A. F.; Didiuk, M.; Xu, Z.; Horau, N. R.; Hoveyda, A. H. *J. Am. Chem. Soc.* **1993**, 115, 6614. (e) Hoveyda, A. H.; Morken, J. P.; *Angew. Chem. Int. Ed. Engl.* **1996**, 35, 1262.
4. Takashashi, T.; Seki, T.; Nitto, Y.; Saburi, M.; Rousset, C. T.; Negishi, E. *J. Am. Chem. Soc.* **1991**, 113, 6266.
5. (a) Lewis, D. P.; Muller, P. M.; Whitby, R. J.; Jones, R. V. H. *Tetrahedron Lett.* **1991**, 32, 6797. (b) Lewis, D. P.; Whitby, R. J.; Jones, R. V. H. *Tetrahedron* **1995**, 51, 4541.
6. Wild, F. P.; Wasiucionek, J.; Hattner, G.; Brintzinger, H. H. *J. Organomet. Chem.* **1985**, 288, 63.
7. Collins, S.; Kuntz, B. A.; Taylor, N. J.; Ward, D. G. *J. Organomet. Chem.* **1988**, 342, 21.
8. Grossman, R. B.; Doyle, R. A.; Buchwald, S. L. *Organometallics*. **1991**, 10, 1501.
9. Diamond, G. M.; Jordan, R. F.; Petersen, J. L. *J. Am. Chem. Soc.* **1996**, 118, 8024.
10. Schafer, A.; Karl, E.; Hunter, G.; Brintzinger, H. H. *J. Organomet. Chem.* **1987**, 328, 87.
11. Hoveyda, A. H.; Morken, J. P. *J. Org. Chem.* **1993**, 58, 4237.
12. Morken, J. P.; Didiuk, M. T.; Hoveyda, A. H. *J. Am. Chem. Soc.* **1993**, 115, 6997.
13. Didiuk, M. T.; Johannes, C. W.; Morken, J. P.; Hoveyda, A. H. *J. Am. Chem. Soc.* **1995**, 117, 7097.
14. Morken, J. P.; Didiuk, M. T.; Visser, M. S.; Hoveyda, A. H. *J. Am. Chem. Soc.* **1994**, 116, 3123.
15. Visser, M. S.; Heron, N. M.; Didiuk, M. T.; Hoveyda, A. H. *Tetrahedron* **1995**, 51, 4383.
16. Hedge, V. R.; Patel, M. G.; Gullo, V. P.; Ganguly, A. K.; Sarre, O.; Puar, M. S.; McPhail, A. T. *J. Am. Chem. Soc.* **1990**, 112, 6403.
17. Komita, K.; Oda, N.; Hoshino, Y.; Ohkusa, N.; Chikazawa, H. *J. Antibiot.* **1991**, 44, 741.
18. (a) Houri, A. F.; Xu, Z.; Cogan, D. A.; Hoveyda, A. H. *J. Am. Chem. Soc.* **1995**, 117, 2943. (b) Xu, Z.; Johannes, C. W.; Houri, A. F.; La, D. S.; Cogan, D. A.; Hofelena, G. E.; Hoveyda, A. H. *J. Am. Chem. Soc.* **1997**, 119, 10302.

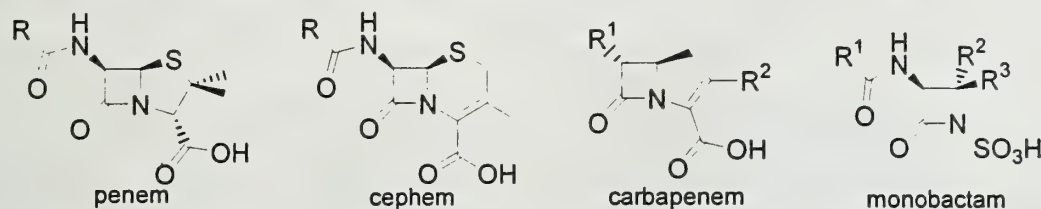
STRATEGIES FOR COMBATING β -LACTAMASE INDUCED ANTIBIOTIC RESISTANCE

Reported by Erika A. Taylor

October 28, 1999

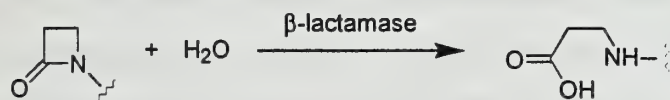
INTRODUCTION

β -Lactam antibiotics, of which penicillin, cephalosporin, carbapenems, and monobactams are four major classes, represent approximately one half of the antibiotics currently prescribed.¹ These antibiotics target both a transpeptidase and a DD-carboxypeptidase that are essential in peptidoglycan synthesis. By inhibiting these enzymes bacteria are unable to effectively synthesize or degrade the cell wall, leading to pore formation and then cell death.²



Bacteria have evolved β -lactamase enzymes to resist β -lactam antibiotics found in nature and in clinical applications. β -Lactamases catalyze the hydrolysis of the β -lactam rings of these antibiotics (Scheme 1), resulting in the inactivation of the drug and thus the proliferation of the bacteria. The gene for this enzyme spreads to progeny via chromosomal DNA, as well as to other bacterial strains via a plasmid-encoded gene.¹ These enzymes are divided into four major classes, designated A to D, based on structural similarities, mechanism, and substrate specificity. Class A enzymes are the most prevalent in clinical isolates.³ β -Lactamases are continually evolving in response to new β -lactam antibiotics administered clinically, resulting in over 250 isolated variants of the enzyme.

Scheme 1. Overall Mechanism



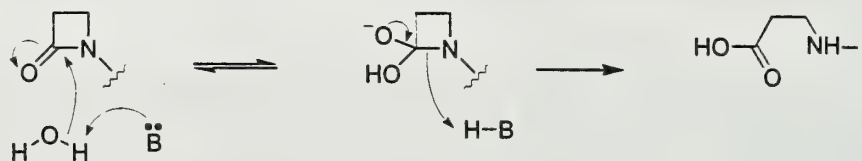
Attempts to discover and develop β -lactamase inhibitors were initiated to combat β -lactamase induced antibiotic resistance. The inhibitors are designed not for antimicrobial activity but for resistance to hydrolysis, thereby blocking the active site and thus preventing degradation of β -lactam antibiotics. Many inhibitors are targeted at class A enzymes, specifically the TEM β -lactamase subgroup, which have an extended-spectrum of hydrolyzable substrates and are often plasmid-encoded.⁴ Many inhibitors have been designed from considerations of transition state and active site models based upon crystal structures of both native and inhibitor bound complexes. These inhibitors utilize a variety of novel mechanisms to inactivate the enzyme.

β -LACTAMASE MECHANISM

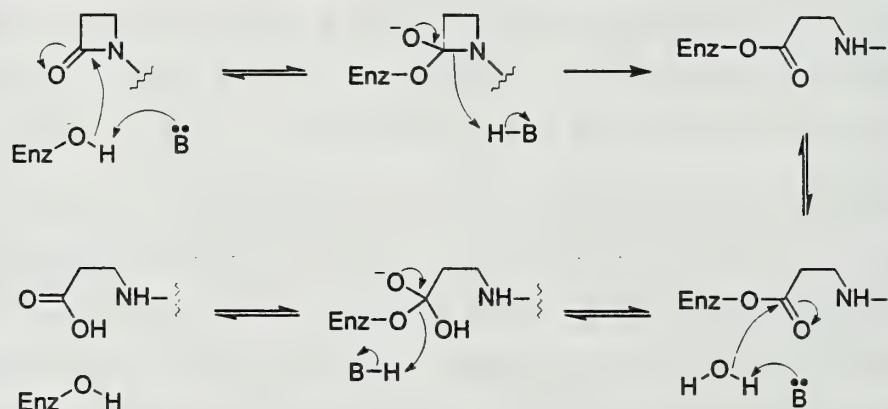
Two mechanisms are used by β -lactamases to hydrolyze the β -lactam ring (Scheme 2). In mechanism A, which is observed in class B β -lactamases, an active site base activates a water molecule, which attacks the lactam carbonyl and displaces the nitrogen leaving group. In mechanism B, as seen in classes A, C, and D, a covalent acyl-enzyme intermediate is formed, followed by the hydrolysis of this intermediate to release the biologically inert β -amino acid.

Scheme 2. Possible enzyme mechanisms.

Mechanism A



Mechanism B

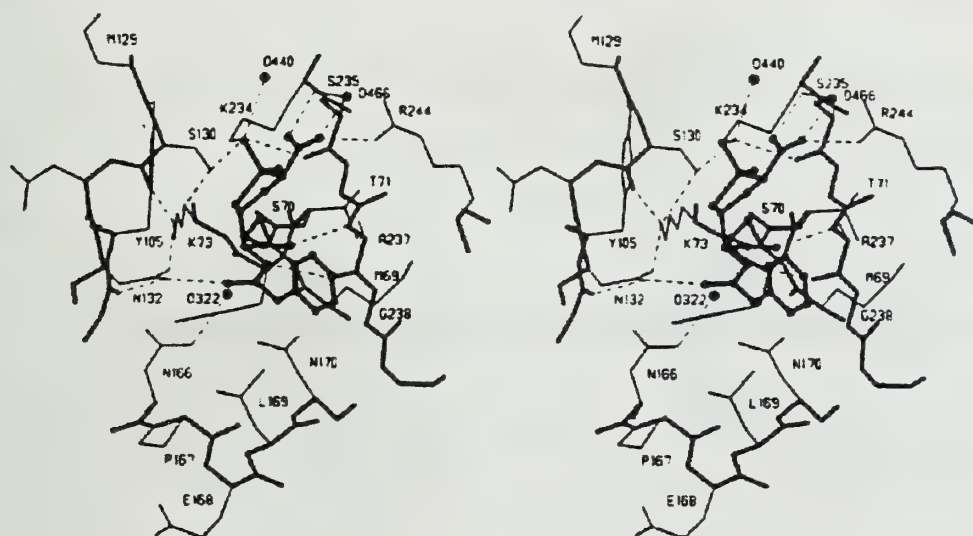


Penicillin-bound intermediate

During the past ten years, crystal structures of various β -lactamases have been determined. The elucidation of crystal structures helped identify the active site residues, but until a structure was determined with a bound substrate, the exact orientations and functions of the residues were uncertain. The mutation of Glu-166 to Asn (E166N), in the TEM-1 β -lactamase from *Escherichia coli*, resulted in an enzyme unable to hydrolyze the acyl-enzyme intermediate.⁵ The determination of the crystal structure of that mutant covalently bound to penicillin G (Pen G) helped assign functions to many of the active site residues (Figure 1). Ser-70, which is covalently bound to Pen G, was identified as the nucleophile involved in attacking the β -lactam carbonyl. Lys-73 was assigned as the general base for the deprotonation of the hydroxyl of Ser-70. Ser-130 was assigned as a general acid that protonates the nitrogen leaving group of the β -lactam ring. Glu-166 was assigned as the general base which deprotonates the hydrolytic water molecule, in agreement with kinetic data and with the observation that

the E166N mutant had the substrate still covalently bound. Residues Ala-237 and Gly-69, whose N-H backbone residues form an oxyanion hole, help stabilize the carbonyl and the negatively charged tetrahedral intermediate. Various groups and water molecules that interact with Pen G via hydrogen bonds or hydrophobic interactions thereby stabilizing its orientation in the active site were also noted. Since the initial assignment of function to these residues, Glu-166 and a water molecule that is activated by Glu-166 have been hypothesized to deprotonate Ser-70. Extensive kinetic and pH studies of the various mutants, as well as numerous inhibitor-bound crystal structures are equivocal so the identity of the general base is still unresolved.^{6,7}

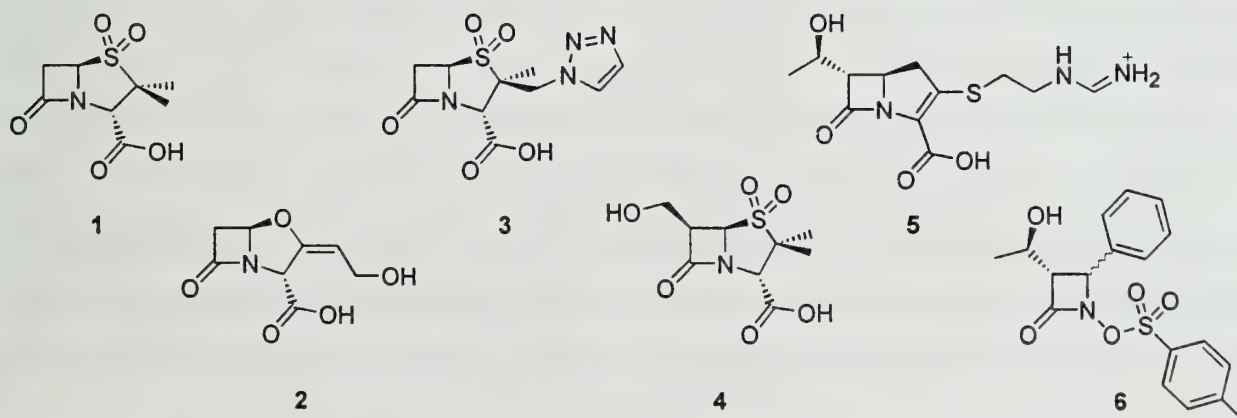
Figure 1. Stereoview of the E166N TEM-1 active site bound with Pen G bound.



ENZYME INHIBITION

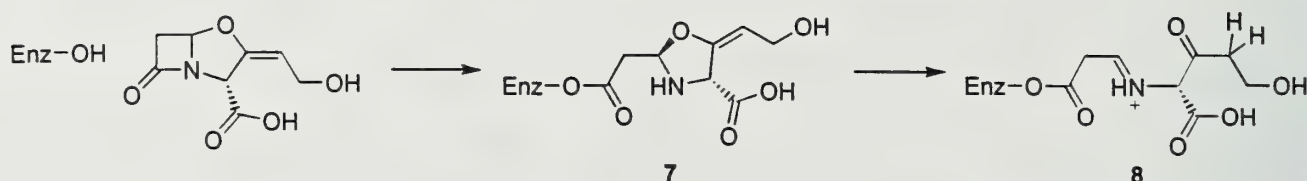
Several known β -lactamase inhibitors are shown in Figure 2. The mechanisms of inhibition exhibited by these compounds include a rearrangement after the formation of the acyl-enzyme intermediate to form an "unhydrolyzable complex," incorporation of functional groups to prevent the attack of the hydrolyzing water, or both.

Figure 2. Mechanism based inhibitors of β -lactamases.



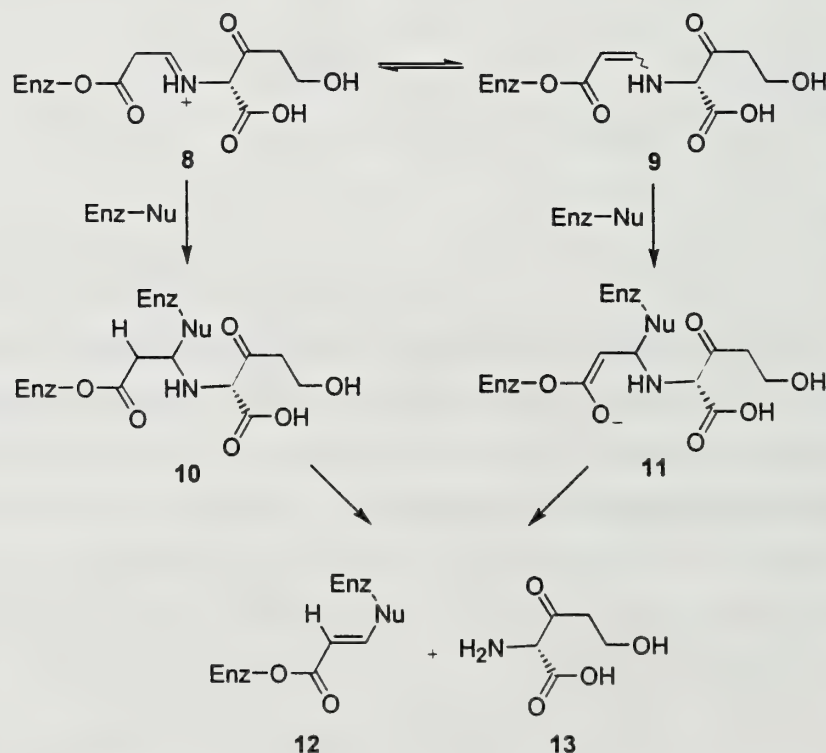
Some clinically utilized inhibitors that work by a rearrangement mechanism are sulbactam (1), clavulanate (2), and tazobactam (3). Clavulanate exemplifies the mechanism of this group of inhibitors (Scheme 3). The mechanism starts with the formation of the acyl-enzyme intermediate, which promotes opening of the remaining penam ring.^{8,9} The acyl-enzyme intermediates 7 and 8 can enter a non-inhibiting pathway, thus being hydrolyzed resulting in the free enzyme and an inactive β -amino acid which then leaves the active site.

Scheme 3. Acyl-enzyme intermediate formation and initial rearrangement.



Alternatively the opened intermediate (8) can proceed to give two different inhibitor complexes (Scheme 4). The enamine complex (9) is a transient inhibitor since the ester linkage can be hydrolyzed, but in the complex where the enzyme is cross-linked with the inhibitor (12), the β -lactamase is irreversibly inactivated.

Scheme 4. Chain-reactions resulting in inactivated enzyme-inhibitor complexes.

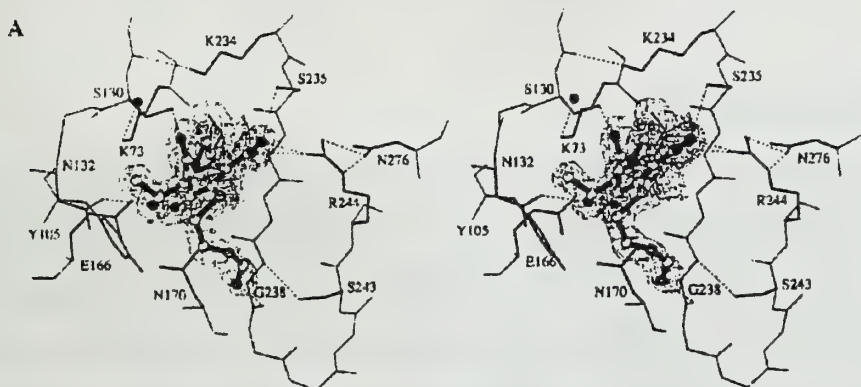


Evidence for the chain-reactions resulting in enzyme inhibition include a crystal structure that corresponds to structure 8 or 9; the resolution was not sufficient to distinguish between the two tautomers.¹⁰ Additionally, HPLC-ESIMS (high-pressure liquid chromatography-electrospray ionizing

mass spectrometry) data show the formation of **12** and that residue Ser-130 is the enzymatic nucleophile.¹¹ These experiments have not allowed the elimination of either of the possible pathways to the irreversible inactivation product.

A second major inhibitor strategy involves the incorporation of a substituent into the inhibitor that interferes sterically with the attack of the water molecule during the final hydrolytic step. Imipenem (**5**) is the only inhibitor of this type with wide clinical use, though many others have been developed.³ Imipenem's 6 α -hydroxyethyl substituent displaces the hydrolytic water molecule from its position in the native enzyme (Figure 3). The hydroxyethyl is also believed to be a hydrogen bond donor with that water molecule, which causes a decrease in its nucleophilicity.¹² Inhibitors of this type have been observed to resist hydrolysis of the acyl-enzyme intermediate.

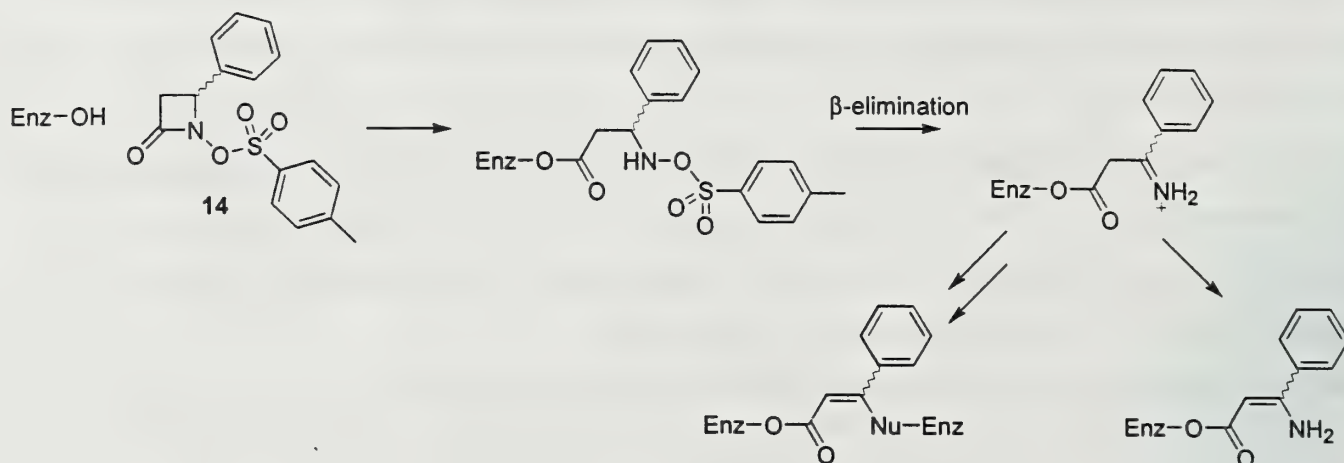
Figure 3. Stereoview of energy minimized TEM-1 with bound imipenem.



Two inhibitors (**4** and **6**), whose structures have been reported within the last 6 months, have combined both strategies into a single molecule. Inhibitor **4** is based on Sulbactam, but a 6 β -hydroxymethyl group has been incorporated into the molecule to prevent further hydrolysis. This addition makes inhibitor **5** even more effective than sulbactam when assayed against bacteria producing TEM-1 β -lactamase, while also having activity against bacteria which produce other classes of β -lactamase enzymes.¹³ Inhibitor **6** is based on an earlier inhibitor design (**14**), and the mechanism of this inhibitor type is shown in Scheme 5.¹⁴ Inhibitor **14** was found to be a rapid acylating agent that could undergo multiple transformations once the tosylate group leaves. The remaining reactions leading to enzyme inhibition follow a mechanism that is effectively the same as seen for clavulanate (Scheme 4). By adding a 6 α -hydroxyethyl group, inhibitor **6** rapidly forms the acyl-enzyme intermediate and the rate of intermediate hydrolysis is decreased. After incubating a TEM-1 β -lactamase with inhibitor **6**, the enzyme was very rapidly inactivated and only 15% of the activity was recovered after 6 days.¹⁵

Compounds **4** and **6** clearly show that effective inhibitors can be developed by combining these two mechanistic strategies.

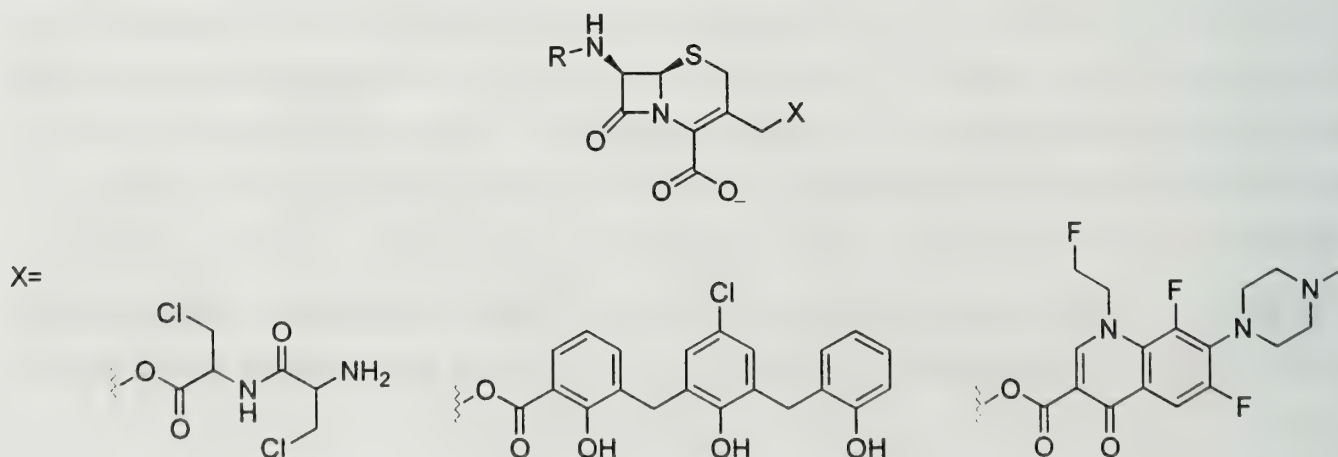
Scheme 5. Fast acylating inhibitor mechanism.



SITE-SPECIFIC-RELEASE PRODRUGS

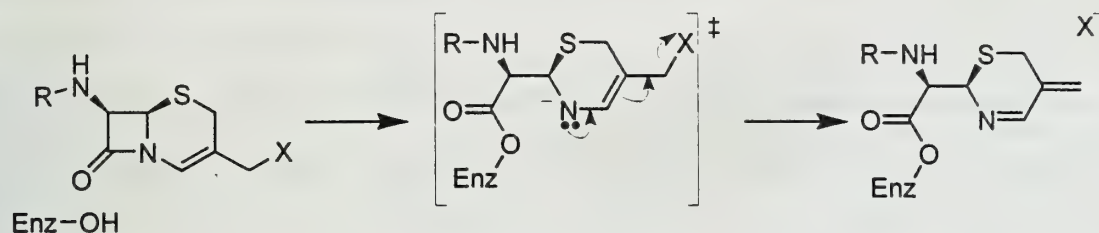
Reliance upon inhibitors has promoted the evolution of inhibitor-resistant enzymes.¹⁶ This problem could potentially be removed by the use of site-specifically-release prodrugs. Prodrugs specific to the β -lactamase enzyme would incorporate a β -lactam ring into their structure and be designed to release bactericidal agents upon hydrolysis. By covalently attaching bactericidal agents to β -lactam carriers, these prodrugs target β -lactamase producing bacteria and are inert to bacteria that do not produce the β -lactamase enzyme. These prodrugs are not specific to the different classes of β -lactamase, since hydrolysis and not the formation of an acyl-enzyme intermediate triggers the drug release. In this way the evolutionary path of the bacteria is potentially shifted from producing better β -lactamases, to a path where bacteria would produce less effective β -lactamase enzymes, or none at all.

Figure 4. Prototype carrier-prodrugs.



Three variants of this type of "carrier" prodrug (Figure 4) were recently developed.^{17, 18, 19} These prodrugs allow the selective delivery of an antibacterial agent from the 3' position (Scheme 6). All of these bactericidal agents target biological processes other than the β -lactamase. Incorporation of latent functionality at the 3' position has been shown to be an effective method for site-directed bacterial targeting. This class of β -lactam antibiotics has not yet been utilized clinically, and the cephalosporin-based carrier is not readily hydrolyzable by all β -lactamases, but these compounds provide a prototype around which further development will likely be forthcoming.

Scheme 6. Drug delivery mechanism by prodrug.



CONCLUSION

Recent developments in inhibitor design have provided novel mechanisms for inhibition of β -lactamases. These inhibitors should be tested for *in vivo* activity in animal systems, and these designs should be explored further to provide clinically effective inhibitors. Research also needs to be expanded to incorporate all four classes of β -lactamase enzymes since the prevalence of the remaining three classes is growing, especially class B and C enzymes which are being isolated in plasmid-encoded forms.¹⁹ Also, the development of prodrug structures that can provide a site-specific scaffold for bactericidal agent delivery should be studied further, since no antibiotics of this type are currently used clinically.

REFERENCES

- 1) Livermore, D. M. *J. Antimicrob. Chemother.* **1998**, 41(Suppl D), 25-41.
- 2) Jelsch, C.; Lenfant, F.; Masson, J. M.; Samama, J. -P. *FEBS Lett.* **1992**, 299, 135-142.
- 3) Maiti, S. N.; Phillips, O. A.; Micetich, R. G.; Livermore, D. M. *Curr. Med. Chem.* **1998**, 5, 441-456.
- 4) Bush, K.; Jacoby, G. *J. Antimicrob. Chemother.* **1997**, 39, 1-3.
- 5) Strynadka, N. J.; Adachi, H.; Jensen, S. E.; Johns, K.; Sielecki, A.; Betzel, C.; Sutoh, K.; James, M. N. G. *Nature* **1992**, 359, 700-705.
- 6) Maveyraud, L.; Pratt, R. F.; Samama J. P. *Biochemistry* **1998**, 37, 2622-2628.
- 7) Page, M. I.; Laws A. P. *Chem. Comm.* **1998**, 16, 1609-1617.
- 8) Yang, Y.; Rasmussen, B. A.; Shaes, D. M. *Pharmacology and Therapeutics* **1999**, 83, 141-151.
- 9) Swaren, P.; Golemi, D.; Cabantous, S.; Bulychev, A.; Maveyraud, L.; Mobashery, S.; Samama, J. -P. *Biochemistry* **1999**, 38, 9570-9576.

- 10) Chem, C. H.; Herzberg, O. *J. Mol. Biol.* **1992**, *224*, 1103-1113.
- 11) Brown, R. P. A.; Äplin, R. T.; Schofield, C. J. *Biochemistry* **1996**, *35*, 12421-12432.
- 12) Maveyraud, L.; Mourey, L.; Kotra, L. P.; Pedelacq, J. -D.; Guillet, V.; Mobashery, S.; Samama, J. *P. J. Am. Chem. Soc.* **1998**, *120*, 9748-9752.
- 13) Bitha, P.; Li, Z.; Francisco, G. D.; Rasmussen, B. A.; Lin, Y. I. *Bioorg. Med. Chem. Lett.* **1999**, *9*, 991-996.
- 14) Bulychev, A.; O'Brien, M. E.; Massova, I.; Teng, M.; Gibson, T. A.; Miller, M. J.; Mobashery S. *J. Am. Chem. Soc.* **1995**, *117*, 5938-5943.
- 15) Swaren, P.; Massova, I.; Bellettini, J. R.; Bulychev, A.; Maveyraud, L.; Kotra, L. P.; Miller, M. J.; Mobashery, S.; Samama, J. *-P. J. Am. Chem. Soc.* **1999**, *121*, 5353-5359.
- 16) Farina, V.; Hauck, S. I.; Firestone, R. A. *Bioorg. Med. Chem. Lett.* **1996**, *6*, 1613-1618.
- 17) Johnston, M.; Lerner, S. A.; Mobashery, S. *J. Am. Chem. Soc.* **1986**, *108*, 1685-1686
- 18) Albrecht, H. A.; Beskid, G. ; Chan, K. -K.; Christenson, J. G.; Cleeland, R.; Dietcher, K. H.; Georgopapadakou, N. H.; Keith, D. D.; Pruess, D. L.; Sepinwall, J.; Specian, A. C.; Then, R. L.; Weigele, M.; West, K. F.; Yang, R. *J. Med. Chem.* **1990**, *33*, 77-86.
- 19) Hwu, J. R.; Moshfegh, A. A.; Tsay, S. C.; Lin, C. C.; Tseng, W. N.; Azaripour, A.; Motaghiam, H.; Hakimelahi, G. H. *J. Med. Chem.* **1997**, *40*, 3434-3441.
- 20) Chaibi, E. B.; Sirot, D.; Paul G.; Labia R. *J. Antimicrob. Chemother.* **1999**, *43*, 447-458.

UNNATURAL AMINO ACIDS IN PROTEINS VIA A BIOSYNTHETIC APPROACH

Reported by Jaisree Moorthy

November 8, 1999

INTRODUCTION

Site-directed mutagenesis is a powerful technique in protein studies. By this method, an amino acid residue at a site of interest along the protein is replaced with another. As a result the environment in the vicinity of the substituted residue is perturbed leading to an altered conformation or change in reactivity of the protein. From systematic changes enzyme mechanisms and other characteristics of the protein can be inferred. However, detailed manipulation of the local environment is not possible due to the limited choice of natural amino acids. Recently techniques¹ have been developed which enable the incorporation of unnatural amino acids (Xaas) into proteins. The broad range of Xaas allows better control of various properties like pK_a , hydrophobicity, size and hydrogen bonding ability. One approach to introduce Xaas is total synthesis of the polypeptide chain. Although this technique allows site-specific replacements, the process is tedious and there are difficulties in making large polypeptides. A second approach involves replacing a fragment of the protein with a synthetic polypeptide. However, only a few methods allow site-specific cleaving and ligation of proteins. *In vivo* approaches include protein biosynthesis with either Xaa or tRNA aminoacylated with Xaa in the medium. Although moderate quantities of the mutant protein are obtained by these methods, the replacements are not site specific. An emerging technique is site-directed mutagenesis with Xaas. This method introduced by Schultz² and Chamberlin³, exploits the biosynthetic machinery affording site-specific replacements by Xaas in moderate yields. The methodology with specific examples will be discussed in this report.

PROTEIN BIOSYNTHESIS

Site-directed mutagenesis with Xaas relies on the natural protein biosynthetic machinery. During *in vivo* protein synthesis,⁴ DNA is transcribed to messenger RNA (mRNA), which forms a template for translation into protein. One or more nucleotide triplet(s) (codon(s)) on mRNA code for each amino acid. During translation, the mRNA is decoded into an amino acid sequence. The key link for this information transfer is provided by transfer RNA (tRNA). The important features of tRNA (Figure 1) are an acceptor arm terminating in a CCA sequence to which an amino acid is bound, and an anticodon loop which is complementary to the codons on the mRNA. The environment for the codon-anticodon interaction and peptide bond formation (between the growing

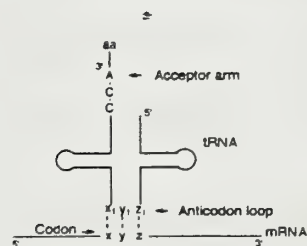


Figure 1. tRNA forms a link between the mRNA and amino acid (aa) via codon (xyz)-anticodon (x₁y₁z₁) interaction.

peptide and amino acid on adjacent tRNAs) is provided by the ribosome complexed to the mRNA. Three termination (or nonsense) codons, UAG, UGA and UAA do not code for any amino acid and in most cases there are no naturally occurring tRNAs identifying them. When any of these codons is encountered, peptide synthesis is terminated and the protein is released with the intervention of cofactors called release factors.

METHODOLOGY

In order to introduce an Xaa selectively into a protein sequence, a tRNA is aminoacylated with an Xaa (mischarged) and the anticodon loop is modified to recognize a unique codon on the mRNA. This complement to the unique codon is included in the DNA, which is transcribed to the mRNA. The transcription and the translation processes are carried out *in vitro* using rabbit or *E. coli* biosynthetic machinery. This process of introducing a unique codon represents an expansion of the genetic code.

The unique codon that is incorporated in the mRNA must be different from any of the codons coding for the natural amino acids. This ensures that only an Xaa is introduced at a specific site. Competition from release factors of the biosynthetic machinery may result in a truncated peptide. The ratio expressed as a percentage of the amount of mutant protein translated compared to the total amount of proteins made, gives the efficiency (suppression efficiency) of the process.

Strategies for Expanding the Genetic Code

Schultz² and Chamberlin³ used one of the termination codon, UAG as the unique codon. The suppression efficiency of the approach is between 0-70% depending on the Xaa. One of the main reasons for the low suppression efficiency is due to competition from the release factors that tend to terminate protein synthesis at UAG. Alternatively, Sisido and coworkers⁵ have introduced a 4-base codon that incorporates Xaas by frame shift mutation; this condition exists when 4 bases code for an amino acid, or a base is skipped on the mRNA during translation. The bases employed were AGGN and CGGN (N indicates any of the 4 bases). The suppression efficiency of this method ranges from 0-100%, the competition being from the tRNA identifying the first 3 bases. Chamberlin and coworkers⁶ also introduced a new base-pair (iso-C iso-G) to incorporate Xaa. Since there is no competition from the biosynthetic machinery for this particular base pair, higher suppression efficiencies (20% higher than the termination codon approach) were observed. However, no further

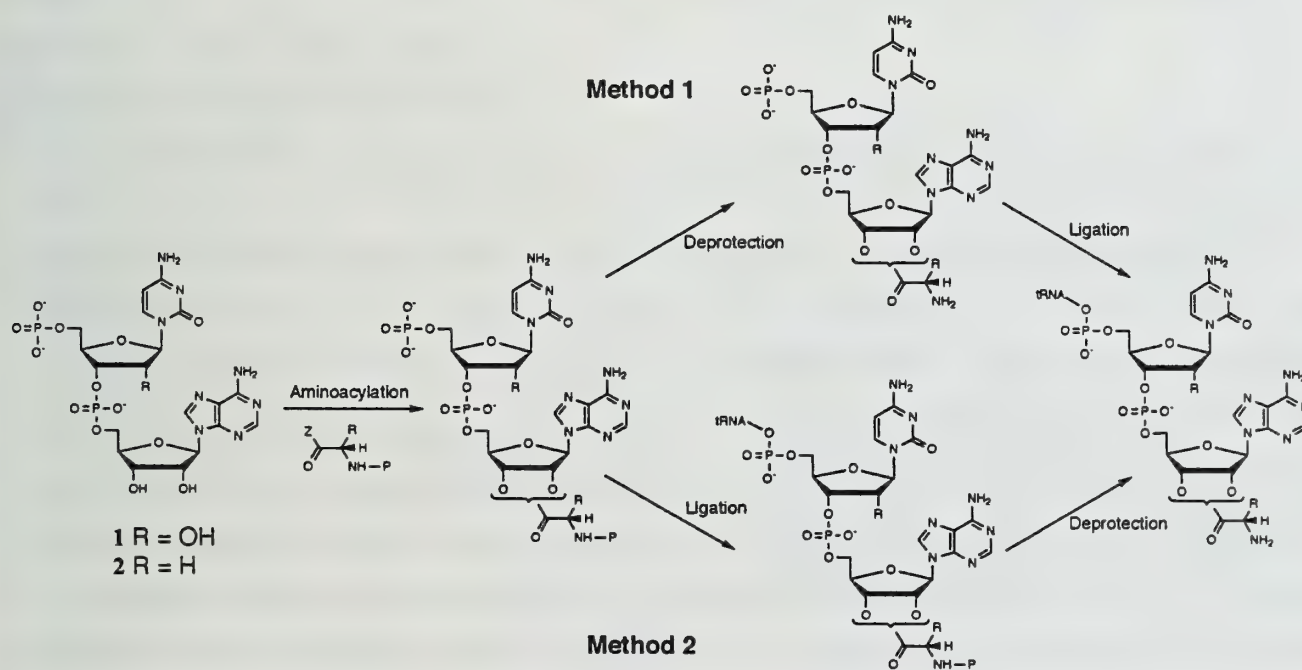
work has been reported on this approach because standardized methods for introducing a new base have yet to be developed.

Synthesis of Mischarged tRNA

One of the major challenges faced in developing this methodology has been making the mischarged tRNA. The tRNA cannot be subjected to direct aminoacylation due to a large number of reactive sites on the macromolecule. Since the terminal CCA sequence is conserved across tRNAs, a general strategy that has been adopted⁷ is aminoacylation of the terminal dinucleotide (CA) followed by ligation with the rest of the macromolecule (tRNA-COH). The tRNA-COH with the modified anticodon loop is made using standard biochemical techniques.⁴

The terminal dinucleotide (CA) is aminoacylated with N-protected Xaas. The protecting group is necessary to afford aminoacylation in high yield and to prevent polymerization of the amino acids during the process. After aminoacylation, two different methods (Scheme 1), differing

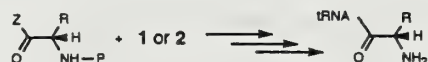
Scheme 1

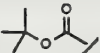

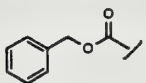
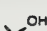
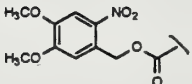

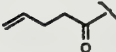



in the order of deprotection and ligation steps were adopted. The choice of a method was based on the deprotection conditions. Under harsh conditions, Method 1 was employed. However, higher yields were obtained in Method 2 when the deprotection of the amino group was performed after ligation (Method 2). To improve the yield further variation in the type of dinucleotide (CA) was investigated. Aminoacylation of dinucleotide 1 gave poor yields due to acylation of 2'-OH of

cytosine and isomerization of the phosphotriester linkage (3'-5', 2'-5') between the nucleotides.⁸ When DNA/RNA hybrid **2** was used as the substrate, better yields of the aminoacylated dinucleotide were obtained. Table 1 summarizes some of the protecting groups investigated, substrates and methods employed, along with the yield obtained in the deprotection step.

Table 1. Mischarging tRNA with Xaa. The substrate and method refer to Scheme 1.



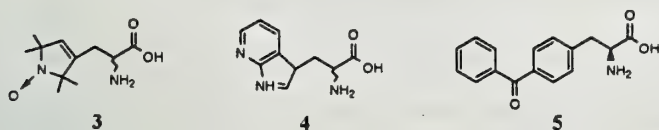
Entry	P	Z	Substrate	Method	Yield %
1			1	1	6
2			2	1	34
3			2	2	95
4			2	2	92

The first successful deprotected mischarged tRNA was synthesized in Brunner's lab.⁸ The amino group of the Xaa was protected as the *tert*-butyl carbamate (BOC) and coupled with dinucleotide **1** as the substrate. After coupling, the deprotection was performed with trifluoroacetic acid in 6% yield (entry 1). Chamberlin and coworkers⁹ used the carbobenzoxy group instead of the BOC group with deprotection by palladium catalyzed hydrogenation giving the aminoacylated dinucleotide **2** in 34% yield (entry 2). The primary reason for the low yield was N-acylation of the dinucleotide. This side product was not observed when the carboxylic acid group was activated by conversion to a cyanoester (entries 3 and 4). By employing the nitroveratriloxycarbonyl (NVOC) group (entry 3), Schultz and coworkers¹⁰ performed the deprotection in 95% yield by irradiating at 350 nm. Similarly, The N-pentenoyl group (entry 4) used in Hecht's lab¹¹ was deprotected via iodolactonization in 92% yield and is compatible with photosensitive groups. Due to the mild deprotection conditions in entries 3 and 4, Method 2 was followed to synthesize the mischarged tRNA.

APPLICATIONS IN PROTEIN STUDIES

A broad range of Xaas has been incorporated in different proteins for investigating enzyme mechanisms, protein stability and various biochemical processes. Some of the amino acid probes that have been introduced are shown in Chart 1. Schultz and coworkers¹² have demonstrated that

Chart 1



spin labels (e.g. 3) and fluorescent tags (e.g. 4) can be incorporated to aid in protein studies. Replacement of natural amino acids by photo cross-linking agent 5 provided a marker that revealed adjacent groups in the

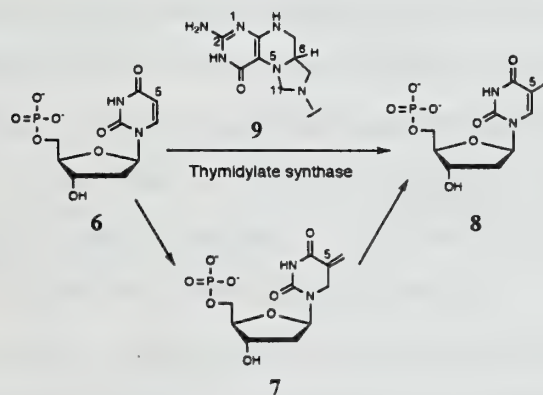
protein structure and contact points with membranes. Photocleaveable groups like NVOC¹³ have been employed to mask amino acids at specific sites on the protein. Upon photolysis, the wild type protein is formed. This process has facilitated time-resolved measurements of biochemical process.¹⁴ The details of some of the enzyme mechanism and protein stability studies will be discussed in the following sections.

Mechanism of Thymidylate Synthetase

A good example of how site-directed mutagenesis with an Xaa has been used to elucidate an enzyme mechanism is seen with thymidylate synthetase. This enzyme catalyzes¹⁵ the methylation of deoxyuridine-5'-monophosphate 6 to make deoxythymidine-5'-monophosphate 8 (Scheme 2).

The methylene C-11 of methylenetetrahydrofolate 9 is transferred to C-5 of 7. Subsequently a hydride is transferred to the intermediate 7 to form 8. The mechanism of methylene transfer has been studied from crystal structures of the enzyme with the substrates. However, it is unclear if the hydride is transferred to 7 in a single or multiple steps. Schultz and coworkers observed¹⁶ that hydride transfer was not efficient when Trp 82 was

Scheme 2



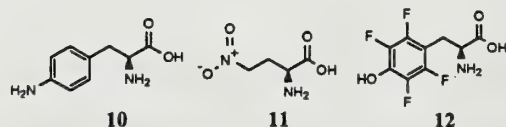
mutated. To understand the importance of the residue, the authors introduced¹⁷ various phenylalanine and tryptophan analogues and studied their effect on the enzymatic activity. They observed that $\log(k_{\text{cat}})$ correlated with the cation stabilizing ability of the corresponding Xaa, suggesting the involvement of a cation intermediate. From this, Schultz and coworkers proposed

that Trp 82 stacks with 9 and facilitates both the transfer of an electron to 7, and the stabilization of the positive charge distributed over the amine on C2, N1 and N5 of 9. This is followed by abstraction of a proton on C6 of 9 by the radical anion of 7.

Hydrogen bond in protein stability

Site-directed mutagenesis with Xaas has also been used to address the debate surrounding the role of hydrogen bonds in protein stability and folding. With a few exceptions, conventional site-directed mutagenesis does not allow direct evaluation of the contribution from hydrogen bonds due to the limited choice of natural amino acids. Schultz and coworkers evaluated the hydrogen bond strength in the side chains and the backbone of the protein. This was estimated from the change in stability $\Delta\Delta G^\circ$ ($= \Delta G^\circ_{\text{wild type(Unfolded} \rightarrow \text{Folded)}} - \Delta G^\circ_{\text{mutant(Unfolded} \rightarrow \text{Folded)}})$ of the protein upon introducing Xaas that vary in hydrogen bonding ability. The values of $\Delta\Delta G^\circ$ were obtained from denaturation curves.

Hydrogen bond strengths between side chains in a protein were evaluated¹⁸ by varying Tyr 27, Tyr 93, Glu 10 and Glu 75 of staphylococcal nuclease (SNase). These residues form hydrogen bonds (Tyr 27—Glu10, Tyr 93—Glu 75) in the 5-stranded β -barrel of this enzyme. The protein



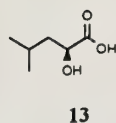
was destabilized to a similar extent (1-2 kcal•mol⁻¹) when tyrosine was replaced with a weak proton donor 10 or when glutamine was substituted with a weak proton acceptor 11. In another study,¹⁹ Tyr 27

was replaced with fluorinated tyrosine analogues varying in their pK_a values. The substitution of tyrosine (phenolic pK_a = 10) by 12 (phenolic pK_a ~ 5) increased the stability of SNase by about 2.3 kcal•mol⁻¹. The linear dependence of an apparent destabilization constant (K_{app}) on the pK_a (Figure 2) indicates a relationship between the stability of the protein and the acidity of the proton donor. These studies provide strong evidence that the side chain hydrogen bonds stabilize the folded protein in preference to the unfolded state in water.

By substituting an amino acid with α -hydroxy acids, the backbone hydrogen bond strength was estimated from the destabilization caused when an amide linkage is replaced with an ester link. Although the ester carbonyl and the amide carbonyl are isosteric, the former is a weaker proton acceptor and therefore the contribution towards hydrogen bond formation is negligible. Upon replacing²⁰ Leu 14 or Ile 72 with α -hydroxy acid 13



Figure 2. Plot of apparent destabilization K_{app} against pK_a at position 27 of SNase



in a β -sheet of SNase, the protein stability decreased by $1.5 - 2 \text{ kcal}\cdot\text{mol}^{-1}$. Similar substitutions²¹ were made at Leu 39 (N-terminal), Ser 44 (middle) and Ile 50 (C-terminal) of an α -helix in T4 Lysozyme. The destabilization caused by mutation in the middle ($\Delta\Delta G^\circ = 1.7 \text{ kcal}\cdot\text{mol}^{-1}$) of the α -helix was twice the destabilization induced by mutation at N and C termini ($\Delta\Delta G^\circ = 0.7\text{-}0.8 \text{ kcal}\cdot\text{mol}^{-1}$). This is consistent with the weakening of 2 hydrogen bonds at middle and one at each terminus.

LIMITATION AND OUTLOOK

Despite the various successes detailed in this report, there are some limitations to the site-directed mutagenesis with Xaa. One relates to the selective nature of the ribosome. Almost no mutant protein is translated when tRNAs mischarged with D-amino acids, β -hydroxy, β - or γ -amines, large side chains or highly polar groups, were employed¹. Also, the selectivity is seen to vary between rabbit and *E. coli* with the *E. coli* ribosome being more selective. Another limitation relates to the small quantities of both mischarged tRNA produced and mutant protein produced.

In conclusion, methods have been developed to site-specifically incorporate unnatural amino acids into proteins. The site-directed mutagenesis with Xaas allows detailed manipulation of the local environment for probing protein structure and function. Recent demonstrations of *in vivo* protein expression¹⁴ and direct aminoacylation²² of the tRNA are promising in improving the amount of mutant protein translated.

REFERENCES

- (1) Gilmore, M. A.; Steward, L. E.; Chamberlin, A. R. *Top. Curr. Chem.* **1999**, *202*, 77-99.
- (2) Noren, C. J.; Anthony-Cahill, S. J.; Griffith, M. C.; Schultz, P. G. *Science* **1989**, *244*, 182-186.
- (3) Bain, J. D.; Glabe, C. G.; Dix, T. A.; Chamberlin, A. R. *J. Am. Chem. Soc.* **1989**, *111*, 8013-8014.
- (4) Watson, J. D.; Hopkins, N. H.; Roberts, J. W.; Stertz, J. A.; Weiner, A. M. *Molecular Biology of the Gene*; 4th ed.; Benjamins/Cummings: California, **1987**.
- (5) Hohsaka, T.; Ashizuka, Y.; Murakami, H.; Sisido, M. *J. Am. Chem. Soc.* **1996**, *118*, 9778-9779.
- (6) Bain, J. D.; Switzer, C.; Chamberlin, A. R.; Benner, S. A. *Nature* **1992**, *356*, 537-539.
- (7) Alford, B. L.; Hecht, S. M. *J. Biol. Chem.* **1978**, *253*, 4844-4850.
- (8) Baldini, G.; Martoglio, B.; Schachenmann, A.; Zugliani, C.; Brunner, J. *Biochemistry*. **1988**, *27*, 7951-7959.
- (9) Bain, J. D.; Wacker, D. A.; Kuo, E. E.; Lyttle, M. H.; Chamberlin, A. R. *J. Org. Chem.* **1991**, *56*, 4615-4625.
- (10) Robertson, S. A.; Ellman, J. A.; Schultz, P. G. *J. Am. Chem. Soc.* **1991**, *113*, 2722-2729.

- (11) Lodder, M.; Golovine, S.; Laikhter, A. L.; Karginov, V. A.; Hecht, S. M. *J. Org. Chem.* **1998**, *63*, 794-803.
- (12) Cornish, V. W.; Benson, D. R.; Altenbach, C. A.; Hideg, K.; Hubbell, W. L.; Schultz, P. G. *Proc. Natl. Acad. Sci. USA* **1994**, *91*, 2910-2914.
- (13) Cook, S. N.; Jack, W. E.; Xiong, X.; Danley, L. E.; Ellman, J. A.; Schultz, P. G.; Noren, C. *J. Angew. Chem., Int. Ed. Engl.* **1995**, *34*, 1629-1630.
- (14) England, P. M.; Lester, H. A.; Davidson, N.; Dougherty, D. A. *Proc. Natl. Acad. Sci. USA* **1997**, *94*, 11025-11030.
- (15) Carreras, C. W.; Santi, D. V. *Annu. Rev. Biochem.* **1995**, *64*, 721-762.
- (16) Barrett, J. E.; Maltby, D. A.; Santi, D. V.; Schultz, P. G. *J. Am. Chem. Soc.* **1998**, *120*, 449-450.
- (17) Barrett, J. E.; Lucero, C. M.; Schultz, P. G. *J. Am. Chem. Soc.* **1999**, *121*, 7965-7966.
- (18) Thorson, J. S.; Chapman, E.; Schultz, P. G. *J. Am. Chem. Soc.* **1995**, *117*, 9361-9362.
- (19) Thorson, J. S.; Chapman, E.; Murphy, E. C.; Schultz, P. G. *J. Am. Chem. Soc.* **1995**, *117*, 1157-1158.
- (20) Chapman, E.; Thorson, J. S.; Schultz, P. G. *J. Am. Chem. Soc.* **1997**, *119*, 7151-7152.
- (21) Koh, J. T.; Cornish, V. W.; Schultz, P. G. *Biochemistry*. **1997**, *36*, 11314-11322.
- (22) Liu, D. R.; Schultz, P. G. *Proc. Natl. Acad. Sci. USA* **1999**, *96*, 4750-4785.

UNIVERSITY OF ILLINOIS-URBANA



3 0112 037715593

Q.547

16s

1999-00:II

ORGANIC SEMINAR ABSTRACTS

1999-00, SEMESTER II

University of Illinois

**Department of Chemistry
600 South Mathews Avenue
271 Roger Adams Laboratory
Urbana, IL 61801**

May 2000

NOTICE: Return or renew all Library Materials! The *Minimum Fee* for each Lost Book is \$50.00.

The person charging this material is responsible for its return to the library from which it was withdrawn on or before the **Latest Date** stamped below.

Theft, mutilation, and underlining of books are reasons for disciplinary action and may result in dismissal from the University.

To renew call Telephone Center, 333-8400

UNIVERSITY OF ILLINOIS LIBRARY AT URBANA-CHAMPAIGN

C. S. COUNTRY LIBRARY

L161—O-1096

54.7
265
99-00:II

Chemistry

SEMINAR TOPICS

SEMESTER II

SPRING 2000

	<u>PAGE</u>
UNDERSTANDING AND APPLICATIONS OF DIELS-ALDER REACTIONS IN WATER.....1 YANTAO ZHU	
NOVEL FLUOROUS PHASE SEPARATION METHODS IN ORGANIC SYNTHESIS9 LILI XIE	
WALKING THE TIGHT ROPE: CATALYST DESIGN IN ARYL-ARYL C-C, C-N, AND C-O COUPLING REACTIONS OF ARYL CHLORIDES AND ARYL SULFONATES17 KEVIN MCCAULEY	
PHAGE PEPTIDE LIBRARY DISPLAY.....25 ANOBEL TAMRAZI	
STEREOSELECTIVE PICTET-SPENGLER REACTIONS33 JING LIU	
DISCOVERY OF NEW CATALYSTS FOR ASYMMETRIC SYNTHESIS: SOLID-PHASE SYNTHESIS OF CATALYST LIBRARIES AND ADVANCES IN RAPID SCREENING TECHNIQUES41 TIMOTHY A. JOHNSON	
TOTAL SYNTHESIS OF HERBICIDIN NUCLEOSIDE ANTIBIOTICS49 CHAD DAVIS	
SYNTHESIS OF CEPHALOSTATINS AND RITTERAZINES: UNSYMMETRICAL DIMERIC STEROID PYRAZINE MARINE ALKALOIDS59 YU FAN	

UNDERSTANDING AND APPLICATIONS OF DIELS-ALDER REACTIONS IN WATER

Reported by Yantao Zhu

February 17, 2000

INTRODUCTION

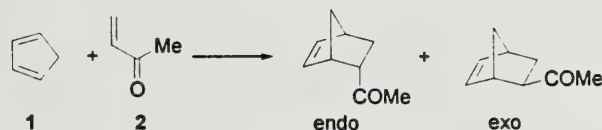
Owing to the insolubility of the reactants and the incompatibility of intermediates in aqueous media, water has typically been ignored as a solvent for decades. However, the low cost, reduced hazards and environmental advantages make water an attractive medium, especially since large aqueous accelerations of some organic reactions have been discovered.¹ To date, many types of organic reactions have been studied in water,² and quite a few of them are subject to large rate enhancements, including the Diels-Alder (DA) reaction.

The DA cycloaddition is a powerful reaction for making new carbon-carbon bonds.³ While early studies showed small or moderate organic solvent effects on DA reactions,⁴ Rideout and Breslow¹ found that these reactions could be greatly accelerated in water. This pioneering discovery set the stage for more detailed studies on the effect of water on DA reactions. In the past twenty years, different explanations have been proposed and examined for the origins of the rate enhancements, and the synthetic potential of aqueous DA reactions has been exploited. A Lewis acid-catalyzed version has also been investigated. This review will focus on recent developments concerning the origins of aqueous rate accelerations, synthetic applications of aqueous DA reactions, and their Lewis acid-catalyzed counterparts.

ORIGINS OF RATE ENHANCEMENT

Aqueous Diels-Alder reactions offer two general advantages over organic solvents: higher endo/exo selectivities and usually significant increases in rate (Table 1).^{1,5} Very little research has been

Table 1. ^{1,5} Solvent Effect on the DA Reaction



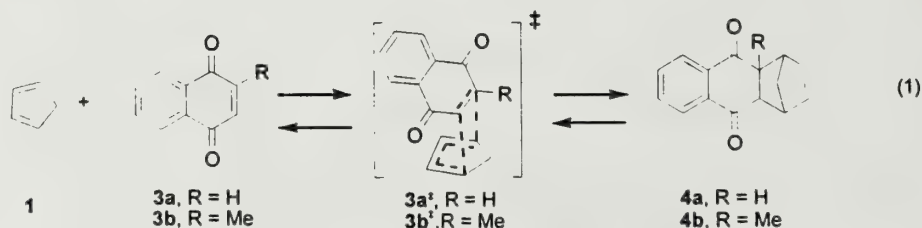
solvent		10 ⁵ × k ₂ (M ⁻¹ s ⁻¹)	
isooctane		5.94	
H ₂ O		4400	
solvent		endo/exo	
1		3.85	
0.015 M 1 in water		21.4	

Copyright © 2000 by Yantao Zhu

carried out on the causes of the higher endo/exo selectivity in water. It is assumed that the more compact endo TS is favored because the surface area exposed to water is minimized. High internal pressure, micellar catalysis, and hydrophobic packing of diene and dienophile have been proposed to explain this aqueous rate enhancement.⁶ However, extensive kinetic studies⁷⁻⁹ and calculations^{10,11} have shown that hydrophobic interactions and hydrogen bonding are the primary causes. DA reactions have negative activation volumes; therefore, the hydrophobic surface area of reactants is reduced on going from the initial state to the transition state. In water, this will lead to the release of water molecules of higher energy in the hydration shell to the bulk water where the free energy of molecules is lower. Therefore, the activation energy is lowered and the reaction is accelerated. "Enforced hydrophobic interaction" is used by Engberts to distinguish the hydrophobic effect during the activation process from the hydrophobic interaction that just pushes organic reactants together.⁷ Hammett ρ values showed that transition states are usually more polar than the initial states for DA reactions.¹² Hydrogen bonding may play another role in accelerating the reaction by stabilizing the polarized transition state more strongly than the initial state when polar activation groups like the carbonyl group are conjugated to the reaction centers. Recent research has attempted to separate and quantify the contribution of these two factors.

The importance of the hydrophobic effect was demonstrated by the dimerization of **1**, and the reaction between acridizinium bromide and **1**.¹³ Accelerations were observed for both cases. Further study¹⁴ on the hydrophobicity of reactants showed that the increased hydrophobicity closer to the reaction center has a larger influence on the rate enhancement. Calculations done by Jorgensen¹⁰ and Gao¹¹ on the reaction between **1** and **2** show different results regarding the relative contribution of the two factors. Jorgensen's calculations indicate that hydrogen bonding is the main factor, while Gao believes both factors contribute equally to the acceleration.

In order to assess the contribution of the two factors in a single reaction, Engberts¹⁵ studied the retro-Diels-Alder (RDA) reaction of **4b** as a model for the hydrogen bonding effect in the DA reaction between **1** and **3a** (eq 1). The RDA reaction is a unimolecular reaction, in which the desolvation and



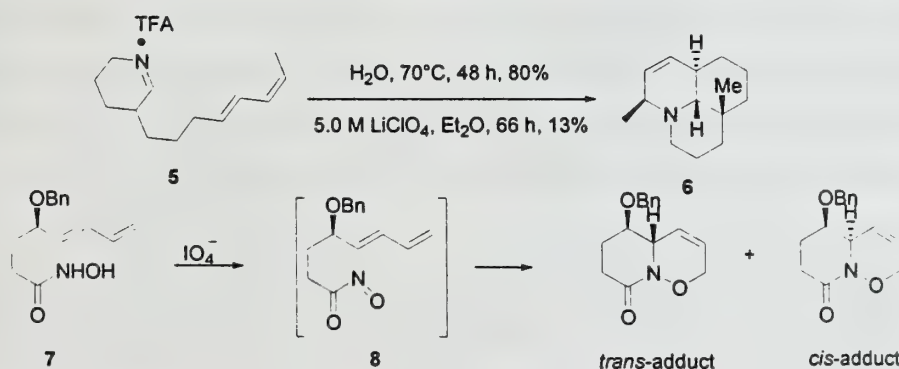
diffusion encounter of reactants are excluded. Furthermore, the absolute value of the activation volume of a RDA reaction is usually close to zero, much smaller than that of a DA reaction. Therefore, in the

absence of a significant hydrophobic effect in the RDA reaction, hydrogen bonding remains as the major contribution to any observed aqueous acceleration. This RDA reaction was found to be 140 times faster in water than in hexane. It is even faster in stronger hydrogen bond-donating solvents, such as 1,1,1,3,3,3-hexafluoroisopropanol (HFIP), which indicates that hydrogen bonding can greatly accelerate the pericyclic reaction without significant hydrophobic interactions. In the reaction between **1** and **3a**, both hydrophobic interactions and hydrogen bonding are available for the rate enhancement. Furthermore, the hydrogen bonding effect resembles that of the RDA reaction of **4b**, since the hydrogen bonding influences both the transition states and the initial states of the two reactions similarly (the number of hydrogen bonding acceptors in **3a** and **4b** is the same; and the TSs of the two reactions **3a**[‡] and **3b**[‡] are quite comparable). The hydrogen bonding effect corresponds to a decrease of 3.0 kcal mol⁻¹ in the $\Delta G^\ddagger_{\text{RDA}}$ of **4b** in water compared to that in hexane. A similar effect should be present in the reaction between **1** and **3a**. Since the $\Delta\Delta G^\ddagger_{\text{DA}}$ of **1** and **3a** in hexane and in water is -5.1 kcal mol⁻¹, the contribution of hydrophobic interactions should be approximately -2.1 kcal mol⁻¹. These values suggest a somewhat larger contribution of hydrogen bonding to the acceleration of this particular reaction.

UNCATALYZED DIELS-ALDER REACTIONS IN WATER

Aqueous media for Diels-Alder reactions have been used to advantage in syntheses directed toward very diverse targets, especially by Grieco et al. They prepared quassinoids via aqueous Diels-Alder reactions and demonstrated improvements in rates, yields, and selectivities in water.¹⁶ Recently, the preparation of nitrogen containing heterocyclic structures by aqueous intramolecular imino DA reaction was reported (Scheme 1).¹⁷ With diethyl ether as solvent, the expected cycloaddition product **6** was obtained in only 13% conversion after 66 h in the presence of 5.0 M LiClO₄. However, the reaction occurred much more efficiently in water at 70°C for 48 h providing **6** in 80% yield.

Scheme 1.



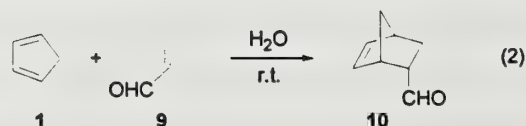
N-Acylnitroso DA reactions usually give poor stereoselectivity in organic solvents. Although these nitroso species are short-lived and may undergo rapid hydrolysis, they behave as good dienophiles

for DA reactions in water (Scheme 1).¹⁸ Typically the trans:cis ratios of the products increased from 1.5:1 in CHCl_3 to 4.5:1 in water. This method has been used in the syntheses of (-)-swainsonine and (-)-pumiliotoxin C.¹⁹ Aqueous DA reactions have also been employed in the highly stereoselective preparation of 1,1,4-trisubstituted tetrahydrofurans with broad-spectrum antifungal activity.²⁰

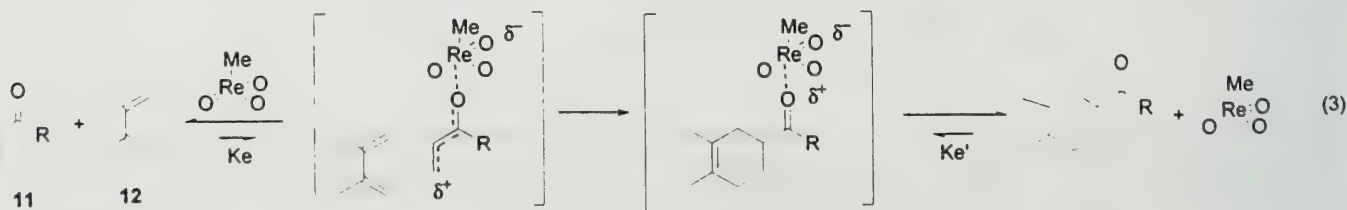
LEWIS ACID-CATALYZED DIELS-ALDER REACTIONS IN WATER

Diels Alder reactions can benefit remarkably from the use of Lewis acids in organic solvents both in terms of reaction rate and endo/exo selectivity.²¹ However, most Lewis acids are water-sensitive requiring thorough drying of both reactants and solvents. To overcome these drawbacks, more researchers turned their attention to water-tolerant Lewis acids. Some catalysts have been proved effective in reactions using a few equivalents of water or water as a co-solvent.^{22,23} In addition, catalyzed DA reactions have been studied in water with the hope that the advantages of using Lewis acids and water as the solvent can be combined.

Loh and coworkers employed InCl_3 as a catalyst for aqueous DA reactions. A typical example is the reaction of compounds **1** and **9** (eq 2).²⁴ The reaction using 20 mol % catalyst gave 100 % conversion in 2 h with 91:9 endo/exo selectivity. The uncatalyzed reaction resulted in only 60% conversion with a 74:26 of endo/exo ratio. The reaction with a dienophile containing amide as chiral auxiliary gave moderate diastereoselectivity (*dr*: 73/27) with 120 mol % InCl_3 . After extraction with organic solvents, the remaining aqueous solution containing the catalyst was reused with comparable yields and selectivity.



Espenson²⁵ and coworkers studied methylrhenium trioxide (MTO) as a catalyst for aqueous DA reactions. As expected, very little difference was observed in the rates of these catalyzed reactions in different organic solvents (CHCl_3 , THF, CH_3CN and acetone). However, the reactions were a few times faster in water than in organic solvents and provided higher endo/exo selectivity. The authors proposed a rapid and reversible interaction between MTO and both dienophile and product (eq 3). The equilibria



Ke and Ke' lie towards the non-coordinated species since no product inhibition was observed and no stable complex was observed by ^1H NMR when dienophile and MTO were mixed together.

Lanthanide (III) triflates were used in the catalysis of aqueous aza Diels-Alder reactions.²⁶ These reactions conveniently combine three reactants (an aldehyde, an amine salt and a diene) to generate nitrogen-containing heterocyclic products. The scope of this hetero annulation reaction has been limited to formaldehyde or activated aldehydes such as glyoxylates. Dienes other than **1** also give poor to moderate yields. In contrast, with the addition of lanthanide (III) salts, less reactive aldehydes (Table 2, entries 1-3) and a variety of dienes (entries 4-6) can also be used. However, the reaction of these less reactive aldehydes with dienes other than **1** is still an unsolved problem. In these reactions, the catalyst

Table 2. ²⁶ Aqueous Aza Diels-Alder Reactions Catalyzed by $\text{Ln}(\text{OTf})_3$

$\text{RCHO} + \text{BnNH}_3^+ \text{Cl}^- + \mathbf{1} \xrightarrow[\text{H}_2\text{O}]{\text{Ln}(\text{OTf})_3}$

$\text{CH}_2\text{O} + \text{H}_2\text{N}-\text{CH}(\text{Ph})-\text{CO}_2\text{Me} + \text{A} \xrightarrow[\text{H}_2\text{O}]{\text{Ln}(\text{OTf})_3}$

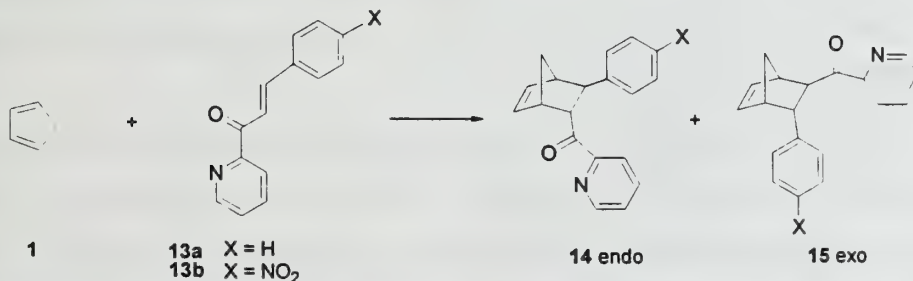
entry	R-	catalyst	yields (%) ^a	entry	A	catalyst	yields (%) ^a
1	$\text{CH}_3(\text{CH}_2)_4-$	$\text{Pr}(\text{OTf})_3$	68 (7)	4	Cyclohexadiene	$\text{Nd}(\text{OTf})_3$	84 (27)
2	CH_3CH_2-	$\text{La}(\text{OTf})_3$	64 (4)	5	2,3-Dimethyl-1,3-butadiene	$\text{Nd}(\text{OTf})_3$	98 (58)
3	PhCH_2-	$\text{Yb}(\text{OTf})_3$	72 (3)	6	2-Methyl-1,3-butadiene	$\text{Nd}(\text{OTf})_3$	96 (37)

^a The yields for uncatalyzed reactions in parentheses.

did not change the endo/exo ratio of the products. The lanthanide catalysts have been used in the synthesis of azasugars,²⁷ which are potential inhibitors of glycoprocessing enzymes.

Engberts and coworkers showed that Cu^{2+} is a good catalyst for the Diels-Alder reaction between compounds **1** and **13** (Table 3)²⁸. It is obvious that the large aqueous acceleration in the uncatalyzed

Table 3. ²⁸ Solvent and Catalyst Effect on the Reaction between **1** and **13**



Solvent	$K_{\text{Uncat},13\text{b}} (\text{M}^{-1}\text{s}^{-1})$	$(k/k_{\text{CH}_3\text{CN}})_{\text{Uncat}}$	$K_{\text{Cat},13\text{b}} (\text{M}^{-1}\text{s}^{-1})$	$(k/k_{\text{CH}_3\text{CN}})_{\text{Cat}}$	endo/exo _{13a}	endo/exo _{13a}
CH_3CN	1.40×10^{-5}	1.00	2.21	1.00	67/33	94/6
EtOH	3.83×10^{-5}	2.74	0.769	0.348	77/23	96/4
H_2O	4.02×10^{-3}	287	3.25	1.47	84/16	93/7

reaction diminished sharply in the catalyzed reaction. A possible explanation involves replacement of hydrogen bonding by water by coordination to Lewis acids in the catalyzed reactions, leaving only hydrophobic effects for the acceleration. The hydrophobic effect may also be decreased since the catalyst can partly disrupt the hydrophobic hydration shell of the activated complex. Although the endo/exo ratio for uncatalyzed reactions is larger in water than it is in organic solvents, the ratio is similar for the catalyzed reactions. Co^{2+} , Ni^{2+} and Zn^{2+} also catalyze this reaction, but they are less effective than Cu^{2+} .²⁸

Although the use of water has long been incompatible with enantioselective DA reactions, the first example of an enantioselective DA reaction in water was achieved when aromatic α -amino acids were used as ligands for the Cu^{2+} -catalyzed DA between **1** and **13b** (Tables 3 and 4).²⁹ Similar endo/exo

Table 4. ²⁹ Influence of Ligand on the Enantioselectivity of the Aqueous DA Reaction^a

entry	ligand	<i>er</i> ^b	entry	ligand	<i>er</i> ^b
1	glycine	50/50	5	N-methyl-L-tyrosine	87/13
2	L-valine	50/50	6	N,N-dimethyl-L-tyrosine	86/14
3	L-leucine	51/49 ^c	7	L-tryptophan	67/33
4	L-tyrosine	68/32	8	N ^{α} -methyl-L-tryptophan	87/13

^a10 mol % of $\text{Cu}(\text{NO}_3)_2$, 17.5 mol % of ligand. ^b results for major isomer.

^c 250 mol % of promoter was used.

ratios of 93:7 were obtained in most cases. The enantioselectivity increased with pH and reached a plateau above pH 5, which indicates that the catalytically active form of the ligands is the amino carboxylate. The similar enantioselectivity with catalyst:dienophile ratios ranging from 8:1 to 1:10 indicates that DA reactions proceed through a ternary dienophile-Cu(II)-ligand complex, and that the displacement of the ligand by the dienophile is insignificant. When only half equivalent of the ligand (entry 8) relative to the copper was used, 76% of the reaction was mediated by the chiral copper-ligand complex. Therefore, ligand-accelerated catalysis must have taken place in this system. A catalytic cycle was proposed based on these observations (Scheme 2).²⁹

The study of different ligands showed a substantial positive influence of N-methylation of the ligand on the enantioselectivity (Table 4, entries 5-8). The trends were rationalized by comparing the four possible geometries of the dienophile-Cu(II)-ligand complex (Figure 1). Because of the arene-arene interaction, one face of the dienophile is partially blocked. Furthermore, the cis complexes are likely to experience a steric repulsion between the pyridine hydrogen and the N-methyl group of the ligand, which does not exist in the trans complexes. Therefore, the cycloaddition presumably takes place preferentially on the more accessible bottom face of the trans complexes. The relatively high

enantioselectivity would suggest a preference between trans-transoid and trans-cisoid. However, which of the two trans complexes is favored is still unknown since the absolute configuration of the product has not been elucidated. This explanation was based on the assumption that similar interactions are involved in transition state. Study of this reaction in different solvents showed higher enantioselectivity in water than in organic solvents, presumably, due to the water enhanced arene-arene interaction.

Scheme 2. Proposed Catalytic Cycle for the Reaction between 1 and 13a

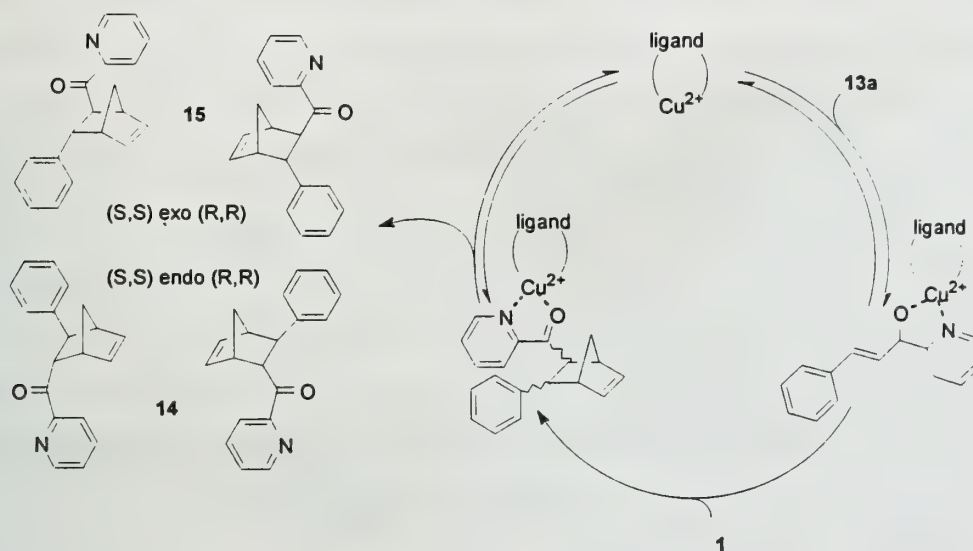
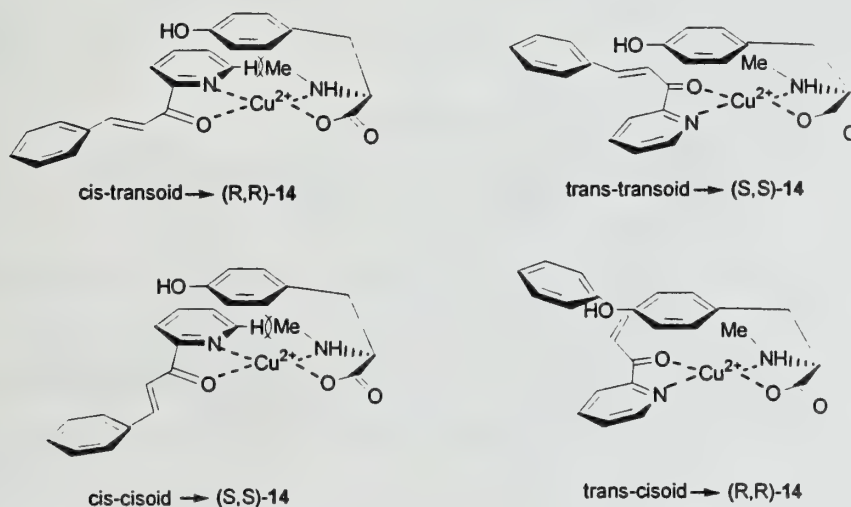


Figure 1. Proposed Structure of Ligand-Cu(II)-dienophile Complex



CONCLUSION

Diels-Alder reactions benefit remarkably from the use of water as a solvent in terms of rate and selectivity. The aqueous rate enhancements are attributed to enforced hydrophobic interactions and

hydrogen bonding. The relative contribution of each factor is still not clear, but experimental data point to a larger role for hydrogen bonding. Aqueous Diels-Alder reactions have been used in the synthesis of a number of natural products. Some water stable, efficient, and reusable Lewis acids were studied in aqueous Diels-Alder reaction. Finally, the first example of a water-enhanced, enantioselective Lewis acid-catalyzed Diels-Alder reaction has been demonstrated. Future work to develop more effective chiral auxiliaries and chiral catalysts is needed.

REFERENCES

- 1) Rideout, D. C.; Breslow, R. *J. Am. Chem. Soc.* **1980**, *102*, 7816-7817.
- 2) Li, C.; Chen, T.-H. *Organic Reactions in Aqueous Media*, Wiley: New York, 1997.
- 3) Sauer, J.; Sustmann, R. *Angew. Chem. Int. Ed. Engl.* **1980**, *19*, 779.
- 4) Breslow, R.; Maitra, U.; Rideout, D. *Tetrahedron Lett.* **1983**, *24*, 1901.
- 5) Selness, S. R. *Chem 435 seminar February 20, 1992*.
- 6) Otto, S.; Blokzijl, W.; Engberts, J. B. F. N. *J. Org. Chem.* **1994**, *59*, 5372-5376.
- 7) Blokzijl, W.; Blandaner, M. J.; Engberts, J. B. F. N. *J. Am. Chem. Soc.* **1991**, *113*, 4241-4246.
- 8) Blokzijl, W.; Engberts, J. B. F. N. *J. Am. Chem. Soc.* **1992**, *114*, 5440-5442.
- 9) Blake, J. F.; Jorgensen, W. L. *J. Am. Chem. Soc.* **1991**, *113*, 7430-7432.
- 10) Furlani, T. R.; Gao, J. *J. Org. Chem.* **1996**, *61*, 5492-5497.
- 11) Sauser, J.; Sustmann, R. *Angew. Chem. Int. Ed. Engl.* **1980**, *19*.
- 12) van der Wel, G. K.; Wijnen, J. W.; Engberts, J. B. F. N. *J. Org. Chem.* **1996**, *61*, 9001-9005.
- 13) Meijer, A.; Otto, S.; Engberts, J. B. F. N. *J. Org. Chem.* **1998**, *63*, 8989-8994.
- 14) Wijnen, J. W.; Engberts, J. B. F. N. *J. Org. Chem.* **1997**, *62*, 2039-2044.
- 15) Grieco, P. A. *Aldrichimica Acta* **1991**, *24*, 59.
- 16) Grieco, P. A.; Kaufman, M. D. *J. Org. Chem.* **1999**, *64*, 6041-6048.
- 17) Naruse, M.; Aoyagi, S.; Kibayashi, C. *Tetrahedron Lett.* **1994**, *35*, 595-598.
- 18) Kibayashi, C.; Aoyagi, S. *Synlett* **1995**, 873-879.
- 19) Saksena, A. K.; Girjavallabhan, V. M.; Chen, Y.; Jao, E.; Pike, R. E.; Desai, J. A.; Rane, D.; Ganguly, A. *Heterocycles* **1993**, *35*, 129-134.
- 20) Pindur, U.; Lutz, G.; Otto, C. *Chem. Rev.* **1993**, *93*, 741-761.
- 21) Kubayashi, S.; Hachiya, I.; Araki, M.; Ishitami, H. *Tetrahedron Lett.* **1993**, *34*, 3755-3758.
- 22) Mikami, K.; Kotera, O.; Motoyama, Y.; Sakaguchi, H. *Synlett* **1995**, 975-977.
- 23) Loh, T.; Pei, J.; Lin, M. *Chem. Commun.* **1996**, 2315-2316.
- 24) Zhu, Z.; Espenson, J. H. *J. Am. Chem. Soc.* **1997**, *119*, 3507-3512.
- 25) Yu, L.; Chen, D.; Wang, P. G. *Tetrahedron Lett.* **1996**, *37*, 2169-2172.
- 26) Yu, L.; Li, J.; Ramirez, J.; Chen, D.; Wang, P. G. *J. Org. Chem.* **1997**, *62*, 903-907.
- 27) Otto, S.; Bertoncin, F.; Engberts, J. B. F. N. *J. Am. Chem. Soc.* **1996**, *118*, 7702-7707.
- 28) Otto, S.; Engberts, J. B. F. N. *J. Am. Chem. Soc.* **1999**, *121*, 6798-6806.

INTRODUCTION

Phase extraction is one of the simplest processes in the purification stage of organic synthesis. Recent developments have been made in a new field called fluorous chemistry which takes advantage of the special properties of perfluorocarbon fluids to facilitate catalyst or reagent separations. Perfluorocarbon fluids are highly fluorinated alkanes, ethers, and amines that are nonpolar, nontoxic solvents. Many of them are commercially available. They are usually immiscible with common organic solvents and water. As a result these unusual solvents can be employed to partition compounds between two liquid phases.¹ If the reagents or catalysts are made fluorous by attaching appropriate solubilizing groups (e.g. $(\text{CH}_2)_x(\text{CF}_2)_y\text{CF}_3$), they can be localized in a fluorous phase and therefore easily separated by extraction processes (Figure 1). This feature has been employed in both organic synthesis and catalysis since Horváth introduced the concept in 1994.²⁻⁸ This review will present recent advances in fluorous synthesis and the design of ligands for fluorous biphasic catalysis.

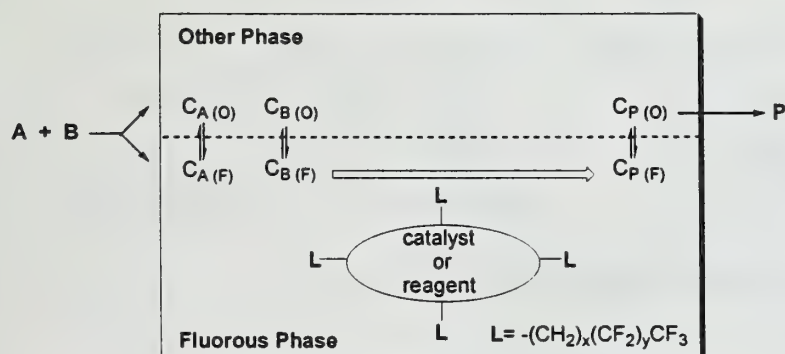


Figure 1. Fluorous Biphasic System.³ (C: partition coefficient)

THE CONCEPT AND OVERVIEW

The term “fluorous” was introduced as the analog to the term “aqueous” by Horváth in 1994.² A fluorous biphasic system (FBS) usually consists of a fluorous phase and a second phase. The fluorous phase contains a fluorous soluble reagent or catalyst while the second phase may be any organic or nonorganic solvent with limited miscibility in the fluorous phase. As illustrated in Figure 1, A and B react to form product P in the presence of fluorous reagent or catalyst under biphasic conditions. After the reaction is complete, the product and the catalyst or reagent partition into different phases which

allows simple separations. Fluoroalkyl groups (so called fluoros ponytails) such as $(\text{CH}_2)_x(\text{CF}_2)_y\text{CF}_3$ can be attached to the catalysts or reagents to promote the solubility of the compounds in the fluoros phase.² The $(\text{CH}_2)_x$ spacers provide a tuning element that can be adjusted to insulate reactive sites from the electron-withdrawing perfluoroalkyl groups by different x values. An empirical value of above 60 w/w % total fluorine content of fluoros complexes was suggested for sufficient fluoros solubility.²

Some organic-fluoros bilayers become miscible at elevated temperature.² Therefore, a fluoros biphasic could combine the advantages of one phase reaction with biphasic product separation. The reaction can be run homogeneously at higher temperature, and the products can be separated at lower temperature (Figure 2).^{2,5} Alternatively, a fluoros biphasic reaction could proceed in either fluoros phase or organic phase if the other solvent is not necessary during the reaction stage. The other possibility is running the reaction in "hybrid solvents" which dissolve both organic and fluoros compounds.⁴ Benzotrifluoride (BTF, $\text{CF}_3\text{C}_6\text{H}_5$) is usually selected for its favorable properties and low cost. After reaction is complete, the solvent is evaporated and the residue is treated with organic/fluoros solvents to perform phase separation.⁹

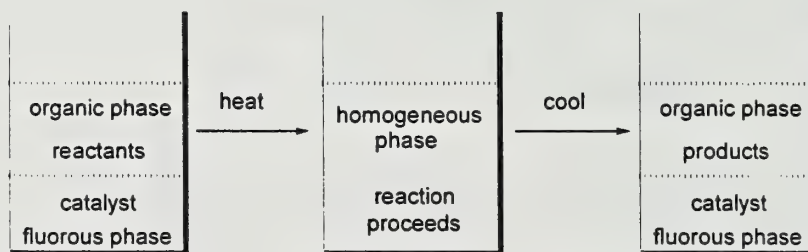


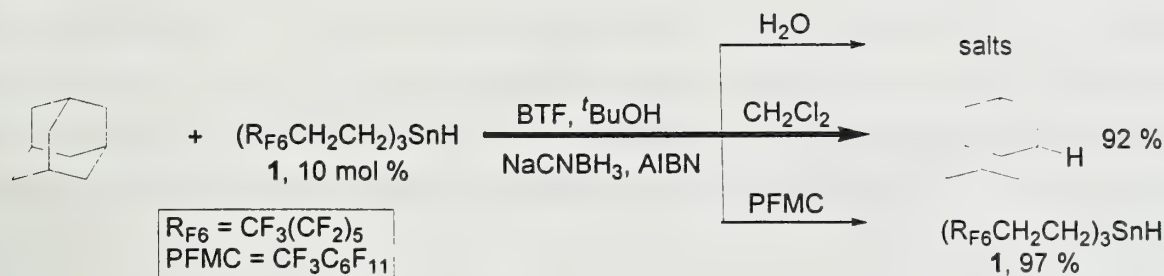
Figure 2. Monophase Reaction and Biphasic Separation.⁵

FLUOROS REAGENTS AND SYNTHESIS

Fluoros reagents facilitate separation in traditional organic synthesis. In addition, they can be recovered easily by phase separation processes. Therefore, fluoros reagents can be recycled which is especially advantageous for expensive or toxic reagents. Recently, Curran and coworkers have developed several fluoros tin reagents which are soluble in fluoros solvents and hybrid solvents such as BTF, but sparingly soluble or insoluble in most organic solvents.⁹ For example, a stoichiometric amount of tri(2-perfluorohexylethyl)tin hydride, $(\text{CF}_3(\text{CF}_2)_5\text{CH}_2\text{CH}_2)_3\text{SnH}$ (1), was used to reduce various functional groups in R-X ($\text{X}=\text{Br}$, SePh , NO_2 , OCS_2CH_3) in good yields in the presence of 10 mol % AIBN. A catalytic procedure for the reduction of 1-bromoadamantane was also carried out using

10 mol % tin hydride **1** and 1.3 equivalent of NaCNBH₃. A three-phase extraction was employed to separate the product, inorganic salts, and **1** (Scheme 1).

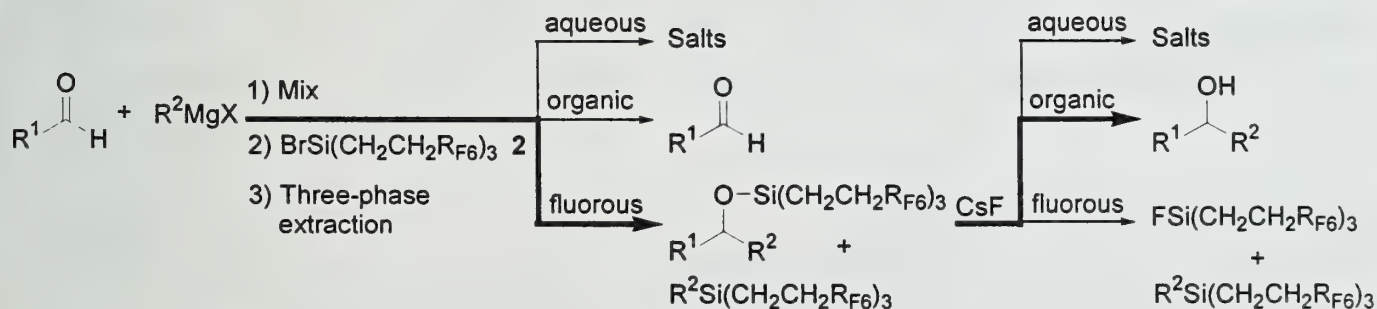
Scheme 1.



The recovered tin hydride **1** was recycled five times with no change in the product yield, and the new reagent proved to be somewhat more reactive than tributyltin hydride ($k_{\text{H}} = 1 \times 10^7 \text{ M}^{-1}\text{s}^{-1}$ vs. $k_{\text{H}} = 6 \times 10^6 \text{ M}^{-1}\text{s}^{-1}$).⁹ This fluorous reagent exhibits excellent potential for large-scale applications.

Phase switching is a common strategy to purify organic reaction mixtures, e.g. acid-base extraction. Similarly, a fluorous phase switch could be triggered by attachment and detachment of the fluorous substituent. An example of this technique is illustrated in Scheme 2.¹⁰

Scheme 2.

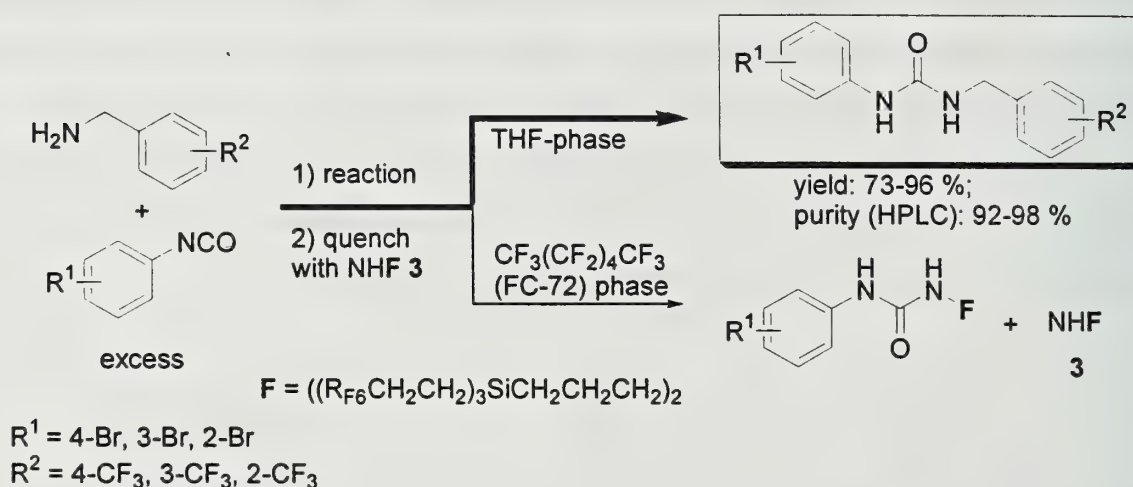


Whether the aldehyde or Grignard reagent is in excess, the pure final product can be obtained by silylation and extraction into the fluorous phase, followed by desilylation and extraction back into the organic phase. Such a fluorous phase switch is also effective for incomplete reactions or reactions with impure starting materials.¹¹ In addition, like solid-phase synthesis, fluorous synthesis is suitable for multistep organic synthesis and multicomponent reactions. If the starting material is labeled with a fluorous group, each fluorous-labelled intermediate can be easily purified by a three-phase extraction in a multistep reaction. Finally the fluorous substituent can be removed to liberate the product.¹⁰

FLUOROUS COMBINATORIAL SYNTHESIS

Combinatorial and parallel syntheses require speed and efficiency. The application of fluororous chemistry in this context is attractive owing to its integration of synthesis and purification strategies. In addition, when all reactions are performed in the liquid phase, the molecular control is better than in solid-phase synthesis. For example, fluororous scavenging agents are effective for rapid purification and isolation of the products formed in a solution phase reaction. The fluororous amine scavenger $((R_FCH_2CH_2)_3SiCH_2CH_2CH_2)_2NH$ (**3**) was applied to the automated solution phase parallel synthesis of a urea library (Scheme 3).¹² Both the yields and purities of the products were good after liquid-liquid extraction.

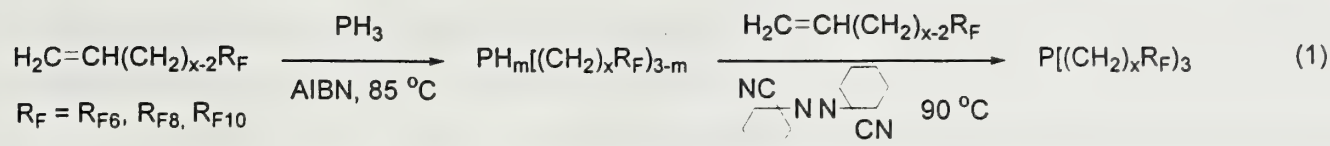
Scheme 3.



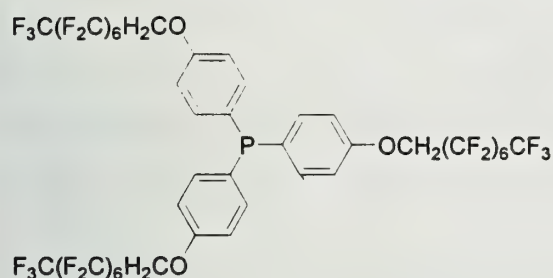
FLUOROUS BIPHASE CATALYSIS

Homogeneous catalysis is widely used in industrial chemical processes. Environmental concerns have led to development of new catalysts that allow for rapid, selective chemical transformations as well as effective catalyst and product recovery. One of the approaches being developed is fluororous biphasic catalysis (FBC).¹³

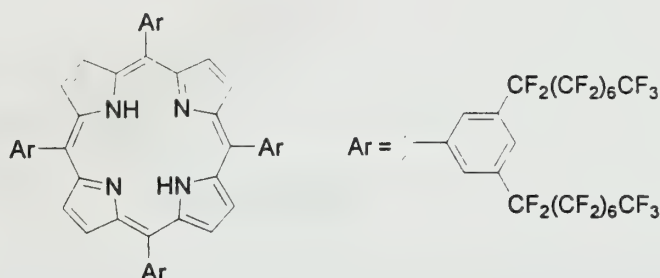
The challenge for FBC is to design ligands for homogeneous catalysts with high solubility in perfluorocarbon fluids, and the usual strategy is to attach fluoroponytails to render them fluororous. A variety of fluororous ligands have been synthesized in the past few years. For example, Gladysz and coworkers recently published the synthesis of perfluoroalkyl phosphines $P[(CH_2)_x(CF_2)_yCF_3]_3$ ($x = 2, y = 5, 7, \text{ or } 9; x = 3 \text{ or } 4, y = 7$) by the radical addition of PH_3 to alkenes (eq 1).¹⁴



However, trialkylphosphines are not as good ligands for most transition metal catalysts as triarylphosphines. Several laboratories therefore are engaged in synthesizing fluorous-soluble, perfluoroalkylated triphenylphosphine (III) ligands (e.g. compound 4) although the applications of these ligands have not been widely investigated yet.¹⁵⁻¹⁷



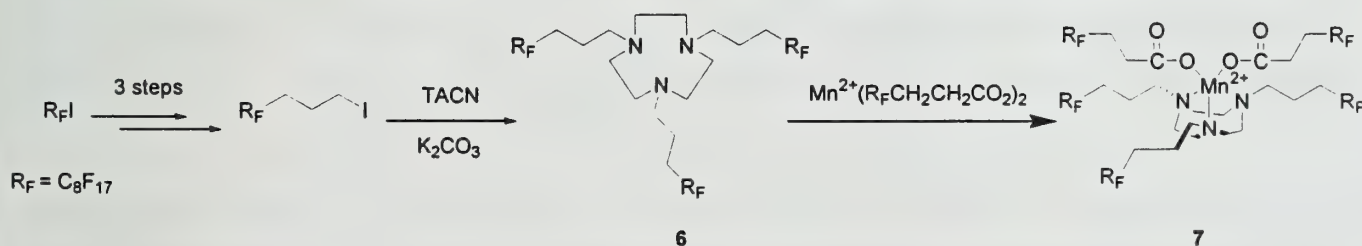
4



5

Perfluorocarbon-soluble tetraarylporphyrin 5 bearing eight C_8F_{17} chains was synthesized by Pozzi and coworkers.¹⁸ Cyclopentadienyl ligands can also be made soluble in fluorous media by attaching fluoroptynyls.¹⁹ Perfluoroalkylated triazacyclononane, $\text{R}_\text{F}\text{TACN}$ (6), synthesized from $\text{R}_\text{F}\text{I}$ (Scheme 4.), forms manganese(II) complex 7 in fluorous phase for oxidation of alkenes and alkanes in the presence of $t\text{BuOOH}$ and O_2 .²⁰

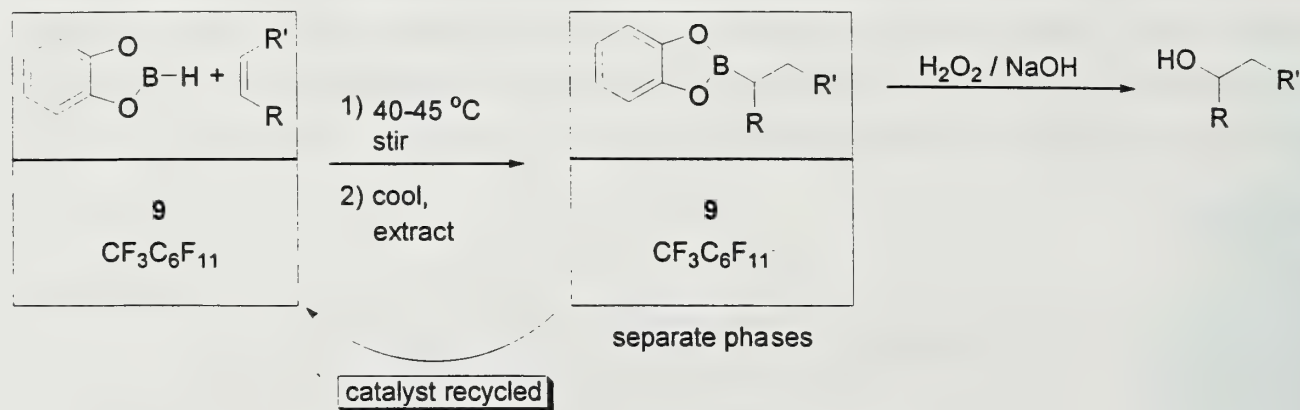
Scheme 4.



Among these achiral ligands, $\text{P}[(\text{CH}_2)_2(\text{CF}_2)_5\text{CF}_3]_3$ (8), has been most extensively studied. A fluorous analog of Wilkinson's catalyst, $\text{RhClP}[(\text{CH}_2)_2(\text{CF}_2)_5\text{CF}_3]_3$ (9), was prepared from $\{[\text{RhCl}(\text{COD})]_2\}$ and 8. The complex is a powerful catalyst for hydrogenation,²¹ hydroboration,²² and hydrosilylation.²³ For example, catalytic hydroboration was carried out in a heterogeneous $\text{CF}_3\text{C}_6\text{F}_{11}$

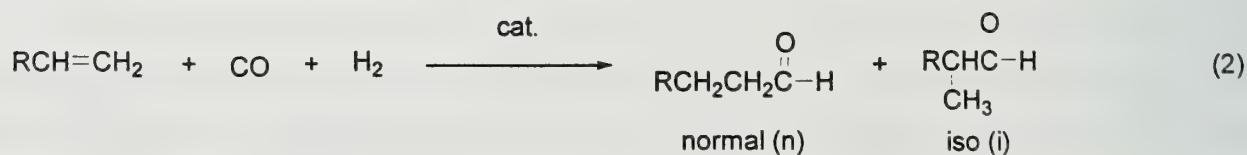
mixture of an alkene, catecholborane, and **9**. After the reaction was complete, the mixture was readily separated by extraction. Catalyst **9** was recycled and the alkylborane intermediate was oxidized in a subsequent step by $\text{H}_2\text{O}_2/\text{NaOH}$ (Scheme 5).²²

Scheme 5.



Catalyst loading of 0.01-0.25 mol % was effective and the turnover value of **9** was higher than 10,000. However, its reactivity was much lower than $\text{ClRh}(\text{PPh}_3)_3$, which is consistent with the observation that Rh/PR_3 (R = alkyl group) complexes are less active hydroboration catalysts than Rh/PPh_3 complexes. This unique example clearly demonstrates the utility of fluorous biphasic catalysis for catalyst recycling.²² In contrast, in the classic hydroboration reactions of alkenes, the valuable transition metal catalysts are usually destroyed at the subsequent oxidation step ($\text{H}_2\text{O}_2/\text{NaOH}$).

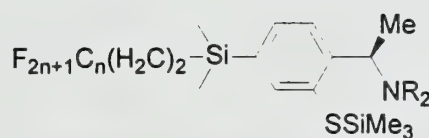
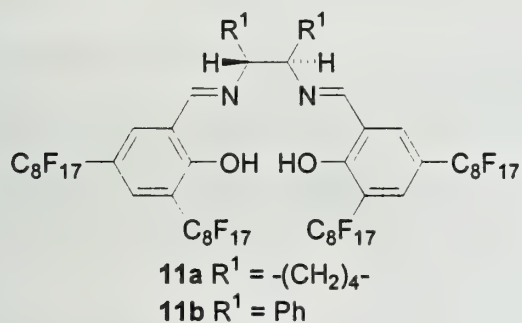
Phosphine ligand **8** was also successfully applied to hydroformylations.²⁴ Hydroformylation is an important industrial process which produces aldehydes from olefins, CO and H_2 in the presence of catalysts (eq 2).



Both catalysts for organic media such as $\text{HRh}(\text{CO})[\text{PPh}_3]_3$ and catalysts for aqueous media such as $\{\text{HRh}(\text{CO})[\text{P}(\text{m}-\text{C}_6\text{H}_4\text{SO}_3\text{Na})_3]_3\}$ ²⁵ have been utilized in these reactions. The new fluorous reagent, $\text{HRh}(\text{CO})\{\text{P}[\text{CH}_2\text{CH}_2(\text{CF}_2)_5\text{CF}_3]_3\}$ (**10**), is the first catalyst that can be used for the hydroformylation of both low and high molecular weight olefins. The reactions were carried out under homogeneous conditions at high temperature ($100\text{ }^\circ\text{C}$), and the products were separated at lower temperature by extraction (Figure 2). The normal/iso (n/i) selectivity of catalyst **10** is similar to Rh/PPh_3 catalyst, but

the activity is an order of magnitude lower which might be attributed to the electronic nature of the ligands.²⁴

A number of other catalysts have been synthesized and applied to various reactions in FBS. However, chiral fluoros catalysts have only recently been investigated. Chiral fluoros reagents and catalysts for asymmetric transformations could offer new tools to synthetic chemists. Aside from the ability to recycle precious chiral reagents or catalysts, it has been proposed that the solution environment provided by perfluorocarbons might afford improved selectivity on reactions.²⁶ Pozzi and co-workers synthesized chiral perfluoroalkylated salen ligands (**11a**, **11b**) which are soluble in perfluorocarbon fluids.²⁷ The manganese (III) complexes of **11a** and **11b** were tested as catalysts in epoxidation of alkenes under FBS conditions in the presence of various oxygen donors. The products were easily separated from catalysts and the catalysts were then recycled. However, enantioselectivities were generally poor except in the case of indene (70-92 % ee).



- 12a** $R = Me, \quad n = 6$
12b $R = Me, \quad n = 10$
12c $R = -(CH_2)_4-, \quad n = 6$

Chiral perfluoroalkyl catalyst precursors (**12a-c**) using $-CH_2CH_2SiMe_2$ units as spacers were prepared by van Koten and co-workers.²⁸ These compounds catalyzed enantioselective addition of diethylzinc to benzaldehyde. Also, Curran and Tukeuchi reported chiral fluoros BINOL derivatives that were applied to the same reaction.²⁹ In both cases, the enantioselectivities were high even after several cycles (ee > 80 %). Thus, we can envision that the fluoros chemistry could lead to the design and synthesis of novel catalysts with high selectivity by simply attaching fluoros ponytails.

CONCLUSION

The fluoros biphasic system has appealing general features, such as the ease of separations of reagents or catalysts from reactants and products, the employment of nontoxic perfluorocarbons, and the ability to recycle the catalysts. However, the cost of the ligands is a serious limitation to possible industrial applications of FBC technology. Furthermore, the solvent effects of fluoros media on

reactions, for example, enantioselectivity, are still unknown. Fluorous biphasic chemistry is still in its infancy, and there is room for more investigations and improvements in this new field.

REFERENCES

- 1) Barthel-Rosa, L. P.; Gladysz, J. A. *Coord. Chem. Rev.* **1999**, 190-192, 587.
- 2) Horváth, I. T.; Rábai, J. S. *Science* **1994**, 266, 72.
- 3) Horváth, I. T. *Acc. Chem. Res.* **1998**, 31, 641.
- 4) Curran, D. P. *Angew. Chem. Int. Ed. Engl.* **1998**, 37, 1174.
- 5) de Wolf, E.; van Koten, G.; Deelman, B. J. *Chem. Soc. Rev.* **1999**, 28, 37.
- 6) Fish, R. H. *Chem. Eur. J.* **1999**, 5, 1677.
- 7) Cavazzini, M.; Montanari, F.; Pozzi, G.; Quici, S. J. *J. Fluorine Chem.* **1999**, 94, 183.
- 8) Cornils, B. *Angew. Chem. Int. Ed. Engl.* **1997**, 36, 2057.
- 9) Curran, D. P.; Hadida, S.; Kim, S. Y.; Luo, Z. *J. Am. Chem. Soc.* **1999**, 121, 6607.
- 10) Studer, A.; Hadida, S.; Ferritto, R.; Kim, S. Y.; Jeger, P.; Wipf, P.; Curran, D. P. *Science* **1997**, 275, 823.
- 11) Curran, D. P.; Hadida, S.; Kim, S. Y. *Tetrahedron* **1999**, 55, 8997.
- 12) Linclau, B.; Singn, A. K.; Curran, D. P. *J. Org. Chem.* **1999**, 64, 2845.
- 13) Baker, R. T.; Tumas, W. *Science* **1999**, 284, 5419.
- 14) Alvey, L. J.; Rutherford, D.; Juliette, J. J. J.; Gladysz, J. A. *J. Org. Chem.* **1998**, 63, 6302.
- 15) Harr, C. M.; Huang, J.; Nolan, S. P. *Organometallics* **1998**, 17, 5018.
- 16) Mathivet, T.; Monflier, E.; Castanet, Y.; Mortreux, A.; Couturier, J. L. *Tetrahedron Lett.* **1999**, 40, 3885.
- 17) Bhattacharyya, P.; Croxtall, B.; Fawcett, J.; Fewcett, J.; Gudmunsen, D.; Hope, E. G. *J. Fluorine Chem.* **2000**, 101, 247.
- 18) Pozzi, G.; Montanari, F.; Quici, S. *Chem. Commun.* **1997**, 69.
- 19) Hughes, R. P.; Trujillo, H. A. *Organometallics* **1996**, 15, 286.
- 20) Vincent, J. M.; Rabion, A.; Yachandra, V. K.; Fish, R. H. *Angew. Chem. Int. Ed. Engl.* **1997**, 36, 2346.
- 21) Rutherford, D.; Juliette, J. J. J.; Rocaboy, C.; Horváth, I. T.; Gladysz, J. A. *Catal. Today.* **1998**, 42, 381.
- 22) Juliette, J. J. J.; Rutherford, D.; Horváth, I. T.; Gladysz, J. A. *J. Am. Chem. Soc.* **1999**, 121, 2696.
- 23) Dinh, L. V.; Gladysz, J. A. *Tetrahedron Lett.* **1999**, 40, 8995.
- 24) Horváth, I. T.; Kiss, G.; Cook, R. A.; Bond, J. E.; Stevens, P. A.; Rábai, J.; Mozoleski, E. *J. Am. Chem. Soc.* **1998**, 120, 3133.
- 25) Herrmann, W. A.; Kohlpaintner, W. *Angew. Chem. Int. Ed. Engl.* **1993**, 32, 1524.
- 26) Gladysz, J. A. *Science* **1994**, 266, 55.
- 27) Pozzi, G.; Cavazzini, M.; Cinato, F.; Montanari, F.; Quici, S. *Eur. J. Org. Chem.* **1999**, 1947.
- 28) Kleijn, H.; Rijnberg, E.; Jastrzebski, J. T.; van Koten, G. *Org. Lett.* **1999**, 1, 853.
- 29) Nakamura, Y.; Takeuchi, S.; Ohgo, Y.; Curran, D. P. *Tetrahedron Lett.* **2000**, 41, 57.

WALKING THE TIGHT ROPE: CATALYST DESIGN IN ARYL-ARYL C-C, C-N, AND C-O COUPLING REACTIONS OF ARYL CHLORIDES AND ARYL SULFONATES

Reported by Kevin M. McCauley

February 24, 2000

INTRODUCTION

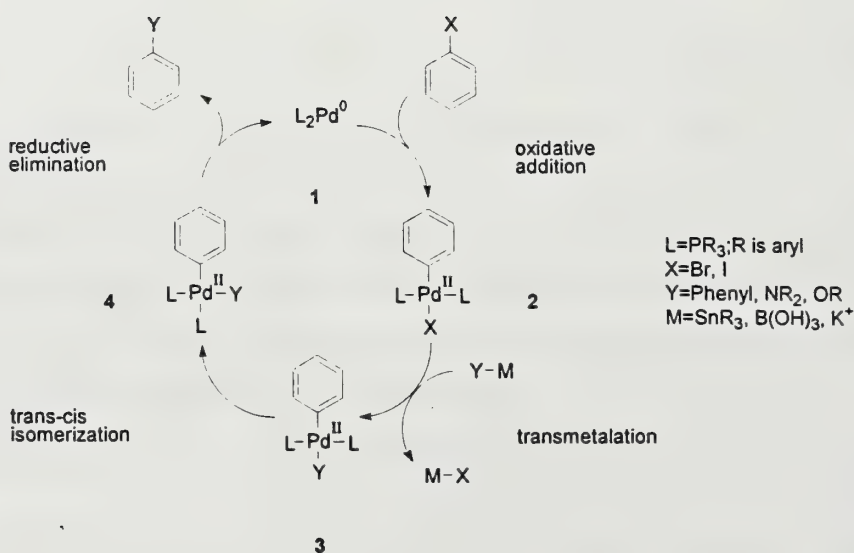
Transition metal catalysis of organic chemical reactions has been extensively investigated. Transformations of particular interest are aryl-aryl coupling reactions, aminations, and etherifications. Some of the most recognizable of these methods are the Stille and Suzuki¹ reactions for carbon-carbon bond formation as well as the more recent coupling reactions involving aminations² and etherifications.³ Aryl iodides and bromides are the substrates most commonly used for these catalytic reactions, while unreactive aryl chlorides and sulfonates are rarely employed.

Recent interest in expanding these reactions to aryl chlorides and aryl sulfonates can be attributed primarily to availability and price.⁴ There is a greater selection of aryl chlorides relative to aryl iodides and bromides, and the aryl chlorides are usually less expensive. The use of aryl sulfonates, which are easily obtained from phenols, would also broaden the scope of these methods. Thus, the design and evaluation of novel catalysts to utilize these unreactive substrates in transition metal catalyzed arylations has become a major focus in chemical research, and will be the subject of this review.

CATALYTIC CYCLE

A general catalytic cycle for aryl-aryl coupling reactions is shown in Scheme 1.¹ The oxidative addition of the palladium(0) catalyst **1** to the carbon halogen bond followed by isomerization gives the trans palladium complex **2**. The halide is displaced by the nucleophile **Y-M** via transmetalation to give **3**. Trans complex **3** isomerizes to the cis isomer **4** which undergoes reductive elimination to regenerate the catalyst **1** and release the product. Aryl aminations and etherifications follow a similar mechanism in which an alkoxy or amine nucleophile displaces the halide, **X**.³ Although oxidative addition of palladium to aryl iodides and aryl bromides occurs readily, reactions of aryl sulfonates are often sluggish, and oxidative addition to aryl chlorides is so slow that effective catalytic turnovers cannot be achieved using the usual aryl phosphine ligands.⁴

Scheme 1



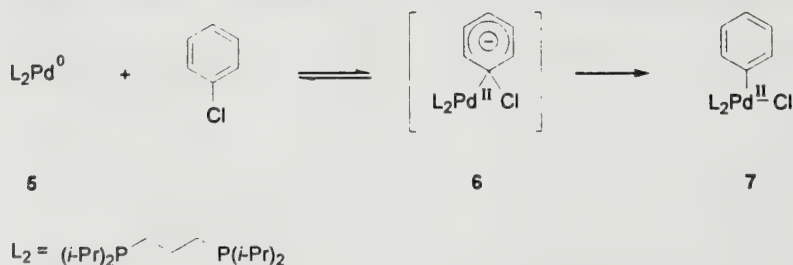
CATALYST DESIGN

Two strategies toward designing new catalysts to accelerate oxidative additions have been devised. One strategy is to use nickel instead of palladium as the transition metal. The second strategy is to tailor the electronic environment around the catalyst by modifying the phosphine ligands. The objective of both strategies is to lower the activation energy for oxidative addition by facilitating electron donation to the aryl chloride or sulfonate.

Oxidative Addition

Until recently, oxidative addition of palladium to aryl chlorides was not well understood owing to its slow rate. However, a number of studies have been reported on the mechanism of the reaction of aryl chlorides with palladium using strong σ donor, chelating phosphine ligands. Although there has been much debate on the mechanism of oxidative addition of aryl iodides and bromides,^{5,6} Portnoy and Milstein^{7,8} have shown that the palladium(0) complex **5** undergoes oxidative addition by a two-electron

Scheme 2

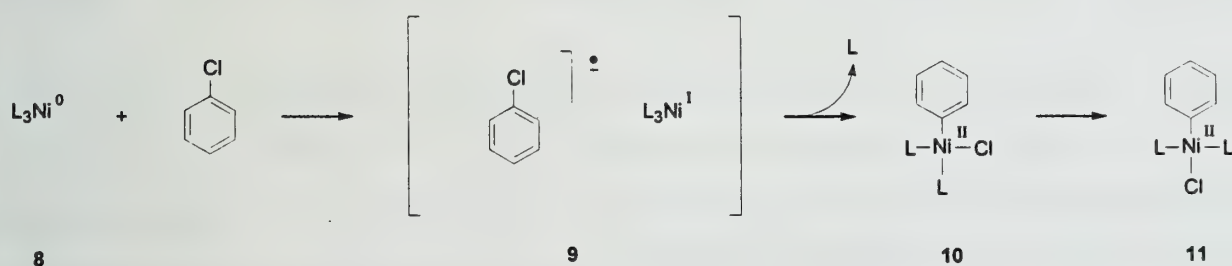


donation (Scheme 2) to form a tetrahedral chloroarene **6**. It should be noted that it is presently unclear whether **6** is a transition state or a short-lived intermediate. Correlations of Hammett σ values and σ^- values have large positive ρ values of +9.2 and +5.2;

respectively, suggesting a negative charge in the transition state. Hammett σ^- values gave stronger correlations indicating the formation of a palladium-carbon bond and delocalization of electrons into the π system of the aromatic ring. The proposed mechanism is similar to a nucleophilic aromatic substitution reaction in which carbon-halide bond cleavage is the rate-determining step. No products resulting from aryl radicals or a palladium(I) species were observed during oxidative addition, which is evidence against a one-electron transfer mechanism. Portnoy and Milstein also proposed that **6** could be stabilized by electron donation from chloride to the electron deficient palladium. The mechanism of oxidative addition of palladium to aryl triflates⁹ is similar to that shown in Scheme 2. However, the intermediate is not stabilized by σ donation because triflates do not strongly coordinate with palladium, and, instead, form ionic complexes.

The mechanism of oxidative addition of nickel(0) is shown in Scheme 3. The first step is a one-electron transfer from the Ni(0) complex **8** to the π^* orbital of chlorobenzene to give the radical anion/Ni(I) tight ion pair **9**. Following cage collapse, Ni(I) inserts into the carbon chloride bond to give

Scheme 3



the cis-Ni(II) complex **10** which isomerizes to the trans isomer **11**. It is unknown whether ligand dissociation occurs before or after cage collapse. This mechanism has been well established by Tsou and Kochi¹⁰ using chemical and electrochemical experiments on aryl halides. Good correlations of substituent effects on the reaction rates of nickel(0) complexes and solvent effects on Ni(II)/Ni(I) product distributions with aryl halides pointed to a common intermediate. Ni(I) halide salts, formed from dissociation of the carbon halide bond, were observed with bromides or iodides indicating a Ni(I) intermediate. However, the absence of nickel(I) chloride salts and products derived from aryl radicals suggests that carbon-halide bond dissociation does not occur with aryl chlorides. Thus, when the halogen is chloride, the tight ion pair gives only nickel(II) products.

Substituting nickel for palladium in the catalyst results in a more reactive catalyst toward less reactive substrates. Typically, nickel(0) complexes have lower oxidation potentials than analogous

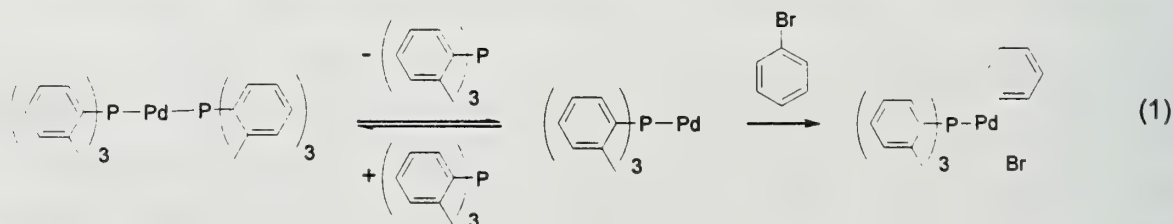
palladium complexes.⁶ The lower oxidation potential of nickel accelerates electron transfer from the metal to the aryl chloride or sulfonate.

Phosphine Ligand Design

Typical protocols for carbon coupling reactions use aryl phosphine ligands, such as $(\text{Ph})_3\text{P}$, to coordinate to the palladium catalyst. However, aryl phosphines are usually not sufficiently electron rich to facilitate oxidative addition of palladium and nickel to aryl chlorides and aryl sulfonates. Only substrates that can be readily reduced, such as aryl iodides and aryl bromides, can be used with aryl phosphine ligands.

The reluctance of aryl chlorides and aryl sulfonates to participate in oxidative addition with the catalyst can be attributed to the electron density surrounding the metal. Replacing the aryl phosphine ligands with alkyl phosphine ligands results in tighter coordination to the metal and lowers the oxidation potential.¹¹ For example, the oxidation potential of $\text{Ni}(\text{PPh}_3)_4$ is -0.45 V while the oxidation potential of $\text{Ni}(\text{PET}_3)_4$ is -0.81 V in THF vs SCE.¹⁰ Initial reports¹² showed that by simply replacing $(\text{Ph})_3\text{P}$ with $(t\text{-Bu})_3\text{P}$, unhindered aryl chlorides could be efficiently coupled with boronic acids using a palladium catalyst.

Another design strategy is to incorporate ortho substituents on the phenyl ring of the phosphine ligand. The steric hindrance results in the coordination of only one phosphine ligand during the oxidative addition step and the rest of the catalytic cycle. Using $(o\text{-tolyl})_3\text{P}$, Hartwig and co-workers¹³ have shown that oxidative addition (eq. 1) is inverse first order in phosphine ligand indicating that the

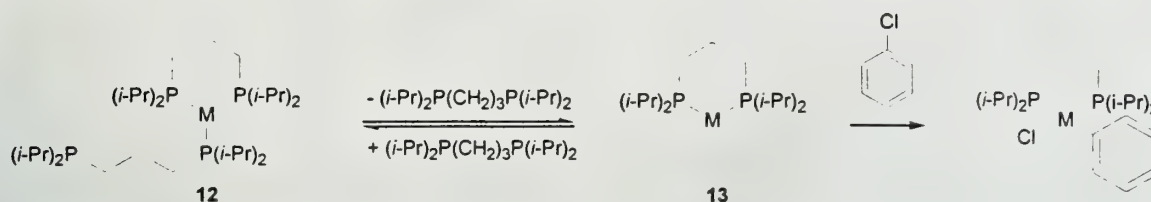


reactive species is a monophosphine catalyst. The coordination of only one ligand is expected to facilitate transmetalation because the tricoordinate complex provides a vacant coordination site for the incoming nucleophile and to accelerate reductive elimination because the slow trans-cis isomerization does not occur.

From mechanistic studies^{7,8} on the addition of palladium to aryl chlorides, Portnoy and Milstein found that chelating alkyl phosphine ligands are more effective than nonchelating alkyl phosphine ligands. After oxidative addition, catalysts bearing monodentate ligands isomerize to the more stable trans complex. After transmetalation, the trans complex slowly reisomerizes to the cis complex to

undergo reductive elimination. However, chelating complexes (Scheme 4) must maintain the cis stereochemistry throughout the cycle, leading to a faster catalytic cycle because the slow isomerization step is avoided. To be effective catalysts, chelate ligands must be able to coordinate and dissociate from the metal complex **12**. Portnoy and Milstein have reported⁸ that ligands based on a trimethylene backbone are usually the most effective because the P-M-P bond angle (bite angle) allows for a facile dissociation of one of the ligands to form the reactive complex **13**. Ligands with smaller bite angles

Scheme 4



form stable, unreactive four coordinate species. Ligands with larger bite angles react at the same rate as complex **13**, but form trans complexes which undergo slow reductive elimination.

Applying the above concepts to catalyst design requires a delicate balance between both steric and electronic properties of the ligands and consideration of the mechanisms by which the metals undergo oxidative addition. In most cases, the design of catalysts that are reactive toward aryl chlorides and sulfonates employs more than one strategy.

APPLICATIONS

The ideas discussed in the preceding paragraphs have been applied to catalyst design for aryl carbon-coupling by Suzuki reactions.^{12,14-19} Aryl chlorides have been linked with various boronic acids using both chelating and nonchelating ligands with nickel and palladium metals. Many improvements in both arene amination^{3,20,21} and etherification^{22,23} have been reported applying the same principles in catalyst design. In some cases, the same ligands employed in aryl-aryl coupling were effective in amination and etherification chemistry.²⁰ The following paragraphs highlight some of the successes, especially with electron-rich aryl chlorides, in catalyst design concerning coupling reactions.

Nickel Catalysts

Both electron-deficient and electron-rich aryl chlorides have been coupled with aryl boronic acids using 1,1'-bis(diphenylphosphino)ferrocene (dppf) as a chelating ligand with yields typically above 80 percent (Table 1).¹⁷ Aryl mesylates have also been linked using nickel and dppf, but in only moderate yields.¹⁸ Dppf and nickel were also effective in catalyzing aminations of aryl chlorides (Table 2).²⁵ Although moderate to high yields were obtained, a disadvantage associated with dppf and nickel is

Table 1. $\text{NiCl}_2(\text{dppf})$ Catalyzed Suzuki Reactions of Aryl Chlorides^a and Aryl Sulfonates^b.

		$\xrightarrow[\text{K}_3\text{PO}_4]{\text{NiCl}_2(\text{dppf})}$	
X	LG	Y	Yield/%
<i>p</i> -CHO	Cl	H	89
<i>p</i> -CO ₂ CH ₃	Cl		87
<i>p</i> -CO ₂ CH ₃	OTf		80
<i>p</i> -CO ₂ CH ₃	OMs		48
<i>p</i> -OCH ₃	Cl		82
<i>p</i> -OCH ₃	OMs		51
<i>p</i> -NH ₂	Cl		90
<i>m</i> -OCH ₃	Cl	<i>p</i> -OCH ₃	91
<i>m</i> -CH ₃	Cl	<i>m</i> -CH ₃	91

^a 1 equiv chloroarene, 1.1 equiv boronic acid, 3 equiv K_3PO_4 nH_2O , 3 mol % $\text{NiCl}_2(\text{dppf})$, 1equiv/Ni dppf, and 4 equiv BuLi in dioxane at 80 °C. ^b 1 equiv chloroarene, 1 equiv boronic acid, 3 equiv K_3PO_4 , 10 mol % $\text{NiCl}_2(\text{dppf})$, and 1.7 equiv Zn in THF at 67 °C.

Table 2. $\text{Ni}(\text{COD})_2/\text{dppf}$ Catalyzed Amination Reactions of Aryl Chlorides.

	NHR_1R_2	$\xrightarrow[\text{NaOt-Bu}]{\text{Ni}(\text{COD})_2(\text{dppf})^a}$	
X	R ₁	R ₂	Yield/%
<i>p</i> -CH ₃	Ph	CH ₃	80
	<i>p</i> -tolyl	H	91
	pyrrolidine		58
<i>p</i> -OCH ₃	<i>o</i> -tolyl	H	88
	Ph	CH ₃	55
<i>m</i> ; <i>p</i> -CH ₃	anisole	H	96
	pyrrolidine		56
	<i>n</i> -hexyl		50

^a 1 equiv aryl chloride, 1.2 equiv amine, 1.4 equiv NaOtBu , 2-5 mol % $\text{Ni}(\text{COD})_2$, and 4-10 mol % dppf in toluene at 100°C.

the requirement for rigorous inert atmosphere conditions. Substrates with nitro groups are not coupled because nitro groups are reduced rapidly to the nitroso group by nickel. Meta-substituted or multiply substituted aryl chlorides or boronic acids were not effectively coupled, and sterically hindered amines gave lower yields.

Palladium Catalysts

Symyx Technologies has recently introduced the bidentate ligand **14** that has shown high reactivity toward aryl chlorides in Suzuki reactions (Table 3).¹⁵ In the presence of palladium, this ligand forms a catalyst which effectively couples a range of substrates, including ortho-substituted aryl chlorides and boronic acids. It also exhibits high reactivity toward electron-rich aryl chlorides. Although the exact structure of the catalyst during the catalytic cycle is unknown, it is speculated that the coordination between oxygen and palladium is weak. Therefore, the electron-rich chelate ligand not only facilitates oxidative addition, but also allows for dissociation of the oxygen leading to a tricoordinate complex, which would favor transmetalation and reductive elimination.

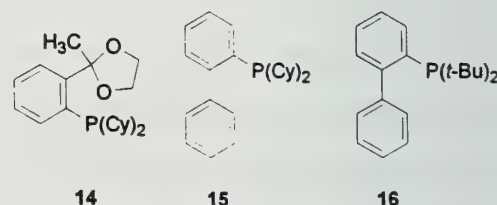
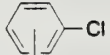
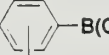
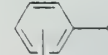


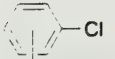
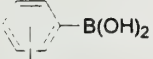
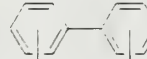
Table 3. Pd-Catalyzed Suzuki Reactions of Aryl Chlorides with Boronic Acids.

		$\xrightarrow[\text{14}]{\text{Pd}(\text{dba})_2^a}$	
X	Y		Yield/%
<i>p</i> -CF ₃			92
<i>p</i> -OPh			94
<i>m</i> -CH ₃ ; <i>m</i> -CH ₃			94
<i>o</i> -CH ₃			95
<i>m</i> -OCH ₃	<i>p</i> -CF ₃		93
<i>o</i> -CH ₃	<i>o</i> -CH ₃		91

^a 1.0 equiv aryl chloride, 1.5 equiv boronic acid, 3.0 equiv CsF , 0.5-1.0 mol % $\text{Pd}(\text{dba})_2$, 1.5 - 3 mol % ligand **14** in toluene or 1,4-dioxane at 100-110 °C. Yields are based on GC.

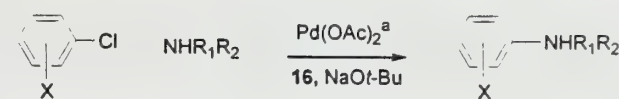
Buchwald and coworkers recently reported¹⁶ two new ligands, **15** and **16** which form highly active palladium catalysts for Suzuki cross coupling reactions (Table 4). In addition, palladium catalysis based on ligand **16** shows promise for both aryl and alkyl amination reactions (Table 5).²⁰ Ligand **16** has

Table 4. Pd-Catalyzed Suzuki Reactions of Aryl Chlorides with Boronic Acids.

		$\xrightarrow[\text{KF, 25 } ^\circ\text{C}]{\text{Pd(OAc)}_2^a}$	
X	Y	Ligand	Yield/%
<i>p</i> -CH ₃		15	95
<i>p</i> -NO ₂			98
<i>o</i> -OCH ₃			96
<i>p</i> -CH ₃	<i>o</i> -OCH ₃		95
<i>p</i> -CO ₂ CH ₃	<i>m</i> -COCH ₃	16	91
<i>o</i> -CH ₃ , <i>m</i> -CH ₃	<i>o</i> -CH ₃		96
<i>m</i> -CH ₃ , <i>m</i> -CH ₃			85

^a 1.0 equiv aryl chloride, 1.5 equiv boronic acid, 3 equiv KF, 1 mol % Pd(OAc)₂, 2 ligand/Pd in THF (1 mL/mmol aryl chloride).

Table 5. Pd-Catalyzed Amination Reactions of Aryl Chlorides.

			
X	R ₁	R ₂	Yield/%
<i>p</i> -CH ₃	Ph	CH ₃	98
	Bu	Bu	81
<i>m</i> -CH ₃ , <i>p</i> -CH ₃	Bn	H	99
<i>o</i> -OCH ₃			99
<i>m</i> -OCH ₃ , <i>m</i> -OCH ₃	Ph	H	97

^a 1.0 equiv aryl chloride, 1.2 equiv amine, 1.4 equiv NaOt-Bu, 1-2 mol % Pd(OAc)₂, 2-4 mol % **16** in toluene (1 mL/mmol aryl chloride).

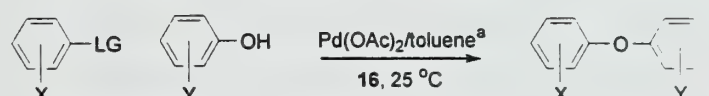
also been reported to be active in aryl etherifications²¹ of electron-poor aryl chlorides and aryl triflates (Table 6). However, application of a broad range of electron-rich aryl chlorides still remains a challenge in aryl etherifications.

Unlike previous catalysts, these ligands not only allow for the coupling of a broad range of substrates, including sterically hindered substrates, but they can also be used at room temperature. Product yields from aryl chlorides are similar to those from aryl bromides and aryl iodides. The alkyl groups bonded to phosphorous ensure that palladium has the appropriate electron density to undergo oxidative addition. The ortho substitution of the biphenyl is necessary to maintain the tricoordinate complex, which enhances the rate of both transmetalation and reductive elimination.

CONCLUSION

Use of unreactive aryl chlorides and sulfonates for aryl carbon coupling reactions has been achieved by modification of the catalysts. Aryl chlorides can now be applied to Suzuki coupling, aminations, and etherifications, expanding the scope of these reactions to a wider variety of starting materials at lower costs. Although initial studies have been completed on the application of aryl

Table 6. Pd Catalyzed Oxygen Coupling Reactions of Aryl Chlorides and Aryl Triflates.

			
X	LG	Y	Yield/%
CN	Cl	H	91
<i>p</i> -COCH ₃	OTf	<i>o</i> -CH ₃	84
<i>p</i> - <i>t</i> -Bu	OTf	<i>o</i> - <i>i</i> -Pr	84

^a 1.0 equiv aryl chloride/triflate, 1.2 equiv phenol, 1.4 equiv NaH or 2.0 equiv K₃PO₄, 2 mol % Pd(OAc)₂, and 3 mol % **16** in toluene at 100 °C.

sulfonates to Suzuki and phenol coupling reactions, further work is needed with these substrates. Walking the tight rope between electronic and steric properties of the phosphine ligand and catalytic metal has brought about these advances in aryl coupling reactions.

REFERENCES

- (1) Miyaura, N.; Suzuki, A. *Chem. Rev.* **1995**, *95*, 2457-2483.
- (2) Curtis, M. D. Organic Seminar Abstracts 1996-97, Semester I; University of Illinois: Urbana, IL, October 7, 1996; p. 33.
- (3) Hartwig, J. F. *Angew. Chem. Int. Ed. Engl.* **1998**, *37*, 2046-2067.
- (4) Grushin, V. V.; Alper, H. *Chem. Rev.* **1994**, *94*, 1047-1062.
- (5) Fauvarque, J., Pflüger, F. *J. Organomet. Chem* **1981**, *208*, 419-427.
- (6) Amatore, C., Pflüger, F. *Organometallics* **1990**, *9*, 2276-2282.
- (7) Portnoy, M.; Milstein, D. *Organometallics* **1993**, *12*, 1665-1673.
- (8) Portnoy, M.; Milstein, D. *Organometallics* **1993**, *12*, 1655-1664.
- (9) Jutand, A.; Mosleh, A. *Organometallics* **1995**, *14*, 1810-1817.
- (10) Tsou, T. T.; Kochi, J. K. *J. Am. Chem. Soc.* **1979**, *101*, 6319-6332.
- (11) Spessard, G. O.; Meissler, G. L. *Organometallic Chemistry*; Prentice Hall: Upper Saddle River, New Jersey, 1996, 171-175.
- (12) Littke, A.; Fu, G. C. *Angew. Chem. Int. Ed. Engl.* **1998**, *37*, 3387-3388.
- (13) Hartwig, J. F.; Paul, F. J. *J. Am. Chem. Soc.* **1995**, *117*, 5373-5374.
- (14) Wolfe, J. P.; Singer, R. A.; Yang, B. H.; Buchwald, S. L. *J. Am. Chem. Soc.* **1999**, *121*, 9550-9561.
- (15) Bei, X.; Turner, H. W.; Weinberg, W. H.; Guram, A. S.; Petersen, J. L. *J. Org. Chem.* **1999**, *64*, 6797-6803.
- (16) Suzuki, A. *J. Organomet. Chem.* **1999**, *576*, 147-168.
- (17) Saito, S.; Oh-tani, S.; Miyaura, N. *J. Org. Chem.* **1997**, *62*, 8024-8030.
- (18) Percec, V.; Bae, J.; Dale, H. *J. Org. Chem.* **1995**, *60*, 1060-1065.
- (19) Ueda, M.; Saitoh, A.; Oh-tani, S.; Miyaura, N. *Tetrahedron* **1998**, *54*, 13079-13086.
- (20) Wolfe, J. P.; Buchwald, S. L. *Angew. Chem. Int. Ed. Engl.* **1999**, *38*, 2413-2416.
- (21) Hartwig, J. F.; Kawatsura, M.; Hauck, S. I.; Shaughnessy, K. H.; Alcazar-Roman, L. M. *J. Org. Chem.* **1999**, *64*, 5575-5580.
- (22) Aranyos, A.; Old, D. W.; Kiyomori, A.; Wolfe, J. P.; Sadighi, J. P.; Buchwald, S. L. *J. Am. Chem. Soc.* **1999**, *121*, 4369-4378.
- (23) Mann, G.; Hartwig, J. F. *J. Org. Chem.* **1997**, *62*, 5413-5418.
- (24) Wolfe, J. P.; Buchwald, S. L. *J. Am. Chem. Soc.* **1997**, *119*, 6054-6058.

INTRODUCTION

In the past few years an increasing emphasis has been placed on using combinatorial methods in biology and chemistry to generate and evaluate large peptide libraries for possible biological activities. Peptide libraries have often been used for mapping complex macromolecular interactions. Selected peptide leads are of particular interest because of their ability to target functionally or biologically relevant sites of a particular protein, such as allosteric or active sites of an enzyme, or ligand-binding domains of receptors.¹ These small peptides can act as mimics of protein-protein interaction surfaces. The structural analysis of protein-peptide complexes may provide insight into the critical molecular interactions required for binding. Peptide leads can be used in developing small non-peptide molecules leading to the development of orally active drugs by chemists.

One of the most widely used combinatorial peptide generation techniques has been filamentous bacteriophage display,² first developed by George Smith in 1985.³ Phage display is the expression of small peptides linked to the *N*-terminal domains of certain proteins on the exterior surface of a bacteriophage particle. Phage display allows for easy assembly and simultaneous expression of 10^8 - 10^{10} different peptides in an inexpensive and rapid manner. The hybrid "fusion" peptides expressed as segments of the bacteriophage capsid proteins usually exhibit the same functional characteristics as their synthetic peptide counterparts. Accessibility of the expressed fusion peptides on the surface of the virus allows for affinity selection of biologically active peptides from a vast peptide library. Finally, the engineered peptide is determined by the DNA sequence encoding its expression. This allows for rapid identification, amplification and facile mutation of selected high affinity peptide leads.

This review will focus on use of peptide libraries for ligand discovery and generation of peptide leads as models for development of non-peptide targets by chemists.

PHAGE DISPLAY OVERVIEW

Filamentous Bacteriophage

Filamentous bacteriophages are viruses containing single-stranded (ss), circular DNA. They infect male (F') strains of *E. coli* by attaching to a threadlike appendage on the bacterium, called the F-

pilus. These phages are flexible, rod-shaped viruses, about 65 Å in diameter and 1 µm in length whose exterior coating or capsid, is composed of five proteins.² The sides of the rod-shaped virus contain approximately 2700 copies of the mostly α-helical, 50-residue major capsid gene VIII protein (gVIIIp). The minor coat protein gIIIp, is present in only 3-5 copies at one end of the virion.⁴ The N-terminal domain of the gIIIp initiates entry of viral DNA into the host through its attachment to the F-pilus of *E. coli*.⁵ Phage proteins are transcribed and translated by the *E. coli* machinery to produce multiple copies of the infecting phage. Several hundred copies of the virion are secreted from each *E. coli*. per division cycle without killing the host (Figure 1).

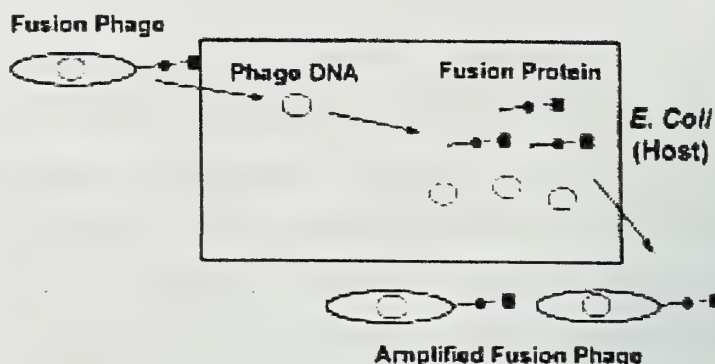


Figure 1. Bacteriophage infection of *E. Coli*.

Expression Of Foreign Peptides On The Surface Of Bacteriophages

Phage peptide libraries are most commonly generated by the fusion of the foreign peptides to the solvent-accessible N-terminal domains of gIIIp and gVIIIp (Figure 2).⁵ Synthetic oligonucleotides coding for the sequence of the desired foreign peptides are inserted within the gene III or VIII of the phage DNA through the use of unique restriction enzymes.⁶ DNA from modified phage is introduced into *E. coli* cells by electroporation transformation. Engineered foreign peptides are expressed as the new solvent exposed N-terminal domains of these phage proteins. Insertion of a foreign peptide sequence into genes III or VIII will

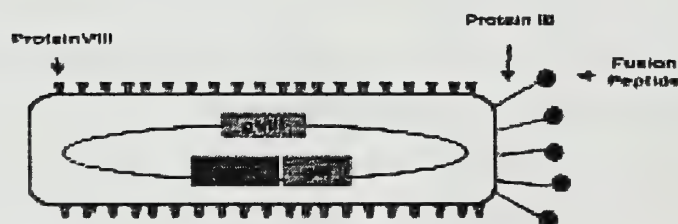


Figure 2. Expression of fusion peptides on phage

result in the expression of the fusion peptide on essentially every copy of the capsid proteins creating a polyvalent expression system.

Valency is the copy number of each peptide on a phage particle, which is an important factor in determining the selection of high vs. low affinity peptides. Screening peptide libraries against targets with multiple binding regions, such as antibodies, can be perturbed by the higher apparent affinity (avidity) if the peptides in the library are presented in a multivalent fashion.

Filamentous phage display has the benefit of allowing the researcher to utilize either multivalent or low valent expression systems, depending on the goals of the experiment. Multivalent expression systems have the advantage of isolating weak binding peptides ($K_a = 10^4$ - 10^6 M⁻¹) owing to increased avidity. However, these multivalent systems prevent identification of high binding affinity peptides ($K_a > 10^7$ M⁻¹) from weakly binding phage clones.⁶ Commercially available low valency expression systems contain two separate genes for gIIIp and gVIIIp respectively. Placing a foreign oligonucleotide in only one of either III or VIII genes generate phages which contain both wild type (wt) and fusion protein versions of that capsid protein.⁴

Construction Of Random And Biased Peptide Libraries

A random phage peptide library is designed using randomly synthesized oligonucleotide inserts. Additionally, a biased peptide library is prepared by designing synthetic inserts corresponding to consensus sequences suggested by earlier peptide leads. A random library is often used as a first step in identifying a consensus sequence. The oligonucleotide insert is a mixture of sequences which includes randomized positions primed with equimolar concentrations of the four nucleotides added to the growing chain. Because the synthetic oligonucleotides are inserted upstream of gIIIp or gVIIIp, the presence of any stop codons in this region would inhibit the expression of a functional capsid protein and produce non-infective progeny. The third position of each random codon (representing one amino acid) is limited to an equal mixture of dG and dT or dG and dC to minimize the appearance of stop codons (Figure 3).⁶ The possible 32 codons generated represent all 20 amino acids and only one stop codon (TAG), which can be suppressed by transforming the ligated phage DNA into certain *E. coli* strains.

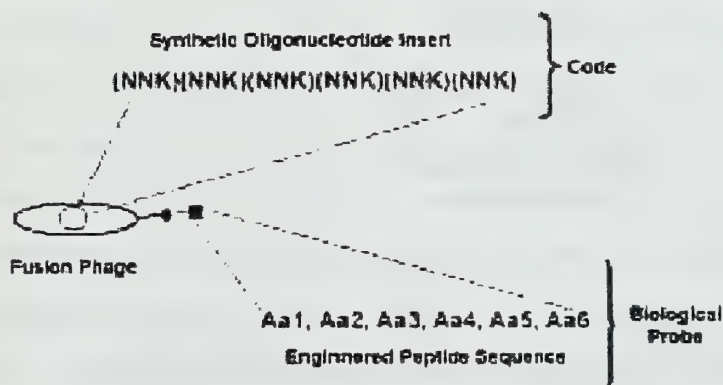


Figure 3. Design of random synthetic oligonucleotides. A single random codon is represented by (NNK), where N = dG, dT, dC or dA, and K = dG/dT or dG/dC

The third position of each random codon (representing one amino acid) is limited to an equal mixture of dG and dT or dG and dC to minimize the appearance of stop codons (Figure 3).⁶ The possible 32 codons generated represent all 20 amino acids and only one stop codon (TAG), which can be suppressed by transforming the ligated phage DNA into certain *E. coli* strains.

A typical randomly generated peptide library contains about a billion phage clones, and is capable of representing most of the 64 million (20^6) unique hexamers possible. However, peptides larger than six amino acids may not be fully represented using filamentous display.⁶ Other constraints on the complete random representation of a phage library include codon degeneracy (each amino acid is not represented by a single codon), codon usage bias, proteolytic stability of generated peptides, and

assembly bias within the inner-membrane of the host cell.⁴ Biased libraries can be constructed upon the isolation of a consensus sequence from early peptide leads to counterbalance these shortcomings.

***In Vitro* Affinity Selection**

There are various methods for the affinity selection of a fusion phage library. Generally a target protein or receptor is tethered on a solid support while a solution of phage particles is passed over the support. Target proteins can be immobilized using polystyrene dishes⁵, or beads in a microtiter plate well.⁷ After a brief incubation period, the heterogeneous mixture is washed to eliminate non-binding phage. Bound phage are recovered by non-specific, specific, or competitive elution protocols. One

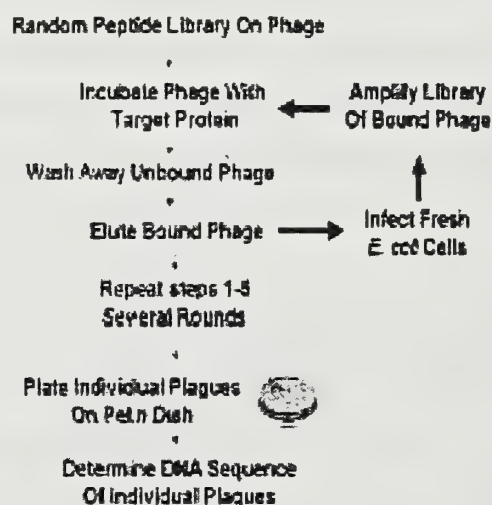


Figure 4. Flow chart for affinity selection of fusion phage particles.

round of purification using immobilized target protein usually results in 10^6 enrichment of specific over non-specific binding phage particles.⁵ After one round of affinity purification, the number of phage particles representing any bound clone is reduced to the point that binding clones may be lost if subjected to a second round of purification. The eluted phage, which are still infective, are introduced to a new batch of *E. coli* cells for amplification to increase the representative populations of each binding clone (Figure 4). After

several rounds of affinity purification and

amplifications, the eluted fusion phage are plated on *E. coli* coated agar plates. Individual plaques corresponding to a unique phage construct are selected, amplified, and identified using standard 2',3'-dideoxyribonucleic acid sequencing protocols.⁷ Comparison of amino acid residues of peptides with affinity for a target protein, can lead to a consensus binding sequence. A consensus binding sequence not only gives information about the target protein, but also can be used to develop pharmaceutical compounds to regulate this protein.

APPLICATIONS

The Streptavidin Model For Ligand Discovery

The streptavidin receptor complexed with its small organic ligand, biotin, has been extensively studied as a model for ligand discovery through phage display. Streptavidin is a tetrameric protein, which binds biotin with high affinity ($K_d = 10^{-15}$ M).⁸ Early experiments with phage display found that fusion peptides containing His-Pro-Gln bound streptavidin and were inhibited from binding in the

presence of biotin.⁹ Streptavidin was chosen as a model to conduct structure-based comparisons between a small organic molecule (biotin), and peptide ligands bound to a common functional motif of a target protein. Crystal structures of streptavidin with a linear peptide, FSHPQNT ($K_d = 125 \mu\text{M}$), and two constricted peptides, cyclo-Ac-[CHPQGPPC]-NH₂ ($K_d = 670 \text{ nM}$) and cyclo-Ac-[CHPQFC]NH₂ ($K_d = 270 \text{ nM}$), were solved and compared to biotin-streptavidin complex.^{8,9} The greater affinity of cyclic over non-cyclic peptides was attributed to a decrease in conformational entropy of the cyclic peptides.⁸ Although peptides with affinity for streptavidin comparable to biotin were not isolated, this model system illustrated that phage-discovered peptides were able to mimic a small organic ligand (biotin). These studies demonstrated that it should also be possible to synthesize small non-peptidic molecules to mimic an initial peptide lead discovered through phage display.

Hormone Ligand Minimization

Erythropoietin receptor (EPOR) belongs to the hematopoietic cytokine receptor superfamily. The hormonal ligand for this receptor, erythropoietin (EPO), is a 34 kD molecule composed of 165 amino acids ($\sim 18.5 \text{ kD}$) and an almost equivalent mass of carbohydrates.¹⁰ Erythropoietin increases the production of red blood cells. EPO is believed to trigger agonist activation by binding and orienting the cell-surface domains of two EPO receptors, initiating an intracellular phosphorylation cascade.¹¹ Whether or not simple dimerization of EPOR on the exterior of the cell initiates the proliferation of precursor cells into red blood cells has been a subject of much speculation.

The lack of an EPO-EPOR crystal structure prompted researchers from Affymax, R.W. Johnson, and The Scripps Research Institute into a collaboration to use phage display along with the EPO receptor

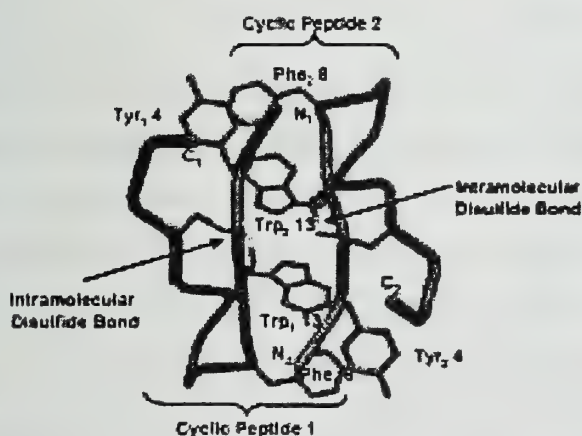


Figure 6. Illustration of the hydrophobic core of two EMP1 peptides from the (EPOR)₂ (EMP1)₂ crystal structure. Figure taken from reference 13

to gain insight into the signal transduction pathway of this complex.¹⁰ Through a combination of multivalent and low valency phage expression systems, along with various affinity selection methodologies, they discovered a series of 20-amino acid cyclic peptides with moderate affinity, $K_d = 200 \text{ nM}$, for EPOR. Surprisingly, these cyclic peptides dimerized the receptor complex and triggered intracellular cascades in an agonist

fashion.^{10,12} Because the peptides emulated the agonist properties of EPO, they were referred to as “erythropoietin-mimetic peptides” (EMPs). The symmetrical crystal structure of the complex revealed

that two peptides dimerized through a series of hydrophobic contacts between the two peptide chains (~2kD each), and that both peptides also came into contact with the surface of both monomers of the EPOR homodimer (Figure 5).¹³ It was predicted through the (EPOR)₂:(EMP)₂ crystal complex, that a covalently linked dimerized version of the EMP would show increased potency as an agonist of EPOR. A covalently-linked dimeric form of EMP1 (EMP1B), showed a pronounced enhancement of potency, with an EC₅₀ of 2 nM compared to 200 nM for the initial monomeric peptide lead EMP1.¹⁴ Although the modified peptide, EMP1B, and EPO had very similar affinities for EPOR, the natural ligand with a potency of 20 pM is still much more potent than any of the phage-derived peptide leads.

Two recent crystal structures of EPOR, one with a modified EPO, and another with a truncated version of EMP1 containing an unnatural 3,5-dibromotyrosine residue (EMP33), published shed some light upon this discrepancy in potency.^{11,15} Although the EMP33 peptide appears to be capable of dimerizing EPOR, it is unable to initiate secondary cascades, thereby acting as an antagonist. A comparison of the three different EPOR complexes with EPO¹¹, EMP1¹² and EMP33¹⁵, yields a noteworthy structure-activity spectrum of EPOR dimer conformations in high, low, and off states of activation with angles between the exterior receptor chains of 120°, 180° and 165°, respectively. Targeting of the EPO receptor with random phage derived peptide libraries illustrates the power of this technique not only in reducing the size of a large natural ligand with pharmaceutical implications, but also for obtaining biochemical insights into molecular interactions.

SH3 Binding Peptides And Structure-Based Design Of Non-Peptide Ligands

The Src homology 3 (SH3) domain is a 50-70 amino acid regulatory unit found in a variety of different proteins playing important roles in signal transduction.⁷ These regulatory domains are known to bind to ligands with short, proline-rich domains.¹⁶ Several groups have screened phage display libraries of peptides to investigate the core and periphery amino acid sequences recognized by various SH3 domains.^{7,16-18} Structural analysis of the peptides obtained has helped to elucidate three distinct binding domains of this receptor.¹⁹ Two classes of SH3 domain peptide ligands, types I and II, have been identified which contain proline rich residues with consensus sequences of RPLPPLXP and APPLPPR.¹⁶ These ligands bind to SH3 in one of two pseudosymmetrical orientations. Receptor-ligand structure studies revealed that these SH3 ligands adopt a polyproline type II helical conformation which places the proline core residues into two conserved binding pockets of the receptor. Flanking residues of the peptide bind in the specificity pocket of an SH3 receptor which mediate specific protein-protein recognition.¹⁹ With this knowledge of receptor-peptide structure in hand, split-pool synthesis was utilized to prepare non-peptide derivatives of an SH3-specific peptide ligand, VSLARRPLPPLP

(VSL12, $K_d = 0.45 \mu\text{M}$), discovered through phage display.^{16,19,20} The most promising non-peptide ligand (**1**) contains only three of the original 12 amino acids of VSL12, while retaining specificity for src-SH3 over Hck-SH3 with a $K_d = 1.6 \mu\text{M}$ (Figure 6).¹⁹ Although the synthesis of non-peptide SH3 ligands may still be in its infancy, knowledge gained through phage display is necessary for both biologists and chemists for the development of potent, orally active drugs.

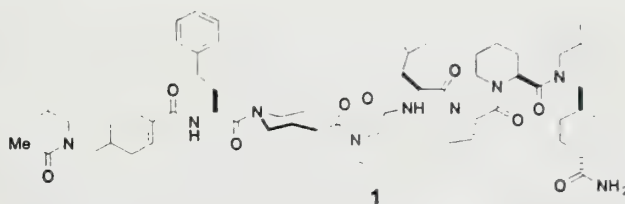


Figure 6. Structure of non-peptide SH3 ligand.

From Peptides To Orally Active Integrin Antagonists

Integrins are heterodimeric transmembrane glycoproteins that modulate cellular adhesion and signal transduction events.^{21,22} Phage peptide libraries have shown a ligand preference of peptides containing core Arg-Gly-Asp (RGD) motifs for a select group of integrins.²¹ Cyclic peptides with flanking Cys residues surrounding an RGD sequence were found to be 20-to 200-fold more potent than their linear counterparts, in inhibiting the attachment of $\alpha_v\beta_3$ or $\alpha_v\beta_5$ integrin-expressing cells to an extracellular matrix protein

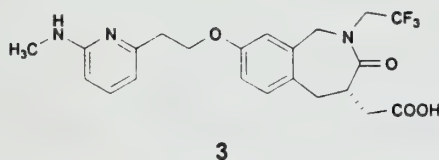
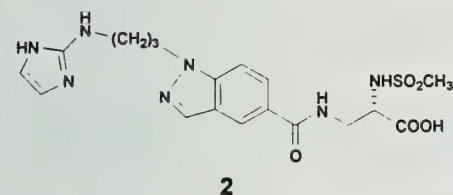


Figure 7. Structure of potent RGD peptidomimetics.

called vitronectin.¹⁸ Early this year, researchers from DuPont and Smith Kline Beecham, reported discoveries of disubstituted indazole (**2**) and a 2-benzazepine²² Gly-Asp mimetic (**3**) as potent, orally active, non-peptide mimics of RGD-containing peptides (Figure 7).^{23,24} Heterocycles **1** and **2** have IC_{50} values of 2.3 and 3.0 nM, respectively, and both show high selectivity for the $\alpha_v\beta_3$ integrin.

CONCLUSION

Filamentous bacteriophage display of peptide libraries has experienced growth as a molecular biology technique since its conception by Smith almost fifteen years ago. Although phage display is still in its infancy period, it is clearly a combinatorial method with applications pertinent to both biologists and chemists interested in ligand discovery and structure-based design of pharmaceutical agents.

REFERENCES

- 1) Kay, B. K.; Kurakin, A. V.; Hyde-DeRuyscher, R. *Drug Discovery Today* **1998**, *3*, 370-378.
- 2) Johnsson, K.; Ge, L. *Curr. Top. Microbiol. Immunol.* **1999**, *243*, 87-105.
- 3) Smith, G. P. *Science* **1985**, *228*, 1315-1316.
- 4) Rodi, D. J.; Makowski, L. *Curr. Opin. Biotechnol.* **1999**, *10*, 87-93.
- 5) Smith, G. P.; Petrenko, V. A. *Chem. Rev.* **1997**, *97*, 391-410.
- 6) Clackson, T.; Wells, J. A. *Trends Biotechnol.* **1994**, *12*, 173-184.
- 7) Sparks, A. B.; Nils, A. B.; Lawrence, Q. A.; Thorn, J. M.; Kay, B. K. *Methods Enzymol.* **1995**, *255*, 498-509.
- 8) Katz, B. A. *Biochemistry* **1995**, *34*, 15421-15429.
- 9) Giebel, L. B.; Cass, R. T.; Milligan, D. L.; Young, D. C.; Arze, R.; Johnson, C. R. *Biochemistry* **1995**, *34*, 15430-15435.
- 10) Wrighton, N. C.; Farrell, F. X.; Chang, R.; Kashyap, A. K.; Barbone, F. P.; Mulcahy, L. S.; Johnson, D. L.; Barrett, R. W.; Jolliffe, L. K.; Dower, W. J. *Science* **1996**, *273*, 458-463.
- 11) Syed, R. S.; Reid, S. W.; Li, C.; Cheetham, J. C.; Aoki, K. H.; Liu, B.; Zhan, H.; Osslund, T. D.; Chirino, A. J.; Zhang, J.; Finer-Moore, J.; Elliott, S.; Sitney, K.; Katz, B. A.; Matthews, D. J.; Wendoloski, J. J.; Egrie, J.; Stroud, R. M. *Nature* **1998**, *395*, 511-516.
- 12) Livnah, O.; Stura, E. A.; Johnson, D. L.; Middleton, S. A.; Mulcahy, L. S.; Wrighton, N. C.; Dower, W. J.; Jolliffe, J. K.; Wilson, I. A. *Science* **1996**, *273*, 464-471.
- 13) Johnson, D. L.; Farrell, F. X.; Barbone, F. P.; McMahon, F. J.; Tullai, J.; Kenway, H.; Livnah, O.; Wrighton, N. C.; Middleton, S. A.; Loughney, D. A.; Stura, E. A.; Dower, W. J.; Mulcahy, L. S.; Wilson, I. A.; Jolliffe, L. K. *Biochemistry* **1998**, *37*, 3699-3710.
- 14) Wrighton, N. C.; Balasubramanian, P.; Barbone, F. P.; Kashyap, A. K.; Farrell, F. X.; Jolliffe, L. K.; Barrett, R. W.; Dower, W. J. *Nat. Biotechnol.* **1997**, *15*, 1261-1265.
- 15) Livnah, O.; Johnson, D. L.; Stura, E. A.; Farrell, F. X.; Barbone, F. P.; You, Y.; Liu, K. D.; Goldsmith, M. A.; He, W.; Krause, C. D.; Pestka, S.; Jolliffe, L. K.; Wilson, I. A. *Nat. Struct. Biol.* **1998**, *5*, 993-1004.
- 16) Rickles, R. J.; Botfield, M. C.; Zhou, X.; Henry, P. A.; Brugge, J. S.; Zoller, M. J. *Proc. Natl. Acad. Sci.* **1995**, *92*, 10909-10913.
- 17) Hiipakka, M.; Poikonen, K.; Saksela, K. *J. Mol. Biol.* **1999**, *293*, 1097-1106.
- 18) Katz, B. A. *Annu. Rev. Biophys. Biomol. Struct.* **1997**, *26*, 27-45.
- 19) Morken, J. P.; Kapoor, T. M.; Feng, S.; Shirai, F.; Schreiber, S. L. *J. Am. Chem. Soc.* **1998**, *120*, 30-36.
- 20) Kapoor, T. M.; Andreotti, A. H.; Schreiber, S. L. *J. Am. Chem. Soc.* **1998**, *120*, 23-29.
- 21) Koivunen, E.; Gay, D. A.; Ruoslahti, E. *J. Biol. Chem.* **1993**, *268*, 20205-20210.
- 22) Rodriguez, A. Organic Seminar Abstracts, Fall 1998; University of Illinois, October 5, **1998**; 11-18.
- 23) Miller, W. H.; Alberts, D. P.; Bhatnagar, P. K.; Bondinell, W. E.; Callahan, J. F.; Calvo, R. R.; Cousins, R. D.; Erhard, K. F.; Heering, D. A.; Keenan, R. M.; Kwon, C.; Manley, P. J.; Newlander, K. A.; Ross, S. T.; Samanen, J. M.; Uzinskas, I. N.; Venslavsky, J. W.; Yuan, C.; Haltiwanger, R. C.; Gowen, M.; Hwang, S. M.; James, I. E.; Lark, M. W.; Rieman, D. J.; Stroup, G. B.; Azzarano, L. M.; Salyers, K. L.; Smith, B. R.; Ward, K. W.; Johanson, K. O.; Huffman, W. F. *J. Med. Chem.* **2000**, *43*, 22-26.
- 24) Batt, D. G.; Petratis, J. J.; Houghton, G. C.; Modi, D. P.; Cain, G. A.; Corjay, M. H.; Mousa, S. A.; Bouchard, P. J.; Forsythe, M. S.; Harlow, P. P.; Barbera, F. A.; Spitz, S. M.; Wexler, R. R.; Jadhav, P. K. *J. Med. Chem.* **2000**, *43*, 41-58.

STEREOSELECTIVE PICTET-SPENGLER REACTIONS

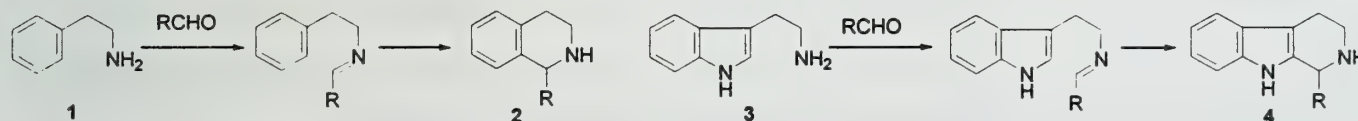
Reported by Jing Liu

March 2, 2000

INTRODUCTION

The Pictet-Spengler (PS) reaction discovered by Ame Pictet and Theodor Spengler in 1911¹ is a heteroannulation that involves the cyclocondensation of arylethylamines **1** or tryptamines **3** with aldehydes or their equivalents (Scheme 1). The imines formed *in situ* undergo cyclization to 1,2,3,4-tetrahydroisoquinolines **2** or 1,2,3,4-tetrahydro- β -carbolines **4**, respectively, which are two important building blocks for alkaloid synthesis. The PS reaction has been applied in syntheses of numerous natural products, including ecteinascidin 743,² fumitremorgin,³ and ajmaline.⁴ With the development of diastereo- and enantioselective versions, the PS reaction is becoming an even more powerful tool for heterocyclic and alkaloid synthesis.⁵ Recent advances in the stereoselective Pictet-Spengler reactions are the focus of this report.

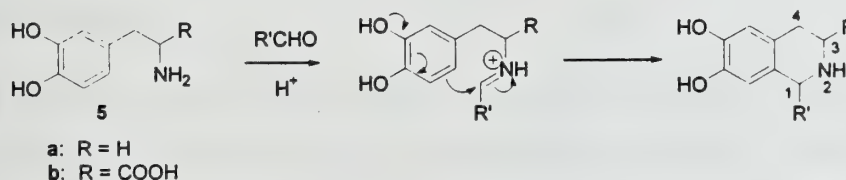
Scheme 1. Pictet-Spengler Reaction.



SYNTHESIS OF TETRAHYDROISOQUINOLINES

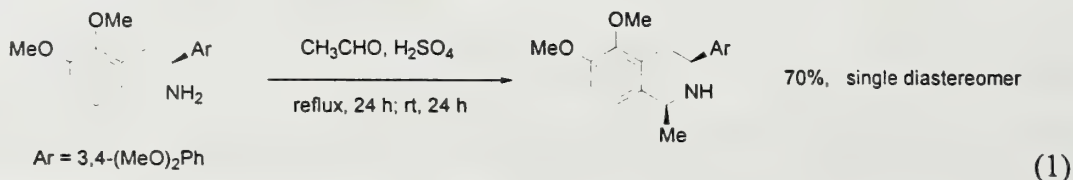
The mechanism of the PS reaction involves initial imine formation, protonation, and subsequent electrophilic attack on the phenyl ring to afford tetrahydroisoquinoline **2**. Hydroxy or alkoxy substituents on the aryl ring greatly facilitate the cyclization step.⁶ Therefore, dopamine (5a) and dopa (5b) derivatives are the most common substrates (Scheme 2).

Scheme 2. Synthesis of Tetrahydroisoquinoline by the Pictet-Spengler Reaction.



During the reaction, a new stereogenic center at C-1 is created. Diastereoselective PS reactions have been carried out using chiral amines, chiral aldehydes, or chiral auxiliaries. Brossi and co-workers

were the first to utilize enantiomerically pure L-dopa in the diastereoselective synthesis of 1,3-cis disubstituted tetrahydroisoquinolines by the PS reaction.⁷ High cis selectivity was also observed in the reaction of an aryl analog.⁸ (eq. 1)

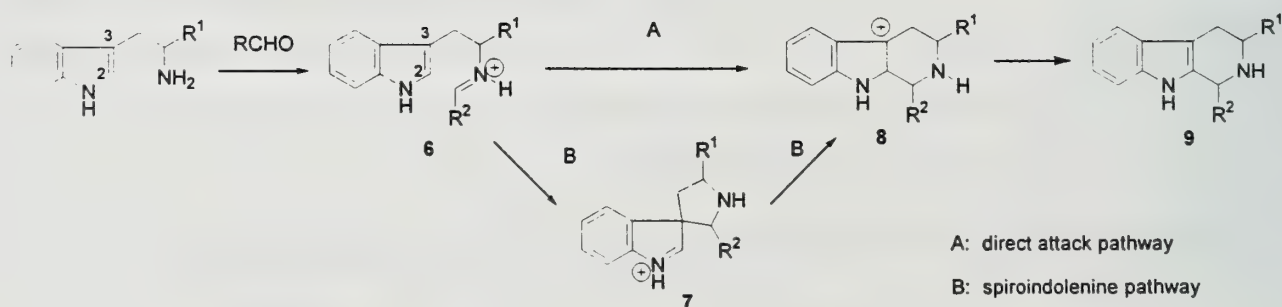


PS reactions of chiral aldehydes from carbohydrates were studied by Czarnocke and co-workers.⁹ As a key step in the synthesis of *threo*-lauranosin, the PS reaction between (*R*)-glyceraldehyde and dopamine hydrochloride afforded the (1*R*, 1'*R*)-tetrahydroisoquinoline product in 80% d.e. The stereochemical outcome can often be explained by the Felkin-Anh model or by intramolecular hydrogen bonding in analogy to carbonyl addition reactions. More recently, a variety of chiral auxiliaries have also been employed with success,¹⁰ including the recently developed borane-10,2-sultam¹¹ and 8-phenylmenthyl¹² auxiliaries.

SYNTHESIS OF TETRAHYDRO- β -CARBOLINES

The PS reactions between aldehydes and tryptamine derivatives afford tetrahydro- β -carboline 4. However, the details of the mechanism are still not clear despite decades of extensive mechanistic studies. Two possible mechanisms proposed for the reaction are shown in Scheme 3.

Scheme 3. Two Possible Mechanisms for Tetrahydro- β -carboline Formation.



Pathway A involves the direct electrophilic attack of iminium ion 6 on the indole β -carbon (C-2). The intermediate carbocation 8 undergoes elimination to provide product 9. Alternatively, in pathway B, the attack of iminium ion 6 occurs on C-3 on the indole ring to form a spiroindolenine intermediate 7. Subsequent 1,2-alkyl migration and elimination of a proton afford the same final product. According to Baldwin's rules, C-2 direct attack pathway A (6-*endo-trig*) should be favored over the spiroindolenine

pathway B (*5-endo-trig*). However, much experimental evidence suggests the existence of spiroindolenines **7**,^{13,14} lending support for the spiroindolenine mechanism (pathway B).

Recent theoretical MNDO calculations by Kowalski and coworkers might provide new insights into the mechanism.¹⁵ According to their results, spiroindolenine **7** should be formed during the course of the reaction, but the following 1,2-alkyl migration is disfavored owing to a high energy barrier for the rearrangement to carbocation **8**. The calculation results suggest that spiroindolenine **7** may exist in equilibrium with the iminium ion **6** but it probably is not on the pathway to the product. Instead, iminium ion **6** is predicted to give the final product **9** via the direct C-2 attack pathway. This hypothesis is consistent with most of the experimental evidence. However, further study is needed to elucidate the mechanism fully.

Because of the uncertainty of the mechanism, it is difficult to rationalize the stereochemical outcome of tetrahydro- β -carboline formation. If the spiroindolenine pathway is dominating, the steric interactions on the five-membered ring should determine the stereoselectivity. However, if the direct C-2 attack pathway is followed, the steric interactions and electronic effects associated with the six-membered ring formation should be considered instead. On the other hand, the stability of the products governs the stereochemistry when the reaction is under thermodynamic control.

Tryptophan Esters as Substrates

The diastereoselectivity of PS reactions can be controlled by using tryptophan ester derivatives as starting material. Two isomeric products may be generated: 1,3-trans- **11** and 1,3-cis-tetrahydro- β -carbolines **12**. With tryptophan methyl ester **10**, moderate cis selectivity was observed when the reaction was carried out at 0°C (Table 1).¹⁶ The steric size of the aldehyde had little influence on the stereoselectivity. Higher temperature led to poor stereoselectivity owing to epimerization of the products at both C-1 and C-3.¹⁷

Table 1. Cis- selectivity with tryptophan methyl esters.

entry	R	d.r. (cis/trans)	yield (%)
1	Ph	82:18	74
2	<i>n</i> -Pr	80:20	72
3	<i>i</i> -Pr	83:17	82
4	C ₆ H ₁₁	71:29	71

In order to improve the trans selectivity, Cook and co-workers studied the reactions with *N*_b-benzyltryptophan methyl esters **13** extensively.¹⁸ The *N*-benzyl substituent greatly enhanced the trans selectivity (Table 2, entry 2), and the utilization of an even bulkier ester group or *N*_b-substituent resulted in exclusive formation of the trans product (Table 2, entries 3-4). The *N*-benzyl group was easily removed by catalytic hydrogenolysis.

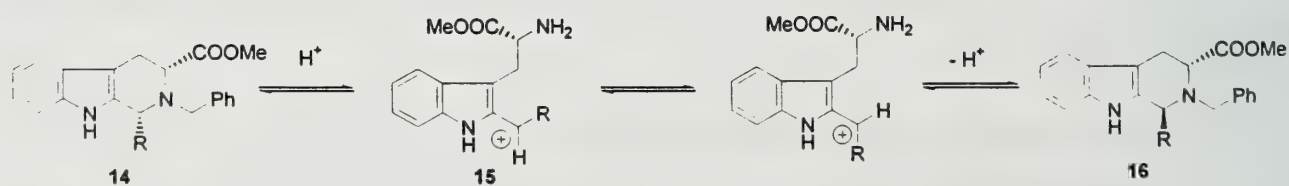
Table 2. Trans selectivity with *N*_b-substituted tryptophan esters.

entry	R ¹	R ²	d.r. (cis/trans)
1	CH ₃	H	75:25
2	CH ₃	PhCH ₂	12:88
3	<i>i</i> -Pr	PhCH ₂	0:100
4	<i>i</i> -Pr	(Ph) ₂ CH	0:100

* Yields were not reported.

The reactions in refluxing benzene were shown to be under kinetic control.¹⁷ In acidic media, the PS reaction of *N*_b-benzyl-tryptophan methyl esters gave even higher trans selectivity. Under these conditions, the 1,3-cis isomers **14** underwent epimerization to form the more stable trans isomers **15** through a separate mechanism involving the formation of carbocation **16** via the C(1)-N(2) bond cleavage (Scheme 4).¹⁸ The assignments of stereochemistry for tetrahydro-β-carbolines were usually based on C¹³ NMR correlations developed by Cook and co-workers.¹⁹ Chemical correlations and X-ray analyses were used to confirm the assignments in many cases.

Scheme 4. Mechanism of cis – trans Epimerization.



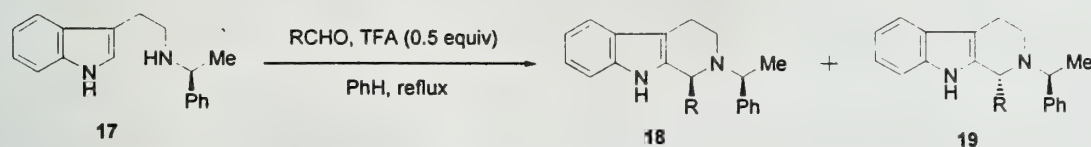
Tryptamines as Substrates

Stereoselective PS reactions of tryptamines can be carried out by employing chiral auxiliaries or chiral Lewis acid promoters. The use of chiral aldehydes²⁰ has not been established as a general method, and the epimerization of aldehydes is often a problem.

α -Arylethyl chiral auxiliaries

Nakagawa and co-workers investigated the use of α -arylethyl chiral auxiliaries.²¹ The reactions of tryptamines **17** bearing the α -phenethyl auxiliaries and benzaldehyde in refluxing benzene afforded the tetrahydro- β -carboline in moderate yields and selectivities (Table 3). The best results were obtained with trifluoroacetic acid (TFA) as catalyst. The substrate scope of this method is limited to benzaldehyde and electron-deficient aromatic aldehydes. Low yields were observed with aliphatic aldehydes owing to side reactions during the long reaction time. The chiral auxiliary was easily removed by catalytic hydrogenation. When α -naphthylethyl auxiliaries were employed under similar conditions, slightly higher stereoselectivities and lower yields were observed.²²

Table 3. Pictet-Spengler reaction with α -phenethyl auxiliary.

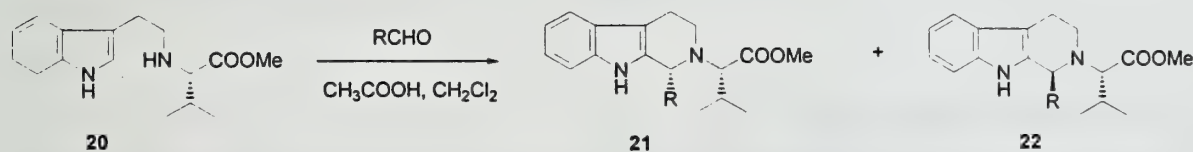


entry	R	time (h)	yield (%)	d.r. (18:19)
1	Ph	24	71	86:14
2	4-NO ₂ -Ph	24	86	68:32
3	4-MeO-Ph	48	39	67:33
4	<i>i</i> -Bu	24	58	69:31

Amino acid-derived chiral auxiliaries

Waldmann and co-workers have used amino acid-derived chiral auxiliaries to control the stereoselectivity of the PS reaction.²³ Among the amino acids tested, valine methyl ester **20** provided the best results (Table 4).

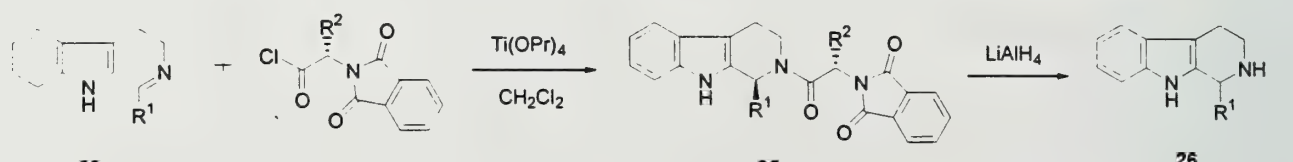
Table 4. Valine methyl ester-derived chiral auxiliary.



entry	R	T (°C)	yield (%)	d.r. 21:22
1	Ph	25	76	90:10
2	4-EtO-Ph	40	85	93:7
3	2,4-di-Cl-Ph	25	78	94:6
4	Me	25	82	60:40

Aromatic aldehydes gave satisfactory yields and good stereoselectivities (entries 1-3). However, aliphatic aldehydes once again led to poor yields owing to side reactions including aldol condensation. The installation and removal of the chiral auxiliary are difficult. In order to improve the method, Waldmann and co-workers employed *N,N*-phthaloyl amino acid-derived auxiliaries.²⁴ Catalyzed by $\text{Ti}(\text{OR})_4$ at room temperature, the reaction of Schiff bases **23** and *N,N*-phthaloyl amino acid chlorides **24** provided β -carboline **25** with excellent stereoselectivities and moderate to good yields (Table 5). The increased yields were attributed to the enhanced reactivity of *N*-acyliminium ion compared to its *N*-alkyl counterpart.

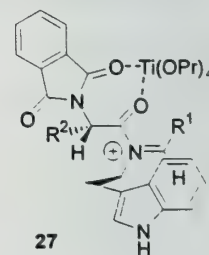
Table 5. PS reactions with *N,N*-phthaloyl amino acid-derived chiral auxiliaries.



entry	R ¹	R ²	yield (%)	25 anti:syn
1	Ph	<i>t</i> -Bu	60	>99:1
2	Me	<i>t</i> -Bu	66	96:4
3	Et	<i>i</i> -Pr	57	97:3
4	<i>i</i> -Pr	<i>i</i> -Pr	99	>99:1

With this method, both aromatic and aliphatic aldehydes proved to be suitable substrates, and the removal of the chiral auxiliary was also greatly simplified. Reduction of **25** with LiAlH_4 afforded the enantiomerically enriched β -carboline **26** in good yield.

Waldmann proved that the reaction was under kinetic control and rationalized the diastereoselectivity by the formation of complex **27** through the $\text{Ti}(\text{IV})$ coordination with the amino acid carbonyl and one of the phthalimide carbonyl groups. Shielding of one face of the imine double bond accounts for the high stereoselectivity.



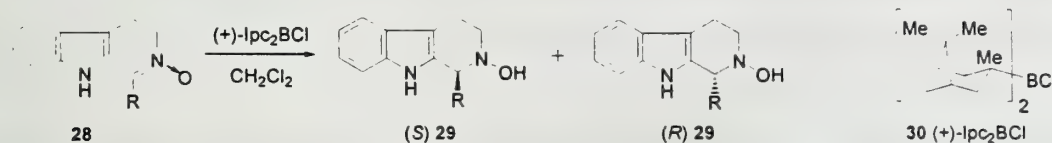
Chiral Lewis acid promoters

The first enantioselective Pictet-Spengler reactions were carried out in 1996 using chiral Lewis acid promoters.²⁵ Nakagawa and co-workers condensed *N*_b-hydroxytryptamine with various aldehydes to form nitrones **28**, which underwent cyclization to give *N*_b-hydroxy- β -carboline **29**. Subsequent Zn/HOAc reduction or catalytic hydrogenation afforded the tetrahydro- β -carboline.

The principle differences between nitrone **28** and the imine counterpart are reactivity and configurational stability. Nitrone **28** is more reactive owing to the electron-withdrawing effect of

oxygen. The configuration of the C=N double bond in **28** is also more stable compared to imines. Only nitrones gave good results in the chiral Lewis acid-promoted Pictet-Spengler reactions studied. Diisopinocampheylchloroborane (Ipc₂BCl) **30** is the first effective Lewis acid promoter (Table 6). The best results were obtained in the reactions of electron-rich aromatic aldehydes at low temperature while aliphatic aldehydes only led to moderate selectivities. The stereochemical outcome was rationalized by semi-empirical calculations of the energies of possible transition states.

Table 6. Ipc₂BCl - promoted nitrone cyclizations.



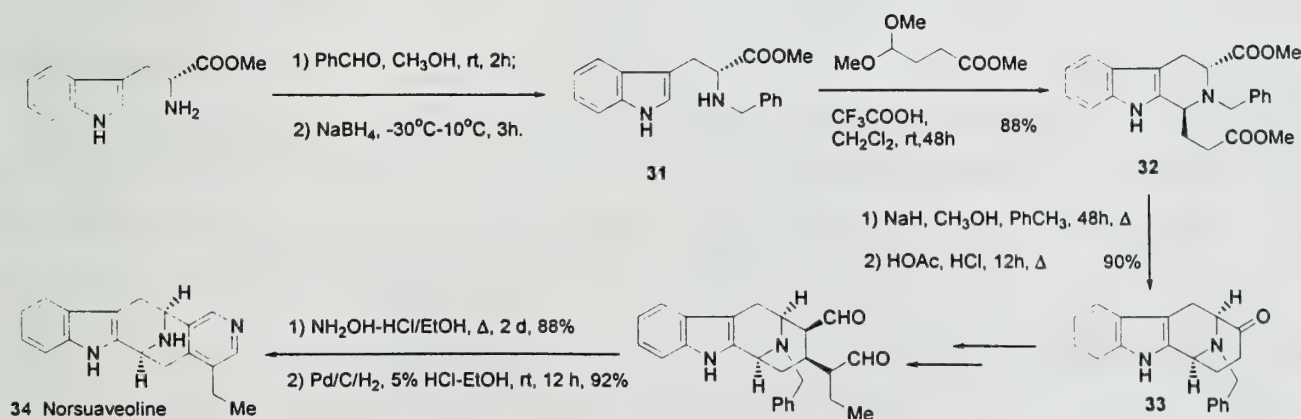
entry	R	T (°C)	yield (%)	e.e. (%) ^a
1	Ph	rt	97	25
2	Ph	-78	92	75
3	4-MeO-Ph	-78	65	90
4	4-NO ₂ -Ph	-78	81	< 1
5	Me	-78	91	43

a) The (*S*)-isomer is the major product.

APPLICATION IN TOTAL SYNTHESIS

The Pictet-Spengler reaction has been applied to numerous heterocyclic syntheses.⁵ One example is the total synthesis of indole alkaloid norsuaveoline **34** (Scheme 6).⁴ The PS reaction of ester **31** under acidic conditions afforded the 1,3-trans product **32** in high yield as a single diastereomer. Subsequent Dieckmann condensation inverted the configuration at C-3 to give the 1,3-cis β -carboline **33**. The *N*-benzyl group was removed by catalytic hydrogenation in the last step of the total synthesis. This example demonstrated the versatility of stereochemical control in PS reactions.

Scheme 6. Total Synthesis of Norsuaveoline.



CONCLUSIONS

As shown in this report, the Pictet-Spengler reaction is a very important method for the preparation of tetrahydroisoquinolines and tetrahydro- β -carbolines. Dopamine, tryptamine, and tryptophan derivatives are the most commonly used starting materials. A variety of methods can be employed to accomplish stereoselective PS reaction. The mechanism of the formation of tetrahydro- β -carbolines still requires extensive investigation. While the asymmetric Pictet-Spengler reactions of tryptophan derivatives are well studied, the counterpart with tryptamine starting materials still needs more investigation. The development of chiral auxiliaries and chiral Lewis acid catalysts are still in their infancy. A catalytic asymmetric version would further enhance the utility of the Pictet-Spengler Reaction.

REFERENCES

- 1) Pictet, A.; Spengler, T. *Ber. Dtsch. Chem. Ges.* **1911**, *44*, 2030.
- 2) Corey, E. J.; Gin, D. Y.; Kania, R. S. *J. Am. Chem. Soc.* **1996**, *118*, 9202.
- 3) Hino, T.; Nakagawa, M. *Heterocycles* **1997**, *46*, 673.
- 4) Li, J.; Wang, T.; Yu, P.; Peterson, A.; Weber, R.; Soerens, D.; Grubisha, D.; Bennett, D.; Cook, J. M. *J. Am. Chem. Soc.* **1999**, *121*, 6998.
- 5) Cox, E. D.; Cook, J. M. *Chem. Rev.* **1995**, *95*, 1797 and references therein.
- 6) Yokoyama, A.; Ohwada, T.; Shudo, K. *J. Org. Chem.* **1999**, *64*, 611.
- 7) Brossi, A.; Focella, A.; Teitel, S. *Helv. Chim. Acta* **1972**, *55*, 15.
- 8) Carrillo, L.; Badia, D.; Dominguez, E.; Anakabe, E.; Osante, I.; Tellitu, I.; Vicario, J. L. *J. Org. Chem.* **1999**, *64*, 1115.
- 9) Czarnocke, Z.; MacLean, D. B.; Szarek, W. *Can. J. Chem.* **1986**, *64*, 2205.
- 10) Rozwadowska, M. D. *Heterocycles* **1994**, *39*, 903.
- 11) Czarnocke, Z.; Arazny, Z. *Heterocycles* **1999**, *51*, 2871.
- 12) Comins, D. L.; Thakker, P. M.; Baevsky, M. F. *Tetrahedron* **1997**, *53*, 16327.
- 13) Ungemach, F.; Cook, J. M. *Heterocycles* **1978**, *9*, 1089 and references therein.
- 14) Kawate, T.; Nakagawa, M.; Ogata, K.; Hino, T. *Heterocycles* **1992**, *33*, 801.
- 15) Kowalski, P.; Mokrosz, J. L. *Bull. Soc. Chim. Belg.* **1997**, *106*, 147.
- 16) Bailey, P. D.; Hollinshead, S. P.; McLay, N. R. *Tetrahedron Lett.* **1987**, *28*, 5177.
- 17) Bailey, P. D.; Hollinshead, S. P.; McLay, N. R.; Morgan, K.; Palmer, S. J.; Prince, S. N.; Reynolds, C. D.; Wood, S. D. *J. Chem. Soc., Perkin Trans. 1* **1993**, 431.
- 18) Cox, E. D.; Hamaker, L. K.; Li, J.; Yu, P.; Czerwinski, K. M.; Deng, L.; Bennett, D. W.; Cook, J. M.; Watson, W. H.; Krawiec, M. *J. Org. Chem.* **1997**, *62*, 44.
- 19) Ungemach, F.; Soerens, D.; Weber, R.; DiPierro, M.; Campos, O.; Mokry, P.; Cook, J. M.; Silverton, J. V. *J. Am. Chem. Soc.* **1980**, *102*, 6976.
- 20) McNulty, J.; Still, I. W. J. *J. Chem. Soc., Perkin Trans. 1* **1994**, 1329.
- 21) Soe, T.; Kawate, T.; Fukui, N.; Hino, T.; Nakagawa, M. *Heterocycles* **1996**, *42*, 347.
- 22) Kawate, T.; Yamanaka, M.; Nakagawa, M. *Heterocycles* **1999**, *50*, 1033.
- 23) Waldmann, H.; Schmidt, G. *Tetrahedron* **1994**, *50*, 11865.
- 24) Waldmann, H.; Schmidt, G.; Henke, H.; Burkard, M. *Chem. Eur. J.* **1996**, *2*, 1566.
- 25) Kawate, T.; Yamada, H.; Soe, T.; Nakagawa, M. *Tetrahedron: Asymmetry* **1996**, *7*, 1249.

DISCOVERY OF NEW CATALYSTS FOR ASYMMETRIC SYNTHESIS: SOLID-PHASE SYNTHESIS OF CATALYST LIBRARIES AND ADVANCES IN RAPID SCREENING TECHNIQUES

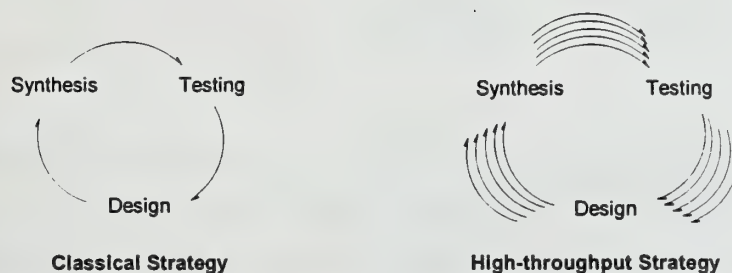
Reported by Timothy A. Johnson

March 6, 2000

INTRODUCTION

Combinatorial synthesis has emerged as a powerful tool for the efficient optimization of desired molecular properties and has led to the discovery of numerous drug candidates and leads for novel materials.¹ The application of this approach to the discovery of catalysts for enantioselective synthesis, a process historically accomplished through design, synthesis, and testing of one candidate at a time, has recently received considerable attention. The classical strategy versus the high-throughput strategy for identification of catalysts for asymmetric reactions is illustrated in Figure 1. In the past five years several groups have used solid-phase, parallel strategies for the optimization of existing catalyst lead structures.² Most recently, and in conjunction with advances in high-throughput screening for reactivity and selectivity, these efforts have evolved and succeeded in identifying novel catalyst leads.³ This review first considers key concepts in this growing field, then details advances in solid-phase, high-throughput synthesis for the optimization and identification of new catalysts, and concludes with a survey of advances in rapid screening techniques.

Figure 1.



KEY CONCEPTS

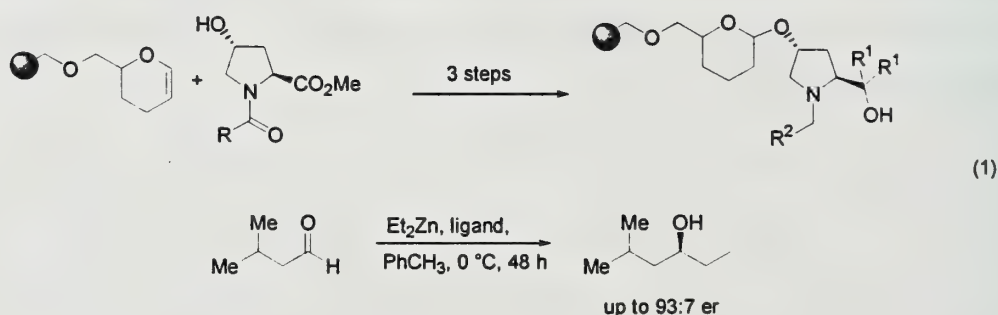
There are several important and non-obvious ideas that need to be recognized in evaluation of chiral catalyst libraries. First, since combinatorial chemistry is barely a decade old, reactions for creating large libraries of compounds are still limited. Second, although split-pool approaches can generate much larger libraries than parallel strategies, the latter has been employed primarily owing to limitations in available screening techniques. This includes the limitation that parallel libraries do not usually generate every possible permutation and the risk that synergistic effects may be overlooked. Third, new catalysts

can be submitted to reaction conditions either without or after cleavage from polymer support. Consequently, assays of product yields and selectivity with bound versus non-bound catalysts can be unreliable because of possible aggregation and conformational effects solid supports and linkers may have on catalytic species. These concepts and limitations will be considered in the context of work presented throughout this review.

LEAD OPTIMIZATION

Initial Approach

The earliest approach to catalyst optimization on the solid phase was based on the successful use of catalytic pyrrolidinemethanol ligands in the asymmetric addition of diethylzinc to aldehydes.⁴ Ellman and coworkers synthesized a small solid-phase, parallel library (10 members) of chiral amino alcohols derived from *trans*-4-hydroxy-L-proline and optimized the catalytic enantioselective addition of diethylzinc to aliphatic aldehydes (eq 1).⁵ This study proved that solid-phase, parallel strategies were indeed suited for chiral catalyst identification and optimization and led to further investigations using this approach.



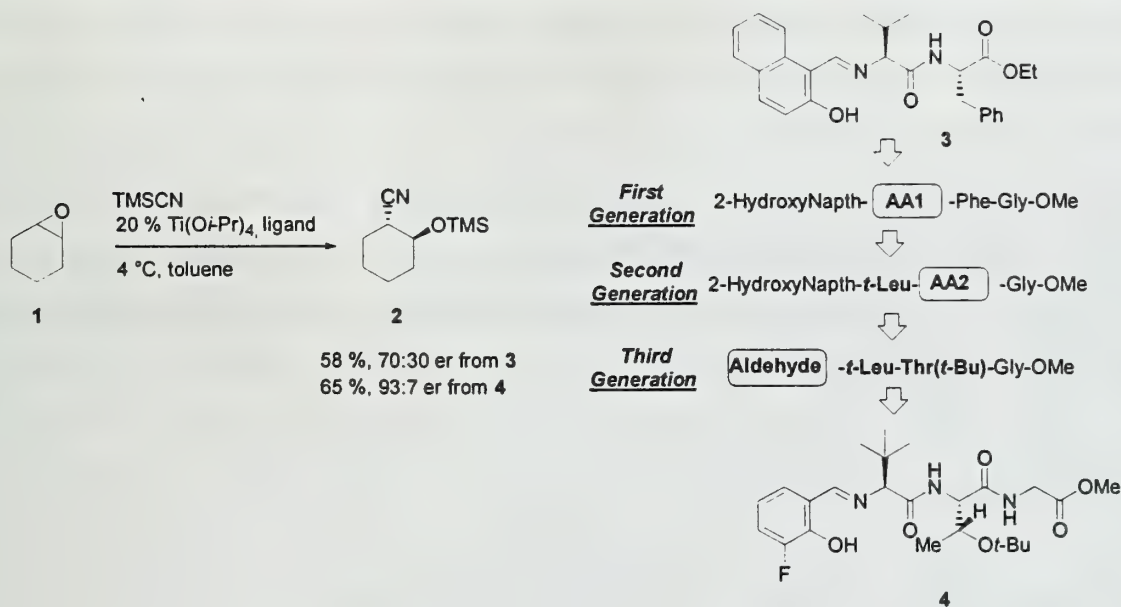
Catalytic Asymmetric Addition of TMSCN to meso Epoxides

Hoveyda and coworkers used a positional scanning approach for ligand optimization in the titanium(IV)-catalyzed asymmetric addition of TMSCN to meso epoxides.⁶ Positional scanning involves the variation of a particular subunit of the library structure, while all others are held constant. The library is screened for the optimized subunit, and following its identification, a new library is prepared varying another subunit, holding the optimized and other un-optimized subunits constant. The process is repeated until all subunits of the library structure are optimal. Based on the knowledge that a known alkoxide Schiff base ligand effectively facilitates the titanium(IV)-catalyzed addition of TMSCN to epoxides,⁷ Hoveyda developed a solid phase parallel library consisting of a glycine linker, two amino acid residues, and a variety of salicylaldehydes. A moderately selective ligand, **3**, for the addition of TMSCN to

cyclohexene oxide, (**1**) (70:30 er) was identified and provided a starting point for the iterative optimization approach (Scheme 1).

Positional scanning of **3** was carried out at amino acid 1 (AA1) with parallel synthesis of ten ligands, maintaining the amino acid 2 (AA2) position and aldehyde. The ligand that induced the largest increase in enantioselectivity for the addition to **1** after cleavage from the resin was used in identification of the optimized AA1 position. Second and third generations were synthesized varying AA2 position and the aldehyde, respectively. This strategy discovered optimal ligand **4**, with an enhancement of the enantiomeric ratio from 70:30 to 93:7.

Scheme 1.



This strategy assumes that the influence of each subunit is independent and additive. Because positional scanning in the reverse order, starting with aldehyde variation and finishing with AA1 variation, also resulted in the identification of **4** as the optimal ligand, the assumption seems valid. However, synergistic effects cannot be discounted without testing every combination of subunits.

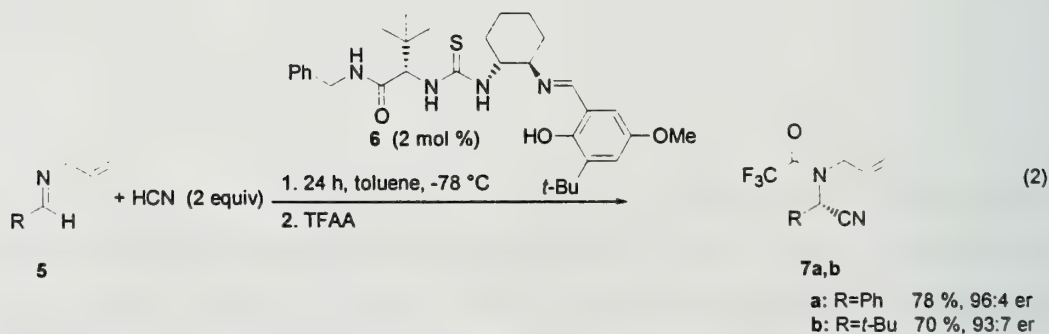
In an effort to increase throughput, Hoveyda and coworkers demonstrated that selective ligands could be identified while bound to the resin.⁸ A reliable solid-solution phase correlation of catalyst selectivity was obtained, particularly for ligands that exhibited higher selectivity. The similarity of the reaction rates, reactivity, and selectivity, as well as observation of a positive non-linear effect in solution indicated that the Ti-ligand complex may be monomeric in solution.

These studies resulted in the efficient ligand optimization for addition of TMSCN to a variety of epoxides. It is also noteworthy that a reversal of enantioselectivity in the addition of TMSCN to

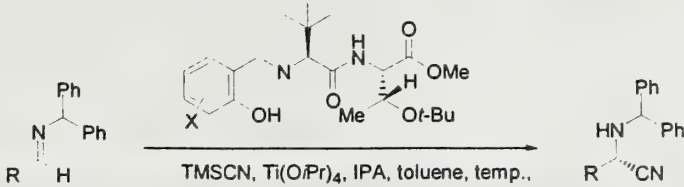
cyclopentene oxide is caused by a subtle variation in constitution, rather than a change in the stereochemical identity at the AA2 position. This emphasizes the importance of maintaining the catalysts in a spatially separated parallel array, because mixtures of enantioselective catalysts could lead to racemic products.

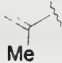
Catalytic Asymmetric Strecker Reaction

Jacobsen and coworkers have utilized solid-phase, parallel synthesis for optimization of Schiff base ligands for the catalytic asymmetric hydrocyanation of imines (the Strecker reaction).⁹ A 48-membered parallel library was prepared from an amino acid, urea, chiral diamine, and salicylaldehyde derivative. This library was based on a lead ligand that catalyzed the asymmetric addition of TBSCN to *N*-allyl-benzaldimine with moderate enantioselectivity (60:40 er). Selectivity analysis of these ligands on the solid phase and identification of key structural characteristics led to synthesis of a second library consisting of 132 thiourea derivatives, incorporating non-polar L-amino acids, and 3-*t*-butyl-substituted salicylaldehyde derivatives. Ligand **6** was identified as the best polymer bound catalyst (90:10 er). The independently synthesized ligand catalyzed the addition of HCN to *N*-allyl-benzaldimine in 96:4 er and 78% yield (eq 2). Ligand **6** also showed excellent activity with a variety of *N*-allyl-aryl imines and bulky aliphatic imines (>65% yield, >85:15 er).



Hoveyda and coworkers have applied their ligand optimization protocol to the titanium(IV)-catalyzed asymmetric addition of TMS-CN to *N*-(diphenylmethyl)aryl and α,β -unsaturated imines.^{10,11} Excellent enantioselectivities were obtained through optimization of ligand **4**, which was previously utilized to enhance enantioselectivity (*vide supra*). In fact, only variation in the aldehyde was necessary to obtain excellent selectivity in a variety of substrates (Table 1).

Table 1. Ti-catalyzed enantioselective addition of cyanide to imines.


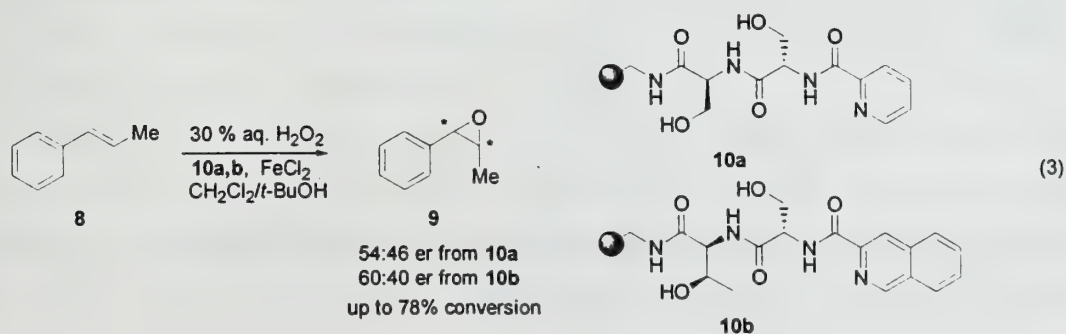
entry	R	schiff base	% cat	temp (°C)	yield (%)	er
1	Ph	X=5-OMe	10	4	82	>99:1
2	<i>t</i> -Bu	X= 3,5-diBr	10	4	97	93:7
3		1-naphthyl	15	-20	80	98:2

LEAD DISCOVERY

Asymmetric Epoxidation Catalysts

Jacobsen and coworkers recently utilized a solid-phase, combinatorial approach to discover new catalyst leads effective in the epoxidation of *trans*- β -methylstyrene (**8**) with H₂O₂ in high yields and measurable enantioselectivity.³ These leads were identified from an extraordinarily large library of 5760 ligand-metal complexes generated by a combination of split-pool and parallel synthesis. This example illustrates the utility of combinatorial methods to discover catalysts with no structural resemblance to previously known ones. The novel catalysts consisted of three FeCl₂ complexes including ligand **10a** derived from two amino acids and a pyridine-containing end cap.

A polystyrene resin-bound parallel library of 96 members derived from four amino acids and eight pyridine-containing end caps was used in ligand optimization. Evaluation of the resin-bound catalysts identified ligand **10b**, which exhibited only a moderate increase in enantioselectivity (eq 3). This example illustrates the true power of combinatorial approaches to screen a truly diverse range of possibilities in catalyst discovery. Future developments will certainly generate libraries of increasing size, and thus the development of rapid catalyst screening techniques is a necessity.



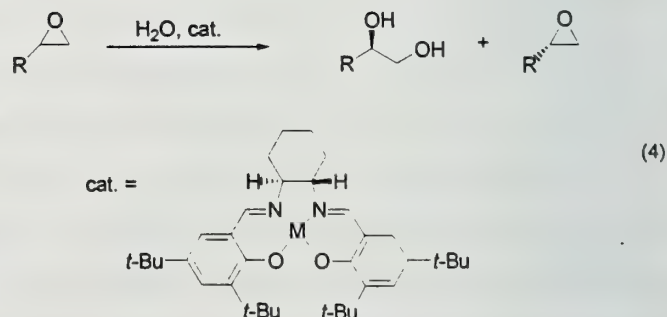
ADVANCES IN HIGH-THROUGHPUT SCREENING

The major limitation of the approaches described thus far is a lack of high-throughput techniques for screening catalytic activity and enantioselectivity. To date, catalyst libraries have been screened through the serial analysis of conversion and selectivity using GC, HPLC, and their chiral variants. The length of time involved in these chromatographic separations and the move toward larger libraries in catalyst discovery has required development of more efficient parallel and high-throughput serial screening techniques.

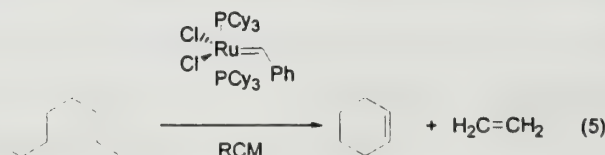
Infrared Thermography

Since high catalytic activity is often a prerequisite for high conversion and selectivity, its efficient assessment is important to catalyst discovery. Reactive dyes,¹² fluorescence signaling,¹³ UV/Vis spectroscopy,¹⁴ and infrared (IR) thermography have been applied to the parallel detection of active catalysts. IR thermography is a powerful tool that measures emitted blackbody radiation and has made spatial resolution of temperatures possible. Since most chemical reactions have a measured heat of reaction, ΔH_r , IR thermography may be used in a variety of catalytic transformations and has been used in efficient parallel screening of a support-bound, split-pool generated catalyst library of 7000 beads.¹⁵

Reetz and coworkers have used time-resolved IR thermography in the parallel assay of chiral transition metal catalyst activity.¹⁶ The exothermic asymmetric ring-opening hydrolysis of epoxides using Jacobsen's salen catalysts (eq 4) was assayed using catalysts with different activities as well as epoxides with different reactivities by the observation of hot spots in parallel wells through an IR camera. The relative reactivity obtained from the IR-thermographic screening was the same as previous reports by Jacobsen in laboratory scale reactions.



The catalytic activity of endothermic and even thermoneutral transition metal-catalyzed reactions has also been monitored using IR thermography. Reetz and coworkers have recently shown that catalytic activity in the endothermic (or thermoneutral) Ru-catalyzed ring closing olefin metathesis (RCM) could be assayed using this technique (eq 5).¹⁷



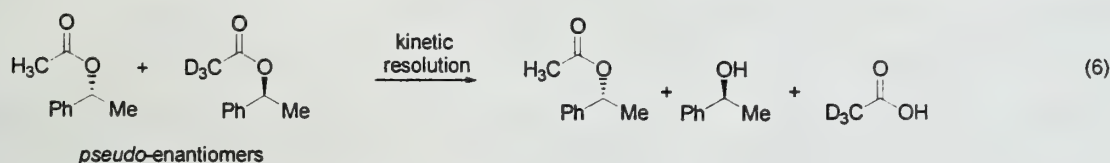
Parallel screening of different catalysts and dienes was accomplished with the observation of cold spots through the IR camera. These spots resulted from a combination of both an endothermic reaction

and evaporation of ethylene as the reaction proceeded. Importantly, IR thermography may be applied to libraries of catalysts generated through split-pool and parallel techniques. The method is limited in that it assays catalytic turnover but not selectivity.

High-Throughput Enantioselectivity Determination

Efficient quantification of the product enantioselectivity for large libraries of chiral catalysts is perhaps the most challenging problem in the discovery process by this approach. To date, a few automated high-throughput serial assays have been developed that can reliably determine the enantioselectivity of approximately 1400 reactions per day.¹⁹

Recent developments in high-throughput screening of enantioselectivity in catalytic kinetic resolutions include the use of electrospray ionization mass spectrometry (ESI-MS).^{18,19} The principle is based on using isotopically labeled substrates in the form of pseudo-enantiomers or pseudo-prochiral compounds. A theoretical example is the determination of the enantioselectivity of the lipase-catalyzed hydrolytic kinetic resolution of pseudo-racemic 1-phenylethyl acetate (eq 6).



Various known pseudo-enantiomeric ratios of 1-phenyl ethyl acetate were detected by ESI-MS using intensity ratios of quasi-molecular ions.¹⁹ Reetz and coworkers have demonstrated the capabilities of automation in the determination of between 700 and 1400 enantiomeric ratios per day, depending on the particular substrate. Control experiments have excluded kinetic isotope effects and it is emphasized that no chromatographic separation of enantiomers or pseudo-enantiomers is involved in this technique.

Circular dichroism (CD) coupled with HPLC has also been used in the high-throughput enantioselectivity determination for catalytic enantioselective syntheses of aryl alcohols. Mikami and coworkers first reported the use of this technique for the catalytic asymmetric addition of diethylzinc to benzaldehyde.²⁰ This method is based on the use of sensitive detectors for HPLC which determine in a parallel manner, both circular dichroism ($\Delta\epsilon$) and the absorption (ϵ) of a sample at a certain wavelength. Normalization of these values gives an anisotropy factor g , which is linearly related to the enantioselectivity and independent of concentration.

Reetz and coworkers have recently developed a reverse phase HPLC analysis which requires just 1.5 minutes for reliable enantioselectivity determinations for the catalytic asymmetric reduction of acetophenone.²¹ It is possible to determine the enantiomeric ratios for 700-900 reactions per day with this approach.

CONCLUSION

Catalyst discovery and optimization of chiral catalysts using solid phase, combinatorial libraries has been very effective. Although this strategy has been limited to relatively smaller libraries, chemists have optimized catalysts very efficiently. Significant advances have been made in the high-throughput screening of the activity and selectivity of catalysts for asymmetric reactions. Future developments in solid phase synthetic methodologies as well as high-throughput screening of larger combinatorial libraries may allow for discovery of enantioselective catalysts with selectivity possessed by enzymes.

REFERENCES

- (1) (a) Czarnik, A. W.; Ellman, J. A. Eds., *Acc. Chem. Res.* **1996**, *29*, 111-170; (b) Szotak, J. Ed., *Chem. Rev.* **1997**, *97*, 347-510; (c) Poole, J. L. Organic Seminar Abstracts 1998-99, Semester II; University of Illinois, Urbana, IL. March 12, 1998; p. 25.
- (2) (a) Hoveyda, A. H.; Snapper, M. L.; Kuntz, K. W. *Curr. Opin. Chem. Biol.* **1999**, *3*, 331-319. (b) Jacobsen, E. N.; Francis, M. B.; Jamison, T. F. *Curr. Opin. Chem. Biol.* **1998**, *2*, 422-428. (c) Hoveyda, A. H. *Chem. Biol.* **1998**, *5*, R187-R191. (d) Kagan, H. B. *J. Organomet. Chem.* **1998**, *567*, 3-6. (e) Hoveyda, A. H.; Snapper, M. L.; Shimizu, K. D. *Chem. Eur. J.* **1998**, *4*, 1885-1889.
- (3) Jacobsen, E. N.; Francis, M. B., *Angew. Chem. Int. Ed. Engl.* **1999**, *38*, 937-941.
- (4) Soai, K.; Ookawa, A.; Kaba, T.; Ogawa, K. *J. Am. Chem. Soc.* **1987**, *109*, 7111-7115.
- (5) Ellman, J. A.; Liu, G. *J. Org. Chem.* **1995**, *60*, 7712-7713.
- (6) Hoveyda, A. H.; Snapper, M. L.; Cole, B.M.; Schimizu, K. D.; Krueger, C. A.; Harrity, J. P. *Angew. Chem. Int. Ed. Engl.* **1996**, *35*, 1668-1671.
- (7) Oguni, N.; Hayashi, M.; Tamura, M. *Synlett* **1992**, 663-664.
- (8) Hoveyda, A. H.; Snapper, M. L.; Cole, B.M.; Schimizu, K. D.; Krueger, C. A.; Kuntz, K. W. *Angew. Chem. Int. Ed. Engl.* **1997**, *36*, 1704-1707.
- (9) Jacobsen, E. N.; Sigman, M. S. *J. Am. Chem. Soc.* **1998**, *120*, 4901-4902.
- (10) Hoveyda, A. H.; Snapper, M. L.; Krueger, C. A.; Kuntz, K. W.; Dzierba, C. D.; Wirshun, W. G.; Gleason, J. D. *J. Am. Chem. Soc.* **1999**, *121*, 4284-4285.
- (11) Hoveyda, A.H.; Snapper, M. L.; Porter, J. R.; Wirshun, W. G.; Kuntz, K. W., manuscript provided by A. H. Hoveyda, Boston College, January 2000.
- (12) Crabtree, R. H.; Cooper, A. C.; McAlexander, L. H.; Lee, D.; Torres, M. T. *J. Am. Chem. Soc.* **1998**, *120*, 9971-9972.
- (13) Miller, S. J.; Copeland, G. T. *J. Am. Chem. Soc.* **1999**, *121*, 4306-4307.
- (14) Reetz, M. T.; Zonta, A.; Schimossek, K.; Liebeton, K.; Jaeger, K.-E. *Angew. Chem. Int. Ed. Engl.* **1997**, *36*, 2830-2832.
- (15) Morken, J. P.; Taylor, S. J. *Science* **1998**, *280*, 267-270.
- (16) Reetz, M. T.; Becker, M. H.; Kuhling, K. M.; Holzwarth A. *Angew. Chem. Int. Ed. Engl.* **1998**, *37*, 2647-2650.
- (17) Reetz, M. T.; Becker, M. H.; Liebl, M.; Fürstner, A., manuscript provided by M. T. Reetz, Max-Planck-Institut für Kohlenforschung, January 2000.
- (18) Finn, M.G.; Siuzdak, G.; Guo, J.; Wu, J. *Angew. Chem. Int. Ed. Engl.* **1999**, *38*, 1755-1758
- (19) Reetz, M. T.; Becker, M. H.; Klein, H. W.; Stockigt, D. *Angew. Chem. Int. Ed. Engl.* **1999**, *38*, 1758-1761.
- (20) Mikami, K.; Ding, K.; Ishii, A. *Angew. Chem. Int. Ed. Engl.* **1999**, *38*, 497-501.
- (21) Reetz, M. T.; Kuhling, K. M.; Hinrichs, H.; Deege, A., manuscript provided by M. T. Reetz, Max-Planck-Institut für Kohlenforschung, January 2000.

TOTAL SYNTHESIS OF HERBICIDIN NUCLEOSIDE ANTIBIOTICS

Reported by Chad Davis

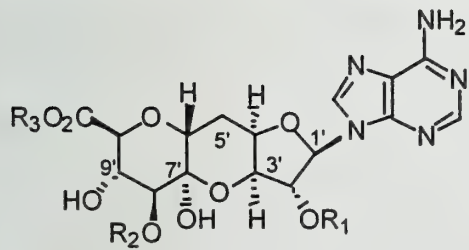
March 9, 2000

INTRODUCTION

The isolation and synthesis of complex nucleoside antibiotics continues to be an active field of natural products chemistry.¹ These molecules are often biologically active and contain interesting structural features. The undecanose skeleton of tunicamycin V, hikizimycin, and the herbicidins is very uncommon and has stimulated several recent total syntheses.¹ This review will cover the isolation, biological activity, and total synthesis of the herbicidins.

ISOLATION AND BIOLOGICAL ACTIVITY

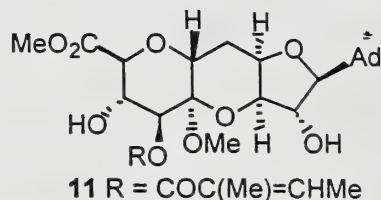
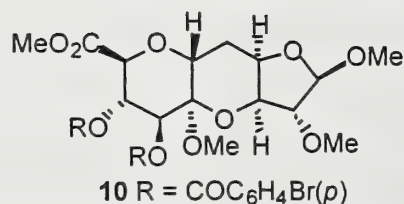
Herbicidins A and B were first isolated in 1976 from the fermentation broth of *Streptomyces saganonensis* by Arai and coworkers (Figure 1).² It was later discovered that herbicidin C and E co-exist in minor proportions with A and B.³ A *S. saganonensis* mutant produced only herbicidins F and G which lead to the conclusion that the latter is a biosynthetic precursor to 1-5.^{4,5} More recently, herbicidin H, aureonuclemycin, and SI-2245 have been discovered.⁶⁻⁸



		R ₁	R ₂	R ₃
Herbicidin A	(1)	Me	COC(CH ₂ OH)=CHMe	Me
Herbicidin B	(2)	Me	H	Me
Herbicidin C	(3)	H	H	Me
Herbicidin E	(4)	Me	COCHMe ₂	Me
Herbicidin F	(5)	Me	COC(Me)=CHMe	Me
Herbicidin G	(6)	H	COC(Me)=CHMe	H
Herbicidin H	(7)	Me	CO(CH ₂ OH)C=CHMe	H
Aureonuclemycin	(8)	H	H	H
SI-2245	(9)	Me	Ac	Me

Figure 1. Structures of the Herbicidins and Related Nucleoside Antibiotics

The structures of the herbicidins were assigned using a combination of IR, UV, NMR spectroscopy; X-ray analysis; and chemical degradation.⁹ In particular, X-ray crystallographic structures were obtained for 10 and 11 which were derived from 2 and 6, respectively. The absolute stereochemistry was determined for 10 using eleven enantiomer-sensitive Bijvoet reflection pairs.



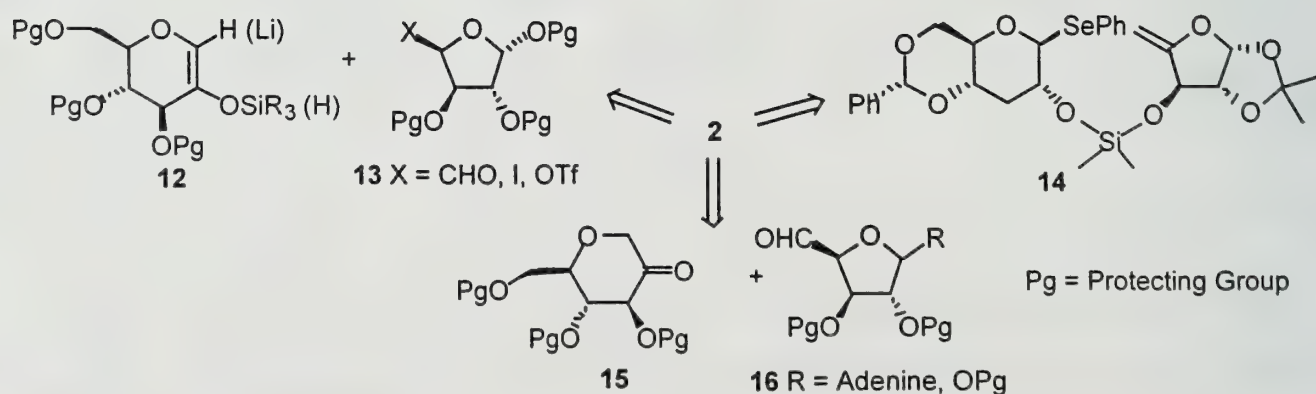
The herbicidins have exhibited a range of biological activities. It was shown that **1-4** inhibit seed germination while **1** and **2** are toxic to certain mono- and dicotyledonous plants.^{2,3} In addition, **1**, **2**, and **8** inhibit the bacterium *Xanthomonas oryzae* which causes leaf blight infection in rice crops.^{2,7} Compounds **1**, **2**, **5**, **6**, and **9** have been shown to inhibit the growth of certain fungi.^{2,4,8}

RETROSYNTHETIC STRATEGIES

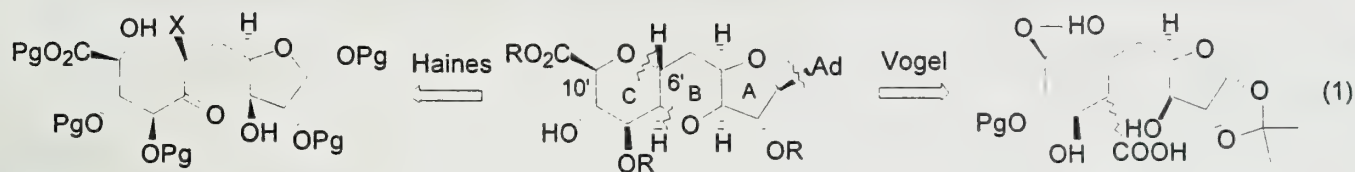
The synthetic strategies revolve primarily around a C5'-C6' disconnection. This approach reflects the general plan to have a ketone group at the C7' position which upon deprotection of a C3' hydroxyl group would cyclize to the hemiketal. Gallagher and Whitting envisioned using silyl enol ethers and vinyl lithium reagents to couple components of general structure **12** and **13** which would avoid problems associated with regioselective enolization (Scheme 1).¹⁰⁻¹⁴ Alternatively, Sinay and coworkers have investigated the radical cyclization of **14** to construct the C5'-C6' bond (Scheme 1).¹⁵

The condensation of ketones **15** with aldehydes **16** offers the advantage that the ketone carbonyl group does not need to be installed later in the synthesis (Scheme 1). However, methods for regioselective enolization were needed. Gallagher and Matsuda have developed methods to control enolization using structural constraints and reductive cleavage.¹⁶⁻²¹

Scheme 1.



The synthetic strategies adopted by Haines and Vogel disconnect the C6'-C10' ether linkage prior to forming the C5'-C6' bond (eq 1),^{22,23} avoiding problems associated with regioselective enolate formation. However, the C-ring must be formed later in the synthesis, thereby rendering this route less convergent.

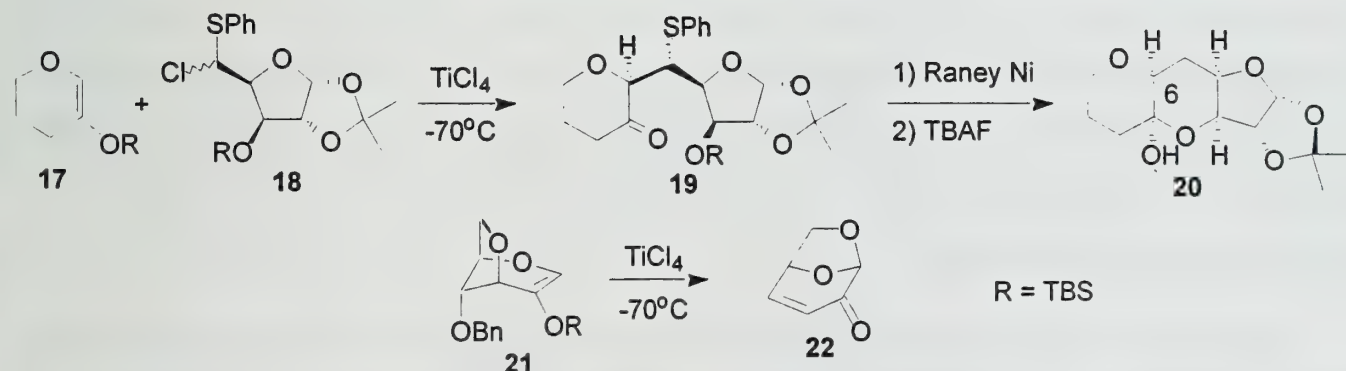


FORWARD SYNTHESIS

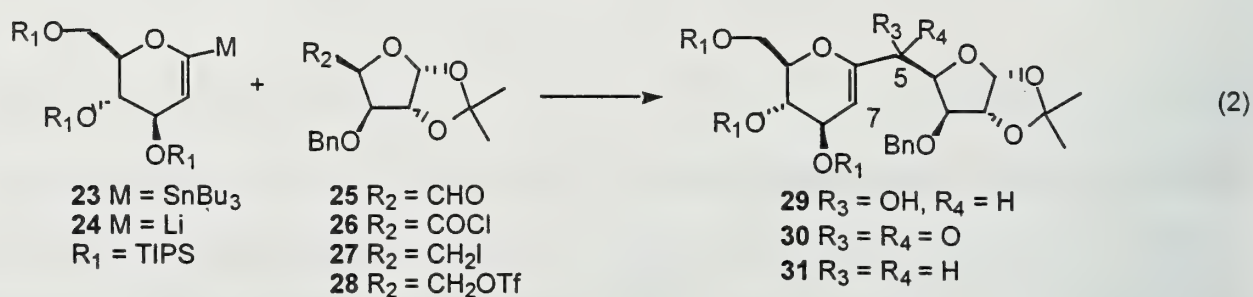
Use of Enol Ethers and Vinyl Lithium Reagents

The early synthetic investigations utilized enol ethers to generate the anomeric nucleophile. The use of β -lithiated enol ethers as synthons in herbicidin synthesis was first envisioned by Gallagher in a model study.^{10,11} Although successful, this approach was quickly abandoned in favor of the milder reaction conditions of Lewis acid-activated silyl enol ethers.¹¹⁻¹³ The alkylation of silyl enol ether **17** with α -chloro sulfide **18** in the presence of TiCl_4 gave a 4:1 mixture of diastereomers in 70% yield (Scheme 2). The major isomer **19** was converted to hemiketal **20** in 50% yield. The structures of **19** and **20** were determined by X-ray crystallography and found to be epimeric at C6 to the herbicidin skeleton. The functionalized silyl enol ether **21** underwent TiCl_4 -catalyzed rearrangement and elimination to give enone **22** (Scheme 2),¹³ precluding its alkylation with **18**.

Scheme 2.



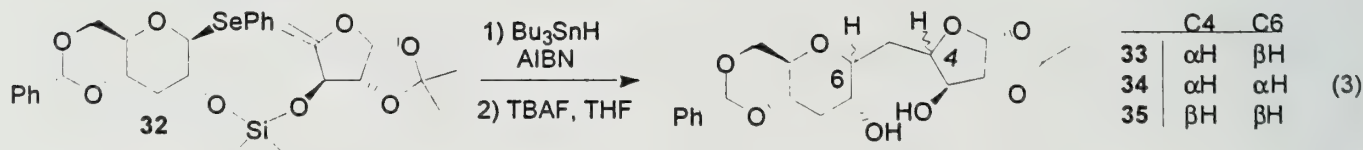
The use of vinyl lithium reagents to form the C5-C6 bond was investigated by Whiting (eq 2).¹⁴ The addition of vinyl lithium **24**, obtained from **23** by tin-lithium exchange, to aldehyde **25** afforded a 2.1:1 mixture of epimeric C5 alcohols **29** (31%). Likewise, reaction of the vinyl lithium reagent with acid chloride **26** gave poor yields (21%) of ketone **30**. Owing to the low yields and problems during C5-deoxygenation, Whiting focused on direct alkylation of the vinyl lithium reagent with iodide **27** and triflate **28**. The iodide gave only a mixture of products; however, the triflate proceeded to give olefin **31** in 41% yield.



Attempts to install the ketone at C7 and control the stereochemistry at C6 via epoxidation of the olefin followed by rearrangement were unsuccessful. Hence, the vinyl lithium approach avoids removal of the C5 hydroxyl group, but conversion of the olefin to the C7 ketone proved to be a disadvantage.

Radical Cyclization Attempt

The use of a radical cyclization protocol to form the C5-C6 bond was employed by Sinay.¹⁵ The seleno glycoside was tethered to the exomethylene furanose via a silyl ether bridge to give **32**. The cyclization reaction followed by deprotection gave a 7.2:2.2:1 mixture of **33**, **34**, and **35** in 62% yield (eq 3). The stereochemistry of the major isomer corresponds to the herbicidin skeleton.

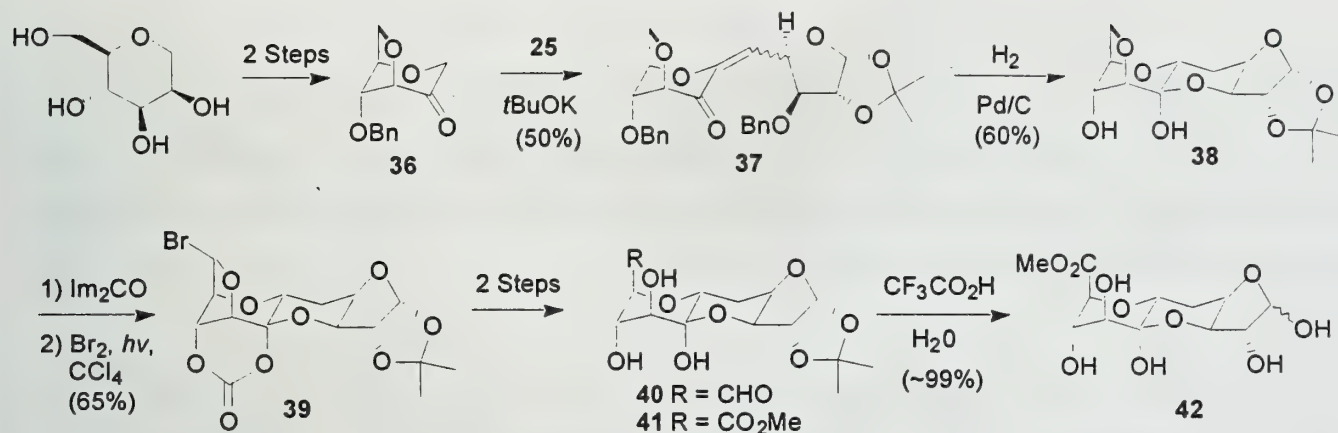


Use of Regio-Controlled Enolates

Gallagher envisioned that the bicyclic constraint of ketone **36** would enforce regioselective enolization (Scheme 3).^{16,17} Therefore, the aldol condensation of ketone **36** with aldehyde **25** gave enone **37** as a single isomer of unknown double bond configuration. The face-selective hydrogenation of

the olefin and removal of the benzyl protecting group initiated cyclization to afford **38**. The 7',9'-diol was protected as the carbonate and ensuing radical bromination gave α -bromo ether **39**. The aldehyde **40** was prepared by methanolysis of the cyclic carbonate followed by Ag(I)-mediated hydrolysis of the α -bromo ether. Finally, the aldehyde was oxidized to the methyl ester **41** (50% from **39**) and the structure was verified by X-ray crystallography. Hydrolysis of the isopropylidene group gave **42** as a 1:1.5 (α : β) mixture of C1 anomers, thereby completing the first synthesis of the undecanose core.

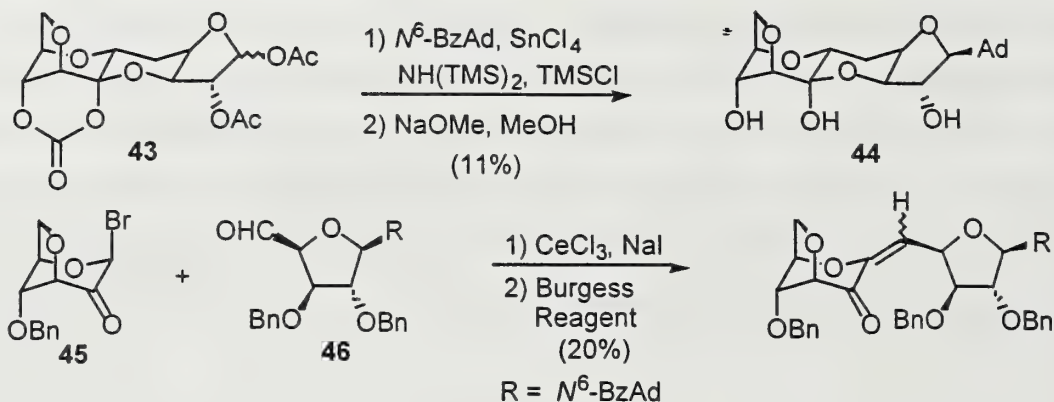
Scheme 3.



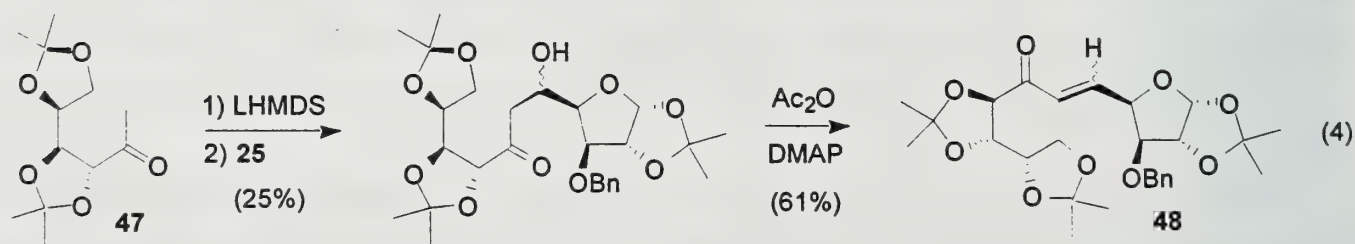
En route to installing the adenine, Gallagher converted the cyclic carbonate of **38** to the corresponding acetates **43** by hydrolysis and acetylation (Scheme 4).¹⁹ Although the heterocycle was successfully introduced by Vorbruggen adenylation to give herbicidin mimic **44**, the adenine unit would not survive the radical bromination conditions used to cleave the bridging ether.

In a strategy to install the adenine unit early in the synthesis, Gallagher prepared the aldehyde **46** from D-glucose in 23% yield.¹⁸ Since aldehyde **46** did not survive the KO^tBu -promoted adol condensation with ketone **36**, investigations were conducted to generate the enolate by reduction of the α -bromo ketone **45** (Scheme 4). This protocol was successful and used to synthesize the corresponding enone. Unfortunately, the preceding problems associated with cleaving the bridging ether prevented access to the herbicidins.

Scheme 4.



The crossed aldol condensation of aldehyde **25** and ketone **47** investigated by Haines gave a 1:1 mixture of alcohols that was dehydrated to enone **48** ($E:Z=95:5$) (eq 4).²² The initial plans to epoxidize the olefin followed by alkoxide-induced ring closure to form the C-ring were abandoned after rearrangements plagued the epoxidation. In an alternative attempt, **48** was treated with iodine to induce cyclization; however, this method was also unsuccessful.

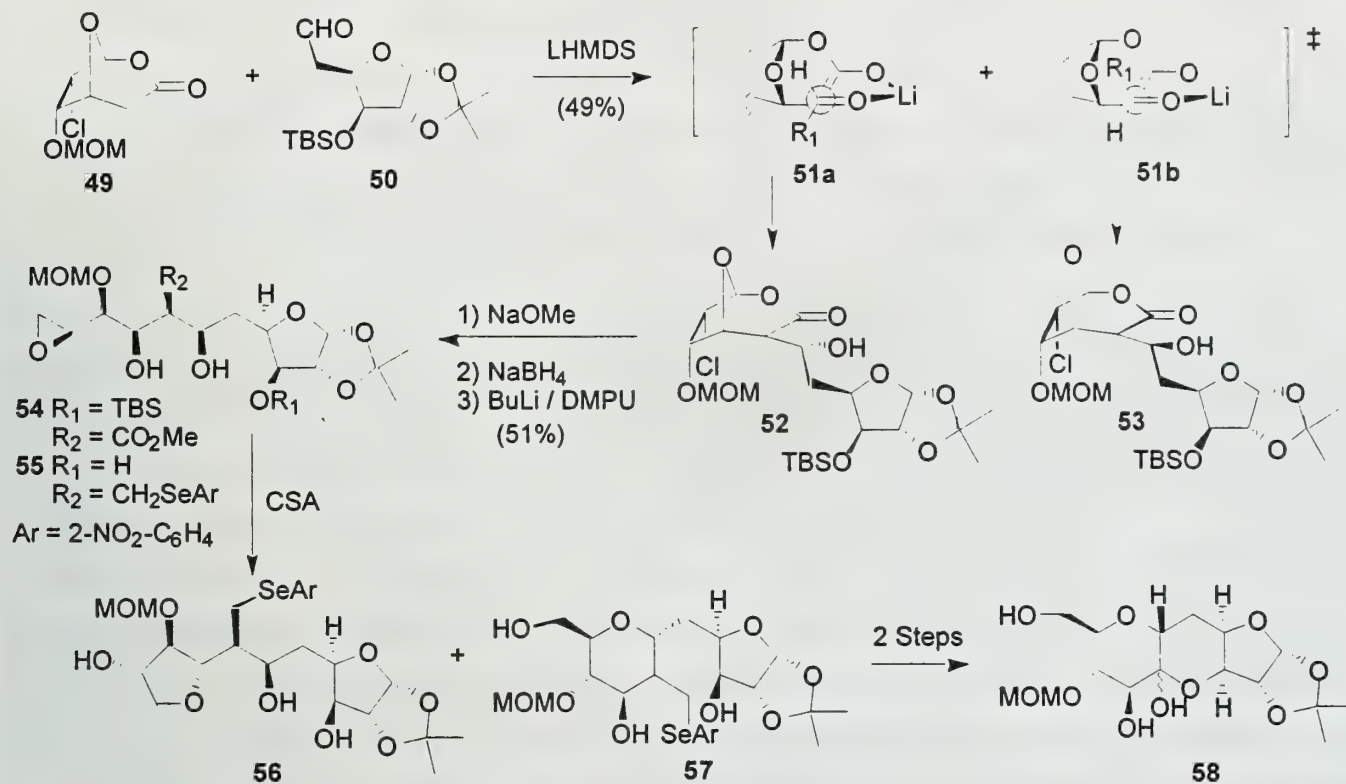


A synthesis of the undecanose core of the herbicidins was completed by Vogel (Scheme 5).²³ The aldol reaction of **49** and **50** gave the exo products exclusively as a 4.5:1 mixture of **52** and **53**, respectively. The C6 stereochemistry was assigned based on the assumption that the major isomer would arise from the sterically less demanding cyclic transition state **51a**. The minor isomer could result from **51b** where the bulky furanose ring would have destabilizing steric interactions with the bridging oxygen. The major isomer was separated by column chromatography and converted to the epoxy diol **54**.

The next stage of the synthesis involved construction of the C-ring. The acid-catalyzed cyclization of **54** failed with a variety of protic and Lewis acids. Reaction of seleno diol **55** with camphorsulfonic acid afforded a 1:2 mixture of **56** and **57** that was converted to the corresponding

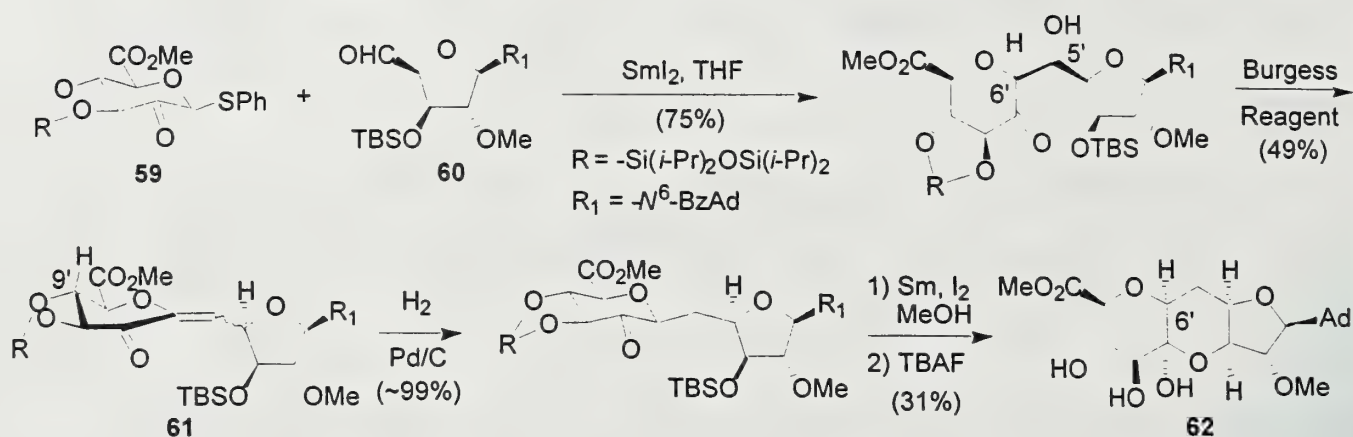
olefins by selenoxide elimination. Finally, separation of the alkenes followed by ozonolysis gave **58** (19% from **55**) as ~2:1 mixture of anomers.

Scheme 5.

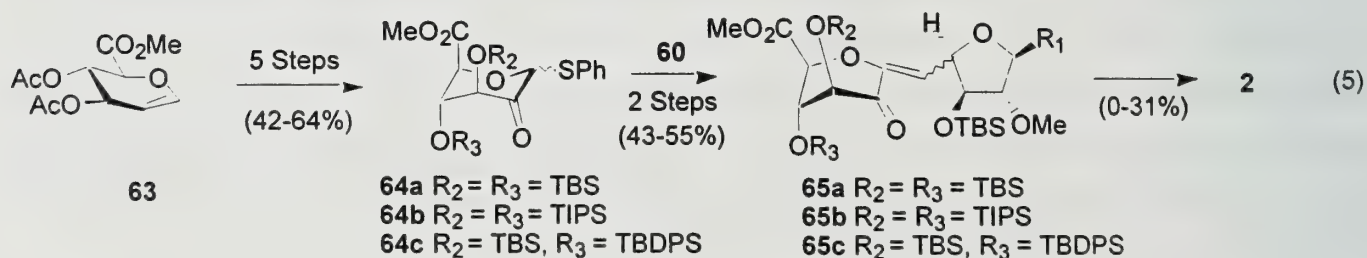


Matsuda developed a regioselective SmI₂-promoted aldol C-glycosidation which was showcased in the first synthesis of herbicidin B.^{20,21} The addition of aldehyde **60** to the samarium enolate from reduction of **59** gave a mixture of keto alcohols that was dehydrated to enone **61** as a mixture of cis/trans isomers (Scheme 6). Catalytic hydrogenation of the enone mixture gave exclusively the C6' epimer of the herbicidins. The selectivity was rationalized based on C6'-isomerization and the steric bias of the C9' axial hydrogen during hydrogenation. Removal of the benzyl and silyl protecting groups was followed by spontaneous ketalization giving 6'-epi-herbicidin B (**62**). Exposure of **62** to both acidic and basic conditions failed effect isomerization to herbicidin B.

Scheme 6.



In order to alter the stereoselectivity of the olefin reduction, Matsuda made use of previous reports demonstrating that bulky protecting groups on vicinal diols favor the $^1\text{C}_4$ -conformation.²⁴ In this conformation, the R_3 -substituent (eq 5) may partially shield the α -face during the reduction. However, if α -face delivery of hydrogen does occur, C6' -isomerization would then give the desired equatorial product. Therefore, the bis silyl ethers **64a-c** were synthesized from glycal **63**. The corresponding enones **65a-c** were prepared in the same manner as single isomers of unknown olefin geometry. The $^1\text{C}_4$ -conformation of the enones was evident from the small coupling constants of the pyranose ring protons ($J_{8'9'} = 0\text{-}2\text{ Hz}$ and $J_{9'10'} = 3\text{-}4\text{ Hz}$). While **65a** proved to be resistant to a variety of reducing conditions, reduction of **65c** with $\text{HCO}_2\text{NH}_4/\text{Pd-C}/\text{MeOH}$ followed by $\text{Sm}/\text{I}_2/\text{MeOH}$ and TBAF/THF to remove the appropriate protecting groups gave herbicidin B. The ^1H NMR spectra and optical rotation data were in accord with those of the authentic sample. This constitutes the first synthesis of (+)-herbicidin B which was accomplished in 10 steps and 10% overall yield.



CONCLUSION

The herbicidins occupy a unique niche within the class of nucleoside antibiotics. The selective herbicidal activity and uncommon undecanose core have made them popular targets for total synthesis. The early model studies used enol ethers, vinyl lithium reagents, and radical cyclizations to construct the C5'-C6' bond. However, these methods have not successfully addressed installation of the adenine or formation of the hemiketal. The aldol condensation of a C7' ketone to form the C5'-C6' bond was accomplished by Gallagher using a bridged ether to control enolization. However, cleavage of the bridged ether ultimately denied access to the herbicidins. The approach adopted by Haines and Vogel avoided the regioselective enolization issue. However, Haines was unable to construct the C-ring and Vogel's synthesis did not address installing the adenine. As an alternative, Matsuda developed a mild regioselective enolization protocol that proved to be amenable to the fragile aldehyde coupling partner. This process in conjunction with the clever use of protecting groups lead to the first successful synthesis of a herbicidin. These syntheses have demonstrated a variety of avenues to generate the anomeric nucleophile. However, Matsuda's highly convergent approach is clearly superior and at the present time would be the method of choice for synthesis of herbicidin analogs.

REFERENCES

- (1) Knapp, S. *Chem. Rev.* **1995**, *95*, 1859.
- (2) a) Arai, M.; Haneishi, T.; Kitahara, N.; Enokita, R.; Kawakubo, K.; Kondo, Y. *J. Antibiot.* **1976**, *29*, 863. b) Haneishi, T.; Terahara, A.; Kayamori, H.; Yabe, J.; Arai, M. *J. Antibiot.* **1976**, *29*, 870.
- (3) Takiguchi, Y.; Yoshikawa, H.; Terahara, A.; Torikata, A.; Terao, M. *J. Antibiot.* **1979**, *32*, 857.
- (4) Takiguchi, Y.; Yoshikawa, H.; Terahara, A.; Torikata, A.; Terao, M. *J. Antibiot.* **1979**, *32*, 862.
- (5) Yoshikawa, H.; Takiguchi, Y.; Terao, M. *J. Antibiot.* **1983**, *36*, 30.
- (6) Kizuka, M.; Enokita, R.; Takahashi, K.; Okamoto, Y.; Otsuka, T.; Shigematsu, Y.; Inoue, Y.; Okazaki, T. *Actinomycetologica* **1998**, *12*, 89.
- (7) Dai, X.; Li, G.; Wu, Z.; Lu, D.; Wang, H.; Li, Z.; Zhou, L.; Chen, X.; Chen, W. Faming Zhuanli Shenqing, Gongkai Shuomingshu CN 87,100,250; *Chem Abstr.* **1989**, *111*, 230661f.
- (8) Tsuzuki, M.; Suzuki, G. Jpn. Kokai Tokkyo Koho JP 62,238,218; *Chem Abstr.* **1988**, *109*, 53206x.
- (9) Terahara, A.; Haneishi, T.; Arai, M. *J. Antibiot.* **1982**, *33*, 1711.
- (10) Cox P.; Mahon, M.F.; Molloy, K.C.; Lister, S.; Gallagher, T. *Tetrahedron Lett.* **1988**, *29*, 1993.
- (11) Cox, P.; Lister, S.; Gallagher, T. *J. Chem. Soc. Perkin Trans. I* **1990**, 3151.
- (12) Cox, P.; Mahon, M.F.; Molloy, K.C.; Lister, S.; Gallagher, T. *Tetrahedron Lett.* **1989**, *30*, 2437.
- (13) Cox, P.J.; Griffin, A.M.; Newcombe, N.J.; Lister, S.; Ramsay, M.; Alker, D.; Gallagher T. *J. Chem. Soc. Perkin Trans. I* **1994**, 1443.
- (14) a) Bearder, J.R.; Dewis, M.L.; Whiting, D. *J. Chem. Soc. Perkin Trans. I* **1995**, 227.

- b) Bearder, J.R.; Dewis, M.L.; Whiting, D. *SynLett* **1993**, 805.
- (15) Fairbanks, A.J.; Perrin, E.; Sinay, P. *Synlett* **1996**, 679.
- (16) Griffin, A.M.; Newcombe, N.J.; Alker, D.; Ramsay, M.; Gallagher, T. *Heterocycles* **1993**, 35, 1247.
- (17) Newcombe, N.; Mahon, M.F.; Molloy, L.C.; Alker, D.; Gallagher, T. *J. Am. Chem. Soc.* **1993**, 115, 6430.
- (18) a) Binch, H.M.; Griffin, A.M.; Gallagher, T. *Pure & Appl. Chem.* **1996**, 589-692. b) Binch, H.M.; Griffin, A.M.; Schwidetzky, S.; Ramsay, M.; Gallagher, T.; Lichtenthaler, F.W. *J. Chem. Soc. Chem. Commun.* **1995**, 967
- (19) Binch, H.M.; Gallagher, T. *J. Chem. Soc., Perkin Trans. 1* **1996**, 401.
- (20) Ichikawa, S.; Shuto, S.; Matsuda, A. *J. Am. Chem. Soc.* **1999**, 121, 10270.
- (21) Ichikawa, S.; Shuto, S.; Matsuda, A. *Tetrahedron Lett.* **1998**, 39, 4525.
- (22) Hines, A.H.; Lamb, A.J. *Carbohydr. Res.* **1999**, 321, 197.
- (23) a) Emery, F.; Vogel, P. *J. Org. Chem.* **1995**, 60, 5843. b) Emery, F.; Vogel, P. *Tetrahedron Lett.* **1993**, 34, 4209.
- (24) a) Walford, C.; Jackson, R.F.W.; Rees, N.H.; Clegg, W.; Heath, S.L. *Chem. Commun.* **1997**, 1855. b) Roush, W.R.; Sebesta, S.P.; Nennett, C.E. *Tetrahedron* **1997**, 53, 8825.

SYNTHESIS OF CEPHALOSTATINS AND RITTERAZINES: UNSYMMETRICAL DIMERIC STEROID PYRAZINE MARINE ALKALOIDS

Reported by Yu Fan

March 24, 2000

INTRODUCTION

Cephalostatins and ritterazines are among the most powerful anticancer agents ever tested by the National Cancer Institute (NCI).¹ The key structural feature of this family of marine natural products (Figure 1) is the pyrazine ring that joins two different steroids together. How these structures are produced in nature and how they are related to the biological activities of the molecules are interesting questions. These dimeric complex steroidal pyrazines are also challenging targets for synthesis. This review will cover the development of methods for formation of unsymmetrical steroidal pyrazines and their application to the synthesis of cephalostatin 1 from an available steroid precursor.

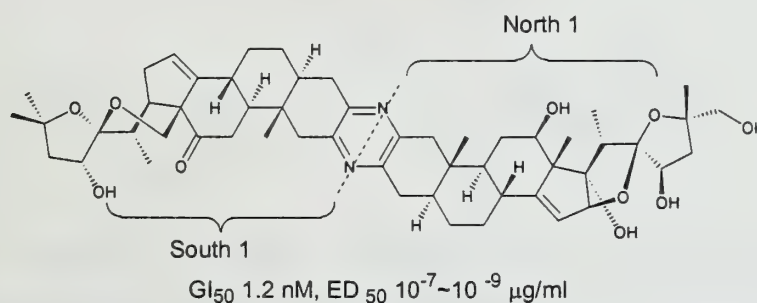


Figure 1. Structure and biological activity data for cephalostatin 1

ISOLATION AND STRUCTURE

To date, forty-five dimeric steroidal pyrazines have been isolated from marine sources. Nineteen cephalostatins were obtained from *Cephalodiscus gilchristi*, a tube marine worm collected off the coast of South Africa. Cephalostatin 1 (Figure 1), the prototype of this family of natural products, was first isolated and characterized in 1988 by Pettit.² Its unusual structure consists of nine fused rings formed by the connection of two steroid units at C2 and C3 via a pyrazine core. In addition, two spiroketal rings terminate each end, generating a total of 13 rings. Over the years, the Pettit group has characterized eighteen additional cephalostatins.^{3a~h} All cephalostatins have fused ring structures formed by dimerizing steroidal units. Interestingly, variations arise mainly in the south half of the molecule, while the north half is identical in 17 members.

Ritterazines were isolated by the Fusetani group from *Ritterella tokioka*, a tunicate collected off the coast of Japan.^{4a~d} The structure of ritterazine A (Figure 2), the first member to be characterized, is closely related to that of cephalostatins. The rearranged north half structure was proposed to be derived,

Copyright © 2000 by Yu Fan

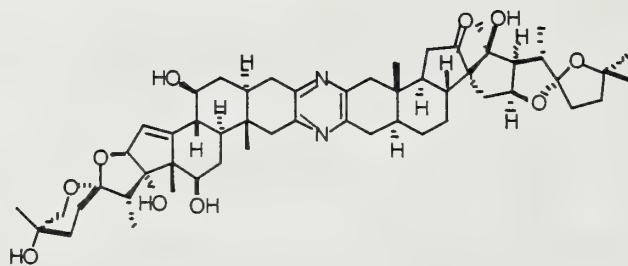
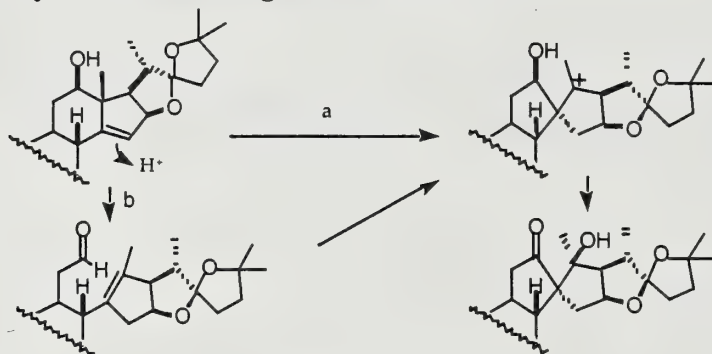


Figure 2. Structure of ritterazine A

biosynthetically, by the protonation of C14 double bond, followed by either a 1,2 Wagner-Meerwein shift (path a) or *retro*-Prins ring opening and the opposite Prins ring closure (path b) (Scheme 1).

Scheme 1. Proposed biosynthetic rearrangement to ritterazine A



This proposal is supported by the subsequent isolation of ritterazine G (Figure 3) with an unrearranged north half structure. Pettit proposed that these dimeric steroid pyrazines are derived from condensation of 3-oxo-2-amino steroids.² However, the details of the biosynthetic pathway and biological functions of the compounds remain unknown.

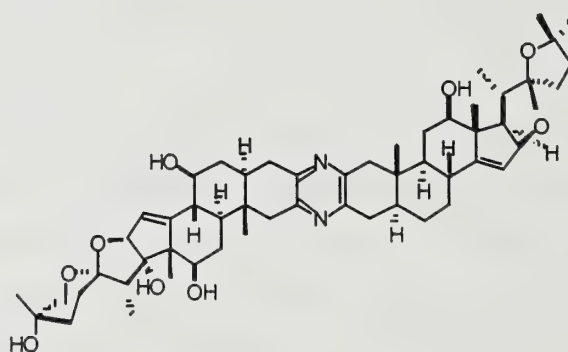


Figure 3. Structure of ritterazine G

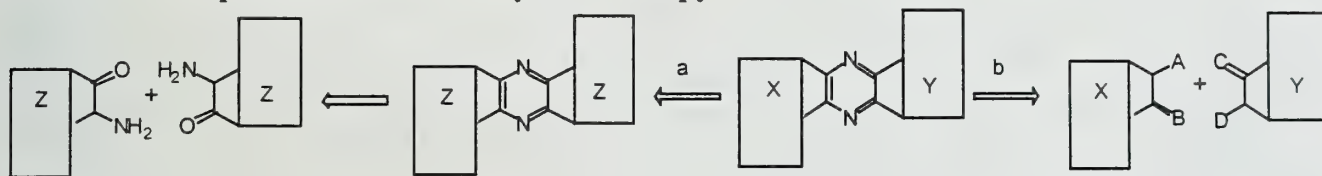
Both cephalostatins and ritterazines were found to be highly cytotoxic to sixty human tumor cell lines in the NCI's new test.^{3c} More interestingly, the cytotoxicity profiles of these pyrazines are different from those of all known anticancer agents. But within the cephalostatin-ritterazine family all

the compounds displayed similar cytotoxicity trends over all sixty tumor cell lines of the test panel, suggesting that these compounds inhibit tumor cell growth by the same as yet unknown mechanism.^{3h}

SYNTHESIS

A wealth of structure activity relationship (SAR) data has been obtained for these natural products. However, the severe difficulty in harvesting the marine sources has hindered clinical trials and efforts on elucidating the mechanism of cytotoxicity. Consequently, synthesis of the cephalostatins and ritterazines has become an urgent task for chemists. Two routes towards these complex molecules can be envisioned, depending on the timing of pyrazine ring formation during the synthesis. The first involves desymmetrization of two identical steroid units after the pyrazine has been formed (Scheme 2, route a). The second is to form an unsymmetrical pyrazine by direct attachment of different subunits (route b). Although route a simplifies the synthesis of the pyrazine core, it would require more linear steps to install two different steroid spiroketals. Route b is more convergent but an efficient method for constructing unsymmetrical pyrazines is necessary for the success of this approach.

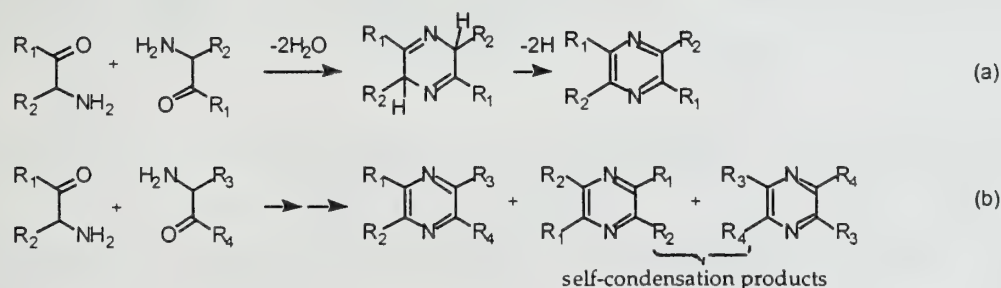
Scheme 2. Two possible routes to unsymmetrical pyrazines



Pyrazine Formation

One general method for pyrazine synthesis involves the dimerization of α -amino ketones followed by mild oxidation to effect aromatization (Scheme 3, eq a).⁵ This self-condensation leads to the formation of symmetrical pyrazines. However, reactions between different α -amino ketones typically provide mixtures of the unsymmetrical pyrazines and the two self-condensation products (eq b). Although this route effects regiospecific formation of symmetrical pyrazines, it is intrinsically inefficient without differentiation between self- and cross- condensation.

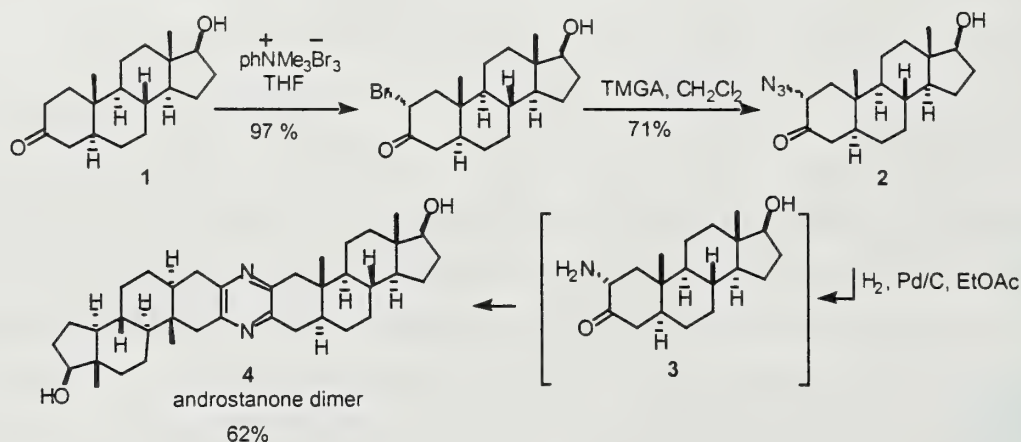
Scheme 3. Regiospecific pyrazine formation from α -amino ketones



Application of this amino ketone condensation-oxidation procedure to symmetrical steroidal pyrazines has been investigated by Fuchs (Scheme 4).⁶ Bromination of androstanone **1**, followed by

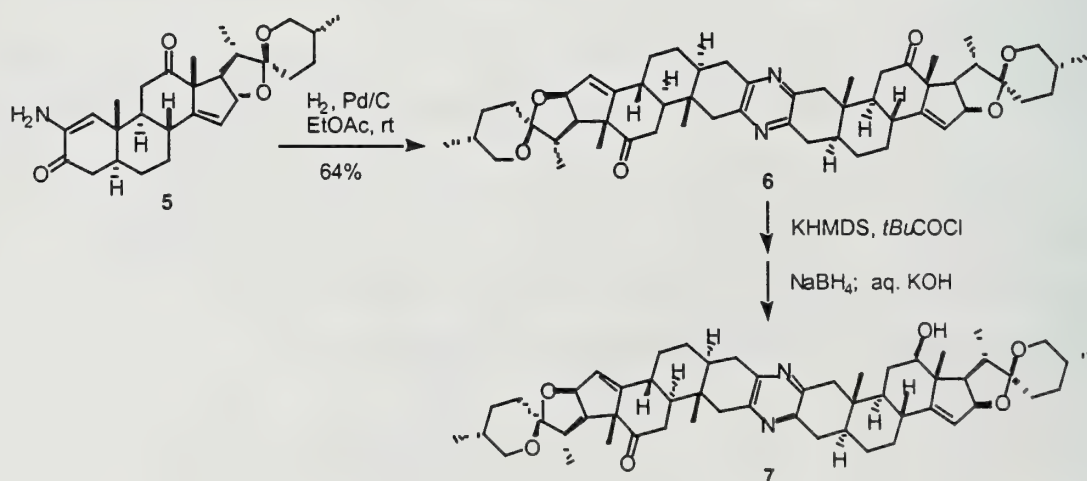
substitution with tetramethylguanidium azide (TMGA) provided α -azido ketone **2**. Hydrogenation afforded amino ketone **3**, which underwent spontaneous self-condensation and air oxidation to dimer **4**.

Scheme 4. Preparation of androstanone pyrazine dimer

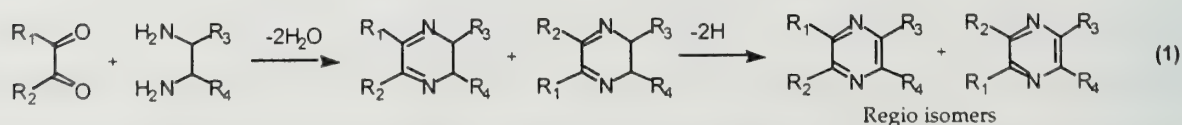


Winterfeldt synthesized pyrazine **6** via reducing enamino ketone **5** (Scheme 5).⁷ Subsequent desymmetrization of **6** was achieved by conversion to the mono enol pivalate, followed by borohydride reduction and hydrolysis to unsymmetrical keto alcohol **7**. These results showed that unsymmetrical steroid pyrazines can be easily prepared from an α -amino ketone steroid precursor.

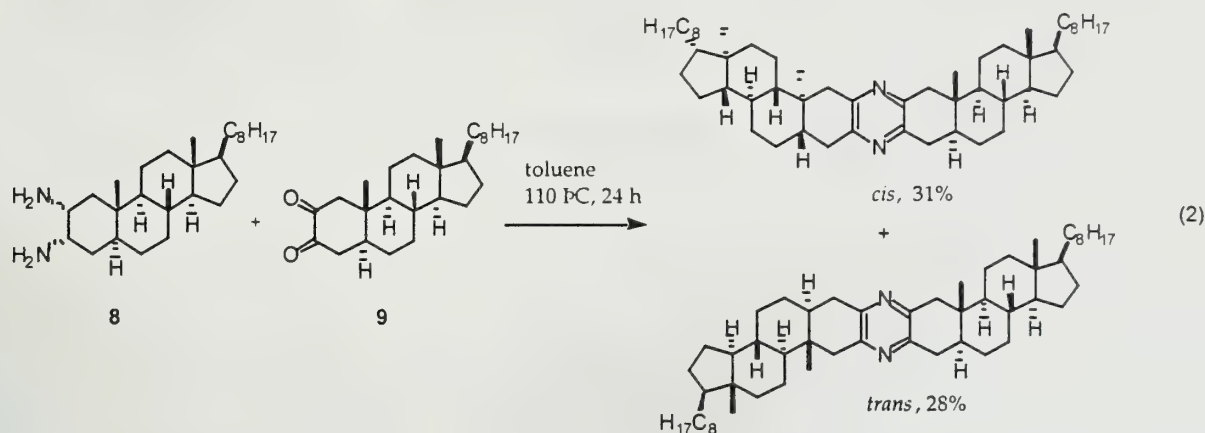
Scheme 5. Synthesis of hecogenin-pyrazine dimer



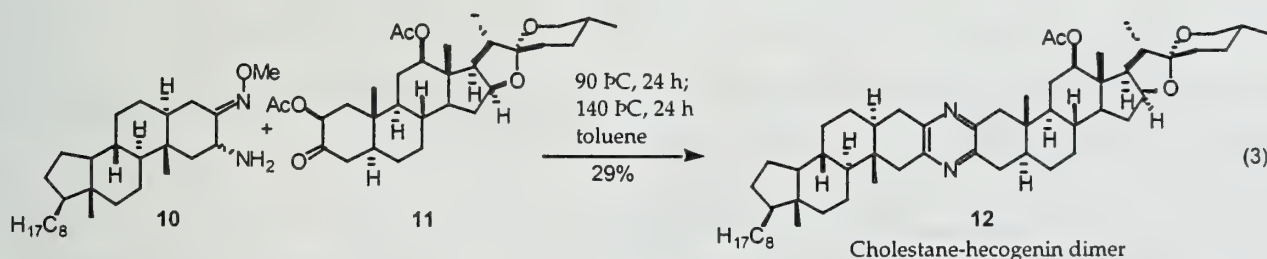
The condensation of 1,2-diketones with 1,2-diamines, followed by oxidation of the dihydropyrazine,



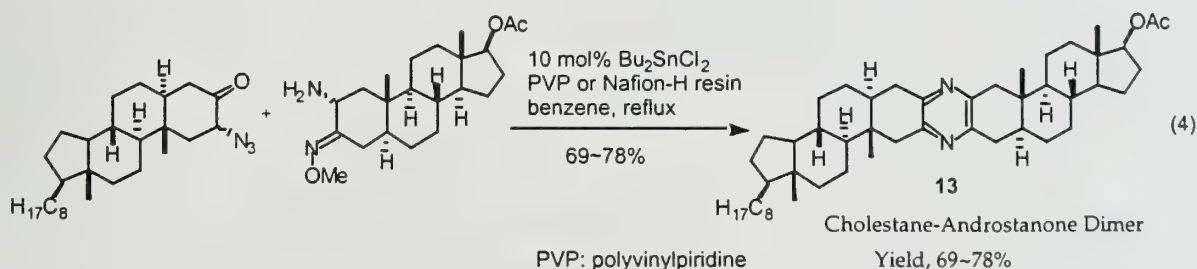
has been widely used for the synthesis of alkyl and aryl pyrazines (Eq 1).⁵ Typically, these reactions provide mixtures of regioisomers from both condensation modes. For example, the reaction of diketone **9** with diamine **8** results in the formation of a 1:1 mixture of *cis* and *trans* products (Eq 2).^{8a}



Heathcock achieved the first synthesis of unsymmetrical dimers by employing a two-stage condensation protocol (Eq 3)^{8b}. α -Amino oxime **10** reacted preferentially with α -acetoxy ketone **11** at 90 °C to form uncharacterized intermediates which proceeded onto the pyrazine **12** at 140 °C. In practice, however, the harsh conditions and the low yield compromise the utility of this method.

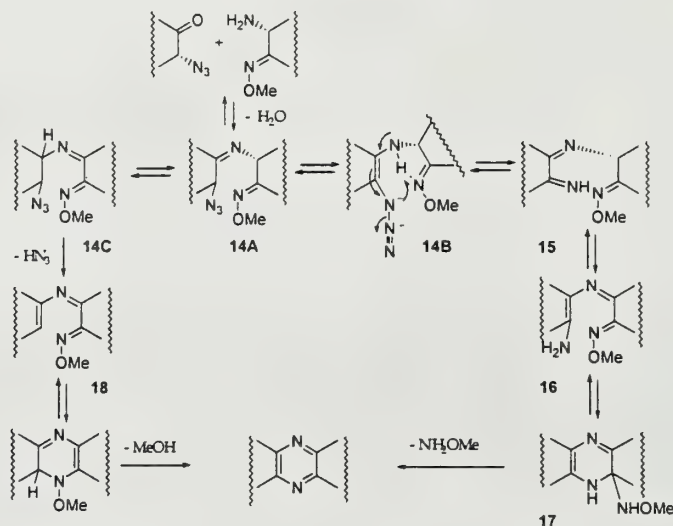


An alternative condensation described by Fuchs in 1996, employs an α -azido ketone as the acceptor instead of the α -acetoxy ketone (Eq 4).⁹ In the presence of 10 mol% catalyst Bu_2SnCl_2 , and either a basic or acidic resin additive, the α -amino *O*-methyloxime and α -azido ketone shown condensed to yield unsymmetrical pyrazine **13** in 69~78% yield. The reaction conditions are much milder and the yield is higher than those reported by Heathcock's protocol.

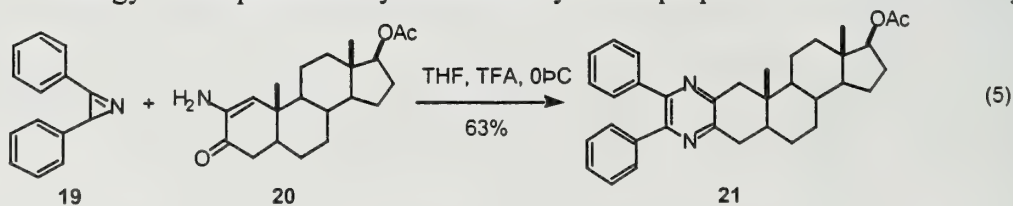


Fuchs proposed two possible mechanisms for the new pyrazine construction method. One involves the formation of the bisimine intermediate **14A** followed by fragmentation of tautomer **14B** and cyclization through intermediates **15**~**17** (Scheme 6). The function of the basic or acidic resin may be to facilitate the tautomerization steps thus improving the yield. Another mechanism involves the thermal rearrangement of intermediate **18**, which may be formed by losing hydrazoic acid from imine intermediate **14A** or its tautomer **14C**.

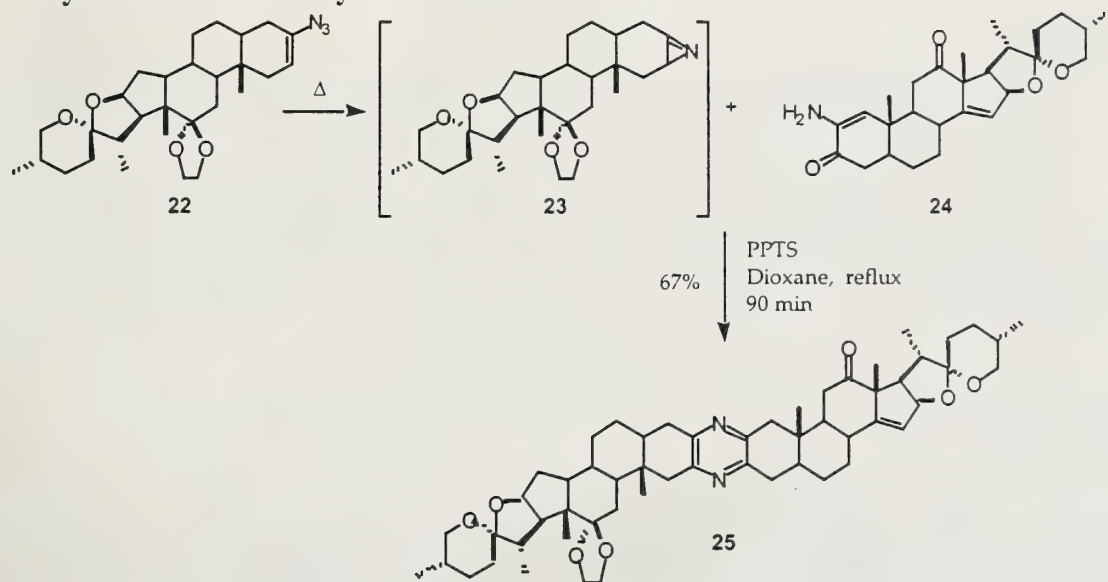
Scheme 6. Proposed mechanisms for pyrazine formation



Another approach to the synthesis of unsymmetrical pyrazines reported by Winterfeldt,¹⁰ employs an azirine as a nondimerizing equivalent of an α -amino ketone. Reaction of azirine **19**, easily prepared from *trans*-stilbene, with enamino ketone **20** and trifluoroacetic acid (TFA) at 0°C in THF provided pyrazine **21** in 63% yield (Eq 5). However, the preparation of the unstable steroidal azirine was unsuccessful. This problem was circumvented by generating the azirine **23** *in situ* through the thermal decomposition of vinyl azide **22** (Scheme 7). In the presence of the enamino ketone **24**, the transient azirine was trapped to provide unsymmetrical pyrazine **25** in 67% yield. However, the potential of this strategy is compromised by the difficulty in the preparation of steroidal vinyl azide.



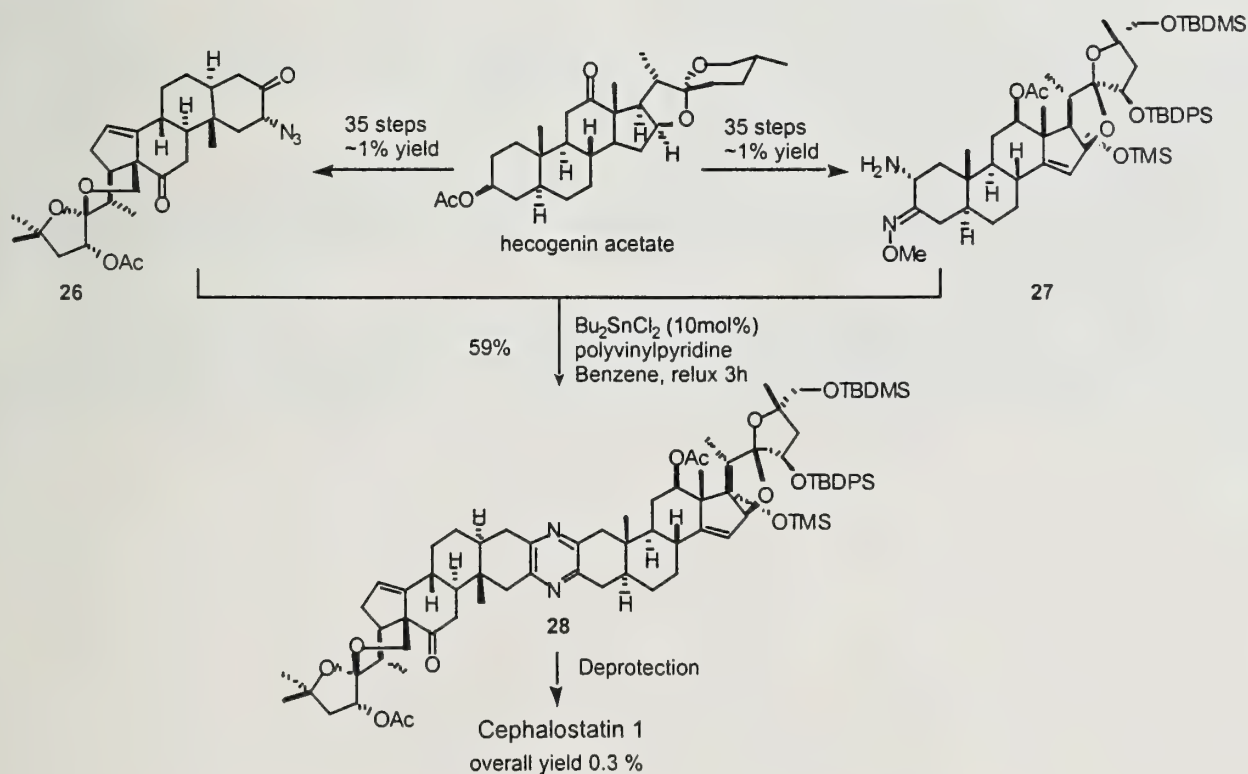
Scheme 7. Pyrazine formation by azirine-enamino ketone condensation



Total Synthesis of Cephalostatin 1 from Hecogenin Acetate

Recently Fuchs accomplished the total synthesis of cephalostatin 1 (Scheme 8).¹¹ The highlight was the successful joining of the highly functionalized steroidal moieties. The condensation between α -azido ketone **26** and α -amino *o*-methyloxime **27** proceeded in 59% yield to the unsymmetrical pyrazine **28**, demonstrating the effectiveness of this protocol in the synthesis of complex dimeric steroidal pyrazine.

Scheme 8. Total synthesis of cephalostatin 1



CONCLUSIONS

The isolation of the cephalostatins by the Pettit group has set the stage for the development of a new class anticancer drugs. Accomplishment of the total synthesis of cephalostatin 1 has started to provide material for clinical trials and demonstrated the effectiveness of total synthesis in drug development. The invention of new methods for unsymmetrical pyrazine formation has opened the way to cephalostatin analogues and provided firm ground for further studies of structure activity relationships.

REFERENCES

- (1) Ganesan, A. *Angew. Chem. Int. Ed. Engl.* **1996**, *35*, 611-614.
- (2) Pettit, G. R.; Inoue, M.; Kamano, Y.; Herald, D. L.; Arm, C.; Dufresne, C.; Christie, N. D.; Schmidt, J. M.; Doubek, D. L.; Krupa, T. S. *J. Am. Chem. Soc.* **1988**, *110*, 2006-2007
- (3) (a) Pettit, G.R. et al. *Chem. Soc. Chem. Commun.* **1988**, 865-867. (b) Pettit, G.R. et al. *Can. J. Chem.* **1989**, *67*, 1509-1513. (c) Pettit, G.R. et al. *J. Org. Chem.* **1992**, *57*, 429-431. (d) Pettit, G.R. et al. *J. Nat. Prod.* **1994**, *57*, 52-63. (e) Pettit, G.R. et al. *Can. J. Chem.* **1994**, *72*, 2260-2267. (f) Pettit, G.R. et al. *Bioorg. Med. Chem. Lett.* **1994**, *4*, 1507-1512. (g) Pettit, G.R. et al. *Bioorg. Med. Chem. Lett.* **1995**, *5*, 2027-2032. (h) Pettit, G.R. et al. *J. Nat. Prod.* **1998**, *61*, 953-957.
- (4) (a) Fukuzawa, S.; Matsunaga, S.; Fusetani, N. *J. Org. Chem.* **1994**, *59*, 6164-6166. (b) Fukuzawa, S.; Matsunaga, S.; Fusetani, N. *J. Org. Chem.* **1995**, *60*, 608-614. (c) Fukuzawa, S.; Matsunaga, S.; Fusetani, N. *J. Tetrahedron* **1995**, *51*, 6707-6716. (d) Fukuzawa, S.; Matsunaga, S.; Fusetani, N. *J. Org. Chem.* **1997**, *62*, 4484-4491.
- (5) Barlin, G. B. In *The Chemistry of Heterocyclic Compounds*; Weissberger, A.; Taylor, E. C., Eds; Wiley: New York, 1982; Vol 41, The Pyrazines.
- (6) Pan, Y.; Merriman, R.L.; Tanzers, L. R.; Fuchs, P. L. *Bioorg. Med. Chem. Lett.* **1992**, *2*, 967-972.
- (7) Kramer, A.; Ullmann, U.; Winterfeldt, E.; *J. Chem. Soc. Perkin. Trans. I* **1993**, 2865-2867.
- (8) (a) Heathcock, C. H.; Smith, S. C.; *J. Org. Chem.* **1992**, *57*, 6379-6380. (b) Heathcock, C. H.; Smith, S. C.; *J. Org. Chem.* **1994**, *57*, 6828-6839.
- (9) Guo, C.; Bhandaru, S.; Fuchs, P. L. *J. Am. Chem. Soc.* **1996**, *118*, 10672-10673
- (10) (a) Drogemuller, M.; Jantelat, R.; Winterfeldt, E.; *Angew. Chem. Int. Ed. Engl.* **1996**, *35*, 1572-1574. (b) Drogemuller, M.; Flessner, T.; Jantelat, R.; Scholz, U.; Winterfeldt, E.; *Eur. J. Org. Chem.* **1998**, 2811-2831.
- (11) (a) LaCour, T. G.; Guo, C.; Bhandaru, S.; Boyd, M. R.; Fuchs, P. L. *J. Am. Chem. Soc.* **1998**, *120*, 692-707. (b) Kim, S.; Sutton, S. C.; Guo, C.; Lacour, T. G.; Fuchs, P. L.; *J. Am. Chem. Soc.* **1999**, *121*, 2056-2070. (c) Jeong, J. U.; Guo, C.; Fuchs, P. L.; *J. Am. Chem. Soc.* **1999**, *121*, 2071-2084.

UNIVERSITY OF ILLINOIS-URBANA



3 0112 056180430

The HF Group

Indiana Plant

T 064384 3 68 00



8/9/2006

UNIVERSITY OF ILLINOIS-URBANA



3 0112 076494282